ISSN 1007-9327 (print)
ISSN 2219-2840 (online)

World Journal of *Gastroenterology*

World J Gastroenterol 2016 April 28; 22(16): 4073-4274

Published by Baishideng Publishing Group Inc

World Journal of Gastroenterology

A peer-reviewed, online, open-access journal of gastroenterology and hepatology

Editorial Board

2014-2017

The *World Journal of Gastroenterology* Editorial Board consists of 1376 members, representing a team of worldwide experts in gastroenterology and hepatology. They are from 68 countries, including Algeria (2), Argentina (7), Australia (31), Austria (9), Belgium (11), Brazil (20), Brunei Darussalam (1), Bulgaria (2), Cambodia (1), Canada (26), Chile (4), China (164), Croatia (2), Cuba (1), Czech (6), Denmark (2), Egypt (9), Estonia (2), Finland (6), France (20), Germany (58), Greece (31), Guatemala (1), Hungary (15), Iceland (1), India (33), Indonesia (2), Iran (10), Ireland (9), Israel (18), Italy (194), Japan (149), Jordan (1), Kuwait (1), Lebanon (7), Lithuania (1), Malaysia (1), Mexico (11), Morocco (1), Netherlands (5), New Zealand (4), Nigeria (3), Norway (6), Pakistan (6), Poland (12), Portugal (8), Puerto Rico (1), Qatar (1), Romania (10), Russia (3), Saudi Arabia (2), Singapore (7), Slovenia (2), South Africa (1), South Korea (69), Spain (51), Sri Lanka (1), Sudan (1), Sweden (12), Switzerland (5), Thailand (7), Trinidad and Tobago (1), Tunisia (2), Turkey (55), United Kingdom (49), United States (180), Venezuela (1), and Vietnam (1).

Gordon Stanley Howarth, *Roseworthy*
Seungha Kang, *Brisbane*
Alfred King Lam, *Gold Coast*
Ian C Lawrance, *PerthFremantle*
Barbara Anne Leggett, *Brisbane*
Daniel A Lemberg, *Sydney*
Rupert W Leong, *Sydney*
Finlay A Macrae, *Victoria*
Vance Matthews, *Melbourne*
David L Morris, *Sydney*
Reme Mountifield, *Bedford Park*
Hans J Netter, *Melbourne*
Nam Q Nguyen, *Adelaide*
Liang Qiao, *Westmead*
Rajvinder Singh, *Adelaide*
Ross Cyril Smith, *StLeonards*
Kevin J Spring, *Sydney*
Debbie Trinder, *Fremantle*
Daniel R van Langenberg, *Box Hill*
David Ian Watson, *Adelaide*
Desmond Yip, *Garran*
Li Zhang, *Sydney*

Austria

Felix Aigner, *Innsbruck*
Gabriela A Berlakovich, *Vienna*
Herwig R Cerwenka, *Graz*
Peter Ferenci, *Wien*
Alfred Gangl, *Vienna*
Kurt Lenz, *Linz*
Markus Peck-Radosavljevic, *Vienna*
Markus Raderer, *Vienna*
Stefan Riss, *Vienna*

Belgium

Michael George Adler, *Brussels*
Benedicte Y De Winter, *Antwerp*
Mark De Ridder, *Jette*
Olivier Detry, *Liege*
Denis Dufrane Dufrane, *Brussels*
Sven M Francque, *Edegem*
Nikos Kotzampassakis, *Liège*
Geert KMM Robaeys, *Genk*
Xavier Sagaert, *Leuven*
Peter Starkel, *Brussels*
Eddie Wisse, *Keerbergen*

Brazil

SMP Balzan, *Santa Cruz do Sul*
JLF Caboclo, *Sao jose do rio preto*
Fábio Guilherme Campos, *Sao Paulo*
Claudia RL Cardoso, *Rio de Janeiro*
Roberto J Carvalho-Filho, *Sao Paulo*
Carla Daltro, *Salvador*
José Sebastiao dos Santos, *Ribeirao Preto*
Eduardo LR Mello, *Rio de Janeiro*
Sthela Maria Murad-Regadas, *Fortaleza*
Claudia PMS Oliveira, *Sao Paulo*
Júlio C Pereira-Lima, *Porto Alegre*
Marcos V Perini, *Sao Paulo*
Vietla Satyanarayana Rao, *Fortaleza*
Raquel Rocha, *Salvador*
AC Simoes e Silva, *Belo Horizonte*
Mauricio F Silva, *Porto Alefre*
Aytan Miranda Sipahi, *Sao Paulo*
Rosa Leonôra Salerno Soares, *Niterói*
Cristiane Valle Tovo, *Porto Alegre*
Eduardo Garcia Vilela, *Belo Horizonte*

Brunei Darussalam

Vui Heng Chong, *Bandar Seri Begawan*

Bulgaria

Tanya Kirilova Kadiyska, *Sofia*
Mihaela Petrova, *Sofia*

Cambodia

Francois Rouet, *Phnom Penh*

Canada

Brian Bressler, *Vancouver*
Frank J Burczynski, *Winnipeg*
Wangxue Chen, *Ottawa*
Francesco Crea, *Vancouver*
Mirko Diksic, *Montreal*
Jane A Foster, *Hamilton*
Hugh J Freeman, *Vancouver*
Shahrokh M Ghobadloo, *Ottawa*
Yuewen Gong, *Winnipeg*
Philip H Gordon, *Quebec*
Rakesh Kumar, *Edmonton*
Wolfgang A Kunze, *Hamilton*
Patrick Labonte, *Laval*
Zhikang Peng, *Winnipeg*
Jayadev Raju, *Ottawa*
Maitreyi Raman, *Calgary*
Giada Sebastiani, *Montreal*
Maida J Sewitch, *Montreal*
Eldon A Shaffer, *Alberta*
Christopher W Teshima, *Edmonton*
Jean Sévigny, *Québec*
Pingchang Yang, *Hamilton*
Pingchang Yang, *Hamilton*
Eric M Yoshida, *Vancouver*
Bin Zheng, *Edmonton*

Chile

Marcelo A Beltran, *La Serena*
Flavio Nervi, *Santiago*
Adolfo Parra-Blanco, *Santiago*
Alejandro Soza, *Santiago*

China

Zhao-Xiang Bian, *Hong Kong*
San-Jun Cai, *Shanghai*
Guang-Wen Cao, *Shanghai*
Long Chen, *Nanjing*
Ru-Fu Chen, *Guangzhou*
George G Chen, *Hong Kong*
Li-Bo Chen, *Wuhan*
Jia-Xu Chen, *Beijing*
Hong-Song Chen, *Beijing*
Lin Chen, *Beijing*
Yang-Chao Chen, *Hong Kong*
Zhen Chen, *Shanghai*
Ying-Sheng Cheng, *Shanghai*
Kent-Man Chu, *Hong Kong*
Zhi-Jun Dai, *Xi'an*
Jing-Yu Deng, *Tianjin*
Yi-Qi Du, *Shanghai*
Zhi Du, *Tianjin*
Hani El-Nezami, *Hong Kong*
Bao-Ying Fei, *Hangzhou*
Chang-Ming Gao, *Nanjing*
Jian-Ping Gong, *Chongqing*
Zuo-Jiong Gong, *Wuhan*
Jing-Shan Gong, *Shenzhen*
Guo-Li Gu, *Beijing*
Yong-Song Guan, *Chengdu*
Mao-Lin Guo, *Luoyang*
Jun-Ming Guo, *Ningbo*
Yan-Mei Guo, *Shanghai*
Xiao-Zhong Guo, *Shenyang*
Guo-Hong Han, *Xi'an*
Ming-Liang He, *Hong Kong*
Peng Hou, *Xi'an*
Zhao-Hui Huang, *Wuxi*
Feng Ji, *Hangzhou*
Simon Law, *Hong Kong*
Yu-Yuan Li, *Guangzhou*
Meng-Sen Li, *Haikou*
Shu-De Li, *Shanghai*
Zong-Fang Li, *Xi'an*
Qing-Quan Li, *Shanghai*
Kang Li, *Lasa*
Han Liang, *Tianjin*
Xing'e Liu, *Hangzhou*
Zheng-Wen Liu, *Xi'an*
Xiao-Fang Liu, *Yantai*
Bin Liu, *Tianjin*
Quan-Da Liu, *Beijing*
Hai-Feng Liu, *Beijing*
Fei Liu, *Shanghai*
Ai-Guo Lu, *Shanghai*
He-Sheng Luo, *Wuhan*
Xiao-Peng Ma, *Shanghai*
Yong Meng, *Shantou*
Ke-Jun Nan, *Xi'an*
Siew Chien Ng, *Hong Kong*
Simon SM Ng, *Hong Kong*
Zhao-Shan Niu, *Qingdao*
Di Qu, *Shanghai*
Ju-Wei Mu, *Beijing*
Rui-Hua Shi, *Nanjing*
Bao-Min Shi, *Shanghai*
Xiao-Dong Sun, *Hangzhou*
Si-Yu Sun, *Shenyang*
Guang-Hong Tan, *Haikou*
Wen-Fu Tang, *Chengdu*
Anthony YB Teoh, *Hong Kong*
Wei-Dong Tong, *Chongqing*
Eric Tse, *Hong Kong*
Hong Tu, *Shanghai*

Stavros Gourgiotis, *Athens*
Leontios J Hadjileontiadis, *Thessaloniki*
Thomas Hyphantis, *Ioannina*
Ioannis Kanellos, *Thessaloniki*
Stylianos Karatapanis, *Rhodes*
Michael Koutsilieris, *Athens*
Spiros D Ladas, *Athens*
Theodoros K Liakakos, *Athens*
Emanuel K Manesis, *Athens*
Spilios Manolakopoulos, *Athens*
Gerassimos John Mantzaris, *Athens*
Athanasios D Marinis, *Piraeus*
Nikolaos Ioannis Nikiteas, *Athens*
Konstantinos X Papamichael, *Athens*
George Sgourakis, *Athens*
Konstantinos C Thomopoulos, *Patras*
Konstantinos Triantafyllou, *Athens*
Christos Triantos, *Patras*
Georgios Zacharakis, *Athens*
Petros Zezos, *Alexandroupolis*
Demosthenes E Ziogas, *Ioannina*

Guatemala

Carlos Maria Parellada, *Guatemala*

Hungary

Mihaly Boros, *Szeged*
Tamás Decsi, *Pécs*
Gyula Farkas, *Szeged*
Andrea Furka, *Debrecen*
Y vette Mandi, *Szeged*
Peter L Lakatos, *Budapest*
Pal Miheller, *Budapest*
Tamás Molnar, *Szeged*
Attila Olah, *Gyor*
Maria Papp, *Debrecen*
Zoltan Rakonczay, *Szeged*
Ferenc Sipos, *Budapest*
Miklós Tanyi, *Debrecen*
Tibor Wittmann, *Szeged*

Iceland

Tryggvi Bjorn Stefánsson, *Reykjavík*

Indiad

Brij B Agarwal, *New Delhi*
Deepak N Amarapurkar, *Mumbai*
Shams ul Bari, *Srinagar*
Sriparna Basu, *Varanasi*
Runu Chakravarty, *Kolkata*
Devendra C Desai, *Mumbai*
Nutan D Desai, *Mumbai*
Suneela Sunil Dhaneshwar, *Pune*
Radha K Dhiman, *Chandigarh*
Pankaj Garg, *Mohali*
Uday C Ghoshal, *Lucknow*
Kalpesh Jani, *Vadodara*
Premashis Kar, *New Delhi*
Jyotdeep Kaur, *Chandigarh*
Rakesh Kochhar, *Chandigarh*
Pradyumna K Mishra, *Mumbai*
Asish K Mukhopadhyay, *Kolkata*
Imtiyaz Murtaza, *Srinagar*
P Nagarajan, *New Delhi*
Samiran Nundy, *Delhi*
Gopal Pande, *Hyderabad*
Benjamin Perakath, *Vellore*
Arun Prasad, *New Delhi*
D Nageshwar Reddy, *Hyderabad*
Lekha Saha, *Chandigarh*
Sundeep Singh Saluja, *New Delhi*
Mahesh Prakash Sharma, *New Delhi*
Sadiq Saleem Sikora, *Bangalore*
Sarman Singh, *New Delhi*
Rajeev Sinha, *Jhansi*
Rupjyoti Talukdar, *Hyderabad*
Rakesh Kumar Tandon, *New Delhi*
Narayanan Thirumoorthy, *Coimbatore*

Indonesia

David Handojo Muljono, *Jakarta*
Andi Utama, *Jakarta*

Iran

Arezoo Aghakhani, *Tehran*
Seyed Mohsen Dehghani, *Shiraz*
Ahad Eshraghian, *Shiraz*
Hossein Khedmat, *Tehran*
Sadegh Massarrat, *Tehran*
Marjan Mohammadi, *Tehran*
Roja Rahimi, *Tehran*
Farzaneh Sabahi, *Tehran*
Majid Sadeghizadeh, *Tehran*
Farideh Siavoshi, *Tehran*

Ireland

Gary Alan Bass, *Dublin*
David J Brayden, *Dublin*
Ronan A Cahill, *Dublin*
Glen A Doherty, *Dublin*
Liam J Fanning, *Cork*
Barry Philip McMahon, *Dublin*
RossMcManus, *Dublin*
Dervla O'Malley, *Cork*
Sinead M Smith, *Dublin*

Israel

Dan Carter, *Ramat Gan*
Jorge-Shmuel Delgado, *Metar*
Eli Magen, *Ashdod*
Nitsan Maharshak, *Tel Aviv*
Shaul Mordechai, *Beer Sheva*
Menachem Moshkowitz, *Tel Aviv*
William Bahij Nseir, *Nazareth*
Shimon Reif, *Jerusalem*
Ram Reifen, *Rehovot*
Ariella Bar-Gil Shitrit, *Jerusalem*
Noam Shussman, *Jerusalem*
Igor Sukhotnik, *Haifa*
Nir Wasserberg, *Petach Tiqwa*
Jacob Yahav, *Rehovot*
Doron Levi Zamir, *Gedera*
Shira Zelber-Sagi, *Haifa*
Romy Zemel, *Petach-Tikva*

Italy

Ludovico Abenavoli, *Catanzaro*
Luigi Elio Adinolfi, *Naples*
Carlo Virginio Agostoni, *Milan*
Anna Alisi, *Rome*
Piero Luigi Almasio, *Palermo*
Donato Francesco Altomare, *Bari*
Amedeo Amedei, *Florence*
Pietro Andreone, *Bologna*
Imerio Angriman, *Padova*
Vito Annese, *Florence*
Paolo Aurello, *Rome*
Salavtore Auricchio, *Naples*
Gian Luca Baiocchi, *Brescia*
Gianpaolo Balzano, *Milan*
Antonio Basoli, *Rome*
Gabrio Bassotti, *San Sisto*
Mauro Bernardi, *Bologna*
Alberto Biondi, *Rome*
Ennio Biscaldi, *Genova*
Massimo Bolognesi, *Padua*
Luigi Bonavina, *Milano*
Aldo Bove, *Chieti*
Raffaele Bruno, *Pavia*
Luigi Brusciano, *Napoli*
Giuseppe Cabibbo, *Palermo*
Carlo Calabrese, *Bologna*
Daniele Calistri, *Meldola*
Vincenza Calvaruso, *Palermo*
Lorenzo Camellini, *Reggio Emilia*
Marco Candela, *Bologna*
Raffaele Capasso, *Naples*
Lucia Carulli, *Modena*
Renato David Caviglia, *Rome*
Luigina Cellini, *Chieti*
Giuseppe Chiarioni, *Verona*
Claudio Chiesa, *Rome*
Michele Cicala, *Roma*
Rachele Ciccocioppo, *Pavia*
Sandro Contini, *Parma*
Gaetano Corso, *Foggia*
Renato Costi, *Parma*
Alessandro Cucchetti, *Bologna*
Rosario Cuomo, *Napoli*
Giuseppe Currò, *Messina*
Paola De Nardi, *Milano*
Giovanni D De Palma, *Naples*
Raffaele De Palma, *Napoli*
Giuseppina De Petro, *Brescia*
Valli De Re, *Aviano*
Paolo De Simone, *Pisa*
Giuliana Decorti, *Trieste*
Emanuele Miraglia del Giudice, *Napoli*
Isidoro Di Carlo, *Catania*
Matteo Nicola Dario Di Minno, *Naples*
Massimo Donadelli, *Verona*
Mirko D'Onofrio, *Verona*
Maria Pina Dore, *Sassari*
Luca Elli, *Milano*
Massimiliano Fabozzi, *Aosta*

Massimo Falconi, *Ancona*
Ezio Falletto, *Turin*
Silvia Fargion, *Milan*
Matteo Fassan, *Verona*
Gianfranco Delle Fave, *Roma*
Alessandro Federico, *Naples*
Francesco Feo, *Sassari*
Davide Festi, *Bologna*
Natale Figura, *Siena*
Vincenzo Formica, *Rome*
Mirella Fraquelli, *Milan*
Marzio Frazzoni, *Modena*
Walter Fries, *Messina*
Gennaro Galizia, *Naples*
Andrea Galli, *Florence*
Matteo Garcovich, *Rome*
Eugenio Gaudio, *Rome*
Paola Ghiorzo, *Genoa*
Edoardo G Giannini, *Genova*
Luca Gianotti, *Monza*
Maria Cecilia Giron, *Padova*
Alberto Grassi, *Rimini*
Gabriele Grassi, *Trieste*
Francesco Greco, *Bergamo*
Luigi Greco, *Naples*
Antonio Grieco, *Rome*
Fabio Grizzi, *Rozzano*
Laurino Grossi, *Pescara*
Simone Guglielmetti, *Milan*
Tiberiu Hershcovici, *Jerusalem*
Calogero Iacono, *Verona*
Enzo Ierardi, *Bari*
Amedeo Indriolo, *Bergamo*
Raffaele Iorio, *Naples*
Paola Iovino, *Salerno*
Angelo A Izzo, *Naples*
Loreta Kondili, *Rome*
Filippo La Torre, *Rome*
Giuseppe La Torre, *Rome*
Giovanni Latella, *L'Aquila*
Salvatore Leonardi, *Catania*
Massimo Libra, *Catania*
Anna Licata, *Palermo*
C armela Loguercio, *Naples*
Amedeo Lonardo, *Modena*
Carmelo Luigiano, *Catania*
Francesco Luzza, *Catanzaro*
Giovanni Maconi, *Milano*
Antonio Macrì, *Messina*
Mariano Malaguarnera, *Catania*
Francesco Manguso, *Napoli*
Tommaso Maria Manzia, *Rome*
Daniele Marrelli, *Siena*
Gabriele Masselli, *Rome*
Sara Massironi, *Milan*
Giuseppe Mazzarella, *Avellino*
Michele Milella, *Rome*
Giovanni Milito, *Rome*
Antonella d'Arminio Monforte, *Milan*
Fabrizio Montecucco, *Genoa*
Giovanni Monteleone, *Rome*
Mario Morino, *Torino*
Vincenzo La Mura, *Milan*
Gerardo Nardone, *Naples*
Riccardo Nascimbeni, *Brescia*
Gabriella Nesi, *Florence*
Giuseppe Nigri, *Rome*
Erica Novo, *Turin*
Veronica Ojetti, *Rome*
Michele Orditura, *Naples*
Fabio Pace, *Seriate*
Lucia Pacifico, *Rome*
Omero Alessandro Paoluzi, *Rome*
Valerio Pazienza, *San Giovanni Rotondo*
Rinaldo Pellicano, *Turin*
Adriano M Pellicelli, *Rome*
Nadia Peparini, *Ciampino*
Mario Pescatori, *Rome*
Antonio Picardi, *Rome*
Alberto Pilotto, *Padova*
Alberto Piperno, *Monza*
Anna Chiara Piscaglia, *Rome*
Maurizio Pompili, *Rome*
Francesca Romana Ponziani, *Rome*
Cosimo Prantera, *Rome*
Girolamo Ranieri, *Bari*
Carlo Ratto, *Tome*
Barbara Renga, *Perugia*
Alessandro Repici, *Rozzano*
Maria Elena Riccioni, *Rome*
Lucia Ricci-Vitiani, *Rome*
Luciana Rigoli, *Messina*
Mario Rizzetto, *Torino*
Ballarin Roberto, *Modena*
Roberto G Romanelli, *Florence*
Claudio Romano, *Messina*
Luca Roncucci, *Modena*
Cesare Ruffolo, *Treviso*
L ucia Sacchetti, *Napoli*
Rodolfo Sacco, *Pisa*
Lapo Sali, *Florence*
Romina Salpini, *Rome*
Giulio Aniello, *Santoro Treviso*
Armando Santoro, *Rozzano*
Edoardo Savarino, *Padua*
Marco Senzolo, *Padua*
Annalucia Serafino, *Rome*
Giuseppe S Sica, *Rome*
Pierpaolo Sileri, *Rome*
Cosimo Sperti, *Padua*
Vincenzo Stanghellini, *Bologna*
Cristina Stasi, *Florence*
Gabriele Stocco, *Trieste*
Roberto Tarquini, *Florence*
Mario Testini, *Bari*
Guido Torzilli, *Milan*
Guido Alberto Massimo, *Tiberio Brescia*
Giuseppe Toffoli, *Aviano*
Alberto Tommasini, *Trieste*
Francesco Tonelli, *Florence*
Cesare Tosetti Porretta, *Terme*
Lucio Trevisani, *Cona*
Guglielmo M Trovato, *Catania*
Mariapia Vairetti, *Pavia*
Luca Vittorio Valenti, *Milano*
Mariateresa T Ventura, *Bari*
Giuseppe Verlato, *Verona*
Marco Vivarelli, *Ancona*
Giovanni Li Volti, *Catania*
Giuseppe Zanotti, *Padua*
Vincenzo Zara, *Lecce*
Gianguglielmo Zehender, *Milan*
Anna Linda Zignego, *Florence*
Rocco Antonio Zoccali, *Messina*
Angelo Zullo, *Rome*

Japan

Yasushi Adachi, *Sapporo*
Takafumi Ando, *Nagoya*
Masahiro Arai, *Tokyo*
Makoto Arai, *Chiba*
Takaaki Arigami, *Kagoshima*
Itaru Endo,*Yokohama*
Munechika Enjoji, *Fukuoka*
Shunji Fujimori, *Tokyo*
Yasuhiro Fujino, *Akashi*
Toshiyoshi Fujiwara, *Okayama*
Yosuke Fukunaga, *Tokyo*
Toshio Fukusato, *Tokyo*
Takahisa Furuta, *Hamamatsu*
Osamu Handa, *Kyoto*
Naoki Hashimoto, *Osaka*
Yoichi Hiasa, *Toon*
Masatsugu Hiraki, *Saga*
Satoshi Hirano, *Sapporo*
Keiji Hirata, *Fukuoka*
Toru Hiyama, *Higashihiroshima*
Akira Hokama, *Nishihara*
Shu Hoteya, *Tokyo*
Masao Ichinose, *Wakayama*
Tatsuya Ide, *Kurume*
Masahiro Iizuka, *Akita*
Toshiro Iizuka, *Tokyo*
Kenichi Ikejima, *Tokyo*
Tetsuya Ikemoto, *Tokushima*
Hiroyuki Imaeda, *Saitama*
Atsushi Imagawa, *Kan-onji*
Hiroo Imazu, *Tokyo*
Shuji Isaji, *Tsu*
Toru Ishikawa, *Niigata*
Toshiyuki Ishiwata, *Tokyo*
Soichi Itaba, *Kitakyushu*
Yoshiaki Iwasaki, *Okayama*
Tatehiro Kagawa, *Isehara*
Satoru Kakizaki, *Maebashi*
Naomi Kakushima, *Shizuoka*
Terumi Kamisawa, *Tokyo*
Akihide Kamiya, *Isehara*
Osamu Kanauchi, *Tokyo*
Tatsuo Kanda, *Chiba*
Shin Kariya, *Okayama*
Shigeyuki Kawa, *Matsumoto*
Takumi Kawaguchi, *Kurume*
Takashi Kawai, *Tokyo*
Soo Ryang Kim, *Kobe*
Shinsuke Kiriyama, *Gunma*
Tsuneo Kitamura, *Urayasu*
Masayuki Kitano, *Osakasayama*
Hirotoshi Kobayashi, *Tokyo*
Hironori Koga, *Kurume*
Takashi Kojima, *Sapporo*
Satoshi Kokura, *Kyoto*
Shuhei Komatsu, *Kyoto*
Tadashi Kondo, *Tokyo*
Yasuteru Kondo, *Sendai*
Yasuhiro Kuramitsu, *Yamaguchi*
Yukinori Kurokawa, *Osaka*
Shin Maeda, *Yokohama*
Koutarou Maeda, *Toyoake*

Hitoshi Maruyama, *Chiba*
Atsushi Masamune, *Sendai*
Hiroyuki Matsubayashi, *Suntogun*
Akihisa Matsuda, *Inzai*
Hirofumi Matsui, *Tsukuba*
Akira Matsumori, *Kyoto*
Yoichi Matsuo, *Nagoya*
Y Matsuzaki, *Ami*
Toshihiro Mitaka, *Sapporo*
Kouichi Miura, *Akita*
Shinichi Miyagawa, *Matumoto*
Eiji Miyoshi, *Suita*
Toru Mizuguchi, *Sapporo*
Nobumasa Mizuno, *Nagoya*
Zenichi Morise, *Nagoya*
Tomohiko Moriyama, *Fukuoka*
Kunihiko Murase, *Tusima*
Michihiro Mutoh, *Tsukiji*
Akihito Nagahara, *Tokyo*
Hikaru Nagahara, *Tokyo*
Hidenari Nagai, *Tokyo*
Koichi Nagata, *Shimotsuke-shi*
Masaki Nagaya, *Kawasaki*
Hisato Nakajima, *Nishi-Shinbashi*
Toshifusa Nakajima, *Tokyo*
Hiroshi Nakano, *Kawasaki*
Hiroshi Nakase, *Kyoto*
Toshiyuki Nakayama, *Nagasaki*
Takahiro Nakazawa, *Nagoya*
Shoji Natsugoe, *Kagoshima City*
Tsutomu Nishida, *Suita*
Shuji Nomoto, *Naogya*
Sachiyo Nomura, *Tokyo*
Takeshi Ogura, *Takatsukishi*
Nobuhiro Ohkohchi, *Tsukuba*
Toshifumi Ohkusa, *Kashiwa*
Hirohide Ohnishi, *Akita*
Teruo Okano, *Tokyo*
Satoshi Osawa, *Hamamatsu*
Motoyuki Otsuka, *Tokyo*
Michitaka Ozaki, *Sapporo*
Satoru Saito, *Yokohama*
Naoaki Sakata, *Sendai*
Ken Sato, *Maebashi*
Toshiro Sato, *Tokyo*
Tomoyuki Shibata, *Toyoake*
Tomohiko Shimatani, *Kure*
Yukihiro Shimizu, *Nanto*
Tadashi Shimoyama, *Hirosaki*
Masayuki Sho, *Nara*
Ikuo Shoji, *Kobe*
Atsushi Sofuni, *Tokyo*
Takeshi Suda, *Niigata*
M Sugimoto, *Hamamatsu*
Ken Sugimoto, *Hamamatsu*
Haruhiko Sugimura, *Hamamatsu*
Shoichiro Sumi, *Kyoto*
Hidekazu Suzuki, *Tokyo*
Masahiro Tajika, *Nagoya*
Hitoshi Takagi, *Takasaki*
Toru Takahashi, *Niigata*
Yoshihisa Takahashi, *Tokyo*
Shinsuke Takeno, *Fukuoka*
Akihiro Tamori, *Osaka*
Kyosuke Tanaka, *Tsu*
Shinji Tanaka, *Hiroshima*
Atsushi Tanaka, *Tokyo*
Yasuhito Tanaka, *Nagoya*
Shinji Tanaka, *Tokyo*
Minoru Tomizawa, *Yotsukaido City*
Kyoko Tsukiyama-Kohara, *Kagoshima*
Takuya Watanabe, *Niigata*
Kazuhiro Watanabe, *Sendai*
Satoshi Yamagiwa, *Niigata*
Takayuki Yamamoto, *Yokkaichi*
Hiroshi Yamamoto, *Otsu*
Kosho Yamanouchi, *Nagasaki*
Ichiro Yasuda, *Gifu*
Yutaka Yata, *Maebashi-city*
Shin-ichi Yokota, *Sapporo*
Norimasa Yoshida, *Kyoto*
Hiroshi Yoshida, *Tama-City*
Hitoshi Yoshiji, *Kashihara*
Kazuhiko Yoshimatsu, *Tokyo*
Kentaro Yoshioka, *Toyoake*
Nobuhiro Zaima, *Nara*

Jordan
Khaled Ali Jadallah, *Irbid*

Kuwait
Islam Khan, *Kuwait*

Lebanon
Bassam N Abboud, *Beirut*
Kassem A Barada, *Beirut*
Marwan Ghosn, *Beirut*
Iyad A Issa, *Beirut*
Fadi H Mourad, *Beirut*
AIa Sharara, *Beirut*
Rita Slim, *Beirut*

Lithuania
Antanas Mickevicius, *Kaunas*

Malaysia
Huck Joo Tan, *Petaling Jaya*

Mexico
Richard A Awad, *Mexico City*
Carlos R Camara-Lemarroy, *Monterrey*
Norberto C Chavez-Tapia, *Mexico City*
Wolfgang Gaertner, *Mexico City*
Diego Garcia-Compean, *Monterrey*
Arturo Panduro, *Guadalajara*
OT Teramoto-Matsubara, *Mexico City*
Felix Tellez-Avila, *Mexico City*
Omar Vergara-Fernandez, *Mexico City*
Saúl Villa-Trevino, *Cuidad de México*

Morocco
Samir Ahboucha, *Khouribga*

Netherlands
Robert J de Knegt, *Rotterdam*
Tom Johannes Gerardus Gevers, *Nijmegen*
Menno Hoekstra, *Leiden*
BW Marcel Spanier, *Arnhem*
Karel van Erpecum, *Utrecht*

New Zealand
Leo K Cheng, *Auckland*
Andrew Stewart Day, *Christchurch*
Jonathan Barnes Koea, *Auckland*
Max Petrov, *Auckland*

Nigeria
Olufunmilayo Adenike Lesi, *Lagos*
Jesse Abiodun Otegbayo, *Ibadan*
Stella Ifeanyi Smith, *Lagos*

Norway
Trond Berg, *Oslo*
Trond Arnulf Buanes, *Krokkleiva*
Thomas de Lange, *Rud*
Magdy El-Salhy, *Stord*
Rasmus Goll, *Tromso*
Dag Arne Lihaug Hoff, *Aalesund*

Pakistan
Zaigham Abbas, *Karachi*
Usman A Ashfaq, *Faisalabad*
Muhammad Adnan Bawany, *Hyderabad*
Muhammad Idrees, *Lahore*
Saeed Sadiq Hamid, *Karachi*
Yasir Waheed, *Islamabad*

Poland
Thomas Brzozowski, *Cracow*
Magdalena Chmiela, *Lodz*
Krzysztof Jonderko, *Sosnowiec*
Anna Kasicka-Jonderko, *Sosnowiec*
Michal Kukla, *Katowice*
Tomasz Hubert Mach, *Krakow*
Agata Mulak, *Wroclaw*
Danuta Owczarek, *Kraków*
Piotr Socha, *Warsaw*
Piotr Stalke, *Gdansk*
Julian Teodor Swierczynski, *Gdansk*
Anna M Zawilak-Pawlik, *Wroclaw*

Portugal
Marie Isabelle Cremers, *Setubal*
Ceu Figueiredo, *Porto*
Ana Isabel Lopes, *LIsbon*
M Paula Macedo, *Lisboa*
Ricardo Marcos, *Porto*
Rui T Marinho, *Lisboa*
Guida Portela-Gomes, *Estoril*

Filipa F Vale, *Lisbon*

Puerto Rico

Caroline B Appleyard, *Ponce*

Qatar

Abdulbari Bener, *Doha*

Romania

Mihai Ciocirlan, *Bucharest*
Dan LucianDumitrascu, *Cluj-Napoca*
Carmen Fierbinteanu-Braticevici, *Bucharest*
Romeo G Mihaila, *Sibiu*
Lucian Negreanu, *Bucharest*
Adrian Saftoiu, *Craiova*
Andrada Seicean, *Cluj-Napoca*
Ioan Sporea, *Timisoara*
Letiţia Adela Maria Streba, *Craiova*
Anca Trifan, *Iasi*

Russia

Victor Pasechnikov, *Stavropol*
Vasiliy Ivanovich Reshetnyak, *Moscow*
Vitaly Skoropad, *Obninsk*

Saudi Arabia

Abdul-Wahed N Meshikhes, *Dammam*
M Ezzedien Rabie, *Khamis Mushait*

Singapore

Brian KP Goh, *Singapore*
Richie Soong, *Singapore*
Ker-Kan Tan, *Singapore*
Kok-Yang Tan, *Singapore*
Yee-Joo Tan, *Singapore*
Mark Wong, *Singapore*
Hong Ping Xia, *Singapore*

Slovenia

Matjaz Homan, *Ljubljana*
Martina Perse, *Ljubljana*

South Korea

Sang Hoon Ahn, *Seoul*
Seung Hyuk Baik, *Seoul*
Soon Koo Baik, *Wonju*
Soo-Cheon Chae, *Iksan*
Byung-Ho Choe, *Daegu*
Suck Chei Choi, *Iksan*
Hoon Jai Chun, *Seoul*
Yeun-Jun Chung, *Seoul*
Young-Hwa Chung, *Seoul*
Ki-Baik Hahm, *Seongnam*
Sang Young Han, *Busan*
Seok Joo Han, *Seoul*
Seung-Heon Hong, *Iksan*
Jin-Hyeok Hwang, *Seoungnam*
Jeong Won Jang, *Seoul*
Jin-Young Jang, *Seoul*
Dae-Won Jun, *Seoul*
Young Do Jung, *Kwangju*
Gyeong Hoon Kang, *Seoul*
Sung-Bum Kang, *Seoul*
Koo Jeong Kang, *Daegu*
Ki Mun Kang, *Jinju*
Chang Moo Kang, *Seodaemun-gu*
Gwang Ha Kim, *Busan*
Sang Soo Kim, *Goyang-si*
Jin Cheon Kim, *Seoul*
Tae Il Kim, *Seoul*
Jin Hong Kim, *Suwon*
Kyung Mo Kim, *Seoul*
Kyongmin Kim, *Suwon*
Hyung-Ho Kim, *Seongnam*
Seoung Hoon Kim, *Goyang*
Sang Il Kim, *Seoul*
Hyun-Soo Kim, *Wonju*
Jung Mogg Kim, *Seoul*
Dong Yi Kim, *Gwangju*
Kyun-Hwan Kim, *Seoul*
Jong-Han Kim, *Ansan*
Sang Wun Kim, *Seoul*
Ja-Lok Ku, *Seoul*
Kyu Taek Lee, *Seoul*
Hae-Wan Lee, *Chuncheon*
Inchul Lee, *Seoul*
Jung Eun Lee, *Seoul*
Sang Chul Lee, *Daejeon*
Song Woo Lee, *Ansan-si*
Hyuk-Joon Lee, *Seoul*
Seong-Wook Lee, *Yongin*
Kil Yeon Lee, *Seoul*
Jong-Inn Lee, *Seoul*
Kyung A Lee, *Seoul*
Jong-Baeck Lim, *Seoul*
Eun-Yi Moon, *Seoul*
SH Noh, *Seoul*
Seung Woon Paik, *Seoul*
Won Sang Park, *Seoul*
Sung-Joo Park, *Iksan*
Kyung Sik Park, *Daegu*
Se Hoon Park, *Seoul*
Yoonkyung Park, *Gwangju*
Seung-Wan Ryu, *Daegu*
Il Han Song, *Cheonan*
Myeong Jun Song, *Daejeon*
Yun Kyoung Yim, *Daejeon*
Dae-Yeul Yu *Daejeon*

Spain

Mariam Aguas, *Valencia*
Raul J Andrade, *Málaga*
Antonio Arroyo, *Elche*
Josep M Bordas, *Barcelona*
Lisardo Boscá, *Madrid*
Ricardo Robles Campos, *Murcia*
Jordi Camps, *Reus*
Carlos Cervera *Barcelona*
Alfonso Clemente, *Granada*
Pilar Codoner-Franch, *Valencia*
Fernando J Corrales, *Pamplona*
Fermin Sánchez de Medina, *Granada*
Alberto Herreros de Tejada, *Majadahonda*
Enrique de-Madaria, *Alicante*
JE Dominguez-Munoz, *Santiago de Compostela*
Vicente Felipo, *Valencia*
CM Fernandez-Rodriguez, *Madrid*
Carmen Frontela-Saseta, *Murcia*
Julio Galvez, *Granada*
Maria Teresa García, *Vigo*
MI Garcia-Fernandez, *Málaga*
Emilio Gonzalez-Reimers, *La Laguna*
Marcel Jimenez, *Bellaterra*
Angel Lanas, *Zaragoza*
Juan Ramón Larrubia, *Guadalajara*
Antonio Lopez-Sanroman, *Madrid*
Vicente Lorenzo-Zuniga, *Badalona*
Alfredo J Lucendo, *Tomelloso*
Vicenta Soledad Martinez-Zorzano, *Vigo*
José Manuel Martin-Villa, *Madrid*
Julio Mayol, *Madrid*
Manuel Morales-Ruiz, *Barcelona*
Alfredo Moreno-Egea, *Murcia*
Albert Pares, *Barcelona*
Maria Pellise, *Barcelona*
José Perea, *Madrid*
Miguel Angel Plaza, *Zaragoza*
María J Pozo, *Cáceres*
Enrique Quintero, *La Laguna*
Jose M Ramia, *Madrid*
Francisco Rodriguez-Frias, *Barcelona*
Silvia Ruiz-Gaspa, *Barcelona*
Xavier Serra-Aracil, *Barcelona*
Vincent Soriano, *Madrid*
Javier Suarez, *Pamplona*
Carlos Taxonera, *Madrid*
M Isabel Torres, *Jaén*
Manuel Vazquez-Carrera, *Barcelona*
Benito Velayos, *Valladolid*
Silvia Vidal, *Barcelona*

Sri Lanka

Arjuna Priyadarsin De Silva, *Colombo*

Sudan

Ishag Adam, *Khartoum*

Sweden

Roland G Andersson, *Lund*
Bergthor Björnsson, *Linkoping*
Johan Christopher Bohr, *Örebro*
Mauro D'Amato, *Stockholm*
Thomas Franzen, *Norrkoping*
Evangelos Kalaitzakis, *Lund*
Riadh Sadik, *Gothenburg*
Per Anders Sandstrom, *Linkoping*
Ervin Toth, *Malmö*
Konstantinos Tsimogiannis, *Vasteras*
Apostolos V Tsolakis, *Uppsala*

Switzerland

Gieri Cathomas, *Liestal*
Jean Louis Frossard, *Geneve*
Christian Toso, *Geneva*
Stephan Robert Vavricka, *Zurich*
Dominique Velin, *Lausanne*

Thailand

Thawatchai Akaraviputh, *Bangkok*
P Yoysungnoen Chintana, *Pathumthani*
Veerapol Kukongviriyapan, *Muang*
Vijittra Leardkamolkarn, *Bangkok*
Varut Lohsiriwat, *Bangkok*
Somchai Pinlaor, *Khaon Kaen*
D Wattanasirichaigoon, *Bangkok*

Trinidad and Tobago

B Shivananda Nayak, *Mount Hope*

Tunisia

Ibtissem Ghedira, *Sousse*
Lilia Zouiten-Mekki, *Tunis*

Turkey

Inci Alican, *Istanbul*
Mustafa Altindis, *Sakarya*
Mutay Aslan, *Antalya*
Oktar Asoglu, *Istanbul*
Yasemin Hatice Balaban, *Istanbul*
Metin Basaranoglu, *Ankara*
Yusuf Bayraktar, *Ankara*
Süleyman Bayram, *Adiyaman*
Ahmet Bilici, *Istanbul*
Ahmet Sedat Boyacioglu, *Ankara*
Züleyha Akkan Cetinkaya, *Kocaeli*
Cavit Col, *Bolu*
Yasar Colak, *Istanbul*
Cagatay Erden Daphan, *Kirikkale*
Mehmet Demir, *Hatay*
Ahmet Merih Dobrucali, *Istanbul*
Gülsüm Ozlem Elpek, *Antalya*
Ayse Basak Engin, *Ankara*
Eren Ersoy, *Ankara*
Osman Ersoy, *Ankara*
Yusuf Ziya Erzin, *Istanbul*
Mukaddes Esrefoglu, *Istanbul*
Levent Filik, *Ankara*
Ozgur Harmanci, *Ankara*
Koray Hekimoglu, *Ankara*
Abdurrahman Kadayifci, *Gaziantep*
Cem Kalayci, *Istanbul*
Selin Kapan, *Istanbul*
Huseyin Kayadibi, *Adana*
Sabahattin Kaymakoglu, *Istanbul*
Metin Kement, *Istanbul*
Mevlut Kurt, *Bolu*
Resat Ozaras, *Istanbul*
Elvan Ozbek, *Adapazari*
Cengiz Ozcan, *Mersin*
Hasan Ozen, *Ankara*
Halil Ozguc, *Bursa*
Mehmet Ozturk, *Izmir*
Orhan V Ozkan, *Sakarya*
Semra Paydas, *Adana*
Ozlem Durmaz Suoglu, *Istanbul*
Ilker Tasci, *Ankara*
Müge Tecder-ünal, *Ankara*
Mesut Tez, *Ankara*
Serdar Topaloglu, *Trabzon*
Murat Toruner, *Ankara*
Gokhan Tumgor, *Adana*
Oguz Uskudar, *Adana*
Mehmet Yalniz, *Elazig*
Mehmet Yaman, *Elazig*
Veli Yazisiz, *Antalya*
Yusuf Yilmaz, *Istanbul*
Ozlem Yilmaz, *Izmir*
Oya Yucel, *Istanbul*
Ilhami Yuksel, *Ankara*

United Kingdom

Nadeem Ahmad Afzal, *Southampton*
Navneet K Ahluwalia, *Stockport*
Yeng S Ang, *Lancashire*
Ramesh P Arasaradnam, *Coventry*
Ian Leonard Phillip Beales, *Norwich*
John Beynon, *Swansea*
Barbara Braden, *Oxford*
Simon Bramhall, *Birmingham*
Geoffrey Burnstock, *London*
Ian Chau, *Sutton*
Thean Soon Chew, *London*
Helen G Coleman, *Belfast*
Anil Dhawan, *London*
Sunil Dolwani, *Cardiff*
Piers Gatenby, *London*
Anil T George, *London*
Pasquale Giordano, *London*
Paul Henderson, *Edinburgh*
Georgina Louise Hold, *Aberdeen*
Stefan Hubscher, *Birmingham*
Robin D Hughes, *London*
Nusrat Husain, *Manchester*
Matt W Johnson, *Luton*
Konrad Koss, *Macclesfield*
Anastasios Koulaouzidis, *Edinburgh*
Simon Lal, *Salford*
John S Leeds, *Aberdeen*
JK K Limdi, *Manchester*
Hongxiang Liu, *Cambridge*
Michael Joseph McGarvey, *London*
Michael Anthony Mendall, *London*
Alexander H Mirnezami, *Southampton*
J Bernadette Moore, *Guildford*
Claudio Nicoletti, *Norwich*
Savvas Papagrigoriadis, *London*
Sylvia LF Pender, *Southampton*
David Mark Pritchard, *Liverpool*
James A Ross, *Edinburgh*
Kamran Rostami, *Worcester*
Xiong Z Ruan, *London*
Frank I Tovey, *London*
Dhiraj Tripathi, *Birmingham*
Vamsi R Velchuru, *Great Yarmouth*
Nicholas T Ventham, *Edinburgh*
Diego Vergani, *London*
Jack Westwood Winter, *Glasgow*
Terence Wong, *London*
Ling Yang, *Oxford*

United States

Daniel E Abbott, *Cincinnati*
Ghassan K Abou-Alfa, *New York*
Julian Abrams, *New York*
David William Adelson, *Los Angeles*
Jonathan Steven Alexander, *Shreveport*
Tauseef Ali, *Oklahoma City*
Mohamed R Ali, *Sacramento*
Rajagopal N Aravalli, *Minneapolis*
Hassan Ashktorab, *Washington*
Shashi Bala, *Worcester*
Charles F Barish, *Raleigh*
P Patrick Basu, *New York*
Robert L Bell, *Berkeley Heights*
David Bentrem, *Chicago*
Henry J Binder, *New Haven*
Joshua Bleier, *Philadelphia*
Wojciech Blonski, *Johnson City*
Kenneth Boorom, *Corvallis*
Brian Boulay, *Chicago*
Carla W Brady, *Durham*
Kyle E Brown, *Iowa City*
Adeel A Butt, *Pittsburgh*
Weibiao Cao, *Providence*
Andrea Castillo, *Cheney*
Fernando J Castro, *Weston*
Adam S Cheifetz, *Boston*
Xiaoxin Luke Chen, *Durham*
Ramsey Cheung, *Palo Alto*
Parimal Chowdhury, *Little Rock*
Edward John Ciaccio, *New York*
Dahn L Clemens, *Omaha*
Yingzi Cong, *Galveston*
Laura Iris Cosen-Binker, *Boston*
Joseph John Cullen, *Lowa*
Mark J Czaja, *Bronx*
Mariana D Dabeva, *Bronx*
Christopher James Damman, *Seattle*
Isabelle G De Plaen, *Chicago*
Punita Dhawan, *Nashville*
Hui Dong, *La Jolla*
Wael El-Rifai, *Nashville*
Sukru H Emre, *New Haven*
Paul Feuerstadt, *Hamden*
Josef E Fischer, *Boston*
Laurie N Fishman, *Boston*
Joseph Che Forbi, *Atlanta*
Temitope Foster, *Atlanta*
Amy E Foxx-Orenstein, *Scottsdale*
Daniel E Freedberg, *New York*
Shai Friedland, *Palo Alto*
Virgilio George, *Indianapolis*
Ajay Goel, *Dallas*
Oliver Grundmann, *Gainesville*
Stefano Guandalini, *Chicago*
Chakshu Gupta, *St. Joseph*
Grigoriy E Gurvits, *New York*

Xiaonan Han, *Cincinnati*
Mohamed Hassan, *Jackson*
Martin Hauer-Jensen, *Little Rock*
Koichi Hayano, *Boston*
Yingli Hee, *Atlanta*
Samuel B Ho, *San Diego*
Jason Ken Hou, *Houston*
Lifang Hou, *Chicago*
K-Qin Hu, *Orange*
Jamal A Ibdah, *Columbia*
Robert Thomas Jensen, *Bethesda*
Huanguang "Charlie" Jia, *Gainesville*
Rome Jutabha, *Los Angeles*
Andreas M Kaiser, *Los Angeles*
Avinash Kambadakone, *Boston*
David Edward Kaplan, *Philadelphia*
Randeep Kashyap, *Rochester*
Rashmi Kaul, *Tulsa*
Ali Keshavarzian, *Chicago*
Amir Maqbul Khan, *Marshall*
Nabeel Hasan Khan, *New Orleans*
Sahil Khanna, *Rochester*
Kusum K Kharbanda, *Omaha*
Hyun Sik Kim, *Pittsburgh*
Joseph Kim, *Duarte*
Jae S Kim, *Gainesville*
Miran Kim, *Providence*
Timothy R Koch, *Washington*
Burton I Korelitz, *New York*
Betsy Kren, *Minneapolis*
Shiu-Ming Kuo, *Buffalo*
Michelle Lai, *Boston*
Andreas Larentzakis, *Boston*
Edward Wolfgang Lee, *Los Angeles*
Daniel A Leffler, *Boston*
Michael Leitman, *New York*
Suthat Liangpunsakul, *Indianapolis*
Joseph K Lim, *New Haven*
Elaine Y Lin, *Bronx*
Henry C Lin, *Albuquerque*
Rohit Loomba, *La Jolla*
James David Luketich, *Pittsburgh*
Li Ma, *Stanford*
Mohammad F Madhoun, *Oklahoma City*
Thomas C Mahl, *Buffalo*
Ashish Malhotra, *Bettendorf*
Pranoti Mandrekar, *Worcester*
John Marks, *Wynnewood*
Wendy M Mars, *Pittsburgh*
Julien Vahe Matricon, *San Antonio*
Craig J McClain, *Louisville*
Tamir Miloh, *Phoenix*
Ayse Leyla Mindikoglu, *Baltimore*
Huanbiao Mo, *Denton*
Klaus Monkemuller, *Birmingham*
John Morton, *Stanford*
Adnan Muhammad, *Tampa*
Michael J Nowicki, *Jackson*
Patrick I Okolo, *Baltimore*
Giusepp Orlando, *Winston Salem*
Natalia A Osna, *Omaha*
Virendra N Pandey, *Newark*
Mansour A Parsi, *Cleveland*
Michael F Picco, *Jacksonville*
Daniel S Pratt, *Boston*
Xiaofa Qin, *Newark*
Janardan K Reddy, *Chicago*
Victor E Reyes, *Galveston*
Jon Marc Rhoads, *Houston*
Giulia Roda, *New York*
Jean-Francois Armand Rossignol, *Tampa*
Paul A Rufo, *Boston*
Madhusudana Girija Sanal, *New York*
Miguel Saps, *Chicago*
Sushil Sarna, *Galveston*
Ann O Scheimann, *Baltimore*
Bernd Schnabl, *La Jolla*
Matthew J Schuchert, *Pittsburgh*
Ekihiro Seki, *La Jolla*
Chanjuan Shi, *Nashville*
David Quan Shih, *Los Angeles*
Shadab A Siddiqi, *Orlando*
William B Silverman, *Iowa City*
Shashideep Singhal, *New York*
Bronislaw L Slomiany, *Newark*
Steven F Solga, *Bethlehem*
Byoung-Joon Song, *Bethesda*
Dario Sorrentino, *Roanoke*
Scott R Steele, *Fort Lewis*
Branko Stefanovic, *Tallahassee*
Arun Swaminath, *New York*
Kazuaki Takabe, *Richmond*
Naoki Tanaka, *Bethesda*
Hans Ludger Tillmann, *Durham*
George Triadafilopoulos, *Stanford*
John Richardson Thompson, *Nashville*
Andrew Ukleja, *Weston*
Miranda AL van Tilburg, *Chapel Hill*
Gilberto Vaughan, *Atlanta*
Vijayakumar Velu, *Atlanta*
Gebhard Wagener, *New York*
Kasper Saonun Wang, *Los Angeles*
Xiangbing Wang, *New Brunswick*
Daoyan Wei, *Houston*
Theodore H Welling, *Ann Arbor*
C Mel Wilcox, *Birmingham*
Jacqueline Lee Wolf, *Boston*
Laura Ann Woollett, *Cincinnati*
Harry Hua-Xiang Xia, *East Hanover*
Wen Xie, *Pittsburgh*
Guang Yu Yang, *Chicago*
Michele T Yip-Schneider, *Indianapolis*
Sam Zakhari, *Bethesda*
Kezhong Zhang, *Detroit*
Huiping Zhou, *Richmond*
Xiao-Jian Zhou, *Cambridge*
Richard Zubarik, *Burlington*

Venezuela

Miguel Angel Chiurillo, *Barquisimeto*

Vietnam

Van Bang Nguyen, *Hanoi*

World Journal of Gastroenterology

Contents

Weekly Volume 22 Number 16 April 28, 2016

NAME OF JOURNAL
World Journal of Gastroenterology

ISSN
ISSN 1007-9327 (print)
ISSN 2219-2840 (online)

LAUNCH DATE
October 1, 1995

FREQUENCY
Weekly

EDITORIAL OFFICE
Jin-Lei Wang, Director
Xiu-Xia Song, Vice Director
World Journal of Gastroenterology
Room 903, Building D, Ocean International Center,
No. 62 Dongsihuan Zhonglu, Chaoyang District,
Beijing 100025, China
Telephone: +86-10-59080039
Fax: +86-10-85381893
E-mail: editorialoffice@wjgnet.com
Help Desk: http://www.wjgnet.com/esps/helpdesk.aspx
http://www.wjgnet.com

PUBLISHER
Baishideng Publishing Group Inc
8226 Regency Drive,
Pleasanton, CA 94588, USA
Telephone: +1-925-223-8242
Fax: +1-925-223-8243
E-mail: bpgoffice@wjgnet.com
Help Desk: http://www.wjgnet.com/esps/helpdesk.aspx
http://www.wjgnet.com

PUBLICATION DATE
April 28, 2016

INSTRUCTIONS TO AUTHORS
Full instructions are available online at http://www.wjgnet.com/bpg/g_info_20160116143427.htm

ONLINE SUBMISSION
http://www.wjgnet.com/esps/

World Journal of Gastroenterology

Submit a Manuscript: http://www.wjgnet.com/esps/
Help Desk: http://www.wjgnet.com/esps/helpdesk.aspx
DOI: 10.3748/wjg.v22.i16.4073

World J Gastroenterol 2016 April 28; 22(16): 4073-4078
ISSN 1007-9327 (print) ISSN 2219-2840 (online)

EDITORIAL

Crohn's disease presenting as acute gastrointestinal hemorrhage

Amareshwar Podugu, Kanwarpreet Tandon, Fernando J Castro

Amareshwar Podugu, Kanwarpreet Tandon, Fernando J Castro, Department of Gastroenterology, Cleveland Clinic Florida, Weston, FL 33331, United States

Author contributions: Podugu A, Tandon T and Castro FJ searched the literature, formulated the tables, and wrote the manuscript; Castro FJ critically reviewed the manuscript.

Conflict-of-interest statement: There is no conflict to declare or no financial disclosures.

Correspondence to: Fernando J Castro, MD, Department of Gastroenterology, Cleveland Clinic Florida, 2950 Cleveland Clinic Blvd, Weston, FL 33331, United States. castrof@ccf.org
Telephone: +1-954-6595646
Fax: +1-954-6595647

Received: February 2, 2016
Peer-review started: February 9, 2016
First decision: March 7, 2016
Revised: March 11, 2016
Accepted: March 30, 2016
Article in press: March 30, 2016
Published online: April 28, 2016

Abstract

Severe gastrointestinal (GI) hemorrhage is a rare complication of Crohn's disease (CD). Although several surgical and non-surgical approaches have been described over the last 2 decades this complication still poses significant diagnostic and therapeutic challenges. Given the relative infrequency of severe bleeding in CD, available medical literature on this topic is mostly in the form of retrospective case series and reports. In this article we review the risk factors, diagnostic modalities and treatment options for the management of CD presenting as GI hemorrhage.

Key words: Crohn's disease; Recurrence; Gastrointestinal hemorrhage; Biologic agents; Risk factors

Core tip: Severe gastrointestinal (GI) hemorrhage is a rare complication of Crohn's disease (CD). With the relative infrequency of severe bleeding in CD, available medical literature on this topic is mostly in the form of retrospective case series and reports. In this article we reviewed the available medical literature and summarized the risk factors, diagnostic modalities and treatment options for the management of CD presenting as GI hemorrhage.

Podugu A, Tandon K, Castro FJ. Crohn's disease presenting as acute gastrointestinal hemorrhage. *World J Gastroenterol* 2016; 22(16): 4073-4078 Available from: URL: http://www.wjgnet.com/1007-9327/full/v22/i16/4073.htm DOI: http://dx.doi.org/10.3748/wjg.v22.i16.4073

INTRODUCTION

Although Crohn's disease (CD) is often associated with mild gastrointestinal (GI) bleeding, severe GI hemorrhage is a rare complication. The first case of hemorrhage due to regional enteritis was described in 1941[1]. Since then, multiple case reports and case series of severe bleeding in CD have been published

with reported incidence ranging from 0.6%-4%[2-7] This presentation poses significant diagnostic and therapeutic challenges for the following reasons: (1) difficulty accurately identifying the origin of the bleed primarily due to presence of multiple areas of inflammation; (2) presence of other complications such as stricturizing CD that can compromise endoscopic evaluation; and (3) increased risk of recurrent bleed[3].

Limitations on available clinical data has made it difficult to formulate a consensus on the definitive diagnostic and treatment modalities for this condition. We will review the current working definition of GI hemorrhage in CD, its pathogenesis, epidemiologic factors, diagnostic and therapeutic options.

DEFINITION OF GI HEMORRHAGE IN PATIENTS WITH CD

The definition of GI hemorrhage in CD has changed over the years. Homan *et al*[8] in 1976 defined it as profuse rectal bleeding that required blood transfusions to maintain normal vital signs. Since then the definition has varied ranging from rectal bleeding requiring more than 4 units of blood over a period of 2 wk[5] to 2-5 units in 24 h[2,7]. In a recent case series the definition was again modified to a drop in hemoglobin (Hb) of 2 g/dL below the baseline +/- hemodynamic instability or an abrupt fall in Hb to less than 9[3,4].

Source and location of bleed

In most patients a definitive bleeding site, defined as a lesion that is either actively bleeding or possesses an adherent clot, is not identified and the bleeding source is attributed to diffuse areas of active inflammation[4]. When found, the source of bleeding is more commonly described as a deep ulcer eroding into a blood vessel[9]. On rare occasions, a large pseudopolyp in the ileum or colon has been identified as the source of bleeding[2,10]. The majority of bleeds originate from the ileum and colon as visualized on pathology after surgery, endoscopy or imaging studies. Only a small number of episodes have been attributed to a jejunal or upper GI source. Isolated colonic bleeding accounts for 3%-50% of hemorrhagic CD, diffuse ileo-colonic lesions for 22.7%-68.5%, and 19%-66% originate from the small bowel[2-5,7]. Although it may seem logical to assume that the presence of significant disease activity and symptomatic CD would result in a higher incidence of acute lower GI bleeding, two series have shown 65%-78% of patients had quiescent CD at the time of bleeding[2,3].

Epidemiology

The incidence of severe lower GI bleeding in CD has ranged from 0.6%-4%. Cirocco *et al*[7] reported an incidence of 0.6% in their 631 patients diagnosed with CD while Kim *et al*[3] reported an incidence of 4% in their study of 1731 patients. Other large series reported incidences from 1.3%-1.6%[4,5]. Some studies describe a similar incidence in males and females[2,5] whereas others have found a higher incidence in males[3,4,7]. The average age of presentation has been around 30 years ranging from 27-45 years[2-5,7]. Since the peak age for the diagnosis of CD is in the 20's, it is possible that patients present with severe bleeding after having the disease for some years.

A study to evaluate risk factors for acute hemorrhage in CD showed that patients on corticosteroids had a higher rate of bleeding when compared to a control group of CD patients with no bleeding but this was not confirmed on multivariate analysis[3]. The same study showed that Azathioprine/6-Mercaptopurine (6-MP) could actually have a role in preventing severe hemorrhage in CD OR = 0.53 (95%CI: 0.30-0.91).

DIAGNOSIS

Available diagnostic modalities include: upper and lower endoscopy, radionuclide bleeding scan, mesenteric angiography, computed tomography (CT) enterography and capsule endoscopy. The following sections describe the utility of these tests.

Endoscopy

Only 2 case series studies have utilized upper endoscopy (EGD) for diagnosis[3,4]. Kim *et al*[3] analyzed 30 patients who underwent an EGD with no diagnostic yield. In the second study, EGD was performed in patients with suspected upper GI bleed or with a negative colonoscopy, and the source of bleeding was identified in 2 patients but there was no mention of the total number of patients undergoing EGD.

There are 3 large case series that have utilized colonoscopy for diagnosis producing variable results as demonstrated in Table 1. Pardi was the first to evaluate the role of colonoscopy in the diagnosis and treatment of hemorrhagic CD. Patients included in this study underwent colonoscopy within 24 h of presentation and the source of bleeding was identified in 78%. Only 3 patients were treated endoscopically with no subsequent recurrence of bleeding[4]. Belaiche *et al*[2] found the yield of colonoscopy in identifying the bleeding site at 60% (18/30). Ulcers located in left and sigmoid colon were recognized as the cause of bleeding in 95% cases while one patient bled from a pseudopolyp. In contrast to the previous two studies, the diagnostic yield for colonoscopy was only 10.6% in a Korean case series. Some of the factors that may have led to a lower yield of colonoscopy in this study include a delay in colonoscopy examination, as its timing was not specified[3], and location of the bleeding site as in most cases in this study the bleeding site originated from the small bowel. As demonstrated in these case series, colonoscopy was not only useful in determining the site of bleeding but also could be used therapeutically.

Table 1 Identification of the bleeding site in case series *n* (%)

Ref.	Study type	*n*	Identification of origin of bleeding	Location	Colonoscopy	Mesenteric angiography	Radionuclide bleeding scan	CT enterography	EGD
Kim *et al*[3] (2012)	Retrospective review	70	22 (31.4)	Small bowel 19 Large bowel 3	5/47 (10.6)	5/19 (26.3)	8/27 (29.6)	9/46 (19.6)	0/30 (0)
Pardi *et al*[4] (1999)	Retrospective review (1989-1996)	31	31 (100.0)	NA	25/31 (78.0)	1/3 (33.0)	3/4 (75.0)	NA	2
Belaiche *et al*[2] (1999)		34	22 (65.0)	Colon (85%) Isolate small bowel (15%)	18/30 (60.0)	3/4 (75.0)	0/2	NA	NA
Robert *et al*[5] (1991)	Retrospective review (1960-1986)	21	2 (10.0)	NA	NA	2/5 (40.0)	NA	NA	NA

CT: Computed tomography; EGD: Esophagogastroduodenoscopy.

Radionuclide bleeding scan and mesenteric angiography

There is very limited literature demonstrating the utility of angiography and radionuclide scan with variable results, success ranging from 26% to 75% for angiography and 0% to 75%[2-4] for radionuclide bleeding scan (Table 1). These modalities do not ascertain if the site of bleeding is resulting from CD but in some instances a presumptive diagnosis can be established based on angiographic signs that have been associated with CD. These signs include the presence of mesenteric neovascularity, an increased contrast staining of bowel loops, early and prominent venous return, skip lesions, and the "zoning" sign[11-13]. The zoning sign refers to a double-layer appearance of the bowel wall with a densely staining inner wall representing a hypervascular submucosa and mucosa and a thick but relatively avascular outer muscle layer.

CT enterography

CT enterography of the small bowel was introduced in 1997 and was found helpful in assessing the extent and severity of CD[14]. The underlying principle was the combination of neutral (low-density) oral contrast with "enteric phase" CT to enhance contrast resolution between mucosa and lumen to better characterize small bowel abnormalities. CT enterography has been utilized in detecting obscure GI bleed[14]. Its utility to detect hemorrhage in patients with CD was demonstrated only in one series where CT enterography diagnosed the site of bleeding in 9/46 (19.6%)[3].

Capsule endoscopy

The role of capsule endoscopy has not been studied in patients with hemorrhagic CD likely due to concern of capsule retention secondary to strictures or previous surgeries[15]. The role of capsule endoscopy has been limited to diagnosing obscure GI bleeds in patients with CD. In these cases capsule endoscopy has been found to be superior to push enteroscopy and small bowel radiography[16].

TREATMENT

In an early case series, 3/21 (14.3%) patients presenting with GI hemorrhage due to CD died from bleeding or associated complications[5]. Later case series have demonstrated decreased mortality in patients with severe hemorrhage from CD with either no mortality in 34 patients[2] or 1/32 (3.1%)[4]. Initial management should always include primary resuscitation with IV fluids and blood transfusion as in any patient with a significant GI bleed. If the patient continues to be hemodynamically unstable the surgical team should be involved early in the course while continuing resuscitation. Treatment consists of medical management, minimally invasive interventions and surgical management.

Medical management

Treatment of CD has evolved over the years. In the early 1990's the most common strategy for the management of CD with hemorrhage was surgery. However beginning in the late 1990's there has been a paradigm shift in the management with a tendency to avoid surgery and instead utilize medical management[2,4]. Besides blood transfusions, medical management consists of medications used to treat CD including corticosteroids, mesalamine, antibiotics and continuation of 6-MP[2,4,17]. Belaiche *et al*[18] successfully achieved hemostasis with the use of infliximab in non-surgical candidates presenting with GI hemorrhage and attributed this success to the high rates of mucosal healing with this medication. Since then, additional case reports and case series have reported the effectiveness of infliximab in cessation of GI hemorrhage[19,20]. Aniwan *et al*[21] recently published a case series in which bleeding was controlled within 24 h in 6/7 patients who received infliximab. No rebleeding episodes were reported after 30 d of follow up and surgery was avoided in all patients. The potential advantage of infliximab in the treatment of patients

with unclear site of bleeding was described. There are at least 11 additional reports of patients presenting with CD related GIB treated with infliximab with successful control of bleeding in all the cases[18,21-25]. Patients selected for treatment with infliximab in these case reports included poor surgical candidates and those who developed recurrent bleeding after undergoing surgery.

There is only one comparative study evaluating medical therapy for CD presenting with severe bleeding in the era of biologics consisting of 70 cases[3]. All patients were initially managed with 5-ASA, azathioprine/ 6-MP or corticosteroids. Eleven patients required additional intervention including embolization, endoscopic management, surgery or infliximab (5 patients) to treat the index bleeding. A total of eleven patients underwent treatment with infliximab (5 first bleeding and 6 rebleeding) and only 1 patient had further bleeding episodes requiring surgery. The benefits of infliximab therapy did not reach statistical significance when compared to patients undergoing other treatments because of the small sample size. The study suggests that medical treatment can have better outcomes than what has been previously reported and surgery could be reserved for patients who fail initial medical treatment or exhibit recurrent bleeding.

There was one case report utilizing recombinant factor VIIa in the management of GI hemorrhage secondary to CD. Recombinant factor VIIa improves hemostasis and has been shown to be effective in treating hemorrhage in patients with hemophilia A or B. The standard dose for these conditions is 90 to 110 μg/kg every 2 to 3 h for two to three doses[26]. In this case report they used 2 doses of 120 μg/kg three hours apart with cessation of bleeding over the next 12 h.

MINIMALLY INVASIVE INTERVENTIONS

Minimally invasive management consists of endoscopic treatment or embolization. Endoscopy may not be feasible in patients with strictures but when possible thermocoagulation alone or combination of epinephrine injection and bipolar coagulation have been described. Application of hemoclips may be compromised in the presence of inflamed and friable mucosa[15,27]. Endoscopic treatment of bleeding lesions was successful in 5/7 cases in one series and 3 (2 upper EGD and 1 colonoscopy) patients in another report underwent therapeutic endoscopy with no recurrent bleeding[2,4].

Superselective embolization can present with complications such as intestinal infarction but recent advances in interventional radiology (microcatheters, embolic agents and microcoils) have reduced the rate of complications[28]. Success rate with this treatment modality ranges from 81% to 93%, with a mortality rate between 0% and 7%[29].

In addition to superselective embolization, there are isolated case reports on the use of arterial vasopressin therapy to control bleeding in cases with diffuse lesions or when superselective catheterization is not technically possible[30]. In these, vasopressin infusion either successfully controlled or reduced the rate of bleeding to stabilize patients before surgery[29-31]. However, vasopressin infusion can result in complications including hypertension, vasoconstriction, cardiac arrhythmia and bowel ischemia[32]. In summary, superselective angiographic embolization has become the standard in treating angiogram positive GI bleeding. In cases where embolization is difficult to perform either because of diffuse pathology or absence of adequate collateralization, vasopressin infusion is an alternative[29].

SURGICAL MANAGEMENT

Papi *et al*[22] summarized 5 series published from 1991-2001[2,4-7]. Of the 101 patients included in this study 37 (36.6%) underwent surgery during the first episode of bleeding and 64 (63.4%) underwent non-operative management. Although the mortality in the medical group was not reported, the mortality in the surgical group was 6.9%. Recurrence of bleeding was noted to be higher in patients who did not undergo surgery (38.5% *vs* 5.7%)[22]. The major challenges they reported with surgery were accurate identification of the bleeding site and the risk of short gut syndrome[33-35].

REBLEEDING

The recurrence rates of severe bleeding have been reported from 19%-41%[2-5] underscoring the high recurrence rate of this complication. An early case series published in 1991 followed 21 patients after GI hemorrhage from Crohn's and found a rate of rebleeding of 4/21 (19%). The rate of rebleeding after medical therapy was 3/10 (30%) compared with 1/11 (9%) in those that received surgical treatment[5]. In another series of 25 patients with a median follow up of 2 years there was a recurrence of bleeding in 35% of patients who were managed with non-operative measures as opposed to no recurrence in surgically managed patients[2].

Kim *et al*[3] reported a total of 64 rebleeding episodes. The rates of rebleeding were 51% in patients treated medically, 50% in those treated endoscopically and 57% in those after embolization. There is limited but promising evidence to support the role of infliximab in prevention of rebleeding. Cumulative probability of rebleeding for 11 patients on infliximab was 9.1% after 1-5 years[3] but the study does not provide information about characteristics of these patients on biologics such as how were these patients selected for infliximab therapy. Based on the available evidence it is prudent to say that the recurrence of bleeding is high and after the management of the initial episode of GI hemorrhage, patients should be

subsequently started on immunomodulator therapy or anti-TNF therapy.

CONCLUSION

CD with acute hemorrhage is a challenging medical condition with evidence for management limited to case reports and few case series. The site of bleeding commonly follows the distribution of disease and is best localized with angiography or endoscopy. Endoscopic or angiographic therapy may be attempted when a source of bleeding is identified. Surgery should be recommended in patients with massive bleeding not stabilized by multiple transfusion (> 4 PRBC/24 h), those who fail medical management or with recurrent massive hemorrhage. Use of infliximab for control of acute hemorrhage is encouraging as limited evidence has demonstrated resolution of bleeding in most patients but additional studies are required to better assess its role.

Recurrent hemorrhage is not unusual and occurs more commonly in non-surgically treated patients. After control of the index bleed, patients should be placed on anti-TNF or immuno-modulator therapy to prevent recurrence.

REFERENCES

1 **Fallis LS**. Massive intestinal hemorrhage in regional enteritis: report of a case. *Am J Surg* 1941; **53**: 512-513 [DOI: 10.1016/S0002-9610(41)90675-X]

2 **Belaiche J**, Louis E, D'Haens G, Cabooter M, Naegels S, De Vos M, Fontaine F, Schurmans P, Baert F, De Reuck M, Fiasse R, Holvoet J, Schmit A, Van Outryve M. Acute lower gastrointestinal bleeding in Crohn's disease: characteristics of a unique series of 34 patients. Belgian IBD Research Group. *Am J Gastroenterol* 1999; **94**: 2177-2181 [PMID: 10445546 DOI: 10.1111/j.1572-0241.1999.01291.x]

3 **Kim KJ**, Han BJ, Yang SK, Na SY, Park SK, Boo SJ, Park SH, Yang DH, Park JH, Jeong KW, Ye BD, Byeon JS, Myung SJ, Kim JH. Risk factors and outcome of acute severe lower gastrointestinal bleeding in Crohn's disease. *Dig Liver Dis* 2012; **44**: 723-728 [PMID: 22497905 DOI: 10.1016/j.dld.2012.03.010]

4 **Pardi DS**, Loftus EV, Tremaine WJ, Sandborn WJ, Alexander GL, Balm RK, Gostout CJ. Acute major gastrointestinal hemorrhage in inflammatory bowel disease. *Gastrointest Endosc* 1999; **49**: 153-157 [PMID: 9925691 DOI: 10.1016/S0016-5107(99)70479-7]

5 **Robert JR**, Sachar DB, Greenstein AJ. Severe gastrointestinal hemorrhage in Crohn's disease. *Ann Surg* 1991; **213**: 207-211 [PMID: 1998401]

6 **Driver CP**, Anderson DN, Keenan RA. Massive intestinal bleeding in association with Crohn's disease. *J R Coll Surg Edinb* 1996; **41**: 152-154 [PMID: 8763176]

7 **Cirocco WC**, Reilly JC, Rusin LC. Life-threatening hemorrhage and exsanguination from Crohn's disease. Report of four cases. *Dis Colon Rectum* 1995; **38**: 85-95 [PMID: 7813353 DOI: 10.1007/BF02053865]

8 **Homan WP**, Tang CK, Thorbjarnarson B. Acute massive hemorrhage from intestinal Crohn disease. Report of seven cases and review of the literature. *Arch Surg* 1976; **111**: 901-905 [PMID: 1085142 DOI: 10.1001/archsurg.1976.01360260069019]

9 **Berg DF**, Bahadursingh AM, Kaminski DL, Longo WE. Acute surgical emergencies in inflammatory bowel disease. *Am J Surg* 2002; **184**: 45-51 [PMID: 12135718 DOI: 10.1016/S0002-9610(02)00879-6]

10 **Renison DM**, Forouhar FA, Levine JB, Breiter JR. Filiform polyposis of the colon presenting as massive hemorrhage: an uncommon complication of Crohn's disease. *Am J Gastroenterol* 1983; **78**: 413-416 [PMID: 6603162]

11 **Barnacle AM**, Aylwin AC, Jackson JE. Angiographic diagnosis of inflammatory bowel disease in patients presenting with gastrointestinal bleeding. *AJR Am J Roentgenol* 2006; **187**: 976-985 [PMID: 16985146]

12 **Asakura H**, Takagi T, Kobayashi K, Aiso S, Hibi T, Sugino Y, Hiramatsu K, Teramoto T, Tsuchiya M. Microangiographic findings of massive intestinal bleeding in a patient with Crohn's disease: a case report. *Angiology* 1985; **36**: 802-808 [PMID: 3877476]

13 **Brahme F**, Hildell J. Angiography in Crohn's disease revisited. *AJR Am J Roentgenol* 1976; **126**: 941-951 [PMID: 178237]

14 **Huprich JE**, Fletcher JG, Alexander JA, Fidler JL, Burton SS, McCullough CH. Obscure gastrointestinal bleeding: evaluation with 64-section multiphase CT enterography--initial experience. *Radiology* 2008; **246**: 562-571 [PMID: 18227546 DOI: 10.1148/radiol.2462061920]

15 **Daperno M**, Sostegni R, Rocca R. Lower gastrointestinal bleeding in Crohn's disease: how (un-)common is it and how to tackle it? *Dig Liver Dis* 2012; **44**: 721-722 [PMID: 22809958 DOI: 10.1016/j.dld.2012.06.006]

16 **Leighton JA**, Triester SL, Sharma VK. Capsule endoscopy: a meta-analysis for use with obscure gastrointestinal bleeding and Crohn's disease. *Gastrointest Endosc Clin N Am* 2006; **16**: 229-250 [PMID: 16644453 DOI: 10.1016/j.giec.2006.03.004]

17 **Kostka R**, Lukás M. Massive, life-threatening bleeding in Crohn's disease. *Acta Chir Belg* 2005; **105**: 168-174 [PMID: 15906908]

18 **Belaiche J**, Louis E. Severe lower gastrointestinal bleeding in Crohn's disease: successful control with infliximab. *Am J Gastroenterol* 2002; **97**: 3210-3211 [PMID: 12492221 DOI: 10.1111/j.1572-0241.2002.07143.x]

19 **Colombel JF**, Sandborn WJ, Reinisch W, Mantzaris GJ, Kornbluth A, Rachmilewitz D, Lichtiger S, D'Haens G, Diamond RH, Broussard DL, Tang KL, van der Woude CJ, Rutgeerts P. Infliximab, azathioprine, or combination therapy for Crohn's disease. *N Engl J Med* 2010; **362**: 1383-1395 [PMID: 20393175 DOI: 10.1056/NEJMoa0904492]

20 **D'haens G**, Van Deventer S, Van Hogezand R, Chalmers D, Kothe C, Baert F, Braakman T, Schaible T, Geboes K, Rutgeerts P. Endoscopic and histological healing with infliximab anti-tumor necrosis factor antibodies in Crohn's disease: A European multicenter trial. *Gastroenterology* 1999; **116**: 1029-1034 [PMID: 10220494 DOI: 10.1016/S0016-5085(99)70005-3]

21 **Aniwan S**, Eakpongpaisit S, Imraporn B, Amornsawadwatana S, Rerknimitr R. Infliximab stopped severe gastrointestinal bleeding in Crohn's disease. *World J Gastroenterol* 2012; **18**: 2730-2734 [PMID: 22690085 DOI: 10.3748/wjg.v18.i21.2730]

22 **Papi C**, Gili L, Tarquini M, Antonelli G, Capurso L. Infliximab for severe recurrent Crohn's disease presenting with massive gastrointestinal hemorrhage. *J Clin Gastroenterol* 2003; **36**: 238-241 [PMID: 12590236]

23 **Tsujikawa T**, Nezu R, Andoh A, Saotome T, Araki Y, Ishizuka Y, Sasaki M, Koyama S, Fujiyama Y. Inflixmab as a possible treatment for the hemorrhagic type of Crohn's disease. *J Gastroenterol* 2004; **39**: 284-287 [PMID: 15065007 DOI: 10.1007/s00535-003-1290-9]

24 **Meyer MM**, Levine EJ. Acute hemorrhagic Crohn's disease controlled with infliximab. *Inflamm Bowel Dis* 2009; **15**: 1456-1457 [PMID: 19107774 DOI: 10.1002/ibd.20840]

25 **Ando Y**, Matsushita M, Kawamata S, Shimatani M, Fujii T, Okazaki K. Infliximab for severe gastrointestinal bleeding in Crohn's disease. *Inflamm Bowel Dis* 2009; **15**: 483-484 [PMID: 18668673 DOI: 10.1002/ibd.20635]

26 **Girona E**, Borrás-Blasco J, Conesa-García V, Navarro-Ruiz A, Solís J, García-Sepulcre MF, Oliver-García I. Successful treatment of severe gastrointestinal bleeding secondary to Crohn disease with recombinant factor VIIa. *South Med J* 2007; **100**: 601-604 [PMID: 17591314 DOI: 10.1097/SMJ.0b013e31804859a4]

27 **Korzenik JR**. Massive Lower Gastrointestinal Hemorrhage in

Crohn's Disease. *Curr Treat Options Gastroenterol* 2000; **3**: 211-216 [PMID: 11097738 DOI: 10.1007/s11938-000-0024-9]

28 **Iiritano E**, Grassia R, Staiano T, Buffoli F. Life-threatening jejunal hemorrhage as first presentation of Crohn's disease. *Inflamm Bowel Dis* 2010; **16**: 1277-1278 [PMID: 20222123 DOI: 10.1002/ibd.21182]

29 **Alla VM**, Ojili V, Gorthi J, Csordas A, Yellapu RK. Revisiting the past: intra-arterial vasopressin for severe gastrointestinal bleeding in Crohn's disease. *J Crohns Colitis* 2010; **4**: 479-482 [PMID: 21122547 DOI: 10.1016/j.crohns.2010.02.011]

30 **Podolny GA**. Crohn's disease presenting with massive lower gastrointestinal hemorrhage. *AJR Am J Roentgenol* 1978; **130**: 368-370 [PMID: 414598 DOI: 10.2214/ajr.130.2.368]

31 **Mellor JA**, Chandler GN, Chapman AH, Irving HC. Massive gastrointestinal bleeding in Crohn's disease: successful control by intra-arterial vasopressin infusion. *Gut* 1982; **23**: 872-874 [PMID: 6981537]

32 **Gomes AS**, Lois JF, McCoy RD. Angiographic treatment of gastrointestinal hemorrhage: comparison of vasopressin infusion and embolization. *AJR Am J Roentgenol* 1986; **146**: 1031-1037 [PMID: 3485897 DOI: 10.2214/ajr.146.5.1031]

33 **Kristensen M**, Lenz K, Nielsen OV, Jarnum S. Short bowel syndrome following resection for Crohn's disease. *Scand J Gastroenterol* 1974; **9**: 559-565 [PMID: 4424368]

34 **Thompson JS**, Iyer KR, DiBaise JK, Young RL, Brown CR, Langnas AN. Short bowel syndrome and Crohn's disease. *J Gastrointest Surg* 2003; **7**: 1069-1072 [PMID: 14675717 DOI: 10.1016/j.gassur.2003.08.007]

35 **Slater G**, Aufses AH. Small bowel length in Crohn's disease. *Am J Gastroenterol* 1991; **86**: 1037-1040 [PMID: 1858740]

P- Reviewer: Furka A, Peng SY, Tsai JF **S- Editor**: Qi Y
L- Editor: A **E- Editor**: Wang CH

World Journal of Gastroenterology

Submit a Manuscript: http://www.wjgnet.com/esps/
Help Desk: http://www.wjgnet.com/esps/helpdesk.aspx
DOI: 10.3748/wjg.v22.i16.4079

World J Gastroenterol 2016 April 28; 22(16): 4079-4090
ISSN 1007-9327 (print) ISSN 2219-2840 (online)

TOPIC HIGHLIGHT

2016 Nonalcoholic Fatty Liver Disease: Global view

Nonalcoholic fatty liver disease as a multi-systemic disease

Hakan Fotbolcu, Elçin Zorlu

Hakan Fotbolcu, Department of Cardiology, Pendik BölgeHastanesi, Istanbul 34000, Turkey

Elçin Zorlu, Istanbul University, Forensic Science Institute, Istanbul 34000, Turkey

Author contributions: Fotbolcu H performed research and wrote the paper; Zorlu E critically revised the manuscript for important intellectual content.

Conflict-of-interest statement: No conflict of interest.

Correspondence to: Hakan Fotbolcu, MD, Department of Cardiology, Pendik BölgeHastanesi, Emek Caddesi, No. 281, Narcity Konutları, A 2b Blok, Kat 9 D 56, Maltepe, Istanbul 34000, Turkey. hakan_fotbolcu@yahoo.com
Telephone: +90-505-6882125
Fax: +90-216-3752212

Received: January 6, 2016
Peer-review started: January 6, 2016
First decision: January 28, 2016
Revised: February 2, 2016
Accepted: March 1, 2016
Article in press: March 2, 2016
Published online: April 28, 2016

Abstract

Nonalcoholic fatty liver disease (NAFLD) is the most common cause of chronic liver disease. NAFLD includes a wide spectrum of liver conditions ranging from simple steatosis to nonalcoholic steatohepatitis and advanced hepatic fibrosis. NAFLD has been recognized as a hepatic manifestation of metabolic syndrome linked with insulin resistance. NAFLD should be considered not only a liver specific disease but also an early mediator of systemic diseases. Therefore, NAFLD is usually associated with cardiovascular disease, chronic kidney disease, type 2 diabetes, obesity, and dyslipidemia. NAFLD is highly prevalent in the general population and is associated with increased cardiovascular morbidity and mortality. The underlying mechanisms and pathogenesis of NAFLD with regard to other medical disorders are not yet fully understood. This review focuses on pathogenesis of NAFLD and its relation with other systemic diseases.

Key words: Nonalcoholic fatty liver disease; Obesity; Insulin resistance; Cardiovascular effect; Multi-systemic disease

Core tip: Nonalcoholic fatty liver disease (NAFLD) is the most common cause of chronic liver disease. NAFLD has been recognized as a hepatic manifestation of metabolic syndrome linked with insulin resistance. NAFLD should be considered not only a liver specific disease but also an early mediator of systemic diseases. Therefore, NAFLD is usually associated with cardiovascular disease, chronic kidney disease, type 2 diabetes, obesity, and dyslipidemia. This review focuses on the pathogenesis of NAFLD and its relation with other systemic diseases.

Fotbolcu H, Zorlu E. Nonalcoholic fatty liver disease as a multi-systemic disease. *World J Gastroenterol* 2016; 22(16): 4079-4090 Available from: URL: http://www.wjgnet.com/1007-9327/full/v22/i16/4079.htm DOI: http://dx.doi.org/10.3748/wjg.v22.i16.4079

INTRODUCTION

Nonalcoholic fatty liver disease (NAFLD) represents a spectrum of diseases from simple steatosis, nonalcoholic steatohepatitis, to liver cirrhosis[1]. The overall prevalence of NAFLD varies between 20% and 50% in Western countries, and it is accepted as the most common type of chronic liver disease[2,3]. Fatty liver and NAFLD occur in all age groups, and its prevalence increases with increases in body weight. Fatty liver is found in 10%-15% of normal weight individuals and 70% of obese subjects[4]. The distribution of excess fat is important, as increased visceral fat increases the risk of hepatic steatosis both in lean and overweight individuals[5].

NAFLD is closely related to obesity, type 2 diabetes mellitus, and dyslipidemia, with a prevalence ranging from 50% to 90% in these patient subgroups[6-8]. Most patients have "simple steatosis" or non-alcoholic fatty liver (NAFL) without inflammation, tissue damage, or fibrosis. However, in a subgroup of patients, nonalcoholic steatohepatitis (NASH), fibrosis, and/or cirrhosis may develop. Progression is more likely in the setting of diabetes, insulin resistance (IR), and other preexisting conditions[4]. The fibrosis stage is the strongest predictor for disease-specific mortality in NAFLD[9]. Biopsy is the gold standard technique for the detection of liver fibrosis, but it may have some disadvantages, such as insufficient sampling, high cost, processing site pain, and intraobserver and interobserver variability[10,11]. It should be reserved for patients with ultrasound-proven fatty liver who have risk factors for NASH or elevated liver enzymes without definitive diagnosis[12]. Consequently, patients with NAFLD who are diagnosed with advanced fibrosis or cirrhosis should be included in surveillance programs that utilize ultrasonography and endoscopy. In addition, recent data have shown that advanced fibrosis in NAFLD predicted not only liver-related mortality but also increased mortality due to cardiovascular events[9,13]. Furthermore, NASH was associated with more metabolic abnormalities compared with NAFL[14], and the increasing severity of NASH was shown to affect adversely renal function[15]. There is some debate about whether NAFL without inflammation is associated with kidney related events. This review focuses on the pathogenesis of NAFLD and its relation with other systemic diseases.

DEFINITION AND PATHOGENESIS

The hallmark histologic feature of NAFLD is the accumulation of fat in the form of triglycerides in hepatocytes without signs of secondary hepatic fat accumulation due to alcohol consumption, steatogenic medication, or hereditary disorders[16]. In 1999, Matteoni *et al*[5] presented the first diagnostic criteria to categorize NAFLD into four different subtypes: NAFLD type 1 with fatty liver alone; type 2 with fatty liver plus lobular inflammation; type 3 with fatty liver plus ballooning degeneration; and type 4 with fat accumulation, ballooning degeneration, and either Mallory-Denk bodies or fibrosis. They revealed that cirrhosis developed in 21%-28% of patients whose liver biopsies displayed NAFLD type 3 or 4, whereas only 4% of patients with NAFLD type 1 and none of those with type 2 developed cirrhosis after a mean follow-up of 10 years. There was a trend for increased liver-related mortality in patients with subtypes 3 and 4 compared with subtypes 1 and 2. Today, subtypes 3 and 4 are considered as NASH[17].

Hepatic lipid content is regulated by balancing hepatic lipid uptake, synthesis, oxidation, and export. Most of the triglycerides are re-esterified fatty acids that come from adipose tissue lipolysis into the liver. Adipose tissue IR is present in the majority of patients with NAFLD, whether they are obese or not[18], and adipose tissue lipolysis provides approximately 60% of the fatty acids used for hepatic triglyceride synthesis. The rest of the hepatic fatty acids come from *de novo* lipogenesis within the liver (25%) and dietary intake (15%)[19]. Excess hepatic fat results in increased very low-density lipoprotein (VLDL) secretion and some of the serum lipid abnormalities noted in metabolic syndrome and NAFLD, including hypertriglyceridemia, decreased high-density lipoprotein (HDL), and higher low-density lipoprotein (LDL)[20]. However, the increased export of triglycerides as VLDL is unable to compensate for the increase in intra-hepatic triglycerides. The high serum glucose and insulin associated with IR further impair liver lipid metabolism by increasing the activity of carbohydrate response element-binding protein (ChREBP) and sterol regulatory-element binding protein 1c (SREBP-1c), the master regulator of hepatic *de novo* lipogenesis[21]. Net lipid accumulation, specifically buildup of the triglyceride precursor diacylglycerol, leads to activation of a serine kinase cascade. This, in turn, inhibits insulin signaling, leading to IR in the liver[22,23].

IR has a strong association with both hepatic steatosis and NASH[18]. In 1998, Day *et al*[24] presented a "two hit" hypothesis to describe the pathogenesis of NAFLD whereby IR contributes to steatosis (first hit), which sensitizes the liver to oxidative stress (second hit) resulting in inflammation, fibrosis, and necrosis[24,25]. Additional theories, such as the multiple-hit hypothesis, suggest other factors, including adipokines and mitochondrial dysfunction, may also contribute to NAFLD[26]. At present, the precise factors leading to inflammation remain unclear, with various metabolites, cytokines, inflammatory cells, and dysregulated processes, such as oxidative stress and autophagy, having been implicated[27]. Elevated fatty acid β-oxidation as a result of increased lipolysis of adipose tissue in NAFLD patients increases reactive oxygen species and activates oxidative stress[28]. The hepatic lipid accumulation and intracellular stresses activate the transcription and release of pro-inflammatory factors, such as

interleukin (IL)-6, tumor necrosis factor-alpha (TNF-α), and C-reactive protein[29,30]. A sedentary lifestyle in conjunction with excessive energy intake promotes obesity and dysfunction of white adipose tissue. White adipose tissue secretes more TNF-α and IL-6 and reduces the secretion of adiponectin[30]. Elevated circulating levels of pro-inflammatory cytokines and reduced levels of anti-inflammatory factors cause a chronic low-grade inflammatory state that is recognized as an important pathogenic mechanism of NAFLD. Among clinical associations, diabetes and metabolic syndrome, advanced age, Hispanic ethnicity, female sex, and obesity are all related to more aggressive liver histology but without a clear distinction of cause and effect[31].

On genetic basis, a lot of single nucleotide polymorphism (SNP) have been identified by genome-wide association studies (GWAS)[32]. Romeo *et al*[33], was the first to report that the rs738409 C>G SNP in the Patatin-like phospholipase domain-containing 3 (PNPLA3) gene, which encodes an isoleucine to methionine variant at protein position 148 (I148M), was strongly associated with increased liver fat content. Since then, several other pieces of evidence have highlighted the role of PNPLA3 in the development and progression of NAFLD. Furthermore, transmembrane 6 superfamily member 2 (TM6SF2) E167K variant is currently emerging as another relevant contributor both for NAFLD pathogenesis and cardiovascular outcomes. Recently, Goffredo *et al*[34] revealed that rs58542926 SNP in the TM6SF2 gene was associated with pediatric NAFLD but may confer protection against cardiovascular risk. As of today, the PNPLA3 gene variant is the most validated susceptibility factor for steatosis, NASH, fibrosis, and hepatocellular carcinoma (HCC), despite a number of other genetic variants contributing to liver damage.

The gastrointestinal tract contains the largest number of bacteria in the human body and serves a variety of physiologic functions, including an active role in glucose and lipid metabolism. The commensal organisms that populate the human gut are dominated by four main phyla: *Firmicutes*, *Bacteroidetes*, *Actinobacteria*, and *Proteobacteria*. Since the liver and intestine are connected anatomically and *via* the hepatic portal system, the gut microbiota and their metabolic products may influence hepatic pathology[35]. The liver is exposed to metabolites originating from intestinal bacteria (such as ethanol and other volatile organic compounds) or the bacteria themselves[36]. The liver acts as a barrier between the gut and the systemic circulation by removing toxins. When Kupffer cells, the specialized macrophages in the hepatic sinusoids, are impaired, or when the gut mucosal barrier is damaged by inflammation or portal hypertension (HTN), a metabolic endotoxinemia may be developed. The high endotoxin level activates Kupffer cells and hepatic stellate cells. Bacteria can also produce lipopolysaccharides, which bind to Toll-like receptor 4 and activate the production of proinflammatory cytokines, subsequently resulting in inflammation[37]. These events may contribute to the pathogenesis of obesity and NAFLD[38,39]. Furthermore, probiotics may modulate gut microbiota, reduce inflammation, increase epithelial barrier function, and increase antibacterial substance production[36]. Current data with probiotic treatment should be considered with caution since related studies were conducted with small group sizes without dietary control. The use of probiotics for NAFLD is not recommended at this moment[40]. The standard treatment of patients with NAFLD has been accepted as weight loss through diet and exercise.

CARDIOVASCULAR DISEASES AND NAFLD

One of the most important mortality and morbidity reasons of NAFLD are cardiovascular events. Multiple pathogenetic conditions contribute to the development of cardiovascular diseases (CVD). Firstly, high levels of LDL have been identified as the most important culprit. The molecular mechanism responsible for the high levels of LDL, oxidized LDL, and their receptors have been clarified, and strategies against high LDL levels have been established using effective cholesterol-lowering drugs, such as statins. Impaired glucose tolerance, HTN, and lipid disorders, including hypertriglyceridemia and low levels of HDL, were recognized as weaker risk factors for CVD compared with high level of LDL. However, the coexistence of multiple risk factors apart from LDL is considered as important as hypercholesterolemia. Such disorders are commonly found in obesity and NAFLD but not in all NAFLD patients. The distribution of excess fat is important in NAFLD patients, as increased visceral fat increases the risk of hepatic steatosis both in lean and overweight individuals[5]. Visceral fat accumulation contributes to the development and/or worsening of various disorders, such as glucose intolerance, hyperlipidemia[41], HTN[42], cardiac dysfunction[43], and sleep apnea syndrome[44]. Even in mildly obese individuals, visceral adiposity is related to a cluster of risk factors and coronary artery disease (CAD)[45]. Recent results from the Framingham Heart study revealed that there was a significant association between NAFLD and subclinical CVD outcomes, independently of many metabolic diseases[46]. Nevertheless, it is not clear if this increased CVD risk is conferred by the presence of several CVD risk factors associated to the metabolic syndrome, which are common in patients with NAFLD, or if NAFLD might be itself a mediator of atherosclerosis.

One of the earliest manifestations of atherosclerosis is the presence of endothelial dysfunction, occurring even in the absence of angiographic evidence of disease. Brachial artery flow-mediated dilation (FMD)

is the most often noninvasive test used for assessing endothelial function as the result of endothelial release of nitric oxide[47]. An impaired FMD was found in a wide variety of CV and metabolic diseases associated to chronic low-grade inflammation, oxidative stress, and metabolic abnormalities[48,49]. Moreover, FMD predicted future CV events in patients with[50] and in those without CVDs[51]. Recently, some studies revealed that NAFLD might affect endothelial function independently from other CVD risk factors, thus suggesting that CVD risk of patients with NAFLD could not be explained entirely by conventional CVD risk factors[52,53]. Increased carotid intima-media thickness (CIMT) is a marker of early generalized atherosclerosis and is associated with increased risk of myocardial infarction, cerebrovascular accident, and peripheral vascular disease[54]. An increasing number of studies, predominantly involving Western population, indicates that the presence of NAFLD is associated with higher CIMT, indicating increased cardiovascular risk[55,56]. Thakur *et al*[57] showed that thicker CIMT and a higher prevalence of atherosclerotic plaques and endothelial dysfunction were observed in patients with NAFLD as compared to those without NAFLD in the Indian population. The presence of NAFLD was independently associated with higher CIMT and impaired FMD, even after taking into account adiposity, blood pressure, lipid levels, and the presence of metabolic syndrome.

Expansion of dysfunctional visceral adipose tissue along with infiltration of mononuclear cells (MNCs) lead to initiation and propagation of inflammatory pathways contributing to IR. Increased expression of inflammatory mediators like inhibitor of kappa light polypeptide gene enhancer in B cells-kinase beta, protein-kinase C-beta 2, suppressor of cytokine signalling-3, and nuclear factor kappa B has been indicated in MNCs from obese subjects[58]. These inflammatory mediators disturb insulin signaling by inhibiting the phosphorylation of insulin receptor (INSR) beta subunit and reducing INSR activity[58]. Increased hydrolysis of adipose tissue triglycerides and flux of free fatty acids to liver result in hepatic steatosis. This coupled with chronic low grade inflammation may progress to steatohepatitis. However, injured liver itself may contribute to systemic inflammation as indicated by increased transcription of proinflammatory genes[59]. Increased production of proinflammatory cytokines by the liver may not only contribute to the progression of liver injury but also induce the proatherogenic effect. Elevated levels of CRP have been observed in patients with NAFLD as compared to controls, with the levels being higher in those with steatohepatitis than in those with simple steatosis[56]. Additionally, chronic inflammatory state in patients with NAFLD is associated with increased expression of biomarkers of endothelial dysfunction. Elevated levels of sICAM-1 have been consistently associated with endothelial dysfunction[60]. In a recent study, patients with NAFLD were observed to have elevated levels of sICAM-1, plasminogen activator inhibitor-1, and soluble CD40 ligand as compared to controls[61]. Uric acid was regulated by a decrease in CPS 1 (a ligase enzyme located in the mitochondria), and it was shown to erect pro-inflammatory and pro-oxidant effects both on adipose tissue and vascular smooth muscles[62,63]. Uric acid may also contribute to IR by inducing local adipose tissue inflammation, which may cause a reduction in the production of adiponectin[64]. Another link may be adiponectin between NAFLD and atherosclerosis[65]. Adiponectin is an adipocyte-specific protein that is abundantly present in the plasma. Since its discovery, numerous experimental and clinical studies have demonstrated that adiponectin has anti-atherogenic, anti-diabetic, and anti-inflammatory properties. Some studies demonstrated the presence of lower adiponectin levels in patients with NASH diagnosed by liver biopsy compared with body mass index-matched controls, or subjects with simple fatty liver, and that in patients with NASH, hypoadiponectinemia correlated with necroinflammatory changes of the liver independent of IR[66,67]. Furthermore, it is well known that adiponectin suppressed (1) tumor necrosis factor alpha-induced expression of adhesion molecules in vascular endothelial cells by inhibiting the nuclear translocation of NF-κB[68]; (2) growth factor-induced proliferation of smooth muscle cells by inhibiting mitogen activated protein kinase pathways[69]; and (3) foam cell transformation of macrophages by suppression of class A scavenger receptor expression[70]. These data suggested that adiponectin provided protection against the development of atherosclerosis. Some clinical studies supported that theory. One of them showed significantly lower plasma concentrations of adiponectin in patients with acute myocardial infarction and unstable angina pectoris compared to those in patients with stable angina pectoris and control subjects[71]. Among patients with CAD, plasma adiponectin levels are lower in subjects with complex coronary lesions associated with plaque vulnerability[72].

Some studies revealed an association between NAFLD and arterial stiffness[73,74]. Arterial stiffness has been shown to be an independent indicator of symptomatic CVD and events as well as a measure of vascular health[75,76]. Arterial stiffness was assessed by carotid-femoral pulse wave velocity (PWV), brachial-ankle pulse wave velocity, or arterial stiffness index. Carotide-femoral PWV has been considered the non-invasive gold standard measure of arterial stiffness. Two studies reported the association of NAFLD with carotid-femoral PWV. In both studies, NAFLD independently increased the carotide-femoral PWV[77,78]. Similarly, in a study of non-hypertensive, non-diabetic individuals without metabolic syndrome, Kim *et al*[79] reported that NAFLD independently predicted increased brachial-ankle PWV. The mechanism underlying the relationship between NAFLD and arterial stiffness is not completely understood. Studies have shown that insulin-resistant states are associated with decreased endothelium-

dependent vasodilation and arterial compliance may be a partially nitric oxide-dependent process[80]. In addition, insulin has been shown to induce vascular smooth muscle proliferation and migration in cell culture[81]. Of interest, recent evidence indicates that TGF-β changes in adventitial collagen may play a role in arterial stiffening[82]. Furthermore, pro-fibrogenic markers, such as endothelin 1 and insulin like growth factor-1, can lead to arterial stiffening[83].

Studies in patients with metabolic syndrome (MetS) have consistently shown increased left ventricular (LV) mass index and diastolic function impairment when compared with controls, which are in the main secondary to the effects of IR, obesity, and HTN on cardiac structure and function[84,85]. Some studies have focused specifically on NAFLD subjects, and the finding of abnormal LV geometry and diastolic dysfunction has been similarly reported[86,87]. Additionally, Kim *et al*[88] found that NAFLD was associated with LV diastolic dysfunction independently of traditional risk factors. Multiple mechanisms may contribute to LV dysfunction in NAFLD, including lipotoxicity associated with cardiac steatosis and lipoapoptosis, alterations in fatty acid metabolism, overproduction of cardio-inhibitory cytokines, upregulation of some neurohormones (especially angiotensin Ⅱ), myocardial fibrosis and chronic overload with LV dilatation and hypertrophy, and increased oxygen consumption[89-91]. IR may represent a link between NAFLD and LV dysfunction. Elevated insulin levels in patients with IR stimulate myocyte growth and interstitial fibrosis. Insulin also causes sodium retention and activates the sympathetic nervous system, which can affect cardiac performance[90,91]. Moreover, alterations in myocardial metabolism, including progressive increases in fatty acid turnover, may impair LV contractility[89]. Finally, chronic sodium retention increases blood pressure levels, which in turn cause myocardial tissue damage, myocardial fibrosis, and impairment of the LV function in response to LV pressure overload[92]. The other possible explanation is that increased aortic stiffness may also increase afterload, which induces myocardial structural changes of the left ventricle and impairs LV diastolic function[73]. Recently, Nakamori *et al*[93] revealed that patients with fatty liver showed decreased myocardial perfusion reserve (MPR) compared to patients without fatty liver. Altered MPR may indicate an early alteration in myocardial tissue and vascular properties in patients with fatty liver. The presence and severity of fatty liver on computed tomography (CT) were closely associated with reduced MPR, independent of classical risk factors. Based on this study, it may be speculated that patients with NAFLD might be prone to subendocardial ischemia in cases of hemodynamic compromise.

Another issue that needs to be discussed is the increase in prothrombotic activity in patients with NAFLD. Platelets producing vasoactive and prothrombotic factors like IL-1β and CD40L play an important role in atherothrombosis[94]. Mean platelet volume (MPV), a simple and inexpensive test, is commonly used to measure platelet size and is also a marker of platelet activity[94]. MPV has been associated with CVD risk factors like diabetes[95], HTN[96], and dyslipidemia[97]. MPV is also associated with acute myocardial infarction[98], arterial and venous thrombosis[99], and ischemic strokes[100]. Recently, Madan *et al*[101] published a meta-analysis suggesting that MPV is significantly higher in patients with NAFLD, indicating the presence of increased platelet activity in such patients. The pathophysiological mechanism for increased platelet volume observed in NAFLD is not yet clearly understood; however, a plausible explanation might be that NAFLD is a chronic inflammatory condition, with increases in various inflammatory mediators, like IL-1, IL-6, and TNF-α[102]. Platelets have been known to respond to these inflammatory mediators by alteration in size measured as MPV[99]. Obesity and the MetS are known to be associated with an increased risk of thromboembolic events[103]. An increase in plasminogen activator inhibitor 1 (PAI-1), fibrinogen, factor Ⅷ, and von Willebrand factor and a decrease in antithrombin Ⅲ are most frequently reported. Recently, Verrijken *et al*[83] showed that NAFLD and NASH independently contributed to the prothrombotic state in obesity by increasing PAI-1, whereas other prothrombotic factors were unaffected by liver status. Large epidemiological studies have shown that elevated plasma level of PAI-1 is a predictor of myocardial infarction[104]. PAI-1 levels are related to the severity of vessel wall damage and are good predictors of subsequent development of a first acute myocardial infarction[105]. It may be hypothesized that the increase in PAI-1 levels by the steatotic and inflamed liver, at least in part, explains the observed link between NAFLD and increased cardiovascular risk.

There is some debate about the association between NAFLD and coronary artery calcification (CAC). Because the CAC score indicates the presence and extent of coronary atherosclerosis, it is not surprising that many studies have reported that a high CAC score is a marker for an increased risk of coronary events[106]. Thus, a CAC score of zero is associated with a very low risk of subsequent coronary events[106], whereas an elevated CAC score is related to a stepwise increase in the risk of subsequent coronary events[106,107]. Several prior studies have demonstrated an increased burden of CAC among individuals with NAFLD independent of traditional risk factors and measures of abdominal adiposity[108,109], whereas others have not[110,111]. However, many of these studies that find a positive correlation included ethnically homogeneous populations of either Africans or Eastern Asians (Taiwan, Korea, Japan). In a sub-study of the Multi-Ethnic Study of Atherosclerosis, 398 participants underwent multi-detector CT to detect liver fat, and no associations were observed with CAC after adjustment for CVD risk factors in a multi-ethnic population[110].

The QT interval represents the duration of electrical depolarization and repolarization of the ventricle. A prolonged QT interval reflects a lengthening of this vulnerable period and increases the risk of malignant arrhythmias[112]. Extreme prolongation of the QT interval is also associated with sudden cardiac death. Moreover, the duration of the QT interval, even within a reference range, is a predictor for cardiovascular death in the general population[113,114]. The QT interval has been shown to be related to cardiac and metabolic disorders, including HTN, diabetes, obesity, and CAD[114,115]. In a recent report of 400 patients with type 2 diabetes, the presence of NAFLD was associated with QT prolongation after adjustment for established confounders[116]. Furthermore, Hung *et al*[117] showed that the severity of NAFLD was associated with prolonged QTc intervals and higher risk for QTc prolongation in the general population with or without diabetes. Their findings suggest that NAFLD-associated QT prolongation might be a link to adverse cardiovascular outcomes among these patients. Recently, two important studies revealed that NAFLD is strongly associated with an increased incidence of atrial fibrillation (AF) in patients with type 2 diabetes even after adjustment for important clinical risk factors for AF[118] and independently associated with the risk of AF in the general population[119]. Increased systemic inflammation and autonomic dysfunction may play a role in the development of AF in patients with NAFLD. Additionally, preliminary studies indicate that there is a strong relationship between NAFLD and early LV diastolic dysfunction in both non-diabetic and type 2 diabetic individuals[73,86]. It is likely that LV diastolic dysfunction plays a role in AF pathogenesis either by increasing pressure that can affect stretch receptors in pulmonary veins triggers and other areas of the atria or by inducing direct structural changes in atrial myocardium[120,121]. It may be thought that the increased incidence of AF may cause an increase in cardiovascular morbidity and mortality in patients with NAFLD.

HTN AND NAFLD

Compared with those with normal blood pressure (BP), prehypertension (PHT) increases the risk of HTN by two to six-fold over 4 years[122]. PHT is also associated with increased risk of mortality and other major cardiovascular events, such as myocardial infarction, stroke, and congestive heart failure[123,124]. Recent studies suggest an independent association between NAFLD and HTN[125,126], and when present among hypertensive patients, NAFLD is associated with CVD complications, such as LV hypertrophy, ventricular dysfunction, and cardiovascular dysautonomia[127-129]. The mechanisms by which BP becomes elevated in the presence of NAFLD and in the absence of MetS are still unclear. However, it is likely that the common pathway between these two pathologies is IR. IR is a major factor in the development of NAFLD[124] and has been implicated in the development of both PHT and HTN independent of other cardiometabolic risk factors[130]. IR is also a proven risk factor of CVD by inducing dyslipidemia and secreting proinflammatory cytokines, such as TNF-α and IL-6, accelerating the arteriosclerosis[131,132]. Under these effects of IR, arterial vascular elasticity and luminal width may be able to decrease to raise BP. In addition, sympathetic activation provoked by IR likely contributed to the development of hypertension. Previous studies showed that IR could raise BP through the sympathetic excitation[133,134]. Elevated insulin level related to IR was reported to induce sympathetic overactivity by direct and indirect action on the central nervous system, and the enhanced uptake of noradrenaline in the arterial wall by hyperinsulinemia increased the vascular sympathetic tone[135]. Accordingly, elevated sympathetic activation related to IR could play a significant role in the development of HTN of NAFLD patients.

OBSTRUCTIVE SLEEP APNEA AND NAFLD

Robust scientific data indicate that obstructive sleep apnea (OSA) is strongly related to NAFLD independently of traditional risk factors[136-138]. Recently, a meta-analysis by Sookoian and Pirola showed that patients with OSA have greater transaminase values and a higher prevalence of NAFLD and liver fibrosis compared to individuals without OSA[133]. Intermittent hypoxia (IH) is a key mediator of OSA and leads to various alterations in biological homeostasis[139]. It activates the sympathetic nervous system *via* the carotid body chemoreceptors, which in turn leads to fat degradation (lipolysis) from adipose tissue. Free fatty acids (FFA) compose the triglycerides, which are transported to different organs to serve as fuel. However, FFA can lead to steatosis and organ inflammation, such as in the setting of NAFLD. At the same time, IH activates hypoxia inducible factors 1 and 2 (HIF-1 and HIF-2 respectively), which leads to decreased lipid metabolism in the liver, increased hepatic fat synthesis, upregulated liver inflammation, and fibrosis. In addition, Vgontzas *et al* included the production of inflammatory cytokines, which led to oxidative stress in patients with chronic sleep apnea, and it may be a possible mechanism contributing to the pathogenesis of NAFLD. This process may not only increase IR seen in patients with NAFLD but also may accelerate the process of liver fibrosis leading to the progression to steatohepatitis, cirrhosis, and its complications[140,141].

CHRONIC KIDNEY DISEASE AND NAFLD

To date, there is uncertainty whether NAFLD poses an independent risk for chronic kidney disease (CKD) (defined as decreased estimated glomerular

filtration rate (GFR) and/or proteinuria) above and beyond known risk factors for CKD. The complex and intertwined interactions among NAFLD, abdominal obesity, and IR make it extremely difficult to dissect out the specific role of the liver and the underlying mechanisms responsible for the association between NAFLD and the risk of developing CKD. NAFLD may contribute to the development and progression of CKD by atherogenic dyslipidemia, systemic/hepatic IR, dysglycemia (increased hepatic glucose production), activation of renin-angiotensin system, and the systemic release of numerous potentially pathogenic mediators (proinflammatory biomarkers and procoagulant and profibrogenic factors)[142]. Choudhary *et al*[143] showed that presence of NAFLD does not adversely affect renal function. In contrast, Machado *et al*[15] found that NASH, particularly lobular inflammation and advanced fibrosis, was associated with mild decreases in e-GFR, suggesting a common inflammatory link between liver and renal lesion in morbid obese patients. Additionally, a recently published a meta-analysis by Musso *et al*[144] revealed that the presence and severity of NAFLD are associated with an increased risk and severity of CKD. The main results of their analysis are the following: (1) NAFLD was associated with an increased prevalence and incidence of CKD; (2) liver disease severity in NAFLD was associated with an increased risk and severity of CKD; and (3) these associations remained statistically significant in diabetic and non-diabetic individuals as well as in studies adjusting for traditional risk factors for CKD and were independent of whole body/abdominal obesity and IR. Finally, large-scale prospective studies are needed to draw firm conclusions about any independent hepatic contribution to the increased risk of CKD observed in patients with NAFLD.

CONCLUSION

To date, growing evidence links NAFLD to CVD and CKD. Dyslipidemia, IR, increased production of proinflammatory cytokines, low adiponectin, high PAI-1, prehypertension, and hyperglycemia are main factors that lead to NAFLD, further aggravate the course of NAFLD, and accelerate the progress of atherosclerosis and the development of CVD. The key questions are whether NAFLD plays a direct role in CVD pathogenesis and whether an inflamed liver (NASH) adds to the CVD risk above the effect of steatosis alone. Therefore, further prospective studies are needed to detect whether NAFLD poses an independent risk for CVD above and beyond known metabolic risk factors. Additional well-conducted large scale studies are also needed to crystallize whether treatment of NAFLD will ultimately prevent or slow the development and progression of CVD and CKD.

REFERENCES

1 **Bambha K**, Belt P, Abraham M, Wilson LA, Pabst M, Ferrell L, Unalp-Arida A, Bass N. Ethnicity and nonalcoholic fatty liver disease. *Hepatology* 2012; **55**: 769-780 [PMID: 21987488 DOI: 10.1002/hep.24726]

2 **Browning JD**, Szczepaniak LS, Dobbins R, Nuremberg P, Horton JD, Cohen JC, Grundy SM, Hobbs HH. Prevalence of hepatic steatosis in an urban population in the United States: impact of ethnicity. *Hepatology* 2004; **40**: 1387-1395 [PMID: 15565570 DOI: 10.1002/hep.20466]

3 **Bedogni G**, Miglioli L, Masutti F, Castiglione A, Crocè LS, Tiribelli C, Bellentani S. Incidence and natural course of fatty liver in the general population: the Dionysos study. *Hepatology* 2007; **46**: 1387-1391 [PMID: 17685472 DOI: 10.1002/hep.21827]

4 **Vernon G**, Baranova A, Younossi ZM. Systematic review: the epidemiology and natural history of non-alcoholic fatty liver disease and non-alcoholic steatohepatitis in adults. *Aliment Pharmacol Ther* 2011; **34**: 274-285 [PMID: 21623852 DOI: 10.1111/j.1365-2036.2011.04724.x]

5 **Matteoni CA**, Younossi ZM, Gramlich T, Boparai N, Liu YC, McCullough AJ. Nonalcoholic fatty liver disease: a spectrum of clinical and pathological severity. *Gastroenterology* 1999; **116**: 1413-1419 [PMID: 10348825]

6 **Ong JP**, Younossi ZM. Epidemiology and natural history of NAFLD and NASH. *Clin Liver Dis* 2007; **11**: 1-16, vii [PMID: 17544968 DOI: 10.1016/j.cld.2007.02.009]

7 **Leite NC**, Salles GF, Araujo AL, Villela-Nogueira CA, Cardoso CR. Prevalence and associated factors of non-alcoholic fatty liver disease in patients with type-2 diabetes mellitus. *Liver Int* 2009; **29**: 113-119 [PMID: 18384521 DOI: 10.1111/j.1478-3231.2008.01718.x]

8 **Assy N**, Kaita K, Mymin D, Levy C, Rosser B, Minuk G. Fatty infiltration of liver in hyperlipidemic patients. *Dig Dis Sci* 2000; **45**: 1929-1934 [PMID: 11117562]

9 **Ekstedt M**, Hagström H, Nasr P, Fredrikson M, Stål P, Kechagias S, Hultcrantz R. Fibrosis stage is the strongest predictor for disease-specific mortality in NAFLD after up to 33 years of follow-up. *Hepatology* 2015; **61**: 1547-1554 [PMID: 25125077 DOI: 10.1002/hep.27368]

10 **Sebastiani G**, Alberti A. Non invasive fibrosis biomarkers reduce but not substitute the need for liver biopsy. *World J Gastroenterol* 2006; **12**: 3682-3694 [PMID: 16773685 DOI: 10.3748/wjg.v12.i23.3682]

11 **West J**, Card TR. Reduced mortality rates following elective percutaneous liver biopsies. *Gastroenterology* 2010; **139**: 1230-1237 [PMID: 20547160 DOI: 10.1053/j.gastro.2010.06.015]

12 **Rinella ME**. Nonalcoholic fatty liver disease: a systematic review. *JAMA* 2015; **313**: 2263-2273 [PMID: 26057287 DOI: 10.1001/jama.2015.5370]

13 **Stål P**. Liver fibrosis in non-alcoholic fatty liver disease - diagnostic challenge with prognostic significance. *World J Gastroenterol* 2015; **21**: 11077-11087 [PMID: 26494963 DOI: 10.3748/wjg.v21.i39.11077]

14 **Choudhary NS**, Duseja A, Kalra N, Das A, Dhiman RK, Chawla YK. Correlation of adipose tissue with liver histology in Asian Indian patients with nonalcoholic fatty liver disease (NAFLD). *Ann Hepatol* 2012; **11**: 478-486 [PMID: 22700629]

15 **Machado MV**, Gonçalves S, Carepa F, Coutinho J, Costa A, Cortez-Pinto H. Impaired renal function in morbid obese patients with nonalcoholic fatty liver disease. *Liver Int* 2012; **32**: 241-248 [PMID: 22098270 DOI: 10.1111/j.1478-3231.2011.02623.x]

16 **Chalasani N**, Younossi Z, Lavine JE, Diehl AM, Brunt EM, Cusi K, Charlton M, Sanyal AJ. The diagnosis and management of non-alcoholic fatty liver disease: practice Guideline by the American Association for the Study of Liver Diseases, American College of Gastroenterology, and the American Gastroenterological Association. *Hepatology* 2012; **55**: 2005-2023 [PMID: 22488764 DOI: 10.1002/hep.25762]

17 **Rafiq N**, Bai C, Fang Y, Srishord M, McCullough A, Gramlich T, Younossi ZM. Long-term follow-up of patients with nonalcoholic fatty liver. *Clin Gastroenterol Hepatol* 2009; **7**: 234-238 [PMID: 19049831 DOI: 10.1016/j.cgh.2008.11.005]

18 **Bugianesi E**, Gastaldelli A, Vanni E, Gambino R, Cassader M, Baldi S, Ponti V, Pagano G, Ferrannini E, Rizzetto M. Insulin resistance in non-diabetic patients with non-alcoholic fatty liver disease: sites and mechanisms. *Diabetologia* 2005; **48**: 634-642 [PMID: 15747110 DOI: 10.1007/s00125-005-1682-x]

19 **Donnelly KL**, Smith CI, Schwarzenberg SJ, Jessurun J, Boldt MD, Parks EJ. Sources of fatty acids stored in liver and secreted via lipoproteins in patients with nonalcoholic fatty liver disease. *J Clin Invest* 2005; **115**: 1343-1351 [PMID: 15864352 DOI: 10.1172/JCI200523621]

20 **Cusi K**. Role of obesity and lipotoxicity in the development of nonalcoholic steatohepatitis: pathophysiology and clinical implications. *Gastroenterology* 2012; **142**: 711-725.e6 [PMID: 22326434 DOI: 10.1053/j.gastro.2012.02.003]

21 **Uyeda K**, Repa JJ. Carbohydrate response element binding protein, ChREBP, a transcription factor coupling hepatic glucose utilization and lipid synthesis. *Cell Metab* 2006; **4**: 107-110 [PMID: 16890538 DOI: 10.1016/j.cmet.2006.06.008]

22 **Jornayvaz FR**, Shulman GI. Diacylglycerol activation of protein kinase Cε and hepatic insulin resistance. *Cell Metab* 2012; **15**: 574-584 [PMID: 22560210 DOI: 10.1016/j.cmet.2012.03.005]

23 **Popov VB**, Lim JK. Treatment of Nonalcoholic Fatty Liver Disease: The Role of Medical, Surgical, and Endoscopic Weight Loss. *J Clin Transl Hepatol* 2015; **3**: 230-238 [PMID: 26623270 DOI: 10.14218/JCTH.2015.00019]

24 **Day CP**, James OF. Steatohepatitis: a tale of two "hits"? *Gastroenterology* 1998; **114**: 842-845 [PMID: 9547102]

25 **Conlon BA**, Beasley JM, Aebersold K, Jhangiani SS, Wylie-Rosett J. Nutritional management of insulin resistance in nonalcoholic fatty liver disease (NAFLD). *Nutrients* 2013; **5**: 4093-4114 [PMID: 24152749 DOI: 10.3390/nu5104093]

26 **Duseja A**, Chawla YK. Obesity and NAFLD: the role of bacteria and microbiota. *Clin Liver Dis* 2014; **18**: 59-71 [PMID: 24274865 DOI: 10.1016/j.cld.2013.09.002]

27 **Tilg H**, Moschen AR. Evolution of inflammation in nonalcoholic fatty liver disease: the multiple parallel hits hypothesis. *Hepatology* 2010; **52**: 1836-1846 [PMID: 21038418 DOI: 10.1002/hep.24001]

28 **Gentile CL**, Pagliassotti MJ. The role of fatty acids in the development and progression of nonalcoholic fatty liver disease. *J Nutr Biochem* 2008; **19**: 567-576 [PMID: 18430557 DOI: 10.1016/j.jnutbio.2007.10.001]

29 **Pirgon Ö**, Bilgin H, Çekmez F, Kurku H, Dündar BN. Association between insulin resistance and oxidative stress parameters in obese adolescents with non-alcoholic fatty liver disease. *J Clin Res Pediatr Endocrinol* 2013; **5**: 33-39 [PMID: 23367495 DOI: 10.4274/Jcrpe.825]

30 **Asrih M**, Jornayvaz FR. Inflammation as a potential link between nonalcoholic fatty liver disease and insulin resistance. *J Endocrinol* 2013; **218**: R25-R36 [PMID: 23833274 DOI: 10.1530/JOE-13-0201]

31 **Argo CK**, Northup PG, Al-Osaimi AM, Caldwell SH. Systematic review of risk factors for fibrosis progression in non-alcoholic steatohepatitis. *J Hepatol* 2009; **51**: 371-379 [PMID: 19501928 DOI: 10.1016/j.jhep.2009.03.019]

32 **Macaluso FS**, Maida M, Petta S. Genetic background in nonalcoholic fatty liver disease: A comprehensive review. *World J Gastroenterol* 2015; **21**: 11088-11111 [PMID: 26494964 DOI: 10.3748/wjg.v21.i39.11088]

33 **Romeo S**, Kozlitina J, Xing C, Pertsemlidis A, Cox D, Pennacchio LA, Boerwinkle E, Cohen JC, Hobbs HH. Genetic variation in PNPLA3 confers susceptibility to nonalcoholic fatty liver disease. *Nat Genet* 2008; **40**: 1461-1465 [PMID: 18820647 DOI: 10.1038/ng.257]

34 **Goffredo M**, Caprio S, Feldstein AE, D'Adamo E, Shaw MM, Pierpont B, Savoye M, Zhao H, Bale AE, Santoro N. Role of TM6SF2 rs58542926 in the pathogenesis of nonalcoholic pediatric fatty liver disease: A multiethnic study. *Hepatology* 2016; **63**: 117-125 [PMID: 26457389 DOI: 10.1002/hep.28283]

35 **Marino L**, Jornayvaz FR. Endocrine causes of nonalcoholic fatty liver disease. *World J Gastroenterol* 2015; **21**: 11053-11076 [PMID: 26494962 DOI: 10.3748/wjg.v21.i39.11053]

36 **Iacono A**, Raso GM, Canani RB, Calignano A, Meli R. Probiotics as an emerging therapeutic strategy to treat NAFLD: focus on molecular and biochemical mechanisms. *J Nutr Biochem* 2011; **22**: 699-711 [PMID: 21292470 DOI: 10.1016/j.jnutbio.2010.10.002]

37 **Miura K**, Seki E, Ohnishi H, Brenner DA. Role of toll-like receptors and their downstream molecules in the development of nonalcoholic Fatty liver disease. *Gastroenterol Res Pract* 2010; **2010**: 362847 [PMID: 21274430 DOI: 10.1155/2010/362847]

38 **Cani PD**, Bibiloni R, Knauf C, Waget A, Neyrinck AM, Delzenne NM, Burcelin R. Changes in gut microbiota control metabolic endotoxemia-induced inflammation in high-fat diet-induced obesity and diabetes in mice. *Diabetes* 2008; **57**: 1470-1481 [PMID: 18305141 DOI: 10.2337/db07-1403]

39 **Alisi A**, Carsetti R, Nobili V. Pathogen- or damage-associated molecular patterns during nonalcoholic fatty liver disease development. *Hepatology* 2011; **54**: 1500-1502 [PMID: 22045668 DOI: 10.1002/hep.24611]

40 **Floch MH**, Walker WA, Madsen K, Sanders ME, Macfarlane GT, Flint HJ, Dieleman LA, Ringel Y, Guandalini S, Kelly CP, Brandt LJ. Recommendations for probiotic use-2011 update. *J Clin Gastroenterol* 2011; **45** Suppl: S168-S171 [PMID: 21992958 DOI: 10.1097/MCG.0b013e318230928b]

41 **Fujioka S**, Matsuzawa Y, Tokunaga K, Tarui S. Contribution of intra-abdominal fat accumulation to the impairment of glucose and lipid metabolism in human obesity. *Metabolism* 1987; **36**: 54-59 [PMID: 3796297 DOI: 10.1016/0026-0495(87)90063-1]

42 **Kanai H**, Matsuzawa Y, Kotani K, Keno Y, Kobatake T, Nagai Y, Fujioka S, Tokunaga K, Tarui S. Close correlation of intra-abdominal fat accumulation to hypertension in obese women. *Hypertension* 1990; **16**: 484-490 [PMID: 2228147 DOI: 10.1161/01.HYP.16.5.484]

43 **Nakajima T**, Fujioka S, Tokunaga K, Matsuzawa Y, Tarui S. Correlation of intraabdominal fat accumulation and left ventricular performance in obesity. *Am J Cardiol* 1989; **64**: 369-373 [PMID: 2756882 DOI: 10.1016/0002-9149(89)90537-7]

44 **Shinohara E**, Kihara S, Yamashita S, Yamane M, Nishida M, Arai T, Kotani K, Nakamura T, Takemura K, Matsuzawa Y. Visceral fat accumulation as an important risk factor for obstructive sleep apnoea syndrome in obese subjects. *J Intern Med* 1997; **241**: 11-18 [PMID: 9042088 DOI: 10.1046/j.1365-2796.1997.63889000.x]

45 **Nakamura T**, Tokunaga K, Shimomura I, Nishida M, Yoshida S, Kotani K, Islam AH, Keno Y, Kobatake T, Nagai Y. Contribution of visceral fat accumulation to the development of coronary artery disease in non-obese men. *Atherosclerosis* 1994; **107**: 239-246 [PMID: 7980698 DOI: 10.1016/0021-9150(94)90025-6]

46 **Mellinger JL**, Pencina KM, Massaro JM, Hoffmann U, Seshadri S, Fox CS, O'Donnell CJ, Speliotes EK. Hepatic steatosis and cardiovascular disease outcomes: An analysis of the Framingham Heart Study. *J Hepatol* 2015; **63**: 470-476 [PMID: 25776891 DOI: 10.1016/j.jhep.2015.02.045]

47 **Al-Qaisi M**, Kharbanda RK, Mittal TK, Donald AE. Measurement of endothelial function and its clinical utility for cardiovascular risk. *Vasc Health Risk Manag* 2008; **4**: 647-652 [PMID: 18827914]

48 **Katz SD**, Hryniewicz K, Hriljac I, Balidemaj K, Dimayuga C, Hudaihed A, Yasskiy A. Vascular endothelial dysfunction and mortality risk in patients with chronic heart failure. *Circulation* 2005; **111**: 310-314 [PMID: 15655134 DOI: 10.1161/01.CIR.0000153349.77489.CF]

49 **Del Ben M**, Fabiani M, Loffredo L, Polimeni L, Carnevale R, Baratta F, Brunori M, Albanese F, Augelletti T, Violi F, Angelico F. Oxidative stress mediated arterial dysfunction in patients with obstructive sleep apnoea and the effect of continuous positive airway pressure treatment. *BMC Pulm Med* 2012; **12**: 36 [PMID: 22824065 DOI: 10.1186/1471-2466-12-36]

50 **Perri L**, Pastori D, Pignatelli P, Violi F, Loffredo L. Flow-mediated

dilation is associated with cardiovascular events in non-valvular atrial fibrillation patients. *Int J Cardiol* 2015; **179**: 139-143 [PMID: 25464433 DOI: 10.1016/j.ijcard.2014.10.039]

51 **Yeboah J**, Folsom AR, Burke GL, Johnson C, Polak JF, Post W, Lima JA, Crouse JR, Herrington DM. Predictive value of brachial flow-mediated dilation for incident cardiovascular events in a population-based study: the multi-ethnic study of atherosclerosis. *Circulation* 2009; **120**: 502-509 [PMID: 19635967 DOI: 10.1161/CIRCULATIONAHA.109.864801]

52 **Pastori D**, Loffredo L, Perri L, Baratta F, Scardella L, Polimeni L, Pani A, Brancorsini M, Albanese F, Catasca E, Del Ben M, Violi F, Angelico F. Relation of nonalcoholic fatty liver disease and Framingham Risk Score to flow-mediated dilation in patients with cardiometabolic risk factors. *Am J Cardiol* 2015; **115**: 1402-1406 [PMID: 25776455 DOI: 10.1016/j.amjcard.2015.02.032]

53 **Pugh CJ**, Spring VS, Kemp GJ, Richardson P, Shojaee-Moradie F, Umpleby AM, Green DJ, Cable NT, Jones H, Cuthbertson DJ. Exercise training reverses endothelial dysfunction in nonalcoholic fatty liver disease. *Am J Physiol Heart Circ Physiol* 2014; **307**: H1298-H1306 [PMID: 25193471 DOI: 10.1152/ajpheart.00306.2014]

54 **Belcaro G**, Nicolaides AN, Laurora G, Cesarone MR, De Sanctis M, Incandela L, Barsotti A. Ultrasound morphology classification of the arterial wall and cardiovascular events in a 6-year follow-up study. *Arterioscler Thromb Vasc Biol* 1996; **16**: 851-856 [PMID: 8673559 DOI: 10.1161/01.ATV.16.7.851]

55 **Fracanzani AL**, Burdick L, Raselli S, Pedotti P, Grigore L, Santorelli G, Valenti L, Maraschi A, Catapano A, Fargion S. Carotid artery intima-media thickness in nonalcoholic fatty liver disease. *Am J Med* 2008; **121**: 72-78 [PMID: 18187076 DOI: 10.1016/j.amjmed.2007.08.041]

56 **Brea A**, Mosquera D, Martín E, Arizti A, Cordero JL, Ros E. Nonalcoholic fatty liver disease is associated with carotid atherosclerosis: a case-control study. *Arterioscler Thromb Vasc Biol* 2005; **25**: 1045-1050 [PMID: 15731489 DOI: 10.1161/01.ATV.0000160613.57985.18]

57 **Thakur ML**, Sharma S, Kumar A, Bhatt SP, Luthra K, Guleria R, Pandey RM, Vikram NK. Nonalcoholic fatty liver disease is associated with subclinical atherosclerosis independent of obesity and metabolic syndrome in Asian Indians. *Atherosclerosis* 2012; **223**: 507-511 [PMID: 22748277 DOI: 10.1016/j.atherosclerosis.2012.06.005]

58 **Ghanim H**, Aljada A, Daoud N, Deopurkar R, Chaudhuri A, Dandona P. Role of inflammatory mediators in the suppression of insulin receptor phosphorylation in circulating mononuclear cells of obese subjects. *Diabetologia* 2007; **50**: 278-285 [PMID: 17180352]

59 **Tilg H**, Moschen AR. Insulin resistance, inflammation, and non-alcoholic fatty liver disease. *Trends Endocrinol Metab* 2008; **19**: 371-379 [PMID: 18929493 DOI: 10.1016/j.tem.2008.08.005]

60 **Rohde LE**, Hennekens CH, Ridker PM. Cross-sectional study of soluble intercellular adhesion molecule-1 and cardiovascular risk factors in apparently healthy men. *Arterioscler Thromb Vasc Biol* 1999; **19**: 1595-1599 [PMID: 10397675 DOI: 10.1161/01.ATV.19.7.1595]

61 **Sookoian S**, Castaño GO, Burgueño AL, Rosselli MS, Gianotti TF, Mallardi P, Martino JS, Pirola CJ. Circulating levels and hepatic expression of molecular mediators of atherosclerosis in nonalcoholic fatty liver disease. *Atherosclerosis* 2010; **209**: 585-591 [PMID: 19896127 DOI: 10.1016/j.atherosclerosis.2009.10.011]

62 **Sirota JC**, McFann K, Targher G, Johnson RJ, Chonchol M, Jalal DI. Elevated serum uric acid levels are associated with non-alcoholic fatty liver disease independently of metabolic syndrome features in the United States: Liver ultrasound data from the National Health and Nutrition Examination Survey. *Metabolism* 2013; **62**: 392-399 [PMID: 23036645 DOI: 10.1016/j.metabol.2012.08.013]

63 **Nakagawa T**, Lomb DJ, Haigis MC, Guarente L. SIRT5 Deacetylates carbamoyl phosphate synthetase 1 and regulates the urea cycle. *Cell* 2009; **137**: 560-570 [PMID: 19410549 DOI: 10.1016/j.cell.2009.02.026]

64 **Johnson RJ**, Nakagawa T, Sanchez-Lozada LG, Shafiu M, Sundaram S, Le M, Ishimoto T, Sautin YY, Lanaspa MA. Sugar, uric acid, and the etiology of diabetes and obesity. *Diabetes* 2013; **62**: 3307-3315 [PMID: 24065788 DOI: 10.2337/db12-1814]

65 **Funahashi T**, Matsuzawa Y. Adiponectin and the cardiometabolic syndrome: an epidemiological perspective. *Best Pract Res Clin Endocrinol Metab* 2014; **28**: 93-106 [PMID: 24417949 DOI: 10.1016/j.beem.2013.09.002]

66 **Hui JM**, Hodge A, Farrell GC, Kench JG, Kriketos A, George J. Beyond insulin resistance in NASH: TNF-alpha or adiponectin? *Hepatology* 2004; **40**: 46-54 [PMID: 15239085 DOI: 10.1002/hep.20280]

67 **Musso G**, Gambino R, Biroli G, Carello M, Fagà E, Pacini G, De Michieli F, Cassader M, Durazzo M, Rizzetto M, Pagano G. Hypoadiponectinemia predicts the severity of hepatic fibrosis and pancreatic Beta-cell dysfunction in nondiabetic nonobese patients with nonalcoholic steatohepatitis. *Am J Gastroenterol* 2005; **100**: 2438-2446 [PMID: 16279898 DOI: 10.1111/j.1572-0241.2005.00297.x]

68 **Ouchi N**, Kihara S, Arita Y, Maeda K, Kuriyama H, Okamoto Y, Hotta K, Nishida M, Takahashi M, Nakamura T, Yamashita S, Funahashi T, Matsuzawa Y. Novel modulator for endothelial adhesion molecules: adipocyte-derived plasma protein adiponectin. *Circulation* 1999; **100**: 2473-2476 [PMID: 10604883 DOI: 10.1161/01.CIR.100.25.2473]

69 **Arita Y**, Kihara S, Ouchi N, Maeda K, Kuriyama H, Okamoto Y, Kumada M, Hotta K, Nishida M, Takahashi M, Nakamura T, Shimomura I, Muraguchi M, Ohmoto Y, Funahashi T, Matsuzawa Y. Adipocyte-derived plasma protein adiponectin acts as a platelet-derived growth factor-BB-binding protein and regulates growth factor-induced common postreceptor signal in vascular smooth muscle cell. *Circulation* 2002; **105**: 2893-2898 [PMID: 12070119 DOI: 10.1161/01.CIR.0000018622.84402.FF]

70 **Ouchi N**, Kihara S, Arita Y, Nishida M, Matsuyama A, Okamoto Y, Ishigami M, Kuriyama H, Kishida K, Nishizawa H, Hotta K, Muraguchi M, Ohmoto Y, Yamashita S, Funahashi T, Matsuzawa Y. Adipocyte-derived plasma protein, adiponectin, suppresses lipid accumulation and class A scavenger receptor expression in human monocyte-derived macrophages. *Circulation* 2001; **103**: 1057-1063 [PMID: 11222466 DOI: 10.1161/01.CIR.103.8.1057]

71 **Nakamura Y**, Shimada K, Fukuda D, Shimada Y, Ehara S, Hirose M, Kataoka T, Kamimori K, Shimodozono S, Kobayashi Y, Yoshiyama M, Takeuchi K, Yoshikawa J. Implications of plasma concentrations of adiponectin in patients with coronary artery disease. *Heart* 2004; **90**: 528-533 [PMID: 15084551 DOI: 10.1136/hrt.2003.011114]

72 **Otsuka F**, Sugiyama S, Kojima S, Maruyoshi H, Funahashi T, Matsui K, Sakamoto T, Yoshimura M, Kimura K, Umemura S, Ogawa H. Plasma adiponectin levels are associated with coronary lesion complexity in men with coronary artery disease. *J Am Coll Cardiol* 2006; **48**: 1155-1162 [PMID: 16978998 DOI: 10.1016/j.jacc.2006.05.054]

73 **Fotbolcu H**, Yakar T, Duman D, Ozden K, Karaahmet T, Tigen K, Kurtoglu U, Dindar I. Aortic elastic properties in nonalcoholic fatty liver disease. *Blood Press Monit* 2010; **15**: 139-145 [PMID: 20414104 DOI: 10.1097/MBP.0b013e328339e2c8]

74 **Sunbul M**, Agirbasli M, Durmus E, Kivrak T, Akin H, Aydin Y, Ergelen R, Yilmaz Y. Arterial stiffness in patients with non-alcoholic fatty liver disease is related to fibrosis stage and epicardial adipose tissue thickness. *Atherosclerosis* 2014; **237**: 490-493 [PMID: 25463079 DOI: 10.1016/j.atherosclerosis.2014.10.004]

75 **Gorgui J**, Doonan RJ, Gomez YH, Kwong C, Daskalopoulou SS. Carotid endarterectomy improves peripheral but not central arterial stiffness. *Eur J Vasc Endovasc Surg* 2013; **45**: 548-553 [PMID: 23540801 DOI: 10.1016/j.ejvs.2013.02.012]

76 **Vlachopoulos C**, Aznaouridis K, Stefanadis C. Prediction of cardiovascular events and all-cause mortality with arterial stiffness: a systematic review and meta-analysis. *J Am Coll Cardiol* 2010; **55**: 1318-1327 [PMID: 20338492 DOI: 10.1016/j.jacc.2009.10.061]

77 **Salvi P**, Ruffini R, Agnoletti D, Magnani E, Pagliarani G, Comandini G, Praticò A, Borghi C, Benetos A, Pazzi P. Increased arterial stiffness in nonalcoholic fatty liver disease: the Cardio-GOOSE study. *J Hypertens* 2010; **28**: 1699-1707 [PMID: 20467324 DOI: 10.1097/HJH.0b013e32833a7de6]

78 **Vlachopoulos C**, Manesis E, Baou K, Papatheodoridis G, Koskinas J, Tiniakos D, Aznaouridis K, Archimandritis A, Stefanadis C. Increased arterial stiffness and impaired endothelial function in nonalcoholic Fatty liver disease: a pilot study. *Am J Hypertens* 2010; **23**: 1183-1189 [PMID: 20634799 DOI: 10.1038/ajh.2010.144]

79 **Kim BJ**, Kim NH, Kim BS, Kang JH. The association between nonalcoholic fatty liver disease, metabolic syndrome and arterial stiffness in nondiabetic, nonhypertensive individuals. *Cardiology* 2012; **123**: 54-61 [PMID: 22986520 DOI: 10.1159/000341248]

80 **Steinberg HO**, Chaker H, Leaming R, Johnson A, Brechtel G, Baron AD. Obesity/insulin resistance is associated with endothelial dysfunction. Implications for the syndrome of insulin resistance. *J Clin Invest* 1996; **97**: 2601-2610 [PMID: 8647954 DOI: 10.1172/JCI118709]

81 **Hu CT**, Chang KC, Wu CY, Chen HI. Acute effects of nitric oxide blockade with L-NAME on arterial haemodynamics in the rat. *Br J Pharmacol* 1997; **122**: 1237-1243 [PMID: 9401792 DOI: 10.1038/sj.bjp.0701496]

82 **Fleenor BS**, Marshall KD, Durrant JR, Lesniewski LA, Seals DR. Arterial stiffening with ageing is associated with transforming growth factor-β1-related changes in adventitial collagen: reversal by aerobic exercise. *J Physiol* 2010; **588**: 3971-3982 [PMID: 20807791 DOI: 10.1113/jphysiol.2010.194753]

83 **Verrijken A**, Francque S, Mertens I, Prawitt J, Caron S, Hubens G, Van Marck E, Staels B, Michielsen P, Van Gaal L. Prothrombotic factors in histologically proven nonalcoholic fatty liver disease and nonalcoholic steatohepatitis. *Hepatology* 2014; **59**: 121-129 [PMID: 24375485 DOI: 10.1002/hep.26510]

84 **Chinali M**, Devereux RB, Howard BV, Roman MJ, Bella JN, Liu JE, Resnick HE, Lee ET, Best LG, de Simone G. Comparison of cardiac structure and function in American Indians with and without the metabolic syndrome (the Strong Heart Study). *Am J Cardiol* 2004; **93**: 40-44 [PMID: 14697463 DOI: 10.1016/j.amjcard.2003.09.009]

85 **Ferrara LA**, Cardoni O, Mancini M, Zanchetti A. Metabolic syndrome and left ventricular hypertrophy in a general population. Results from the Gubbio Study. *J Hum Hypertens* 2007; **21**: 795-801 [PMID: 17508012 DOI: 10.1038/sj.jhh.1002232]

86 **Karabay CY**, Kocabay G, Kalayci A, Colak Y, Oduncu V, Akgun T, Kalkan S, Guler A, Kirma C. Impaired left ventricular mechanics in nonalcoholic fatty liver disease: a speckle-tracking echocardiography study. *Eur J Gastroenterol Hepatol* 2014; **26**: 325-331 [PMID: 24161963 DOI: 10.1097/MEG.0000000000000008]

87 **Fotbolcu H**, Yakar T, Duman D, Karaahmet T, Tigen K, Cevik C, Kurtoglu U, Dindar I. Impairment of the left ventricular systolic and diastolic function in patients with non-alcoholic fatty liver disease. *Cardiol J* 2010; **17**: 457-463 [PMID: 20865675]

88 **Kim NH**, Park J, Kim SH, Kim YH, Kim DH, Cho GY, Baik I, Lim HE, Kim EJ, Na JO, Lee JB, Lee SK, Shin C. Non-alcoholic fatty liver disease, metabolic syndrome and subclinical cardiovascular changes in the general population. *Heart* 2014; **100**: 938-943 [PMID: 24721975 DOI: 10.1136/heartjnl-2013-305099]

89 **Peterson LR**, Herrero P, Schechtman KB, Racette SB, Waggoner AD, Kisrieva-Ware Z, Dence C, Klein S, Marsala J, Meyer T, Gropler RJ. Effect of obesity and insulin resistance on myocardial substrate metabolism and efficiency in young women. *Circulation* 2004; **109**: 2191-2196 [PMID: 15123530 DOI: 10.1161/01.CIR.0000127959.28627.F8]

90 **Wong CY**, O'Moore-Sullivan T, Leano R, Byrne N, Beller E, Marwick TH. Alterations of left ventricular myocardial characteristics associated with obesity. *Circulation* 2004; **110**: 3081-3087 [PMID: 15520317 DOI: 10.1161/01.CIR.0000147184.13872.0F]

91 **Di Bello V**, Santini F, Di Cori A, Pucci A, Palagi C, Delle Donne MG, Fierabracci P, Marsili A, Talini E, Giannetti M, Biadi O, Balbarini A, Mariani M, Pinchera A. Obesity cardiomyopathy: is it a reality? An ultrasonic tissue characterization study. *J Am Soc Echocardiogr* 2006; **19**: 1063-1071 [PMID: 16880104 DOI: 10.1016/j.echo.2006.03.033]

92 **Capasso JM**, Palackal T, Olivetti G, Anversa P. Left ventricular failure induced by long-term hypertension in rats. *Circ Res* 1990; **66**: 1400-1412 [PMID: 2335033 DOI: 10.1161/01.RES.66.5.1400]

93 **Nakamori S**, Onishi K, Nakajima H, Yoon YE, Nagata M, Kurita T, Yamada T, Kitagawa K, Dohi K, Nakamura M, Sakuma H, Ito M. Impaired myocardial perfusion reserve in patients with fatty liver disease assessed by quantitative myocardial perfusion magnetic resonance imaging. *Circ J* 2012; **76**: 2234-2240 [PMID: 22664721 DOI: 10.1253/circj.CJ-11-1487]

94 **Chu SG**, Becker RC, Berger PB, Bhatt DL, Eikelboom JW, Konkle B, Mohler ER, Reilly MP, Berger JS. Mean platelet volume as a predictor of cardiovascular risk: a systematic review and meta-analysis. *J Thromb Haemost* 2010; **8**: 148-156 [PMID: 19691485 DOI: 10.1111/j.1538-7836.2009.03584.x]

95 **Papanas N**, Symeonidis G, Maltezos E, Mavridis G, Karavageli E, Vosnakidis T, Lakasas G. Mean platelet volume in patients with type 2 diabetes mellitus. *Platelets* 2004; **15**: 475-478 [PMID: 15763888 DOI: 10.1080/09537100420002677O7]

96 **Nadar S**, Blann AD, Lip GY. Platelet morphology and plasma indices of platelet activation in essential hypertension: effects of amlodipine-based antihypertensive therapy. *Ann Med* 2004; **36**: 552-557 [PMID: 15513305 DOI: 10.1080/07853890410017386]

97 **Pathansali R**, Smith N, Bath P. Altered megakaryocyte-platelet haemostatic axis in hypercholesterolaemia. *Platelets* 2001; **12**: 292-297 [PMID: 11487381 DOI: 10.1080/09537100120058810]

98 **Avramakis G**, Papadimitraki E, Papakonstandinou D, Liakou K, Zidianakis M, Dermitzakis A, Mikhailidis DP, Ganotakis ES. Platelets and white blood cell subpopulations among patients with myocardial infarction and unstable angina. *Platelets* 2007; **18**: 16-23 [PMID: 17365849 DOI: 10.1080/09537100600800412]

99 **Gasparyan AY**, Stavropoulos-Kalinoglou A, Mikhailidis DP, Douglas KM, Kitas GD. Platelet function in rheumatoid arthritis: arthritic and cardiovascular implications. *Rheumatol Int* 2011; **31**: 153-164 [PMID: 20390282 DOI: 10.2174/138161211795049804]

100 **O'Malley T**, Langhorne P, Elton RA, Stewart C. Platelet size in stroke patients. *Stroke* 1995; **26**: 995-999 [PMID: 7762052 DOI: 10.1161/01.STR.26.6.995]

101 **Madan SA**, John F, Pitchumoni CS. Nonalcoholic Fatty Liver Disease and Mean Platelet Volume: A Systemic Review and Meta-analysis. *J Clin Gastroenterol* 2016; **50**: 69-74 [PMID: 25984978 DOI: 10.1097/MCG.0000000000000340]

102 **Targher G**, Day CP, Bonora E. Risk of cardiovascular disease in patients with nonalcoholic fatty liver disease. *N Engl J Med* 2010; **363**: 1341-1350 [PMID: 20879883 DOI: 10.1056/NEJMra0912063]

103 **Poirier P**, Giles TD, Bray GA, Hong Y, Stern JS, Pi-Sunyer FX, Eckel RH. Obesity and cardiovascular disease: pathophysiology, evaluation, and effect of weight loss: an update of the 1997 American Heart Association Scientific Statement on Obesity and Heart Disease from the Obesity Committee of the Council on Nutrition, Physical Activity, and Metabolism. *Circulation* 2006; **113**: 898-918 [PMID: 16380542 DOI: 10.1161/CIRCULATIONAHA.106.171016]

104 **Mertens I**, Van Gaal LF. Obesity, haemostasis and the fibrinolytic system. *Obes Rev* 2002; **3**: 85-101 [PMID: 12120424 DOI: 10.1046/j.1467-789X.2002.00056.x]

105 **Thögersen AM**, Jansson JH, Boman K, Nilsson TK, Weinehall L, Huhtasaari F, Hallmans G. High plasminogen activator inhibitor and tissue plasminogen activator levels in plasma precede a first acute myocardial infarction in both men and women: evidence for the fibrinolytic system as an independent primary risk factor. *Circulation* 1998; **98**: 2241-2247 [PMID: 9826309 DOI: 10.1161/01.CIR.98.21.2241]

106 **Bonow RO**. Clinical practice. Should coronary calcium screening be used in cardiovascular prevention strategies? *N Engl J Med* 2009; **361**: 990-997 [PMID: 19726773 DOI: 10.1056/NEJMcp0902177]

107 **Greenland P**, LaBree L, Azen SP, Doherty TM, Detrano RC.

Coronary artery calcium score combined with Framingham score for risk prediction in asymptomatic individuals. *JAMA* 2004; **291**: 210-215 [PMID: 14722147 DOI: 10.1001/jama.291.2.210]

108 **Santos RD**, Nasir K, Conceição RD, Sarwar A, Carvalho JA, Blumenthal RS. Hepatic steatosis is associated with a greater prevalence of coronary artery calcification in asymptomatic men. *Atherosclerosis* 2007; **194**: 517-519 [PMID: 17335826 DOI: 10.1016/j.atherosclerosis.2007.01.026]

109 **Kim D**, Choi SY, Park EH, Lee W, Kang JH, Kim W, Kim YJ, Yoon JH, Jeong SH, Lee DH, Lee HS, Larson J, Therneau TM, Kim WR. Nonalcoholic fatty liver disease is associated with coronary artery calcification. *Hepatology* 2012; **56**: 605-613 [PMID: 22271511 DOI: 10.1002/hep.25593]

110 **Ding J**, Kritchevsky SB, Hsu FC, Harris TB, Burke GL, Detrano RC, Szklo M, Criqui MH, Allison M, Ouyang P, Brown ER, Carr JJ. Association between non-subcutaneous adiposity and calcified coronary plaque: a substudy of the Multi-Ethnic Study of Atherosclerosis. *Am J Clin Nutr* 2008; **88**: 645-650 [PMID: 18779279]

111 **VanWagner LB**, Ning H, Lewis CE, Shay CM, Wilkins J, Carr JJ, Terry JG, Lloyd-Jones DM, Jacobs DR, Carnethon MR. Associations between nonalcoholic fatty liver disease and subclinical atherosclerosis in middle-aged adults: the Coronary Artery Risk Development in Young Adults Study. *Atherosclerosis* 2014; **235**: 599-605 [PMID: 24956534 DOI: 10.1016/j.atherosclerosis.2014.05.962]

112 **Sauer AJ**, Moss AJ, McNitt S, Peterson DR, Zareba W, Robinson JL, Qi M, Goldenberg I, Hobbs JB, Ackerman MJ, Benhorin J, Hall WJ, Kaufman ES, Locati EH, Napolitano C, Priori SG, Schwartz PJ, Towbin JA, Vincent GM, Zhang L. Long QT syndrome in adults. *J Am Coll Cardiol* 2007; **49**: 329-337 [PMID: 17239714 DOI: 10.1016/j.jacc.2006.08.057]

113 **Robbins J**, Nelson JC, Rautaharju PM, Gottdiener JS. The association between the length of the QT interval and mortality in the Cardiovascular Health Study. *Am J Med* 2003; **115**: 689-694 [PMID: 14693320 DOI: 10.1016/j.amjmed.2003.07.014]

114 **Straus SM**, Kors JA, De Bruin ML, van der Hooft CS, Hofman A, Heeringa J, Deckers JW, Kingma JH, Sturkenboom MC, Stricker BH, Witteman JC. Prolonged QTc interval and risk of sudden cardiac death in a population of older adults. *J Am Coll Cardiol* 2006; **47**: 362-367 [PMID: 16412861 DOI: 10.1016/j.jacc.2005.08.067]

115 **Zhang Y**, Post WS, Blasco-Colmenares E, Dalal D, Tomaselli GF, Guallar E. Electrocardiographic QT interval and mortality: a meta-analysis. *Epidemiology* 2011; **22**: 660-670 [PMID: 21709561 DOI: 10.1097/EDE.0b013e318225768b]

116 **Targher G**, Valbusa F, Bonapace S, Bertolini L, Zenari L, Pichiri I, Mantovani A, Zoppini G, Bonora E, Barbieri E, Byrne CD. Association of nonalcoholic fatty liver disease with QTc interval in patients with type 2 diabetes. *Nutr Metab Cardiovasc Dis* 2014; **24**: 663-669 [PMID: 24594085 DOI: 10.1016/j.numecd.2014.01.005]

117 **Hung CS**, Tseng PH, Tu CH, Chen CC, Liao WC, Lee YC, Chiu HM, Lin HJ, Ho YL, Yang WS, Wu MS, Chen MF. Nonalcoholic Fatty Liver Disease Is Associated With QT Prolongation in the General Population. *J Am Heart Assoc* 2015; **4**: pii e001820 [PMID: 26199227 DOI: 10.1161/JAHA.115.001820]

118 **Targher G**, Valbusa F, Bonapace S, Bertolini L, Zenari L, Rodella S, Zoppini G, Mantovani W, Barbieri E, Byrne CD. Non-alcoholic fatty liver disease is associated with an increased incidence of atrial fibrillation in patients with type 2 diabetes. *PLoS One* 2013; **8**: e57183 [PMID: 23451184 DOI: 10.1371/journal.pone.0057183]

119 **Käräjämäki AJ**, Pätsi OP, Savolainen M, Kesäniemi YA, Huikuri H, Ukkola O. Non-Alcoholic Fatty Liver Disease as a Predictor of Atrial Fibrillation in Middle-Aged Population (OPERA Study). *PLoS One* 2015; **10**: e0142937 [PMID: 26571029 DOI: 10.1371/journal.pone.0142937]

120 **Lip GY**, Tse HF, Lane DA. Atrial fibrillation. *Lancet* 2012; **379**: 648-661 [PMID: 22166900 DOI: 10.1016/S0140-6736(11)61514-6]

121 **Rosenberg MA**, Gottdiener JS, Heckbert SR, Mukamal KJ. Echocardiographic diastolic parameters and risk of atrial fibrillation: the Cardiovascular Health Study. *Eur Heart J* 2012; **33**: 904-912 [PMID: 21990265 DOI: 10.1093/eurheartj/ehr378]

122 **Vasan RS**, Larson MG, Leip EP, Kannel WB, Levy D. Assessment of frequency of progression to hypertension in non-hypertensive participants in the Framingham Heart Study: a cohort study. *Lancet* 2001; **358**: 1682-1686 [PMID: 11728544 DOI: 10.1016/S0140-6736(01)06710-1]

123 **Shen L**, Ma H, Xiang MX, Wang JA. Meta-analysis of cohort studies of baseline prehypertension and risk of coronary heart disease. *Am J Cardiol* 2013; **112**: 266-271 [PMID: 23608614 DOI: 10.1016/j.amjcard.2013.03.023]

124 **Vasan RS**, Larson MG, Leip EP, Evans JC, O'Donnell CJ, Kannel WB, Levy D. Impact of high-normal blood pressure on the risk of cardiovascular disease. *N Engl J Med* 2001; **345**: 1291-1297 [PMID: 11794147 DOI: 10.1056/NEJMoa003417]

125 **Aneni EC**, Oni ET, Martin SS, Blaha MJ, Agatston AS, Feldman T, Veledar E, Conçeicao RD, Carvalho JA, Santos RD, Nasir K. Blood pressure is associated with the presence and severity of nonalcoholic fatty liver disease across the spectrum of cardiometabolic risk. *J Hypertens* 2015; **33**: 1207-1214 [PMID: 25693058 DOI: 10.1097/HJH.0000000000000532]

126 **Vasunta RL**, Kesäniemi YA, Ylitalo AS, Ukkola OH. High ambulatory blood pressure values associated with non-alcoholic fatty liver in middle-aged adults. *J Hypertens* 2012; **30**: 2015-2019 [PMID: 22940679 DOI: 10.1097/HJH.0b013e3283576faf]

127 **Fallo F**, Dalla Pozza A, Sonino N, Lupia M, Tona F, Federspil G, Ermani M, Catena C, Soardo G, Di Piazza L, Bernardi S, Bertolotto M, Pinamonti B, Fabris B, Sechi LA. Non-alcoholic fatty liver disease is associated with left ventricular diastolic dysfunction in essential hypertension. *Nutr Metab Cardiovasc Dis* 2009; **19**: 646-653 [PMID: 19278843 DOI: 10.1016/j.numecd.2008.12.007]

128 **Mantovani A**, Zoppini G, Targher G, Golia G, Bonora E. Non-alcoholic fatty liver disease is independently associated with left ventricular hypertrophy in hypertensive Type 2 diabetic individuals. *J Endocrinol Invest* 2012; **35**: 215-218 [PMID: 22490991]

129 **Liu YC**, Hung CS, Wu YW, Lee YC, Lin YH, Lin C, Lo MT, Chan CC, Ma HP, Ho YL, Chen CH. Influence of non-alcoholic fatty liver disease on autonomic changes evaluated by the time domain, frequency domain, and symbolic dynamics of heart rate variability. *PLoS One* 2013; **8**: e61803 [PMID: 23626730 DOI: 10.1371/journal.pone.0061803]

130 **Kawamoto R**, Kohara K, Tabara Y, Abe M, Kusunoki T, Miki T. Insulin resistance and prevalence of prehypertension and hypertension among community-dwelling persons. *J Atheroscler Thromb* 2010; **17**: 148-155 [PMID: 20145357]

131 **Kern PA**, Di Gregorio GB, Lu T, Rassouli N, Ranganathan G. Adiponectin expression from human adipose tissue: relation to obesity, insulin resistance, and tumor necrosis factor-alpha expression. *Diabetes* 2003; **52**: 1779-1785 [PMID: 12829646 DOI: 10.2337/diabetes.52.7.1779]

132 **Targher G**, Arcaro G. Non-alcoholic fatty liver disease and increased risk of cardiovascular disease. *Atherosclerosis* 2007; **191**: 235-240 [PMID: 16970951 DOI: 10.1016/j.atherosclerosis.2006.08.021]

133 **Landsberg L**, Young JB. Insulin-mediated glucose metabolism in the relationship between dietary intake and sympathetic nervous system activity. *Int J Obes* 1985; **9** Suppl 2: 63-68 [PMID: 3934092]

134 **Anderson EA**, Hoffman RP, Balon TW, Sinkey CA, Mark AL. Hyperinsulinemia produces both sympathetic neural activation and vasodilation in normal humans. *J Clin Invest* 1991; **87**: 2246-2252 [PMID: 2040704 DOI: 10.1172/JCI115260]

135 **Bhagat B**, Burke WJ, Dhalla NS. Insulin-induced enhancement of uptake of noradrenaline in atrial strips. *Br J Pharmacol* 1981; **74**: 325-332 [PMID: 6274461 DOI: 10.1111/j.1476-5381.1981.tb09975.x]

136 **Musso G**, Cassader M, Olivetti C, Rosina F, Carbone G, Gambino R. Association of obstructive sleep apnoea with the presence and severity of non-alcoholic fatty liver disease. A systematic review and meta-analysis. *Obes Rev* 2013; **14**: 417-431 [PMID: 23387384

DOI: 10.1111/obr.12020]
137 **Minville C**, Hilleret MN, Tamisier R, Aron-Wisnewsky J, Clement K, Trocme C, Borel JC, Lévy P, Zarski JP, Pépin JL. Nonalcoholic fatty liver disease, nocturnal hypoxia, and endothelial function in patients with sleep apnea. *Chest* 2014; **145**: 525-533 [PMID: 24264333 DOI: 10.1378/chest.13-0938]
138 **Sookoian S**, Pirola CJ. Obstructive sleep apnea is associated with fatty liver and abnormal liver enzymes: a meta-analysis. *Obes Surg* 2013; **23**: 1815-1825 [PMID: 23740153 DOI: 10.1007/s11695-013-0981-4]
139 **Drager LF**, Jun JC, Polotsky VY. Metabolic consequences of intermittent hypoxia: relevance to obstructive sleep apnea. *Best Pract Res Clin Endocrinol Metab* 2010; **24**: 843-851 [PMID: 21112030 DOI: 10.1016/j.beem.2010.08.011]
140 **Vgontzas AN**, Papanicolaou DA, Bixler EO, Hopper K, Lotsikas A, Lin HM, Kales A, Chrousos GP. Sleep apnea and daytime sleepiness and fatigue: relation to visceral obesity, insulin resistance, and hypercytokinemia. *J Clin Endocrinol Metab* 2000; **85**: 1151-1158 [PMID: 10720054]
141 **Musso G**, Olivetti C, Cassader M, Gambino R. Obstructive sleep apnea-hypopnea syndrome and nonalcoholic fatty liver disease: emerging evidence and mechanisms. *Semin Liver Dis* 2012; **32**: 49-64 [PMID: 22418888 DOI: 10.1055/s-0032-1306426]
142 **Targher G**, Chonchol MB, Byrne CD. CKD and nonalcoholic fatty liver disease. *Am J Kidney Dis* 2014; **64**: 638-652 [PMID: 25085644 DOI: 10.1053/j.ajkd.2014.05.019]
143 **Choudhary NS**, Saraf N, Kumar N, Rai R, Saigal S, Gautam D, Lipi L, Rastogi A, Goja S, Bhangui P, Ramchandra SK, Soin AS. Nonalcoholic fatty liver is not associated with incident chronic kidney disease: a large histology-based comparison with healthy individuals. *Eur J Gastroenterol Hepatol* 2016; **28**: 441-443 [PMID: 26636408 DOI: 10.1097/MEG.0000000000000531]
144 **Musso G**, Gambino R, Tabibian JH, Ekstedt M, Kechagias S, Hamaguchi M, Hultcrantz R, Hagström H, Yoon SK, Charatcharoenwitthaya P, George J, Barrera F, Hafliðadóttir S, Björnsson ES, Armstrong MJ, Hopkins LJ, Gao X, Francque S, Verrijken A, Yilmaz Y, Lindor KD, Charlton M, Haring R, Lerch MM, Rettig R, Völzke H, Ryu S, Li G, Wong LL, Machado M, Cortez-Pinto H, Yasui K, Cassader M. Association of non-alcoholic fatty liver disease with chronic kidney disease: a systematic review and meta-analysis. *PLoS Med* 2014; **11**: e1001680 [PMID: 25050550 DOI: 10.1371/journal.pmed.1001680]

P- Reviewer: Elalfy H, Peltec A, Sirin G, Souza-Mello V, Sutti S, Wang GY **S- Editor**: Qi Y **L- Editor**: Filipodia **E- Editor**: Ma S

World Journal of Gastroenterology

Submit a Manuscript: http://www.wjgnet.com/esps/
Help Desk: http://www.wjgnet.com/esps/helpdesk.aspx
DOI: 10.3748/wjg.v22.i16.4091

World J Gastroenterol 2016 April 28; 22(16): 4091-4108
ISSN 1007-9327 (print) ISSN 2219-2840 (online)

ORIGINAL ARTICLE

Basic Study

Adult mouse model of early hepatocellular carcinoma promoted by alcoholic liver disease

Aditya Ambade, Abhishek Satishchandran, Benedek Gyongyosi, Patrick Lowe, Gyongyi Szabo

Aditya Ambade, Abhishek Satishchandran, Benedek Gyongyosi, Patrick Lowe, Gyongyi Szabo, Department of Medicine, University of Massachusetts Medical School, Worcester, MA 01605, United States

Author contributions: Ambade A and Szabo G designed research and wrote the manuscript; Ambade A did the DEN injections and the Lieber DeCarli alcohol diet feeding, analyzed and interpreted all the data; Ambade A, Satishchandran A, Gyongyosi B and Lowe P performed the animal sacrifice; Szabo G obtained the funding and provided overall study supervision.

Supported by NIH/ NIAAA, No. AA011576 to Szabo G.

Institutional review board statement: The study protocol was approved by the Institutional Animal Use and Care Committee of the University of Massachusetts Medical School.

Institutional animal care and use committee statement: All procedures were performed in accordance with the policies of Institutional Animal Use and Care Committee of the University of Massachusetts Medical School. The study protocol was reviewed and approved by the Institutional Animal Use and Care Committee of the University of Massachusetts Medical School.

Conflict-of-interest statement: The authors do not have any conflict-of-interest to declare.

Data sharing statement: No additional data available.

Correspondence to: Gyongyi Szabo, MD, PhD, Department of Medicine, University of Massachusetts Medical School, 364 Plantation Street, Worcester, MA 01605, United States. gyongyi.szabo@umassmed.edu
Telephone: +1-508-8565276
Fax: +1-528-8565033

Received: December 16, 2015
Peer-review started: December 17, 2015
First decision: January 13, 2016
Revised: March 9, 2016
Accepted: March 18, 2016
Article in press: March 18, 2016
Published online: April 28, 2016

Abstract

AIM: To establish a mouse model of alcohol-driven hepatocellular carcinoma (HCC) that develops in livers with alcoholic liver disease (ALD).

METHODS: Adult C57BL/6 male mice received multiple doses of chemical carcinogen diethyl nitrosamine (DEN) followed by 7 wk of 4% Lieber-DeCarli diet. Serum alanine aminotransferase (ALT), alpha fetoprotein (AFP) and liver Cyp2e1 were assessed. Expression of F4/80, CD68 for macrophages and Ly6G, MPO, E-selectin for neutrophils was measured. Macrophage polarization was determined by IL-1β/iNOS (M1) and Arg-1/IL-10/CD163/CD206 (M2) expression. Liver steatosis and fibrosis were measured by oil-red-O and Sirius red staining respectively. HCC development was monitored by magnetic resonance imaging, confirmed by histology. Cellular proliferation was assessed by proliferating cell nuclear antigen (PCNA).

RESULTS: Alcohol-DEN mice showed higher ALTs than pair fed-DEN mice throughout the alcohol feeding without weight gain. Alcohol feeding resulted in increased ALT, liver steatosis and inflammation compared to pair-fed controls. Alcohol-DEN mice had reduced steatosis and increased fibrosis indicating

advanced liver disease. Molecular characterization showed highest levels of both neutrophil and macrophage markers in alcohol-DEN livers. Importantly, M2 macrophages were predominantly higher in alcohol-DEN livers. Magnetic resonance imaging revealed increased numbers of intrahepatic cysts and liver histology confirmed the presence of early HCC in alcohol-DEN mice compared to all other groups. This correlated with increased serum alpha-fetoprotein, a marker of HCC, in alcohol-DEN mice. PCNA immunostaining revealed significantly increased hepatocyte proliferation in livers from alcohol-DEN compared to pair fed-DEN or alcohol-fed mice.

CONCLUSION: We describe a new 12-wk HCC model in adult mice that develops in livers with alcoholic hepatitis and defines ALD as co-factor in HCC.

Key words: Alpha-fetoprotein; Macrophage polarization; Steatohepatitis; Proliferating cell nuclear antigen; Liver tumor

Core tip: Chronic alcohol consumption leads to broad spectrum of disorders from steatosis to steatohepatitis to cirrhosis and hepatocellular cancer (HCC). Currently there are no animal models of HCC that evaluate effect of alcoholic liver disease (ALD) on HCC acceleration. We describe a new 12-wk HCC model in adult mice that develops in livers with alcoholic hepatitis and defines ALD as co-factor in HCC. Our model involves sequential step-wise progression of ALD to HCC and highlights the role of alcohol as a tumor promoting agent. Importantly, our model shows inflammation, cellular regeneration, and fibrosis, all the features of human HCC pathogenesis.

Ambade A, Satishchandran A, Gyongyosi B, Lowe P, Szabo G. Adult mouse model of early hepatocellular carcinoma promoted by alcoholic liver disease. *World J Gastroenterol* 2016; 22(16): 4091-4108 Available from: URL: http://www.wjgnet.com/1007-9327/full/v22/i16/4091.htm DOI: http://dx.doi.org/10.3748/wjg.v22.i16.4091

INTRODUCTION

Hepatocellular carcinoma (HCC) is the most common liver cancer, and worldwide it represents the fifth most common primary cancer diagnosed in patients[1]. HCC is also the third leading cause of cancer related mortality globally. In the United States, the incidence of HCC has tripled over the last two decades[2]. Unlike many other cancers with known associated risk factors, the underlying molecular pathophysiology for HCC is still not completely known. Most commonly, the incidence of HCC is linked to known risk factors including hepatitis B and C, aflatoxin and chronic alcohol drinking[3]. About 40% of individuals who chronically consume alcohol develop fatty liver, the first pathological condition that, with continued alcohol use, can advance to alcoholic hepatitis and cirrhosis[4]. In humans, alcohol is a known causal agent in the development of HCC[1]. Most HCC patients have a history of chronic liver disease and cirrhosis and cirrhosis remains the single common precursor to HCC development[5].

Increasing evidence suggests that chronic tissue inflammation promotes tumor development[6]. In alcoholic hepatitis recruitment of macrophages and neutrophils to the liver and activation of resident Kupffer cells results in high levels of pro-inflammatory cytokines (TNFα, IL-1β, MCP-1, IL-6) both in the liver and systemic circulation[7]. Because alcoholic liver disease (ALD) and alcoholic hepatitis are characterized by significant liver inflammation, here we hypothesized that the alcoholic liver environment may expedite HCC development.

Hepatocarcinogenesis is a multistep, multistage process that involves genetic and epigenetic alterations that ultimately lead to malignant transformation of hepatocytes[8]. Several animal models have been reported that mimic different steps leading to HCC. These models have helped to identify molecular mechanisms that underlay the development of HCC including genetically modified mouse models, transgenic models expressing viral genes, transgenic mice over-expressing oncogenes and transgenic models over-expressing growth factors[9,10]. Although valuable in facilitating detailed investigation of molecular pathways, the genetically modified animal models have been shown to vary significantly in their pattern of HCC development[10]. Of the chemically induced HCC animal models, the N-nitrosodiethylamine (DEN) based models are the most widely used and accepted. DEN acts as alkylating agent for DNA bases which initiates the formation of neoplasms[11].

Chronic alcohol consumption causes morbidity and leads to broad spectrum of disorders from steatosis to steatohepatitis to cirrhosis and hepatocellular cancer[12]. Currently there are no animal models of HCC that evaluates the effect of ALD on HCC acceleration. In this study, we administered 6 doses of DEN to 4 wk old adult C57bl/6 male mice followed by 7 wk of Lieber DeCarli alcohol diet feeding. We report up-regulation of liver inflammatory cell infiltration and fibrotic markers in mice receiving alcohol + DEN. Further, alcohol + DEN mice showed characteristic appearance of intrahepatic cysts and hepatic neoplastic foci at the end of the alcohol feeding compared to mice exposed to alcohol alone and DEN alone, respectively, supporting acceleration of HCC by ALD.

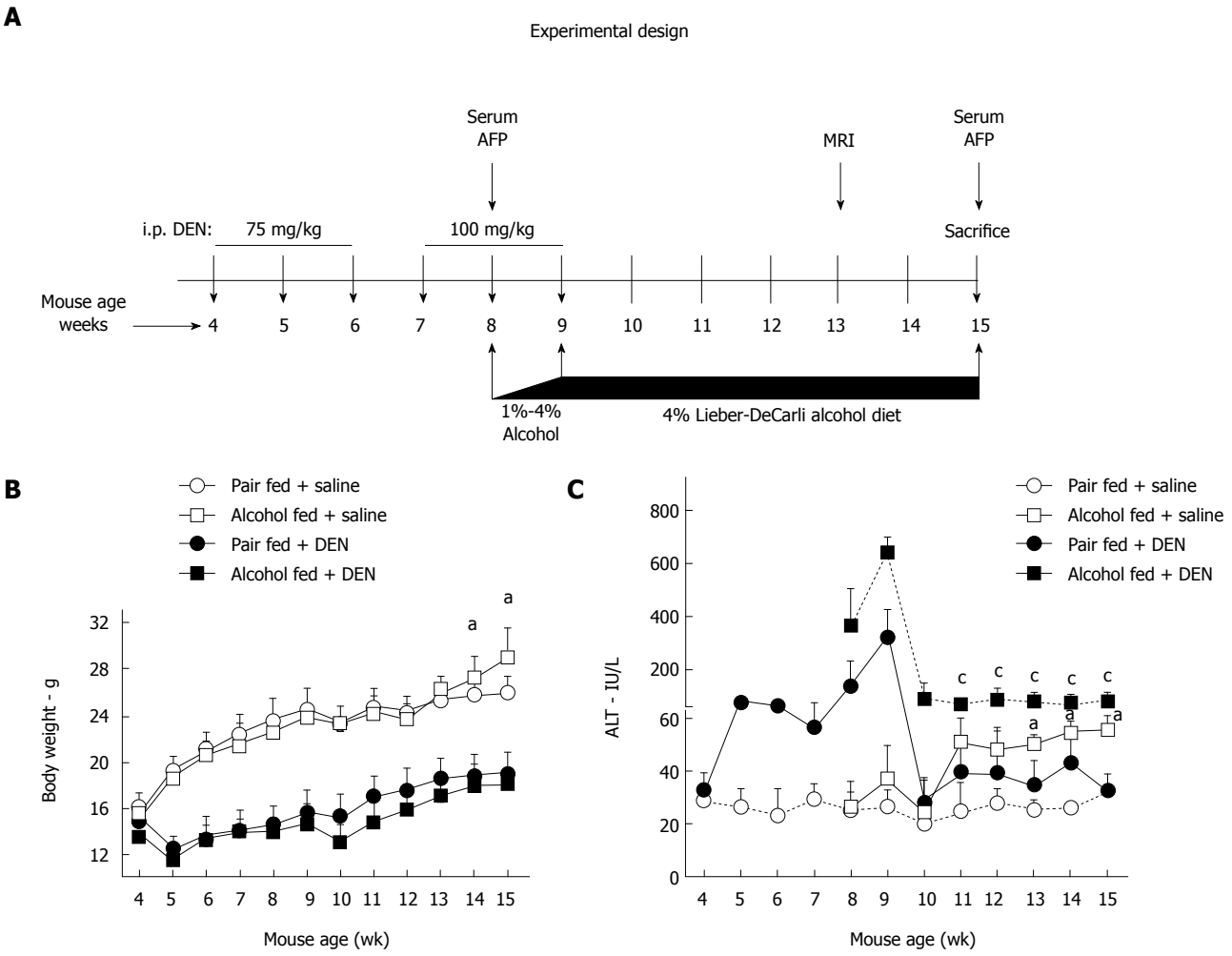

Figure 1 Chronic alcohol enhances DEN induced hepatic injury. A: Experimental design of the adult mouse model of early hepatocellular carcinoma. B: Body weight of mice in each group per week. C: Three - five mice from each experimental group were bled every week and serum ALT was measured. The graph represents mean ALT levels of each group. In graphs B and C, values are given as mean ± SD, Dunnett's multiple comparison were used to compare the means of multiple groups; ($^{a}P < 0.05$ *vs* pair fed saline injected mice, $^{c}P < 0.05$ *vs* pair fed DEN injected mice). ALT: Alanine aminotransferase; DEN: Diethyl nitrosamine; AFP: α-fetoprotein; MRI: Magnetic resonance imaging.

MATERIALS AND METHODS

Animal model of HCC

To establish a mouse model of hepatocellular cancer based on the Lieber-DeCarli alcohol diet, we injected 4 wk old C57bl/6 male mice with total 6 doses of DEN (Sigma, MO, United States) intraperitoneally. As shown in Figure 1A, a dose of 75 mg/kg DEN was administered weekly for the first 3 wk followed by a dose of 100 mg/kg DEN for next 3 wk. At week 8, the mice were randomly divided into alcohol and pair fed (control) groups. Age matched groups of mice without DEN were included in the study to understand the effect of chronic alcohol feeding. Depending on the experimental design, mice were fed 4% Lieber-Decarli alcohol diet or calorie matched control diet (Pair fed), (Bio-Serv, Flemington, NJ, United States) for 7 wk (Figure 1A). At sacrifice, blood and liver tissues were collected for further assays. The study protocol was approved by the Institutional Animal Use and Care Committee of the University of Massachusetts Medical School.

Magnetic resonance imaging

Magnetic resonance imaging (MRI) of liver was performed to monitor hyperplastic changes in liver. Images were obtained using 3T Philips Achieva whole-body MR scanner (Philips Medical Systems, Best, Netherlands) with a custom-made solenoid T/R coil with a diameter of 30 mm. The animals were anesthetized with 5% isoflurane mixed with carbogen (95% O_2/5% CO_2) and were maintained with 1% to 2% isofluorane. Coronal T2-weighted spin echo images were acquired with respiratory triggering to reduce the motion artifacts. The respiration rate was monitored with an optical probe (Model 1025T Monitoring and Gating System, SA Instruments Inc, Stony Brook, NY, United States). The output signal from the respiration monitor was used to trigger, in real time, the MR acquisition. As a consequence

of the triggered acquisition, the TR value of around 2000 ms, corresponding to the respiration rate of around 30 bpm, was determined. Other imaging parameters were: echo time (TE) of 70 ms, flip angel of 90 degrees, TSE-factor of 8, number of average = 4, matrix size of 148 × 120, field of view of 30 × 25 mm^2, slice thickness of 1 mm with no gap, acquisition time around 4 min for 22 slices. Hyperplastic nodules were distinguished from normal liver tissues on basis of differences in homogeneity and signal intensity. Pixel based nodule area quantitation was performed using ImageJ software.

Biochemical assays

Serum alanine aminotransferase (ALT) activity was determined using a kinetic method (D-TEK LLC, PA, United States). Serum AFP was assayed by ELISA (R&D systems, Minneapolis, MN, United States). Serum bilirubin was estimated using bilirubin assay kit (Abnova, Walnut, CA, United States) and the endotoxin levels were measured using *LAL Chromogenic Endotoxin Quantitation Kit* (Thermo Scientific, Rockford, IL, United States). Liver triglycerides were assayed in liver whole cell lysates using L-Type TriGlyceride M kit (Wako Diagnostics, Richmond, VA, United States).

RNA extraction and real-time PCR

Total RNA was extracted using the Direct-zol RNA MiniPrep according to the manufacturer's instructions (Zymo Research, Irvin, CA, United States). RNA was quantified using Nanodrop 2000 (Thermo Scientific, Wilmington, DE). Complementary DNA (cDNA) synthesis was performed by reverse transcription of total RNA using the iScript Reverse Transcription Supermix (BIO-RAD, Hercules, CA, United States). Real-time quantitative PCR was performed using the CFX96 real-time detection system (Bio-Rad Laboratories, Hercules, CA, United States). Primers were synthesized by IDT, Inc. (Coralville, IA, United States). Accumulation of PCR products was detected by monitoring the increase in fluorescence of double-stranded DNA-binding dye SYBR Green during amplification. Relative gene expression was calculated by the comparative cycle threshold (Ct) method. The expression of target genes was normalized to the house-keeping gene, 18S rRNA, in each sample and the fold-change in the target gene expression between experimental groups was expressed as a ratio. Melt-curve analysis was used to confirm the authenticity of the PCR products.

Western blotting

Whole cell lysates, were prepared from mouse livers as described previously[13]. Proteins of interest were detected by immunoblotting with specific primary antibodies against: Cyp2e1 (ab1252 Millipore), β-actin-HRP (ab49900; Abcam). Respective horseradish peroxidase-labeled secondary antibodies were from Santacruz Biotechnology (Dallas, TX, United States). The specific immunoreactive bands of interest were detected by chemiluminescence (Bio-Rad, Hercules, CA, United States). The immunoreactive bands were quantified by densitometric analysis using the UVP System (Bio-Rad Laboratories, Hercules, CA, United States).

Histopathological analysis

Sections of formalin-fixed, paraffin-embedded livers were stained with hematoxylin and eosin, or Sirius Red and assessed for histological features of carcinoma and fibrosis. To assess steatosis, Oil Red O staining was performed on cryofrozen liver tissue sections (OCT). Immunohistochemistry staining for PCNA (ab29; Abcam), MPO (ab9535; Abcam) was performed on formalin-fixed, paraffin-embedded livers according to the manufacturer's instructions. Images were acquired on a Nikon microscope at magnification mentioned in figure legends. The quantitation of the Oil Red O, Sirius Red staining was performed using ImageJ software.

Statistical analysis

Statistical significance was determined using two-tailed *t*-test; ANOVA and Dunnett's multiple comparison post-test were used to compare the means of multiple groups. Data are shown as mean ± SD and were considered statistically significant at $P < 0.05$. GraphPad Prism 6.02 (GraphPad Software Inc., La Jolla, CA, United States) was used for analysis.

RESULTS

Chronic alcohol enhances DEN-induced hepatic injury

ALD and alcoholic cirrhosis are major risk factors for HCC development in humans[14]. Here we hypothesized that the alcoholic liver environment expedites liver tumor development after repeated administration of a chemical carcinogen, DEN. In this study, male C57bl/6 mice received 6 weekly DEN injections, starting at age of 4 wk followed by 7 wk of chronic alcohol administration (Figure 1A). Weekly body weight monitoring showed that compared to pair-fed mice, alcohol-fed saline-injected mice gained weight significantly after 7 wk of alcohol feeding. Both DEN injected pair-fed and DEN-injected alcohol-fed mice showed attenuated weight gain during the entire course of experiment compared to mice without DEN injection (Figure 1B).

Serum ALT, a marker of hepatic injury, was significantly increased after the first DEN administration and remained elevated after repeated doses. In addition, co-administration of DEN and alcohol further increased ALT (weeks 8-9) that remained elevated in alcohol-fed mice. Introduction of alcohol feeding even in the saline injected group resulted in a significant

and sustained increase in ALT compared to pair-fed control diet (Figure 1C). These results suggested that while DEN and alcohol, respectively induce liver injury, their combination results in synergistic hepatic injury leading to sustained high serum ALT levels.

Macrophage and neutrophil activation in the liver is increased in DEN exposed ALD

Previous reports showed that chronic alcohol feeding results in significant liver inflammation[15]. Human alcoholic hepatitis is characterized by liver injury, increased serum transaminases, increased bilirubin and inflammatory cell infiltration into the liver[16]. Thus, first, we assessed serum bilirubin which is increased in alcoholic hepatitis as well as in human HCC[17]. We found that similar to human patients with alcoholic hepatitis, serum bilirubin was increased in mice after chronic alcohol administration (Figure 2A). Serum bilirubin was also increased in mice that received DEN alone (Figure 2A). However, the greatest extent of serum bilirubin increase was found in alcohol-fed DEN-injected mice compared to any other experimental groups. This was indicative of advanced liver disease and raised the possibility of HCC (Figure 2A).

Chronic alcohol exposure also induces Kupffer cell activation and infiltration of macrophages into the liver and results in secretion of pro-inflammatory cytokines that drive inflammation in alcoholic hepatitis[18]. Kupffer cells and macrophages are the most abundant pro-inflammatory cell type in the liver and are known to contribute to ALDs[19]. Thus, next, we assessed the expression of the macrophage/Kupffer cell markers, F4/80, CD68 in the liver. The expression of the pan-macrophage marker, F4/80, was significantly elevated in all alcohol-fed mice with or without DEN. The macrophage activation marker, CD68, was up regulated to greater extent in alcohol-fed DEN-injected mice as compared to alcohol-fed saline-injected mice suggesting the presence of activated inflammatory macrophages in the liver (Figure 2B). Recent literature suggests that macrophages can be further classified into pro-inflammtory M1 or anti-inflammatory M2 macrophages[20]. These macrophage subtypes express unique markers[21]. We found a significant increase in the expression of M1 macrophage markers, IL-1β and iNOS, (Figure 2C) in livers of alcohol fed mice. Importantly, iNOS expression was significantly higher in alcohol fed-DEN injected mice compared to alcohol alone (Figure 2C). Livers from alcohol fed mice also showed higher expression of M2 macrophage markers, Arg1, CD163, IL-10 and CD206, compared to non-alcohol controls (Figure 2D) and CD206 the highest in alcohol fed-DEN injected mice (Figure 2D). These observations suggested increased macrophage recruitment to precancerous liver with mixed M1/M2 phenotype.

Neutrophils play a significant role in alcoholic hepatitis and also contribute to HCC[22]. Other studies have shown that alcohol alone upregulated expression of the characteristic neutrophil markers, Ly6G, MPO and E-selectin[23]. In our study, messenger RNA levels of these neutrophil markers were significantly up-regulated in alcohol-fed (Figure 3A) compared to pair-fed mice. The highest expression of Ly6G, MPO and E-selectin was found in alcohol-fed DEN-injected mice as compared to any other experimental groups (Figure 3A). DEN alone resulted in no change in neutrophil marker expression compared to saline injected controls (Figure 3A). We also confirmed the upregulation of MPO at the protein level using MPO immunostaining (Figure 3B) that showed significantly increased numbers of infiltrating neutrophils in alcohol-fed saline-injected mice compared to pair-fed controls (Figure 3B). Moreover, the highest levels of MPO staining, confirming neutrophil infiltration and activation, were present in the livers of DEN-injected alcohol-fed mice (Figure 3C). Taken together, our data showed a significant increase in key features of alcoholic hepatitis including increased serum bilirubin, a clinically relevant diagnostic marker, elevated macrophage, neutrophil after alcohol administration and an even greater elevation in all of these indices in the alcohol + DEN treated mice markers in our experimental model.

Chronic alcohol synergizes with DEN in induction of liver fibrosis

As we found sustained and increased liver injury and inflammation after DEN + alcohol administration, we next analyzed steatosis and fibrosis in the livers. There was a significant increase in steatosis in the livers of alcohol-fed mice compared to the pair-fed control as indicated by Oil-Red-O staining (Figure 4A). Interestingly, alcohol-induced liver steatosis was attenuated in DEN-injected mice compared to saline-injected alcohol-fed mice (Figure 4A). DEN alone did not induce steatosis (Figure 4A and B). Alcohol induced steatosis was further confirmed by measuring hepatic triglyceride content, which also showed reduction in alcohol-fed DEN-injected mice as compared to alcohol-fed saline-injected mice (Figure 4C). While steatosis is an early presentation of ALD, prolonged liver disease results in fibrosis that is considered as a sequential step towards HCC development[24]. Hence, we assessed the extent of fibrosis using Sirius Red staining. As shown in Figure 4D, alcohol-fed DEN-injected mice showed significantly increased fibrosis by Sirius Red staining indicating the presence of liver fibrosis compared to all other groups (Figure 4D). The increased fibrosis was quantified in Figure 4E. Thus, our experimental model of HCC with DEN + alcohol

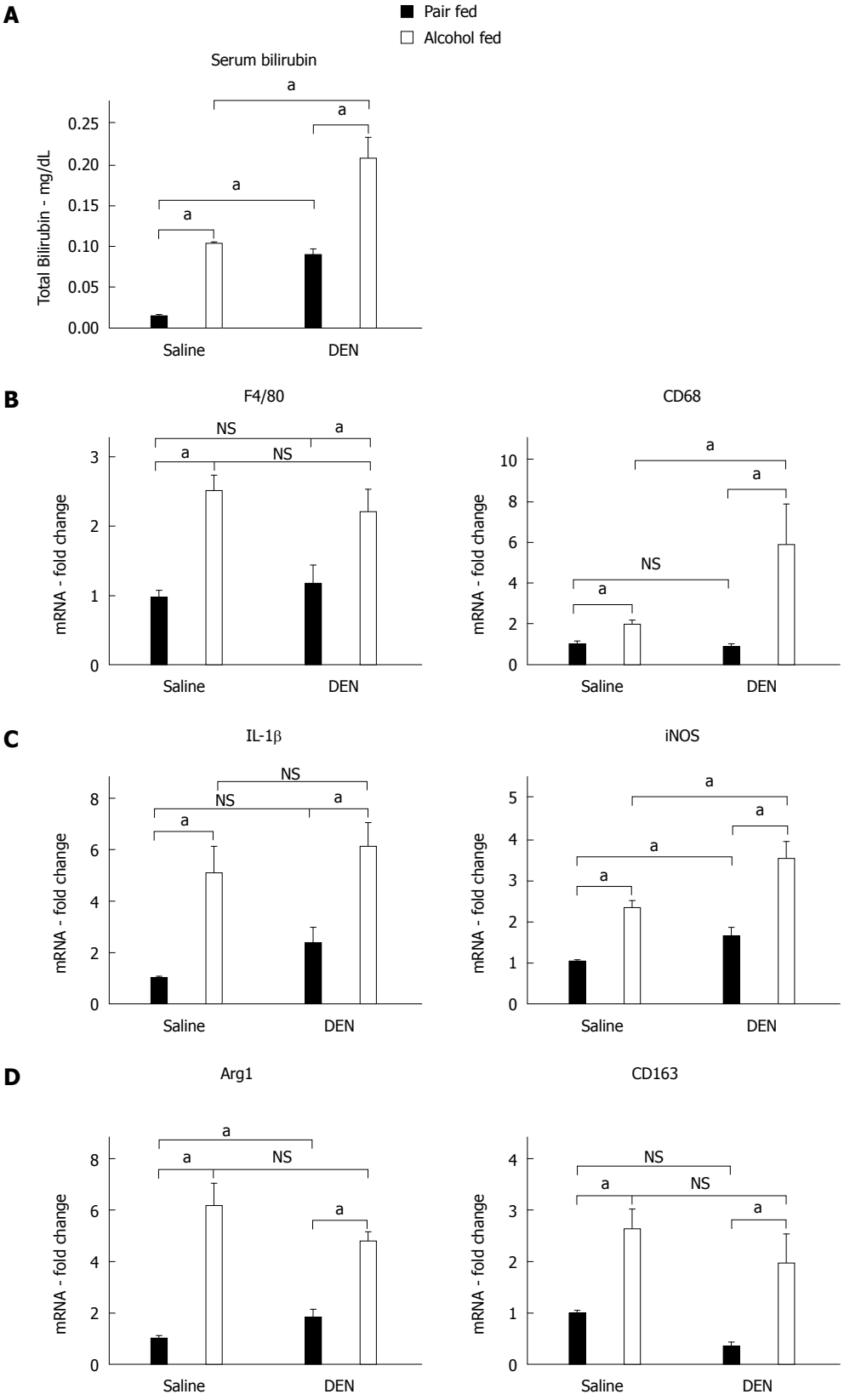
A
Pair fed
Alcohol fed
Serum bilirubin
Total Bilirubin - mg/dL
0.25
0.20
0.15
0.10
0.05
0.00
a
a
a
a
Saline
DEN
B
F4/80
mRNA - fold change
3
2
1
0
NS
a
a
NS
Saline
DEN
CD68
mRNA - fold change
10
8
6
4
2
0
a
a
NS
a
Saline
DEN
C
IL-1β
mRNA - fold change
8
6
4
2
0
NS
NS
a
a
Saline
DEN
iNOS
mRNA - fold change
5
4
3
2
1
0
a
a
a
a
Saline
DEN
D
Arg1
mRNA - fold change
8
6
4
2
0
a
a
NS
a
Saline
DEN
CD163
mRNA - fold change
4
3
2
1
0
NS
a
NS
a
Saline
DEN

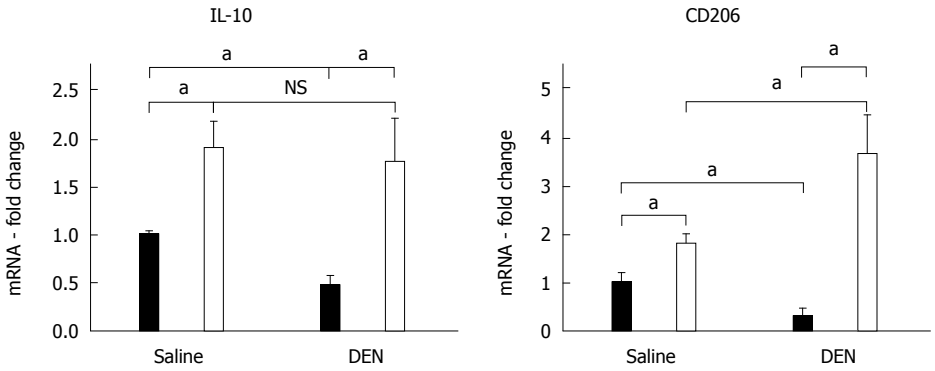

Figure 2 Alcoholic hepatitis induces macrophage polarization. A: Serum bilirubin was measured in serum samples at week 15; B: Liver mRNA levels of macrophage markers, F4/80, CD68; C: Liver mRNA levels of M1 macrophage markers, IL-1β, iNOS; D: Liver mRNA levels of M2 macrophage markers, Arg1, CD163, IL-10, and CD206. In graphs, values are given as mean ± SD, Dunnett's multiple comparison were used to compare the means of multiple groups; $^{a}P < 0.05$. NS: Not significant; DEN: Diethyl nitrosamine; IL: Interleukin; iNOS: Inducible nitric oxide synthase.

showed minimal steatosis and significant fibrosis indicative of advanced liver disease.

Chronic alcohol induces serum endotoxin and activates Cyp2e1

Chronic alcohol exposure leads to an increase in levels of circulating endotoxin, which can activate the immune cells in the liver causing inflammation[25]. TLR4 signaling has been shown to contribute to HCC[26]. We observed a significant increase in serum endotoxin levels after alcohol feeding while there was no significant difference between the endotoxin levels of alcohol-fed DEN injected mice and alcohol alone fed mice, at the time of sacrifice (Figure 5A). Cyp2e1, the enzyme that metabolizes alcohol in liver, was upregulated at both mRNA and liver protein levels in alcohol fed mice (Figure 5B and C) as compared to pair fed or DEN alone mice. Interestingly, the liver protein levels of Cyp2e1 in alcohol + DEN mice were significantly lower than alcohol alone fed mice (Figure 5D). This data supported the hypothesis of increased inflammation and Cyp2e1 activation after alcohol exposure in our experimental model.

Chronic alcohol induces cellular proliferation and expedites HCC

To ascertain the liver tumor and HCC development, we performed MRI on all experimental groups before sacrifice, at week 13 of age. The liver MRI revealed a few bright spots, characteristics of intrahepatic cysts, in DEN treated mice, however significantly higher numbers of hepatic cysts were present in the DEN + alcohol mice (Figure 6A). The increased numbers of intrahepatic cysts in DEN + alcohol mice were further confirmed by histology (Figure 6B). Livers of pair-fed or alcohol alone fed mice showed no lesions on MRI. The area of cysts from MRI data was quantified using ImageJ and shown in Figure 6C. In addition to hepatic cysts, histology evaluation revealed the presence of numerous liver nodules characterized by hepatic hyperplasia exclusively in alcohol-fed DEN-injected mice compared to all other experimental groups (Figure 6D). The pair-fed DEN-injected mice had very few intrahepatic cysts and no hepatic hyperplastic nodules. None of the alcohol fed or pair fed mice had cysts or hyperplastic nodules. These results indicated that alcoholic hepatitis expedited early liver tumor development.

Next, we assessed the expression of characteristic HCC markers. The expression of AFP is directly associated with hepatocyte differentiation and HCC progression[27]. More importantly, AFP is the most commonly used noninvasive marker for HCC diagnosis[17]. We measured serum AFP levels at week 8 (at the beginning of alcohol feeding) and at week 15 (at the end of alcohol feeding). DEN alone increased serum AFP at both 8 and 15 wk while alcohol alone increased AFP only at 15 wk (Figure 7A). Importantly, there was a significant increase in serum AFP in alcohol + DEN mice compared to the DEN alone or alcohol alone groups not only at 8 but also at 15 wk, indicating early regeneration and potentially, HCC development (Figure 7A and B).

Chronic alcohol feeding is reported to induce hepatic proliferation[28]. Thus, to estimate cell proliferation, we performed PCNA staining on liver tissue sections (Figure 7C). Immunohistochemistry staining for PCNA showed significantly higher number of PCNA positive nuclei in alcohol-fed DEN-injected mice compared to all other groups (Figure 7C). Of note, both alcohol-fed saline-injected and pair-fed DEN-injected mice showed increased numbers of PCNA positive nuclei compared to pair-fed saline-injected controls (Figure 7D). Taken together, our experimental model showed hepatic hyperplasia confirmed on histology, significant up regulation in AFP and cell proliferation, providing evidence for the synergistic action of alcohol as a tumor promoting agent in DEN-induced early HCC.

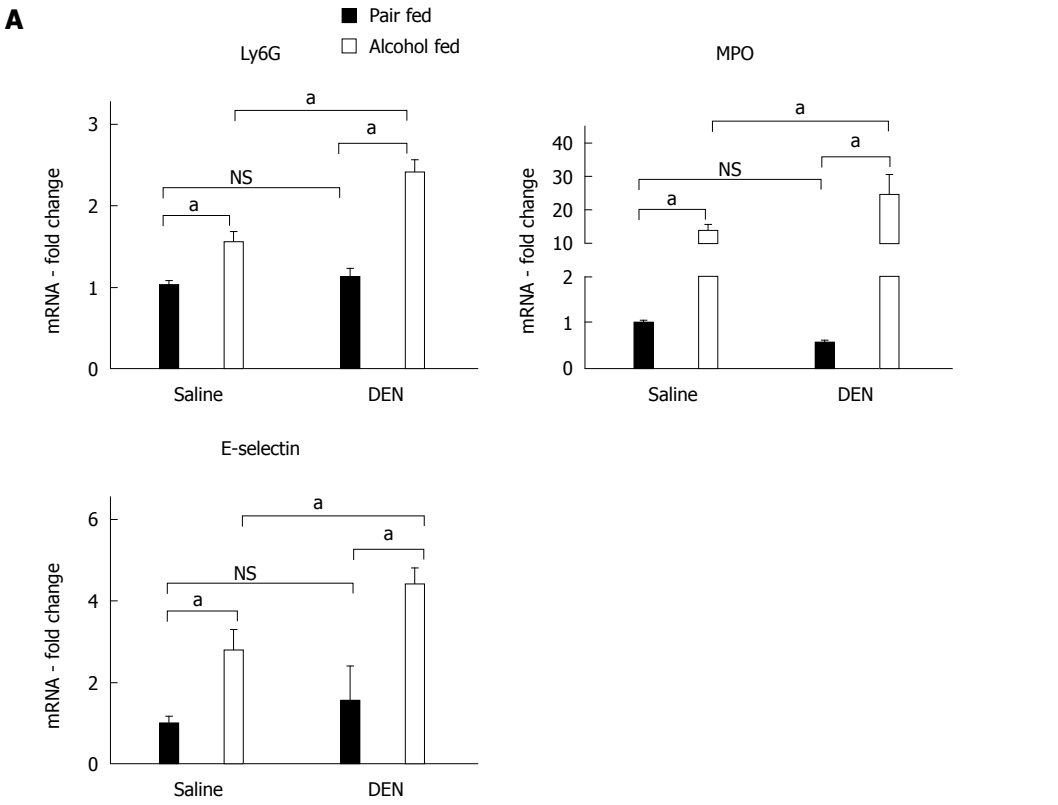
A
Pair fed
Alcohol fed
Ly6G
MPO
E-selectin
mRNA - fold change
Saline
DEN
NS
a

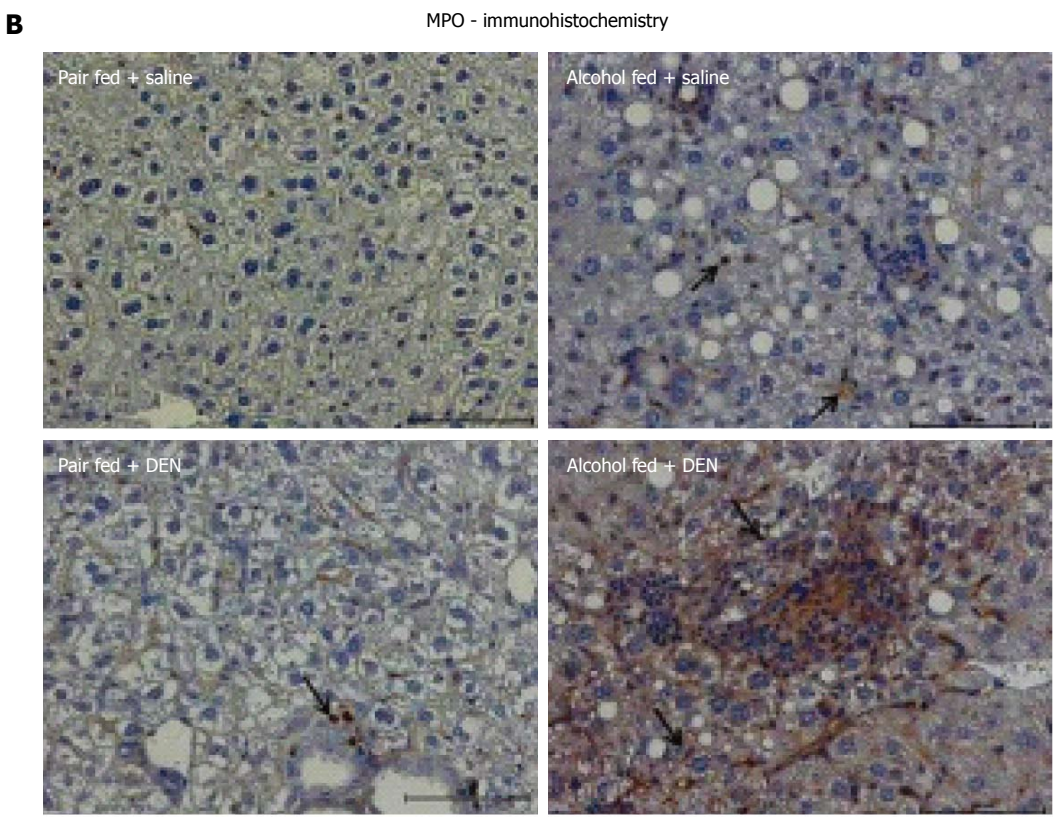
B
MPO - immunohistochemistry
Pair fed + saline
Alcohol fed + saline
Pair fed + DEN
Alcohol fed + DEN

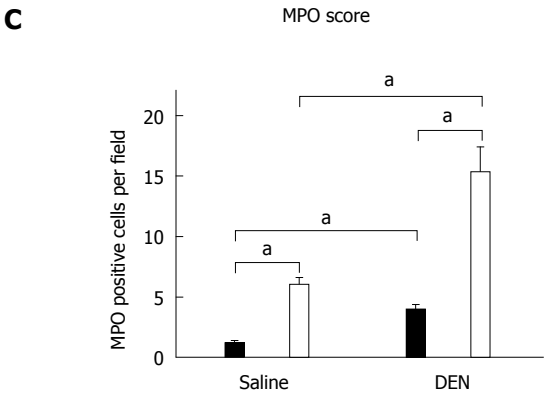

Figure 3 Alcoholic hepatitis induces neutrophil infiltration. A: Liver mRNA levels of neutrophil markers, Ly6G, MPO and E-selectin; B: Representative myeloperoxidase (MPO) immunohistochemistry of hepatic sections (magnification × 200) from all experimental groups at 15 wk. Black arrows point to the positive staining; C: MPO positive cells were scored in at least 3 different microscopic fields for each mouse and plotted as bar graph. ($n \geqslant 5$ mice per group). In graphs, values are given as mean ± SD, Dunnett's multiple comparison were used to compare the means of multiple groups; $^{a}P < 0.05$. NS: Not significant; DEN: Diethyl nitrosamine.

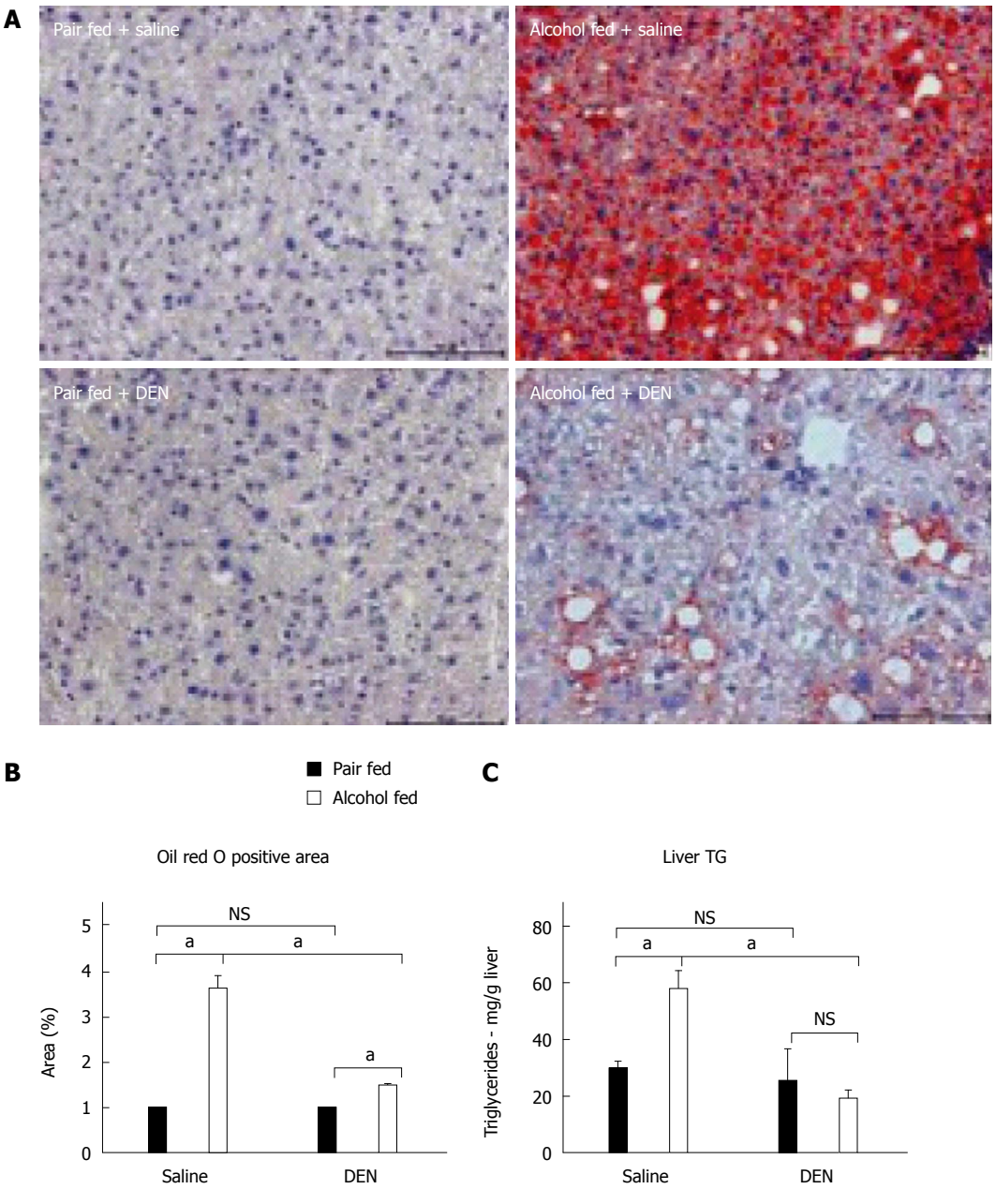

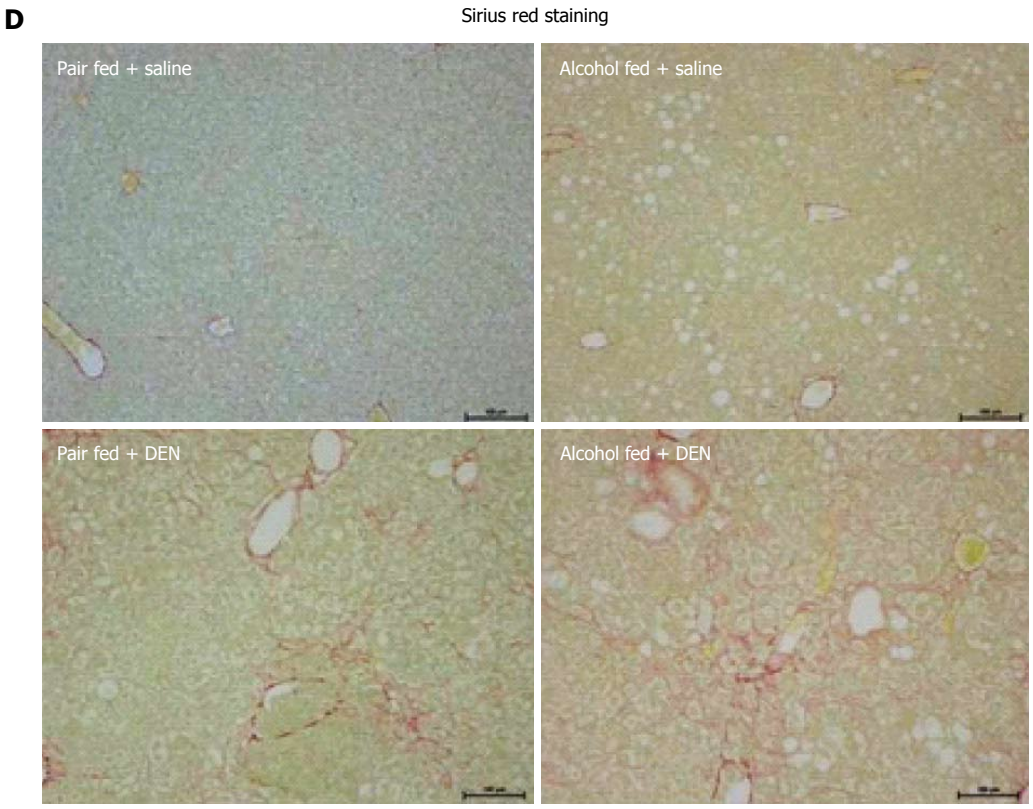

Figure 4 Chronic alcohol synergizes with diethyl nitrosamine in hepatocellular carcinoma development. A: Representative Oil Red O staining of hepatic sections (200 × magnification) from all experimental groups at 15 wk; B: Bar graph shows percent Oil Red O stained area in groups that was quantified using ImageJ software. For quantification, at least 3 different microscope fields were scored for each mouse ($n \geqslant 5$ mice per group); C: Liver triglycerides were estimated at week 15; D: Representative Sirius Red staining of hepatic sections (magnification × 100) from all experimental groups at 15 wk. E: For quantification of fibrosis, at least 3 different microscope fields at 10x magnification were scored for each mouse ($n \geqslant 5$ mice per group). Bar graph shows percent Sirius Red positive area quantified using ImageJ. In graphs, values are given as mean ± SD, Dunnett's multiple comparison were used to compare the means of multiple groups; $^{a}P < 0.05$. NS: Not significant; DEN: Diethyl nitrosamine.

DISCUSSION

Chronic alcohol use leads to alcoholic hepatitis and cirrhosis[14]. Epidemiological data suggests that chronic heavy alcohol consumption and ALD is a significant risk factor towards the development of HCC[29]. In this study, we introduce a mouse model that demonstrates that chronic alcohol feeding resulting in alcoholic hepatitis in adult mice, expedites DEN (chemical) induced early liver tumor development. We found that features of human alcoholic hepatitis including inflammation, steatosis and fibrosis were all present in DEN-injected mice after alcohol feeding and resulted in present numbers of early HCC neoplastic foci (Figure 8). Our data indicate that increased neutrophil and macrophage activation is triggered in the alcoholic liver tissue microenvironment and may contribute to acceleration of HCC (Figure 8). In addition to steatohepatitis, liver fibrosis was also present in DEN + alcohol treated mice as indicated by Sirius Red staining. Further, our model showed increased numbers of intrahepatic cysts by the MRI that were confirmed as hepatobiliary cysts by histology and are features of early hepatobiliary cancer. Our model also

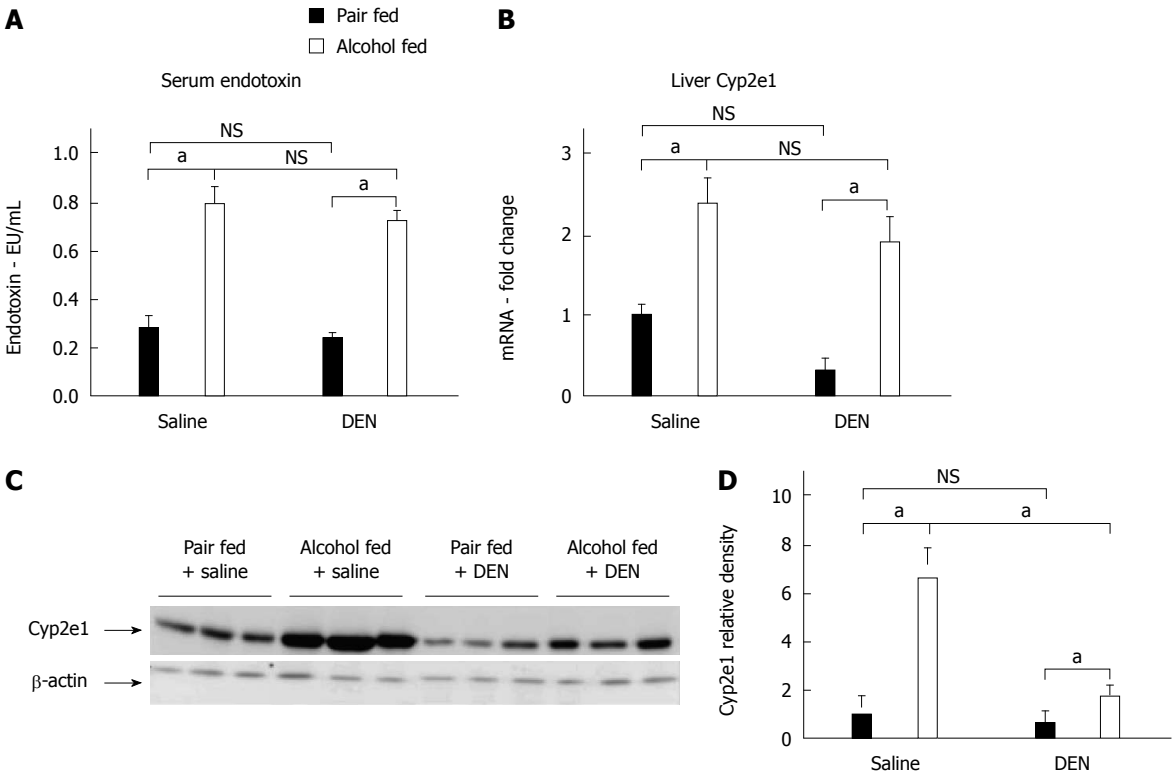

Figure 5 Chronic alcohol increases serum endotoxin levels and activates Cyp2e1. A: Serum endotoxin; B: Liver Cyp2e1 mRNA levels; C: Representative western blot showing liver Cyp2e1 protein levels. β-actin was used as loading control for western blot; D: Relative density of Cyp2e1 western blot signal. In graphs, values are given as mean ± SD, Dunnett's multiple comparison were used to compare the means of multiple groups; $^{a}P < 0.05$. NS: Not significant; DEN: Diethyl nitrosamine.

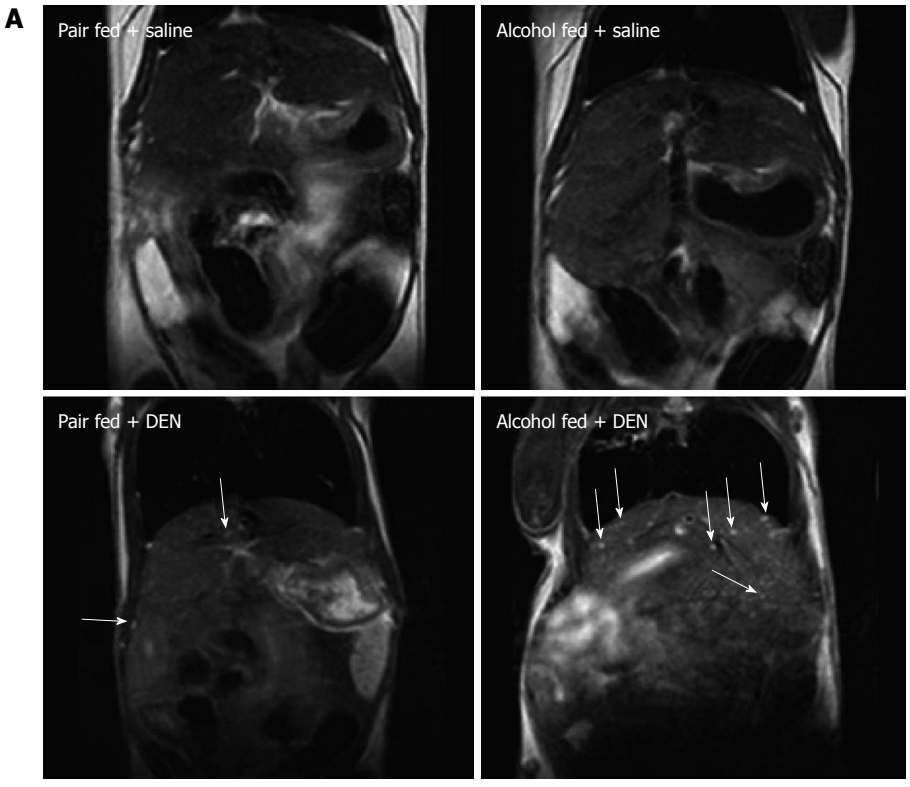

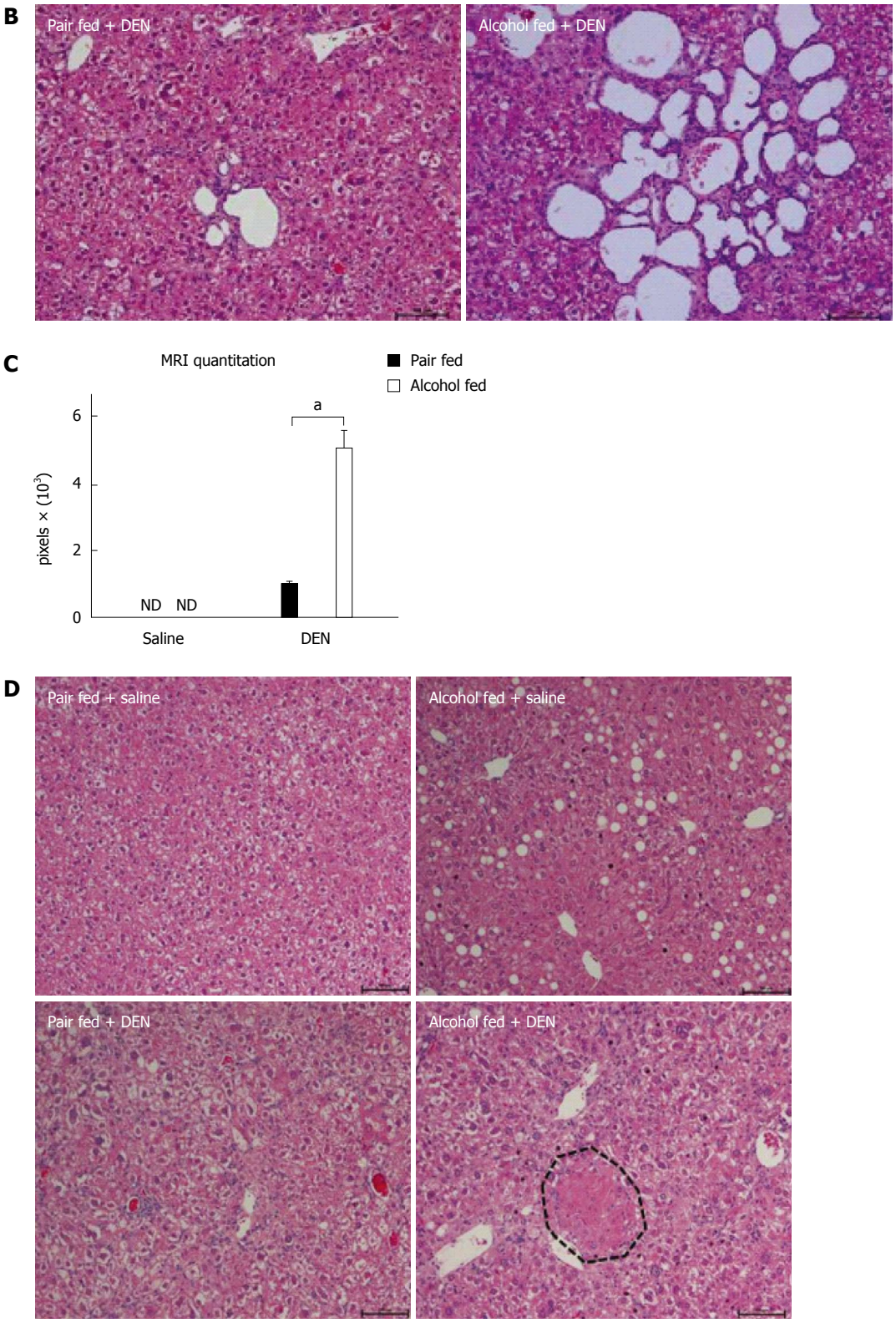

Figure 6 Chronic alcohol expedites hepatocellular carcinoma development. A: T2-weighted MRI of liver in coronal section at week 13. Arrows denote intrahepatic cysts. B: Representative HE stained intrahepatic cysts observed in all DEN injected mice (100X magnification). Note the higher number of cysts in alcohol + DEN mice. C: Quantification of cyst area using ImageJ. D: Representative HE stained liver sections from all treatment groups (magnification × 100) at week 15. The hepatic hyperplasia (encircled in black dotted line) was exclusively observed in alcohol + DEN mice. In graph (C), values are given as mean ± SD, Dunnett's multiple comparison were used to compare the means of multiple groups; $^{a}P < 0.05$, pair fed *vs* alcohol fed. ND: Not detected; DEN: Diethyl nitrosamine.

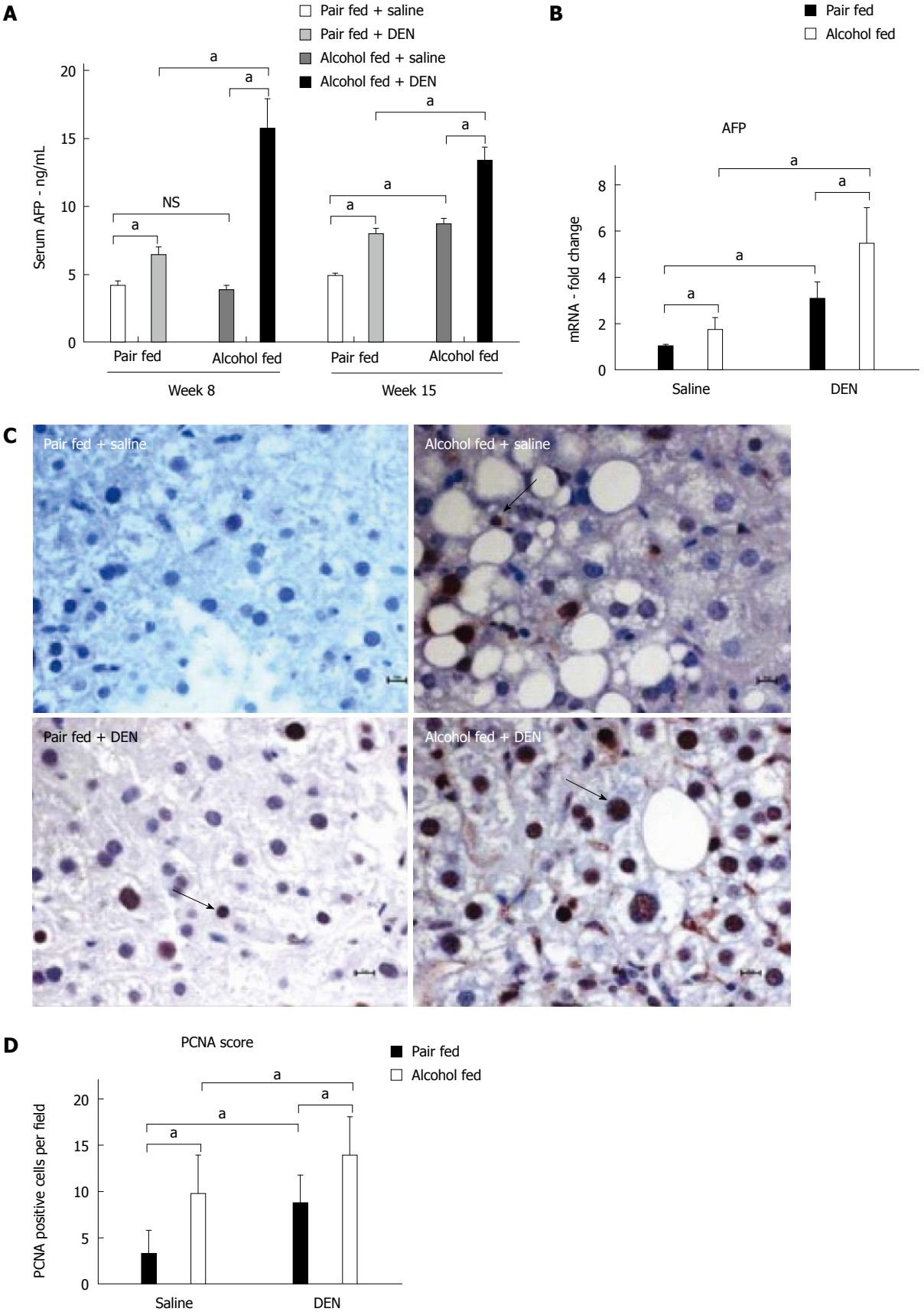

Figure 7 Chronic alcohol induces serum AFP and cellular proliferation. A: Fold changes in serum AFP levels at week 8 and week 15; B: Liver AFP mRNA levels at week 15; C: Representative immunostaining images for proliferating cell nuclear antigen (PCNA) at week 15 (magnification × 400). Arrows point to positive staining; D: PCNA positive nuclei were scored in at least 3 different microscopic fields for each mouse and plotted as bar graph on the right. ($n \geqslant 5$ mice per group). In graphs, values are given as mean ± SD, Dunnett's multiple comparison were used to compare the means of multiple groups; $^{a}P < 0.05$. NS: Not significant; DEN: Diethyl nitrosamine; AFP: α-fetoprotein.

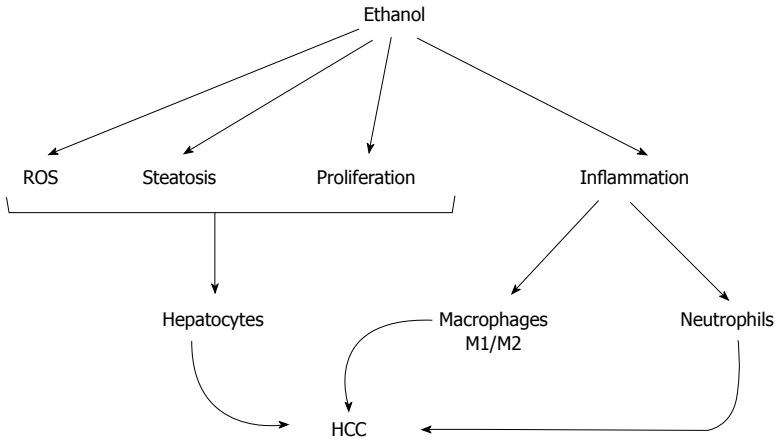

Figure 8 Multi-factorial effects of ethanol in hepatocellular carcinoma acceleration. HCC: Hepatocellular carcinoma.

showed significant induction in serum AFP, one of the well-established markers of HCC, upon alcohol feeding in the DEN-injected mice. Finally, our data showed enhanced cellular proliferation in response to chronic alcohol feeding which promoted progression to HCC.

DEN has been used since the 1960s to induce HCCs in laboratory animals, and is the most widely used chemical to induce liver cancer in mice[10]. DEN undergoes metabolic activation in hepatocytes by enzymes of the cytochrome P450 family and acts as a complete carcinogen, if injected in mice younger than 2 wk, when hepatocytes are still actively proliferating[30]. When administered to adult mice, tumor promotion is required and can be achieved by phenobarbital, carbon tetrachloride, partial hepatectomy. Our experimental model used 4 wk old male mice and provided evidence for the role of alcohol as tumor promoting agent in adult mice. In our study, male mice were chosen because of the higher prevalence of HCC in males compared to females in humans[3]. Irrespective of the promoting agent used, DEN based HCC models take at least 5 mo to show the first signs of tumor. Our model using alcohol as a tumor promoting agent demonstrated the first signs of early HCC in a much shorter time of 3 mo.

Although several carcinogen initiated HCC animal models have been described, none of them so far evaluated alcoholic hepatitis and ALD as a tumor promoting factor in wild-type mice[9]. A recent study performed in neonate mice combined chronic alcohol exposure in the drinking water with DEN injection and showed tumors at 48 wk[12]. However, alcohol administration in the drinking water does not cause ALD[31]. In our study, we employed the Lieber-DeCarli alcohol feeding model that results in features of human ALD including steatosis, inflammation and liver fibrosis[32]. By utilizing adult mice and the Lieber-DeCarli alcohol diet, our model shows acceleration of early hepatobiliary tumors after a chemical carcinogen exposure with some histopathological resemblance to human ALD.

Chemical toxins and viral agents are the two well known etiologies of hepatocellular cancer[1]. Irrespective of the underlying etiology, cellular inflammation is the common feature that has been shown to be present in human HCC patients as well as animal models[33]. It is also known that persistent inflammation in the absence of infection increases the risk and expedites the development of cancer. Inflammation in the liver is one of the hallmarks of alcoholic hepatitis[33] and it was prominent in our model with the highest level in alcohol-fed DEN treated mice. Activation and recruitment of neutrophils and macrophages to the liver is a well-known feature of alcoholic hepatitis[19,22], steatohepatitis and ALD[34]. In our experiments, we found increased expression and activation of neutrophils and macrophages in alcohol-fed mice and markers of inflammation were even higher in mice with liver tumors after DEN + alcohol feeding. Alcohol-induced sensitization of liver macrophages to portal endotoxin is a hallmark of ALD[35]. LPS recognition by TLR4 on macrophages and other cell types in the liver, activation of downstream signaling pathways culminating in activation of transcription factors such as NF-κB, AP-1 leads to increased inflammatory cytokine production in ALD. Recent literature suggests that macrophages can be further classified into pro-inflammatory M1 or anti-inflammatory M2 macrophages[20]. The M1 phenotype is characterized by the expression of high levels of proinflammatory cytokines, high production of reactive nitrogen and oxygen intermediates, promotion of Th1 response, and strong microbicidal and tumoricidal activity[20,36]. The alternatively activated or M2 macrophages are often referred to as tumor associated macrophages (TAMs)[20]. We observed a significant induction of both M1 (TNFα, iNOS) and M2 markers (Arg1, CD163, CD206) in our experimental model. The presence of M1 macrophages is consistent with the increased proinflammatory activation in ALD. This

increase in M2 macrophage is likely suggestive of the presence of TAMs in the liver. TAMs represent the major inflammatory component of the stroma of liver cancer and can affect different aspects of the neoplastic transformation of the tissue. Many observations indicate that TAMs express several M2-associated pro-tumoural functions, including promotion of angiogenesis, matrix remodeling and suppression of adaptive immunity. The pro-tumoural role of TAMs in cancer is further supported by clinical studies that found a correlation between the high macrophage content of tumors and poor patient prognosis. TAMs represent a unique and distinct M2-skewed myeloid population and are now recognized as a potential target for anti-cancer therapy[37]. Therefore, we mixed M1/M2 MΦ presence with the increase in M2 macrophage markers observed in our model may be responsible for promoting tumor development in the DEN exposed alcohol-fed mice.

Alcohol is primarily metabolized in hepatocytes and its metabolites generate ROS, cause inflammation and steatosis. Long term alcohol exposure induces a state of chronic inflammation in the liver[38]. Both DEN and alcohol induce Cyp2E1, and the chronic alcoholic injury induced in our model synergized with the chemical injury to increase hepatocyte proliferation leading to appearance of early neoplastic foci found in our experimental model. In the context of cancer-related inflammation, key intracellular signal transducers have been identified both in preneoplastic cells as well as in inflammatory cells. Among these signaling pathways, sustained activation of transcription factors including NF-κB, p53, HIF-1α, β-catenin/Wnt, and Nrf2 in liver leads to chronic inflammation that is responsible for cancer progression[39]. Thus, the inflammation associated with alcoholic hepatitis may be a significant contributing factor to HCC development in alcohol fed DEN injected mice.

In addition to cellular inflammation, the alcohol fed DEN injected mice showed sustained higher ALT levels. Increased ALT levels are indicator of hepatocyte damage and can be used reliably as a marker of liver injury[40]. Initially in our experimental model, the ALT levels were significantly higher in all DEN injected mice and ALT returned to baseline after cessation of DEN administration. However, the alcohol fed mice showed sustained the higher ALT levels suggesting sustained liver injury. DEN acts as an alkylating agent for DNA bases which initiates the formation of neoplasms[11]. It has been proposed that the charged nucleophilic intermediates of DEN attack DNA bases thereby leading to mutations which initiate cellular transformation[11]. Chemical carcinogens including DEN exert their effect by generating ROS during their metabolism in the liver, which is responsible for DNA damage associated with increased risk of cancer development[39]. Importantly, DEN is metabolized in the liver by Cyp2E1, the same enzyme that metabolizes alcohol[41]. We also observed significantly higher TBARS in alcohol fed DEN injected mice, compared to alcohol alone mice (data not shown). Hence, it is possible that the hepatocytes from alcohol fed DEN injected mice are exposed to extremely higher ROS in addition to DNA damage which may expedite their transformation into early HCC observed in this group exclusively.

The expression of AFP is directly associated with hepatocyte differentiation[27]. Elevated levels of serum AFP are reported in alcoholic hepatitis patients[42]. However, as compared to alcoholic hepatitis patients, the AFP levels are much higher in human HCC patients[43]. Some reports show a clinical correlation between serum AFP and severity of liver disease[44]. Our data of serum AFP levels at week 8 and 15 clearly show the role of alcohol in stimulating AFP expression which can be correlated to advanced liver disease such as HCC. In addition to hepatocytes, the liver progenitor cells (LPC) also produce AFP during their cellular differentiation[45]. The LPCs play an important role in liver regeneration and homeostasis[46,47]. Increased serum AFP in our experimental model is also indicative of enhanced proliferation of LPCs which may be responding to chronic liver injury caused by alcohol feeding. This regenerative response by LPCs may also contribute to HCC development.

Chronic alcohol feeding is reported to induce Cyclin D1 protein that corresponds with enhanced hepatic proliferation[28]. More recently, Lanthier *et al*[48] reported that alcoholic hepatitis patients demonstrated a significant invasion of LPC and a higher number of proliferating hepatocytes compared to controls. This study on human alcoholic hepatitis patients suggests that hepatic cell proliferation plays a pivotal role in the prognosis of alcoholic hepatitis and HCC. A significantly higher number of PCNA positive cells in DEN + alcohol mice provide another evidence for the role of alcohol as inducer of hepatocyte and LPC proliferation.

Chronic liver injury such as long term alcohol exposure leads to steatohepatitis, hepatitis which can progress to fibrosis[24]. Hepatic fibrosis is an injury healing process in which excessive connective tissue accumulates in the liver[49]. The profibrotic factors like collagen are overproduced to assist the expansion of new hepatocytes. Hepatic fibrosis can progress to cirrhosis and in few cases to HCC[24]. In our experimental model of HCC, the alcohol fed DEN injected mice showed significantly higher fibrosis as compared to alcohol fed (alone) or DEN injected (alone) mice. The molecular pathways associated with fibrosis are very similar to liver regeneration, a cellular process in which mature terminally differentiated hepatocytes proliferate to replace the injured cells[50]. In adult mice, mature hepatocytes exist in a growth-arrested (G_0) state which, after liver injury, leave their G_0 state and enter the proliferative stages of the cell cycle during which they duplicate necessary components and

synthesize new proliferation-specific molecules (G_1 phase), replicate their DNA (S phase), and divide (M phase)[51]. It is conceivable that in our experimental model, hepatocytes with damaged DNA undergo multiple rounds of proliferation to complete the regeneration response. However, due to their damaged DNA, continue to proliferate leading to HCC. Other probable explanation could be that the hepatocytes with DEN induced DNA damage are exposed to increased amount of ROS and inflammation due to chronic alcohol exposure, which leads to their constant proliferation resulting in HCC development. These hypotheses can be the focus of future studies.

In conclusion, by combining multiple injections of DEN prior to chronic Lieber-DeCarli alcohol diet feeding, we developed a mouse model that displays the features of early HCC. Importantly, our model involves adult mice with alcoholic hepatitis, liver inflammation, cellular regeneration, and fibrosis, all the features associated with pathogenesis of human HCC. We believe that availability of such a model will provide unique opportunities to understand alcohol associated molecular and cellular mechanisms related to HCC.

ACKNOWLEDGMENTS

The authors would like to thank members of the Szabo lab for their stimulating intellectual discussions and scientific input. The help provided by Shao-Kuan Zheng (Department of Radiology) in acquisition of MRI data is acknowledged. We thank Merin MacDonald and Candice Dufour for assistance with formatting the manuscript. The authors are grateful to services provided by DERC (histology and immunostaining) and CFAR (Primer Synthesis) core facilities at UMASS Medical School. CFAR core facility is supported by the University of Massachusetts Center for AIDS Research (P30 AI042845).

COMMENTS

Background

Hepatocellular carcinoma (HCC) is the most common liver cancer, and worldwide it represents the fifth most common primary cancer diagnosed in patients. Chronic alcohol consumption causes morbidity and leads to broad spectrum of disorders from steatosis to steatohepatitis to cirrhosis and hepatocellular cancer.

Research frontiers

Several animal models have been reported that mimic different steps leading to HCC. Currently there are no animal models of HCC that evaluate the effect of alcoholic liver disease on HCC acceleration.

Innovations and breakthrough

In this study, the authors administered 6 doses of diethyl nitrosamine (DEN) to 4 wk old adult C57bl/6 male mice followed by 7 wk of Lieber-DeCarli alcohol diet feeding. They found that features of human alcoholic hepatitis including inflammation, steatosis and fibrosis were all present in DEN-injected mice after alcohol feeding and resulted in higher numbers of early HCC neoplastic foci. The data indicate that increased neutrophil and macrophage activation is triggered in the alcoholic liver tissue microenvironment and may contribute to acceleration of HCC.

Applications

This combination of carcinogen pre-exposure and chronic alcohol consumption presents one of the most unique phenomenons of chronic alcohol leading to progression of HCC that occurs in humans. This availability of such a model will provide unique opportunities to understand alcohol associated molecular and cellular mechanisms related to HCC.

Terminology

Lieber-DeCarli diet, a commercially available, carefully designed and well characterized rodent diet intended to mimic the clinical situation in which the various effects of alcohol occur in the setting of liver changes characterized by a fatty liver and inflammation.

Peer-review

This is an interesting manuscript devoted to increased DEN-induced HCC development by alcohol. An important aspect of this study is that mice were fed not ethanol in water, but ethanol in Lieber-DeCarli diet (pair-feeding), which by itself induces liver injury.

REFERENCES

1 **El-Serag HB**. Hepatocellular carcinoma. *N Engl J Med* 2011; **365**: 1118-1127 [PMID: 21992124 DOI: 10.1056/NEJMra1001683]
2 **Torre LA**, Bray F, Siegel RL, Ferlay J, Lortet-Tieulent J, Jemal A. Global cancer statistics, 2012. *CA Cancer J Clin* 2015; **65**: 87-108 [PMID: 25651787 DOI: 10.3322/caac.21262]
3 **Altekruse SF**, Henley SJ, Cucinelli JE, McGlynn KA. Changing hepatocellular carcinoma incidence and liver cancer mortality rates in the United States. *Am J Gastroenterol* 2014; **109**: 542-553 [PMID: 24513805 DOI: 10.1038/ajg.2014.11]
4 **Szabo G**, Dolganiuc A. Hepatitis C core protein - the "core" of immune deception? *J Hepatol* 2008; **48**: 8-11 [PMID: 18023495 DOI: 10.1016/j.jhep.2007.10.005]
5 **Sanyal AJ**, Yoon SK, Lencioni R. The etiology of hepatocellular carcinoma and consequences for treatment. *Oncologist* 2010; **15** Suppl 4: 14-22 [PMID: 21115577 DOI: 10.1634/theoncologist.2010-S4-14]
6 **Grivennikov SI**, Greten FR, Karin M. Immunity, inflammation, and cancer. *Cell* 2010; **140**: 883-899 [PMID: 20303878 DOI: 10.1016/j.cell.2010.01.025]
7 **Szabo G**, Petrasek J. Inflammasome activation and function in liver disease. *Nat Rev Gastroenterol Hepatol* 2015; **12**: 387-400 [PMID: 26055245 DOI: 10.1038/nrgastro.2015.94]
8 **Villanueva A**, Newell P, Chiang DY, Friedman SL, Llovet JM. Genomics and signaling pathways in hepatocellular carcinoma. *Semin Liver Dis* 2007; **27**: 55-76 [PMID: 17295177 DOI: 10.1055/s-2006-960171]
9 **Li Y**, Tang ZY, Hou JX. Hepatocellular carcinoma: insight from animal models. *Nat Rev Gastroenterol Hepatol* 2012; **9**: 32-43 [PMID: 22025031 DOI: 10.1038/nrgastro.2011.196]
10 **Bakiri L**, Wagner EF. Mouse models for liver cancer. *Mol Oncol* 2013; **7**: 206-223 [PMID: 23428636 DOI: 10.1016/j.molonc.2013.01.005]
11 **Verna L**, Whysner J, Williams GM. N-nitrosodiethylamine mechanistic data and risk assessment: bioactivation, DNA-adduct formation, mutagenicity, and tumor initiation. *Pharmacol Ther* 1996; **71**: 57-81 [PMID: 8910949]
12 **Brandon-Warner E**, Walling TL, Schrum LW, McKillop IH. Chronic ethanol feeding accelerates hepatocellular carcinoma progression in a sex-dependent manner in a mouse model of hepatocarcinogenesis. *Alcohol Clin Exp Res* 2012; **36**: 641-653 [PMID: 22017344 DOI: 10.1111/j.1530-0277.2011.01660.x]
13 **Ambade A**, Catalano D, Lim A, Kopoyan A, Shaffer SA, Mandrekar P. Inhibition of heat shock protein 90 alleviates steatosis and macrophage activation in murine alcoholic liver injury. *J*

Hepatol 2014; **61**: 903-911 [PMID: 24859453 DOI: 10.1016/j.jhep.2014.05.024]
14 **O'Shea RS**, Dasarathy S, McCullough AJ; Practice Guideline Committee of the American Association for the Study of Liver Diseases; Practice Parameters Committee of the American College of Gastroenterology. Alcoholic liver disease. *Hepatology* 2010; **51**: 307-328 [PMID: 20034030 DOI: 10.1002/hep.23258]
15 **Hritz I**, Mandrekar P, Velayudham A, Catalano D, Dolganiuc A, Kodys K, Kurt-Jones E, Szabo G. The critical role of toll-like receptor (TLR) 4 in alcoholic liver disease is independent of the common TLR adapter MyD88. *Hepatology* 2008; **48**: 1224-1231 [PMID: 18792393 DOI: 10.1002/hep.22470]
16 **Wang HJ**, Gao B, Zakhari S, Nagy LE. Inflammation in alcoholic liver disease. *Annu Rev Nutr* 2012; **32**: 343-368 [PMID: 22524187 DOI: 10.1146/annurev-nutr-072610-145138]
17 **Drinane M**, Shah VH. Alcoholic Hepatitis: Diagnosis and Prognosis. *Clinical Liver Disease* 2013; **2**: 80-83 [DOI: 10.1002/cld.164]
18 **Szabo G**. Gut-liver axis in alcoholic liver disease. *Gastroenterology* 2015; **148**: 30-36 [PMID: 25447847 DOI: 10.1053/j.gastro.2014.10.042]
19 **Thakur V**, McMullen MR, Pritchard MT, Nagy LE. Regulation of macrophage activation in alcoholic liver disease. *J Gastroenterol Hepatol* 2007; **22** Suppl 1: S53-S56 [PMID: 17567466 DOI: 10.1111/j.1440-1746.2006.04650.x]
20 **Martinez FO**, Gordon S. The M1 and M2 paradigm of macrophage activation: time for reassessment. *F1000Prime Rep* 2014; **6**: 13 [PMID: 24669294 DOI: 10.12703/P6-13]
21 **Lee J**, French B, Morgan T, French SW. The liver is populated by a broad spectrum of markers for macrophages. In alcoholic hepatitis the macrophages are M1 and M2. *Exp Mol Pathol* 2014; **96**: 118-125 [PMID: 24145004 DOI: 10.1016/j.yexmp.2013.09.004]
22 **Xu R**, Huang H, Zhang Z, Wang FS. The role of neutrophils in the development of liver diseases. *Cell Mol Immunol* 2014; **11**: 224-231 [PMID: 24633014 DOI: 10.1038/cmi.2014.2]
23 **Bertola A**, Park O, Gao B. Chronic plus binge ethanol feeding synergistically induces neutrophil infiltration and liver injury in mice: a critical role for E-selectin. *Hepatology* 2013; **58**: 1814-1823 [PMID: 23532958 DOI: 10.1002/hep.26419]
24 **Gao B**, Bataller R. Alcoholic liver disease: pathogenesis and new therapeutic targets. *Gastroenterology* 2011; **141**: 1572-1585 [PMID: 21920463 DOI: 10.1053/j.gastro.2011.09.002]
25 **Wang Y**, Liu Y, Kirpich I, Ma Z, Wang C, Zhang M, Suttles J, McClain C, Feng W. Lactobacillus rhamnosus GG reduces hepatic TNFα production and inflammation in chronic alcohol-induced liver injury. *J Nutr Biochem* 2013; **24**: 1609-1615 [PMID: 23618528 DOI: 10.1016/j.jnutbio.2013.02.001]
26 **Machida K**, Tsukamoto H, Mkrtchyan H, Duan L, Dynnyk A, Liu HM, Asahina K, Govindarajan S, Ray R, Ou JH, Seki E, Deshaies R, Miyake K, Lai MM. Toll-like receptor 4 mediates synergism between alcohol and HCV in hepatic oncogenesis involving stem cell marker Nanog. *Proc Natl Acad Sci USA* 2009; **106**: 1548-1553 [PMID: 19171902 DOI: 10.1073/pnas.0807390106]
27 **Abelev GI**, Eraiser TL. Cellular aspects of alpha-fetoprotein reexpression in tumors. *Semin Cancer Biol* 1999; **9**: 95-107 [PMID: 10202131 DOI: 10.1006/scbi.1998.0084]
28 **Apte UM**, McRee R, Ramaiah SK. Hepatocyte proliferation is the possible mechanism for the transient decrease in liver injury during steatosis stage of alcoholic liver disease. *Toxicol Pathol* 2004; **32**: 567-576 [PMID: 15603541 DOI: 10.1080/01926230490508812]
29 **Ferlay J**, Soerjomataram I, Dikshit R, Eser S, Mathers C, Rebelo M, Parkin DM, Forman D, Bray F. Cancer incidence and mortality worldwide: sources, methods and major patterns in GLOBOCAN 2012. *Int J Cancer* 2015; **136**: E359-E386 [PMID: 25220842 DOI: 10.1002/ijc.29210]
30 **Swann PF**, Coe AM, Mace R. Ethanol and dimethylnitrosamine and diethylnitrosamine metabolism and disposition in the rat. Possible relevance to the influence of ethanol on human cancer incidence. *Carcinogenesis* 1984; **5**: 1337-1343 [PMID: 6435899 DOI: 10.1093/carcin/5.10.1337]
31 **Cook RT**, Schlueter AJ, Coleman RA, Tygrett L, Ballas ZK, Jerrells TR, Nashelsky MB, Ray NB, Haugen TH, Waldschmidt TJ. Thymocytes, pre-B cells, and organ changes in a mouse model of chronic ethanol ingestion--absence of subset-specific glucocorticoid-induced immune cell loss. *Alcohol Clin Exp Res* 2007; **31**: 1746-1758 [PMID: 17681030 DOI: 10.1111/j.1530-0277.2007.00478.x]
32 **Lieber CS**, DeCarli LM. The feeding of alcohol in liquid diets: two decades of applications and 1982 update. *Alcohol Clin Exp Res* 1982; **6**: 523-531 [PMID: 6758624 DOI: 10.1111/j.1530-0277.1982.tb05017.x]
33 **Berasain C**, Castillo J, Perugorria MJ, Latasa MU, Prieto J, Avila MA. Inflammation and liver cancer: new molecular links. *Ann N Y Acad Sci* 2009; **1155**: 206-221 [PMID: 19250206 DOI: 10.1111/j.1749-6632.2009.03704.x]
34 **Donohue TM**. Alcohol-induced steatosis in liver cells. *World J Gastroenterol* 2007; **13**: 4974-4978 [PMID: 17854140 DOI: 10.3748/wjg.v13.i37.4974]
35 **Mandrekar P**, Szabo G. Signalling pathways in alcohol-induced liver inflammation. *J Hepatol* 2009; **50**: 1258-1266 [PMID: 19398236 DOI: 10.1016/j.jhep.2009.03.007]
36 **Sica A**, Mantovani A. Macrophage plasticity and polarization: in vivo veritas. *J Clin Invest* 2012; **122**: 787-795 [PMID: 22378047 DOI: 10.1172/JCI59643]
37 **Sica A**, Schioppa T, Mantovani A, Allavena P. Tumour-associated macrophages are a distinct M2 polarised population promoting tumour progression: potential targets of anti-cancer therapy. *Eur J Cancer* 2006; **42**: 717-727 [PMID: 16520032 DOI: 10.1016/j.ejca.2006.01.003]
38 **Meadows GG**, Zhang H. Effects of Alcohol on Tumor Growth, Metastasis, Immune Response, and Host Survival. *Alcohol Res* 2015; **37**: 311-322 [PMID: 26695753]
39 **Waris G**, Ahsan H. Reactive oxygen species: role in the development of cancer and various chronic conditions. *J Carcinog* 2006; **5**: 14 [PMID: 16689993 DOI: 10.1186/1477-3163-5-14]
40 **Kim WR**, Flamm SL, Di Bisceglie AM, Bodenheimer HC; Public Policy Committee of the American Association for the Study of Liver Disease. Serum activity of alanine aminotransferase (ALT) as an indicator of health and disease. *Hepatology* 2008; **47**: 1363-1370 [PMID: 18366115 DOI: 10.1002/hep.22109]
41 **Chowdhury G**, Calcutt MW, Nagy LD, Guengerich FP. Oxidation of methyl and ethyl nitrosamines by cytochrome P450 2E1 and 2B1. *Biochemistry* 2012; **51**: 9995-10007 [PMID: 23186213 DOI: 10.1021/bi301092c]
42 **Mendenhall CL**, Chedid A, French SW, Ray M, Roselle GA, Grossman CJ, Weesner RE, Gartside PS. Alpha-fetoprotein alterations in alcoholics with liver disease. V.A. Cooperative Study Groups. *Alcohol Alcohol* 1991; **26**: 527-534 [PMID: 1725107]
43 **Gowda S**, Desai PB, Hull VV, Math AA, Vernekar SN, Kulkarni SS. A review on laboratory liver function tests. *Pan Afr Med J* 2009; **3**: 17 [PMID: 21532726]
44 **Farinati F**, Marino D, De Giorgio M, Baldan A, Cantarini M, Cursaro C, Rapaccini G, Del Poggio P, Di Nolfo MA, Benvegnù L, Zoli M, Borzio F, Bernardi M, Trevisani F. Diagnostic and prognostic role of alpha-fetoprotein in hepatocellular carcinoma: both or neither? *Am J Gastroenterol* 2006; **101**: 524-532 [PMID: 16542289 DOI: 10.1111/j.1572-0241.2006.00443.x]
45 **Sell S**, Leffert HL. Liver cancer stem cells. *J Clin Oncol* 2008; **26**: 2800-2805 [PMID: 18539957 DOI: 10.1200/JCO.2007.15.5945]
46 **Itoh T**, Miyajima A. Liver regeneration by stem/progenitor cells. *Hepatology* 2014; **59**: 1617-1626 [PMID: 24115180 DOI: 10.1002/hep.26753]
47 **Miyajima A**, Tanaka M, Itoh T. Stem/progenitor cells in liver development, homeostasis, regeneration, and reprogramming. *Cell Stem Cell* 2014; **14**: 561-574 [PMID: 24792114 DOI: 10.1016/j.stem.2014.04.010]
48 **Lanthier N**, Rubbia-Brandt L, Lin-Marq N, Clément S, Frossard JL, Goossens N, Hadengue A, Spahr L. Hepatic cell proliferation plays a pivotal role in the prognosis of alcoholic hepatitis. *J Hepatol* 2015; **63**: 609-621 [PMID: 25872168 DOI: 10.1016/j.jhep.2015.04.003]

49 **Brenner DA**. Molecular pathogenesis of liver fibrosis. *Trans Am Clin Climatol Assoc* 2009; **120**: 361-368 [PMID: 19768189]
50 **Marquardt JU**, Seo D, Gómez-Quiroz LE, Uchida K, Gillen MC, Kitade M, Kaposi-Novak P, Conner EA, Factor VM, Thorgeirsson SS. Loss of c-Met accelerates development of liver fibrosis in response to CCl(4) exposure through deregulation of multiple molecular pathways. *Biochim Biophys Acta* 2012; **1822**: 942-951 [PMID: 22386877 DOI: 10.1016/j.bbadis.2012.02.012]
51 **Diehl AM**. Alcohol and liver regeneration. *Clin Liver Dis* 1998; **2**: 723-738 [DOI: 10.1016/S1089-3261(05)70038-6]

P- Reviewer: Osna NA, Takahashi T
S- Editor: Gong ZM **L- Editor**: A **E- Editor**: Liu XM

World Journal of Gastroenterology

Submit a Manuscript: http://www.wjgnet.com/esps/
Help Desk: http://www.wjgnet.com/esps/helpdesk.aspx
DOI: 10.3748/wjg.v22.i16.4109

World J Gastroenterol 2016 April 28; 22(16): 4109-4119
ISSN 1007-9327 (print) ISSN 2219-2840 (online)

ORIGINAL ARTICLE

Basic Study

Functional analysis and drug response to zinc and D-penicillamine in stable *ATP7B* mutant hepatic cell lines

Gursimran Chandhok, Judit Horvath, Annu Aggarwal, Mohit Bhatt, Andree Zibert, Hartmut HJ Schmidt

Gursimran Chandhok, Andree Zibert, Hartmut HJ Schmidt, Klinik für Transplantationsmedizin, Universitätsklinikum Münster, D-48149 Münster, Germany

Judit Horvath, Institut für Humangenetik, Westfälische Wilhelms-Universität, D-48149 Münster, Germany

Annu Aggarwal, Mohit Bhatt, Kokilaben Dhirubhai Ambani Hospital and Medical Research Institute, Mumbai 400103, India

Author contributions: Chandhok G, Aggarwal A, Bhatt M, Zibert A and Schmidt HHJ designed the experiments; Chandhok G and Horvath J performed the experiments; Chandhok G interpreted the data and performed statistical analysis; Chandhok G, Zibert A and Schmidt HHJ wrote the manuscript; all authors read and approved the final manuscript.

Conflict-of-interest statement: The authors declare no conflict of interest associated with this manuscript.

Data sharing statement: No additional data are available.

Correspondence to: Hartmut HJ Schmidt, MD, Professor, Klinik für Transplantationsmedizin, Universitätsklinikum Münster, Albert-Schweitzer-Campus 1, Gebäude A14, D-48149 Münster, Germany. hepar@ukmuenster.de
Telephone: +49-251-8357935
Fax: +49-251-8357771

Received: December 5, 2015
Peer-review started: December 7, 2015
First decision: January 13, 2016
Revised: January 24, 2016
Accepted: February 20, 2016

Article in press: February 22, 2016
Published online: April 28, 2016

Abstract

AIM: To study the effect of anti-copper treatment for survival of hepatic cells expressing different *ATP7B* mutations in cell culture.

METHODS: The most common Wilson disease (WD) mutations p.H1069Q, p.R778L and p.C271*, found in the *ATP7B* gene encoding a liver copper transporter, were studied. The mutations represent major genotypes of the United States and Europe, China, and India, respectively. A human hepatoma cell line previously established to carry a knockout of *ATP7B* was used to stably express WD mutants. mRNA and protein expression of mutant *ATP7B*, survival of cells, apoptosis, and protein trafficking were determined.

RESULTS: Low temperature increased ATP7B protein expression in several mutants. Intracellular ATP7B localization was significantly impaired in the mutants. Mutants were classified as high, moderate, and no survival based on their viability on exposure to toxic copper. Survival of mutant p.H1069Q and to a lesser extent p.C271* improved by D-penicillamine (DPA) treatment, while mutant p.R778L showed a pronounced response to zinc (Zn) treatment. Overall, DPA treatment resulted in higher cell survival as compared to Zn treatment; however, only combined Zn + DPA treatment fully restored cell viability.

CONCLUSION: The data indicate that the basic impact of a genotype might be characterized by analysis of mutant hepatic cell lines.

Key words: ATP7B; D-penicillamine; Zinc; Mutations; Wilson disease; Therapy

Core tip: Copper overload in Wilson disease (WD) is treated with anti-copper therapy. However, the effect of treatment has not been studied using human hepatic cells lacking the *ATP7B* copper transporter. Using a previously established *ATP7B* KO cell line, we generated stable mutant cell lines to study functional analysis and response to zinc (Zn) and D-penicillamine (DPA). All mutants showed individual response rates following copper and anti-copper treatment. Highest rescue from copper toxicity was observed after combined Zn and DPA treatment. The study provides novel insights into genotype-phenotype correlations and genotype-specific treatment of WD.

Chandhok G, Horvath J, Aggarwal A, Bhatt M, Zibert A, Schmidt HHJ. Functional analysis and drug response to zinc and D-penicillamine in stable *ATP7B* mutant hepatic cell lines. *World J Gastroenterol* 2016; 22(16): 4109-4119 Available from: URL: http://www.wjgnet.com/1007-9327/full/v22/i16/4109.htm DOI: http://dx.doi.org/10.3748/wjg.v22.i16.4109

INTRODUCTION

Wilson disease (WD; MIM No. 277900) is an autosomal recessive disorder resulting from mutation of the *ATP7B* gene[1]. More than 600 mutations of *ATP7B* are known (www.hgmd.org). Due to improved genetic diagnosis, novel mutations are being found around the world. The WD gene consists of 21 exons that span a genomic region of about 80 kb and is located on the long arm of chromosome 13 (13q14.1)[2,3]. *ATP7B* encodes a large membrane protein of 1465 amino acids that was characterized to be a copper (Cu) transporting P-type adenosine triphosphatase (ATPase) which has high homology to the amino acid sequence of the gene responsible for Menkes disease (MIM No. 300011). Apart from involvement of *ATP7B* in causing rare inherited disease, its role in Cu homeostasis is central to the function of important biochemical pathways[4]. Of note, anti-copper therapy effective for treatment of WD patients was recently recognized to represent an alternative for the treatment of other diseases[5,6]. The effect of anti-copper treatment for hepatocytes, the major target cell of the disease, and the correlation to individual WD genotypes have yet to be determined.

ATP7B is mainly expressed in the liver and to a lesser extent in the brain and other organs. *ATP7B* has two functions in the liver which are central for Cu homeostasis[4,7]. ATP7B protein transports Cu into the trans Golgi network (TGN) where the metal is transferred to apoceruloplasmin that is finally released as ceruloplasmin into the blood. Excess Cu is sequestered by ATP7B into vesicles that are subsequently released from the body *via* bile canaliculi. ATP7B protein normally resides in the TGN but is believed to traffic to the endocytic vesicles under high Cu conditions for biliary Cu excretion. Impaired ATP7B function due to mutations in the *ATP7B* gene results in toxic Cu accumulation, ultimately leading to cell death.

Hallmarks of WD include Cu accumulation in the liver and the brain, a low ceruloplasmin activity, and the presence of Kayser-Fleischer (KF) corneal rings[1]. Diagnosis is difficult since individual abnormalities could be absent or at borderline. A wide spectrum of clinical presentations is observed, including liver damage and/or neurological symptoms, ranging from asymptomatic phenotypes which show only mild abnormalities of Cu homeostasis, to patients having liver cirrhosis, acute liver failure, or severe neurological disability. Onset of disease is also highly variable and is often observed at childhood but also in adolescence and even in late adults[8]. Unrelated proteins that mediate uptake, delivery, and efflux of Cu have been implicated to modify disease; however, an understanding of the molecular mechanisms that are involved in the complex, highly variable phenotype, including the toxic events observed in hepatocytes, is far from being achieved.

The type and location of *ATP7B* mutation has been suggested to be one determinant of the disease phenotype indicating that individual mutations of *ATP7B* may be linked to a phenotype. However, prognosis of the disease related to a specific WD mutation expressed in patients has not been established. Therefore, there is a pressing need for an optimal treatment regimen of unknown genotypes in various regions, including China where novel genotypes have increasingly been identified[9-12]. The majority of WD mutations are missense but deletions and insertions are also observed. Since most WD patients carry compound heterozygous *ATP7B* mutations that may modulate the phenotypic expression of an individual mutation, the analysis of homozygous mutations has helped to explore links of *ATP7B* genotype and phenotype, *e.g.*, in studies of large families in specific regions[13,14]. Recently, functional characterization of individual ATP7B mutations expressed in various cell lines was suggested to improve the understanding of the clinical impact of a given mutation[15-17].

WD is a fatal disease when not appropriately treated by anti-coppering drugs and can lead to early death. The two most commonly used drugs for therapy of WD are D-penicillamine (DPA) and zinc (Zn) that involve de-coppering by chelation or metallothionein induction, respectively[18]. Both lines of drugs are associated with side effects and the correct choice of treatment, including the survival of hepatocytes, is still under debate. In a significant portion of patients with WD, treatment is not effective leading to discontinuation of therapy[18]. Chelation therapy seems to be most beneficial in European WD patients, whereas Chinese patient benefit most from Zn treat-

ment[19-21]. Whether poor response to therapy may relate to the genotype is not known, since a standard therapy regimen for WD has not been established.

We addressed the functional characterization of *ATP7B* mutations following anti-copper treatment in a novel hepatic *ATP7B* knockout (KO) cell line that was previously established by us[22]. The effect of Cu on intracellular trafficking, viability, and apoptosis was studied.

MATERIALS AND METHODS

Cell culture

HepG2 (human hepatocellular carcinoma) cells purchased from American Type Culture Collection (ATCC) and derivatives of *ATP7B* knockout cells[22] were cultured in RPMI media (Lonza) containing 10% fetal bovine serum (FBS) and supplemented with 100 U/mL penicillin/streptomycin (PAA). Cell lines were maintained in 5% CO_2 at 37 ℃ in a humidified chamber.

Site-Directed Mutagenesis and generation of stable ATP7B mutant cell lines

Wild type *ATP7B* cDNA was cloned into pGCsamENATP7B retroviral vector encoding blasticidin resistance[23]. Site-directed mutagenesis was performed using QuikChange II XL Site-Directed Mutagenesis Kit (Agilent Technologies) according to the manufacturer's instructions. Mutagenized cDNA was sequenced to confirm the presence of the selected variant and exclude secondary mutations. KO cells were transduced with the plasmid containing the WD mutation. KO cells harbouring wild type *ATP7B* plasmid were used as a control. Cells were selected in media containing 6 μg/mL blasticidin (Invitrogen).

Confocal staining

Cell lines were grown on cover slips coated with 0.1% gelatin to about 80% confluency. For studying Cu induced trafficking under low and high Cu conditions, cells were either maintained in RPMI basal cell culture media or treated by addition of 100 μmol/L Cu for 3 h. Cells were then washed with PBS, fixed using 4% paraformaldehyde (Electron Microscopy Sciences) and permeabilized with 0.25% triton X-100 (Sigma). Cells were blocked for 30 min with 3% bovine serum albumin (Sigma), followed by staining with primary anti-ATP7B (kind gift of Dr. I. Sandoval, Madrid, Spain) and anti-lamp2 (Santa Cruz Biotechnology, sc-18822) antibodies. Secondary antibody incubation was done using goat anti-rabbit 594 and goat anti-mouse 488 (Life technologies, A-11012 and A-11001, respectively) for 45 min. Confocal images were recorded with a Nikon A1 confocal laser scanning microscope and an ECLIPSE Ti with a CFI Plan Fluor 40 × (NA 1.3 oil) lens (Nikon, Japan). The images were analyzed using NIS-elements software.

Western blot analysis

Western blot was performed as described previously[22]. Briefly, cells were lysed in RIPA buffer containing 60 mmol/L Tris-HCl, 150 mmol/L NaCl, 2% Na-deoxycholate, 2% triton X-100, 0.2% SDS and 15 mmol/L EDTA supplemented with protease inhibitors (Roche, Complete Mini, EDTA-free). Protein concentration was determined by Bradford assay (Bio-Rad, Protein Assay). 10 μg of protein was loaded onto a 9% SDS gel and blotting was performed using a 0.45 μmol/L nitrocellulose membrane (GE Healthcare). Polyclonal anti-rabbit ATP7B antibody was used for protein detection. HSC70 (Santa Cruz Biotechnology, sc-1059) staining was used as a protein loading control. Densitometric analysis was performed using ImageJ 1.46 software (http://imagej.nih.gov/ij/docs/guide/). Relative expression was normalized to KO cells expressing wild type *ATP7B*.

MTT assay

10^4 cells were seeded in triplicates in a 96 well plate and cultivated overnight in 100 μL RPMI media lacking phenol red (PAA). Cells were then exposed to different Cu concentrations ($CuCl_2$; Sigma Aldrich). After 48 h, viability was determined by MTT assay as previously described[22]. For testing drug efficacy, cells were preincubated with 200 μmol/L Zn ($ZnCl_2$; AppliChem) for 2 h[24] and washed twice with phosphate buffered saline (PBS, PAA) prior to Cu addition. D-penicillamine (Dako) was added at 6.25 mmol/L simultaneously with Cu. Cells were incubated for 48 h. Cell rescue was determined as percentage of treated, viable compared to untreated cells.

Determination of apoptosis

10^6 cells were incubated with 100 μmol/L Cu at 37 ℃ for 24 h. Supernatants and cells were collected and subjected to Annexin-V and propidium iodide staining (Roche Annexin-V-FLUOS kit) and analyzed using flow cytometry (Epics XL.MCL, Beckman Coulter).

Real-time PCR analysis

PCR analysis was performed as described previously[25]. Briefly, isolation of total RNA was performed by RNeasy kit (Qiagen). 1 μg of RNA was transcribed using SuperScript II (Invitrogen) according to the instructions of the manufacturer. For quantitative real time PCR (qPCR) the RT product was incubated with SYBR Green PCR Core Plus (Eurogentec, Belgium) and 150 nmol/L of primers. PCR was analyzed on the ABI Prism 7900 HT Sequence Detection System (PE Applied Biosystems). Each sample was tested in three independent experiments. Ct values were normalized to the expression of the house-keeping GAPDH gene ($^{\Delta\Delta}$ct method).

Statistical analysis

Statistical analysis was performed by Kruskal-Wallis

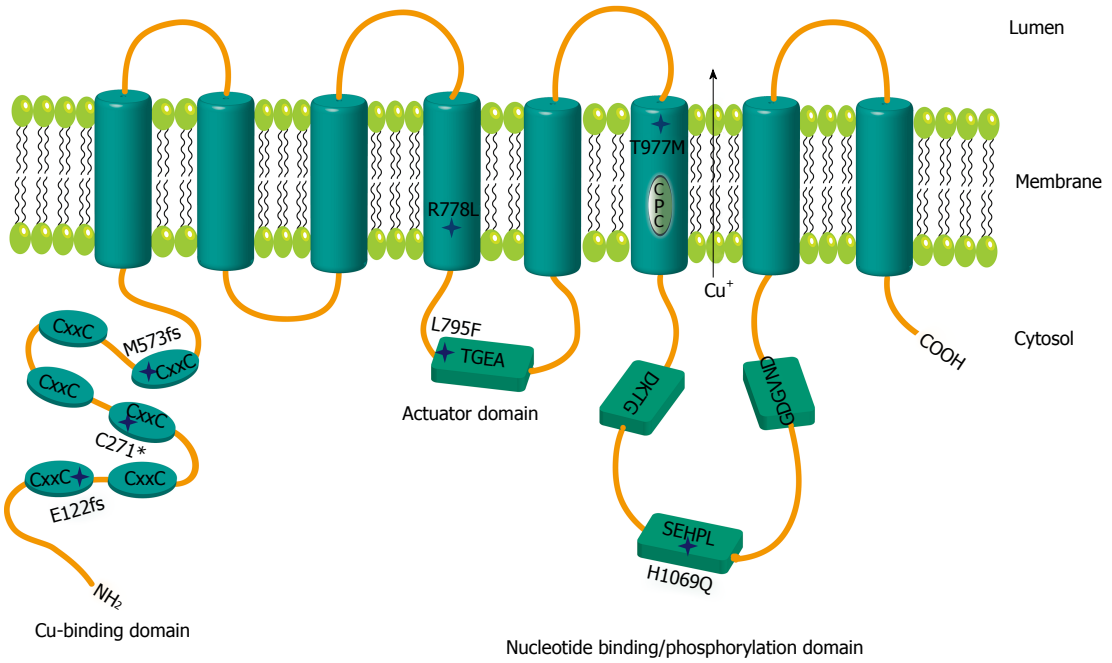

Figure 1 Schematic representation of mutations within ATP7B. Relative positions of the mutations are shown by stars. The six metal binding domains at the N terminal are indicated by CxxC. Sequence motifs TGEA, DKTG, SEHPL, GDGVND, and CPC depict conserved elements of copper (Cu) ATPases.

one-way ANOVA and Student's *t*-test using SPSS 22.0 software. Data are given as mean ± SE.

RESULTS

Establishment of hepatic cells expressing ATP7B mutations

In order to analyze the impact of various WD mutants for survival of hepatic cells, we generated stable cell lines in an *ATP7B* knockout (KO) human hepatoma cell line[22]. The three major *ATP7B* mutations reported from WD patients around the world (p.H1069Q, p.R778L and p.C271*) were chosen for this study (Supplementary Table 1)[26-30]. In addition, mutations from a recently identified cohort of Western India (p.L795F, p.T977M, p.M573fs, and p.E122fs) were also included[26]. The selected four missense and three mutations encoding incomplete reading frames are located throughout different functional domains of ATP7B (Figure 1). The presence of the desired mutations and the absence of any other aberration within *ATP7B* were confirmed in the cell lines by sequencing of chromosomal DNA (data not shown). In order to characterize *ATP7B* mRNA expression of the cell lines, real time PCR analysis was performed indicating that expression was in the same range as compared to KO cells expressing wild type *ATP7B* (KO.wt) (Figure 2A). To explore the stability of ATP7B protein expression in different mutants, Western blot analysis of the cell lines was performed. Cells were either maintained at 37 ℃ or at 30 ℃ prior to Western blot analysis to determine unstable ATP7B expression that is known to be augmented by lower temperature[31]. At 37 ℃, only mutant cell line KO.L795F showed ATP7B expression levels similar to KO.wt cells (Figure 2B). Cell lines KO.H1069Q and KO.T977M showed a lower ATP7B protein expression. Lowest ATP7B expression was observed for cell line KO.R778L. Cell lines KO.M573fs, KO.C271* and KO.E122fs that have abrogated reading frames showed no detectableATP7B protein. Incubation of cells at 30 ℃ prominently increased protein expression in cell lines KO.L795F, KO.H1069Q and KO.T977M (Figure 2C). Relative increase of protein expression was highest for cell line KO.R778L, although overall expression was still low (Supplementary Table 2).

ATP7B trafficking in hepatic mutant cell lines

Trafficking of ATP7B from TGN to vesicular compartments upon exposure of cells to high Cu levels has been reported[31]. We addressed whether trafficking of ATP7B in response to elevated Cu is impaired in the mutant hepatic cells[32]. Subcellular trafficking of ATP7B was determined under two different Cu conditions (Figure 3) using lamp2, a late endosome-lysosome marker[33,34]. First we established that trafficking of exogenous ATP7B in KO.wt was similar to HepG2 cells (Supplementary Figure 1). Using low Cu conditions, KO.wt cells showed a perinuclear localization of ATP7B. Upon exposure of cells to 0.1 mmol/L Cu, KO.wt cells displayed a dispersed punctate staining pattern of ATP7B distant from the perinuclear region towards the cytosolic vesicular compartment. Co-localization of ATP7B with lamp2 was predominantly observed in KO.wt cells under high Cu conditions. A similar staining pattern was observed with HepG2 cells (data not shown).

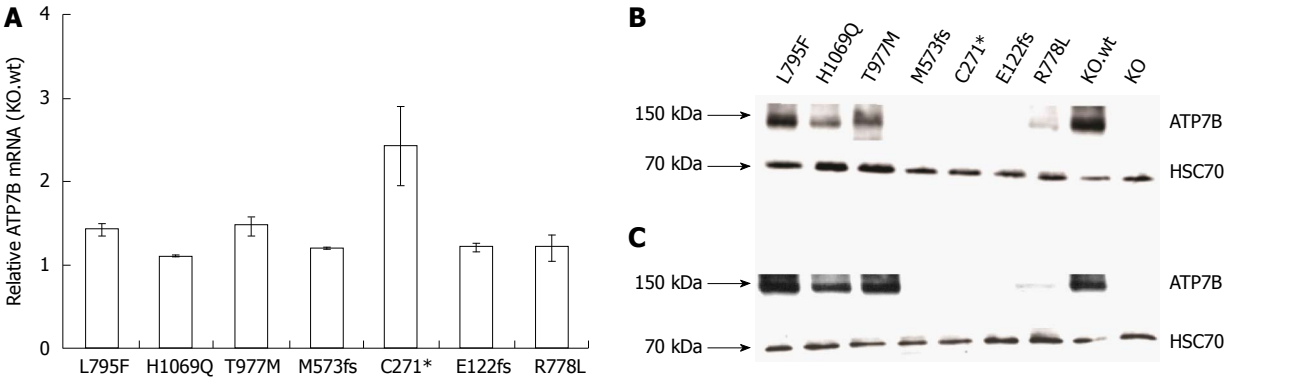

Figure 2 ATP7B mRNA and protein expression in mutant cell lines. A: Relative ATP7B mRNA expression in mutant cell lines was determined. The expression was normalized to GAPDH housekeeping gene. Gene expression as factor fold change relative to KO cells expressing wild type was calculated; B and C: Representative Western blots showing ATP7B protein at 37 ℃ and 30 ℃, respectively.

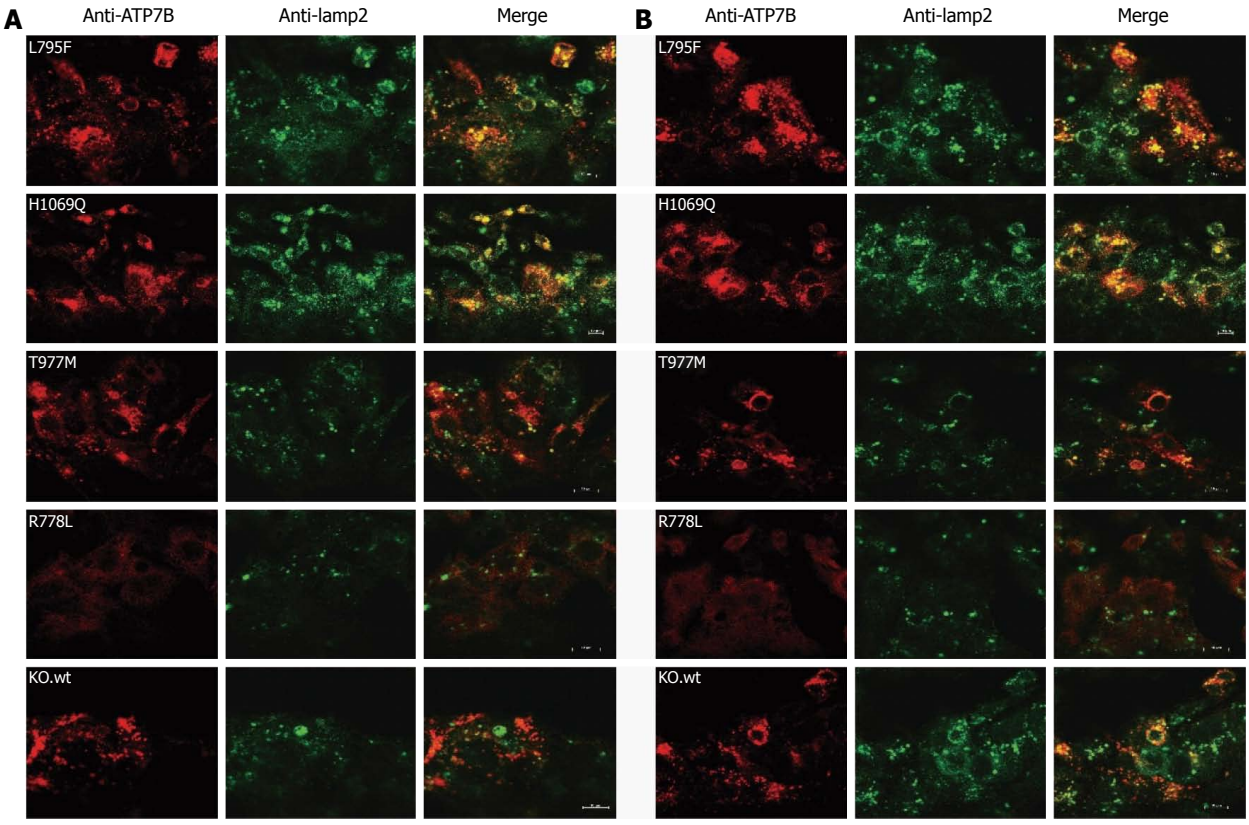

Figure 3 Localization of ATP7B mutant protein in stably transfected KO cells. Co-localization studies were performed with lamp2 at low copper (Cu) (A) and in the presence of 100 μmol/L Cu (B). Bars represent 10 μm. A representative photograph is shown for each mutant cell line.

In cell line KO.L795F ATP7B staining was found to be dispersed in the cytoplasm under both low and high Cu conditions, although a higher co-localization with lamp2 was observed at high Cu. As compared to KO.wt cells, no co-localization with vesicle-like structures was seen in cell line KO.L795F. ATP7B staining pattern of cell line KO.H1069Q was partially dispersed. A high overlap with lamp2 was observed. Only minor differences as compared to low Cu were observed upon exposure to high Cu. Cell line KO.T977M showed a perinuclear staining pattern of ATP7B at low Cu. Under high Cu conditions, ATP7B was somewhat dispersed with only a slight overlap with lamp2. Cell line KO.R778L showed a diffuse staining pattern suggesting an extensively mislocalized ATP7B dispersed throughout the cell. No co-localization of ATP7B was observed with lamp2 in cell line KO.R778L. The cell lines KO.M573fs, KO.C271*, KO.E122fs and KO did not show any ATP7B-specific staining (data not shown).

Viability of hepatic mutant cell lines following copper exposure

Since most ATP7B mutant cell lines showed defects in trafficking, we further assessed whether expression

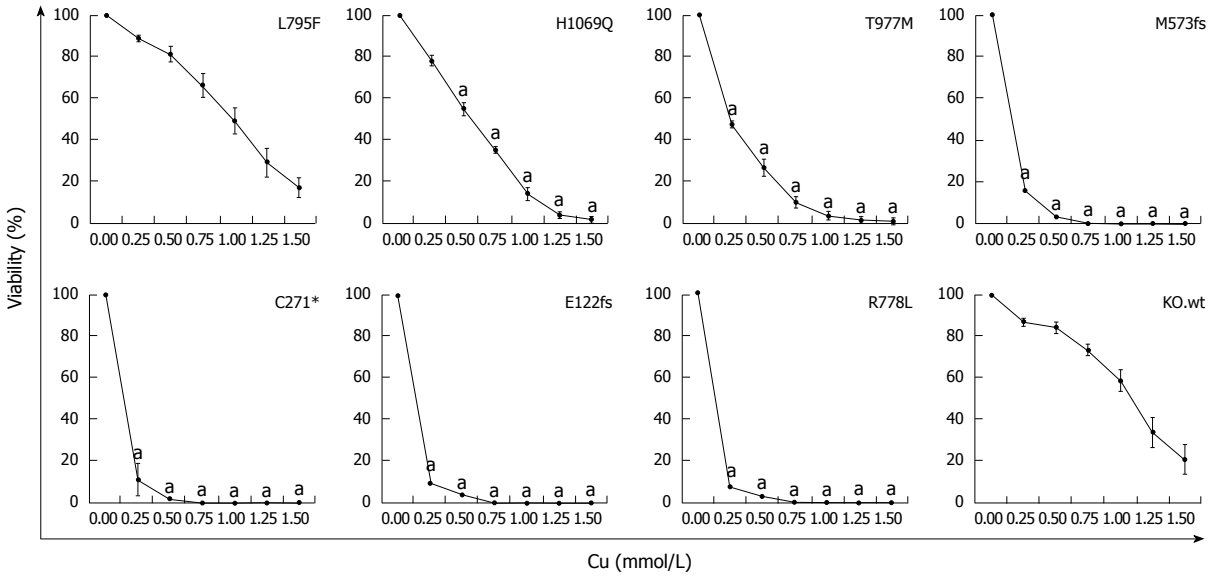

Figure 4 Survival of *ATP7B* mutant cell lines after copper exposure. Cell survival of ATP7B mutant cell lines relative to control (no copper) was determined by MTT assay after 48 h copper (Cu) exposure. Data is represented as mean ± SE of at least three independent experiments. Significance ($^{a}P < 0.05$) as compared to KO.wt.

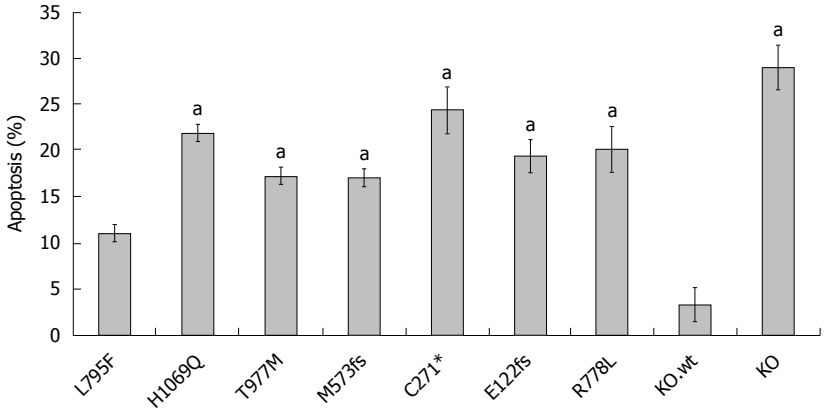

Figure 5 Rate of apoptosis in *ATP7B* mutant cell lines after copper exposure. Cells were exposed to 100 μmol/L Cu for 24 h. Induction of apoptosis was determined by Annexin-V staining followed by flow cytometry analysis. Data is represented as mean ± SE of at least three independent experiments. $^{a}P < 0.05$ *vs* KO cells expressing wild type *ATP7B*.

of ATP7B mutations can lead to escape of cells from toxic Cu. The viability of the cell lines at various Cu concentrations was determined (Figure 4). Cell line KO.L795F showed high viability at 0.25 mmol/L Cu (89.0% ± 1%) which slowly decreased to 16.9% ± 5% at 1.5 mmol/L Cu concentration. Cell lines KO.H1069Q and KO.T977M displayed lower levels of Cu resistance with a viability of 78.2% ± 3% and 47.3% ± 2%, respectively at 0.25 mmol/L Cu. Viability significantly dropped in these mutants below 2.0% ± 1% at highest Cu concentration. In contrast, the three mutant cell lines encoding incomplete reading frames and KO.R778L showed Cu resistance similar to KO cells[22] with values below 16.2% ± 5% at 0.25 mmol/L Cu that further dropped to almost 0.0% at higher Cu concentrations. Values calculated for IC50 (Supplementary Table 2) suggested that only cell lines KO.L795F, KO.H1069Q and KO.T977M displayed significant survival after toxic Cu exposure.

Induction of apoptosis

Cu is also known as an inducer of apoptosis[35]. Having shown that WD mutations affect cell survival, we assessed induction of apoptosis following Cu exposure (Figure 5). Experiments were carried out at 0.1 mmol/L Cu since significant necrosis was observed at higher Cu concentrations (data not shown). KO.wt and HepG2 cells showed similar rates of apoptosis (Supplementary Figure 2). Induction of apoptosis was low (11.1% ± 1%) for cell line KO.L795F underscoring that cell line KO.L795F can resist high concentrations of Cu as shown above. All other cell lines displayed higher rates of apoptosis (range 17.1% ± 1% to 24.4% ± 3%) suggesting that although cell lines KO.H1069Q and

KO.T977M can escape high Cu, significant levels of apoptosis are induced by Cu.

Zinc and DPA treatment of mutant cell lines

We addressed whether the individual rates of survival and apoptosis observed in the ATP7B mutant cell lines may also have an impact on the response to Zn and DPA treatment. In order to determine the treatment response for different ATP7B mutants, KO mutant cell lines were exposed to Zn, DPA and Zn + DPA at different Cu concentrations (Figure 6). Upon treatment, all mutant cell lines showed a significant higher survival at Cu concentrations $\geqslant$ 0.25 mmol/L (mean 55.1% ± 3%; median 63.1%) as compared to untreated control (mean 18.1% ± 4%; median 3.6 %) indicating that all three treatments are highly efficient. Overall, Zn treatment alone was less effective (mean 35.6% ± 5%) and significantly outperformed by DPA treatment (mean 57.8% ± 5 %). Combined treatment Zn + DPA resulted in highest cell survival (mean 69.7% ± 2 %) suggesting a synergistic effect of both modalities as compared to single treatments as shown before for KO cells[22].

Some of the mutations showed unique response rates to the treatments. Relative increase of viability by Zn treatment (gain) was highest for mutant cell line KO.R778L (mean 26.9% ± 8%). Following DPA treatment, only cell lines KO.L795F and KO.H1069Q showed full restoration of viability as compared to KO.wt cells. Relative increase of viability by DPA treatment was mostly gradual ($\leqslant$ 1.0 mmol/L Cu) for cell lines KO.L795F and KO.H1069Q whereas most of the other mutant cell lines, in particular KO.M573fs, showed a plateau of high values (> 65%) at Cu concentrations of 0.5-1.0 mmol/L Cu. Relative increase of viability by combination as compared to DPA treatment was highest in cell line KO.C271* (mean 57.8% ± 6% and 29.2% ± 11%, respectively).

DISCUSSION

Our results indicate that the analysis of hepatic cell lines resulted in a functional classification of WD mutations. Mutant cell lines showed different degrees of cell survival and characteristic responses upon treatment with Zn and DPA. The findings provide first *in vitro* evidence that survival of hepatic cells following anti-copper treatment may depend on the *ATP7B* mutation, an observation that may further lead to a better prognosis of unknown WD mutants and improved knowledge on WD genotype to phenotype associations.

HepG2 cells are widely used for analysis of Cu toxicity and apoptosis[36,37]. By using *ATP7B* KO cells derived from HepG2[22], we assessed viability of hepatic cells without interference by intrinsic *ATP7B* or impairment by hybrid protein sequences[31,37] reflecting a situation close to human WD hepatocytes. Mutant p.H1069Q was observed in this study to have a moderately reduced impact on cell survival underlining previous results obtained in other systems[17,37]. Localisation of protein p.H1069Q was reported to be close to the ER[17,31,37]. The observed stabilization of p.H1069Q protein expression in hepatic cells by low temperature confirmed previous results obtained in human kidney cells[31] suggesting that improper folding of the mutant protein is not cell type specific. Mutant p.R778L did not show detectable levels of cell survival in contrast to the other missense mutants underscoring that it may be difficult to predict activity from sequence analysis alone. ATP7B expression and improvement of survival were not detected for the three mutations encoding incomplete reading frames underlining previous observations[16,17,38].

Based on cell survival, WD mutants could be classified into groups having high (p.L795F, p.H1069Q), moderate (p.T977M), and no survival (p.M573fs, p.C271*, p.E122fs and p.R778L). Homozygous mutation p.L795F was associated in WD patients from India with late onset and neurological disease[26]. For mutation p.H1069Q an association with late and neurological presentation has been observed[8,30,39,40]. A high cell survival may thus be associated to a relatively late, predominantly neurologic phenotype, possibly due to the almost wild type activity of *ATP7B* that can prevent severe disease, at least in the early years. Of note, in two patients having compound heterozygous mutation p.L795F together with frameshift mutation p.M769fs, late onset of disease was significantly reduced[26] suggesting that one allele of mutation p.L795F is sufficient to prevent early onset of disease when combined with a putative non-functional mutation. Homozygous mutation p.T977M was observed in Indian WD patients who had an early onset of disease (around year 4) predominantly affecting liver and resulting in moderate neurological impairment[26]. In European WD patients, mutation p.T977M was however relatively mild[41]. On the other hand, *ATP7B* frameshift and nonsense mutations have been implicated to result in early onset and a more severe manifestation of WD[42-44]. The phenotypes that were associated with homozygous mutations p.M573fs, p.C271* and p.E122fs are mostly severe including high disease burden and relatively early onset of diseases, at least for p.M573fs and p.C271* (around years 7-10). Overall disease burden according to the Tier 1 score[26] was highest for mutation p.E122fs within this group, except that osseomuscular disease was completely missing in patients having this mutation. Mutation p.R778L has a high frequency in WD patients from Asia, especially in China, Japan, South Korea and was associated with severe hepatic disease and with a relatively early onset (about 10 years)[9,45-49], however, a later onset of disease mostly associated with cerebral symptoms was noted in a different cohort[50]. In addition to the common genotypes, there are an increasing number of novel genotypes identified, especially in China, which may benefit from genotype-

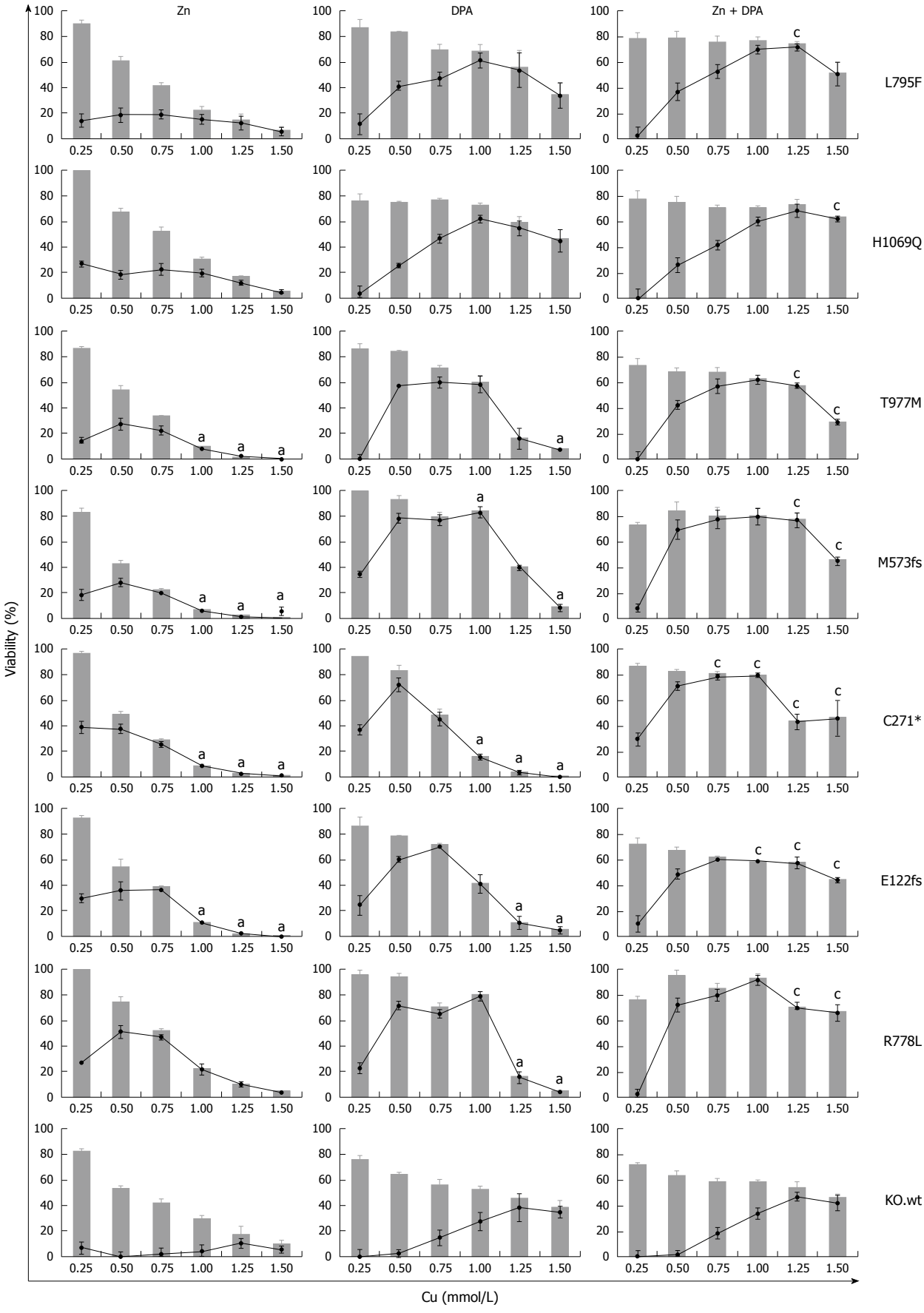

Figure 6 Survival of *ATP7B* mutant cell lines after zinc and D-penicillamine treatment. Cells were treated with zinc (Zn), D-penicillamine (DPA), and Zn + DPA followed by determination of viability at 48 h. Bar graphs indicate cell viability after treatment relative to untreated cells [0 mmol/L copper (Cu)]. Relative increase of viability by individual treatment (gain) is indicated by line graph. Data is represented as mean ± SE of at least three independent experiments. Viability of KO cells expressing *ATP7B* wild type is shown as control. [a]$P < 0.05$ *vs* KO.wt cells, [c]$P < 0.05$ *vs* DPA treatment.

specific therapy approaches[10,12].

Zn and DPA are effective treatments for WD[51,52] and are implemented in current guidelines for treatment. While DPA is reducing overall Cu load in the body due to chelation, the first line defence of Zn is thought to take place in the intestine where Cu is expelled *via* metallothionein. The mechanism of both drugs at the level of the hepatocyte has been explored[24,53], however, to the best of our knowledge this is the first study on Zn and DPA in human hepatic cells expressing mutant *ATP7B*. The results indicate that the survival of hepatic cells following treatment might depend on the genotype of *ATP7B*. With the exception of mutant p.R778L, efficacy of Zn treatment for hepatic cells is mostly confined to low Cu concentrations. Previous data indicate that metallothionein is induced in hepatic cells even when *ATP7B* is absent[22] suggesting that high metallothionein expression is insufficient for rescue of cells.

Our study indicates as shown before for KO cells[22] that combined treatment by Zn and DPA resulted in the highest survival of hepatic cells suggesting that a synergism by both drugs is needed to resist maximal liver Cu concentrations that can be up to 3 mg/g dry weight[1]. While our own experience with combined treatment is limited to small WD patient cohorts and standardized treatment regimen has not been established, a possible translation of our results awaits further *in vivo* studies and regimens that minimize interference of both drugs[18,51,54]. Notably, in support of our *in vitro* findings WD patients having mutation p.R778L were observed to benefit largely from Zn monotherapy corroborating the importance of Zn treatment in different Asian countries, including China[20,21,55]. In addition, our finding of a general reduced hepatic cell survival after Zn treatment as compared to DPA is corroborated by clinical findings from large WD cohorts[19,52] and also from Indian patients (AA, MB, unpublished data). Apart from the WD genotype, many variables are likely to contribute to the phenotype and drug response, including the genetic background in different populations, diet, type of disease manifestation, and local preferences of anti-Cu treatment regimens. In addition, combination of the two drugs *in vitro* and *in vivo* may act by different mechanism. Given the limitations of our *in vitro* study, functional characterization of cells following Cu exposure and Zn/DPA treatment may however indicate the basic impact of a given WD genotype.

ACKNOWLEDGMENTS

We thank Oksana Nadzemova for technical support and Alexander Zibert for mathematical analysis.

COMMENTS

Background

Wilson disease (WD) is a rare autosomal recessive disorder of Cu accumulation, especially in the liver and brain, where Cu toxicity results in a varying presentation of liver disease, neurological, and psychiatric conditions. Lifelong treatment currently involves Cu chelating compounds and zinc salts. A standard anti-Cu treatment has not been established for therapy of WD. The rarity of disease and the high number of compound heterozygote mutations aggravate genotype to phenotype correlations.

Research frontiers

Specific *ATP7B* mutations are often found to be concentrated in certain geographical populations. Over 600 different mutations of *ATP7B* have so far been identified, and it is thought - although not proven - that the range of symptoms presented by individual WD patients and the response to therapy has partly a genetic basis.

Innovations and breakthroughs

Previous work allowed the functional characterization of WD genotypes in different *in vitro* cellular systems. In this report, using human hepatic cells that have no intrinsic *ATP7B* expression, the impact of the WD genotype with regard to treatment by standard anti-Cu drugs was addressed. Unique insights into the genotype-phenotype correlations of the most prominent WD mutations that refer to more than 50% of patients in some regions of the world are presented.

Applications

Findings on a WD genotype-specific response of hepatic cells to anti-Cu treatment are important to stimulate further clinical and molecular studies to assess genotype to phenotype correlations, genotype-specific treatment regimens, and the prognosis of novel genotypes.

Terminology

ATP7B mutations have been studied in various mammalian tissue culture cells, however, intrinsic *ATP7B* expression or non-hepatic cells have blurred a direct correlation of the results. The study of primary hepatocytes from WD patients is difficult, since such cells cannot be propagated in tissue culture. Hepatic cells expressing homozygote WD mutations may represent a novel platform to study the impact of individual mutants.

Peer-review

Interesting paper with the novel idea how to learn more about genotype/phenotype correlations and potential genotype influence on reaction to therapy in WD. Presented results provide for a first time that the response of hepatic cells depends on the WD mutation, most interesting after treatment with penicillamine and zinc.

REFERENCES

1 **Ala A**, Walker AP, Ashkan K, Dooley JS, Schilsky ML. Wilson's disease. *Lancet* 2007; **369**: 397-408 [PMID: 17276780 DOI: 10.1016/s0140-6736(07)60196-2]

2 **Bull PC**, Thomas GR, Rommens JM, Forbes JR, Cox DW. The Wilson disease gene is a putative copper transporting P-type ATPase similar to the Menkes gene. *Nat Genet* 1993; **5**: 327-337 [PMID: 8298639 DOI: 10.1038/ng1293-327]

3 **Tanzi RE**, Petrukhin K, Chernov I, Pellequer JL, Wasco W, Ross B, Romano DM, Parano E, Pavone L, Brzustowicz LM. The Wilson disease gene is a copper transporting ATPase with homology to the Menkes disease gene. *Nat Genet* 1993; **5**: 344-350 [PMID: 8298641 DOI: 10.1038/ng1293-344]

4 **Lutsenko S**, Barnes NL, Bartee MY, Dmitriev OY. Function and regulation of human copper-transporting ATPases. *Physiol Rev* 2007; **87**: 1011-1046 [PMID: 17615395 DOI: 10.1152/physrev.00004.2006]

5 **Brady DC**, Crowe MS, Turski ML, Hobbs GA, Yao X, Chaikuad A, Knapp S, Xiao K, Campbell SL, Thiele DJ, Counter CM. Copper is required for oncogenic BRAF signalling and tumorigenesis. *Nature* 2014; **509**: 492-496 [PMID: 24717435 DOI: 10.1038/nature13180]

6 **Martinelli D**, Travaglini L, Drouin CA, Ceballos-Picot I, Rizza T, Bertini E, Carrozzo R, Petrini S, de Lonlay P, El Hachem M, Hubert

L, Montpetit A, Torre G, Dionisi-Vici C. MEDNIK syndrome: a novel defect of copper metabolism treatable by zinc acetate therapy. *Brain* 2013; **136**: 872-881 [PMID: 23423674 DOI: 10.1093/brain/awt012]

7 **Wu F**, Wang J, Pu C, Qiao L, Jiang C. Wilson's disease: a comprehensive review of the molecular mechanisms. *Int J Mol Sci* 2015; **16**: 6419-6431 [PMID: 25803104 DOI: 10.3390/ijms16036419]

8 **Ferenci P**, Członkowska A, Merle U, Ferenc S, Gromadzka G, Yurdaydin C, Vogel W, Bruha R, Schmidt HT, Stremmel W. Late-onset Wilson's disease. *Gastroenterology* 2007; **132**: 1294-1298 [PMID: 17433323 DOI: 10.1053/j.gastro.2007.02.057]

9 **Liu Y**, Zhou H, Guo H, Bai Y. Genetic and Clinical Analysis in a Cohort of Patients with Wilson's Disease in Southwestern China. *Arch Med Res* 2015; **46**: 164-169 [PMID: 25704634 DOI: 10.1016/j.arcmed.2015.02.001]

10 **Li XH**, Lu Y, Ling Y, Fu QC, Xu J, Zang GQ, Zhou F, De-Min Y, Han Y, Zhang DH, Gong QM, Lu ZM, Kong XF, Wang JS, Zhang XX. Clinical and molecular characterization of Wilson's disease in China: identification of 14 novel mutations. *BMC Med Genet* 2011; **12**: 6 [PMID: 21219664 DOI: 10.1186/1471-2350-12-6]

11 **Li K**, Zhang WM, Lin S, Wen L, Wang ZF, Xie D, Wei M, Qiu ZQ, Dai Y, Lin MC, Kung HF, Yao FX. Mutational analysis of ATP7B in north Chinese patients with Wilson disease. *J Hum Genet* 2013; **58**: 67-72 [PMID: 23235335 DOI: 10.1038/jhg.2012.134]

12 **Wang LH**, Huang YQ, Shang X, Su QX, Xiong F, Yu QY, Lin HP, Wei ZS, Hong MF, Xu XM. Mutation analysis of 73 southern Chinese Wilson's disease patients: identification of 10 novel mutations and its clinical correlation. *J Hum Genet* 2011; **56**: 660-665 [PMID: 21796144 DOI: 10.1038/jhg.2011.76]

13 **Barada K**, El-Atrache M, El-Hajj II, Rida K, El-Hajjar J, Mahfoud Z, Usta J. Homozygous mutations in the conserved ATP hinge region of the Wilson disease gene: association with liver disease. *J Clin Gastroenterol* 2010; **44**: 432-439 [PMID: 20485189 DOI: 10.1097/MCG.0b013e3181ce5138]

14 **Wu ZY**, Wang N, Lin MT, Fang L, Murong SX, Yu L. Mutation analysis and the correlation between genotype and phenotype of Arg778Leu mutation in chinese patients with Wilson disease. *Arch Neurol* 2001; **58**: 971-976 [PMID: 11405812]

15 **Braiterman LT**, Murthy A, Jayakanthan S, Nyasae L, Tzeng E, Gromadzka G, Woolf TB, Lutsenko S, Hubbard AL. Distinct phenotype of a Wilson disease mutation reveals a novel trafficking determinant in the copper transporter ATP7B. *Proc Natl Acad Sci USA* 2014; **111**: E1364-E1373 [PMID: 24706876 DOI: 10.1073/pnas.1314161111]

16 **Huster D**, Kühne A, Bhattacharjee A, Raines L, Jantsch V, Noe J, Schirrmeister W, Sommerer I, Sabri O, Berr F, Mössner J, Stieger B, Caca K, Lutsenko S. Diverse functional properties of Wilson disease ATP7B variants. *Gastroenterology* 2012; **142**: 947-956.e5 [PMID: 22240481 DOI: 10.1053/j.gastro.2011.12.048]

17 **Payne AS**, Kelly EJ, Gitlin JD. Functional expression of the Wilson disease protein reveals mislocalization and impaired copper-dependent trafficking of the common H1069Q mutation. *Proc Natl Acad Sci USA* 1998; **95**: 10854-10859 [PMID: 9724794]

18 **Schilsky ML**. Treatment of Wilson's disease: what are the relative roles of penicillamine, trientine, and zinc supplementation? *Curr Gastroenterol Rep* 2001; **3**: 54-59 [PMID: 11177695]

19 **Weiss KH**, Gotthardt DN, Klemm D, Merle U, Ferenci-Foerster D, Schaefer M, Ferenci P, Stremmel W. Zinc monotherapy is not as effective as chelating agents in treatment of Wilson disease. *Gastroenterology* 2011; **140**: 1189-1198.e1 [PMID: 21185835 DOI: 10.1053/j.gastro.2010.12.034]

20 **Abuduxikuer K**, Wang JS. Zinc mono-therapy in pre-symptomatic Chinese children with Wilson disease: a single center, retrospective study. *PLoS One* 2014; **9**: e86168 [PMID: 24475083 DOI: 10.1371/journal.pone.0086168]

21 **Ni W**, Dong QY, Zhang Y, Wu ZY. Zinc monotherapy and a low-copper diet are beneficial in patients with Wilson disease after liver transplantation. *CNS Neurosci Ther* 2013; **19**: 905-907 [PMID: 24119323 DOI: 10.1111/cns.12167]

22 **Chandhok G**, Schmitt N, Sauer V, Aggarwal A, Bhatt M, Schmidt HH. The effect of zinc and D-penicillamine in a stable human hepatoma ATP7B knockout cell line. *PLoS One* 2014; **9**: e98809 [PMID: 24892424 DOI: 10.1371/journal.pone.0098809]

23 **Sauer V**, Siaj R, Todorov T, Zibert A, Schmidt HH. Overexpressed ATP7B protects mesenchymal stem cells from toxic copper. *Biochem Biophys Res Commun* 2010; **395**: 307-311 [PMID: 20362556 DOI: 10.1016/j.bbrc.2010.03.158]

24 **Schilsky ML**, Blank RR, Czaja MJ, Zern MA, Scheinberg IH, Stockert RJ, Sternlieb I. Hepatocellular copper toxicity and its attenuation by zinc. *J Clin Invest* 1989; **84**: 1562-1568 [PMID: 2478589 DOI: 10.1172/JCI114333]

25 **Siaj R**, Sauer V, Stöppeler S, Spiegel HU, Köhler G, Zibert A, Schmidt HH. Dietary copper triggers onset of fulminant hepatitis in the Long-Evans cinnamon rat model. *World J Gastroenterol* 2012; **18**: 5542-5550 [PMID: 23112546 DOI: 10.3748/wjg.v18.i39.5542]

26 **Aggarwal A**, Chandhok G, Todorov T, Parekh S, Tilve S, Zibert A, Bhatt M, Schmidt HH. Wilson disease mutation pattern with genotype-phenotype correlations from Western India: confirmation of p.C271* as a common Indian mutation and identification of 14 novel mutations. *Ann Hum Genet* 2013; **77**: 299-307 [PMID: 23551039 DOI: 10.1111/ahg.12024]

27 **Chuang LM**, Wu HP, Jang MH, Wang TR, Sue WC, Lin BJ, Cox DW, Tai TY. High frequency of two mutations in codon 778 in exon 8 of the ATP7B gene in Taiwanese families with Wilson disease. *J Med Genet* 1996; **33**: 521-523 [PMID: 8782057]

28 **Curtis D**, Durkie M, Balac (Morris) P, Sheard D, Goodeve A, Peake I, Quarrell O, Tanner S. A study of Wilson disease mutations in Britain. *Hum Mutat* 1999; **14**: 304-311 [PMID: 10502777 DOI: 10.1002/(SICI)1098-1004(199910)14::4<304::AID-HUMU5>3.0.CO;2-W]

29 **Shah AB**, Chernov I, Zhang HT, Ross BM, Das K, Lutsenko S, Parano E, Pavone L, Evgrafov O, Ivanova-Smolenskaya IA, Annerén G, Westermark K, Urrutia FH, Penchaszadeh GK, Sternlieb I, Scheinberg IH, Gilliam TC, Petrukhin K. Identification and analysis of mutations in the Wilson disease gene (ATP7B): population frequencies, genotype-phenotype correlation, and functional analyses. *Am J Hum Genet* 1997; **61**: 317-328 [PMID: 9311736 DOI: 10.1086/514864]

30 **Stapelbroek JM**, Bollen CW, van Amstel JK, van Erpecum KJ, van Hattum J, van den Berg LH, Klomp LW, Houwen RH. The H1069Q mutation in ATP7B is associated with late and neurologic presentation in Wilson disease: results of a meta-analysis. *J Hepatol* 2004; **41**: 758-763 [PMID: 15519648 DOI: 10.1016/j.jhep.2004.07.017]

31 **van den Berghe PV**, Stapelbroek JM, Krieger E, de Bie P, van de Graaf SF, de Groot RE, van Beurden E, Spijker E, Houwen RH, Berger R, Klomp LW. Reduced expression of ATP7B affected by Wilson disease-causing mutations is rescued by pharmacological folding chaperones 4-phenylbutyrate and curcumin. *Hepatology* 2009; **50**: 1783-1795 [PMID: 19937698 DOI: 10.1002/hep.23209]

32 **Forbes JR**, Cox DW. Copper-dependent trafficking of Wilson disease mutant ATP7B proteins. *Hum Mol Genet* 2000; **9**: 1927-1935 [PMID: 10942420]

33 **Polishchuk EV**, Concilli M, Iacobacci S, Chesi G, Pastore N, Piccolo P, Paladino S, Baldantoni D, van IJzendoorn SC, Chan J, Chang CJ, Amoresano A, Pane F, Pucci P, Tarallo A, Parenti G, Brunetti-Pierri N, Settembre C, Ballabio A, Polishchuk RS. Wilson disease protein ATP7B utilizes lysosomal exocytosis to maintain copper homeostasis. *Dev Cell* 2014; **29**: 686-700 [PMID: 24909901 DOI: 10.1016/j.devcel.2014.04.033]

34 **Jain S**, Farías GG, Bonifacino JS. Polarized sorting of the copper transporter ATP7B in neurons mediated by recognition of a dileucine signal by AP-1. *Mol Biol Cell* 2015; **26**: 218-228 [PMID: 25378584 DOI: 10.1091/mbc.E14-07-1177]

35 **Lang PA**, Schenck M, Nicolay JP, Becker JU, Kempe DS, Lupescu A, Koka S, Eisele K, Klarl BA, Rübben H, Schmid KW, Mann K, Hildenbrand S, Hefter H, Huber SM, Wieder T, Erhardt A, Häussinger D, Gulbins E, Lang F. Liver cell death and anemia in Wilson disease involve acid sphingomyelinase and ceramide. *Nat Med* 2007; **13**: 164-170 [PMID: 17259995 DOI: 10.1038/nm1539]

36 **Strand S**, Hofmann WJ, Grambihler A, Hug H, Volkmann M, Otto G,

Wesch H, Mariani SM, Hack V, Stremmel W, Krammer PH, Galle PR. Hepatic failure and liver cell damage in acute Wilson's disease involve CD95 (APO-1/Fas) mediated apoptosis. *Nat Med* 1998; **4**: 588-593 [PMID: 9585233]

37 **Huster D**, Hoppert M, Lutsenko S, Zinke J, Lehmann C, Mössner J, Berr F, Caca K. Defective cellular localization of mutant ATP7B in Wilson's disease patients and hepatoma cell lines. *Gastroenterology* 2003; **124**: 335-345 [PMID: 12557139 DOI: 10.1053/gast.2003.50066]

38 **Wan L**, Tsai CH, Hsu CM, Huang CC, Yang CC, Liao CC, Wu CC, Hsu YA, Lee CC, Liu SC, Lin WD, Tsai FJ. Mutation analysis and characterization of alternative splice variants of the Wilson disease gene ATP7B. *Hepatology* 2010; **52**: 1662-1670 [PMID: 20931554 DOI: 10.1002/hep.23865]

39 **Figus A**, Angius A, Loudianos G, Bertini C, Dessi V, Loi A, Deiana M, Lovicu M, Olla N, Sole G. Molecular pathology and haplotype analysis of Wilson disease in Mediterranean populations. *Am J Hum Genet* 1995; **57**: 1318-1324 [PMID: 8533760]

40 **Houwen RH**, Juyn J, Hoogenraad TU, Ploos van Amstel JK, Berger R. H714Q mutation in Wilson disease is associated with late, neurological presentation. *J Med Genet* 1995; **32**: 480-482 [PMID: 7666402]

41 **Waldenström E**, Lagerkvist A, Dahlman T, Westermark K, Landegren U. Efficient detection of mutations in Wilson disease by manifold sequencing. *Genomics* 1996; **37**: 303-309 [PMID: 8938442 DOI: 10.1006/geno.1996.0564]

42 **Gromadzka G**, Schmidt HH, Genschel J, Bochow B, Rodo M, Tarnacka B, Litwin T, Chabik G, Członkowska A. Frameshift and nonsense mutations in the gene for ATPase7B are associated with severe impairment of copper metabolism and with an early clinical manifestation of Wilson's disease. *Clin Genet* 2005; **68**: 524-532 [PMID: 16283883 DOI: 10.1111/j.1399-0004.2005.00528.x]

43 **Merle U**, Eisenbach C, Weiss KH, Tuma S, Stremmel W. Serum ceruloplasmin oxidase activity is a sensitive and highly specific diagnostic marker for Wilson's disease. *J Hepatol* 2009; **51**: 925-930 [PMID: 19720421 DOI: 10.1016/j.jhep.2009.06.022]

44 **Panagiotakaki E**, Tzetis M, Manolaki N, Loudianos G, Papatheodorou A, Manesis E, Nousia-Arvanitakis S, Syriopoulou V, Kanavakis E. Genotype-phenotype correlations for a wide spectrum of mutations in the Wilson disease gene (ATP7B). *Am J Med Genet A* 2004; **131**: 168-173 [PMID: 15523622 DOI: 10.1002/ajmg.a.30345]

45 **Liu XQ**, Zhang YF, Liu TT, Hsiao KJ, Zhang JM, Gu XF, Bao KR, Yu LH, Wang MX. Correlation of ATP7B genotype with phenotype in Chinese patients with Wilson disease. *World J Gastroenterol* 2004; **10**: 590-593 [PMID: 14966923 DOI: 10.3748/wjg.v10.i4.590]

46 **Kim EK**, Yoo OJ, Song KY, Yoo HW, Choi SY, Cho SW, Hahn SH. Identification of three novel mutations and a high frequency of the Arg778Leu mutation in Korean patients with Wilson disease. *Hum Mutat* 1998; **11**: 275-278 [PMID: 9554743 DOI: 10.1002/(SICI)1098-1004(1998)11::4<275::AID-HUMU4>3.0.CO;2-L]

47 **Okada T**, Shiono Y, Hayashi H, Satoh H, Sawada T, Suzuki A, Takeda Y, Yano M, Michitaka K, Onji M, Mabuchi H. Mutational analysis of ATP7B and genotype-phenotype correlation in Japanese with Wilson's disease. *Hum Mutat* 2000; **15**: 454-462 [PMID: 10790207 DOI: 10.1002/(SICI)1098-1004(200005)15::5<454::AID-HUMU7>3.0.CO;2-J]

48 **Gu YH**, Kodama H, Du SL, Gu QJ, Sun HJ, Ushijima H. Mutation spectrum and polymorphisms in ATP7B identified on direct sequencing of all exons in Chinese Han and Hui ethnic patients with Wilson's disease. *Clin Genet* 2003; **64**: 479-484 [PMID: 14986826]

49 **Wu Z**, Wang N, Murong S, Lin M. Identification and analysis of mutations of the Wilson disease gene in Chinese population. *Chin Med J* (Engl) 2000; **113**: 40-43 [PMID: 11775208]

50 **Fan Y**, Yu L, Jiang Y, Xu Y, Yang R, Han Y, Cui Y, Ren M, Zhao S. Identification of a mutation hotspot in exon 8 of Wilson disease gene by cycle sequencing. *Chin Med J* (Engl) 2000; **113**: 172-174 [PMID: 11775546]

51 **Chang H**, Xu A, Chen Z, Zhang Y, Tian F, Li T. Long-term effects of a combination of D-penicillamine and zinc salts in the treatment of Wilson's disease in children. *Exp Ther Med* 2013; **5**: 1129-1132 [PMID: 23599735 DOI: 10.3892/etm.2013.971]

52 **Weiss KH**, Thurik F, Gotthardt DN, Schäfer M, Teufel U, Wiegand F, Merle U, Ferenci-Foerster D, Maieron A, Stauber R, Zoller H, Schmidt HH, Reuner U, Hefter H, Trocello JM, Houwen RH, Ferenci P, Stremmel W. Efficacy and safety of oral chelators in treatment of patients with Wilson disease. *Clin Gastroenterol Hepatol* 2013; **11**: 1028-35.e1-2 [PMID: 23542331 DOI: 10.1016/j.cgh.2013.03.012]

53 **McQuaid A**, Lamand M, Mason J. The interactions of penicillamine with copper in vivo and the effect on hepatic metallothionein levels and copper/zinc distribution: the implications for Wilson's disease and arthritis therapy. *J Lab Clin Med* 1992; **119**: 744-750 [PMID: 1593220]

54 **Brewer GJ**. Zinc and tetrathiomolybdate for the treatment of Wilson's disease and the potential efficacy of anticopper therapy in a wide variety of diseases. *Metallomics* 2009; **1**: 199-206 [PMID: 21305118 DOI: 10.1039/b901614g]

55 **Wu ZY**, Lin MT, Murong SX, Wang N. Molecular diagnosis and prophylactic therapy for presymptomatic Chinese patients with Wilson disease. *Arch Neurol* 2003; **60**: 737-741 [PMID: 12756138 DOI: 10.1001/archneur.60.5.737]

P- Reviewer: Czlonkowska A, Pan JJ **S- Editor**: Yu J **L- Editor**: A
E- Editor: Wang CH

World Journal of Gastroenterology

Submit a Manuscript: http://www.wjgnet.com/esps/
Help Desk: http://www.wjgnet.com/esps/helpdesk.aspx
DOI: 10.3748/wjg.v22.i16.4120

World J Gastroenterol 2016 April 28; 22(16): 4120-4135
ISSN 1007-9327 (print) ISSN 2219-2840 (online)

ORIGINAL ARTICLE

Basic Study

Combined mesenchymal stem cell transplantation and interleukin-1 receptor antagonism after partial hepatectomy

Jian-Feng Sang, Xiao-Lei Shi, Bing Han, Xu Huang, Tao Huang, Hao-Zhen Ren, Yi-Tao Ding

Jian-Feng Sang, Xiao-Lei Shi, Bing Han, Xu Huang, Tao Huang, Hao-Zhen Ren, Yi-Tao Ding, Department of General Surgery, the Affiliated Drum Tower Hospital of Nanjing University Medical School, Nanjing 210008, Jiangsu Province, China

Author contributions: Sang JF and Shi XL contributed equally to this work; Sang JF and Shi XL designed the research; Sang JF, Han B, Huang T, Huang X, and Ren HZ performed the research; Ding YT provided new reagents/analytic tools; Sang JF and Han B analyzed the data and wrote the paper. All authors have read and approved the final manuscript.

Supported by The National Natural Science Foundation of China, No. 81300338; 863 National Science and Technology Plans, No. 2013aa020102; and Project Fund of Clinical Medical Center of Digestive Diseases in Jiangsu Province, No. bl2012001.

Institutional review board statement: The study was reviewed and approved by the Nanjing Drum Tower Hospital Institutional Review Board.

Institutional animal care and use committee statement: All animal procedures were approved by the Animal Care Ethics Committee of Nanjing Drum Tower Hospital, Nanjing, China.

Conflict-of-interest statement: The authors declare that there is no conflict of interest related to this study.

Data sharing statement: No additional data are available.

Correspondence to: Dr. Yi-Tao Ding, Professor, Department of Hepatobiliary Surgery, Nanjing Drum Tower Hospital, No. 321 Zhongshan Road, Nanjing 210008, Jiangsu Province, China. yitaoding@hotmail.com
Telephone: +86-25-83304616-66866
Fax: +86-25-83317016

Received: July 3, 2015
Peer-review started: July 6, 2015
First decision: August 26, 2015
Revised: September 24, 2015
Accepted: December 12, 2015
Article in press: December 14, 2015
Published online: April 28, 2016

Abstract

AIM: To study the therapeutic effects of mesenchymal stem cells (MSCs) and an interleukin-1 receptor antagonist (IL-1Ra) in acute liver failure.

METHODS: Chinese experimental miniature swine (15 ± 3 kg, 5-8 mo) were obtained from the Laboratory Animal Centre of the Affiliated Drum Tower Hospital of Nanjing University Medical School. Acute liver failure was induced *via* 85% hepatectomy, and animals were treated by MSC transplantation combined with IL-1Ra injection. Blood samples were collected for hepatic function analysis, and the living conditions and survival time were recorded. Liver injury was histologically analyzed. Hepatic cell regeneration and apoptosis were studied by Ki67 immunohistochemistry and terminal deoxynucleotidyl transferase dUTP nick end labeling, respectively. The levels of protein kinase B and nuclear factor-κB expression were analyzed by Western blotting.

RESULTS: MSCs were infected with a lentivirus for expression of green fluorescent protein (GFP) for subsequent identification; 97.3% of the MSCs were positive for GFP as assessed by flow cytometry.

Additional flow cytometric analysis of cell surface marker expression demonstrated that > 90% of GFP-expressing MSCs were also positive for CD29, CD44, and CD90, indicating that most of these cells expressed typical markers of MSCs, and the population of MSCs was almost pure. Transplantation of MSCs in combination with 2 mg/kg IL-1Ra therapy significantly improved survival time compared to the acute liver failure model group (35.3 ± 6.7 d *vs* 17.3 ± 5.5 d, $P < 0.05$). Combined therapy also promoted improvement in serum inflammatory cytokines and biochemical conditions. The observed hepatic histopathologic score was significantly lower in the group with combined therapy than in the model group (3.50 ± 0.87 *vs* 8.17 ± 1.26, $P < 0.01$). In addition, liver cell apoptosis in the combined therapy group was significantly inhibited (18.1 ± 2.1% *vs* 70.8 ± 3.7%, $P < 0.01$), and hepatic cell regeneration increased. A significant increase in protein kinase B expression and decrease in nuclear factor-κB expression were observed ($P < 0.01$), which supports their important roles in liver regeneration.

CONCLUSION: MSCs and IL-1Ra had a synergistic effect in liver regeneration *via* regulation of inflammation and apoptotic signaling.

Key words: Mesenchymal stem cells; Interleukin-1 receptor antagonist; Stem cell transplantation; Acute liver failure; Hepatoectomy

Core tip: Combination therapy is superior to any method of mesenchymal stem cell (MSC) transplantation used alone. This study shows that combination therapy improved liver function, inhibited apoptosis, and prolonged the survival of swine with acute liver failure (ALF). Transplanted MSCs may participate in liver regeneration by promoting proliferation and inhibiting apoptosis during the initial stage of ALF following antagonism of interleukin-1 inflammatory signaling. Combination therapy with MSC transplantation and an interleukin-1 receptor antagonist, which enables restoration from ALF and liver reconstruction in swine, is a promising treatment option for ALF patients in the future.

Sang JF, Shi XL, Han B, Huang X, Huang T, Ren HZ, Ding YT. Combined mesenchymal stem cell transplantation and interleukin-1 receptor antagonism after partial hepatectomy. *World J Gastroenterol* 2016; 22(16): 4120-4135 Available from: URL: http://www.wjgnet.com/1007-9327/full/v22/i16/4120.htm DOI: http://dx.doi.org/10.3748/wjg.v22.i16.4120

INTRODUCTION

Acute liver failure (ALF) is characterized by severe liver cell damage due to virus infection, drugs, toxins, alcohol, or as a result of hepatectomy. ALF leads to hepatic encephalopathy, hepatorenal syndrome, severe infection, multiple organ failure, and even death[1]. Combating ALF requires either reduction of liver cell necrosis or stimulation of liver cell regeneration. This can be achieved with drug therapy, artificial liver therapy, stem cell transplantation, and liver transplantation[2]. Even though artificial liver therapy has the potential to reduce mortality, its efficacy is limited[3]. So far, liver transplantation is the most effective treatment for ALF. However, it has its own limitations due to many difficulties, including severe donor shortage, numerous complications, immune rejection, use of immunosuppressive agents, and high medical costs[4].

In recent years, stem cell therapy has become a new area of investigation for ALF treatment. This is mainly because stem cells are abundant, show low immunogenicity, and have the potential to differentiate into hepatocyte-like cells[5]. A large body of evidence suggests that mesenchymal stem cells (MSCs) could differentiate *in vitro* and *in vivo* into liver-like cells with partial hepatic functions under appropriate environmental conditions[6,7]. Given that autologous cell transplantation helps to prevent immunologic rejection, which is always a major obstacle for orthotopic liver transplantation, MSCs could be regarded as seeding cells for transplantation in relation to the treatment of liver diseases[8].

Severe inflammation as a result of ALF leads to necrosis of a large number of liver cells and is caused by acetaminophen, idiosyncratic drug reactions, hepatitis B, or seronegative hepatitis. The occurrence of ALF also involves various inflammatory factors and cytokines, and its pathogenesis is closely related to liver cell apoptosis[9-11]. In recent years, experimental studies have demonstrated that microcirculatory dysfunction and an inflammatory environment are determinants of ALF, and proinflammatory mediators such as interleukin (IL)-1, IL-2, and tumor necrosis factor (TNF)-α are the key players[12]. One study showed that the levels of these cytokines in patients with ALF were significantly higher than in healthy individuals and patients with chronic hepatitis[13]. IL-1 may be a main driver of late inflammation, which leads to further injury. IL-1 is considered to be a primary proinflammatory cytokine because of its ability to stimulate expression of many inflammation-associated genes through the IL-1 signaling cascade[14].

The IL-1 receptor antagonist (IL-1Ra) is a natural IL-1 antagonist that can block the inflammatory process by competitively binding to the IL-1 receptor with equal avidity to IL-1. IL-1Ra inhibits the stimulation of downstream signaling, thereby reducing inflammation[15]. Imbalance between IL-1 and IL-1Ra has been observed in a variety of inflammatory diseases including ALF[16]. IL-1Ra, which is significantly associated with the level of liver inflammation, is an independent marker unaffected by obesity, alcohol

consumption, or insulin resistance[17]. IL-1Ra can inhibit hepatocellular apoptosis in mice with ALF induced by acetaminophen and significantly improve their survival rate[18]. Therefore, we hypothesized that reducing inflammation in acutely injured liver would benefit the efficacy of MSC transplantation in patients with ALF. In this study, IL-1Ra was injected through the portal vein along with MSCs to reduce liver inflammation in a swine model of ALF. Liver function before and after MSC transplantation with or without IL-Ra was compared by measuring the changes in serum levels of alanine aminotransferase (ALT), aspartate transaminase (AST), alkaline phosphatase (ALP), and γ-glutamyl transpeptidase (γ-GT). In addition, pathologic injury and hepatic cell apoptosis were also examined. The outcome of this study appears promising and may improve the clinical application of MSCs.

MATERIALS AND METHODS

Animals

Chinese experimental miniature swine (15 ± 3 kg, 5-8 mo) were obtained from the Laboratory Animal Centre of the Affiliated Drum Tower Hospital of Nanjing University Medical School. Animals were maintained under standard conditions. All animal procedures were approved by the Animal Care Ethics Committee of Nanjing Drum Tower Hospital. Every effort was made to minimize any suffering of the animals used in this study.

MSC isolation, culture, and characterization

Porcine MSCs were isolated as described previously[19]. Bone marrow aspirates were collected from the iliac crests. MSCs were separated by density gradient centrifugation over a Ficoll histopaque layer (20 min, 400 × *g*, density: 1.077 g/mL) (TBD, Tianjin, China) and cultured in low-glucose Dulbecco's modified Eagle's medium (Gibco of Thermo Fisher Scientific, Waltham, MA, United States) supplemented with 10% fetal bovine serum (Gibco), 100 IU/mL penicillin, and 100 μg/mL streptomycin (Gibco). The non-adherent cells were removed after the first 24 h incubation, and medium was changed every 3-4 d. When the cells reached 80% confluence, they were trypsinized using 2.5 g/L trypsin-EDTA (Gibco) and replated at a density of 1 × 10^4/cm^2 for further expansion. The cells were infected with a lentivirus encoding the gene for green fluorescent protein (GFP), and the multiplicity of infection was determined by fluorescence inverted phase-contrast microscopy and flow cytometry. MSCs were characterized by flow cytometry (FACScan; Becton Dickinson, Franklin Lakes, NJ, United States) with phycoerythrin-conjugated antibodies against CD29 (VMRD, Pullman, WA, United States), CD44, and CD90 (Becton Dickinson); isotypic antibodies were used as controls.

Swine hepatectomy model of ALF

The swine model of ALF was established as described previously[20]. The swine were starved for 8 h before the operation. Initial sedation was achieved with a deep intramuscular injection of ketamine (15-20 mg/kg) and chlorpromazine (6-8 mg/kg), administered 15 min after atropine (0.01 mg/kg). Oxygen saturation and heart rate were monitored throughout the operation, and anesthesia was maintained using 1.5% halothane in oxygen titrated to provide anesthesia. Normal saline (1 L) and 5% dextrose (500 mL) were administered intravenously during the surgical procedure. For 85% hepatectomy, left trilobectomy was performed, together with partial right-posterior-lobe resection but without hepatic pedicle occlusion. Parts of the right posterior and caudate lobes were retained to leave a residual hepatic volume of 15% of the normal volume. Computed tomography (CT) and CT reconstruction were performed to visualize the residual liver volume after hepatectomy, and B-scan ultrasound examination was performed to detect ascites.

Postoperative management

All animals received the following subcutaneous injections: 5 mL 10% glucose, 0.1 mL analgesics (ketorolac; Whanin Pharm, Seoul, South Korea), and 0.1 mL ceftriaxone (Rocephin; Roche Holding AG, Basel, Switzerland). Animals had *ad libitum* access to 20% glucose solution for drinking and standard laboratory chow.

Experimental groups and treatments

Twenty-four swine with injured livers were randomly divided into four groups (n = 6 each): a model control group, a group receiving IL-1Ra *via* peripheral vein injection, a group receiving MSC transplantation *via* portal vein injection, and a combined therapy group. The model control group received 40 mL normal saline *via* the portal vein 1 d after surgery. The IL-1Ra group received an injection of 2 mg/kg IL-1Ra (Institute of Process Engineering, Chinese Academy of Sciences, China) *via* the ear vein at 18 h, 2 d, and 4 d after surgery. The MSC transplant group received 1 × 10^8 GFP-MSCs suspended in 40 mL normal saline *via* the portal vein 24 h after surgery. The combined therapy group received 2 mg/kg IL-1Ra *via* the ear vein 18 h after surgery, followed by MSC transplantation 6 h after IL-1Ra injection, and finally 2 mg/kg IL-1Ra was again injected *via* the ear vein at 2 d and 4 d after surgery.

Blood and serum analysis

Blood samples were collected before and after MSC transplantation. Venous blood samples were drawn preoperatively and at 1 d, 3 d, 5 d, 7d, and 14 d after MSC transplantation (day 0) for biochemical analysis. Serum levels of ALT, AST, ALP, and γ-GT were monitored, and the degree of liver function estimated.

Inflammatory cytokines IL-1β, IL-6, and TNF-α were also measured by ELISA (Corbett Life Science, Sydney, Australia) preoperatively, intraoperatively, and at 1 d, 3 d, 5 d, 7 d, and 14 d after MSC transplantation.

Histologic assessment

Seven days after cell transplantation, animal liver tissues were surgically collected under general anesthesia. To trace transplanted MSCs, GFP expression in frozen tissue sections was analyzed by fluorescent microscopy. For histologic analysis, liver tissue was fixed in 10% neutral-buffered formalin and embedded in paraffin. Sections of 5-μm thickness were affixed to slides, deparaffinized, and stained with hematoxylin and eosin to determine morphologic changes. Liver injury was histologically interpreted and scored in all samples. Histopathology was independently evaluated by three pathologists blinded to the treatment and scored in terms of steatosis, necrosis, and inflammation as follows: 0, normal; 1, mild changes; 2, mild to moderate severity; 3, moderate severity; and 4, maximum severity. The scores were added for each animal to create a composite score. Sections were photographed with a Leitz Aristoplan microscope (Wetzlar, Germany). The slices were subjected for further anti-Ki67 (EnoGene Biotech Co., Ltd., New York, NY, United States) immunohistochemical staining. To determine liver cell proliferation, six high-powered fields from each section were analyzed to obtain an average number of $Ki67^+$ cells (Ki67 index).

Terminal deoxynucleotidyl transferase dUTP nick end labeling assay

Hepatic apoptosis was detected by terminal deoxynucleotidyl transferase dUTP nick end labeling (TUNEL) assay (BioBox, Nanjing, China)[21]. Paraffin sections for histologic assessment were deparaffinized, rehydrated, and then rinsed in PBS. After endogenous peroxidase activity was blocked by methanol, a permeability solution (1 g/L Triton X-100 in 0.1% sodium citrate), TUNEL reaction solution, and Converter-POD were added. Each slice was stained by 3,3-diaminobenzidine, and apoptosis was observed by microscopy. The brown staining in the nucleus represented apoptotic cells. Three fields were randomly selected in each slice under high-power field (400 ×) and the percentage of $TUNEL^+$ cells was used to estimate the apoptosis rate.

Western blotting

Western blotting was performed as previously described[22]. Seven days after cell transplantation, surgically collected animal liver tissues were frozen in liquid nitrogen and lysed with buffer containing 20 mmol/L Tris (pH 7.4), 250 mmol/L NaCl, 2 mmol/L EDTA (pH 8.0), 0.1% Triton X-100, 0.01 mg/mL aprotinin, 0.005 mg/mL leupeptin, 0.4 mmol/L PMSF, and 4 mmol/L $NaVO_4$. The protein content was measured using a Bio-Rad colorimetric protein assay kit (Bio-Rad Laboratories, Hercules, CA, United States) and an equal amount of protein was separated by SDS-PAGE. After separation, the proteins were electrotransferred onto nitrocellulose membranes and blotted with primary antibodies against protein kinase B (Akt), nuclear factor (NF)-κB p65, and β-actin (EnoGene) at 1:1000 dilutions. The membranes were washed and exposed to horseradish-peroxidase-conjugated secondary antibody for 1 h, and signals were finally detected by ECL reagent (GE Healthcare, Little Chalfont, United Kingdom). The signal band intensities were analyzed using Image J software and the results are expressed as fold change relative to the internal control (β-actin).

Statistical analysis

All assays were repeated three times to ensure reproducibility. Results are expressed as mean ± SD. Differences between the control and treated groups were analyzed by Student's unpaired *t* test and one-way analysis of variance. The comparison of survival time was achieved using the Kruskal-Wallis test. For the survival time, two-tailed *P* values $\leqslant$ 0.05 were considered as statistically significant. Analyses were performed with SPSS version 17.0 statistical software (SPSS Inc., Chicago, IL, United States).

RESULTS

MSC phenotype

MSCs formed colonies after 24 h of plating when observed under microscope. They grew rapidly like fibroblasts, with a single nucleus. After passage 1, they looked like spindles or asters with a slim body. However, after passage 4, most of the miscellaneous cells were eliminated, leaving the uniformly fibroblast-like cells, which were MSCs. Infecting these cells with lentivirus expressing GFP protein resulted in nearly complete transfection as observed by fluorescence microscopy (Figure 1A and B). Flow cytometry revealed that approximately 97.3% of MSCs were GFP positive (Figure 1C). In addition, flow cytometry analysis of cell surface-marker expression demonstrated that > 90% of GFP-MSCs were positive for CD29, CD44, and CD90 expression (Figure 1D).

Survival of swine after ALF

CT examination and reconstruction analysis of the residual liver volume in the hepatectomized animals indicated that approximately 85% of the liver was resected compared with normal swine liver (Figure 2A-D). After hepatectomy, animals displayed typical liver failure characteristics, such as a prolonged recovery time, hypobulia, drowsiness, reduced movement, weak response to stimulation, and emerging ocular hemorrhage. B-scan ultrasound revealed massive

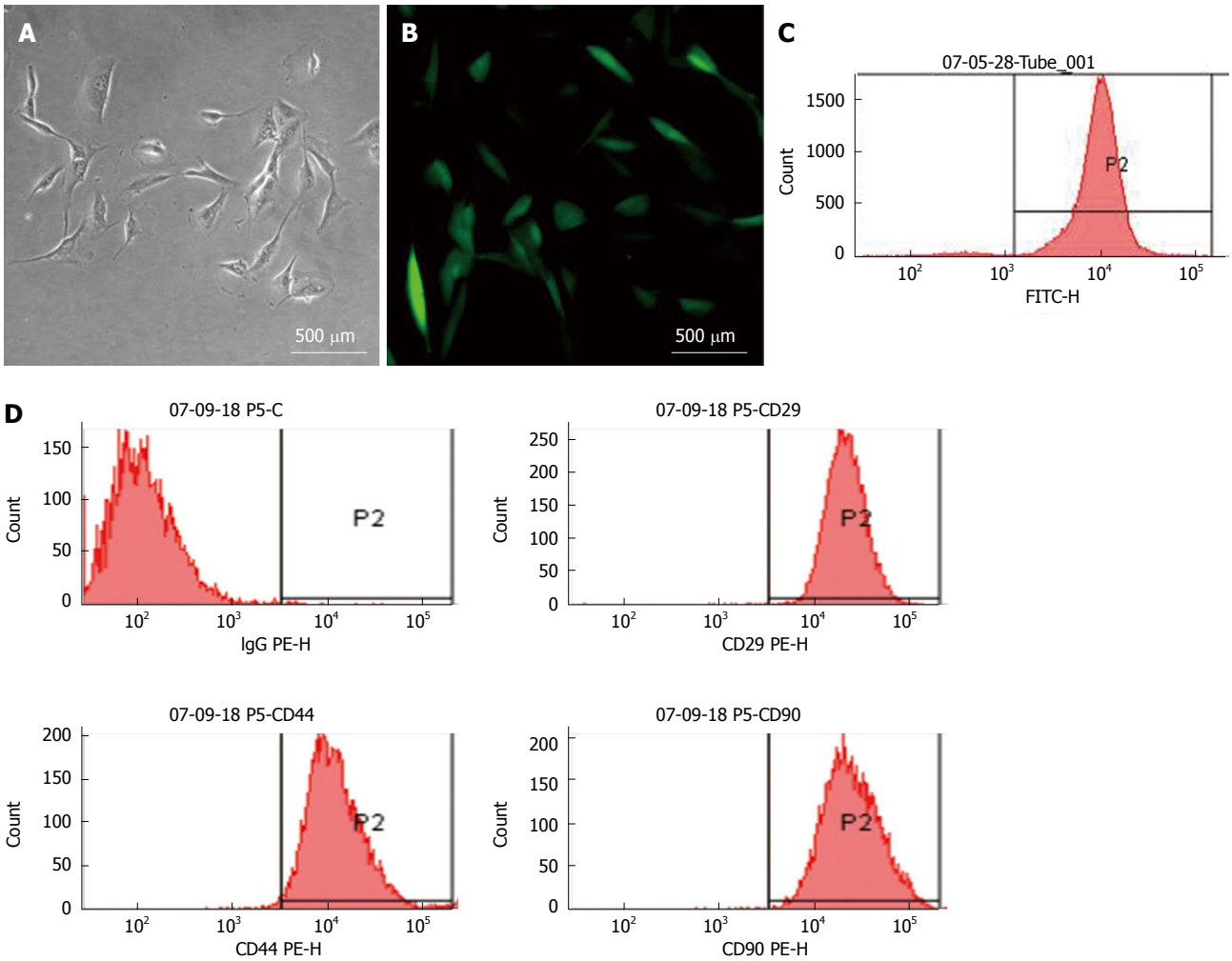

Figure 1 Characterization of mesenchymal stem cells (MSCs). MSCs transfected with a lentiviral vector encoding green fluorescent protein (GFP) were cultured for 3 d *in vitro* and observed by A: Light and B: Fluorescent microscopy (magnification × 200, scale bar = 500 μm); C: Flow cytometry of MSCs revealed > 97% expressed GFP after propagation; D: Surface markers of the cultured MSCs were identified by flow cytometry: > 90% of GFP-MSCs were positive for CD29 (upper right), CD44 (lower left) and CD90 (lower right); isotypic antibodies served as the control (upper left).

ascites (Figure 2E).

All swine in the hepatectomy group (no treatment) died within 25 d after surgery; the average survival time was 17.3 ± 5.5 d. No abdominal bleeding or vascular embolism was detected during autopsy examinations, indicating that animals died from liver failure and not surgical complications. However, the 25-d survival rates of the treatment group were 33.3%, 66.7%, and 100% in the IL-1Ra group, MSC transplantation group, and combined therapy group, respectively, with average survival times of 21.7 ± 4.7 d, 24.3 ± 4.0 d, and 35.3 ± 6.7 d, respectively. The difference in survival time between the hepatectomy and combined therapy groups was significant (P < 0.05) (Figure 3).

Estimation of liver function

Preoperative and serial postoperative measurements of serum ALT, AST, ALP, and γ-GT are shown in Figure 4. Serum levels of ALT and AST were significantly elevated within 1-7 d after hepatectomy, whereas ALP levels were significantly elevated within 1-14 d after hepatectomy (all P < 0.05). γ-GT level was significantly elevated within 3-7 d (P < 0.05 or < 0.01) after hepatectomy. These data demonstrated that acute liver injury was successfully achieved after hepatectomy. Postoperative measurements revealed that the greatest improvements were found in the combined therapy group. The serum levels of ALT in the model group were significantly lower than in the combined therapy group on days 5 (P < 0.05) and 7 (P < 0.01), in the IL-1Ra group on day 5 (P < 0.05), and the MSC transplantation group on day 7 (P < 0.05). Similarly, the serum levels of AST were significantly lower in the combined therapy group than in the model group on days 3, 5, 7, and 14 (P < 0.01), and significantly lower than in the IL-1Ra and MSC transplantation groups on days 3 (P < 0.05), 5, and 7 (P < 0.01). The serum levels of ALP were significantly lower in the combined therapy group than in the model group on days 3 (P < 0.01), 5, 7, and 14 (P < 0.05), and significantly lower than in the IL-1Ra and MSC transplantation groups on

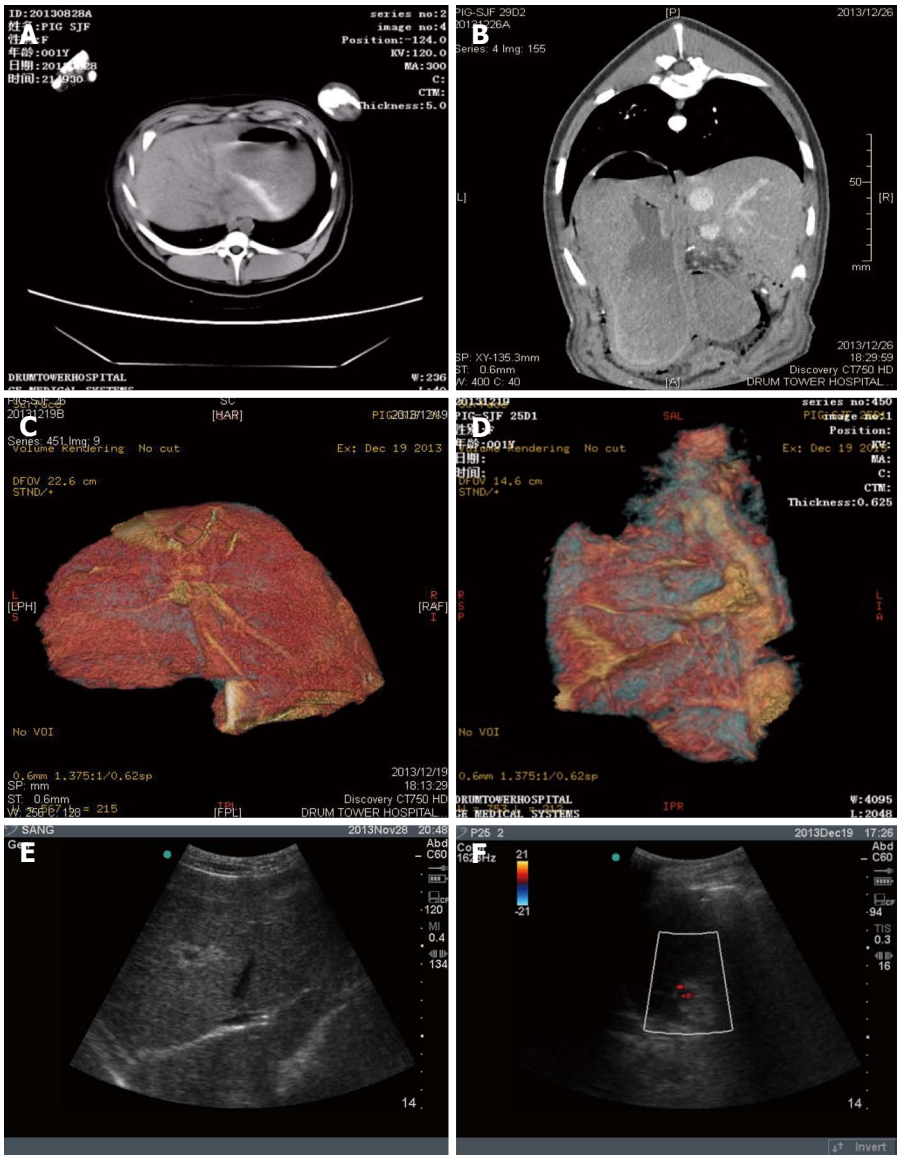

Figure 2 Imaging evaluation of residual liver volume after hepatectomy. A and B: CT examination; C and D: CT reconstruction analysis indicated that an average 85% of liver was resected; E and F: B-scan ultrasound was performed to examine ascites (A, C, E: Sham-operated swine; B, D, F: Hepatectomized swine).

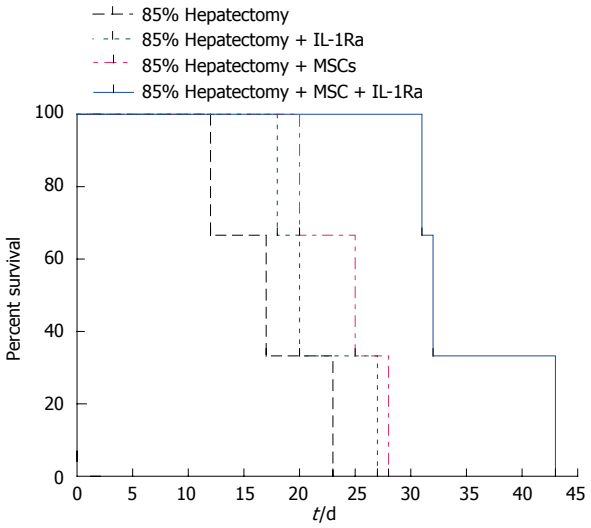

Figure 3 Survival rate after partial (85%) liver hepatectomy. IL-1Ra: Interleukin-1 receptor antagonist; MSC: Mesenchymal stem cell transplantation.

days 3 ($P < 0.01$) and 5 ($P < 0.05$). The serum levels of γ-GT in the model group were significantly lower than in the combined therapy group on days 3 ($P < 0.05$), 5 ($P < 0.01$), and 7 ($P < 0.05$), and lower than the IL-1Ra group on day 5 ($P < 0.05$). There was no significant difference from the MSC transplantation group.

Analysis of serum inflammatory cytokines

Following hepatectomy, the levels of inflammatory cytokines IL-1β, IL-6, and TNF-α increased significantly in all groups, reaching a peak within 3 d and lasting > 2 wk before gradually declining (Figure 5). The combined therapy group had the lowest levels of inflammatory cytokines, with IL-1β, IL-6 and TNF-α levels significantly lower than in the model group on days 1-14 (all $P < 0.05$). The IL-1Ra group also had significantly decreased IL-1β levels on days 3-14 (all $P < 0.05$), decreased IL-6 levels on days 1-14 (all $P <$

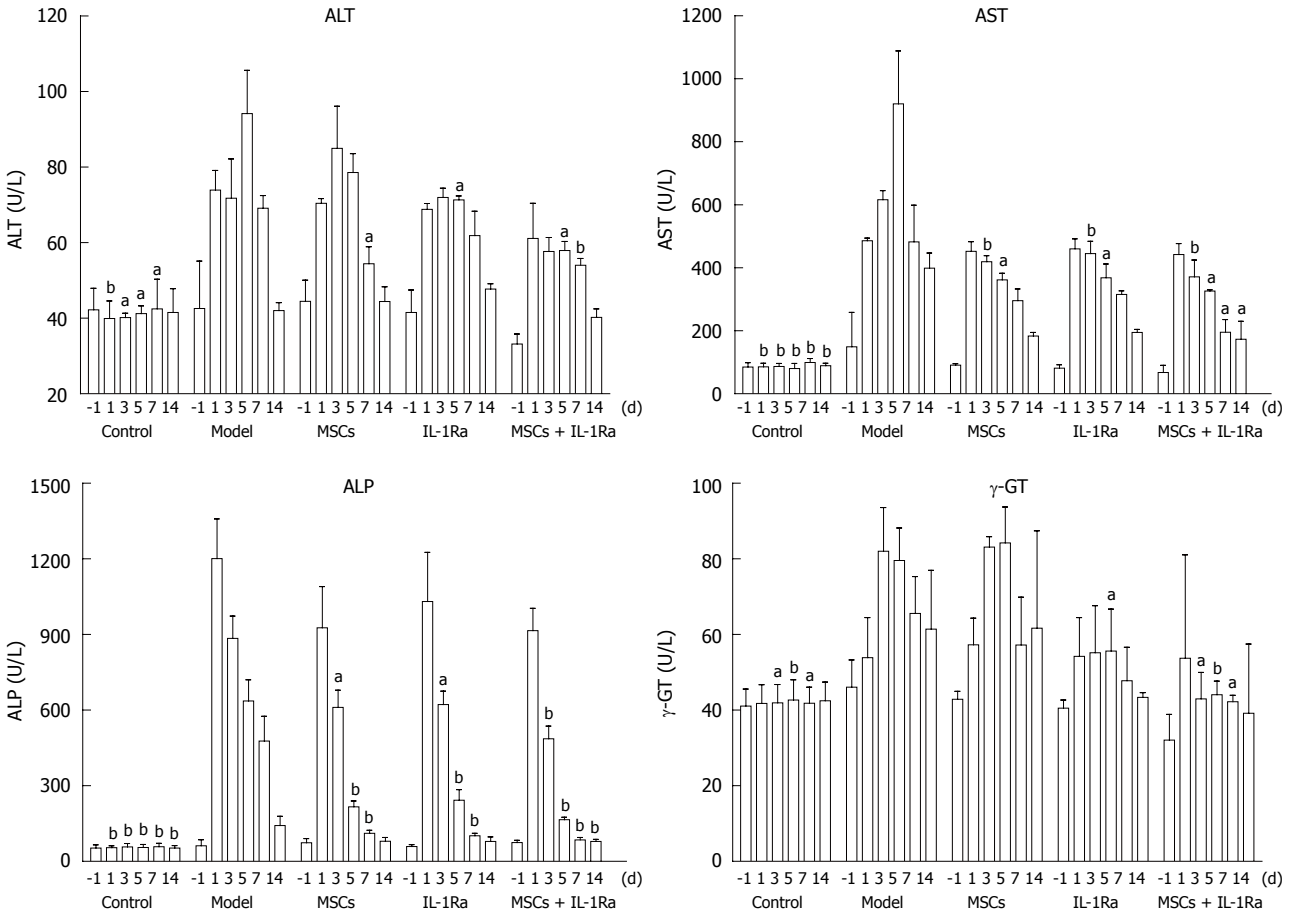

Figure 4 Serologic analyses. Serum samples collected at various times before (-1 d) and after (1 d, 3, d, 5 d, 7 d, and 14 d) surgery were analyzed for levels of alanine aminotransferase (ALT), aspartate transaminase (AST), alkaline phosphatase (ALP), and γ-glutamyl transpeptidase (γ-GT); $^{a}P < 0.05$, $^{b}P < 0.01$ compared with model group. IL-1Ra: Interleukin-1 receptor antagonist; MSC: Mesenchymal stem cell transplantation.

0.05), and decreased TNF-α levels on day 3 ($P < 0.05$). MSC transplantation alone had a weaker influence on inflammatory cytokines, as IL-1β levels were only significantly decreased on day 14 ($P < 0.05$), IL-6 levels decreased only on days 3 and 14 ($P < 0.05$), and TNF-α levels decreased only on day 3 ($P < 0.05$).

Histologic analysis

Histopathologic studies of swine liver tissue from normal sham-operated animals showed that the liver lobular structure was clear, arranged radially around the central vein in liver cells, and liver lobules were separated by slender connective tissue. In biliary epithelium, no cell degeneration, necrosis, or non-proliferation was observed (Figure 6A). However, liver tissue samples from the injured model group after hepatectomy demonstrated diffuse necrosis with extensive bridging and proliferation of inflammatory cells around the periportal area. Severe hepatic necrosis was seen in most of the lobules, along with hepatic sinusoidal dilatation, congestion, and hemorrhage. Liver cell necrosis appeared in the hemorrhagic area. Only a small number of liver cells remained on the edges of the hepatic lobules (Figure 6B). This group showed the most severe liver damage, while in contrast, the therapy groups had less inflammatory cell infiltration and relatively complete lobular architectures. The combined therapy group displayed the most apparent improvements among all the groups. The lobular architecture could be recognized and liver cells were arranged radially around the central vein. Liver lobules were surrounded by interlobular connective tissue, and few inflammatory cells were observed. Combined therapy substantially protected against liver injury, relieved liver sinusoidal dilatation and congestion, and reduced the level of liver cell degeneration and necrosis (Figure 6E).

After hepatic resection, the pathologic score was 8.17 ± 1.26, which was significantly higher than that of the sham-operated group (0.33 ± 0.29; $P < 0.01$) (Figure 6F). The histopathologic score in the combined therapy group (3.50 ± 0.87) was significantly decreased compared with hepatectomized model group ($P < 0.01$). However, there was no significant difference in the IL-1Ra (6.67 ± 1.04) and MSC transplantation (5.83 ± 0.76) groups (Figure 6F). In addition, frozen sections of liver tissue were examined using fluorescence microscopy. The green fluorescent signal for GFP-MSCs and the blue staining (DAPI)

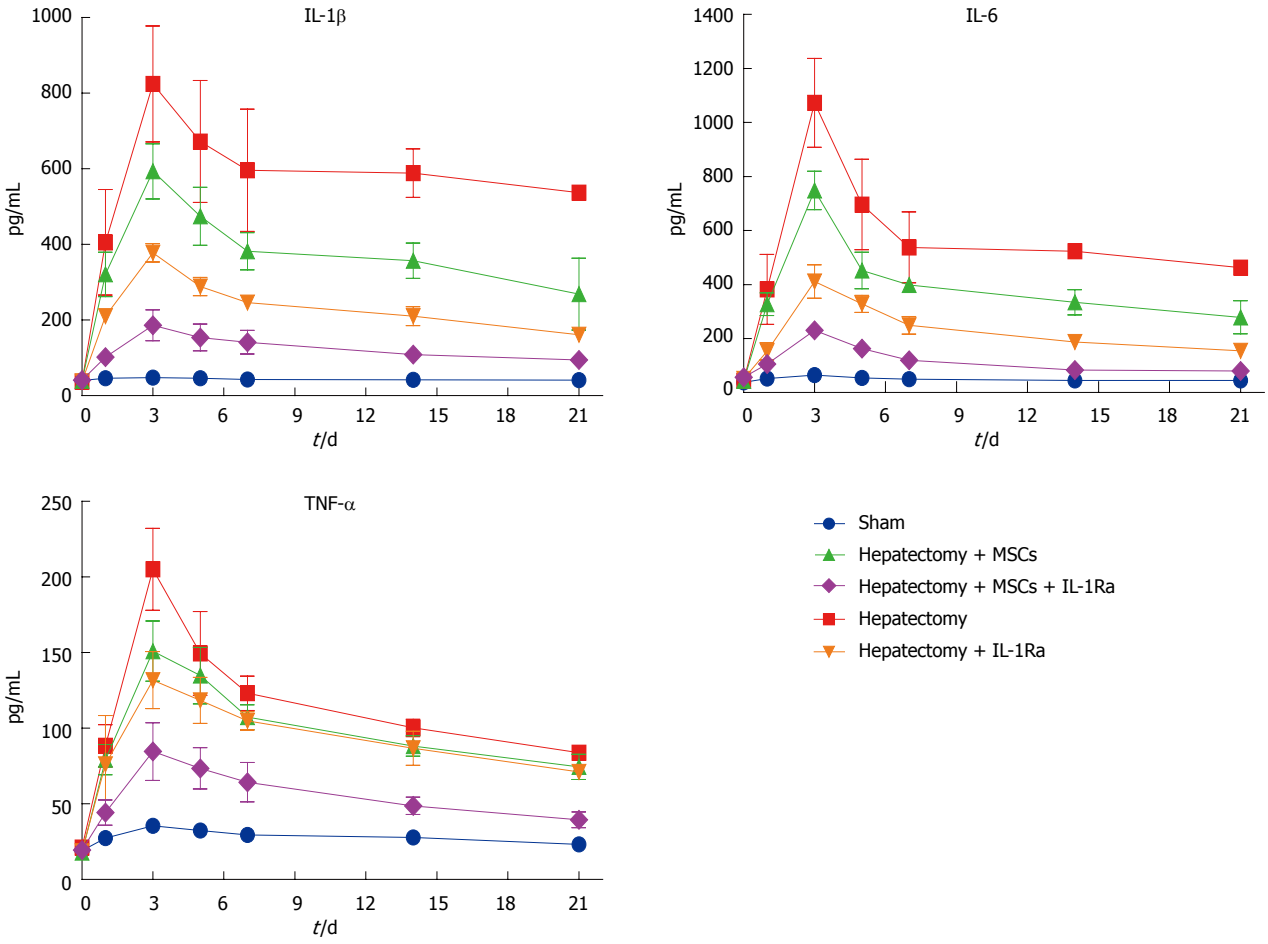

Figure 5 Serum levels of inflammatory cytokines. Serum samples collected at various times (0 d, 1 d, 3, d, 5 d, 7 d, 14 d, and 21 d) after surgery were analyzed for levels of IL-1β, IL-6, and TNF-α by ELISA. IL: Interleukin; IL-1Ra: IL-1 receptor antagonist; MSC: Mesenchymal stem cell transplantation; TNF: Tumor necrosis factor.

signal for nuclei were distributed around the hepatic lobules in the combined therapy group, representing even distribution of MSCs (Figure 7).

Assessment of hepatic apoptosis and regeneration

To determine the effect of combination therapy on ALF-related apoptosis, a TUNEL assay was performed (Figure 8). The cells in the model control group had many positively stained apoptotic cells that were round with brown nuclei (Figure 8B). The percentage of TUNEL-positive cells relative to the total cell count was used to estimate the apoptosis rate. The number of apoptotic cells in the sham group was low (0.8% ± 0.2%), while their number significantly increased following hepatectomy (70.8% ± 3.7%; $P < 0.01$) (Figure 8F). Apoptotic cells were also detected in the combined therapy group (Figure 8E); however, the apoptosis rate (18.1% ± 2.1%) was significantly lower compared to the IL-1Ra and MSC transplantation groups (39.5% ± 1.2% and 54.5% ± 6.0%, respectively) ($P < 0.01$) (Figure 8F).

To quantify hepatic regeneration, the expression of Ki67 was analyzed by immunohistochemistry (Figure 9). The expression of Ki67 was significantly increased in the hepatectomy group compared with the sham group ($P < 0.05$). The Ki67 index was also upregulated in the MSC transplantation and IL-1Ra groups, but the differences were not significant. By contrast, Ki67 expression was significantly increased in the combined therapy group ($P < 0.01$).

Analysis of cell signaling

To investigate whether Akt and NF-κB signaling pathways mediate hepatocyte injury, the expression levels of these two proteins were assessed by Western blotting. The expression levels of Akt and NF-κB were significantly increased in the model group compared with the sham group ($P < 0.05$) (Figure 10). Compared to the model group, the MSC transplantation group had significantly decreased expression of NF-κB ($P < 0.01$), but similar levels of Akt expression. Conversely, the IL-1Ra group showed significantly increased Akt expression ($P < 0.05$), with no change in NF-κB compared to the model group. In the combined therapy group, expression levels of both Akt and NF-κB were significantly different compared to

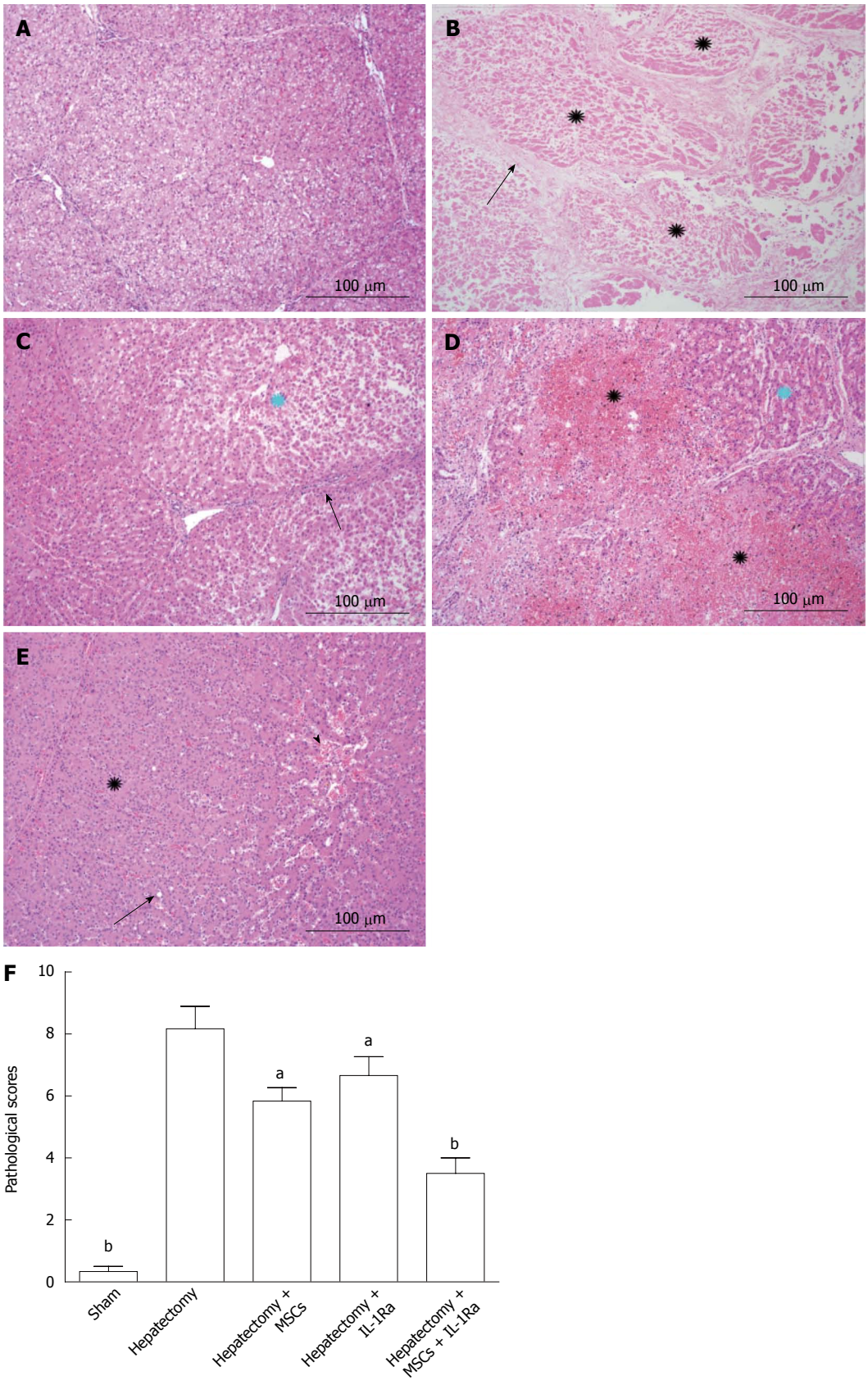

Figure 6 Histologic analysis of liver tissues. Hematoxylin and eosin staining of liver sections taken seven days post-hepatectomy in A: Normal, sham-operated control; B: After hepatectomy (black stars indicate complete necrosis in liver organization; black arrow represents interlobular fiber structure); C: With MSC transplantation (blue star shows a hepatic lobule near the central part and necrosis of hepatocytes; black arrow shows the fibrous tissue and some inflammatory cell infiltration); D: Treatment with IL-1Ra (black stars show hemorrhage and necrosis in the hepatic lobe; blue star represents the liver cells in the hemorrhagic area); E: Combined MSC transplantation and IL-1Ra treatment (black star shows a normal hepatic lobule; black arrows indicate fatty degeneration of hepatocytes and hepatic sinus dilation with hyperemia in central hepatic lobe) (magnification × 100, scale bar = 100 μm); F: Histopathologic scores of liver tissues after hepatectomy. $^{a}P < 0.05$ *vs* hepatectomy + MSCs + IL-1Ra; $^{b}P < 0.01$ *vs* hepatectomy. IL-1Ra: Interleukin-1 receptor antagonist; MSC: Mesenchymal stem cell transplantation.

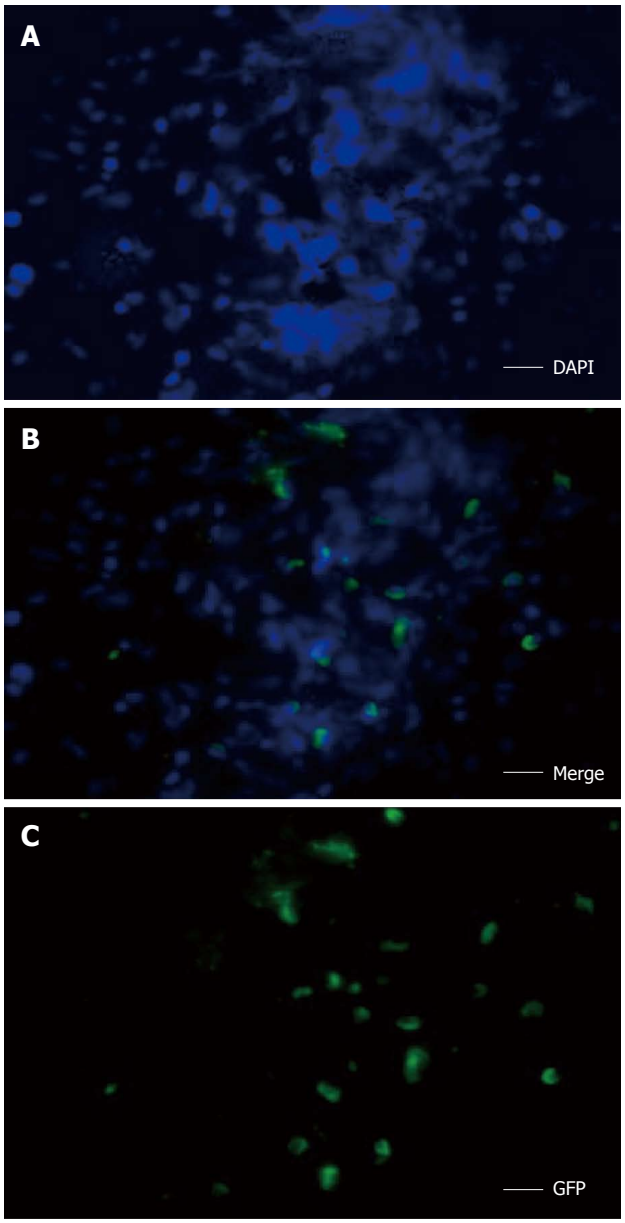

Figure 7 Fluorescence microscopy of green fluorescent protein (GFP)-expressing mesenchymal stem cells. Transplanted cells in the combined therapy group were distributed around the hepatic lobule (nuclei are stained blue with DAPI; scale bar = 20 μm).

the model group ($P < 0.01$).

DISCUSSION

ALF is a severe disease that aggravates liver cell necrosis. Partial hepatectomy leads to compensatory hypertrophy and hyperplasia in the remaining lobes of the liver to replace the lost functional mass. However, large-scale hepatectomy may cause ALF, the biggest problem in clinical settings. Bone-marrow-derived MSCs may thus be a potential therapeutic choice, because their mesodermal origin represents multipotent adult stem cells with the potential for self-renewal[23]. Petersen *et al*[24] and Schwartz *et al*[25] showed that MSCs possess the ability to differentiate into hepatocytes, both *in vitro* and *in vivo*. However, despite the ability of MSCs to differentiate, the limited MSC transplantation efficiency is a major obstacle due to microcirculatory dysfunction and inflammatory environment. Proinflammatory mediators, such as IL-1, IL-2, and TNF-α, create an inflammatory environment in ALF, leading to reduced survival and differentiation of the transplanted MSCs, thereby limiting the therapeutic role of the transplantation[26]. Increased levels of proinflammatory cytokines, including IL-1β, IL-6, and TNF-α, are seen in all hepatectomized animals[27].

Exogenous IL-1Ra reduces some proinflammatory mediators, thus providing a better inflammatory environment[28]. This results in increased liver cell proliferation and enhanced MSC transplantation efficiency. This effect may last at least three weeks with combined therapy. Indeed, in the combined therapy group, a continuous reduction in proinflammatory mediators was observed, which could be attributed to the disrupted inflammatory cycle caused by IL-1Ra in the early phase. This reduction was slightly ameliorated when MSCs were transplanted alone, but better results were achieved in the combined therapy group.

In our study, combined therapy resulted in: (1) reduction of liver injury biomarkers; (2) improvement in hepatic functional parameters; and (3) increased survival, as compared with IL-1Ra or MSC transplantation alone. Combined therapy improved liver serology of ALT, AST, ALP, and γ-GT, and provided a long-term survival benefit, observed as a significantly higher survival time compared to untreated animals. Furthermore, the histopathologic scores in the combined therapy group were significantly decreased compared with those in the model group. Combined therapy inhibited hepatocellular apoptosis and promoted liver cell proliferation in swine with ALF, thereby significantly improving their survival rate. Higher MSC transplantation efficiency may directly lead to a higher hepatocyte differentiation rate, proliferation level, and better liver function. In addition, proliferation in the combined therapy group was significantly higher than in the IL-1Ra or MSC transplantation groups alone. Therefore, we conclude that the combined therapy group had the best liver function. These results also suggest that the animals with lower levels of inflammatory cytokines have a higher MSC implantation rate. It is therefore important to improve the efficacy of MSC transplantation and to reduce the inflammation levels.

We further studied the potential mechanism of combined therapy in hepatic protection. Although much is known about the cytokines (hepatocyte priming) and growth factors (stimulating cell cycle progression) involved, a link between these two signaling pathways has yet to be illustrated. Akt has been shown to play

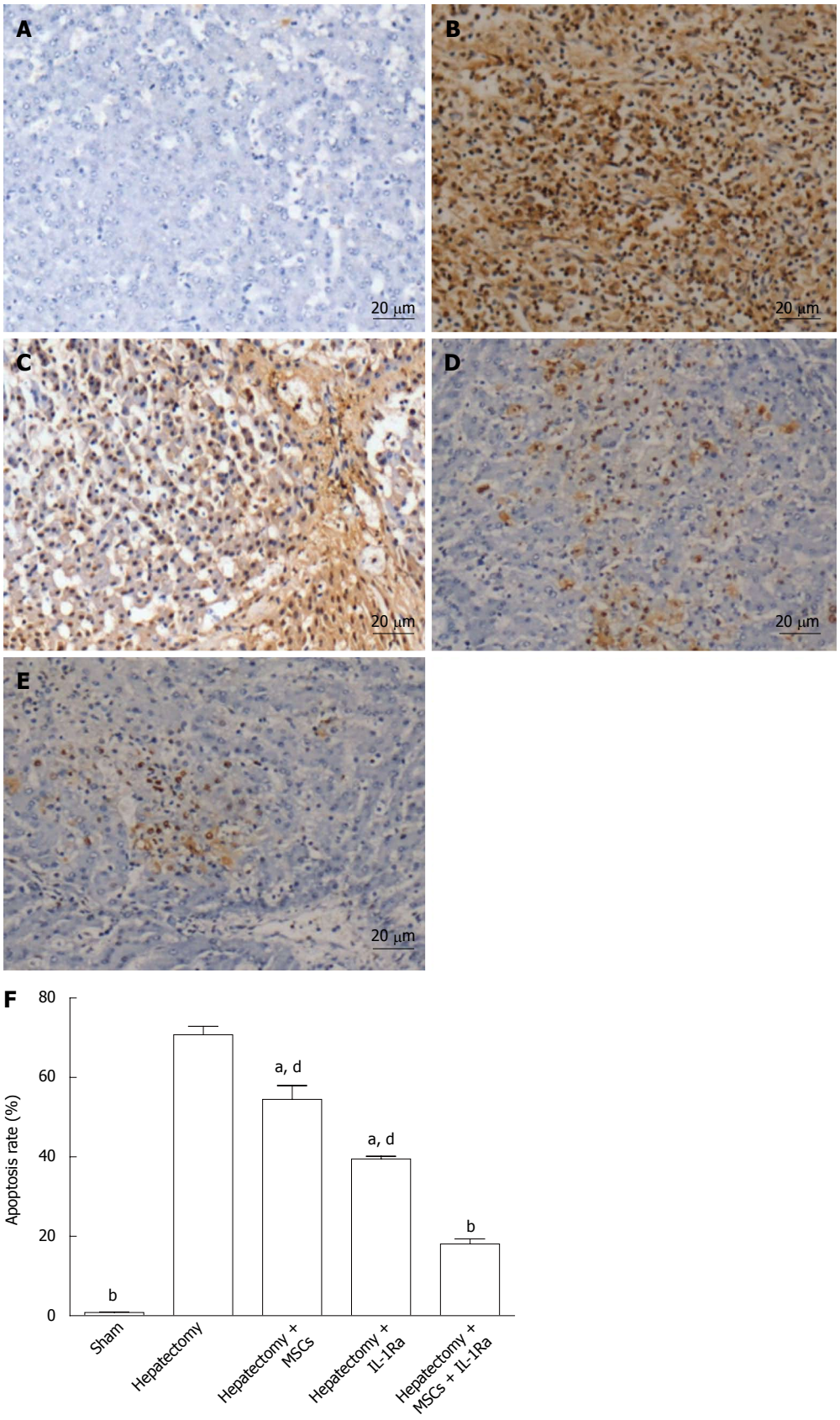

Figure 8 Assessment of apoptosis seven days after hepatectomy. Apoptotic cells were visualized by TUNEL staining in A: Normal, sham-operated control; B: After hepatectomy; C: With MSC transplantation; D: Treatment with IL-1Ra; and E: Combined MSC transplantation and IL-1Ra (magnification × 100; scale bar = 20 μm); F: Percentage of TUNEL-positive cells relative to the total cell count was used to estimate the apoptosis rate. [a]$P < 0.05$, [b]$P < 0.01$ *vs* hepatectomy model group; [d]$P < 0.01$ *vs* hepatectomy + MSCs + IL-1Ra combination therapy group. IL-1Ra: Interleukin-1 receptor antagonist; MSC: Mesenchymal stem cell transplantation; TUNEL: Terminal deoxynucleotidyl transferase dUTP nick end labeling.

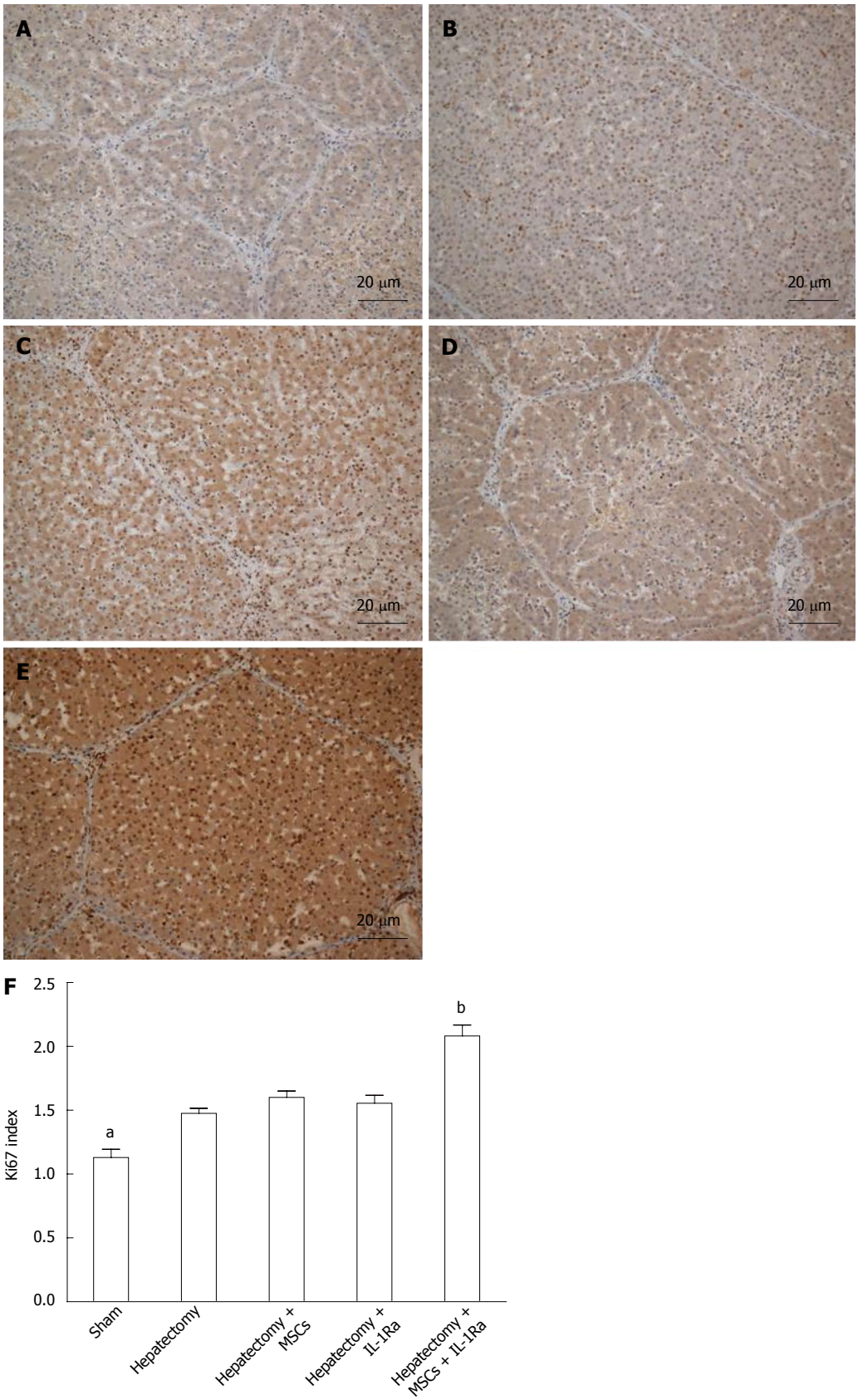

Figure 9 Hepatic cell proliferation. Expression of Ki67 protein was determined by immunohistochemistry in A: Normal, sham-operated control; B: After hepatectomy; C: With MSC transplantation; D: Treatment with IL-1Ra; and E: Combined MSC transplantation and IL-1Ra (magnification × 100; scale bar = 20 μm); F: Percentage of Ki67-stained hepatocytes per total number of hepatocytes was used as calculate the Ki67 index. $^{a}P < 0.05$, $^{b}P < 0.01$ *vs* hepatectomy. IL-1Ra: Interleukin-1 receptor antagonist; MSC: Mesenchymal stem cell transplantation.

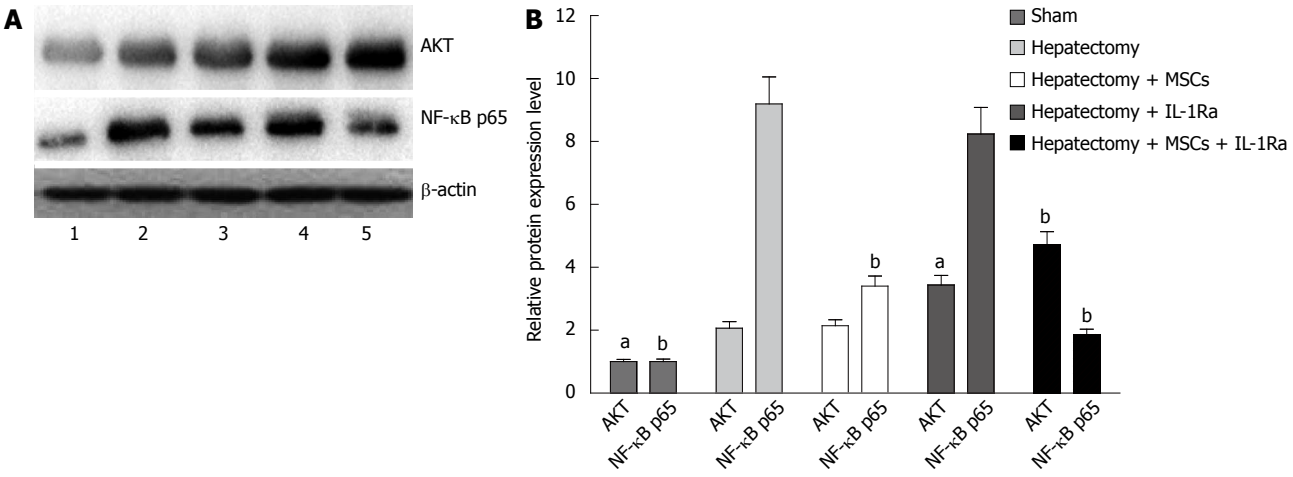

Figure 10 Western blot analysis for expression of Akt and NF-κB after acute liver injury. A: Representative Western blot showing Akt, NF-κB, and β-actin (lane 1, normal control; lane 2, hepatectomy; lane 3, with IL-1Ra treatment; lane 4, with MSC transplantation; lane 5, with MSC transplantation and IL-1Ra treatment. B: Band densitometry was expressed as fold change relative to the internal control (n = 6). $^{a}P < 0.05$, $^{b}P < 0.01$ *vs* hepatectomy. Akt: Protein kinase B; IL-1Ra: Interleukin-1 receptor antagonist; MSC: Mesenchymal stem cell transplantation; NF-κB: Nuclear factor κB.

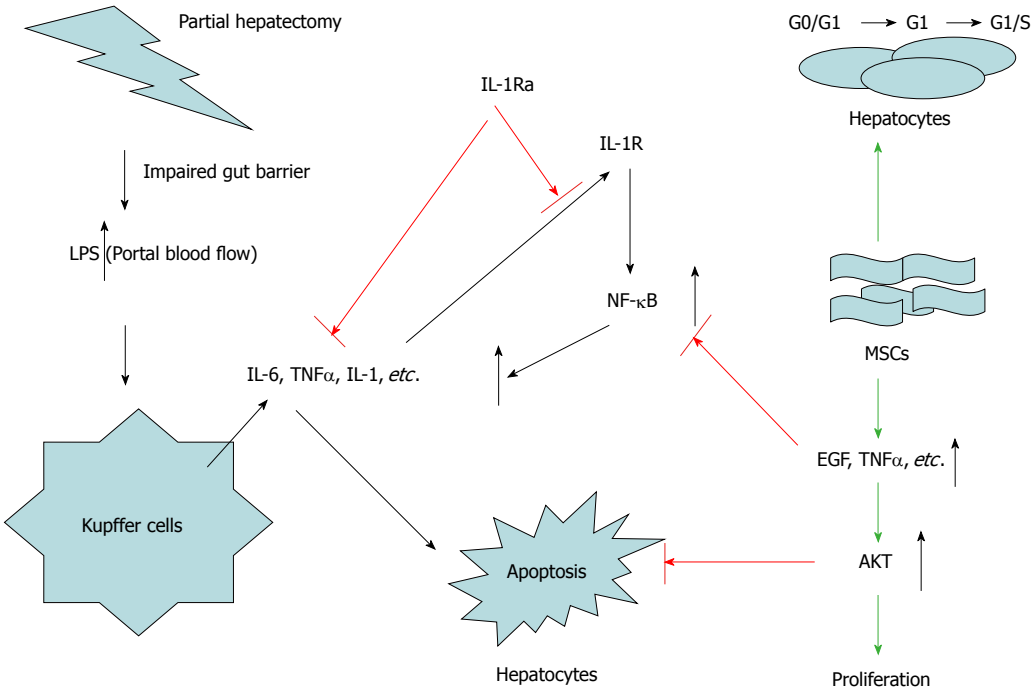

Figure 11 Schematic illustrating the proposed dual mechanism of action of combination therapy. (1) Inhibition of NF-κB leads to decreased IL-1, IL-6, and TNF-α expression, which appears to be the central mechanism by which IL-1Ra combines with MSC transplantation to promote regeneration of liver cells. (2) Upregulation of Akt expression due to EGF and TGF-α growth factors induces hepatocyte survival, DNA synthesis, and cell division. Cytokines, including IL-1, IL-6, and TNF-α, are secreted by nonparenchymal cells, such as Kupffer cells and sinusoidal epithelial cells, following hepatectomy. Exogenous IL-1Ra blocks IL-1R, reducing proinflammatory mediators, and enhancing MSC transplantation efficiency. This benefits initial priming of hepatocytes, with the transition of quiescent hepatocytes from the G0 to G1 stage of the cell cycle. Effective MSC transplantation may induce upregulation of growth factors such as hepatocyte growth factor, EGF and TGF-α, which promote Akt signaling pathways, producing an antiapoptotic effect and benefiting liver regeneration. Akt: Protein kinase B; EGF: Epidermal growth factor; IL: Interleukin; IL-1Ra: IL-1 receptor antagonist; MSC: Mesenchymal stem cell transplantation; NF-κB: Nuclear factor κB; TGF: Transforming growth factor; TNF: Tumor necrosis factor.

an important role in the compensatory recovery of liver mass following resection by regulating hepatocyte hypertrophy[29]. In addition to its role in leukocyte trafficking, signaling and phagocytosis, Akt also plays an important role in cell survival and proliferation. Similarly, elevation of Akt expression in the combined therapy group in our study supports higher liver cell proliferation and inhibition of apoptosis.

Hepatectomy-induced liver injury results in increased hepatocellular apoptosis as well as inflammation. This strongly inhibits the therapeutic effect of MSC transplantation. Effective MSC transplantation may

induce secretion of growth factors that participate in the priming phase of liver regeneration, which makes hepatocytes responsive to growth factors such as hepatocyte growth factor, epidermal growth factor, and transforming growth factor-α, and promotes hepatocyte replication and liver growth *in vivo*[30]. Pathways such as Akt signaling are central to protecting hepatocytes from apoptosis and to enhanced hepatic repair after liver injury. Inactivation of the Akt pathway results in delayed liver regeneration in mice[31]. The antiapoptotic effect of the Akt signaling pathway is *via* activation of Bcl-2, which in turn inhibits the apoptotic mediator, caspase-3[32].

The production of cytokines is a consequence of extensive liver necrosis as well as infection/sepsis, which frequently complicates ALF. Hepatectomy leads to increased levels of endotoxin in the portal circulation, thereby activating Kupffer cells to produce toxic mediators that cause liver injury[33]. Transcription factor NF-κB, a key regulator of genes involved in inflammation, is activated by endotoxin or oxidative stress, which results in its translocation to the nucleus and subsequent transcription of target genes[34]. NF-κB has long been considered as a prototypical proinflammatory signaling molecule, largely due to the activation of NF-κB by proinflammatory cytokines such as IL-1 and TNF-α. In the present study, hepatectomy caused a compensatory increase in Akt and NF-κB expression. However, combined therapy decreased NF-κB levels, which likely then results in reduced expression of genes involved in inflammation, an effect that is important for MSC transplantation and liver regeneration after hepatectomy. It is generally considered that inhibition of apoptosis and promotion of cell proliferation are possible major outcomes of intraportal MSC transplantation with IL-1Ra administration.

As Akt and NF-κB are important regulators of hepatic regeneration following partial hepatectomy, we propose a dual-action mechanism for combination therapy involving these two signaling molecules: (1) inhibition of NF-κB leads to decreased IL-1, IL-6, and TNF-α expression, which results in better MSC transplantation with IL-Ra administration, thus promoting regeneration of liver cells; (2) upregulation of Akt expression due to growth factors (hepatocyte growth factor, epidermal growth factor, transforming growth factor-α) induces hepatocyte survival, DNA synthesis and cell division (Figure 11).

In summary, combination therapy appears to be superior to MSC transplantation alone. Our data revealed that combination therapy could improve liver function, inhibit apoptosis, and prolong the survival time of swine with ALF. The transplanted MSCs may quickly participate in liver regeneration by promoting proliferation and inhibiting apoptosis during the initial stage of ALF, after the IL-1 inflammation signaling pathway is blocked by IL-Ra. Combination therapy with IL-1Ra and MSC transplantation, which enables restoration from acute liver injury and reconstruction in swine, is a promising treatment option for patients with ALF. This increased understanding of the liver regeneration cascade in MSC transplantation combined with IL-1Ra administration could lead to improved clinical outcomes for treatment of acute or chronic liver failure.

COMMENTS

Background

Acute liver failure (ALF) is characterized by severe liver cell damage caused by virus infection, drugs, toxins, alcohol, or hepatectomy. ALF leads to hepatic encephalopathy, hepatorenal syndrome, severe infection, multiple organ failure, and even death. Combating ALF requires either reduction of liver cell necrosis or stimulation of liver cell regeneration. So far, liver transplantation is the most effective treatment for ALF. However, it has its own limitations, including severe donor shortage, numerous complications, immune rejection, use of immunosuppressive agents, and high medical costs.

Research frontiers

In recent years, therapy with stem cells has become a new area of investigation for ALF treatment. This is mainly attributable to their abundant availability, low immunogenicity, and potential of differentiating into hepatocyte-like cells. Experimental studies have demonstrated that microcirculatory dysfunction and an inflammatory environment are determinants of ALF, and proinflammatory mediators such as interleukin (IL)-1, IL-2, and tumor necrosis factor-α are the key players in ALF.

Innovations and breakthroughs

In this study, the authors hypothesized that reducing inflammation in the acutely injured liver can benefit the efficacy of mesenchymal stem cell (MSC) transplantation in ALF patients. IL-1 receptor antagonist (IL-1Ra) was injected to reduce liver inflammation, in addition to MSC transplantation through the portal vein in a swine model of ALF. The liver functions before and after MSC transplantation with or without IL-Ra were compared by measuring the changes in serum levels of alanine aminotransferase, aspartate transaminase, alkaline phosphatase, and γ-glutamyl transpeptidase. In addition, pathologic injury and hepatic cell apoptosis were also examined.

Applications

This study revealed that combination therapy improves liver function, inhibits apoptosis, and prolongs the survival of swine with ALF. The transplanted MSCs may quickly participate in liver regeneration by promoting proliferation and inhibiting apoptosis during the initial stage of ALF, after the IL-1 inflammation signaling pathway is blocked by IL-Ra. Combination therapy with IL-1Ra and MSC transplantation, which enables restoration from acute liver injury and reconstruction in swine, is a promising treatment option for patients with ALF in the future. This enhanced understanding of the liver regeneration cascade in MSC transplantation combined with IL-1Ra administration could lead to improved clinical outcomes for the treatment of acute or chronic liver failure.

Terminology

IL-1Ra is a natural IL-1 antagonist that can block the inflammatory process by competitively binding to the IL-1 receptor with equal avidity to IL-1. It inhibits the stimulation of downstream signaling and thereby reduces inflammation.

Peer-review

This study provided a new way to restore or treat ALF. The result of the study showed that combination therapy with MSCs and IL-1Ra can increase liver regeneration after hepatectomy in a swine model of ALF. The study appears promising and demonstrates the preclinical application of MSCs.

REFERENCES

1 **Bernal W**, Wendon J. Acute liver failure. *N Engl J Med* 2013; **369**:

2525-2534 [PMID: 24369077 DOI: 10.1056/NEJMra1208937]
2 **Hoyer DP**, Munteanu M, Canbay A, Hartmann M, Gallinat A, Paul A, Saner FH. Liver transplantation for acute liver failure: are there thresholds not to be crossed? *Transpl Int* 2014; **27**: 625-633 [PMID: 24606197 DOI: 10.1111/tri.12302]
3 **Pan XN**, Zheng LQ, Lai XH. Bone marrow-derived mesenchymal stem cell therapy for decompensated liver cirrhosis: a meta-analysis. *World J Gastroenterol* 2014; **20**: 14051-14057 [PMID: 25320545 DOI: 10.3748/wjg.v20.i38.14051]
4 **O'Grady J**. Timing and benefit of liver transplantation in acute liver failure. *J Hepatol* 2014; **60**: 663-670 [PMID: 24211740 DOI: 10.1016/j.jhep.2013.10.024]
5 **Buzhor E**, Leshansky L, Blumenthal J, Barash H, Warshawsky D, Mazor Y, Shtrichman R. Cell-based therapy approaches: the hope for incurable diseases. *Regen Med* 2014; **9**: 649-672 [PMID: 25372080 DOI: 10.2217/rme.14.35]
6 **Ma HC**, Shi XL, Ren HZ, Yuan XW, Ding YT. Targeted migration of mesenchymal stem cells modified with CXCR4 to acute failing liver improves liver regeneration. *World J Gastroenterol* 2014; **20**: 14884-14894 [PMID: 25356048 DOI: 10.3748/wjg.v20.i40.14884]
7 **Deng C**, Qin A, Zhao W, Feng T, Shi C, Liu T. Up-regulation of CXCR4 in rat umbilical mesenchymal stem cells induced by serum from rat with acute liver failure promotes stem cells migration to injured liver tissue. *Mol Cell Biochem* 2014; **396**: 107-116 [PMID: 25098450 DOI: 10.1007/s11010-014-2147-7]
8 **Volarevic V**, Nurkovic J, Arsenijevic N, Stojkovic M. Concise review: Therapeutic potential of mesenchymal stem cells for the treatment of acute liver failure and cirrhosis. *Stem Cells* 2014; **32**: 2818-2823 [PMID: 25154380 DOI: 10.1002/stem.1818]
9 **Raicevic G**, Najar M, Najimi M, El Taghdouini A, van Grunsven LA, Sokal E, Toungouz M. Influence of inflammation on the immunological profile of adult-derived human liver mesenchymal stromal cells and stellate cells. *Cytotherapy* 2015; **17**: 174-185 [PMID: 25455740 DOI: 10.1016/j.jcyt.2014.10.001]
10 **Qingqing M**, Xin Z, Meizhong S. Bone marrow mesenchymal stem cells altered the immunoregulatory activities of hepatic natural killer cells. *Clin Res Hepatol Gastroenterol* 2014; **38**: 689-698 [PMID: 25241998 DOI: 10.1016/j.clinre.2014.06.001]
11 **Xiao JQ**, Shi XL, Ma HC, Tan JJ, Lin-zhang Q, Ding YT. Administration of IL-1Ra chitosan nanoparticles enhances the therapeutic efficacy of mesenchymal stem cell transplantation in acute liver failure. *Arch Med Res* 2013; **44**: 370-379 [PMID: 23916885 DOI: 10.1016/j.arcmed.2013.06.004]
12 **Nguyen NT**, Vierling JM. Acute liver failure. *Curr Opin Organ Transplant* 2011; **16**: 289-296 [PMID: 21519261 DOI: 10.1097/MOT.0b013e328346c8ee]
13 **Nakae H**, Yonekawa T, Narita K, Endo S. Are proinflammatory cytokine concentrations reduced by plasma exchange in patients with severe acute hepatic failure? *Res Commun Mol Pathol Pharmacol* 2001; **109**: 65-72 [PMID: 11458986]
14 **Jensen LE**, Muzio M, Mantovani A, Whitehead AS. IL-1 signaling cascade in liver cells and the involvement of a soluble form of the IL-1 receptor accessory protein. *J Immunol* 2000; **164**: 5277-5286 [PMID: 10799889 DOI: 10.4049/jimmunol.164.10.5277]
15 **Volarevic V**, Al-Qahtani A, Arsenijevic N, Pajovic S, Lukic ML. Interleukin-1 receptor antagonist (IL-1Ra) and IL-1Ra producing mesenchymal stem cells as modulators of diabetogenesis. *Autoimmunity* 2010; **43**: 255-263 [PMID: 19845478 DOI: 10.3109/08916930903305641]
16 **Sekiyama KD**, Yoshiba M, Thomson AW. Circulating proinflammatory cytokines (IL-1 beta, TNF-alpha, and IL-6) and IL-1 receptor antagonist (IL-1Ra) in fulminant hepatic failure and acute hepatitis. *Clin Exp Immunol* 1994; **98**: 71-77 [PMID: 7923888 DOI: 10.1111/j.1365-2249.1994.tb06609.x]
17 **Pihlajamäki J**, Kuulasmaa T, Kaminska D, Simonen M, Kärjä V, Grönlund S, Käkelä P, Pääkkönen M, Kainulainen S, Punnonen K, Kuusisto J, Gylling H, Laakso M. Serum interleukin 1 receptor antagonist as an independent marker of non-alcoholic steatohepatitis in humans. *J Hepatol* 2012; **56**: 663-670 [PMID: 22027586 DOI: 10.1016/j.jhep.2011.10.005]
18 **Hu J**, Yan D, Gao J, Xu C, Yuan Y, Zhu R, Xiang D, Weng S, Han W, Zang G, Yu Y. rhIL-1Ra reduces hepatocellular apoptosis in mice with acetaminophen-induced acute liver failure. *Lab Invest* 2010; **90**: 1737-1746 [PMID: 20644519 DOI: 10.1038/labinvest.2010.127]
19 **Brückner S**, Tautenhahn HM, Winkler S, Stock P, Jonas S, Dollinger M, Christ B. Isolation and hepatocyte differentiation of mesenchymal stem cells from porcine bone marrow--"surgical waste" as a novel MSC source. *Transplant Proc* 2013; **45**: 2056-2058 [PMID: 23769107 DOI: 10.1016/j.transproceed.2013.01.101]
20 **Eshkenazy R**, Dreznik Y, Lahat E, Zakai BB, Zendel A, Ariche A. Small for size liver remnant following resection: prevention and management. *Hepatobiliary Surg Nutr* 2014; **3**: 303-312 [PMID: 25392842 DOI: 10.3978/j.issn.2304-3881.2014.09.08]
21 **Yuan H**, Li L, Zheng W, Wan J, Ge P, Li H, Zhang L. Antidiabetic drug metformin alleviates endotoxin-induced fulminant liver injury in mice. *Int Immunopharmacol* 2012; **12**: 682-688 [PMID: 22330083 DOI: 10.1016/j.intimp.2012.01.015]
22 **Zhang ZF**, Lu J, Zheng YL, Hu B, Fan SH, Wu DM, Zheng ZH, Shan Q, Liu CM. Purple sweet potato color protects mouse liver against d-galactose-induced apoptosis via inhibiting caspase-3 activation and enhancing PI3K/Akt pathway. *Food Chem Toxicol* 2010; **48**: 2500-2507 [PMID: 20600541 DOI: 10.1016/j.fct.2010.06.023]
23 **Zhang S**, Chen L, Liu T, Zhang B, Xiang D, Wang Z, Wang Y. Human umbilical cord matrix stem cells efficiently rescue acute liver failure through paracrine effects rather than hepatic differentiation. *Tissue Eng Part A* 2012; **18**: 1352-1364 [PMID: 22519429 DOI: 10.1089/ten.TEA.2011.0516]
24 **Petersen BE**, Bowen WC, Patrene KD, Mars WM, Sullivan AK, Murase N, Boggs SS, Greenberger JS, Goff JP. Bone marrow as a potential source of hepatic oval cells. *Science* 1999; **284**: 1168-1170 [PMID: 10325227 DOI: 10.1126/science.284.5417.1168]
25 **Schwartz RE**, Reyes M, Koodie L, Jiang Y, Blackstad M, Lund T, Lenvik T, Johnson S, Hu WS, Verfaillie CM. Multipotent adult progenitor cells from bone marrow differentiate into functional hepatocyte-like cells. *J Clin Invest* 2002; **109**: 1291-1302 [PMID: 12021244 DOI: 10.1172/JCI15182]
26 **Vollmar B**, Menger MD. The hepatic microcirculation: mechanistic contributions and therapeutic targets in liver injury and repair. *Physiol Rev* 2009; **89**: 1269-1339 [PMID: 19789382 DOI: 10.1152/physrev.00027.2008]
27 **Xu CS**, Jiang Y, Zhang LX, Chang CF, Wang GP, Shi RJ, Yang YJ. The role of Kupffer cells in rat liver regeneration revealed by cell-specific microarray analysis. *J Cell Biochem* 2012; **113**: 229-237 [PMID: 21898544 DOI: 10.1002/jcb.23348]
28 **Petrasek J**, Bala S, Csak T, Lippai D, Kodys K, Menashy V, Barrieau M, Min SY, Kurt-Jones EA, Szabo G. IL-1 receptor antagonist ameliorates inflammasome-dependent alcoholic steatohepatitis in mice. *J Clin Invest* 2012; **122**: 3476-3489 [PMID: 22945633 DOI: 10.1172/JCI60777]
29 **Jackson LN**, Larson SD, Silva SR, Rychahou PG, Chen LA, Qiu S, Rajaraman S, Evers BM. PI3K/Akt activation is critical for early hepatic regeneration after partial hepatectomy. *Am J Physiol Gastrointest Liver Physiol* 2008; **294**: G1401-G1410 [PMID: 18388186 DOI: 10.1152/ajpgi.00062.2008]
30 **Vandermeulen M**, Grégoire C, Briquet A, Lechanteur C, Beguin Y, Detry O. Rationale for the potential use of mesenchymal stromal cells in liver transplantation. *World J Gastroenterol* 2014; **20**: 16418-16432 [PMID: 25469010 DOI: 10.3748/wjg.v20.i44.16418]
31 **Pan N**, Lv X, Liang R, Wang L, Liu Q. Suppression of graft regeneration, not ischemia/reperfusion injury, is the primary cause of small-for-size syndrome after partial liver transplantation in mice. *PLoS One* 2014; **9**: e93636 [PMID: 24709852 DOI: 10.1371/journal.pone.0093636]
32 **Wang W**, Du Z, Yan J, Ma D, Shi M, Zhang M, Peng C, Li H. Mesenchymal stem cells promote liver regeneration and prolong survival in small-for-size liver grafts: involvement of C-Jun

N-terminal kinase, cyclin D1, and NF-κB. *PLoS One* 2014; **9**: e112532 [PMID: 25479410 DOI: 10.1371/journal.pone.0112532]

33 **Nanji AA**, Jokelainen K, Tipoe GL, Rahemtulla A, Thomas P, Dannenberg AJ. Curcumin prevents alcohol-induced liver disease in rats by inhibiting the expression of NF-kappa B-dependent genes. *Am J Physiol Gastrointest Liver Physiol* 2003; **284**: G321-G327 [PMID: 12388178 DOI: 10.1152/ajpgi.00230.2002]

34 **Lawrence T**. The nuclear factor NF-kappaB pathway in inflammation. *Cold Spring Harb Perspect Biol* 2009; **1**: a001651 [PMID: 20457564 DOI: 10.1101/cshperspect.a001651]

P- Reviewer: Gao B, Mendez I, Wang GY **S- Editor**: Gong ZM
L- Editor: Filipodia **E- Editor**: Zhang DN

World Journal of Gastroenterology

Submit a Manuscript: http://www.wjgnet.com/esps/
Help Desk: http://www.wjgnet.com/esps/helpdesk.aspx
DOI: 10.3748/wjg.v22.i16.4136

World J Gastroenterol 2016 April 28; 22(16): 4136-4148
ISSN 1007-9327 (print) ISSN 2219-2840 (online)

ORIGINAL ARTICLE

Basic Study

Recombinant adenovirus containing hyper-interleukin-6 and hepatocyte growth factor ameliorates acute-on-chronic liver failure in rats

Dan-Dan Gao, Jia Fu, Bo Qin, Wen-Xiang Huang, Chun Yang, Bei Jia

Dan-Dan Gao, Jia Fu, Bo Qin, Wen-Xiang Huang, Chun Yang, Bei Jia, Chongqing Key Laboratory of Infectious Diseases and Parasitic Diseases, Department of Infectious Diseases, The First Affiliated Hospital of Chongqing Medical University, Chongqing 400016, China

Author contributions: Jia B, Yang C, Qin B, Gao DD and Huang WX conceived and designed the study; Gao DD performed the experiments and wrote the paper; Fu J provided the mutants; Jia B and Gao DD analysed the data; and Jia B reviewed and edited the manuscript. Yang C and Jia B made equal contributions to this work.

Supported by Natural Science Foundation of Chongqing, No. cstc2012jjA10052; and Young High-End Medical Reserve Personnel Training Plan Foundation of Chongqing, China.

Institutional review board statement: The study was reviewed and approved by Chongqing Science and Technology Committee with protocol number cstc2012jjA10052.

Institutional animal care and use committee statement: All of the procedures involving animals were reviewed and approved by the Institutional Animal Care and Use Committee of the Ethical Committee on Animal Experiments at First Affiliated Hospital of Chongqing Medical University (Chongqing, China) with the reference number 2015-3.

Conflict-of-interest statement: The authors declare no conflict of interest.

Data sharing statement: No additional data are available.

Correspondence to: Bei Jia, PhD, Chongqing Key Laboratory of Infectious Diseases and Parasitic Diseases, Department of Infectious Diseases, The First Affiliated Hospital of Chongqing Medical University, No. 1 Youyi Road, Yu Zhong District, Chongqing 400016, China. beijia7410@163.com
Telephone: +86-23-89012427
Fax: +86-23-89012430

Received: November 25, 2015
Peer-review started: November 26, 2016
First decision: December 30, 2015
Revised: February 1, 2016
Accepted: March 1, 2016
Article in press: March 2, 2016
Published online: April 28, 2016

Abstract

AIM: To investigate the protective efficacy of recombinant adenovirus containing hyper-interleukin-6 (Hyper-IL-6, HIL-6) and hepatocyte growth factor (HGF) (Ad-HGF-HIL-6) compared to that of recombinant adenovirus containing either HIL-6 or HGF (Ad-HIL-6 or Ad-HGF) in rats with acute-on-chronic liver failure (ACLF).

METHODS: The recombinant adenoviruses containing HIL-6 and/or HGF were constructed. We established an ACLF model, and rats were randomly assigned to control, model, Ad-GFP, Ad-HIL-6, Ad-HGF or Ad-HGF-HIL-6 group. We collected serum and liver tissue samples to test pathological changes, biochemical indexes and molecular biological indexes.

RESULTS: Attenuated alanine aminotransferase, prothrombin time, high-mobility group box 1 (HMGB1), endotoxin, tumour necrosis factor (TNF)-α and interferon-γ were observed in the Ad-HGF-, Ad-HIL-6- and Ad-HGF-HIL-6-treated rats with ACLF. Likewise, reduced hepatic

damage and apoptotic activity, as well as reduced HMGB1 and Bax proteins, but raised expression of Ki67 and Bcl-2 proteins and Bcl-2/Bax ratio were also observed in the Ad-HGF-, Ad-HIL-6- and Ad-HGF-HIL-6-treated rats with ACLF. More significant changes were observed in the Ad-HGF-HIL-6 treatment group without obvious side effects. Furthermore, caspase-3 at the protein level decreased in the Ad-HIL-6 and Ad-HGF-HIL-6 treatment groups, more predominantly in the latter group.

CONCLUSION: This study identifies that the protective efficacy of Ad-HGF-HIL-6 is more potent than that of Ad-HGF or Ad-HIL-6 in ACLF rats, with no significant side effects.

Key words: Acute-on-chronic liver failure; Recombinant adenovirus; Hyper-interleukin-6; Hepatocyte growth factor; Inflammatory cytokines

Core tip: The purport of our study was to analyse the protective efficacy of recombinant adenovirus containing hyper-interleukin-6 (Hyper-IL-6, HIL-6) and hepatocyte growth factor (HGF) (Ad-HGF-HIL-6) compared to that of recombinant adenovirus HIL-6 or HGF (Ad-HIL-6 or Ad-HGF) in rats with acute-on-chronic liver failure (ACLF). In summary, our results suggest that Ad-HGF-HIL-6 may confer a more powerful protective effect against ACLF than do Ad-HGF or Ad-HIL-6 in rats and can restrain the secretion of diverse inflammatory cytokines and reduce the apoptosis of hepatocytes. Ad-HGF-HIL-6 is likely to be a feasible protective therapy for serious liver injury.

Gao DD, Fu J, Qin B, Huang WX, Yang C, Jia B. Recombinant adenovirus containing hyper-interleukin-6 and hepatocyte growth factor ameliorates acute-on-chronic liver failure in rats. *World J Gastroenterol* 2016; 22(16): 4136-4148 Available from: URL: http://www.wjgnet.com/1007-9327/full/v22/i16/4136.htm DOI: http://dx.doi.org/10.3748/wjg.v22.i16.4136

INTRODUCTION

Acute-on-chronic liver failure (ACLF) refers to the patients with chronic liver diseases that have the raised perils of multiple organ failure or death following one or a few precipitating incidents, such as infection or bleeding. It still lacks an effective treatment so far. Viral vectors have been engineered for gene therapy against various types of infectious diseases[1,2]. The adenovirus vector has become the ideal vehicle for liver diseases due to its hepatotropism[3].

Previous studies have reported that IL-6 plays a critical and unique role during the process of early-stage hepatic regeneration response[4]. Hyper-interleukin-6 (Hyper-IL-6, HIL-6) is an artificial protein involving IL-6 connected with a variant of glycoprotein 80 (soluble interleukin 6 receptor, sIL-6R) by an artificial short linker. HIL-6 is a steady protein expressing biological activity dozens of times or even one thousand times stronger than that of IL-6/sIL-6R complex *in vitro* or *in vivo*[5]. HGF initiates liver regeneration after liver excision or chemical injuries[6-8]. The coadministration of IL-6 and HGF most effectively raised both the weight of unoccluded lobes and the DNA synthesis of hepatocytes in animals that underwent portal branch ligation (PBL) of the median branches and left lateral[9], suggesting a possible synergistic effect of these two factors. Our study assessed the protective effect of recombinant adenovirus containing HIL-6 and HGF compared to that of recombinant adenovirus containing either HIL-6 or HGF in an ACLF rat model.

MATERIALS AND METHODS

HEK293 cell culture

HEK (Human Embryonic Kidney) 293 is a cell line derived from human embryonic kidney cells grown in tissue culture. This particular line was initiated by the transformation and culturing of normal HEK cells with sheared adenovirus 5 DNA. HEK293 cells are used to produce viruses for biomedical research purposes. We culture the cell line in Dulbecco's modified Eagle's medium (Hyclone, Logan, UT, United States) supplemented with 10% foetal calf serum (Hyclone, Logan, UT, United States). Being cultured at 37 ℃ in 5% CO_2 provided a favorable growth environment for HEK293 cells. Medium was renewed 2-3 times a week, and cell counting was kept between 1×10^5 and 3×10^5 cells per millilitre.

Adenovirus vector and genes

Adenovirus vector GV314 (pDC315-3FLAG-sv40-EGFP) was used in this study. The vector and the primers for amplifying the Hyper-IL-6, HGF or HGF-IRES-Hyper-IL-6 ORF were purchased from Genechem Incorporation, Shanghai, China. pDC315-3FLAG-sv40-HGF-EGFP (Ad-HGF), pDC315-3FLAG-sv40-Hyper-IL-6-EGFP (Ad-HIL-6) and pDC315-3FLAG-sv40-HGF-IRES-Hyper-IL-6-EGFP (Ad-HGF-HIL-6) were constructed as previously described[10]. An "empty" vector pDC315-3FLAG-sv40-EGFP (Ad-GFP) was used as a negative control. The recombinant adenoviruses were greatly propagated with HEK293 cells for enhancing titre. Viruses for animal experimentation were purified by caesium chloride gradients as previously described[11].

Animals

Female Sprague-Dawley rats weighing 150-170 g were purchased from the Experimental Animal Centre of Chongqing Medical University (Chongqing, China).

Housing conditions were as detailed previously[12]. All rats were given humanitarian care in conformity to the international guidelines.

Induction of ACLF in rats

An ACLF rat model was performed as formerly depicted[13]. Briefly, human serum albumin (HAS; Octapharma m.b.H, Austria) was compounded with physiological saline in the proportion of 8 g/L and then emulsified with incomplete Freund's adjuvant of an equal amount. The rats received 0.5 mL of the prepared solution by multipoint subcutaneous injections four times in total (The first two times had a 14-d interval, and a 10-d intervals between the latter two). After that, the rats were given 4 mg HSA by tail intravenous injection twice in one week for a total of 6 wk. Finally, we induced ACLF in rats by intraperitoneal injection of D-galactosamine (D-GalN; 400 mg/kg) with lipopolysaccharide (LPS; 100 μg/kg) (Sigma-Aldrich Co., United States).

Experimental design

All the rats were divided into a control group (normal rats, n = 16), a model group (ACLF model rats, n = 16), an Ad-GFP group (Ad-GFP treated ACLF rats, n = 42), an Ad-HIL-6 group (Ad-HIL-6 treated ACLF rats, n = 42), an Ad-HGF group (Ad-HGF treated ACLF rats, n = 42), and an Ad-HGF-HIL-6 group (Ad-HGF-HIL-6 treated ACLF rats, n = 42). Adenoviruses were administered by caudal vein injection at a dose of 1×10^{10} viral particles in 100 μL (diluted with physiological saline) 3 h after the ACLF model had been induced. Meanwhile, the rats of the control and model groups received physiological saline by tail intravenous injection. The time of administration of adenovirus was marked as baseline (0 time point). Rats of all of the groups were sacrificed randomly for hepatic tissue and blood collection after adenovirus or physiological saline had been given for 24 h and 48 h.

Determinations of serum and plasma samples

An Automatic Hitachi Analyzer (Hitachi Inc., Japan) was utilized to test serum alanine aminotransferase (ALT). We also chose to avail of plasma prothrombin time (PT) to determine liver function. Serum endotoxin was tested with a commercial kit (Houshiji, Xiamen, China) in accordance with the instructions of the kit. ELISA kits (HMGB1 ELISA kit was purchased from Westang Co., China, tumour necrosis factor (TNF)-α and interferon (IFN)-γ ELISA kits were purchased from EBioscience Co., United Kingdom, respectively) were employed to measure serum levels of HMGB1, TNF-α and IFN-γ on the basis of the manufacturer's instructions.

Histopathology and immunohistochemistry

We used light microscopy to assess the histopathological changes of the liver. Parts of the right lobe of liver specimens were treated with 10% neutral formalin. Paraffin-embedded specimens were cut into 5 μm sections and stained with haematoxylin and eosin (HE). The extent of injury was determined by the criteria as the literature[14] described.

Ki67-related antigen is mainly localized in the nucleus by immunohistochemistry. The proliferation of hepatocytes was evaluated by Ki67-staining. After deparaffinised, sections were incubated in a prediluted monoclonal anti-Ki67 antibody (Roche Ventana) on an automatized medical system (BenchmarkXT, Ventana) utilizing a diaminobenzidin detection kit (Ventana/VIEW 3,30) based on the manufacturer's instructions.

Determinations of hepatocyte apoptosis by TUNEL assay

A detection kit (In Situ Cell Death Kit; Roche Diagnostics GmbH, Mannheim, Germany) was employed for accurate evaluation of the typical biochemical and morphological characteristics of apoptosis. We used proteinase K to treat paraffin-embedded liver sections, and so, hydrogen peroxide hampered the endogenous peroxidase activity. The sections were incubated in a terminal TdT/nucleotide compound at 37 ℃ for 1 h. Following that, the slides were washed in phosphate-buffered saline. Nuclear labeling was performed with horseradish peroxidase and diaminobenzidine. We performed counterstaining using hematoxylin. The apoptotic cells were observed and photographed under an optical microscope (Positive cells were dyed brown in nuclei.). Apoptosis was determined in eight liver samples of each group by counting 1000 cells from five sections of each sample. The percentage of positive cells was used to present apoptosis rates (%).

Determinations of HMGB1, Bcl-2, Bax and caspase-3 proteins by Western blot

Briefly, proteins extracted from liver samples were subjected to 10% SDS-PAGE, and transferred to PVDF membranes for 2 h. Western blots were then performed in accordance with a method previously described[15]. Glyceraldehyde-3-phosphate dehydrogenase (GAPDH; Santa Cruz Co., United States) was used as a control. Anti-HMGB1 antibody was purchased from Abcam Co., United Kingdom; Anti-caspase-3, -Bcl-2 and -Bax antibodies were purchased from CST Co., United States. Finally, an Odyssey infrared imaging system (LI-COR Co.) was used to detect the signals.

Real-time quantitative PCR for detection of Hyper-IL-6 and HGF

Trizol reagent (Invitrogen Co., United States) was used to extract total RNA from liver samples in accordance with the manufacturer's recommendations. Total RNA was reverse-transcribed employing a reagent kit (PrimeScript RT; TaKaRa Co. Ltd., Dalian, China) in accordance with standard instructions. The expression

Table 1 Primers for real-time PCR

Gene	Primer sequences
Hyper IL-6	Forward: 5'-GTCAGATCTATGCTGGCCGTCGGCTGC-3'
	Reverse: 5'-CCGGAATTCCTACATTTGCCGAAGAGCCCTC-3'
HGF	Forward: 5′-ATGATGTGGGGGACCAAA-3′
	Reverse: 5′-CAACTTGTATGTCAAAATTACTTTGTG-3′
β-*actin*	Forward: 5′-TGACGAGGCCCAGAGCAAGA-3′
	Reverse: 5′-ATGGGCACAGTGTGGGTGAC-3′

of the target genes in the liver was detected with SYBR Premix Ex TaqTM (Takara, Otsu, Japan), and a Real-Time PCR system (ABI PRISM 7500; Applied Biosystems, United States) was employed to perform the procedure. Designing specific primers for HIL-6, HGF and β-actin originated from known human sequences (Table 1) was performed using Oligo 7.0 Software. The PCR procedure for HIL-6, HGF and β-actin was composed of 95 ℃ for 10 min, 40 cycles of 94 ℃ for 5 s, 55 ℃ for 30 s and 72 ℃ for 30 s, and then 94 ℃ for 15 s. The data were collected automatically using the LightCycler (Roche, Switzerland), and then the value of the threshold cycle (Ct) was analysed on the basis of the $2^{-\Delta\Delta Ct}$ method[16].

Statistical analysis

The Kruskal-Wallis test was used to analyse histopathological score, Ki67 proliferation index and apoptosis rates (%) in our study. Two-way analysis of variance followed by Tukey's Honestly Significant Difference (HSD) test for independent samples was adopted to evaluate the other parameters in this study. We used SPSS 19.0 to perform statistical analysis, and regarded a *P*-value < 0.05 as having statistical significance.

RESULTS

Effect of recombinant adenovirus containing Hyper-IL-6 and HGF on plasma PT, serum ALT, HMGB1, endotoxin, TNF-α and IFN-γ

As shown in Figure 1, plasma PT, serum ALT, HMGB1, endotoxin, TNF-α and IFN-γ of the control group were 10.34 ± 0.69 s, 48.88 ± 7.29 IU/L, 454.15 ± 18.45 pg/mL, 0.013 ± 0.001 EU/mL, 59.85 ± 14.45 pg/mL and 46.21 ± 6.18 pg/mL at 24 h, and 9.69 ± 1.10 s, 51.77 ± 9.56 IU/L, 465.76 ± 46.84 pg/mL, 0.013 ± 0.001 EU/mL, 59.84 ± 6.94 pg/mL and 58.20 ± 15.04 pg/mL at 48 h, respectively. Plasma PT, serum ALT, HMGB1, endotoxin, TNF-α and IFN-γ increased significantly in the model group at 24 h and 48 h (24 h: 34.71 ± 2.79 s, 1206.13 ± 154.29 IU/L, 1115.02 ± 33.58 pg/mL, 0.049 ± 0.002 EU/mL, 257.84 ± 29.85 pg/mL and 172.17 ± 16.12 pg/mL, respectively, $P < 0.01$; 48 h: 42.76 ± 4.77 s, 2889.34 ± 305.46 IU/L, 1817.57 ± 121.50 pg/mL, 0.061 ± 0.002 EU/mL, 356.86 ± 14.34 pg/mL and 268.79 ± 8.34 pg/mL, respectively, $P < 0.01$) compared to the control group, however, the model group and the Ad-GFP group (Ad-GFP group at 24 h: 31.89 ± 3.88 s, 1255.25 ± 156.52 IU/L, 1121.35 ± 35.94 pg/mL, 0.048 ± 0.003 EU/mL, 260.07 ± 50.23 pg/mL and 174.70 ± 15.99 pg/mL, respectively; 48 h: 40.87 ± 5.13 s, 3034.15 ± 156.52 IU/L, 1810.71 ± 138.75 pg/mL, 0.051 ± 0.001 EU/mL, 357.81 ± 14.17 pg/mL and 267.53 ± 10.68 pg/mL, respectively) showed no statistical discrepancy at the two time points ($P > 0.05$).

Compared to the Ad-GFP group, plasma PT, serum ALT, HMGB1, endotoxin and IFN-γ were markedly lower in the Ad-HGF group (24 h: 25.95 ± 2.16 s, 285.00 ± 29.05 IU/L, 973.14 ± 46.55 pg/mL, 0.039 ± 0.001 EU/mL, 133.02 ± 15.13 pg/mL, respectively, $P < 0.01$; 48 h: 31.98 ± 5.79 s, 1342.87 ± 325.09 IU/L, 1233.17 ± 24.63 pg/mL, 0.046 ± 0.003 EU/mL, 193.64 ± 9.16 pg/mL, respectively, $P < 0.01$), Ad-HIL-6 group (24 h: 26.98 ± 2.22 s, 310.75 ± 24.38 IU/L, 1026.41 ± 49.25 pg/mL, 0.043 ± 0.002 EU/mL, 150.07 ± 20.60 pg/mL, respectively, $P < 0.01$; 48 h: 30.66 ± 4.87 s, 1127.54 ± 217.88 IU/L, 1303.32 ± 107.31 pg/mL, 0.051 ± 0.002 EU/mL, 205.64 ± 9.18 pg/mL, respectively, $P < 0.01$) and Ad-HGF-HIL-6 group (24 h: 19.88 ± 4.72 s, 227.38 ± 32.78 IU/L, 925.67 ± 32.95 pg/mL, 0.036 ± 0.002 EU/mL and 111.87 ± 11.24 pg/mL, respectively, $P < 0.01$; 48 h: 23.77 ± 5.31 s, 578.87 ± 87.47 IU/L, 1093.40 ± 35.86 pg/mL, 0.041 ± 0.001 EU/mL and 163.97 ± 12.89 pg/mL, respectively, $P < 0.01$) at 24 h and 48 h, and the changes were more predominant in the latter group at two time points ($P < 0.05$). Serum TNF-α also decreased in ACLF rats with the administration of Ad-HGF-HIL-6 (24 h: 166.43 ± 22.20 pg/mL; 48 h: 279.68 ± 30.31 pg/mL), Ad-HGF (24 h: 191.11 ± 28.30 pg/mL; 48 h: 302.13 ± 12.69 pg/mL) OR Ad-HIL-6 (24 h: 203.76 ± 13.73 pg/mL; 48 h: 313.52 ± 27.39 pg/mL) compared to rats in the Ad-GFP group (24 h: 257.84 ± 29.85 pg/mL, 48 h: 357.81 ± 14.17 pg/mL; $P < 0.01$) at 24 h and 48 h. A greater effect in reducing serum levels of TNF-α of ACLF rats was observed from the administration of Ad-HGF-HIL-6 compared to Ad-HIL-6 ($P < 0.05$), but serum TNF-α between the Ad-HGF-HIL-6 group and Ad-HGF group or between the model group (24 h: 260.07 ± 50.23 pg/mL, 48 h: 356.86 ± 14.34 pg/mL) and Ad-GFP group had no significant differences ($P > 0.05$).

Effect of recombinant adenovirus containing Hyper-IL-6 and HGF on liver histopathology and Ki67 expression

HE staining revealed neither the necrosis nor the degeneration of hepatic lobule in the liver samples of the control group (Figure 2). However, widespread necrosis was detected in the model and Ad-GFP groups, whereas histology of samples was significantly ameliorated in rats of all of the recombinant adenovirus (not including Ad-GFP) treatment groups, which displayed an obvious diminish of inflammatory cell infiltration, amelioration of liver cell swelling, and less pyrenolysis. These changes were more obvious in the Ad-HGF-HIL-6 group. The histopathological score comparison is

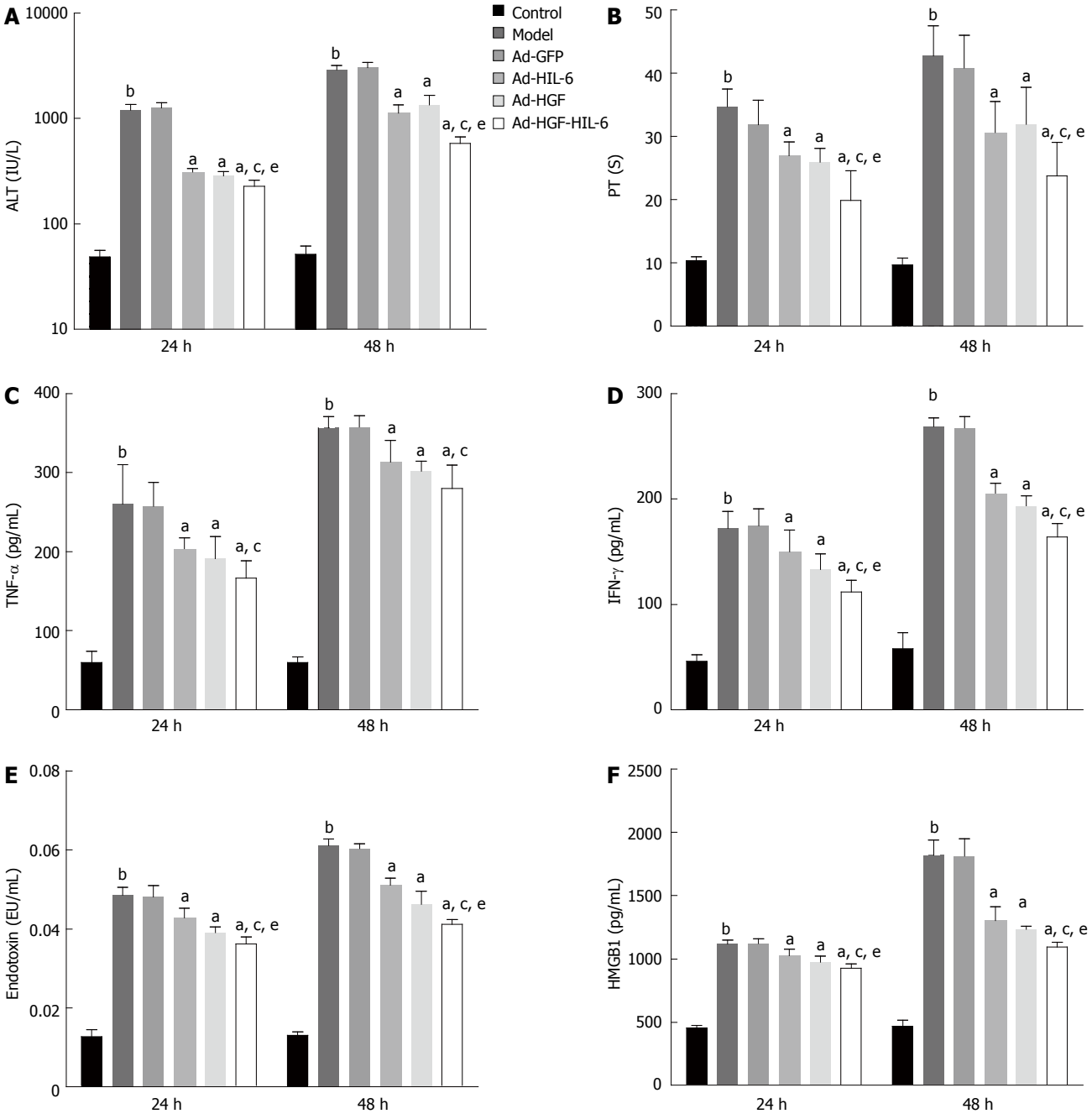

Figure 1 Effect of pDC315-3FLAG-sv40-HGF-IRES-Hyper-IL-6-EGFP on the hepatic enzyme, prothrombin time, inflammatory cytokines, serum endotoxin and high mobility group box-1 in a rat acute-on-chronic liver failure model compared to those of pDC315-3FLAG-sv40-HGF-EGFP or pDC315-3FLAG-sv40-Hyper-IL-6-EGFP. A: Alanine transaminase (ALT); B: Prothrombin time (PT); C: Tumour necrosis factor-α (TNF-α); D: Interferon-γ (IFN-γ); E: Endotoxin; F: High mobility group box-1 (HMGB1). $^{a}P < 0.05$ *vs* Ad-GFP treated, $^{b}P < 0.01$ *vs* control, $^{c}P < 0.05$ *vs* Ad-HIL-6 treated, $^{e}P < 0.05$ *vs* Ad-HGF treated. The results are expressed as the mean ± SD, $n = 6$. Control: Normal liver; model: ACLF liver; Ad-GFP: pDC315-3FLAG-sv40-EGFP; Ad-HIL-6: pDC315-3FLAG-sv40-Hyper-IL-6-EGFP; Ad-HGF: pDC315-3FLAG-sv40-HGF-EGFP; Ad-HGF-HIL-6: pDC315-3FLAG-sv40-HGF-IRES-Hyper-IL-6-EGFP.

presented in Figure 2.

We stained the nuclear Ki67 of hepatocytes (Figure 3). As shown in Figure 3, the expression of Ki67 was higher in the Ad-HGF group (24 h: 6.27%; 48 h: 5.29%), Ad-HIL-6 group (24 h: 5.94%; 48 h: 4.90%) and Ad-HGF-HIL-6 group (24 h: 11.95%; 48 h: 9.10%) compared to the Ad-GFP group (24 h: 0.17% ; 48 h: 0.11%; $P < 0.01$) at 24 h and 48 h, and the expression of Ki67 was more predominant in the Ad-HGF-HIL-6 group at both two time points ($P < 0.05$). However, the expression of Ki67 in the model group (24 h: 0.13%; 48 h: 0.09%) had no statistical significance compared to the Ad-GFP group at the two time points ($P > 0.05$).

Effect of recombinant adenovirus containing Hyper-IL-6 and HGF on hepatic apoptosis

As shown in Figure 4, TUNEL assay displayed that apoptotic cells had irregular and condensed nuclei, and the nuclei was brown-stained. Apoptosis could scarcely

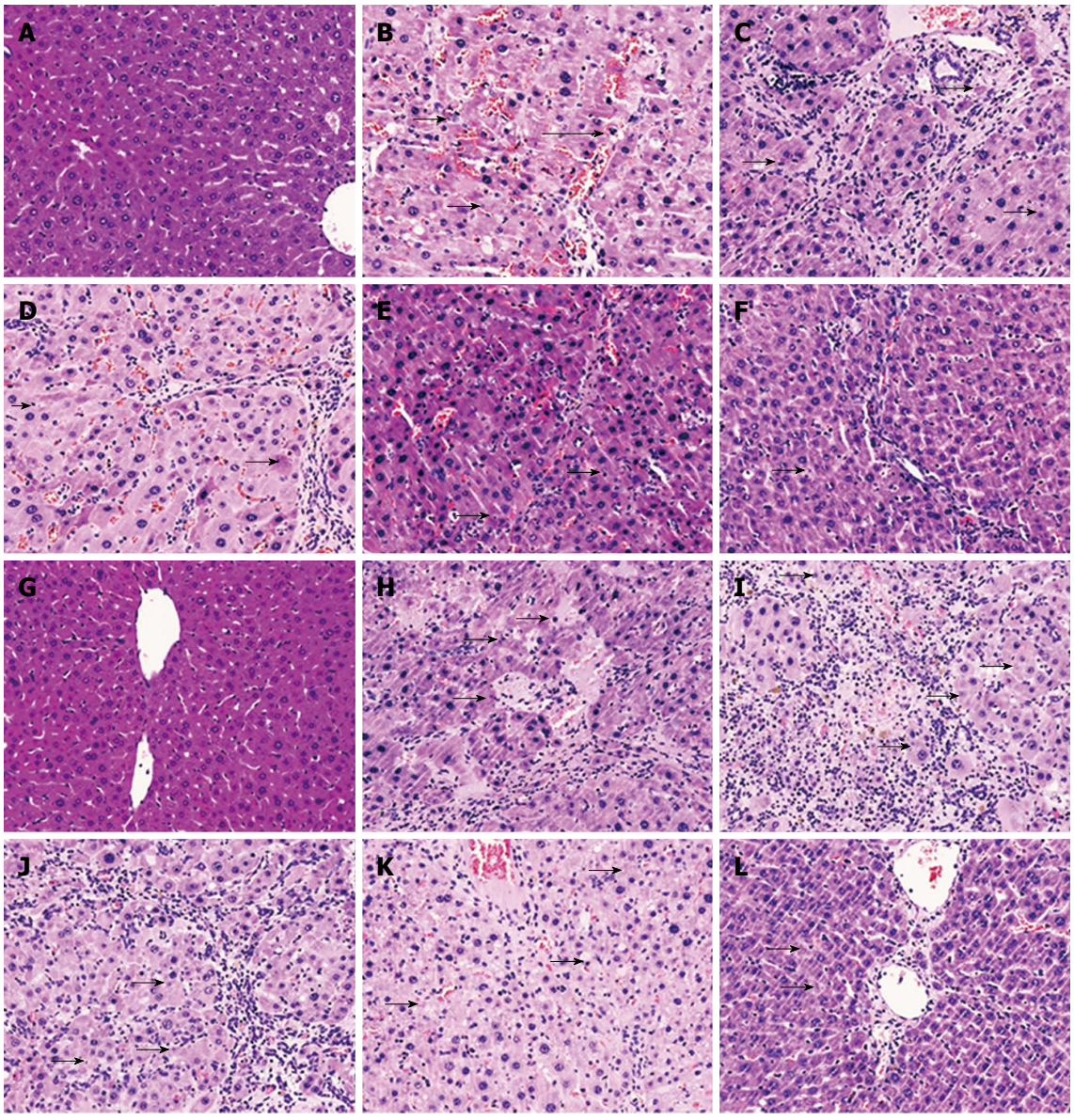

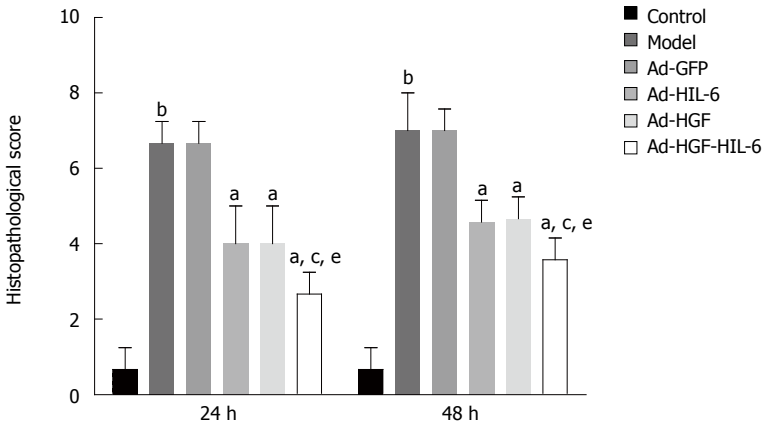

Figure 2 Effect of pDC315-3FLAG-sv40-HGF-IRES-Hyper-IL-6-EGFP on liver histology (HE staining, original magnification × 100) compared to those of pDC315-3FLAG-sv40-HGF-EGFP or pDC315-3FLAG-sv40-Hyper-IL-6-EGFP and comparison of histopathological scores for all types of treated liver. Arrow indicates an apoptotic or necrotic cell. [a]*P* < 0.05 *vs* Ad-GFP treated, [b]*P* < 0.01 *vs* control, [c]*P* < 0.05 *vs* Ad-HIL-6 treated, and [e]*P* < 0.05 *vs* Ad-HGF treated. The results are expressed as the mean ± SEM, *n* = 8. Control: Normal liver; Model: ACLF liver; Ad-GFP: pDC315-3FLAG-sv40-EGFP; Ad-HIL-6: pDC315-3FLAG-sv40-Hyper-IL-6-EGFP; Ad-HGF: pDC315-3FLAG-sv40-HGF-EGFP; Ad-HGF-HIL-6: pDC315-3FLAG-sv40-HGF-IRES-Hyper-IL-6-EGFP; A: Control at 24 h; B: Model at 24 h; C: Ad-GFP at 24 h; D: Ad-HIL-6 at 24 h; E: Ad-HGF at 24 h; F: Ad-HGF-HIL-6 at 24 h; G: Control at 48 h; H: Model at 48 h; I: Ad-GFP at 48 h; J: Ad-HIL-6 at 48 h; K: Ad-HGF at 48 h; L: Ad-HGF-HIL-6 at 48 h.

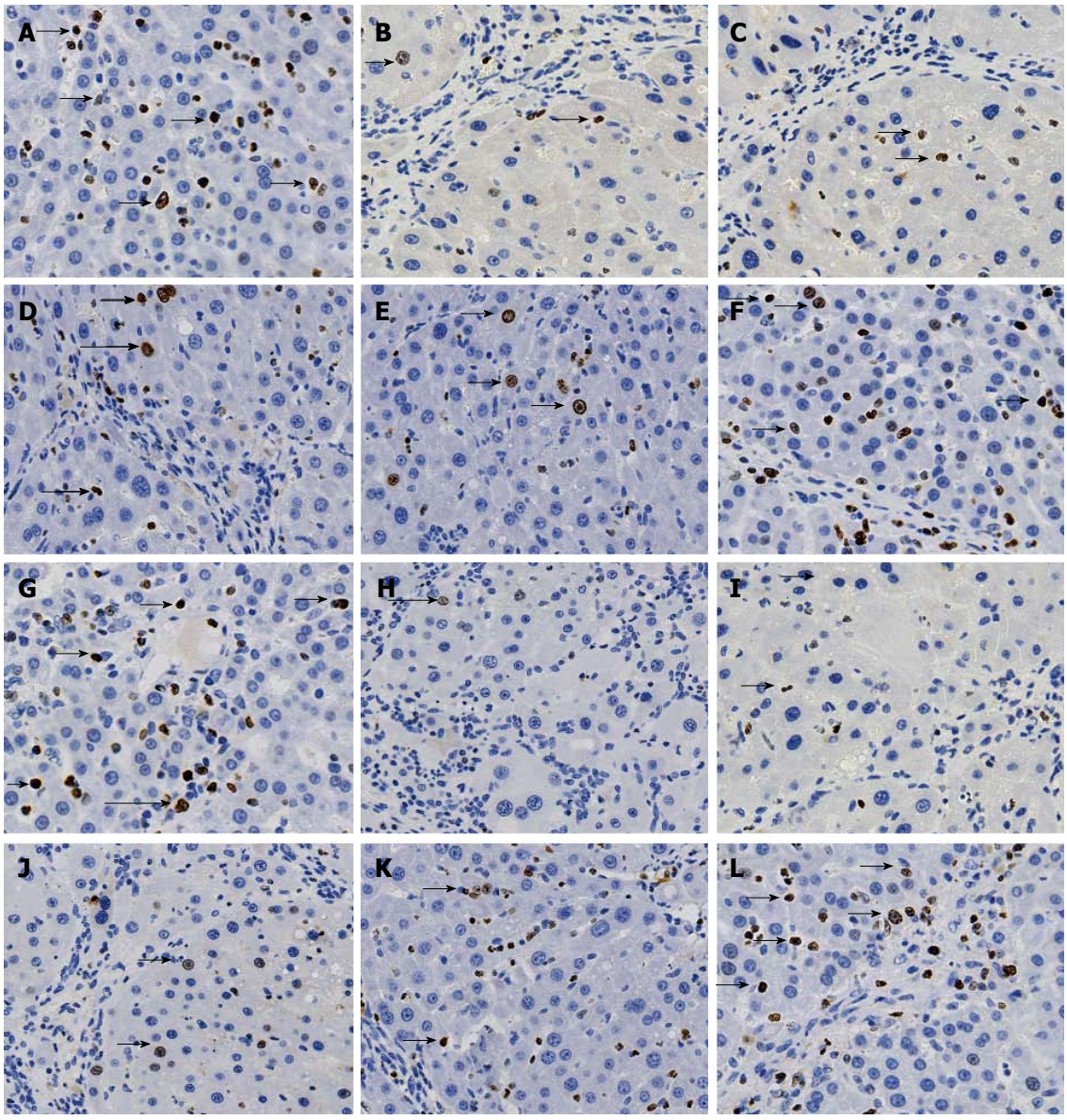

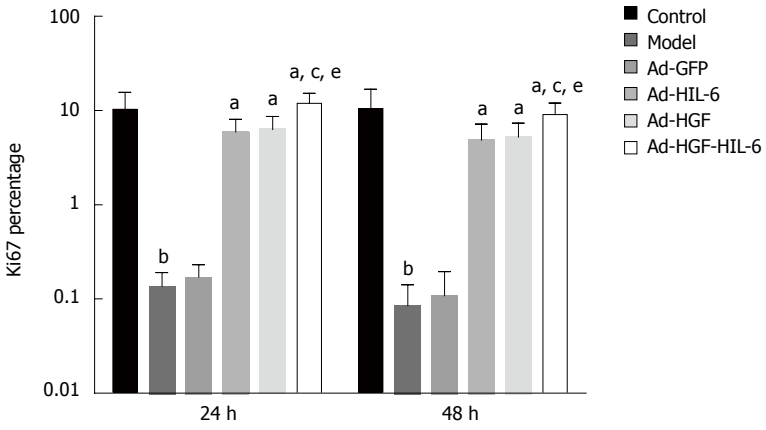

Figure 3 Effect of pDC315-3FLAG-sv40-HGF-IRES-Hyper-IL-6-EGFP on Ki67 proliferation index (immunohistochemistry, original magnification × 200) compared to those of pDC315-3FLAG-sv40-HGF-EGFP or pDC315-3FLAG-sv40-Hyper-IL-6-EGFP and quantification for Ki67$^+$ hepatocytes versus total counted cells for all types of treated liver. $^aP < 0.05$ *vs* Ad-GFP treated, $^bP < 0.01$ *vs* control, $^cP < 0.05$ *vs* Ad-HIL-6 treated, $^eP < 0.05$ *vs* Ad-HGF treated. The results are expressed as the mean ± SEM, $n = 8$. Arrow is a Ki67$^+$ cell. Control: Normal liver; model: ACLF liver; Ad-GFP: pDC315-3FLAG-sv40-EGFP; Ad-HIL-6: pDC315-3FLAG-sv40-Hyper-IL-6-EGFP; Ad-HGF: pDC315-3FLAG-sv40-HGF-EGFP; and Ad-HGF-HIL-6: pDC315-3FLAG-sv40-HGF-IRES-Hyper-IL-6-EGFP; A: Control at 24 h; B: Model at 24 h; C: Ad-GFP at 24 h; D: Ad-HIL-6 at 24 h; E: Ad-HGF at 24 h; F: Ad-HGF-HIL-6 at 24 h; G: Control at 48 h; H: Model at 48 h; I: Ad-GFP at 48 h; J: Ad-HIL-6 at 48 h; K: Ad-HGF at 48 h; L:Ad-HGF-HIL-6 at 48 h.

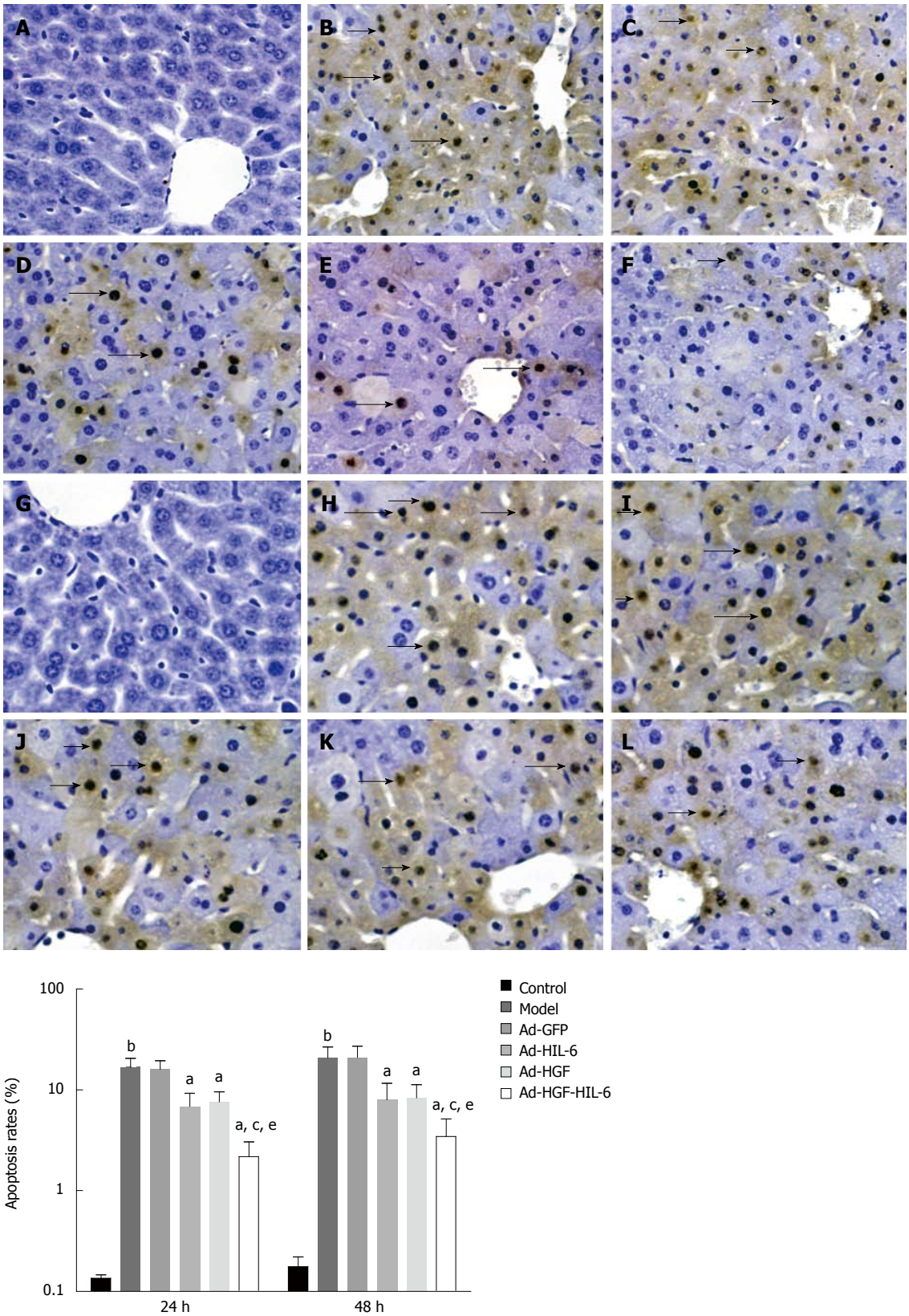

Figure 4 Effect of pDC315-3FLAG-sv40-HGF-IRES-Hyper-IL-6-EGFP on apoptotic index by TUNEL assays (Images are represented at × 400 magnification) compared to those of pDC315-3FLAG-sv40-HGF-EGFP or pDC315-3FLAG-sv40-Hyper-IL-6-EGFP and comparison of the apoptosis rates (%) for all types of treated liver. Arrow indicates an apoptotic cell. [a]$P < 0.05$ *vs* Ad-GFP treated, [b]$P < 0.01$ *vs* control, [c]$P < 0.05$ *vs* Ad-HIL-6 treated, and [e]$P < 0.05$ *vs* Ad-HGF treated. The results are expressed as the mean ± SEM, $n = 8$. Control: Normal liver; model: ACLF liver; Ad-GFP: pDC315-3FLAG-sv40-EGFP; Ad-HIL-6: pDC315-3FLAG-sv40-Hyper-IL-6-EGFP; Ad-HGF: pDC315-3FLAG-sv40-HGF-EGFP; Ad-HGF-HIL-6: pDC315-3FLAG-sv40-HGF-IRES-Hyper-IL-6-EGFP; A: Control at 24 h; B: Model at 24 h; C: Ad-GFP at 24 h; D: Ad-HIL-6 at 24 h; E: Ad-HGF at 24 h; F: Ad-HGF-HIL-6 at 24 h; G: Control at 48 h; H: Model at 48 h; I: Ad-GFP at 48 h; J: Ad-HIL-6 at 48 h; K: Ad-HGF at 48 h; L:Ad-HGF-HIL-6 at 48 h.

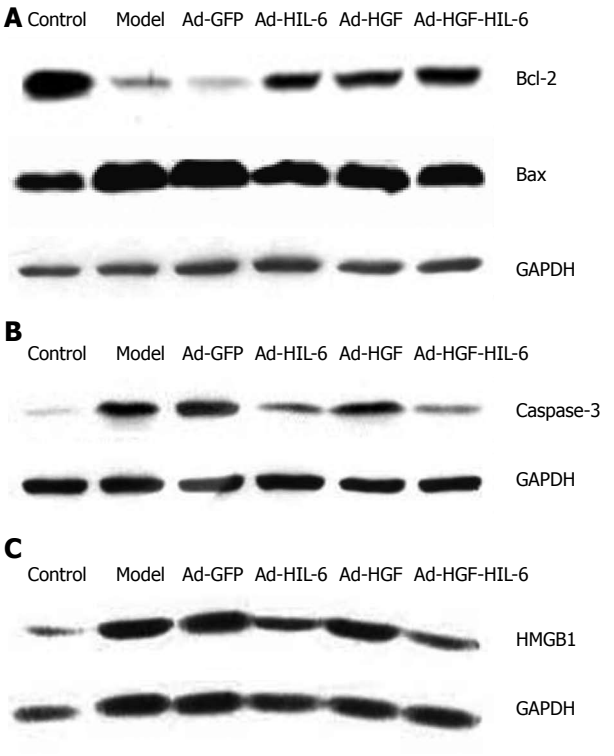

Figure 5 Western blot assays showing the protein expression of Bcl-2, Bax, Caspase-3 and HMGB1 for all types of treated liver. n = 6. A: Bcl-2, Bax; B: Caspase-3; C: HMGB1. Control: Normal liver; Model: ACLF liver; Ad-GFP: pDC315-3FLAG-sv40-EGFP; Ad-HIL-6: pDC315-3FLAG-sv40-Hyper-IL-6-EGFP; Ad-HGF: pDC315-3FLAG-sv40-HGF-EGFP; Ad-HGF-HIL-6: pDC315-3FLAG-sv40-HGF-IRES-Hyper-IL-6-EGFP. ACLF: Acute-on-chronic liver failure.

ever be detected in the liver tissue slices of the control group, while apoptosis increased in the model and Ad-GFP groups. Recombinant adenovirus (except Ad-GFP) administration dramatically reduced apoptotic rates compared to Ad-GFP.

The percentage of apoptotic hepatocytes significantly increased in the model group (24 h: 16.8%; 48 h: 20.87%) compared to the control group (24 h: 0.14%, 48 h: 0.18%; $P < 0.01$). In contrast, the apoptotic index markedly decreased ($P < 0.01$) in the Ad-HGF-HIL-6 (24 h: 2.18%; 48 h: 3.46%), Ad-HIL-6 (24 h: 6.88%; 48 h: 7.98%) and Ad-HGF (24 h: 7.60%; 48 h: 8.35%) groups compared to the Ad-GFP group (24 h: 15.97%, 48 h: 21.13%; $P < 0.01$). The lowest apoptotic rates were observed in the Ad-HGF-HIL-6 group ($P < 0.05$). At the detected time points, there were no statistically significances ($P > 0.05$) in the apoptotic index between the model and Ad-GFP groups.

As shown in Figure 5A and B and Figure 6A-D, Bax and caspase-3 proteins in the model group (1.23 ± 0.23; 0.67 ± 0.19) were dramatically enhanced compared to the control group (0.97 ± 0.20, 0.15 ± 0.14; $P < 0.01$), however, there was no statistically significance between the model group and Ad-GFP group (1.21 ± 0.20; 0.68 ± 0.31, $P > 0.05$). The Ad-HIL-6 (1.18 ± 0.21; 0.40 ± 0.21) and Ad-HGF-HIL-6 (1.01 ± 0.12; 0.25 ± 0.14) treatments evidently decreased the levels of Bax and caspase-3 proteins compared to Ad-GFP ($P < 0.05$), and the effect of Ad-HGF-HIL-6 treatment was more obvious ($P < 0.05$). The levels of Bax protein in the Ad-HGF group were lower than those of the Ad-GFP group (1.12 ± 0.27, $P < 0.01$) but significantly higher than those of the Ad-HGF-HIL-6 group ($P < 0.05$). However, Ad-HGF treatment failed to decrease the expression of caspase-3 protein levels (0.59 ± 0.22) compared to Ad-GFP ($P > 0.05$). Bcl-2 protein of the model group (0.24 ± 0.03) was remarkably lower than that of the control group (1.85 ± 0.40, $P < 0.01$). The Ad-HIL-6 (0.54 ± 0.19), Ad-HGF (0.81 ± 0.20) and Ad-HIL-6-HGF (0.93 ± 0.41) treatments dramatically enhanced Bcl-2 protein expression compared to Ad-GFP ($P < 0.01$), and the effect of Ad-HGF-HIL-6 was more obvious ($P < 0.05$). The trends of Bcl-2/Bax (protein levels; ratio) in each group were consistent with those of Bcl-2. In addition, Bcl-2 protein and Bcl-2/Bax displayed no statistical discrepancy between the model and Ad-GFP groups ($P > 0.05$).

Hyper-IL-6 and HGF gene expression

As shown in Figure 7, real-time quantitative PCR revealed that the expression of HIL-6 or HGF mRNA in the liver samples in the Ad-HIL-6 or Ad-HGF group had no significant difference compared to the Ad-HGF-HIL-6 group (HIL-6: 4.27 ± 3.69 *vs* 4.92 ± 1.34, HGF: 1.68 ± 5.13 *vs* 2.56 ± 7.79; $P > 0.05$) and had a very small intersection of false-positive expression in the control (HIL-6: 1.02 ± 0.27, HGF: 1.01 ± 0.21; $P < 0.01$), model (HIL-6: 0.64 ± 0.28, HGF: 0.57 ± 0.04; $P < 0.01$), Ad-GFP (HIL-6: 1.08 ± 0.15, HGF: 0.64 ± 0.16; $P < 0.01$), HIL-6 (HGF: 0.63 ± 0.25; $P < 0.01$) and HGF (HIL-6: 0.49 ± 0.01; $P < 0.01$) groups.

Effect of recombinant adenovirus containing Hyper-IL-6 and HGF on HMGB1 protein expression

As shown in Figure 5C and Figure 6E, the Western blot assay exhibited that the HMGB1 protein expression in liver samples was dramatically enhanced in the model group (1.12 ± 0.00) compared to the control group (0.41 ± 0.01, $P < 0.01$); however, it was remarkably reduced in the Ad-HGF (1.02 ± 0.02), Ad-HIL-6 (0.80 ± 0.01) and Ad-HGF-HIL-6 (0.59 ± 0.02) groups compared to the Ad-GFP group ($P < 0.01$), and the change was more considerable in the Ad-HGF-HIL-6 group ($P < 0.01$). Meanwhile, the HMGB1 protein expression had no statistical significance between the model and Ad-GFP groups (1.12 ± 0.06, $P > 0.05$).

DISCUSSION

Various strategies have been attempted *in vivo* to search for effective ways to treat ACLF[17-21]. In our study, an ACLF rat model was used to perform a comparative study on the efficacy of Ad-HGF, Ad-HIL-6 or Ad-HGF-HIL-6 in ACLF. We demonstrated that Ad-HGF-HIL-6 significantly improved pathological damage

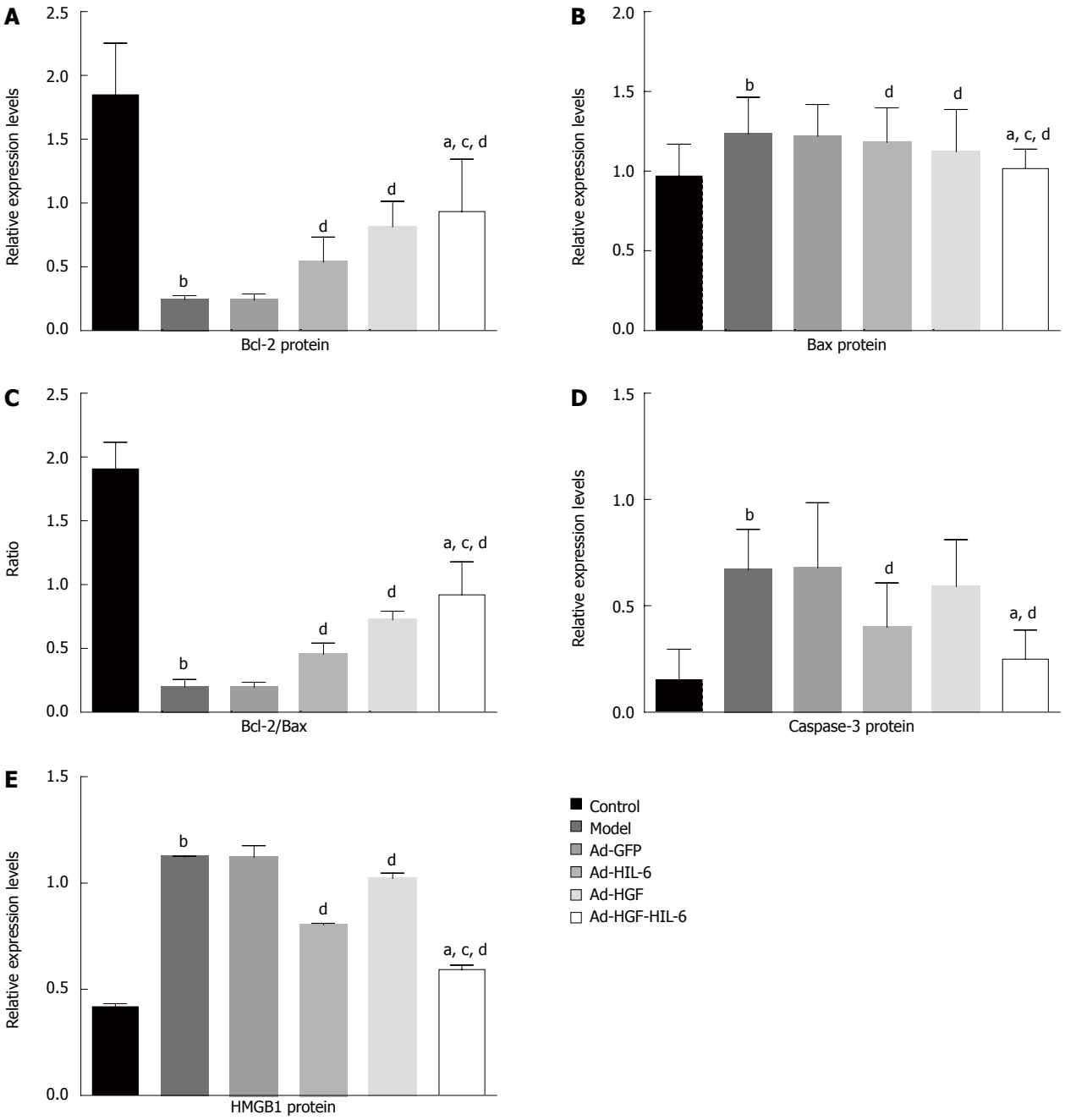

Figure 6 Protein levels of Bcl-2, Bax, Caspase-3 and HMGB1 detected by Western blot, revealing the relative protein expression of Bcl-2, Bax, Caspase-3 and HMGB1, and the ratio of Bcl-2/Bax of all treated livers. A: Bcl-2 protein; B: Bax protein; C: the ratio of Bcl-2/Bax; D: Caspase-3 protein; E: HMGB1 protein. A, B, D, E: The Y axis represents the relative protein expression of Bcl-2, Bax Caspase-3 and HMGB1 compared to that of glyceraldehyde-3-phosphate dehydrogenase (GAPDH) for all types of treated liver; C: The Y axis represents the ratio of the relative protein expression of Bcl-2/Bax for all types of treated liver. $^{a}P < 0.05$ *vs* Ad-HIL-6 treated, $^{b}P < 0.01$ *vs* control, $^{c}P < 0.05$ *vs* Ad-HGF treated, $^{d}P < 0.01$ *vs* Ad-GFP treated. The results are expressed as the mean ± SD, $n = 6$. Control: Normal liver; Model: ACLF liver; Ad-GFP: pDC315-3FLAG-sv40-EGFP; Ad-HIL-6: pDC315-3FLAG-sv40-Hyper-IL-6-EGFP; Ad-HGF: pDC315-3FLAG-sv40-HGF-EGFP; Ad-HGF-HIL-6: pDC315-3FLAG-sv40-HGF-IRES-Hyper-IL-6-EGFP.

compared to Ad-HGF and Ad-HIL-6 in ACLF rats. Meanwhile, greater effects in correcting coagulation and liver function were observed in ACLF rats with Ad-HGF-HIL-6 treatment. Ki67 is an important index for evaluating the regeneration of hepatocytes. At the 24 h and 48 h detection points of our study, Ad-HGF-HIL-6 treatment significantly enhanced the frequency of $Ki67^{+}$ hepatocytes compared to Ad-HGF or Ad-HIL-6, indicating a better ability to promote hepatocyte regeneration.

The apoptosis of hepatocytes plays a significant part in the development of multifarious liver diseases[22,23]. By reducing the hepatocyte injury that proceeds apoptosis, HGF may prevent or diminish the initiation of the apoptotic cascade[24]. In our study, we also detected that Ad-HGF-HIL-6 remarkably enhanced Bcl-2 (anti-apoptotic) protein expression and apparently reduced Bax (pro-apoptotic) protein expression in hepatocytes of

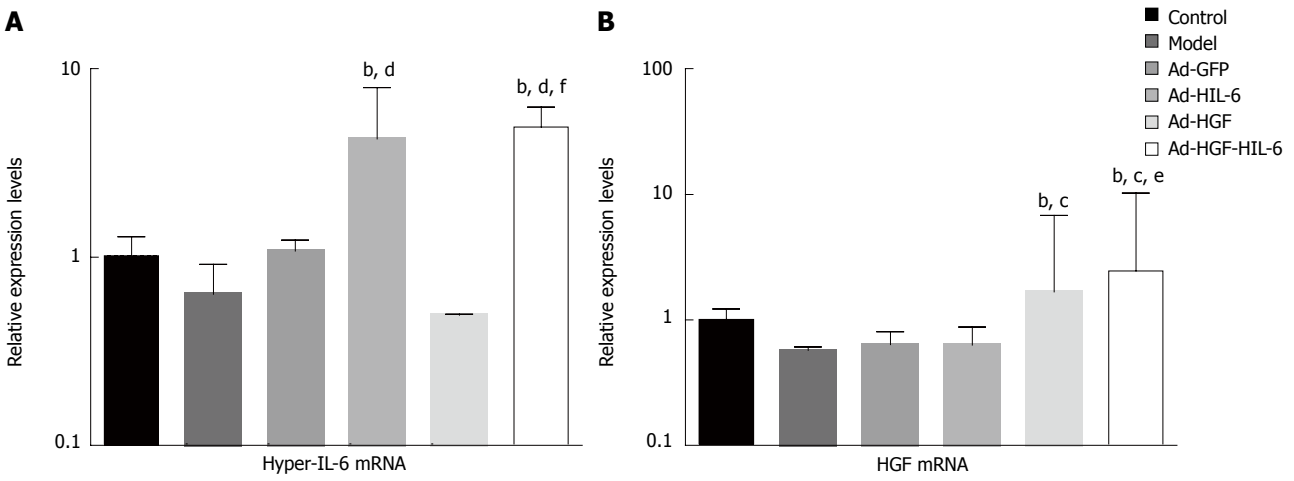

Figure 7 Expression of mRNA levels of hyper-IL-6 or HGF as detected by representative reverse transcription-polymerase chain reaction. A: Hyper-IL-6 mRNA; B: HGF mRNA. The Y axis represents the relative mRNA expression of Hyper-IL-6 or HGF compared to that of the house-keeping gene β-actin for all types of treated liver. $^{b}P < 0.01$ *vs* Ad-GFP treated, $^{c}P < 0.01$ *vs* Ad-HIL-6 treated, $^{d}P < 0.01$ *vs* Ad-HGF treated, $^{e}P > 0.05$ *vs* Ad-HGF treated and $^{f}P > 0.05$ *vs* Ad-HIL-6 treated. The results are expressed as the mean ± SD, $n = 6$. Control: Normal liver; Model: ACLF liver; Ad-GFP: pDC315-3FLAG-sv40-EGFP; Ad-HIL-6: pDC315-3FLAG-sv40-Hyper-IL-6-EGFP; Ad-HGF: pDC315-3FLAG-sv40-HGF-EGFP; and Ad-HGF-HIL-6: pDC315-3FLAG-sv40-HGF-IRES-Hyper-IL-6-EGFP.

ACLF rats compared to Ad-HGF or Ad-HIL-6. Although both Ad-HGF-HIL-6 and Ad-HIL-6 could conspicuously decrease the activities of caspase-3, the former had a more significant effect. In addition, apoptotic characteristics were viewed by the TUNEL assay of liver tissues. These results displayed that Ad-HGF-HIL-6 could protect the liver of rats against ACLF more effectively by reducing apoptosis.

HMGB1 positively reacts upon various inflammatory diseases[20,25-27]. A protective effect against ACLF is detected by blockading HMGB1 at 24 h since the ACLF model was established[21]. A previous study proved that the high level of HMGB1 plays a considerable part in the pathogenic mechanism of liver failure[28]. Our study found that Ad-HGF-HIL-6 could significantly decrease the serum and tissue HMGB1 concentrations in ACLF compared to Ad-HGF or Ad-HIL-6, suggesting reduced inflammatory response and necrotic hepatocytes. These results further indicate that the mechanism of Ad-HGF-HIL-6 in protecting against ACLF is likely to be related to HMGB1 signalling, which is worthy of future research.

In the progress of ACLF, systemic inflammatory response is tightly related to its prognosis[29]. Anti-TNF treatment protects against experimental hepatic damage due to bacteria endotoxin[30], demonstrating that TNF-α plays a pivotal part in the development of liver failure. In the current research, serum TNF-α in the Ad-HGF, Ad-HIL-6 and Ad-HGF-HIL-6 groups significantly decreased compared with the Ad-GFP group; however, there was no statistical discrepancy between the Ad-HGF-HIL-6 and Ad-HGF treatments at 24 h and 48 h, but these levels were lower than those of the Ad-HIL-6 treatment. TNF-α can mediate apoptosis by interacting with TNF-R1, giving rise to the activation of caspase cascades[21], as confirmed by the similar alteration trend between TNF-α and the apoptotic indicator caspase-3 in this experiment. Similarly, Ad-HGF-HIL-6 inhibited the release of IFN-γ and endotoxin more effectively than did Ad-HGF or Ad-HIL-6, also suggesting the alleviation of the liver inflammatory response.

Our study confirmed the functional synergistic effect of HIL-6 and HGF by combining them into an adenovirus vector. Real-time PCR results suggest that the constructions of recombinant adenovirus were successful, as the expression of the two genes in the liver tissues of ACLF rats was excellent and did not produce mutual interference. Moreover, the enhancement of treatment did not increase immunogenicity or toxicity.

In summary, our results suggest that Ad-HGF-HIL-6 may confer a more powerful protective effect against ACLF than do Ad-HGF or Ad-HIL-6 in rats and can restrain the release of various inflammatory cytokines, reduce the apoptosis of hepatocytes, and protect rats against experimental ACLF even 48 h since ACLF model was established, although the precise molecular events and cell signalling pathways warrant further studies. Our findings indicate that Ad-HGF-HIL-6 is likely to be a feasible and neoteric protective agent for severe liver injury.

COMMENTS

Background

Acute-on-chronic liver failure (ACLF) is a life-threatening medical emergency, which is usually associated with a precipitating event and results in high mortality. Therefore, it is urgent to develop new therapeutic reagents for ACLF. Gene therapy by delivering a target gene to the patients *via* viral and non-viral vectors appears to be a promising approach for the treatment of ACLF. Previous studies have shown that hyper-interleukin-6 (HIL-6), comprising interleukin-6 (IL-6) and the soluble IL-6 receptor, can reduce the necrosis of remnant liver cells during the process of liver failure, and hepatocyte growth factor (HGF) can stimulate the DNA synthesis of hepatocytes, suggesting a possible protective

effect of these two factors on liver injury.

Research frontiers

IL-6 is the crucial transcriptional factor during the process of early-stage hepatic regeneration response. Hyper-IL-6 is an artificial fusion cytokine comprising IL-6 linked by an artificial linker with a soluble variant of gp80 (sIL-6R). HIL-6 is a stable protein displaying biological activity *in vitro* or *in vivo* 10-1000-fold higher than that of IL-6/sIL-6R soluble complex. HGF initiates liver regeneration after liver excision or chemical injuries. The coadministration of IL-6 and HGF most effectively increased both the wet weight of the unoccluded lobes and the hepatocellular DNA synthesis of the animals that underwent PBL of the left lateral and median branches, suggesting a possible synergistic effect of these two factors. In the current study, the authors evaluated the protective efficacy of recombinant adenovirus containing HIL-6 and HGF (Ad-HGF-HIL-6) compared to that of recombinant adenovirus HIL-6 (Ad-HIL-6) or HGF (Ad-HGF) in an ACLF rat model.

Innovations and breakthroughs

ACLF is a condition with acute liver function decompensation secondary to chronic liver diseases. Infectious etiologies constitute the majority of acute insults in the East. In this study, the authors established a rat model of ACLF by immune system-induced liver cirrhosis induced with HSA, and later with D-galactosamine and lipopolysaccharide. Since this practical animal model can well simulate the pathophysiological processes of ACLF, the experimental results of treatment with Ad-HGF-HIL-6 are more persuasive. On the other hand, they sought to deliver two genes by a recombinant adenovirus vector into rats simultaneously but avoiding significant side effects. These findings demonstrated that the protective efficacy of Ad-HGF-HIL-6 is more potent than that of Ad-HGF or Ad-HIL-6 in ACLF rats, with no significant side effects.

Applications

These findings indicate that Ad-HGF-HIL-6 is likely to be a potential and novel protective agent for severe liver inflammatory injury.

Terminology

ACLF refers to an acute deterioration of known or unknown chronic liver disease. It is primarily caused by bleeding and infections, which could result in a series of pathophysiological process, including systemic hemodynamic changes, systemic inflammatory response syndrome, hepatorenal syndrome, and hepatic encephalopathy. IL-6 is a pleiotropic cytokine mediating acute-phase responses, cell regeneration, and transition from innate to acquired immunity. In the classical pathway, IL-6 binds to a membrane bound IL-6R and the complex associates with gp130, for intracellular signalling. Interactions of the IL-6/sIL-6R complex with gp130 provides IL-6 sensitivity to many cell types that do not express IL-6R, thereby expanding biological effects. HIL-6 is a chimera of recombinant human IL-6 bound to IL-6Rα by a short peptide chain. Compared to IL-6/IL-6Rα, HIL-6 has a 10-1000-fold higher receptor binding affinity while the half-life is similar to IL-6. HIL-6 has enhanced and longer activation of mitogen-activated protein kinase pathways. HGF initiates liver regeneration after liver excision or chemical injuries. The coadministration of IL-6 and HGF most effectively increased both the wet weight of the unoccluded lobes and the hepatocellular DNA synthesis of the animals that underwent portal branch ligation of the left lateral and median branches, suggesting a possible synergistic effect of these two factors. In the current study, we evaluated the therapeutic efficacy of recombinant adenovirus containing HIL-6 and HGF compared to that of recombinant adenovirus HIL-6 or HGF in an ACLF rat model.

Peer-review

This is a very well designed research and the literature relating to the principle for using this recombinant adenovirus in the ACLF model in rats to explicate its potential effects has been exhaustively explored. The study is well presented in terms of its aims and purposes. There are confident data to indicate that Ad-HGF-HIL-6 may be explored as a potential therapeutic agent for severe liver inflammatory injury.

REFERENCES

1 **Limbach KJ**, Richie TL. Viral vectors in malaria vaccine development. *Parasite Immunol* 2009; **31**: 501-519 [PMID: 19691555 DOI: 10.1111/j.1365-3024.2009.01141.x]

2 **Robert-Guroff M**. Replicating and non-replicating viral vectors for vaccine development. *Curr Opin Biotechnol* 2007; **18**: 546-556 [PMID: 18063357 DOI: 10.1016/j.copbio.2007.10.010]

3 **Kato H**, Shimomura T, Murai R, Gonda K, Ishii K, Yoshida Y, Kanbe T, Hashiguchi K, Sakabe T, Takubo K, Okano J, Tsuchiya H, Hoshikawa Y, Kurimasa A, Shiota G. Regulation of hepatic oval cell proliferation by adenoviral mediated hepatocyte growth factor gene transfer and signal transduction inhibitors. *Hepatogastroenterology* 2007; **54**: 821-825 [PMID: 17591071]

4 **Fausto N**, Campbell JS, Riehle KJ. Liver regeneration. *Hepatology* 2006; **43**: S45-S53 [PMID: 16447274 DOI: 10.1002/hep.20969]

5 **Peters M**, Blinn G, Solem F, Fischer M, Meyer zum Büschenfelde KH, Rose-John S. In vivo and in vitro activities of the gp130-stimulating designer cytokine Hyper-IL-6. *J Immunol* 1998; **161**: 3575-3581 [PMID: 9759879]

6 **Makino H**, Shimizu H, Ito H, Kimura F, Ambiru S, Togawa A, Ohtsuka M, Yoshidome H, Kato A, Yoshitomi H, Sawada S, Miyazaki M. Changes in growth factor and cytokine expression in biliary obstructed rat liver and their relationship with delayed liver regeneration after partial hepatectomy. *World J Gastroenterol* 2006; **12**: 2053-2059 [PMID: 16610056 DOI: 10.3748/wjg.v12.i13.2053]

7 **Hamada T**, Eguchi S, Takatsuki M, Yamanouchi K, Sugiyama N, Kawashita Y, Okudaira S, Tajima Y, Ishii T, Kanematsu T. Low-dose recombinant human hepatocyte growth factor enhances effect of hepatocyte transplantation in rats treated with retrorsine. *Hepatogastroenterology* 2009; **56**: 1466-1470 [PMID: 19950811]

8 **Franco-Gou R**, Roselló-Catafau J, Casillas-Ramirez A, Massip-Salcedo M, Rimola A, Calvo N, Bartrons R, Peralta C. How ischaemic preconditioning protects small liver grafts. *J Pathol* 2006; **208**: 62-73 [PMID: 16261637 DOI: 10.1002/path.1859]

9 **Kaido T**, Oe H, Imamura M. Interleukin-6 augments hepatocyte growth factor-induced liver regeneration; involvement of STAT3 activation. *Hepatogastroenterology* 2004; **51**: 1667-1670 [PMID: 15532800]

10 **Bramson JL**, Hitt M, Addison CL, Muller WJ, Gauldie J, Graham FL. Direct intratumoral injection of an adenovirus expressing interleukin-12 induces regression and long-lasting immunity that is associated with highly localized expression of interleukin-12. *Hum Gene Ther* 1996; **7**: 1995-2002 [PMID: 8930660 DOI: 10.1089/hum.1996.7.16-1995]

11 **Hitt MM**, Addison CL, Graham FL. Human adenovirus vectors for gene transfer into mammalian cells. *Adv Pharmacol* 1997; **40**: 137-206 [PMID: 9217926]

12 **Balasubramaniyan V**, Wright G, Sharma V, Davies NA, Sharifi Y, Habtesion A, Mookerjee RP, Jalan R. Ammonia reduction with ornithine phenylacetate restores brain eNOS activity via the DDAH-ADMA pathway in bile duct-ligated cirrhotic rats. *Am J Physiol Gastrointest Liver Physiol* 2012; **302**: G145-G152 [PMID: 21903766 DOI: 10.1152/ajpgi.00097.2011]

13 **Liu XH**, Chen Y, Wang TL, Lu J, Zhang LJ, Song CZ, Zhang J, Duan ZP. [Establishment of a D-galactosamine/lipopolysaccharide induced acute-on-chronic liver failure model in rats]. *Zhonghua Gan Zang Bing Za Zhi* 2007; **15**: 771-775 [PMID: 17963606]

14 **Ni HM**, Chen X, Ding WX, Schuchmann M, Yin XM. Differential roles of JNK in ConA/GalN and ConA-induced liver injury in mice. *Am J Pathol* 2008; **173**: 962-972 [PMID: 18772342 DOI: 10.2353/ajpath.2008.080358]

15 **Takahashi K**, Imaeda H, Fujimoto T, Ban H, Bamba S, Tsujikawa T, Sasaki M, Fujiyama Y, Andoh A. Regulation of eotaxin-3/CC chemokine ligand 26 expression by T helper type 2 cytokines in human colonic myofibroblasts. *Clin Exp Immunol* 2013; **173**: 323-331 [PMID: 23607908 DOI: 10.1111/cei.12117]

16 **Livak KJ**, Schmittgen TD. Analysis of relative gene expression data using real-time quantitative PCR and the 2(-Delta Delta C(T)) Method. *Methods* 2001; **25**: 402-408 [PMID: 11846609 DOI: 10.1006/meth.2001.1262]

17 **Hu C**, Shen S, Zhang A, Ren B, Lin F. The liver protective effect of methylprednisolone on a new experimental acute-on-chronic

liver failure model in rats. *Dig Liver Dis* 2014; **46**: 928-935 [PMID: 25022338 DOI: 10.1016/j.dld.2014.06.008]
18 **Xu Y**, Wang H, Bao S, Tabassam F, Cai W, Xiang X, Zhao G, Wu H, Gao T, Li H, Xie Q. Amelioration of liver injury by continuously targeted intervention against TNFRp55 in rats with acute-on-chronic liver failure. *PLoS One* 2013; **8**: e68757 [PMID: 23874752 DOI: 10.1371/journal.pone.0068757]
19 **Yang F**, Li X, Wang LK, Wang LW, Han XQ, Zhang H, Gong ZJ. Inhibitions of NF-κB and TNF-α result in differential effects in rats with acute on chronic liver failure induced by d-Gal and LPS. *Inflammation* 2014; **37**: 848-857 [PMID: 24385241 DOI: 10.1007/s10753-013-9805-x]
20 **Wang LW**, Wang LK, Chen H, Fan C, Li X, He CM, Gong ZJ. Ethyl pyruvate protects against experimental acute-on-chronic liver failure in rats. *World J Gastroenterol* 2012; **18**: 5709-5718 [PMID: 23155311 DOI: 10.3748/wjg.v18.i40.5709]
21 **Li X**, Wang LK, Wang LW, Han XQ, Yang F, Gong ZJ. Blockade of high-mobility group box-1 ameliorates acute on chronic liver failure in rats. *Inflamm Res* 2013; **62**: 703-709 [PMID: 23591781 DOI: 10.1007/s00011-013-0624-1]
22 **Tsamandas AC**, Thomopoulos K, Zolota V, Kourelis T, Karatzas T, Ravazoula P, Tepetes K, Petsas T, Karavias D, Karatza C, Bonikos DS, Gogos C. Potential role of bcl-2 and bax mRNA and protein expression in chronic hepatitis type B and C: a clinicopathologic study. *Mod Pathol* 2003; **16**: 1273-1288 [PMID: 14681329 DOI: 10.1097/01.MP.0000097367.56816.5E]
23 **Zhang M**, He W, Liu F, Zou P, Xiao J, Zhong ZD, Hu ZB. Inhibition of mouse hepatocyte apoptosis via anti-Fas ribozyme. *World J Gastroenterol* 2004; **10**: 2567-2570 [PMID: 15300908 DOI: 10.3748/wjg.v10.i17.2567]
24 **Thatch KA**, Schwartz MZ, Yoo EY, Mendelson KG, Duke DS. Modulation of the inflammatory response and apoptosis using epidermal growth factor and hepatocyte growth factor in a liver injury model: a potential approach to the management and treatment of cholestatic liver disease. *J Pediatr Surg* 2008; **43**: 2169-2173 [PMID: 19040928 DOI: 10.1016/j.jpedsurg.2008.08.045]
25 **Tsung A**, Sahai R, Tanaka H, Nakao A, Fink MP, Lotze MT, Yang H, Li J, Tracey KJ, Geller DA, Billiar TR. The nuclear factor HMGB1 mediates hepatic injury after murine liver ischemia-reperfusion. *J Exp Med* 2005; **201**: 1135-1143 [PMID: 15795240 DOI: 10.1084/jem.20042614]
26 **Suda K**, Kitagawa Y, Ozawa S, Saikawa Y, Ueda M, Ebina M, Yamada S, Hashimoto S, Fukata S, Abraham E, Maruyama I, Kitajima M, Ishizaka A. Anti-high-mobility group box chromosomal protein 1 antibodies improve survival of rats with sepsis. *World J Surg* 2006; **30**: 1755-1762 [PMID: 16850155 DOI: 10.1007/s00268-005-0369-2]
27 **Yang R**, Miki K, Oksala N, Nakao A, Lindgren L, Killeen ME, Mennander A, Fink MP, Tenhunen J. Bile high-mobility group box 1 contributes to gut barrier dysfunction in experimental endotoxemia. *Am J Physiol Regul Integr Comp Physiol* 2009; **297**: R362-R369 [PMID: 19494177 DOI: 10.1152/ajpregu.00184.2009]
28 **Wang LW**, Chen H, Gong ZJ. High mobility group box-1 protein inhibits regulatory T cell immune activity in liver failure in patients with chronic hepatitis B. *Hepatobiliary Pancreat Dis Int* 2010; **9**: 499-507 [PMID: 20943459]
29 **Cazzaniga M**, Dionigi E, Gobbo G, Fioretti A, Monti V, Salerno F. The systemic inflammatory response syndrome in cirrhotic patients: relationship with their in-hospital outcome. *J Hepatol* 2009; **51**: 475-482 [PMID: 19560225 DOI: 10.1016/j.jhep.2009.04.017]
30 **van der Poll T**, Levi M, van Deventer SJ, ten Cate H, Haagmans BL, Biemond BJ, Büller HR, Hack CE, ten Cate JW. Differential effects of anti-tumor necrosis factor monoclonal antibodies on systemic inflammatory responses in experimental endotoxemia in chimpanzees. *Blood* 1994; **83**: 446-451 [PMID: 8286742]

P- Reviewer: Grizzi F, Wei D **S- Editor**: Ma YJ
L- Editor: Wang TQ **E- Editor**: Zhang DN

World Journal of Gastroenterology

Submit a Manuscript: http://www.wjgnet.com/esps/
Help Desk: http://www.wjgnet.com/esps/helpdesk.aspx
DOI: 10.3748/wjg.v22.i16.4149

World J Gastroenterol 2016 April 28; 22(16): 4149-4159
ISSN 1007-9327 (print) ISSN 2219-2840 (online)

ORIGINAL ARTICLE

Basic Study

Thymoquinone inhibits proliferation in gastric cancer *via* the STAT3 pathway *in vivo* and *in vitro*

Wen-Qian Zhu, Jun Wang, Xu-Feng Guo, Zhou Liu, Wei-Guo Dong

Wen-Qian Zhu, Jun Wang, Xu-Feng Guo, Zhou Liu, Wei-Guo Dong, Department of Gastroenterology, Renmin Hospital of Wuhan University, Key Laboratory of Hubei Province for Digestive System Disease, Wuhan 430060, Hubei Province, China

Author contributions: Zhu WQ and Wang J contributed equally to this work; Zhu WQ, Wang J, Guo XF, Liu Z and Dong WG designed research; Zhu WQ, Wang J, Guo XF and Liu Z performed research; Wang J, Zhu WQ and Guo XF contributed new reagents/analytic tools; Wang J, Zhu WQ, Guo XF and Liu Z analyzed data; and Zhu WQ and Wang J wrote the paper.

Supported by The National Natural Science Foundation of China, No. 81372551.

Institutional review board statement: This study was reviewed and approved by the Wuhan University Institutional Review Board.

Institutional animal care and use committee statement: All procedures involving animals were reviewed and approved by the Institutional Animal Care and Use Committee of the Wuhan University.

Conflict-of-interest statement: We declare that we have no financial and personal relationships with other people or organizations that can inappropriately influence our work, there is no professional or other personal interest of any nature or kind in any product, service and/or company that could be construed as influencing the position presented in, or the review of, the manuscript entitled, "Thymoquinone inhibits proliferation in gastric cancer *via* the STAT3 pathway *in vivo* and *in vitro*".

Data sharing statement: Technical appendix, original data, images, and statistical code of this manuscript are available from the corresponding author at dwg@whu.edu.cn. Participants gave informed consent for data sharing.

Correspondence to: Dr. Wei-Guo Dong, Professor, Department of Gastroenterology, Renmin Hospital of Wuhan University, Key Laboratory of Hubei Province for Digestive System Disease, Hubei Zhang Road, Wuhan 430060, Hubei Province, China. dwg@whu.edu.cn
Telephone: +86-27-88041911
Fax: +86-27-88042292

Received: January 23, 2016
Peer-review started: January 25, 2016
First decision: February 18, 2016
Revised: February 26, 2016
Accepted: March 18, 2016
Article in press: March 18, 2016
Published online: April 28, 2016

Abstract

AIM: To elucidate the mechanism of thymoquinone (TQ)-induced apoptosis in human gastric cancer cells *in vitro* and *in vivo*.

METHODS: HGC27, BGC823, and SGC7901 cells were cultured *in vitro* and treated with TQ (0, 10, 25, 50, 75, 100, 125 μmol/L) for 12 h, 24 h, and 36 h, and then the proliferation inhibitory rates were detected by methylthiazole tetrazolium assay. Apoptosis was observed after Hoechst staining. The protein expressions of signal transducer and activator of transcription (STAT)3, p-STAT3, STAT5, p-STAT5, phospho-janus-activated kinase 2 (JAK2), JAK2, p-Src, Src, glyceraldehyde-3-phosphate dehydrogenase, lamin-A, survivin, Cyclin D, Bcl-2, Bax, peroxisome proliferator activated receptor, and caspase-3,7,9 were detected by western blot. Cell cycle and apoptosis were

determined with flow cytometry. TQ induced dose-dependent apoptotic cell death in HGC27 cells was measured by Annexin V-fluorescein isothiocyanate (FITC)/propidium iodide (PI) analysis and Hoechst 33258.

RESULTS: TQ inhibited the phosphorylation of STAT3 but not STAT5. TQ-induced downregulation of STAT3 activation was associated with a reduction in JAK2 and c-Src activity. TQ also downregulated the expression of STAT3-regulated genes, such as Bcl-2, cyclin D, survivin, and vascular endothelial growth factor, and activated caspase-3,7,9. Consistent with the *in vitro* results, TQ was significantly effective as an antitumor agent in a xenograft tumor mouse model.

CONCLUSION: This study provides strong evidence that downregulation of the STAT3 signaling pathway mediates TQ-induced apoptosis in gastric cancer.

Key words: Thymoquinone; Gastric cancer; STAT3; Proliferation; Apoptosis

Core tip: Thymoquinone (TQ) has been demonstrated to exert biological activity in gastric cancer. However, the specific mechanism of TQ in gastric cancer has not been examined. In order to elucidate the mechanism of TQ-induced apoptosis in human gastric cancer cells, we investigated the effects of TQ on signal transducer and activator of transcription (STAT)3 and its related pathway *in vitro* and *in vivo*.

Zhu WQ, Wang J, Guo XF, Liu Z, Dong WG. Thymoquinone inhibits proliferation in gastric cancer *via* the STAT3 pathway *in vivo* and *in vitro*. *World J Gastroenterol* 2016; 22(16): 4149-4159 Available from: URL: http://www.wjgnet.com/1007-9327/full/v22/i16/4149.htm DOI: http://dx.doi.org/10.3748/wjg.v22.i16.4149

INTRODUCTION

Based on the Global Burden of Cancer Study (GLOBOCAN) estimates, about 14.1 million new cancer cases and 8.2 million deaths occurred in 2012 worldwide[1]. Among them, gastric cancer ranks fourth and third for incidence rate and mortality rate, respectively, in male patients and ranks fifth in female patients[1]. Chemotherapy is commonly used in the treatment of gastric cancer. Commonly used chemotherapy drugs are 5-fluorouracil (5-FU), cisplatin, and doxorubicin, but they are limited by toxic side effects, the development of resistance, and other defects[2]. Therefore, it is important to search for low toxicity and efficient anti-cancer drugs that inhibit gastric cancer development.

Thymoquinone (TQ, also called 2-isopropyl-5-methyl-1,4-benzo-quinone, $C_{10}H_{12}O_2$) is the active constituent of black cumin (Nigella sativa) seed oil (Figure 1A) and was first extracted by EI-Dakhakhany[3]. TQ has been shown to suppress proliferation and induce apoptosis and drug resistance in various tumor cells, including colorectal carcinoma, pancreatic carcinoma, breast adenocarcinoma, prostate cancer, *etc.*[4-9]. A phase I study reported that in adult patients with solid tumors or hematological malignancies who were treated with TQ, there were no significant systemic toxicities[10]. It was also reported that the human body could tolerate a dose of 75 to 2600 TQ mg/d. Because of its high efficiency, low toxicity, and natural features in cancer prevention and treatment, TQ has gradually attracted the attention of scholars worldwide, but studies on tumors of the digestive system, especially gastric cancer, are rare.

Signal transducer and activator of transcription (STAT) has been shown to be a fundamental factor in tumor cell survival and proliferation[11]. STAT3, a member of the STAT protein family, is a critical molecule of the janus-activated kinase (JAK)/STAT signaling pathway through many signals, such as interleukin (IL)-6, tumor necrosis factor (TNF)-α, and vascular endothelial growth factor (VEGF). STAT3 can be activated by a variety of ligands related to these signals[12]. It was reported in a variety of human malignancies, such as gastric, colon, breast, and lung, that abnormal expression and constitutive activation of STAT3 are involved[12,13]. Once activated, STAT3 would continue to promote phosphorylation-induced homodimerization, leading to nuclear translocation, DNA binding, and subsequent gene transcription (*e.g.*, Bcl-xL, Bcl-2, survivin, cyclin D, Mcl-1). In addition, STAT3 could also control VEGF expression, which is necessary for angiogenesis and the maintenance of tumor vasculature[14]. STAT3 has been implicated in the inhibition of immune responses to tumor growth by blocking expression of pro-inflammatory factors. A previous study showed that TQ could induce apoptosis and augment 5-FU-induced apoptosis in gastric cancer cells[15]. However, specific mechanisms underlying the effects of TQ in gastric cancer have not been examined.

Based on preliminary studies, we explored the specific mechanisms of TQ-induced regulation of proliferation and apoptosis in gastric cancer cells.

MATERIALS AND METHODS

Cell culture and reagents

Three human gastric cancer cells (HGC27, BGC823, and SGC7901) were obtained from Key Laboratory of Hubei Province for Digestive System Disease (Wuhan University). The cells were maintained in continuous exponential growth in Dulbecco's Modified Eagle's Medium (DMEM)/F12 medium supplemented with heat-inactivated 10% fetal bovine serum (FBS) and 1% antibiotics (100 IU penicillin and 100 μg/mL

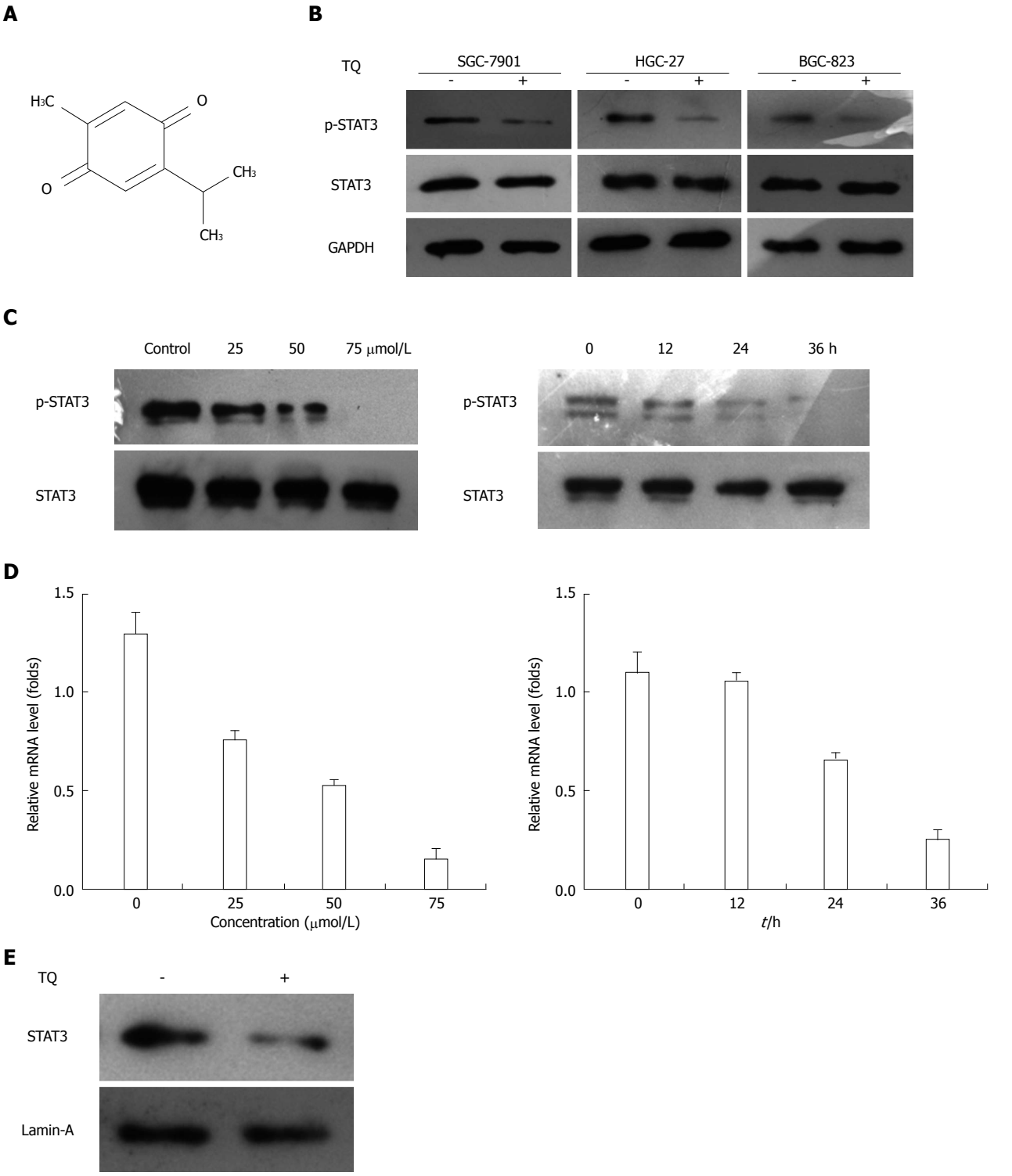

Figure 1 Thymoquinone suppresses constitutive STAT3 activation in three gastric cancer cell lines. A: Human gastric cancer cells (HGC27, BGC823, and SGC7901) were incubated with 50 μmol/L thymoquinone (TQ) for 24 h, and western blotting was performed as described previously; B: The same blots were stripped and reprobed with the GAPDH antibody to verify equal protein loading; C: TQ suppressed phospho-STAT3 levels in a concentration- and time-dependent manner. HGC27 cells (1 × 10^6/mL) were treated with the indicated concentrations of TQ for 24 h, and western blotting was performed (left). HGC27 cells (1 × 10^6/mL) were treated with 50 μmol/L TQ for the indicated times, and western blotting was performed (right). The same blots were stripped and reprobed with the STAT3 antibody to verify equal protein loading; D: TQ suppressed STAT3 gene levels in a concentration- and time-dependent manner. HGC27 cells (1 × 10^6/mL) were treated with the indicated concentrations of TQ for 24 h, and real-time RT-PCR was performed (left). HGC27 cells (1 × 10^6/mL) were treated with 50 μmol/L TQ for the indicated times, and real-time RT-PCR was performed (right); E: TQ suppressed STAT3 nuclear translocation. HGC27 cells (1 × 10^6/mL) cells were treated with or without 50 μmol/L TQ for 24h, and nuclear extracts were assessed for the detection nuclear accumulation of STAT3. Lamin-A was used as a nuclear extract marker. GAPDH: Glyceraldehyde-3-phosphate dehydrogenase; RT-PCR: Reverse transcription polymerase chain reaction; STAT: Signal transducer and activator of transcription.

streptomycin) in a humidified incubator at 37 ℃ and 5% CO_2.

Western blot analysis

Protein expression levels were assessed by western blot analysis. Briefly, cells were collected, washed twice, and lysed with lysis buffer. Cell lysates were kept on ice for 30 min and centrifuged at 4 ℃. Samples were then boiled in loading buffer and separated by 10% SDS-PAGE. After electrophoresis, protein was transferred onto a nitrocellulose membrane (Millipore, Bedford, MA, United States), which was incubated with blocking solution [10% non-fat dry milk in Tris-buffered saline with tween (TBST) containing 0.05% Tween-20] for 2 h and immunoblotted with primary antibodies, including STAT3, p-STAT3, STAT5, p-STAT5, p-JAK2, JAK2, p-Src, Src, glyceraldehyde-3-phosphate dehydrogenase (GAPDH), Lamin-A, survivin, Cyclin D, Bcl-2, Bax, peroxisome proliferator activated receptor, caspase-3,7,9 (Cell Signaling Technology, Beverly, MA, United States, 1:1000), overnight at 4 ℃. After washing with TBST, the membranes were incubated with anti-rabbit (or anti-mouse) immunoglobulin conjugated to horseradish peroxidase secondary antibody (Promega, Madison, WI, United States, 1:500) for 2 h at room temperature, developed using the enhanced chemiluminescence (ECL) western blotting kit (Millipore, Bedford, MA, United States), and then exposed to Kodak X-ray Film. Protein band intensities were determined densitometrically using the video imaging CMIASWIN system (BioRad, Hercules, CA, United States).

Real-time reverse transcription polymerase chain reaction

Total RNA and complementary DNA (cDNA) were extracted from the cells for real-time reverse transcription polymerase chain reaction (RT-PCR) analysis as described previously[16]. The cDNA was used as the template in an SYBR Green Real-Time PCR Master Mix (Invitrogen, Carlsbad, CA, United States). The PCR reaction was performed with an ABI PRISM 7300 PCR and detection system (Applied Biosystems, Carlsbad, CA, United States). The following primers were used: STAT3 sense 5′- GCCCTTTGGAACGAAGGGTA-3′ and STAT3 antisense 5′- TGGTATTGCTGCAGGTCGTT-3′; GAPDH sense, 5′-TTTGGTATCGTGGAAGGAC-3′, and GAPDH antisense, 5′- GTGGAGGAGTGGGTGTCGC-3′. The relative levels of STAT3 mRNA transcripts were normalized to the control GAPDH. For relative quantification, the expression levels of the *STAT3* gene were calculated based on the method of $2^{-\Delta\Delta Ct}$[17].

STAT3-Luciferase reporter gene assay

Cells were seeded into 12-well plates at a density of 5 × 10^4 cells/well prior to transfection. Cells were transfected with p-STAT3-TA-luc (Clontech, Palo Alto, CA, United States) or control vector using Genefectin transfection reagent (Genetrone Biotech, Seoul, South Korea). After 24 h of transfection, cells were treated with TQ for an additional 24 h, and cell lysis was carried out with 1 × reporter lysis buffer. After mixing the cell lysates with luciferase substrate (Promega), luciferase activity was measured using a luminometer (Tecan Trading AG, Shanghai, China). The β-galactosidase assay was carried out according to the supplier's instructions (Promega Enzyme Assay System) for normalizing the luciferase activity, and the results are expressed as fold transactivation.

Cell proliferation assay

Cell proliferation was assessed with 3-(4,5-dimethylthiazolyl-2)-2,5-diphenyltetrazolium bromide (MTT) (Sigma St. Louis, MO, United States) colorimetric method. Gastric cancer cells were cultured in a 96-well plate in the presence of 0, 25, 50, 75, or 100 μmol/L TQ for 12, 24, or 36 h. MTT reagent (20 μL) was added into each well and incubated for 4 h at 37 ℃. After the purple precipitate was visible, the cells were added with 150 μL dimethylsulfoxide and incubated at room temperature in the dark for 2 h. The absorbance was recorded at 490 nm. For each experiment, the total procedure was repeated three times.

Hoechst 33258 staining for apoptotic cells

Gastric cancer cells in exponential growth were placed at a final concentration of 5 × 10^5 cells per well in a six-well plate, which was pretreated with 25 μmol/L, 50 μmol/L, or 75 μmol/L TQ for 24 h. The cells were subsequently fixed, washed three times with phosphate buffered saline (PBS), and stained with Hoechst 33258 (Sigma-Aldrich) according to the manufacturer's protocol. Apoptotic features were assessed by analyzing chromatin condensation and by staining the fragments under an inverted fluorescent microscope (Olympus, Center Valley, PA, United States).

Annexin V staining for apoptosis

Gastric cancer cells were cultured in six-well plates at 1 × 10^6 cells/well in DMEM medium supplemented with 0.5% FBS and different concentrations of TQ as described above. Cells were washed twice with cold PBS and centrifuged, and then incubated with 5 mL of Annexin V-fluorescein isothiocyante (FITC) and 10 mL of propidium iodide (PI) at room temperature for 5 min in the dark. Flow cytometric analysis was performed with a FACSCalibur using the CellQuest software (BDIS, San Jose, CA, United States). For each experiment, the total procedure was repeated three times.

Xenograft tumor model

Female BALB/c athymic nude mice (4-wk-old) were obtained from the Center of Experimental Animals of Wuhan University, and all procedures were performed in compliance with the National Institutes of Health

Guide for the Care and Use of Laboratory Animals. Nude mice were divided into four groups, and mice were housed (four animals per cage) in standard mouse plexiglass cages in a light and temperature-controlled environment. Mice were provided with food and water *ad libitum*. Gastric cancer cells were harvested from subconfluent cultures, washed in serum-free medium, and resuspended in PBS. Cells (5×10^6) resuspended in 0.2 mL PBS were subcutaneously inoculated into the lower right flank of nude mice. When the developing tumors reached 100-150 mm^3 in size, mice were randomly assigned to the following treatment groups ($n = 5$): (1) untreated control, equal volume physiologic saline; (2) 10 mg/kg TQ; (3) 20 mg/kg TQ; and (4) 30 mg/kg TQ. All therapies were administered three times per week *via* intraperitoneal injection. Next, the mice were weighed, and the size of each tumor and its central necrotic area was monitored using calipers every 3 d. Following the last dose of TQ, all mice were sacrificed on day 30. During the autopsy procedure, the tumor was neatly excised and weighed. One part of the tissue was fixed in formalin, and another part was frozen in liquid nitrogen. Ethical approval was obtained prior to the start of the experiments.

TdT-mediated dUTP-biotin nick end-labeling assay

For histological examination, tumor tissues were fixed in 10% buffered formalin and embedded in paraffin, and tissue sections (4 μm) were prepared. The TdT-mediated dUTP-biotin nick end-labeling (TUNEL) assay for apoptosis was conducted using an apoptosis detection kit (Roche Diagnostics, Branchburg, NJ, United States) according to the manufacturer's instructions. Positive cells were counted as the number of TUNEL-labeled cells per 100 epithelial cancer cells in 10 fields of the most affected tumor areas with 400 × magnification and analyzed using light microscopy (Carl Zeiss, Thornwood, NY, United States).

Statistical analysis

Results were analyzed by SPSS version 17.0 (SPSS, Inc., Chicago, IL, United States). All data are presented as the mean ± standard deviation (SD). One-way analysis of variance (ANOVA, multiple comparisons) and *t*-tests (two groups comparisons) were performed accordingly. $P < 0.05$ was considered to be statistically significant.

RESULTS

TQ inhibited constitutive STAT3 phosphorylation and nuclear translocation in gastric cancer cells

Since HGC27, BGC823, and SGC7901 cells were shown to express constitutive STAT3 activation, we determined whether TQ could inhibit this activation in these cells. Based on western blot results, the protein level of p-STAT3 was significantly reduced in all three types of cancer cells treated with TQ compared to cells not treated with TQ (Figure 1B). These findings suggest that TQ inhibited STAT3 activation in all these cells in a concentration- and time-dependent manner, with maximum inhibition occurring at 75 μmol/L (Figure 1C). Although TQ did not affect protein levels of STAT3 (Figure 1B, lower panel), it did suppress the mRNA expression of STAT3 in a concentration- and time-dependent manner, as demonstrated by real-time RT-PCR (Figure 1D). Because the active dimer of STAT3 is capable of translocating to the nucleus and inducing transcription of specific target genes[18], we determined whether TQ suppresses the nuclear translocation of STAT3. Western blot clearly demonstrated that TQ blocked the translocation of STAT3 into the nucleus in HGC27 cells (Figure 1E). The phosphorylation of STAT5 and the expression of STAT5 were not affected by TQ (Figure 2A and B), indicating that TQ specifically inhibits STAT3 tyrosine phosphorylation.

TQ suppressed constitutive activation of other proteins

Since JAK2 and c-Src kinase are two of the main kinases involved in the activation of STAT3[19,20], we examined the effect of TQ on the expression and phosphorylation of these two proteins. As shown in Figure 2C, JAK2 was constitutively active in HGC27 cells, and pretreatment with TQ clearly suppressed its phosphorylation in a time-dependent manner. TQ treatment did not affect total JAK2 levels. In addition, we found that TQ suppressed the constitutive phosphorylation of c-Src kinase in a time-dependent manner (Figure 2D), while the levels of total c-Src kinase remained unchanged under the same conditions (Figure 2D, lower panel).

TQ suppresses STAT3-dependent reporter gene expression

STAT3 is constitutively active in gastric cancer and plays a critical role in cell proliferation through transcriptional activation of pro-survival genes[21]. We found that TQ reduced STAT3 reporter gene activity in HGC27 cells transiently transfected with STAT3-luc vector (Figure 3A). Moreover, TQ attenuated the protein expression of STAT3 target gene products, such as survivin, cyclin-D, VEGF, and Bcl-2 and increased the expression levels of Bax (Figure 3B and C).

TQ activated caspase activity and induced PARP cleavage

Next, we investigated whether suppression of constitutively active STAT3 in HGC27 cells by TQ caused cell apoptosis. In HGC27 cells, TQ activated procaspase-3,7,9 in a concentration-dependent manner (Figure 3D). Activation of downstream procaspase-3 led to the cleavage of a 116 kDa poly(ADP-ribose)-polymerase (PARP) protein into an 85 kDa fragment (Figure 3C). These results clearly suggested that TQ induces caspase-3-dependent apoptosis in HGC27 cells.

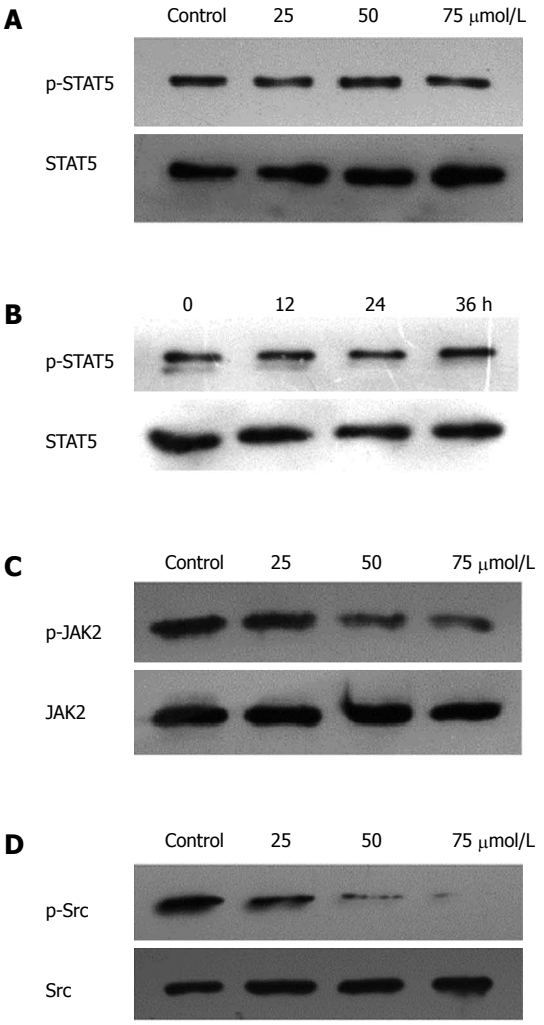

Figure 2 Thymoquinone suppresses phospho-JAK2 and phospho-Src levels, but not STAT5 levels. A: HGC27 cells (1 × 10^6/mL) were treated with the indicated concentrations of thymoquinone (TQ) for 24 h, and western blotting was performed; B: HGC27 cells (1 × 10^6/mL) were treated with 50 μmol/L TQ for the indicated times, and western blotting was performed. The same blots were stripped and reprobed with the STAT5 antibody to verify equal protein loading; C: TQ suppressed phospho-JAK2 levels in a concentration -dependent manner. HGC27 cells (1 × 10^6/mL) were treated with the indicated concentrations of TQ for 24 h, and Western blotting was performed. The same blots were stripped and reprobed with the JAK2 antibody to verify equal protein loading; D: TQ suppressed phospho-Src levels in a concentration -dependent manner. HGC27 cells (1 × 10^6/mL) were treated with the indicated concentrations of TQ for 24 h, and Western blotting was performed. The same blots were stripped and reprobed with the Src antibody to verify equal protein loading. JAK: Janus-activated kinase.

TQ inhibited proliferation and induces apoptosis

According to the results of the MTT assay, cell viability was reduced in the presence of TQ (25, 50 or 75 μmol/L) in a time- and concentration-dependent manner (Figure 4). Annexin V staining of cells treated with the indicated concentrations of TQ showed that the compound induced apoptosis in a concentration-dependent manner (Figure 5A). In addition, Hoechst 33258 staining was performed in TQ treated cells and showed that apoptotic bodies containing nuclear fragments were generated in apoptotic cells (Figure 5B).

Anti-tumor effects in vivo

Based on the induction of apoptosis in gastric cancer cell *in vitro*, the antitumor effect of TQ was dose-dependent. In a xenograft tumor mouse model, the treatments of intraperitoneally administered injections of TQ for 30 d led to significant decreases in tumor weight and size compared to the control group mice ($P < 0.05$). (Figure 6A and B). Tumor tissues isolated from the xenograft mice of the four groups were processed for TUNEL assay, and the results showed (Figure 6C and D) that the tumors derived from high doses of TQ treated mice exhibited a markedly higher count of apoptotic bodies compared with that from control group mice. In addition, we measured the levels of STAT3 in tumor tissue by western blot and found that TQ inhibited STAT3 phosphorylation *in vivo* (Figure 6E).

DISCUSSION

As the second most common cause of cancer-related death in the world, gastric cancer has been reported to have particularly high incidence and mortality rates in eastern Asia. Its survival rate is substantially lower than that of patients with other types of cancers[22].

TQ, the active constituent of black cumin seed oil, was shown to inhibit the proliferation of various types of tumor cells, including lung carcinoma, breast adenocarcinoma, pancreatic cancer, colorectal cancer, acute lymphoblastic leukemia, and prostate cancer[23,24]. It has also been shown to enhance detoxification and inhibit benzo(a)pyrene (BP)-induced fore-stomach tumors in a female Swiss albino mouse model[25]. TQ was also induced apoptosis and augmented 5-FU-induced apoptosis in gastric cancer cells[15]. In this study, we found that TQ inhibited phosphorylation of STAT3 in three gastric cancer cells. TQ also inhibited the expression of the *STAT3* gene in a concentration- and time-dependent manner, as demonstrated by real-time RT-PCR.

Phosphorylation of STAT3 is required for its activation and results in dimerization, nuclear translocation, DNA binding, and transcriptional activation of target genes[26]. To investigate the mechanism of TQ-induced STAT3 inhibition in HGC27 cells, we analyzed the activation of upstream protein kinases, such as JAK and Src. We found that TQ could inhibit JAK2 and Src phosphorylation, and presumably the suppression of STAT3 phosphorylation at Tyr705 was due to the inhibition of JAK2 and Src activity. Interestingly, TQ-induced inhibition of tyrosine phosphorylation was only observed for STAT3, not STAT5. These results suggest that TQ specifically inhibited phosphorylation of STAT3 at Tyr705.

We also observed that TQ suppressed the expression of several STAT3-regulated genes, including proliferative (cyclin D1), anti-apoptotic (Bcl-2, survivin), and angiogenic (VEGF) gene products in HGC27 cells. Activation of

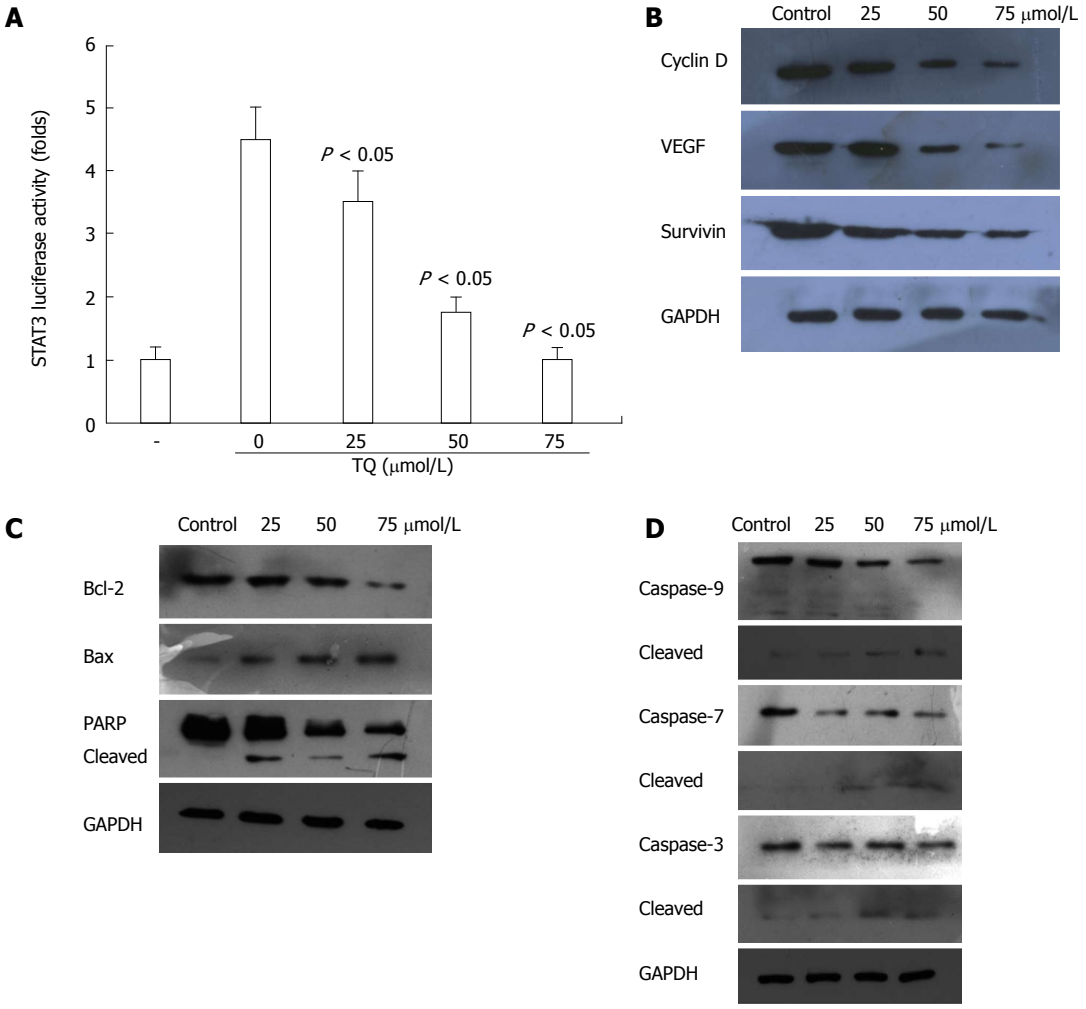

Figure 3 Thymoquinone suppresses STAT3-dependent reporter gene expression and activates caspase activity. A: Thymoquinone (TQ) suppressed STAT3 transcriptional activity. HGC27 cells (1 × 10^6/mL) were transfected with STAT3-luciferase (STAT3-Luc) plasmid, incubated for 24 h, and treated with 25, 50, and 75 μmol/L TQ for 24 h. Whole-cell extracts were then prepared and analyzed for luciferase activity. The results shown are representative of three independent experiments; B: TQ inhibited the expression of Cyclin D, survivin, and VEGF. HGC27 cells (1 × 10^6/mL) were treated with the indicated concentrations of TQ for 24 h, and western blotting was performed. The same blots were stripped and reprobed with the GAPDH antibody to verify equal protein loading; C: HGC27 cells (1 × 10^6/mL) were treated with the indicated concentrations of TQ for 24 h, and whole-cell extracts were prepared, separated by SDS-PAGE, and subjected to western blot against Bcl-2, Bax, and PARP antibody. The same blot was stripped and reprobed with GAPDH antibody to show equal protein loading; (D) TQ activates caspase activity. HGC27 cells (1 × 10^6/mL) were treated with the indicated concentrations of TQ for 24 h, and western blotting was performed. The results shown are representative of three independent experiments. PARP: Poly(ADP-ribose)polymerase

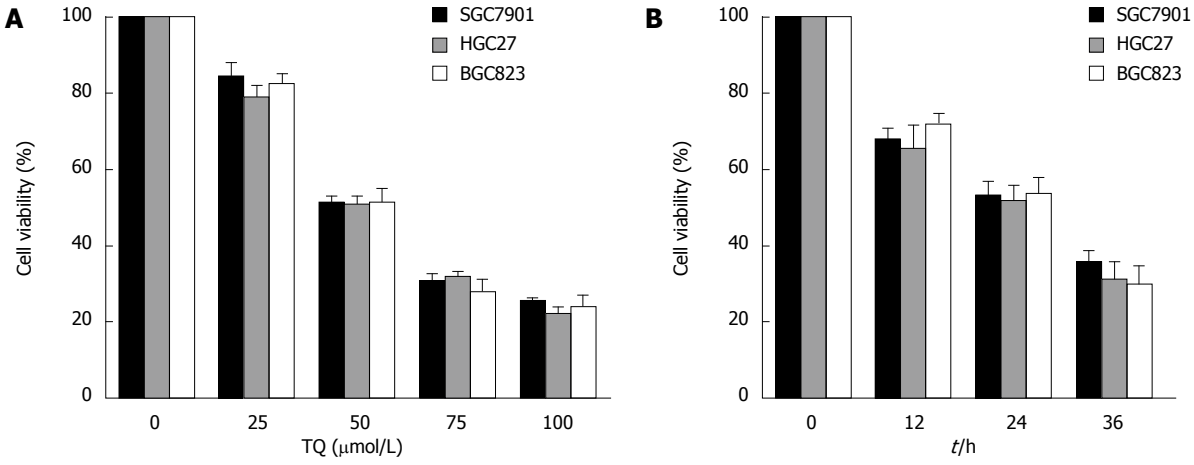

Figure 4 Thymoquinone inhibits proliferation in gastric cancer cells. A: Gastric cancer cells were treated with 25 μmol/L, 50 μmol/L, or 100 μmol/L TQ for 24 h, after which an MTT assay was performed; B: Cells were treated with 50 μmol/L TQ for 12, 24, or 36 h, and an MTT assay was performed. TQ: Thymoquinone.

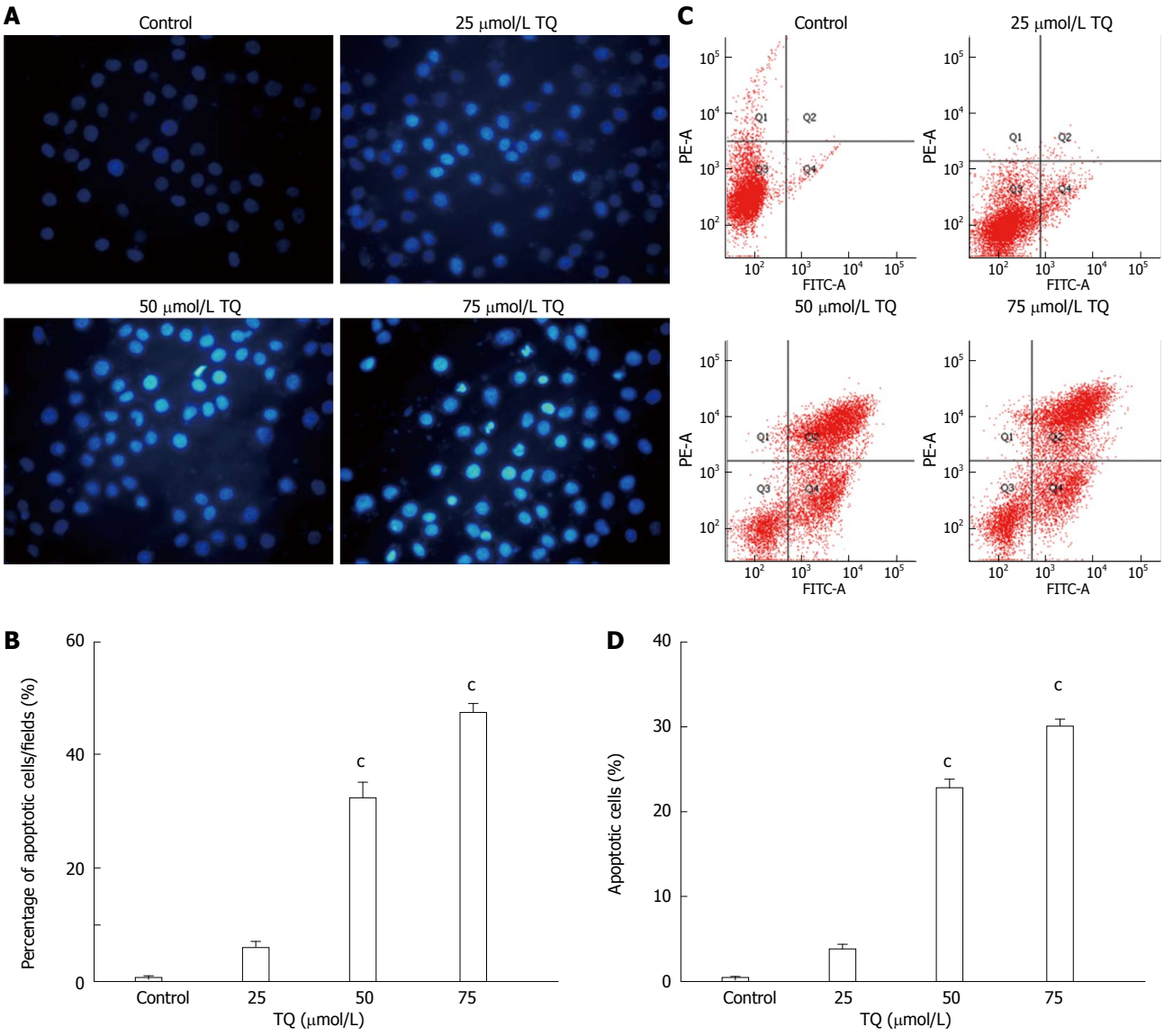

Figure 5 Thymoquinone induces apoptosis in HGC27 cells. A: Detection of apoptosis *via* Annexin V/PI staining (X-axis: annexin V; Y-axis: PI). The proportion of non-apoptotic cells (Q3), early apoptotic cells (Q4), late apoptotic/necrotic cells (Q2), and cell debris or death cell (Q1); B: Data shown are mean ± SD from three independent experiments; C: Apoptosis was assessed using Hoechst 33258, and apoptotic features were assessed by observing chromatin condensation and fragment staining (original magnification, × 200); D: Quantitative analysis of apoptotic cells is represented as the mean ± SD from three independent experiments. $^{c}P < 0.05$, *vs* control and 25 μmol/L TQ. PI: Propidium iodide; TQ: Thymoquinone.

STAT3 signaling was thought to induce survivin gene expression and confer resistance to apoptosis in human breast cancer cells[27]. It was reported that blocking cell death by Bcl-2 and Bcl-xL could be induced by a variety of chemotherapeutic agents, in parallel with an increase in chemoresistance[28,29]. Thus, we considered that the downregulation of the expression of Bcl-2, Bcl-xL, and survivin was likely to be linked with the ability of TQ to induce apoptosis in HGC27 cells, as evidenced by cleavage of PARP. In addition, we observed that TQ could activate caspase-3,7,9 activities in a concentration-dependent manner. The MTT assay showed that TQ could inhibit cell viability in a concentration- and time-dependent manner. TQ dose-dependently induced apoptotic cell death in HGC27 cells, as estimated by Annexin V-FITC/PI analysis and Hoechst33258.

In addition to these *in vitro* studies, we further analyzed the effect of TQ on xenograft tumor *in vivo*. We found that TQ treatment exhibited obvious antitumor effects in a xenograft tumor mouse model. The therapeutic effect was demonstrated by TUNEL analysis, which displayed obvious cell death in the tumor masses *via* apoptosis. Moreover, STAT3 protein was measured in tumor tissue, and we found that the levels of p-STAT3 in the tumor tissue were significantly decreased after TQ treatment.

In conclusion, the present study demonstrated that TQ inhibited proliferation and induced apoptosis *via* down-regulation of the STAT3 signaling pathway.

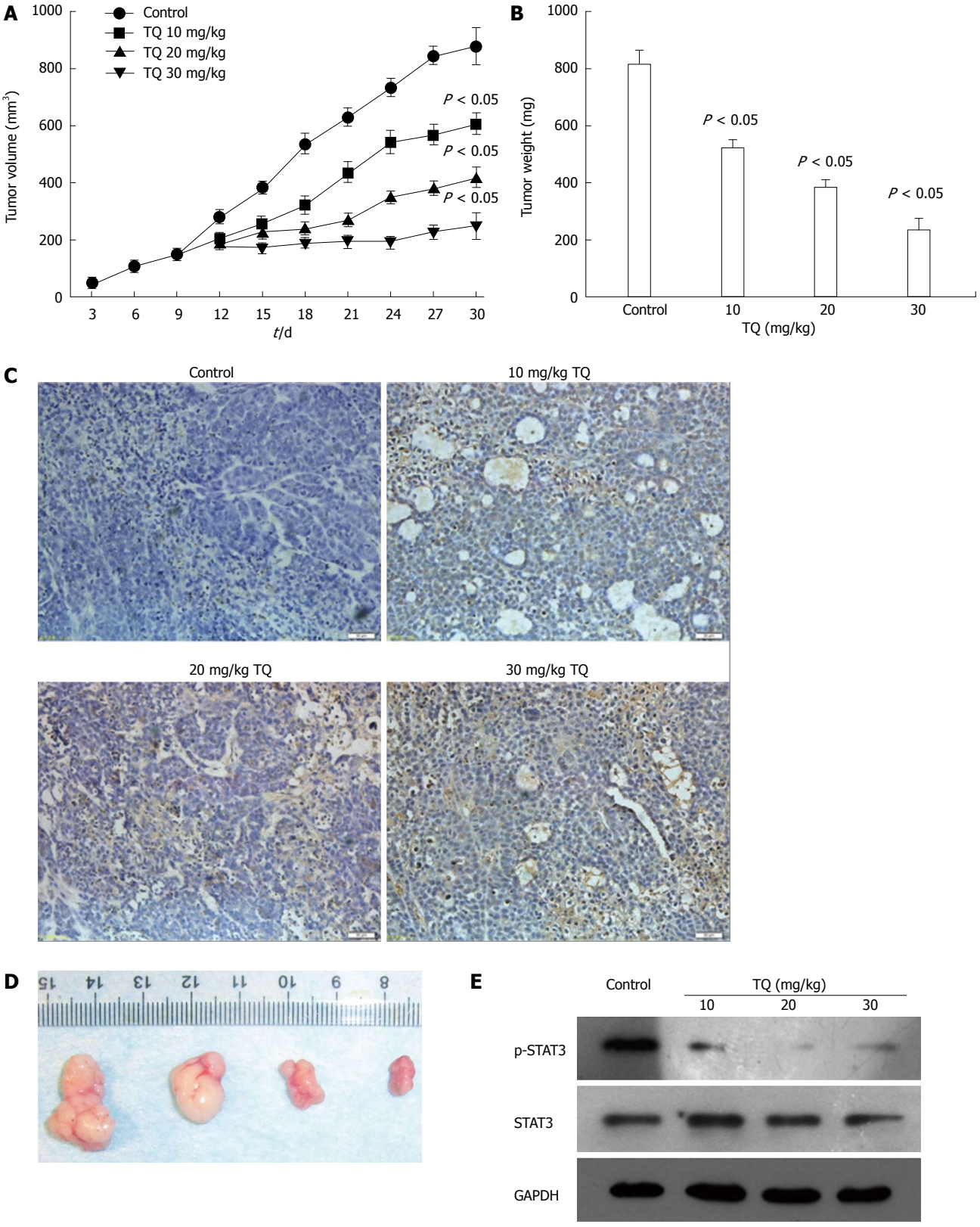

Figure 6 Thymoquinone inhibits tumor growth in a gastric mouse xenograft model. A: Tumor volumes of the xenograft tumors derived from 0, 25, 50, or 75 μmol/L TQ group. Each time point represents the mean tumor volume for each group; B: Tumor weight was obtained at the end of the experiment. Error bars represent the standard error of the mean ± SD; C: Detection of apoptotic cells in tumor tissue by TUNEL assay. Control: equal-volume physiologic saline; Treatment group: different doses of TQ: 10 mg/kg TQ; 20 mg/kg TQ; 30 mg/kg TQ; all therapies were administered three times per week *via* intraperitoneal injection. The brown color indicating apoptotic signals is shown by the arrows. Scale bar represents 50 mL. Original magnification: 400 ×; D: Photographs of tumors from control and TQ treatment groups. From left to right: control group, 10 mg/kg TQ; 20 mg/kg TQ; 30 mg/kg TQ group; E: TQ suppresses phosphor-STAT3 *in vivo*. The tumor tissue extracts were prepared, after which Western blotting was performed. The same blots were stripped and reprobed with the GAPDH antibody to verify equal protein loading. TQ: Thymoquinone; TUNEL: TdT-mediated dUTP-biotin nick end-labeling.

TQ may be a promising candidate as a cancer chemo-preventive or chemotherapeutic agent.

COMMENTS

Background

Thymoquinone (TQ) has been demonstrated to exert biological activity in gastric cancer. However, the specific mechanism by which TQ affects gastric cancer remains to be examined. In order to elucidate the mechanism of TQ-induced apoptosis in human gastric cancer cells, we investigated the effects of TQ on signal transducer and activator of transcription (STAT)3 activation and its relative pathway both *in vitro* and *in vivo*.

Research frontiers

In 2014, Kundu *et al* found in human colon cancer HCT116 cells that TQ induced apoptosis through inactivation of STAT3 by blocking janus-activated kinase (JAK)2- and Src-mediated phosphorylation of endothelial growth factor (EGF) receptor tyrosine kinase. This finding is similar with the authors' study, thus they examined JAK2- and Src as well.

Innovations and breakthroughs

It was previously shown that TQ could induce apoptosis in gastric cancer cells. However, the specific mechanism of TQ in gastric cancer had not been examined. Our study demonstrated in gastric tumor cells that TQ inhibited proliferation and induced apoptosis though downregulation of the STAT3 signaling pathway. These findings suggest that TQ may be a potential chemopreventive or chemotherapeutic candidate for gastric cancer.

Applications

Since STAT3 is one of the main signaling pathways involved in TQ-mediated inhibition of gastric cancer, TQ may be used safely clinically. However, it remains to be determined if TQ will be useful in gastric cancer with drug resistance. In the future, this will be examined.

Terminology

Thymoquinone (TQ, also called 2-isopropyl-5-methyl-1,4-benzo-quinone, $C_{10}H_{12}O_2$) is the active constituent of black cumin (Nigella sativa) seed oil (Figure 1A) and was first extracted by El-Dakhakhany. STAT refers to signal transducer and activator of transcription. VEGF refers to vascular endothelial growth factor.

Peer-review

In this article, the authors analyzed the mechanism underlying the effect of TQ in the treatment of gastric cancer. This study has practical research significance, providing important information to guide the clinical administration of TQ in the future.

REFERENCES

1 **Torre LA**, Bray F, Siegel RL, Ferlay J, Lortet-Tieulent J, Jemal A. Global cancer statistics, 2012. *CA Cancer J Clin* 2015; **65**: 87-108 [PMID: 25651787 DOI: 10.3322/caac.21262]

2 **Ohtsu A**. Chemotherapy for metastatic gastric cancer: past, present, and future. *J Gastroenterol* 2008; **43**: 256-264 [PMID: 18458840 DOI: 10.1007/s00535-008-2177-6]

3 **El-Dakhakhany M**. Studies on the chemical constitution of Egyptian N. Sativa L. seeds. *Planta Medica* 1963; **11**: 465-470 [DOI: 10.1055/s-0028-1100266]

4 **Gali-Muhtasib H**, Kuester D, Mawrin C, Bajbouj K, Diestel A, Ocker M, Habold C, Foltzer-Jourdainne C, Schoenfeld P, Peters B, Diab-Assaf M, Pommrich U, Itani W, Lippert H, Roessner A, Schneider-Stock R. Thymoquinone triggers inactivation of the stress response pathway sensor CHEK1 and contributes to apoptosis in colorectal cancer cells. *Cancer Res* 2008; **68**: 5609-5618 [PMID: 18632613 DOI: 10.1158/0008-5472.CAN-08-0884]

5 **Chehl N**, Chipitsyna G, Gong Q, Yeo CJ, Arafat HA. Anti-inflammatory effects of the Nigella sativa seed extract, thymoquinone, in pancreatic cancer cells. *HPB (Oxford)* 2009; **11**: 373-381 [PMID: 19768141 DOI: 10.1111/j.1477-2574.2009.00059.x]

6 **Connelly L**, Barham W, Onishko HM, Sherrill T, Chodosh LA, Blackwell TS, Yull FE. Inhibition of NF-kappa B activity in mammary epithelium increases tumor latency and decreases tumor burden. *Oncogene* 2011; **30**: 1402-1412 [PMID: 21076466 DOI: 10.1038/onc.2010.521]

7 **Kaseb AO**, Chinnakannu K, Chen D, Sivanandam A, Tejwani S, Menon M, Dou QP, Reddy GP. Androgen receptor and E2F-1 targeted thymoquinone therapy for hormone-refractory prostate cancer. *Cancer Res* 2007; **67**: 7782-7788 [PMID: 17699783 DOI: 10.1158/0008-5472.CAN-07-1483]

8 **Das S**, Dey KK, Dey G, Pal I, Majumder A, MaitiChoudhury S, kundu SC, Mandal M. Antineoplastic and apoptotic potential of traditional medicines thymoquinone and diosgenin in squamous cell carcinoma. *PLoS One* 2012; **7**: e46641 [PMID: 23077516 DOI: 10.1371/journal.pone.0046641]

9 **Attoub S**, Sperandio O, Raza H, Arafat K, Al-Salam S, Al Sultan MA, Al Safi M, Takahashi T, Adem A. Thymoquinone as an anticancer agent: evidence from inhibition of cancer cells viability and invasion in vitro and tumor growth in vivo. *Fundam Clin Pharmacol* 2013; **27**: 557-569 [PMID: 22788741 DOI: 10.1111/j.1472-8206.2012.01056.x]

10 **Al-Amri AM**, Bamosa AO. Phase I safety and clinical activity study of thymoquinone in patients with advanced refractory malignant disease. *Shiraz E-Med J* 2009; **10**: 107-111

11 **Ihle JN**. The Stat family in cytokine signaling. *Curr Opin Cell Biol* 2001; **13**: 211-217 [PMID: 11248555 DOI: 10.1016/S0955-0674(00)00199-X]

12 **Xiong A**, Yang Z, Shen Y, Zhou J, Shen Q. Transcription Factor STAT3 as a Novel Molecular Target for Cancer Prevention. *Cancers (Basel)* 2014; **6**: 926-957 [PMID: 24743778 DOI: 10.3390/cancers6020926]

13 **Kanda N**, Seno H, Konda Y, Marusawa H, Kanai M, Nakajima T, Kawashima T, Nanakin A, Sawabu T, Uenoyama Y, Sekikawa A, Kawada M, Suzuki K, Kayahara T, Fukui H, Sawada M, Chiba T. STAT3 is constitutively activated and supports cell survival in association with survivin expression in gastric cancer cells. *Oncogene* 2004; **23**: 4921-4929 [PMID: 15077160 DOI: 10.1038/sj.onc.1207606]

14 **Niu G**, Wright KL, Huang M, Song L, Haura E, Turkson J, Zhang S, Wang T, Sinibaldi D, Coppola D, Heller R, Ellis LM, Karras J, Bromberg J, Pardoll D, Jove R, Yu H. Constitutive Stat3 activity up-regulates VEGF expression and tumor angiogenesis. *Oncogene* 2002; **21**: 2000-2008 [PMID: 11960372 DOI: 10.1038/sj.onc.1205260]

15 **Lei X**, Lv X, Liu M, Yang Z, Ji M, Guo X, Dong W. Thymoquinone inhibits growth and augments 5-fluorouracil-induced apoptosis in gastric cancer cells both in vitro and in vivo. *Biochem Biophys Res Commun* 2012; **417**: 864-868 [PMID: 22206670 DOI: 10.1016/j.bbrc.2011.12.063]

16 **Song J**, Peng XL, Ji MY, Ai MH, Zhang JX, Dong WG. Hugl-1 induces apoptosis in esophageal carcinoma cells both in vitro and in vivo. *World J Gastroenterol* 2013; **19**: 4127-4136 [PMID: 23864775 DOI: 10.3748/wjg.v19.i26.4127]

17 **Livak KJ**, Schmittgen TD. Analysis of relative gene expression data using real-time quantitative PCR and the 2(-Delta Delta C(T)) Method. *Methods* 2001; **25**: 402-408 [PMID: 11846609 DOI: 10.1006/meth.2001.1262]

18 **Yu CL**, Meyer DJ, Campbell GS, Larner AC, Carter-Su C, Schwartz J, Jove R. Enhanced DNA-binding activity of a Stat3-related protein in cells transformed by the Src oncoprotein. *Science* 1995; **269**: 81-83 [PMID: 7541555 DOI: 10.1126/science.7541555]

19 **Ihle JN**. STATs: signal transducers and activators of transcription. *Cell* 1996; **84**: 331-334 [PMID: 8608586 DOI: 10.1016/S0092-8674(00)81277-5]

20 **Schreiner SJ**, Schiavone AP, Smithgall TE. Activation of STAT3 by the Src family kinase Hck requires a functional SH3 domain.

J Biol Chem 2002; **277**: 45680-45687 [PMID: 12244095 DOI: 10.1074/jbc.M204255200]

21 **Aggarwal BB**, Kunnumakkara AB, Harikumar KB, Gupta SR, Tharakan ST, Koca C, Dey S, Sung B. Signal transducer and activator of transcription-3, inflammation, and cancer: how intimate is the relationship?. *Ann N Y Acad Sci* 2009; **1171**: 59-76 [PMID: 19723038 DOI: 10.1111/j.1749-6632.2009.04911.x]

22 **Shen L**, Shan YS, Hu HM, Price TJ, Sirohi B, Yeh KH, Yang YH, Sano T, Yang HK, Zhang X, Park SR, Fujii M, Kang YK, Chen LT. Management of gastric cancer in Asia: resource-stratified guidelines. *Lancet Oncol* 2013; **14**: e535-e547 [PMID: 24176572 DOI: 10.1016/S1470-2045(13)70436-4]

23 **Banerjee S**, Kaseb AO, Wang Z, Kong D, Mohammad M, Padhye S, Sarkar FH, Mohammad RM. Antitumor activity of gemcitabine and oxaliplatin is augmented by thymoquinone in pancreatic cancer. *Cancer Res* 2009; **69**: 5575-5583 [PMID: 19549912 DOI: 10.1158/0008-5472.CAN-08-4235]

24 **Kundu J**, Choi BY, Jeong CH, Kundu JK, Chun KS. Thymoquinone induces apoptosis in human colon cancer HCT116 cells through inactivation of STAT3 by blocking JAK2- and Src-mediated phosphorylation of EGF receptor tyrosine kinase. *Oncol Rep* 2014; **32**: 821-828 [PMID: 24890449]

25 **Badary OA**, Al-Shabanah OA, Nagi MN, Al-Rikabi AC, Elmazar MM. Inhibition of benzo(a)pyrene-induced forestomach carcinogenesis in mice by thymoquinone. *Eur J Cancer Prev* 1999; **8**: 435-440 [PMID: 10548399 DOI: 10.1097/00008469-199910000-00009]

26 **Groner B**, Lucks P, Borghouts C. The function of Stat3 in tumor cells and their microenvironment. *Semin Cell Dev Biol* 2008; **19**: 341-350 [PMID: 18621135 DOI: 10.1016/j.semcdb.2008.06.005]

27 **Gritsko T**, Williams A, Turkson J, Kaneko S, Bowman T, Huang M, Nam S, Eweis I, Diaz N, Sullivan D, Yoder S, Enkemann S, Eschrich S, Lee JH, Beam CA, Cheng J, Minton S, Muro-Cacho CA, Jove R. Persistent activation of stat3 signaling induces survivin gene expression and confers resistance to apoptosis in human breast cancer cells. *Clin Cancer Res* 2006; **12**: 11-19 [PMID: 16397018 DOI: 10.1158/1078-0432.CCR-04-1752]

28 **Simonian PL**, Grillot DA, Nuñez G. Bcl-2 and Bcl-XL can differentially block chemotherapy-induced cell death. *Blood* 1997; **90**: 1208-1216 [PMID: 9242554]

29 **Tu Y**, Renner S, Xu F, Fleishman A, Taylor J, Weisz J, Vescio R, Rettig M, Berenson J, Krajewski S, Reed JC, Lichtenstein A. BCL-X expression in multiple myeloma: possible indicator of chemoresistance. *Cancer Res* 1998; **58**: 256-262 [PMID: 9443402]

P- Reviewer: Caboclo JLF, Martin-Villa JM **S- Editor**: Ma YJ
L- Editor: Filipodia **E- Editor**: Zhang DN

World Journal of Gastroenterology

Submit a Manuscript: http://www.wjgnet.com/esps/
Help Desk: http://www.wjgnet.com/esps/helpdesk.aspx
DOI: 10.3748/wjg.v22.i16.4160

World J Gastroenterol 2016 April 28; 22(16): 4160-4167
ISSN 1007-9327 (print) ISSN 2219-2840 (online)

ORIGINAL ARTICLE

Case Control Study

Total pancreatectomy with islet cell transplantation *vs* intrathecal narcotic pump infusion for pain control in chronic pancreatitis

Mohamad Mokadem, Lama Noureddine, Thomas Howard, Lee McHenry, Stuart Sherman, Evan L Fogel, James L Watkins, Glen A Lehman

Mohamad Mokadem, Division of Gastroenterology and Hepatology, Roy J. and Lucille A. Carver College of Medicine, University of Iowa, Iowa, IA 52242, United States

Lama Noureddine, Division of Nephrology and Hypertension, Roy J. and Lucille A. Carver College of Medicine, University of Iowa, Iowa, IA 52242, United States

Thomas Howard, Community Health Network, Indianapolis, IN 46219, United States

Lee McHenry, Stuart Sherman, Evan L Fogel, James L Watkins, Glen A Lehman, Division of Gastroenterology and Hepatology, Indiana University Medical Center, Indianapolis, IN 46202, United States

Author contributions: Mokadem M and Lehman GA designed the study; Mokadem M, Noureddine L, Howard T, McHenry L, Sherman S, Fogel EL, Watkins JL and Lehman GA executed the experiments; Mokadem M and Lehman GL drafted manuscript; Mokadem M, Noureddine L, Howard T, McHenry L, Sherman S, Fogel EL, Watkins JL and Lehman GA critically revised the manuscript.

Institutional review board statement: All experiments were in compliance with the ethics of the Institutional Review Board of Indiana University Medical Center.

Informed consent statement: Oral informed consent was obtained from all patients before performing the questionnaire.

Conflict-of-interest statement: All authors declare no conflicts of interest.

Data sharing statement: All collected data is present within the core of the manuscript.

Correspondence to: Mohamad Mokadem, MD, Division of Gastroenterology and Hepatology, Roy J. and Lucille A. Carver College of Medicine, University of Iowa, 200 Hawkins Drive, 4570 JCP, Iowa, IA 52242,
United States. mohamad-mokadem@uiowa.edu
Telephone: +1- 319-3846178
Fax: +1-319-3547981

Received: December 18, 2015
Peer-review started: December 20, 2015
First decision: December 30, 2015
Revised: January 20, 2016
Accepted: February 20, 2016
Article in press: February 22, 2016
Published online: April 28, 2016

Abstract

AIM: To evaluate pain control in chronic pancreatitis patients who underwent total pancreatectomy with islet cell transplantation or intrathecal narcotic pump infusion.

METHODS: We recognized 13 patients who underwent intrathecal narcotic pump (ITNP) infusion and 57 patients who underwent total pancreatectomy with autologous islet cell transplantation (TP + ICT) for chronic pancreatitis (CP) pain control between 1998 and 2008 at Indiana University Hospital. All patients had already failed multiple other modalities for pain control and the decision to proceed with either intervention was made at the discretion of the patients and their treating

physicians. All patients were evaluated retrospectively using a questionnaire inquiring about their pain control (using a 0-10 pain scale), daily narcotic dose usage, and hospital admission days for pain control before each intervention and during their last follow-up.

RESULTS: All 13 ITNP patients and 30 available TP + ICT patients were evaluated. The mean age was approximately 40 years in both groups. The median duration of pain before intervention was 6 years and 7 years in the ITNP and TP + ICT groups, respectively. The median pain score dropped from 8 to 2.5 (on a scale of 0-10) in both groups on their last follow up. The median daily dose of narcotics also decreased from 393 mg equivalent of morphine sulfate to 8 mg in the ITNP group and from 300 mg to 40 mg in the TP + ICT group. No patient had diabetes mellitus (DM) before either procedure whereas 85% of those who underwent pancreatectomy were insulin dependent on their last evaluation despite ICT.

CONCLUSION: ITNP and TP + ICT are comparable for pain control in patients with CP however with high incidence of DM among those who underwent TP + ICT. Prospective comparative studies and longer follow up are needed to better define treatment outcomes.

Key words: Chronic pancreatitis; Intractable pain; Total pancreatectomy; Islet cell transplantation; Intrathecal narcotic pump infusion

Core tip: Total pancreatectomy (TP) is the last resort offered to chronic pancreatitis (CP) patients with intractable pain when other interventions have failed. We wanted to compare pain control and rate of insulin-dependent diabetes in CP patients after TP and autologous islet cell transplantation (ICT) or intrathecal narcotic pump infusion, which is a relatively new and less invasive technique used for chronic analgesia in multiple other clinical settings. We found that pain control was similar between the two interventions after a median follow-up of 3 years yet the rate of insulin-dependent diabetes was still high in the surgical resection group despite the ICT.

Mokadem M, Noureddine L, Howard T, McHenry L, Sherman S, Fogel EL, Watkins JL, Lehman GA. Total pancreatectomy with islet cell transplantation *vs* intrathecal narcotic pump infusion for pain control in chronic pancreatitis. *World J Gastroenterol* 2016; 22(16): 4160-4167 Available from: URL: http://www.wjgnet.com/1007-9327/full/v22/i16/4160.htm DOI: http://dx.doi.org/10.3748/wjg.v22.i16.4160

INTRODUCTION

Abdominal pain remains the most common and difficult to treat complaint for patients with chronic pancreatitis as it can often be severe and debilitating. There is still lack of full understanding of the exact mechanism of pain in chronic pancreatitis (CP) and factors contributing to it are only partially defined[1-3]. The general goals of treatment include pain relief in addition to prevention and management of disease related complications such as pseudocysts, strictures, malabsorption (exocrine failure) and diabetes mellitus (endocrine failure). Opiates, however, remain the most frequently used analgesics in the background of all other treatment options. It is the generally acceptable approach to start with the least invasive intervention first, such as alcohol and smoking abstinence, and then advance in a stepwise manner as the method fails[4-6]. Total pancreatectomy (TP) is considered the final resort offering additional pain control to most patients with remaining intractable pain at the expense of developing insulin dependent diabetes. The addition of autologous islet cell transplantation (ICT) to TP has been shown to have variable success in prevention of insulin dependence from zero up to a maximum of 40% based on the performing center and the duration of follow up[7-9]. Neuroaxial blockage modalities such as spinal cord stimulation or intrathecal analgesia are among the newer modalities that may have a role in CP. Experience in this field, however, has been limited to case reports[10-12]. Among these, the intrathecal narcotic pump infusion (ITNP) is the most studied modality for control of intractable pain in cancer as well as non-cancer patients but with variable level of success[13-16]. The ITNP consists of a channeled catheter intrathecally (into the subarachnoidal space) that is connected to a small battery-powered programmable pump which is placed in the subcutaneous tissue of the abdominal wall. In our institution, we used a Medtronic Synchro MedII pump that possesses a 40 mL drug reservoir that is filled via a transcutaneous route under sterile conditions every 1-6 mo[17]. The literature has been scarce regarding its role and efficacy in patients with CP. In 2009, Kongkam *et al*[17] published a pilot study from the same center suggesting a promising role of ITNP in these patients.

MATERIALS AND METHODS

Using hospital electronic records and the endoscopic retrograde cholangiopancreatography (ERCP) database at Indiana University Medical Center from 1998 to 2008, we identified 13 patients who underwent ITNP infusion and 57 patients who underwent TP + ICT for CP and control of pain. The goal was to assess pain control in a cohort of surgical patients that is at least two fold the previously reported cohort of ITNP patients. All patients were managed at the discretion of their gastroenterology treating physicians at Indiana University and different approaches were selected based on clinical judgment and patient preferences. When patients' final decision was to undergo ITNP, the

Table 1 Etiology of chronic pancreatitis among patients who underwent intrathecal narcotic pump or total pancreatectomy + islet cell transplantation *n* (%)

	Idiopathic	Pancreatic divisum	Alcohol induced	Gallstone induced	Auto-immune
ITNP group	6/13 (46.1)	3/13 (23.1)	1/13 (7.7)	2/13 (15.4)	1/13 (7.7)
TP + ICT group	19/30 (63.3)	5/30 (16.7)	4/30 (13.3)	2/30 (6.7)	0/30 (0)

ITNP: Intrathecal narcotic pump; TP: Total pancreatectomy; ICT: Islet cell transplantation.

procedure was arranged and performed at Indiana University Hospital. On the other hand, when patients decided to proceed with TP + ICT, the surgery was arranged to be performed in one of three different surgical centers that offer this procedure- including Indiana University Hospital- based on patients' preferences and proximity to their household. Patients with persistent evidence of increased duct pressure were offered surgical or endoscopic decompression procedures - as appropriate - before being considered for total resection. All patients available for follow up answered a phone call-based questionnaire inquiring about their pain level, their daily narcotic use and the number and duration of hospital admissions for pain control.

The phone call inquiry about pain control is part of the standard care provided by the gastroenterology group at Indiana University. Verbal informed consent was obtained from all patients before proceeding with the questions. The study design abides by the ethical guidelines of the "World Medical Association Declaration of Helsinki - Ethical Principles for Medical Research Involving Human Subjects". Pain was assessed subjectively using a zero to ten scales (0 being no pain and 10 being maximum pain) before each procedure and on the last follow up available. All the daily narcotics used before and after the procedures were recorded and converted to milligram (mg) equivalent of oral morphine sulfate using a pharmacologic online converter http://www.globalrph.com/narcotic.cgi.

The number of in-hospital days per year for pain control was defined as the number of in-hospital admissions multiplied by the average duration of each admission (in days) divided by the total number of pain-years. This was recorded in each group before and after each intervention. Finally, the diabetes mellitus status, the average units of insulin used per day and the last HbA1C (glycosylated hemoglobin) were also recorded among the surgical group candidates on their last follow up.

Statistical analysis

All data are presented as median or mean ± standard deviation. Only *P*-values that are less than 0.05 were considered statistically significant. Experiments comparing two means were analyzed using Student's *t*-test with Welch's correction if appropriate.

RESULTS

The thirty patients who answered the phone call questionnaire constituted the surgery study group while no data was available from the remaining 27 surgical candidates. All 13 ITNP patients (5 male, 8 female) and the 30 TP + ICT patients (6 male, 24 female) contacted were Caucasians with a mean age of 40.6 years (± 9.6) and 39.9 years (± 14) respectively. The median duration of pain was 6 years (range 2-22) in the ITNP group and 7 years (range 1-21) in the TP + ICT group before each procedure. The median duration of follow up was 3 years in both groups with a range of 0.5 to 9 years in the ITNP group and 0.5 to 10 years in the TP + ICT group. The most common etiology of CP was idiopathic in the TP + ICT group (approximately 63%) followed by pancreatic divisum (approximately 17%), while it was pancreatic divisum (46%) followed by idiopathic in the ITNP group (approximately 23%). Alcohol constituted 15% of the ITNP group and approximately 7% of the surgery group (Table 1).

One ITNP patient developed serious meningitis requiring permanent removal of the catheter and pump and was excluded from the study. Three surgical patients were reported dead by their families upon contact, leaving 12 ITNP and 27 TP + ICT patients for retrospective comparison. All patients underwent multiple interventions for attempted pain control before either procedures such as ERCP with sphincterotomy (100% in both groups), celiac plexus neurolysis (46% of ITNP and 50% of TP + ICT), enteral tube feeding for bowel rest (61% of ITNP and approximately 33% of TP + ICT), and surgery (approximately 61% in ITNP and approximately 33% in TP + ICT).

The most common surgical procedure performed was denervation (bilateral splanchnicectomy) in the ITNP group and decompression (Puestow procedure) in the TP + ICT group (Table 2).

Pain control

The pain score dropped from a mean of 8.1 (± 1.4) and a median of 8 before the ITNP to a mean of 2.5 (± 2.2) and a median of 2.5 on the last follow up (Figure 1A). Similarly, the pain score dropped from a mean of 8.0 (± 1.7) and a median of 8 before the TP+ICT to a mean of 2.7 (± 2.9) and a median of 2.5 on the last follow up (Figure 1B). No ITNP patients

Table 2 Multiple interventions performed in patients with chronic pancreatitis for pain control before undergoing intrathecal narcotic pump or total pancreatectomy + islet cell transplantation *n* (%)

	ERCP with sphincterotomy	Celiac Block (EUS or CT)	Jejunal or Gastro-Jejunal tube insertion	Surgeries (denervation or decompression)
ITNP group	13/13 (100)	6/13 (46)	8/13 (61)	8/13 (61)
TP + ICT group	30/30 (100)	15/30 (50)	10/30 (33)	10/30 (33)

ITNP: Intrathecal narcotic pump; TP: Total pancreatectomy; ICT: Islet cell transplantation; EUS: Endoscopic ultrasonography; CT: Computed tomography; ERCP: Endoscopic retrograde cholangiopancreatography.

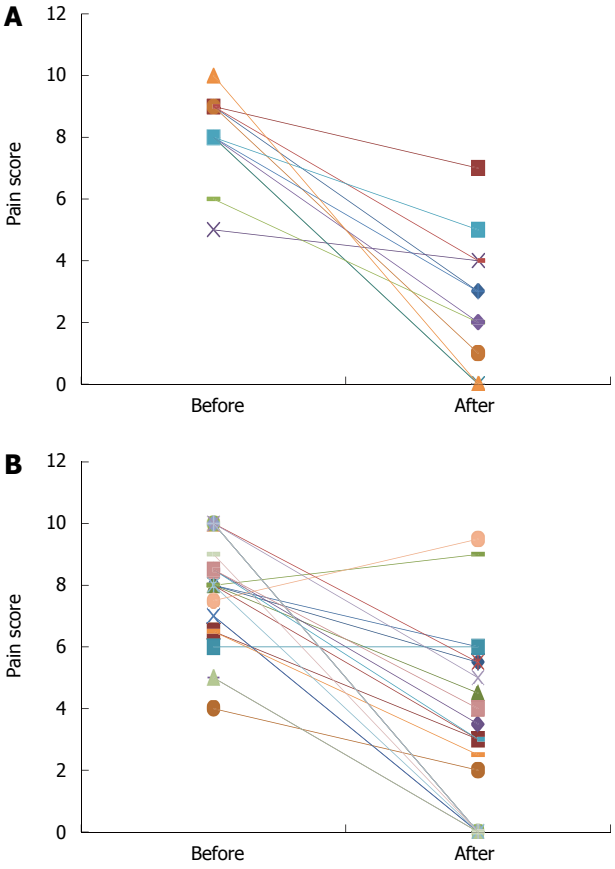

Figure 1 The average daily pain scores (on a scale of 0-10) in chronic pancreatitis patients before undergoing intrathecal narcotic pump infusion (A) and total pancreatectomy + islet cell transplantation (B) at the last follow-up.

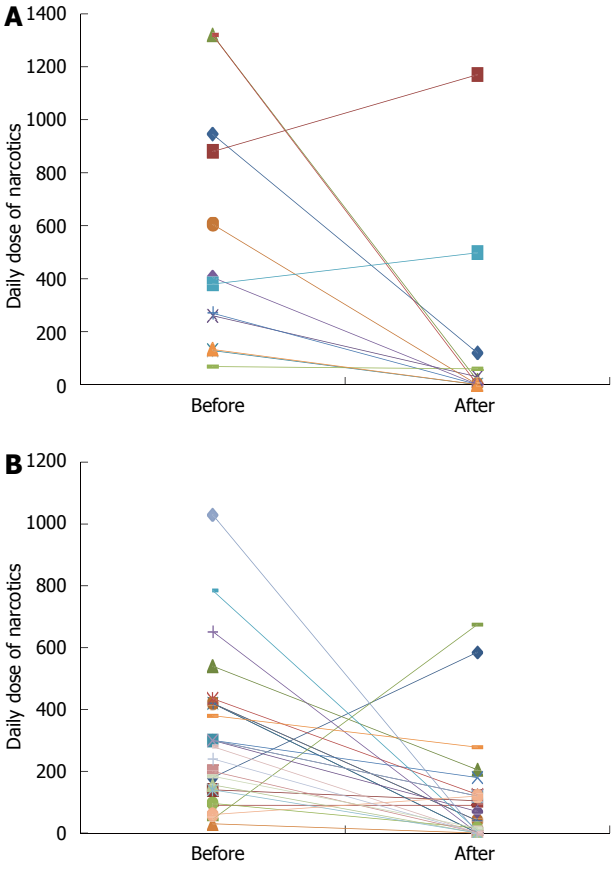

Figure 2 The average daily dose of narcotics (in mg equivalents of oral morphine sulfate) in chronic pancreatitis patients before undergoing intrathecal narcotic pump infusion (A) and total pancreatectomy + islet cell transplantation (B) at the last follow-up.

reported increase in their pain score and 3 out of 12 were still pain free on their last follow up (duration of last follow up was 0.5, 5, and 9 years respectively). Two TP + ICT patients reported worsening of their pain after surgery and one reported no change. 12 surgical patients were still pain free on their last follow up with a median duration of 4 years. The daily narcotics usage among ITNP patients decreased from a median of 393 mg equivalent of morphine sulfate and a mean of 553 mg (± 448) before intervention to a median of 8 mg and a mean of 158 mg (± 349) on their last clinic follow up, respectively ($P < 0.05$) (Figure 2A). Likewise, TP + ICT patients experienced a drop in their daily narcotics usage from a median of 300 mg equivalent of morphine sulfate and a mean of 316 mg (± 234) before surgery to a median of 40 mg and a mean of 104 mg (± 170) on their last clinic follow up, respectively ($P < 0.05$) (Figure 2B).

Two ITNP patients had increase in their oral daily narcotic requirements, one patient had very minimal decrease in his dose and six were narcotic free on their last follow up. The duration of follow up for these patients ranged from 0.5 to 7 years with a median of 1.5 years. The average dose of intrathecal morphine was 7.5 mg (2-10 mg). Three TP + ICT had increase in their daily narcotic requirements and 9 patients were narcotic free on their last follow up. The duration of follow up ranged from 1 to 10 years with a median of 4 years. These same 9 patients also reported zero pain (Figure 2A and B).

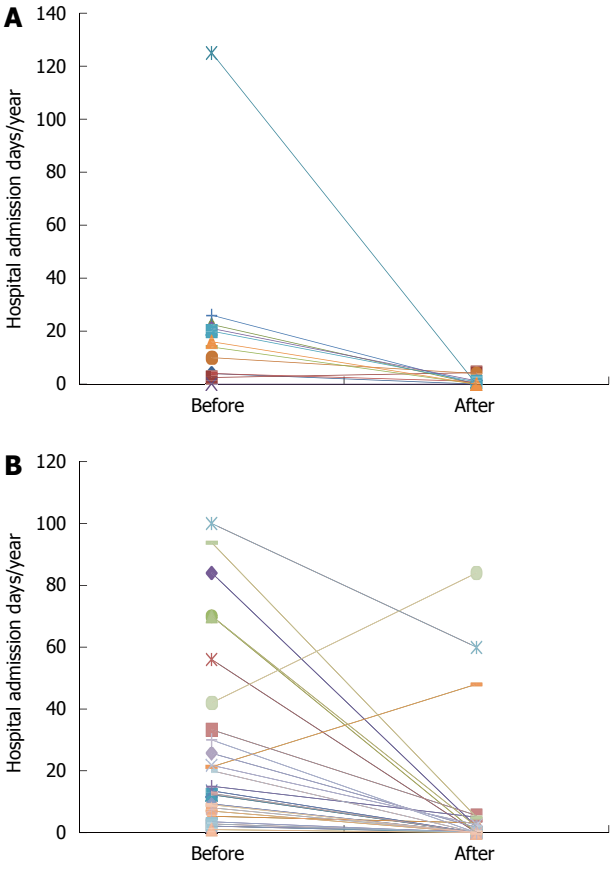

Figure 3 Number of hospital admission days per year for pain control among chronic pancreatitis patients before undergoing intrathecal narcotic pump infusion (A) and total pancreatectomy + islet cell transplantation (B) at the last follow-up.

Hospital admissions

The number of in-hospital days per year (d/year) for pain control decreased from a mean of 22 d/year (± 34) and a median of 15 d/year before ITNP to a mean of 1 d/year (± 1.5) and a median of zero thereafter. Only one patient reported increase in his hospital admission days per year for pain control and 7 patients (64%) have not been admitted to the hospital for pain control as of their last follows up. Likewise, the number of hospital days dropped from a mean of 29 d/year (± 30) and a median of 15 d/year before total pancreatectomy to a mean of 8 d/year (± 2) and a median of zero on the last follow up. Two patients reported increase in their hospital admission days per year and 15 patients (55%) have not been admitted to the hospital for pain control as of their last follow up (Figure 3A and B).

Complications

No patient had diabetes mellitus before either intervention in both groups. Only 4 out of the 27 surgical patients (approximately 15%) were insulin free on their last follow up despite the autologous islet cell transplantation. The average insulin dose per day was 25 units among the new diabetics with a median of 21 units (range = 4-54 units). The last HbA1c reported by the TP + ICT patients had an average of 7.35% and a median of 6.6% (Table 3). There were 3 deaths in the TP + ICT group (10% mortality rate), 2 were due to sepsis occurring at 3 wk and 1 mo after surgery as reported by family. However, no further information was available for the third death case. One TP + ICT patient had abscess formation in the abdomen post-surgery requiring drainage. No other major surgical complications were reported by patients during the questionnaire; however, no surgical records were available for patients operated on at other institutions. No death to date occurred in our series among the ITNP group. Two out of the 13 patients who underwent the ITNP infusion had bacterial meningitis. One of them was serious enough to necessitate catheter and pump removal and was excluded from the study. One patient had CSF leak (7.7%) that was surgically repaired with no further reported complications.

DISCUSSION

Here we report two relatively similar series of patients with intractable pain due to chronic pancreatitis who underwent either an intrathecal narcotic pump infusion or total pancreatectomy with islet cell transplantation as a terminal procedure for pain control after failure of multiple other modalities. We considered two ITNP patients to have failed treatment because of higher narcotic use and increased hospital admission days upon their last follow up despite having lower pain scores.

Likewise, three TP + ICT patients can also be reported as failure due to worsening pain, higher narcotic use and increase in hospital admissions in 2 of them, and only higher narcotic use in the remaining one. Therefore, in our case series, success rate was observed as 77% (10/13) among the ITNP group and 80% (24/30) among the TP + ICT group for pain control. Most of the published case series reported a post-operative morbidity range (*e.g.* infections, anastomosis leak, *etc.*) between 25 and 68% but major complications constituted approximately 14%-18% based on their reporting[7,9,18]. Several series from single centers reported a peri-operative mortality rate (usually defined as mortality within 2 wk of surgery) of 0% to 3.5% from total pancreatectomy[7-9,18-20]. Our multi-center based data was incomplete as we were unable to record the morbidity and mortality among all 57 surgical patients. However, the thirty-day mortality, which may not reflect the exact peri-operative mortality, is found to be at best 3.5% (3 out of 57) and at worst 10% (3 out of 30). The rate of serious complications (like bacterial meningitis, CSF leak and pump or catheter migration) from intrathecal analgesia is not clear in the literature but reports vary from 0% to 20% depending on the center, the population studied, and duration of follow up[14-16]. Anderson *et al*[16] and Kumar *et al*[14] reported a success rate of 50% and 75% respectively using

Table 3 Status of insulin-dependent diabetes among all surgical patients before and after total pancreatectomy with islet cell transplantation

	Number of patients with insulin independence	Average dose of insulin/day (units)	Average HbA1c
Before TP + ICT	30/30 (100%)	0	N/A
After TP + ICT	4/27 (approximately 15%)	25	7.35%

ITNP: Intrathecal narcotic pump; TP: Total pancreatectomy; ICT: Islet cell transplantation.

Table 4 Summary of outcomes among patients with intrathecal narcotic pump and those with total pancreatectomy and islet cell transplantation

	ITNP	TP + ICT	Comparison
Reversibility of the procedure	Yes	No	Different
Success rate for pain control	77%	80%	Similar
Residual narcotic dose usage (mg equivalent of oral morphine sulfate)	Mean = 158 mg/d Median = 8 mg/d	Mean = 104 mg/d Median = 40 mg/d	Similar
Percentage of patients with poor pain control	16.7%	11.1%	Similar
Percentage of patients with new insulin dependent diabetes	0%	Approximately 85%	Different
Procedure related death	0%	10%	Different

ITNP: Intrathecal narcotic pump; TP: Total pancreatectomy; ICT: Islet cell transplantation.

intrathecal morphine in patients with chronic non-malignant pain after an average duration of follow up of approximately 2 years. This, however, drops to 30% and 44% respectively when success rate is defined as more than 50% reduction in visual pain scores[14,16]. It is important to note that all our successful ITNP patients (10 out of 13) had more than 50% reduction in their pain scores with an average intrathecal morphine dose of 7.5 mg/d (range 2.5-10 mg/d).

Our results from TP + ICT have been consistent with several previous series reporting successful pain control and narcotic independence in 70%-80% of subjects within 6-12 mo after surgery[8,9,18,19]. Garcea *et al*[20] reported in a a series of 85 pts who underwent TP + ICT for CP that narcotic-free patients dropped from 90% after surgery to 40% at 1 year and ultimately to l6% at 5 years. On the other hand, Riediger *et al*[21] reported 87% improvement in pain control of 224 patients as far as 10 years after pancreatic head resection. However, 72% of these patients were back on narcotic medications despite using lower doses. Therefore, the success rate of pain control after pancreatectomy seems to depend largely on the definition of "success"[21]. Nonetheless, the most effective and most durable pancreatic surgeries performed for pain control in chronic pancreatitis seem to involve resection of the head of pancreas when compared with denervation or decompression procedures[18-21].

Our series had a 3 years median duration of follow up raising the question about the durability of the reported rate of 80%. The complete success of the autologous islet cell graft with resulting insulin independence has variably been reported to range from zero up to 40% within duration of follow up between 6 and 24 mo[8,9,18,19]. Garcea *et al*[20] again showed in his series that insulin independence dropped from 14.1% post engraftment to 5.9% after a median follow up duration of 8 years. However, there still might be a role for ICT in diabetes management after TP since there is evidence of partial graft function in patients with insulin-dependent diabetes after pancreatectomy but with relatively low insulin requirements. Therefore, ICT may probably add some protection against hypoglycemia events and long-term diabetes complications. However, this need to be evaluated independently[20,22]. Female gender, lower body weight and higher number of islet cells transplanted have been suggested to be positive predictive factors of graft survival[8,18,19]. Our data show a complete preservation of islet cells graft function in 15% of pts after a median follow up of 3 years (range 0.5-10 years) and an acceptable glucose control (average HbA1c 7.35%) with moderate insulin requirements (average 25 units/d) compared to patients with type 1 diabetes. Further follow-up of these patients is very important in order to assess for any further change in the islet cell graft viability and insulin requirements as in Garcea's report[20]. The incidence of diabetes mellitus complications awaits further follow up. Positive outcomes were very similar among both treatment modalities (Table 4) but major limitations still exist in our series.

First, the study is retrospective as it will be difficult to prospectively design a large population study in patients with CP, especially when it involves very extensive surgery such as total pancreatectomy with islet cell transplantation a procedure performed in only few selected centers in the United States. Second, the ITNP and surgical interventions were performed in different institutions which make comparison more difficult given the variability in technical performance.

This discrepancy was due to the fact that ITNP was offered at Indiana University Hospital by the treating gastroenterologist there as a one day procedure like all other interventions provided. However, when the ultimate decision was to go for TP + ICT and since some patients came from out-of-state, the surgical center was chosen based on proximity to patients' homes and social support. Third, not all surgical patients were assessed due to the fact that many surgeries were performed in multiple institutions and medical records were not available to us for review. In addition, three years median duration of follow up is still considered modest for CP. Larger comparative series with longer duration of follow up are needed to better characterize the optimal management of intractable pain in patients with chronic pancreatitis.

In conclusion, our case series compared two advanced interventions offered to chronic pancreatitis patients who failed several conventional therapies and continued to have high reported levels of daily pain coupled with consumption of large dosages of narcotics. Total pancreatectomy is a morbid surgery associated with well-known short and long term peri-operative risks with insulin-dependent diabetes being one of its major sequelae. Based on our data, the addition of islet cell transplantation to total pancreatectomy may offer a protective effect from insulin dependence at least for few years. This surgical procedure is not readily accessible to many patients within the United States or around the world.

On the other hand, intrathecal narcotic pump infusion is a relatively newer, less invasive therapeutic technique that delivers significantly lower doses of narcotics to the spinal fluid, therefore minimizing major systemic side effects of narcotics such as tolerance and constipation. There is very limited data of its long term efficacy and complications in chronic pancreatitis patients but observations can be extrapolated from reported patients with central nervous system disorders. Based on our data, ITNP seems to have a promising role as it showed comparable effect to total pancreatectomy on pain control with the additional benefit of preserving glucose and insulin metabolism. Future prospective studies in selected patients with chronic pancreatitis will better define its future role in pain management.

ACKNOWLEDGMENTS

We would like to thank all staff and personnel of the Division of Gastroenterology and Hepatology at Indiana University Medical Center who helped in the execution of this study.

COMMENTS

Background

Chronic pancreatitis (CP) patients who still have intractable abdominal pain despite undergoing several endoscopic and surgical interventions for analgesia are left with very few options short of having a complete resection of their pancreas. Total pancreatectomy is associated with adverse effect of insulin-dependent diabetes which may be reversed or delayed by performing islet cell transplantation *via* infusion of isolated islet cells into the portal system. However, this surgery carries a significant risk of morbidity and mortality and is usually reserved as the last resort for pain control in chronic pancreatitis.

Research frontiers

Intrathecal narcotic pump infusion is a minimally invasive procedure aimed at delivering very low dose of narcotics to the spinal fluid through a small catheter for the purpose of analgesia with minimal narcotic's side effects. This pump is currently used to manage severe pain in patients with refractory abdominal malignancies and in those with central nervous system injury and secondary spasms.

Innovations and breakthroughs

The authors examine - in a rare comparison - multiple markers of pain control in chronic pancreatitis patients who underwent either total pancreatectomy with islet cell transplantation or the less invasive yet relatively new procedure of intrathecal narcotic pump infusion.

Applications

The intrathecal narcotic pump (ITNP) infusion seems to have similar pain control to total pancreatectomy with islet cell transplantation (TP + ICT) with significant lower incidence of insulin-dependent diabetes. This modality may be considered as an option in chronic pancreatitis patients with intractable pain who refuse or do not qualify for total pancreatectomy.

Peer-review

This is a retrospective study of TP + ICT and ITNP for the control of intractable pain in CP. The aim is to evaluate pain control in patients with CP from a single center. Small series, but exceptionally well conducted, analyzed, and written. This is an important message that there may be a viable non-surgical alternative to TP and ICT for intractable pain in CP.

REFERENCES

1 **Gachago C**, Draganov PV. Pain management in chronic pancreatitis. *World J Gastroenterol* 2008; **14**: 3137-3148 [PMID: 18506917 DOI: 10.3748/wjg.14.3137]
2 **Warshaw AL**, Banks PA, Fernández-Del Castillo C. AGA technical review: treatment of pain in chronic pancreatitis. *Gastroenterology* 1998; **115**: 765-776 [PMID: 9721175 DOI: 10.1016/S0016-5085(98)70157-X]
3 **Layer P**, Yamamoto H, Kalthoff L, Clain JE, Bakken LJ, DiMagno EP. The different courses of early- and late-onset idiopathic and alcoholic chronic pancreatitis. *Gastroenterology* 1994; **107**: 1481-1487 [PMID: 7926511 DOI: 10.1016/0016-5085(94)90553-3]
4 **Steer ML**, Waxman I, Freedman S. Chronic pancreatitis. *N Engl J Med* 1995; **332**: 1482-1490 [PMID: 7739686 DOI: 10.1056/NEJM199506013322206]
5 **Abdel Aziz AM**, Lehman GA. Current treatment options for chronic pancreatitis. *Curr Treat Options Gastroenterol* 2007; **10**: 355-368 [PMID: 17897574 DOI: 10.1007/s11938-007-0036-9]
6 **Singh VV**, Toskes PP. Medical therapy for chronic pancreatitis pain. *Curr Gastroenterol Rep* 2003; **5**: 110-116 [PMID: 12631450 DOI: 0.1007/s11894-003-0079-6]
7 **Behrman SW**, Mulloy M. Total pancreatectomy for the treatment of chronic pancreatitis: indications, outcomes, and recommendations. *Am Surg* 2006; **72**: 297-302 [PMID: 16676850]
8 **Wahoff DC**, Papalois BE, Najarian JS, Kendall DM, Farney AC, Leone JP, Jessurun J, Dunn DL, Robertson RP, Sutherland DE. Autologous islet transplantation to prevent diabetes after pancreatic resection. *Ann Surg* 1995; **222**: 562-575; discussion 575-579 [PMID: 7574935 DOI: 10.1097/00000658-199522240-00013]
9 **Argo JL**, Contreras JL, Wesley MM, Christein JD. Pancreatic resection with islet cell autotransplant for the treatment of severe chronic pancreatitis. *Am Surg* 2008; **74**: 530-536; discussion 536-537 [PMID: 18556996]

10 **Kapural L**, Rakic M. Spinal cord stimulation for chronic visceral pain secondary to chronic non-alcoholic pancreatitis. *J Clin Gastroenterol* 2008; **42**: 750-751 [PMID: 18496389 DOI: 10.1097/01.mcg.0000225647.77437.45]

11 **Paicius RM**, Bernstein CA, Lempert-Cohen C. Peripheral nerve field stimulation in chronic abdominal pain. *Pain Physician* 2006; **9**: 261-266 [PMID: 16886036]

12 **Verheijen R**, Slappendel R, Jansen JB, Crul BJ, van Dongen RT. [Intrathecal administration of morphine and bupivacaine in the treatment of severe pain in chronic pancreatitis]. *Ned Tijdschr Geneeskd* 1996; **140**: 1410-1412 [PMID: 8766685]

13 **Newsome S**, Frawley BK, Argoff CE. Intrathecal analgesia for refractory cancer pain. *Curr Pain Headache Rep* 2008; **12**: 249-256 [PMID: 18625101 DOI: 10.1007/s11916-008-0043-0]

14 **Kumar K**, Kelly M, Pirlot T. Continuous intrathecal morphine treatment for chronic pain of nonmalignant etiology: long-term benefits and efficacy. *Surg Neurol* 2001; **55**: 79-86; discussion 86-88 [PMID: 11301086 DOI: 10.1016/S0090-3019(01)00353-6]

15 **Thimineur MA**, Kravitz E, Vodapally MS. Intrathecal opioid treatment for chronic non-malignant pain: a 3-year prospective study. *Pain* 2004; **109**: 242-249 [PMID: 15157684 DOI: 10.1016/j.pain.2004.01.003]

16 **Anderson VC**, Burchiel KJ. A prospective study of long-term intrathecal morphine in the management of chronic nonmalignant pain. *Neurosurgery* 1999; **44**: 289-300; discussion 300-301 [PMID: 9932882 DOI: 10.1097/00006123-199902000-00026]

17 **Kongkam P**, Wagner DL, Sherman S, Fogel EL, Whittaker SC, Watkins JL, McHenry L, Lehman GA. Intrathecal narcotic infusion pumps for intractable pain of chronic pancreatitis: a pilot series. *Am J Gastroenterol* 2009; **104**: 1249-1255 [PMID: 19367269 DOI: 10.1038/ajg.2009.54]

18 **Rodriguez Rilo HL**, Ahmad SA, D'Alessio D, Iwanaga Y, Kim J, Choe KA, Moulton JS, Martin J, Pennington LJ, Soldano DA, Biliter J, Martin SP, Ulrich CD, Somogyi L, Welge J, Matthews JB, Lowy AM. Total pancreatectomy and autologous islet cell transplantation as a means to treat severe chronic pancreatitis. *J Gastrointest Surg* 2003; **7**: 978-989 [PMID: 14675707 DOI: 10.1016/j.gassur.2003.09.008]

19 **Ahmad SA**, Lowy AM, Wray CJ, D'Alessio D, Choe KA, James LE, Gelrud A, Matthews JB, Rilo HL. Factors associated with insulin and narcotic independence after islet autotransplantation in patients with severe chronic pancreatitis. *J Am Coll Surg* 2005; **201**: 680-687 [PMID: 16256909 DOI: 10.1016/j.jamcollsurg.2005.06.268]

20 **Garcea G**, Weaver J, Phillips J, Pollard CA, Ilouz SC, Webb MA, Berry DP, Dennison AR. Total pancreatectomy with and without islet cell transplantation for chronic pancreatitis: a series of 85 consecutive patients. *Pancreas* 2009; **38**: 1-7 [PMID: 18665009 DOI: 0.1097/MPA.0b013e3181825c00]

21 **Riediger H**, Adam U, Fischer E, Keck T, Pfeffer F, Hopt UT, Makowiec F. Long-term outcome after resection for chronic pancreatitis in 224 patients. *J Gastrointest Surg* 2007; **11**: 949-959; discussion 959-960 [PMID: 17534689 DOI: 10.1007/s11605-007-0155-6]

22 **Webb MA**, Illouz SC, Pollard CA, Gregory R, Mayberry JF, Tordoff SG, Bone M, Cordle CJ, Berry DP, Nicholson ML, Musto PP, Dennison AR. Islet auto transplantation following total pancreatectomy: a long-term assessment of graft function. *Pancreas* 2008; **37**: 282-287 [PMID: 18815550 DOI: 0.1097/mpa.0b013e31816fd7b6]

P- Reviewer: Bradley EL 3rd, Fu DL, Sperti C **S- Editor**: Gong ZM
L- Editor: A **E- Editor**: Zhang DN

World Journal of Gastroenterology

Submit a Manuscript: http://www.wjgnet.com/esps/
Help Desk: http://www.wjgnet.com/esps/helpdesk.aspx
DOI: 10.3748/wjg.v22.i16.4168

World J Gastroenterol 2016 April 28; 22(16): 4168-4182
ISSN 1007-9327 (print) ISSN 2219-2840 (online)

ORIGINAL ARTICLE

Case Control Study

Early detection of hepatocellular carcinoma co-occurring with hepatitis C virus infection: A mathematical model

Abdel-Rahman Nabawy Zekri, Amira Salah El-Din Youssef, Yasser Mabrouk Bakr, Reham Mohamed Gabr, Ola Sayed Ahmed, Mostafa Hamed Elberry, Ahmed Mahmoud Mayla, Mohamed Abouelhoda, Abeer A Bahnassy

Abdel-Rahman Nabawy Zekri, Amira Salah El-Din Youssef, Yasser Mabrouk Bakr, Reham Mohamed Gabr, Ola Sayed Ahmed, Mostafa Hamed Elberry, Ahmed Mahmoud Mayla, Molecular Virology and Immunology Unit, Cancer Biology Department, National Cancer Institute, Cairo University, Cairo 11976, Egypt

Mohamed Abouelhoda, Systems and Biomedical Engineering Department, Faculty of Engineering, Cairo University, Giza 16453, Egypt

Mohamed Abouelhoda, Center for Informatics Sciences, Nile University, Sheikh Zayed City, Giza 16453, Egypt

Abeer A Bahnassy, Pathology Department, National Cancer Institute, Cairo University, Cairo 11976, Egypt

Author contributions: Zekri AR designed the study, edited the manuscript and helped in creating the model; Youssef AS participated in sample collection and manuscript writing and editing; Bakr YM assisted with the practical work and statistical analysis; Gabr RM and Ahmed OS assisted with the practical work; Elberry MH, Mayla AM and Bahnassy AA assisted with editing the manuscript; Abouelhoda M assited with creating the model.

Supported by National Cancer Institute, Cairo University, Cairo, Egypt.

Institutional review board statement: The study was approved by the Ethics Committee of National Cancer Institute, Cairo University, Cairo, Egypt (IRB No. 00004025, IORG. 0003381).

Informed consent statement: All patients gave informed consent.

Conflict-of-interest statement: No benefits in any form have been received or will be received from a commercial party related directly or indirectly to the subject of this article.

Data sharing statement: The technical appendix, statistical code, and dataset are available from the corresponding author at ncizekri@yahoo.com.

Correspondence to: Abdel-Rahman Nabawy Zekri, PhD, Head, Molecular Virology and Immunology Unit, Cancer Biology Department, National Cancer Institute, Cairo University, Kasr Al-Aini street, Fom El-Khaleeg, Cairo 11976, Egypt. ncizekri@yahoo.com
Telephone: +20-2-22742607
Fax: +20-2-23644720

Received: November 30, 2015
Peer-review started: December 2, 2015
First decision: January 13, 2016
Revised: February 16, 2016
Accepted: March 1, 2016
Article in press: March 2, 2016
Published online: April 28, 2016

Abstract

AIM: To develop a mathematical model for the early detection of hepatocellular carcinoma (HCC) with a panel of serum proteins in combination with α-fetoprotein (AFP).

METHODS: Serum levels of interleukin (IL)-8, soluble intercellular adhesion molecule-1 (sICAM-1), soluble tumor necrosis factor receptor Ⅱ (sTNF-R Ⅱ), proteasome, and β-catenin were measured in 479 subjects categorized into four groups: (1) HCC concurrent with hepatitis C virus (HCV) infection

(*n* = 192); (2) HCV related liver cirrhosis (LC) (*n* = 96); (3) Chronic hepatitis C (CHC) (*n* = 96); and (4) Healthy controls (*n* = 95). The R package and different modules for binary and multi-class classifiers based on generalized linear models were used to model the data. Predictive power was used to evaluate the performance of the model. Receiver operating characteristic curve analysis over pairs of groups was used to identify the best cutoffs differentiating the different groups.

RESULTS: We revealed mathematical models, based on a binary classifier, made up of a unique panel of serum proteins that improved the individual performance of AFP in discriminating HCC patients from patients with chronic liver disease either with or without cirrhosis. We discriminated the HCC group from the cirrhotic liver group using a mathematical model (-11.3 + 7.38 × Prot + 0.00108 × sICAM + 0.2574 × β-catenin + 0.01597 × AFP) with a cutoff of 0.6552, which achieved 98.8% specificity and 89.1% sensitivity. For the discrimination of the HCC group from the CHC group, we used a mathematical model [-10.40 + 1.416 × proteasome + 0.002024 × IL + 0.004096 × sICAM-1 + (4.251 × 10^{-4}) × sTNF + 0.02567 × β-catenin + 0.02442 × AFP] with a cutoff 0.744 and achieved 96.8% specificity and 89.7% sensitivity. Additionally, we derived an algorithm, based on a binary classifier, for resolving the multi-class classification problem by using three successive mathematical model predictions of liver disease status.

CONCLUSION: Our proposed mathematical model may be a useful method for the early detection of different statuses of liver disease co-occurring with HCV infection.

Key words: Mathematical model; Hepatocellular carcinoma; α-fetoprotein; Soluble intercellular adhesion molecule-1; β-catenin; Interleukin-8; Soluble tumor necrosis factor receptor Ⅱ; Proteasome

Core tip: Hepatocellular carcinoma is one of the most common liver malignancies. We sought to create a mathematical model from a panel of serum proteins (intercellular adhesion molecules, beta catenin, interleukin-8, the proteasome, and soluble tumor necrosis factor receptor Ⅱ) in combination with α-fetoprotein to aid in early detection of hepatocellular carcinoma. This panel was measured in 384 subjects infected with hepatitis C virus (HCV) as well as 95 healthy control subjects negative for HCV. Finally, we created mathematical models that may be valuable tools for the early detection of different statuses of liver disease co-occurring with HCV infection.

Zekri AR, Youssef AS, Bakr YM, Gabr RM, Ahmed OS, Elberry MH, Mayla AM, Abouelhoda M, Bahnassy AA. Early detection of hepatocellular carcinoma co-occurring with hepatitis C virus infection: A mathematical model. *World J Gastroenterol* 2016; 22(16): 4168-4182 Available from: URL: http://www.wjgnet.com/1007-9327/full/v22/i16/4168.htm DOI: http://dx.doi.org/10.3748/wjg.v22.i16.4168

INTRODUCTION

Hepatocellular carcinoma (HCC) is one of the most common primary liver malignancies and the third leading cause of cancer related mortality, and it is predominant in males[1,2]. Among the risk factors for developing HCC is the hepatitis C virus (HCV), which has been considered to be the second most common cause of HCC and the most common cause in Egypt, Japan, and the United States[3]. Egypt has the highest prevalence of HCV (genotype 4, predominately) worldwide, estimated to be 14.7% nationally[4].

Using the serum α-fetoprotein (AFP) level, the most widely used tumor biomarker, for the early diagnosis of HCC has several limitations[5]. Because of its low sensitivity, only 44% of patients are diagnosed at a localized disease stage, and only 30% of HCC patients are candidates for potentially curative treatments[6]. Moreover, the heterogeneity of HCC due to the coexistence of inflammation and cirrhosis makes the early detection of HCC difficult[7]. This complication highlights the need to identify valuable biomarkers for the early detection of HCC. Although single markers lack sensitivity and specificity for accurate cancer detection[8], specific panels of markers may offer an improvement in diagnostic performance**.** The ability of novel biomarkers to accurately detect HCC depends on their capacity to discriminate HCC from benign diseases of the liver, such as chronic hepatitis and liver cirrhosis.

Novel biomarkers for early diagnosis should meet the following criteria: first, they should achieve high accuracy; second, sample collection for detecting the markers should be easily operable and non-invasive; and third, the detection method should be cost effective[9].

Emerging key candidate biomarkers include mediators of the tumor microenvironment and the host response, notably cytokines involved in the immune system, inflammation, tumor development, and metastasis, *e.g.*, interleukin (IL)-8 and tumor necrosis factor (TNF)-α[10-12]; enzymes and isozymes involved in basic cellular processes, such as cell-cycle regulation, apoptosis, transcriptional regulation, and antigen processing, *e.g.*, proteasomes[13,14]; proteantigen mediated adhesion-dependent cell-cell interactions facilitating cell metastasis and evading the immune system, *e.g.*, soluble intercellular adhesion molecule-1 (sICAM-1)-1[15,16]; and proteantigen mediated Wnt/wingless (Wg) signaling pathway, which is involved in a large variety of developmental processes, including cell

fate regulation, proliferation and self-renewal of stem and progenitor cells, *e.g.*, β-catenin[17,18].

Our current study was conducted as a confirmatory study of our four previously published papers: Zekri *et al*[19-22], to address the potential roles of sICAM-1, β-catenin, the proteasome, IL-8 and sTNFR-Ⅱ in the early detection of HCC. Additionally, it was conducted as a complementary study to our previously published paper by Zekri *et al*[23], to address the potential role of combinations of sICAM-1, β-catenin, IL-8, the proteasome, and soluble soluble tumor necrosis factor receptor Ⅱ (sTNF-RⅡ) or subsets of these biomarkers with AFP, using logistic disease predictor models, in the early detection of HCC in a normal population and in high risk patients (patients with chronic hepatitis C and liver cirrhosis). We revealed that mathematical models identified a unique panel of biomarkers that improved the individual performance of AFP for the discrimination of HCC patients from patients with benign liver disease. Moreover, in the presence of inflammation and cirrhosis, whereas AFP offered relatively poor discrimination of HCC patients from benign disease patients, our mathematical model afforded better discrimination.

MATERIALS AND METHODS

Study design and grouping

This is a retrospective case-control study conducted on 384 adult patients with HCV related chronic diseases classified into: 192 patients with HCC recruited from the multidisciplinary HCC clinic, Tropical Medicine Department, Faculty of Medicine and National Cancer Institute (NCI) Outpatients Clinic, Cairo University; 96 patients with liver cirrhosis (LC) recruited from the Endemic Medicine Department, Faculty of Medicine, Cairo University and 96 chronic hepatitis C (CHC) patients recruited from the Kasr El Aini Viral Hepatitis Center, Faculty of Medicine, Cairo University, in addition to 95 healthy subjects enrolled as the control group from May 2012 to April 2013. The study was approved by the Investigation and Ethics Committee of NCI and written informed consent was obtained from all persons involved.

Patients with HCC were diagnosed by abdominal ultrasonography and triphasic computed tomography (CT) of the abdomen, and serum AFP and were confirmed histopathologically. The patients also showed no evidence of local invasion or distant metastasis. Notably, diabetes mellitus is a risk factor for HCC development. All of the 192 HCC patients, diabetic or not, were included in the mathematical modeling process. However, patients with HCV related liver cirrhosis were diagnosed by abdominal ultrasonography, and the diagnoses were confirmed histopathologically. Patients with chronic hepatitis C were characterized by persistent increases of the alanine aminotransferase (ALT) values to more than three times normal level for at least 6 mo. The control group showed no clinical or biochemical evidence of liver disease with normal abdominal ultra-sonography.

The exclusion criteria included being free of HBV and HCV infection, as confirmed by ELISA and PCR, as well as being free of diabetes. Regarding the groups with HCV liver related diseases, patients having HBV infection or those who received previous treatment or antiviral therapy for HCV were excluded from the study. In addition, all alcoholic subjects were excluded.

Serum sample collection

Five milliliters of venous blood was collected and allowed to coagulate for 30 min before centrifugation at 5000 rpm for 10 min. The serum fraction was aliquoted into cryotubes and stored at -80 ℃ until use.

Measurement of serum biomarkers

Serum levels of sICAM-1, IL-8, and sTNF-RⅡ were measured with an enzyme linked immunosorbent assay (ELISA) kit from R&D Systems Inc, Minneapolis, MN, United States, Proteasome levels were measured by an ELISA kit from Enzo Life Sciences, Inc., Switzerland and β-catenin was measured by an ELISA kit from Glory Science Co., Ltd, United States according to the manufacturers' instructions. These assays used the quantitative sandwich enzyme immunoassay technique. A monoclonal antibody specific for sICAM-1, IL-8, sTNF-RⅡ, β-catenin, or proteasomes was used. The average of the duplicate readings for each standard, control, and sample was taken, and the average zero standard optical density was subtracted. A standard curve was constructed by plotting the mean absorbance for each standard on the Y-axis against the concentration on the X-axis, and a best fit curve was drawn through the points on the graph**.** By interpolation, the unknown concentrations of sICAM-1, IL-8, sTNF-RⅡ, β-catenin, and proteasomes could be determined.

Statistical analysis

The SPSS software package (version 15) and the R programming environment were used to analyze the data. Continuous variables were expressed as the mean ± SD, median and interquartile range. Comparisons between groups were analyzed by non-parametric one-way ANOVA for continuous variables and by the χ^2 test for categorical variables. *P* values $\leqslant$ 0.05 were considered significant. Correlations between the variables were analyzed using Spearman's correlation coefficient.

In our model construction, we followed two strategies: The first was using the glmnet function as a multi-class classifier based on multinomial logit regression to differentiate between the four classes in our study including the control, cirrhotic, non-cirrhotic, and HCC groups. The second was using the glm function to study different pairwise combinations

among the classes. The details are as follows:

Use of the multi-class classifier: We used the glmnet function to analyze the input data based on the multinomial logit mode. To find the best fit, we used the cross validation version of the glmnet, which tested different values of the lambda parameter. The four classes were labeled with discrete values between 1 and 4. To evaluate the performance of the model, we used the predict function to compute the response after applying the model. The predicted values were float values ranging between 1 and 5. To find the best cutoffs differentiating among different classes, we used receiver operating characteristic (ROC) curve analysis over pairs of classes.

The use of the binary-class classifier over pairs of classes: We tested different pairwise class combinations in nine combinations: (1) disease *vs* control; (2) HCV *vs* control; (3) HCC *vs* HCV; (4) HCC *vs* LC; (5) LC *vs* CHC; (6) CHC *vs* control; (7) HCC *vs* non-HCC; (8) LC *vs* control; and (9) HCC *vs* LC. For each of these combinations, we used the glm function to analyze the input data based on the binomial logit mode. We used the predict function in combination with ROC curve analysis to find the best cutoffs differentiating the two classes in each combination. Visualization of the results was performed using different R packages and functions.

RESULTS

The clinical data of the studied groups are shown in (Table 1). The mean age of the HCC group was significantly higher than that in other groups ($P < 0.001$). Thus, there was a trend of increasing age with the progression of the disease from chronic hepatitis through liver cirrhosis to hepatocellular carcinoma.

Regarding gender differences, in the majority of the HCV related liver disease patients in the three groups were male. Risk factors for HCC such as diabetes mellitus (DM) were reported in 22.5% of HCC patients, 23% of LC patients, 8% of CHC patients, and 0% of controls. The percentage of diabetic patients was significantly higher in patients with HCC and LC compared to the CHC group and the control group ($P < 0.001$).

Cigarette smokers comprised 39% of the HCC group, 27% of the LC group, 21% of the CHC group, and 3% of the control group, with a significant difference between patients with (HCC and CHC) and the control group ($P < 0.001$). There was no significance between the LC group and either the HCC group or the CHC group.

Regarding liver function, the median value of ALT was significantly higher in the HCV related liver disease patients in the three patient groups than in the control group ($P < 0.001$). The median value of AST was significantly higher in the HCC group than in the other groups ($P < 0.001$), whereas there was no significant difference in the median AST value between the LC group and the CHC group. The median value of T-bilirubin was significantly higher in the LC group than in the other groups ($P < 0.001$). The median value of albumin was significantly higher in the normal group than in the HCV related liver disease patients in the three patient groups ($P < 0.001$). The median value of albumin in patients with LC was significantly lower than in the patients (HCC and CHC) and healthy controls ($P < 0.001$).

Regarding ascites, 42% of the HCC group and 78% of the LC group showed ascites, and there was a significant difference between the two groups ($P < 0.001$). The severity of liver disease in the HCC and cirrhotic groups was assessed using the child score; 36% of HCC group scored child A, 36% scored child B, and 28% scored child C compared to 12.5%, 28%, and 59.5% in the LC group, respectively ($P < 0.001$), consistently with the conclusion that the LC group had a more decompensated pattern than the HCC group.

Spearman's rank analysis of the studied serological markers for the control group showed a maximum rho of -0.218, indicating little or no correlation between age and analyte level in the control group, because the rho value was in the range of 0-(-0.25), as shown in Supplementary Table 1.

Serological marker levels in patients diagnosed with HCC, liver cirrhosis, and chronic hepatitis C and in healthy controls

The levels of the studied biomarkers in the different studied groups were expressed as box plots with scattered measurement points (Figure 1); more details such as the mean ± SD, median and range are shown in (Table 2).

The median proteasome serum concentration was significantly elevated in patients with HCC compared with patients with LC and CHC and healthy controls ($P < 0.001$) with mean values 0.91 ± 0.6, 0.25 ± 0.25, 0.68 ± 0.58, and 0.19 ± 0.3 μg/mL, respectively. However, the median proteasome concentration was significantly elevated in patients with CHC compared with patients with LC and the healthy controls ($P < 0.001$).

Moreover, the median concentration of serum IL-8 was significantly higher in patients with HCC and LC than in patients with CHC and the healthy controls, with mean values of 518.19 ± 656.23 pg/mL, 552.9 ± 732.2 pg/mL, 283.76 ± 442.7 pg/mL, and 238.8 ± 431.6 pg/mL, respectively ($P < 0.001$). However, there was no significant difference in the median proteasome concentrations in patients with HCC and LC ($P = 0.09$). Additionally, no significant difference was observed in median proteasome concentrations in patients with CHC and healthy controls.

Additionally, the median serum concentration of

Table 1 Clinical data of the studied groups *n* (%)

	HCC (*n* = 192)	Cirrhotic (*n* = 96)	Non-cirrhotic (*n* = 96)	Control (*n* = 95)	*P* value
Age, mean ± SD (range)	56.7 ± 7.7[a] (29-80)	54.01 ± 8.3[b] (27-66)	40.54 ± 8.82[c] (22-61)	33.37 ± 11[d] (19-62)	< 0.001
Gender					
Male	152[a] (79)	67[a] (70)	78[a] (81)	21[b] (22)	< 0.001
Female	40[a] (21)	29[a] (30)	18[a] (19)	74[b] (78)	
Smoker					
Yes	75[a] (39)	26[ab] (27)	20[b] (21)	3[c] (3)	< 0.001
No	117[a] (61)	70[ab] (73)	76[b] (79)	92[c] (97)	
DM					
Yes	43[a] (22)	22[a] (23)	8[b] (8)	0[c] (0)	< 0.001
No	149[a] (78)	74[a] (77)	88[b] (92)	95[c] (100)	
HCV Ab					
Present	168[a] (88)	90[a] (94)	96[b] (100)	0[c]	< 0.001
Absent	24[a] (12)	6[a] (6)	0[b] (0)	95[c] (100)	
HBs Ag					
Present	0 (0)	0 (0)	0 (0)	0 (0)	0.57
Absent	191 (100)	96 (100)	96 (100)	95 (100)	
Ascites					
Yes	86[a] (45)	75[b] (78)	0[c] (0)	0[c] (0)	< 0.001
No	106[a] (55)	21[b] (22)	96[c] (100)	95[c] (100)	
Child score					
A	69[a] (36)	12[b] (12)			< 0.001
B	69[a] (36)	27[a] (28)			
C	49[a] (28)	57[b] (60)			
ALT,					
mean	64.79 ± 52.737	63.6 ± 42.54	63.41 ± 44.22	21.84 ± 5.04	< 0.001
(range)	(5-395)	(6-290)	(10-223)	(11-33)	
median	51[a]	60[a]	54[a]	22[b]	
AST,					
mean	94.39 ± 105.61	53.91 ± 31.72	47.53 ± 29.04	26.68 ± 5.07	< 0.001
(range)	(16-1155)	(16-176)	(8-167)	(15-37)	
median	77[a]	46.5[b]	39.5[b]	27[c]	
T-Bil,					
mean	2.4 ± 2.63	3.25 ± 2.51	0.88 ± 0.49	0.79 ± 0.16	< 0.001
(range)	(0.3-25.8)	(0.2-19.7)	(0.3-5)	(0.5-1.1)	
median	1.7[a]	2.86[b]	0.84[c]	0.8[c]	
Albumin,					
mean	3.02 ± 0.63	2.55 ± 0.51	4.28 ± 0.4	4.45 ± 0.34	< 0.001
(range)	(1.8-4.8)	(1.7-4.3)	(3.2-5.4)	(3.8-5.2)	
median	3.1[a]	2.5[b]	4.2[c]	4.5[d]	
AFP,					
mean	3933.25 ± 16142	35.21 ± 40.1	18.19 ± 29.62		< 0.001
(range)	(1.5-114170)	(1.7-190)	(0.65-112)	0	
median	152[a]	17.95[b]	4.6[c]	0[d]	

[a-d]Groups bearing different initials are significantly different. ALT: Alanine aminotransferase; AST: Aspartate aminotransferase; AFP: α-fetoprotein; DM: Diabetes mellitus; T-Bil: Total bilirubin.

sICAM-1 was significantly elevated in patients in the HCC group compared to patients with LC and CHC and the healthy controls with mean values of 1034.73 ± 373.7 ng/mL, 978.17 ± 540.17 ng/mL, 570 ± 287 ng/mL, and 493 ± 188 ng/mL, respectively (P < 0.001). However, there was no significant difference in median sICAM-1 concentrations in patients with CHC and the healthy controls (P = 0.07). Moreover, the median serum concentration of sTNF-RⅡ was significantly higher in patients with LC compared to patients with HCC, CHC, and the control group with mean values of 6984.5 ± 626.8 pg/mL, 7058.31 ± 1338.78 pg/mL, 5456 ± 1531.7 pg/mL, and 3400 ± 1519 pg/mL, respectively (P < 0.001). Also, the median sTNR-RⅡ serum concentration was significantly elevated in patients with HCC compared with patients with CHC and the healthy controls (P < 0.001).

Additionally, the median concentration of β-catenin was significantly higher in patients with HCC than in patients with (LC and CHC) and healthy controls (P < 0.001) with mean values 11.26 ± 5.49 ng/mL, 9.34 ± 5.13 ng/mL, 8.8 ± 4.07 ng/mL, and 7.5 ± 3.2 ng/mL, respectively, whereas there were no significant differences in its median β-catenin concentrations in patients with LC and CHC (P = 0.76).

Correlation analysis of the studied serological markers

Correlation analysis of the studied serological markers performed with Spearman's correlation coefficient (Table 3) revealed a moderately positive correlation between sTNF-RⅡ and sICAM-1 or β-catenin (r = 0.482, 0.264; P < 0.01), respectively, and the rho

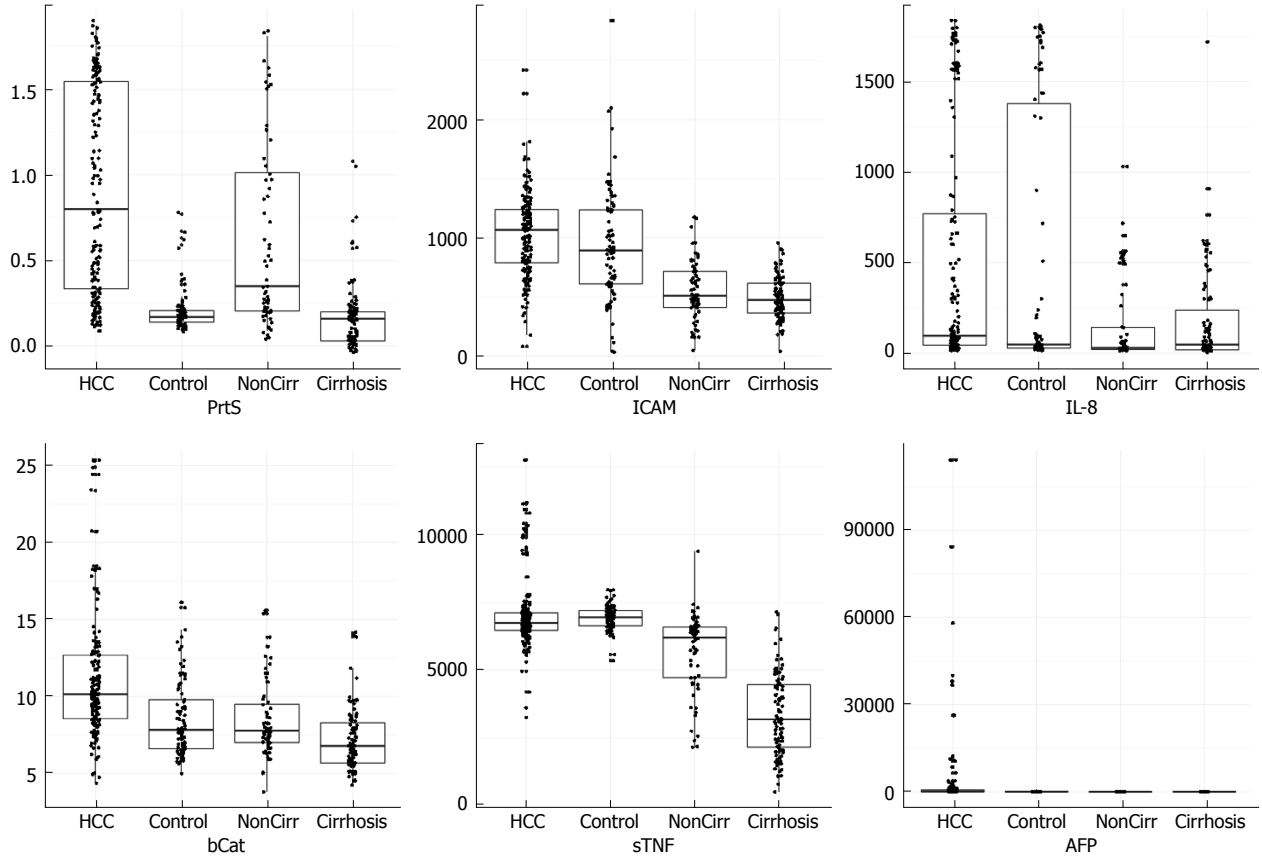

Figure 1 Box plots with scattered measurement points showing distribution of measured serum markers levels in different investigated groups. Sample groups on x axis and protein concentrations on Y axis. The markers from left to right are proteosome (PrtS), ICAM (sICAM-1), IL-8, β-catenin (bCat), sTNF-RⅡ (sTNF), and AFP. The box defines the boundaries of the first and third quartiles of data and the median values are indicated by horizontal lines within the boxes.

values were in the range of (0.25-0.5). However, there was little positive correlation or no correlation between the levels of IL-8 and the proteasome, sICAM-I, sTNF-RⅡ, or β-catenin levels (r = 0.240, 0.233, 0.184, 0.141; P < 0.01), respectively. Additionally, there was little positive correlation or no correlation between the proteasome levels and sICAM-I, β-catenin, and sTNF-RⅡ (r = 0.240, 230, 0.18; P < 0.01), respectively. Moreover, there was little positive correlation or no correlation between the levels of β-catenin and sICAM-1 (r = 0.222; P < 0.01), because the rho values were in the range of (0-0.25).

Application of the mathematical model in data analysis

Further analyses of the data using ROC analysis curves and the corresponding area under the curve were performed to investigate the diagnostic accuracy of the individual studied markers and combined markers with AFP.

Table 4 summarizes the area under the curve (AUC) for individual serum markers and combined markers, using two different methods, in different comparisons of the studied groups. Method 1 was the implementation of a multi-class classifier based on logistic regression, whereas method 2 was the implementation of a binary-class classifier based on logistic regression. Individual serum marker results revealed that sTNF-RⅡ had the highest diagnostic performance in discriminating LC cases from healthy controls (AUC = 0.981); CHC cases from healthy controls (AUC = 0.857); LC cases from CHC cases (AUC = 0.829); diseased cases (patients with HCC, LC, and CHC) from healthy controls (AUC = 0.951); and HCV cases (patients with LC and CHC) from healthy controls (AUC = 0.928). However, the proteasome levels had the highest diagnostic performance in discriminating HCC cases from LC cases (AUC = 0.981). AFP had the highest diagnostic performance in discriminating HCC cases from HCV cases (AUC = 0.849); HCC cases from non-HCC cases (healthy controls, LC group, CHC group) (AUC = 0.902); HCC cases from CHC cases (AUC = 0.908), and HCC cases from healthy controls (AUC = 0.986).

Additionally, the results in the table showed that Method 2 (the binary-class classifier) over the different pairwise comparison of the studied groups was superior to both Method 1 (the multi-class one) and individual markers, as shown in (Figures 2 and 3). For the discrimination of HCC cases from LC cases; Method 2 offered improved diagnostic performance (AUC = 0.962) over Method 1 (AUC = 0.840) and the top performing marker, proteasome levels (AUC = 0.911).

Table 2 Levels of the studied serological markers in different investigated groups

	HCC (n = 192)	Cirrhotic (n = 96)	Non-Cirrhotic (n = 96)	Control (n = 95)	P value
Proteosome,					
median	0.8[a]	0.17[b]	0.4[c]	0.16[d]	< 0.001
mean ± SD	0.91 ± 0.6	0.25 ± 0.25	0.68 ± 0.58	0.18 ± 0.3	
range	0.13-1.87	0.12-1.67	0.09-1.83	0.01-2.22	
IL-8,					
median	107[a]	55[a]	36.5[b]	47[b]	< 0.001
mean ± SD	518.19 ± 656.23	552.9 ± 732.2	283.76 ± 442.7	238.8 ± 431.6	
range	14-1837	14-1811	8-1734	3-1719	
sICAM-1,					
median	1072.5[a]	892[b]	510.5[c]	473[c]	< 0.001
mean ± SD	1034.73 ± 372.7	978.17 ± 540.17	570 ± 287	493 ± 188	
range	79-2419	31-2838	46-1654	37-1078	
sTNF-RII,					
median	6785[a]	7011.5[b]	5948.5[c]	3190.5[d]	< 0.001
mean ± SD	7058.31 ± 1338.78	6984.5 ± 626.8	5456 ± 1531.7	3400 ± 1519	
range	3250-12776	4351-9919	1772-9403	495-7157	
β-catenin,					
median	10.1[a]	7.95[b]	7.85[b]	6.8[c]	< 0.001
mean ± SD	11.26 ± 5.49	9.34 ± 5.13	8.81 ± 4.07	7.5 ± 3.2	
range	4.3-55.4	5.0-49.2	3.8-41.6	4.3-28.4	

[a-d]Groups bearing different initials are significantly different. IL-8: Interleukin-8; sTNF-RII: Soluble tumor necrosis factor receptor II; sICAM-1: Soluble intercellular adhesion molecule-1.

Table 3 Correlation analysis of different studied markers showing Spearman's rho value and *P* value

	Proteosome	IL-8	sICAM-1	sTNF-RII	β-catenin
Proteosome	1	0.240[1]	0.240[1]	0.185[1]	0.230[1]
		0.000	0.000	0.000	0.000
IL-8	0.240[1]	1	0.233[1]	0.184[1]	0.141[1]
	0.000		0.000	0.000	0.003
sICAM-1	0.240[1]	0.233[1]	1	0.547[1]	0.222[1]
	0.000	0.000		0.000	0.000
sTNF-RII	0.185[1]	0.184[1]	0.547[1]	1	0.264[1]
	0.000	0.000	0.000		0.000
β-catenin	0.230[1]	0.141[1]	0.222[1]	0.264[1]	1
	0.000	0.003	0.000	0.000	

[1]Correlation is significant at the 0.01 level (2-tailed). IL-8: Interleukin-8; sTNF-RII: Soluble tumor necrosis factor receptor II; sICAM-1: Soluble intercellular adhesion molecule-1.

For the discrimination of HCC cases from CHC cases, Method 2 offered improved diagnostic performance (AUC = 0.972) over Method 1 (AUC = 0.967) and the top performing marker, AFP (AUC = 0.908). For the discrimination of HCC cases from healthy controls, Method 2 offered improved diagnostic performance (AUC = 1) over Method 1(AUC = 0.998) and the top performing marker, AFP (AUC = 0.986).

Table 5 presents the best cutoff based on Youden statistics for each model and the related statistical measures of the performance for the binary-class classifier. All models over different pairwise comparisons of the studied groups achieved high diagnostic performance using all measures: the sensitivity ranged from 80.5% to 100%; the specificity ranged from 90.5% to 100%; the accuracy ranged from 88.9% to 100%; the PPV (positive predictive values) ranged from 87.9% to 100%; and the NPV (negative predictive values) ranged from 81.3% to 100%.

Table 6 presents the different binary-class classifier based mathematical models that best fit the data for each pairwise comparison. Table 7 presents the reduced models with the most significant markers (significance level at $P < 0.05$) and with the best cut-off. From these models, only three markers (sTNF-R Ⅱ, proteasome, and AFP) were able to discriminate healthy controls from all other groups. For further discrimination between the other studied groups; sICAM-1, IL-8, and β-catenin were also needed in addition to sTNF-R Ⅱ, the proteasome, and AFP.

The algorithmic use of different models for making a final prediction among different groups (accordingly solving the multi-class classification problem) could be performed as follows: First, use the mathematical model involving sTNF-R Ⅱ, the proteasome, and AFP with a cut-off of 0.764 to discriminate disease cases from healthy controls. Second, for disease cases, discriminate HCC cases from HCV cases by using

Table 4 Area under curve of individual markers *vs* combined one using (method 1 and 2) in different combinations of groups

	Method 1	Method 2	Proteasome	IL-8	sICAM-1	sTNF-RII	β-catenin	AFP
Disease *vs* Control	0.979	0.992	0.834	0.612	0.825	0.951	0.768	0.923
HCC *vs* LC	0.841	0.962	0.911	0.576	0.585	0.424	0.718	0.804
HCC *vs* HCV	0.866	0.952	0.799	0.639	0.705	0.568	0.723	0.849
HCC *vs* Non-HCC	0.917	0.970	0.848	0.652	0.787	0.724	0.771	0.902
HCV *vs* Control	0.957	0.983	0.726	0.543	0.716	0.928	0.677	0.850
LC *vs* CHC	0.695	0.951	0.220	0.648	0.769	0.829	0.494	0.736
CHC *vs* Control	0.917	0.968	0.846	0.471	0.571	0.857	0.678	0.749
LC *vs* Control	0.990	1.000	0.637	0.597	0.825	0.981	0.676	0.924
HCC *vs* Control	0.998	1.000	0.927	0.672	0.917	0.970	0.846	0.986
HCC *vs* CHC	0.967	0.971	0.648	0.724	0.867	0.762	0.730	0.908

Method 1 is based on multi-class classifier and Method 2 is based on binary-class classifier. HCV group: Include LC and CHC groups; Disease group: HCC, CHC and LC groups. CHC: Chronic hepatitis C; LC: Liver cirrhosis; AFP: α-fetoprotein; HCV: Hepatitis C virus.

the corresponding mathematical model in the table involving the levels of sTNF-RⅡ, the proteasome, sICAM-1, β-catenin, and AFP with a cut-off of 0.712. Third, for HCV cases, proceed to discriminate LC cases from CHC cases by using the respective mathematical model with a cut-off of 0.582. The decision tree representing this algorithm is shown in (Figure 4).

DISCUSSION

Hepatocellular carcinoma (HCC) is a common disorder worldwide that ranks as the fifth and eighth most common cancer among men and women, respectively[24]. In Egypt, HCC is the first and second most common cancer among men and women, respectively[24]. The rising incidence of HCC in Egypt may be explained by the high prevalence of HCV[25], estimated nationally to be approximately 14%[4].

Early diagnosis is crucial for improving the survival rate of patients. The serum level of AFP is often not significantly elevated in patients with early-stage, potentially curable, HCC[5].

Therefore, finding a new appropriate panel of serum markers rather than a single marker is necessary for the early detection of HCC in normal populations (healthy controls) and in high risk patients (CHC and LC patients).

Our study was conducted as a complementary study to our previously published papers by Zekri *et al*[23], 2015 to investigate whether combinations of serum sICAM-1, β-catenin, IL-8, proteasome, and sTNF-RⅡ levels or subsets of these biomarkers with AFP, using logistic disease predictor models, could facilitate the early detection of HCC.

Our study revealed that the serum level of AFP was significantly elevated in the HCC group than the other groups, a finding in concordance with those from previous studies by many authors[26,27].

The serum level of sICAM-1 was significantly elevated in the HCC group compared with other groups ($P < 0.001$). However, there was no significant difference between the CHC group and the control group. These data are consistent with those from previous studies by Shimizu *et al*[28], 1995 and Moriyama *et al*[29], 2006, which have reported that increasing levels of sICAM-1 over time represent a significant HCC risk factor in patients with HCV-associated CH or LC. ROC curve analysis of the individual markers revealed that serum levels of sICAM-1 had excellent diagnostic accuracy for the discrimination of the HCC group from the control group, because the AUC was in the range of (0.9-1), and had good diagnostic accuracy in discriminating the HCC group from the CHC group as AUC was in the range of (0.8-0.89), whereas it failed to have diagnostic accuracy in discriminating the HCC group from the LC group, because the AUC was in the range of (0.5-0.59). Thus, regular measurements of sICAM-1 concentrations may be used as a diagnostic marker for the early detection of HCC in healthy controls and CHC patients.

Serum levels of β-catenin were significantly higher in the HCC group than in the other groups ($P < 0.001$), whereas there was no significant difference in the levels in the LC group and the CHC group. These results are is consistent with those from our previous study, Zekri *et al*[22], 2011, which has found that serum levels of β-catenin are higher in patients with HCC compared with CH, ASC (chronic HCV with persistent normal alanine aminotransferase levels) and healthy control groups. In agreement with our results, previous studies by Li *et al*[30] and Guan *et al*[27] have reported higher nuclear accumulation of β-catenin in HCC tissue than in the corresponding para-carcinoma, cirrhotic, and normal tissues. ROC curve analysis of the individual markers revealed that serum levels of β-catenin had good diagnostic accuracy for the discrimination of the HCC group from the control group, because the AUC was in the range of (0.8-0.89), and had fair diagnostic accuracy in discriminating between the HCC group and the LC group, and between the HCC group and the CHC group, because the AUC was in the range of (0.7-0.79). These data suggested that serum levels of β-catenin may be used as a diagnostic marker for the early detection of HCC in the normal population, CHC, and LC patients.

Serum levels of proteasome were significantly

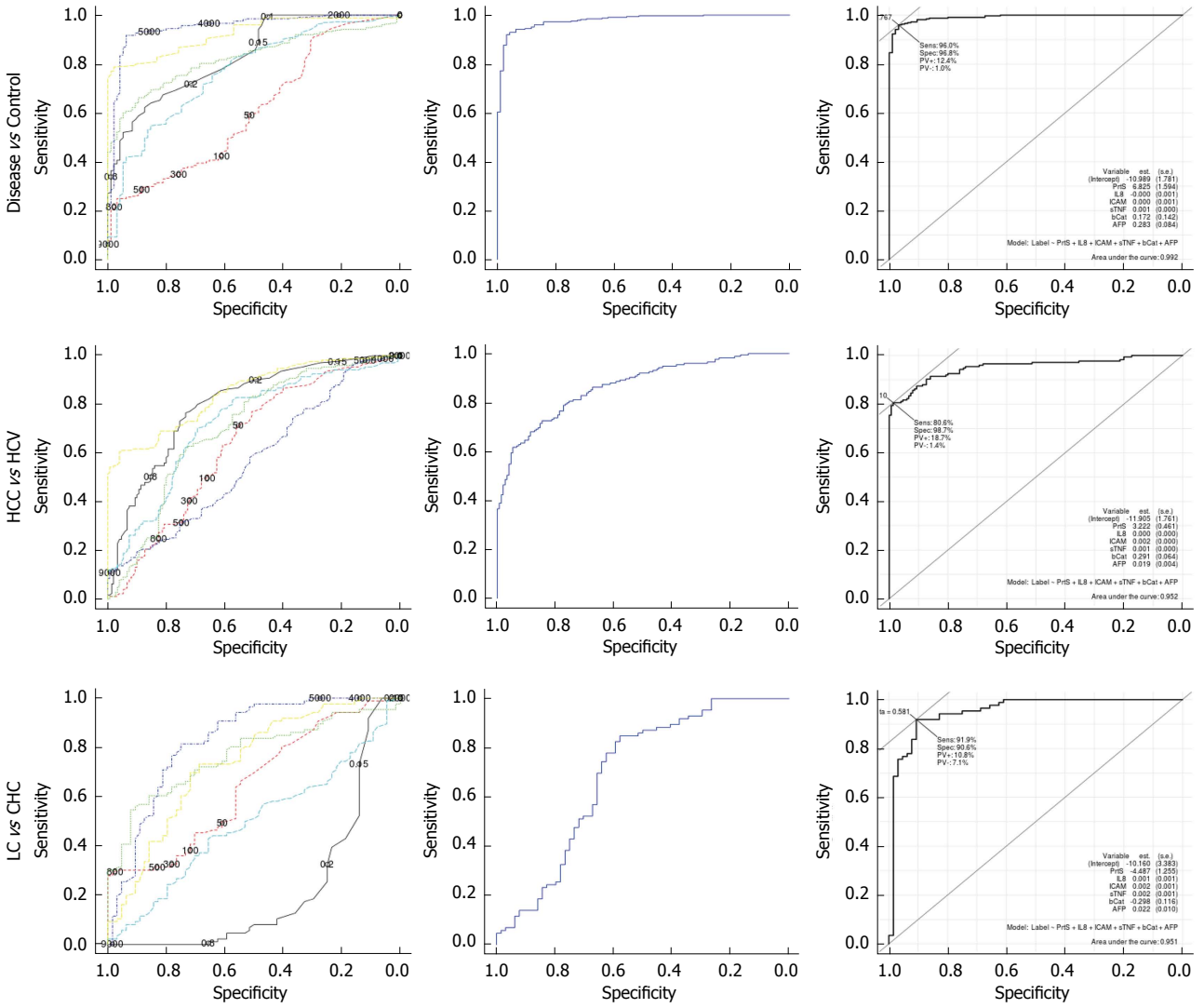

Figure 2 Receiver operating characteristic curves for the three pairwise comparisons of investigated groups used in our algorithm. The leftmost column includes receiver operating characteristic (ROC) curves for individual markers, The middle columns includes ROC curves for Method 1 based on for the multi-class classifier, and the rightmost column includes ROC curves for Method2 based on binary class classifiers. On the ROC curve of Method 2, we depict the respective model and appropriate cut-offs. The different ROC curves for proteasome, IL-8, sICAM-1, sTNF-RⅡ, β-catenin, and AFP in the leftmost column are colored black, red, green, blue, cyan, and yellow, respectively. Prts: Proteasome.

higher in the HCC group than in the other groups (P < 0.001). This result is consistent with results from a previous study by Henry *et al*[13], which has found that plasma proteasome levels are significantly higher in patients with HCC compared with the LC group and the control group. However, serum levels of proteasome were also significantly elevated in the CHC group than in the LC group and the control group (P < 0.001). ROC curve analysis of the individual markers revealed that serum proteasome levels showed excellent diagnostic accuracy in discriminating between the HCC group and the LC group, and also between the HCC group and the control group, because the AUC was in the range of (0.9-1). However, it showed poor diagnostic accuracy between in discriminating the HCC group from the CHC group, with an AUC in the range of (0.6-0.69). These data suggested that serum levels of proteasome are a reliable diagnostic marker for the early detection of HCC in normal populations and LC patients.

Serum levels of sTNF-RⅡ were significantly higher in patients with HCC than in the CHC group and the control group (P < 0.001). This result is concordant with results from our previous study, Zekri *et al*[21], which has reported significantly elevated serum levels of sTNF-RⅡ in patients with HCC than in patients with CLD (chronic liver disease associated with elevated liver enzyme levels), ASC (a symptomatic liver disease associated with normal liver enzyme levels), and the control group. However, the serum level of sTNF-RⅡ was significantly higher in patients with LC than in HCC patients in our current study (P < 0.001). The ROC curve analysis of the individual markers revealed that the serum level of sTNF-RⅡ had excellent diagnostic

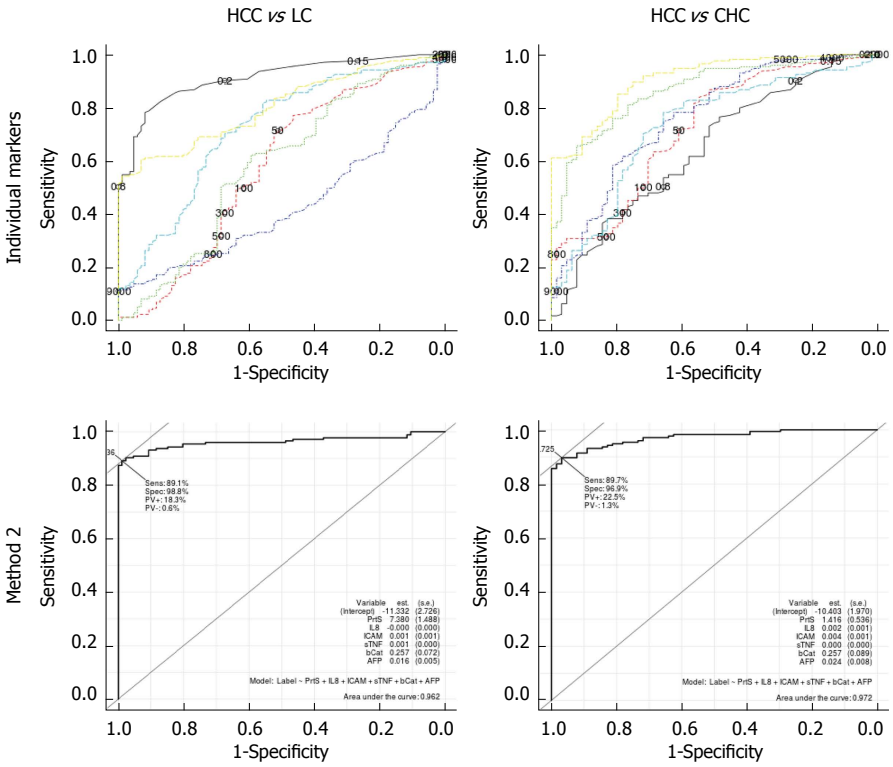

Figure 3 Receiver operating characteristic curves of individual markers *vs* Method 2 (based on binary class-calssifier) over different pairwise comparisons discriminating hepatocellular carcinoma groups from liver cirrhosis group and chronic hepatitis C group. CHC: Chronic hepatitis C; LC: Liver cirrhosis; HCC: Hepatocellular carcinoma.

Table 5 Statistical measurements of the diagnostic performance for the binary classifier over different pairwise comparison of the investigated groups

	AUC	BT_Y	Spec (%)	Sen (%)	Acc (%)	TN	TP	FN	FP	NPV (%)	PPV (%)
Disease *vs* Control	0.992	0.764	96.8	96.0	96.2	92	312	13	3	87.6	99.0
HCC *vs* LC	0.962	0.655	98.8	89.1	92.3	85	156	19	1	81.7	99.3
HCC *vs* HCV	0.952	0.712	98.7	80.5	88.9	148	141	34	2	81.3	98.6
HCC *vs* Others	0.970	0.378	91.0	91.4	91.2	223	160	15	22	93.7	87.9
HCV *vs* Control	0.983	0.764	96.8	91.3	93.5	92	137	13	3	87.6	97.8
LC *vs* CHC	0.950	0.581	90.6	91.9	91.3	58	79	7	6	89.2	92.9
CHC *vs* Control	0.968	0.341	90.5	93.7	91.8	86	60	4	9	95.5	86.9
LC *vs* Control	1.000	0.500	100.0	100.0	100.0	95	86	0	0	100.0	100.0
HCC *vs* Control	1.000	0.500	100.0	100.0	100.0	95	175	0	0	100.0	100.0
HCC *vs* CHC	0.971	0.745	96.8	89.7	91.6	62	157	18	2	77.5	98.7

BT_Y: Best cut off computed using Youden statistics, TP: True positive; TN: True negative; FP: False positive; FN: False negative; Sen: Sensitivity; Spec: Specificity; Acc: Accuracy; PPV: Positive predictive value; NPV: Negative predictive value; HCC: Hepatocellular carcinoma; HCV: Hepatitis C virus.

accuracy in discriminating the HCC group from the control group, because the AUC was in the range of (0.9-1), and fair diagnostic accuracy in discriminating the HCC group from the CHC group, because the AUC was in the range of (0.7-0.79), whereas its diagnostic accuracy in discriminating between the HCC group and LC group was insignificant, because the AUC was below 0.5. This result suggests that sTNF-RⅡ may be used as a diagnostic marker for the early detection of HCC in the normal population and CHC patients.

The serum level of IL-8 was significantly elevated in patients with HCC and LC compared with the CHC group and healthy controls ($P < 0.001$). This result is concordant with results from a previous study by Elewa *et al*[31], which has reported that the serum level of IL-8 is significantly higher in patients with HCV-associated HCC than in patients with chronic hepatitis C without HCC and healthy controls, as well as a previous study by Ren *et al*[10], which has reported that the IL-8 serum level is significantly higher in patients with HCC than in the control group. Moreover, this result is in agreement with those from a previous study by Zimmermann *et al*[32], which has reported that the level of serum IL-8 is significantly higher in patients with LC than in those with CH and healthy controls. However, in the present study, there was no significant difference between the HCC group and the LC group, or between the CHC group and control group. ROC curve analysis of the

Table 6 Disease logistic predictive models based on binary-class classifier over different pairwise comparisons of the investigated groups

Combination	Model
Disease *vs* Control	[-11 + 6.83 × Prot + (-5.99 × 10^{-5}) × IL-8 + 3.12 × 10^{-4} × sICAM + 0.0013 × sTNF-RII + 0.172aβ-catenin + 0.283 × AFP] [*P* values = 6.83E-10, 1.86E-05, 0.938962, 0.764414, 6.79E-08, 0.225761, 0.000818]
HCC *vs* LC	[11.33 + 7.380 × Prot + (-2.047 × 10^{-4}) × IL-8 + 0.0011 × sICAM + 6.299 × 10^{4} × sTNF + 0.26 × β-catenin + 0.016 × AFP] [*P* values = 3.22E-05, 7.11E-07, 0.591834, 0.041838, 0.056595, 0.000357, 0.000638]
HCC *vs* HCV	[-11.9 + 3.222 × Prot + (3.813 × 10^{-4}) × IL + 0.00152 × sICAM + (6.481 × 10^{-4}) × sTNF + 0.0291 × β-catenin + 0.019 × AFP] [*P* values = 1.39E-11, 2.63E-12, 0.231248, 0.000928, 0.000952, 5.41E-06, 5.09E-06]
HCC *vs* Non-HCC	[-12.27 + 3.3 × Prot + 0.0004 × IL + 0.00155 × sICAM + (6.803 × 10^{-4}) × sTNF + 0.294 × β-catenin + 0.02 × AFP] [*P* values = 5.26E-13, 4.14E-13, 0.211689, 0.000767, 0.000388, 3.89E-06, 3.42E-06]
HCV *vs* Control	[-10.84 + 6.80 × Prot + (2.68 × 10^{-5}) × IL-8 + 0.00017 × ICAM + 0.00126 × sTNF + 0.1742 × β-catenin + 0.278 × AFP] [*P* values = 1.12E-09, 1.87E-05, 0.972804, 0.875503, 9.02E-08, 0.227858, 0.000935]
LC *vs* CHC	[-10.16 + (-4.487) × Prot + 0.00134 × IL-8 + 0.0021 × sICAM + 0.0018 × sTNF + (-0.2984) × β-catenin + 0.0217 × AFP] [*P* values = 0.002674, 0.000351, 0.052275., 0.021958, 0.000211, 0.009838, 0.030621]
CHC *vs* Control	[-9.354 + 6.634 × Proteasome + (-0.00166) × IL-8 + (-0.00126) × sICAM + 0.001111 × sTNF + 0.208624 × β-catenin + 0.24604 × AFP] [*P* values = 1.40E-07, 1.64E-05, 0.2627, 0.3799, 8.55E-06, 0.1477, 0.0016]
LC *vs* Control	[-515.7 + 108.7 × Proteasome + 0.01295 × IL-8 + 0.0194 × sICAM + 0.05745 × sTNF + 4.485 × β-catenin + 12.59 × AFP] [*P* values = 0.997, 0.998, 0.999, 0.999, 0.998, 0.998, 0.995]
HCC *vs* Control	[-375.640 + 122.598 × Prot + (-0.0577) × IL + 0.0368 × sICAM + 0.0427 × sTNF + 1.1533 × β-catenin + 13.584 × AFP] [*P* values = 0.737, 0.802, 0.823, 0.917, 0.812, 0.923, 0.66]
HCC *vs* CHC	[-10.40 + 1.416 × Prot + 0.002024 × IL-8 + 0.0041 × sICAM + (4.251 × 10^{-4}) × sTNF + 0.2.67 × β-catenin + 0.0244 × AFP] [*P* values = 1.28E-07, 0.00826, 0.01827, 5.52E-05, 0.04942, 0.00391, 0.00354]

The values between brackets were the *P* values for the corresponding term parameter in the model respectively. Terms with *P* value < 0.05 are considered significant. The first *P* value was for overall model.

Table 7 Final reduced disease logistic predictive models based on binary classifier with the most significant markers (achieved regression *P* < 0.05)

	Final reduced model (with relevant terms)	Best threshold
Disease *vs* Control	(-11 + 6.83 × Prot + 0.00129 × sTNF + 0.283 × AFP)	0.764
HCC *vs* LC	(-11.3 + 7.38 × Prot + 0.00108 × sICAM + 0.2574 × β-catenin + 0.01597 × AFP)	0.655
HCC *vs* HCV	[-11.91 + 3.222 × Prot + 0.001518 × sICAM + (6.481 × 10^{-4}) × sTNF + 0.291 × β-catenin + 0.0193 × AFP]	0.712
HCC *vs* Non-HCC	[-12.27 + 3.299 × Prot + 0.001548 × sICAM + (6.803 × 10^{-4}) × sTNF + 0.2936 × β-catenin + 0.0198 × AFP]	0.378
HCV *vs* Control	(-10.84 + 6.803 × Prot + 0.00126 × sTNF + 0.2783 × AFP)	0.764
LC *vs* CHC	[-10.16 + (-4.487) × Prot + 0.002086 × sICAM + 0.001858 × sTNF + (-0.2984) × β-catenin + 0.02169 × AFP]	0.582
CHC *vs* Control	(-9.353476 + 6.63414 × Prot + 0.001111 × sTNF + 0.24604 × AFP)	0.341
HCC *vs* CHC	[-10.40 + 1.416 × Prot + 0.002024 × IL-8 + 0.004096 × sICAM + (4.251 × 10^{-4}) × sTNF + 0.2567 × β-catenin + 0.02442 × AFP]	0.745

CHC: Chronic hepatitis C; LC: Liver cirrhosis; AFP: α-fetoprotein; HCC: Hepatocellular carcinoma; HCV: Hepatitis C virus.; sICAM-1: Soluble intercellular adhesion molecule; sTNF: Soluble tumor necrosis factor.

individual markers revealed that the serum level of IL-8 had fair diagnostic accuracy in discriminating the HCC group from the CHC group, because the AUC was in the range of (0.7-0.79), and had poor diagnostic accuracy in discriminating the HCC group from the control group, because the AUC was in the range of (0.6-0.69), whereas it failed to have diagnostic accuracy in discriminating between the HCC group and the LC group, because the AUC was in the range of (0.5-0.59). This result suggested that the serum level of IL-8 may be used as diagnostic marker for the early detection of HCC in CHC patients.

Correlation studies (Figure 5) showing the interplay between the studied markers revealed a moderately positive correlation between sTNF-RⅡ and sICAM-1. A possible explanation of this result is that ICAM-1 expression is regulated through four primary pathways: NF-κB, JAK/STAT and IFN-g, AP-1 and MAP Kinase, and PKC pathways. Ultimately, ICAM-1 is regulated at the level of transcription by one of these signaling cascades[33]. It has previously been reported that binding of TNF-α causes trimerization of TNFR-Ⅱ, enabling its direct interaction with TRAF-Ⅱ, resulting in the activation of transcription factors NF-κB or AP-1[34], and in turn leading to subsequent expression of ICAM-1. Additionally, there was a moderately positive correlation between sTNF-RⅡ and β-catenin. A possible explanation for this result is that TNF-RⅡ can also activate endothelial/epithelial tyrosine kinase (Etk) independently of TRAF2. Active Etk mediates crosstalk with vascular endothelial growth factor receptor 2 (VEGFR2) through reciprocal phosphorylation, resulting in the activation of the phosphatidylinositol 3-kinase (PI3K)-Akt angiogenic pathway[34]. PI3K (phosphatidylinositol 3-Kinase)-mediated activation of Akt/PKB (protein kinase-B) negatively regulates

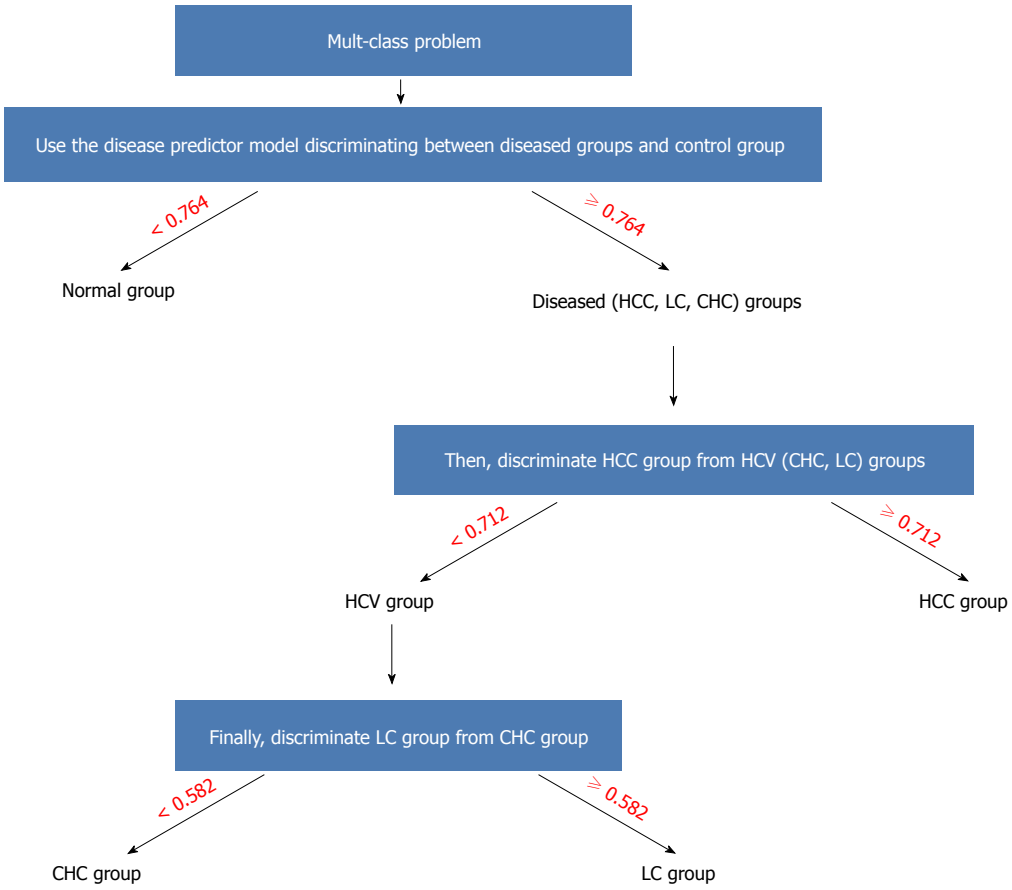

Figure 4 Algorithm of the disease predictor model for identifying muti-class problem. Each discrimination step in the algorithm has its own mathematical model with the appropriate cutoff that was conceived from Table 7. CHC: Chronic hepatitis C; LC: Liver cirrhosis; HCC: Hepatocellular carcinoma.

GSK3[35]. When GSK3 is active, it phosphorylates APC and β-catenin and stimulates an interaction between β-catenin and Beta-TRCP (Beta-transducin repeat-containing protein), a regulator of E3 ubiquitin ligase, which degrades β-catenin in proteasomes[36]. Thus, the inactivation of GSK3 inhibits β-catenin phosphorylation and subsequent degradation, leading to the nuclear accumulation of β-catenin. Moreover, our previous study, Zekri *et al*[20] has used correlation analysis of the expressed genes in HCC cases associated with HCV infection to reveal a significant negative correlation between GSK3B and AKT (P = 0.04), characterized by GSK3B downregulation with overexpression of AKT at the m-RNA level.

Further analysis of the data, using the R package and different modules for binary and multi-class classifiers based on generalized linear models, was carried out to model the top performing markers with AFP, in order to improve the diagnostic performance and the predictive power for the early detection of HCC. ROC curve analysis of the different modules revealed that using a binary classifier over different pairwise comparisons was superior to using the multi-class classification. Additionally, using a binary classifier based on a linear model offered an improvement in the diagnostic performance over using the top performing individual marker in each pairwise comparison. The performance of the binary classifier based linear model was evaluated by measuring the predictive power (PPV). The performance of the model was high, because the PPV was in the range of (87%-100%) over different pairwise comparisons.

From these models (Table 7), only three markers (sTNF-RⅡ, proteasome, and AFP) were able to discriminate the control group from all other groups. To discriminate among different other groups, sICAM-1, β-catenin, and IL-8 were required. The use of different models for resolving the multi-class classification problem may be performed as follows: First, use the mathematical model based on the binary classifier (-11 + 6.83 × proteasome + 0.00129 × sTNF + 0.283 × AFP) with the cutoff of 0.764 to discriminate controls from disease cases. For disease cases, first discriminate HCC cases from HCV cases (cases with LC and CHC) using the mathematical model based on the binary classifier [-11.91 + 3.222 × proteasome + (3.813×10^{-4}) × IL-8 + 0.001518 × sICAM + (6.481×10^{-4}) × sTNF + 0.2906 × β-catenin + 0.01931 × AFP] with the cutoff of 0.712. If the cases have HCV, proceed to discriminate LC cases from CHC cases using the mathematical model based on the binary classifier [-10.16+ (-4.487) × proteasome + 0.002086

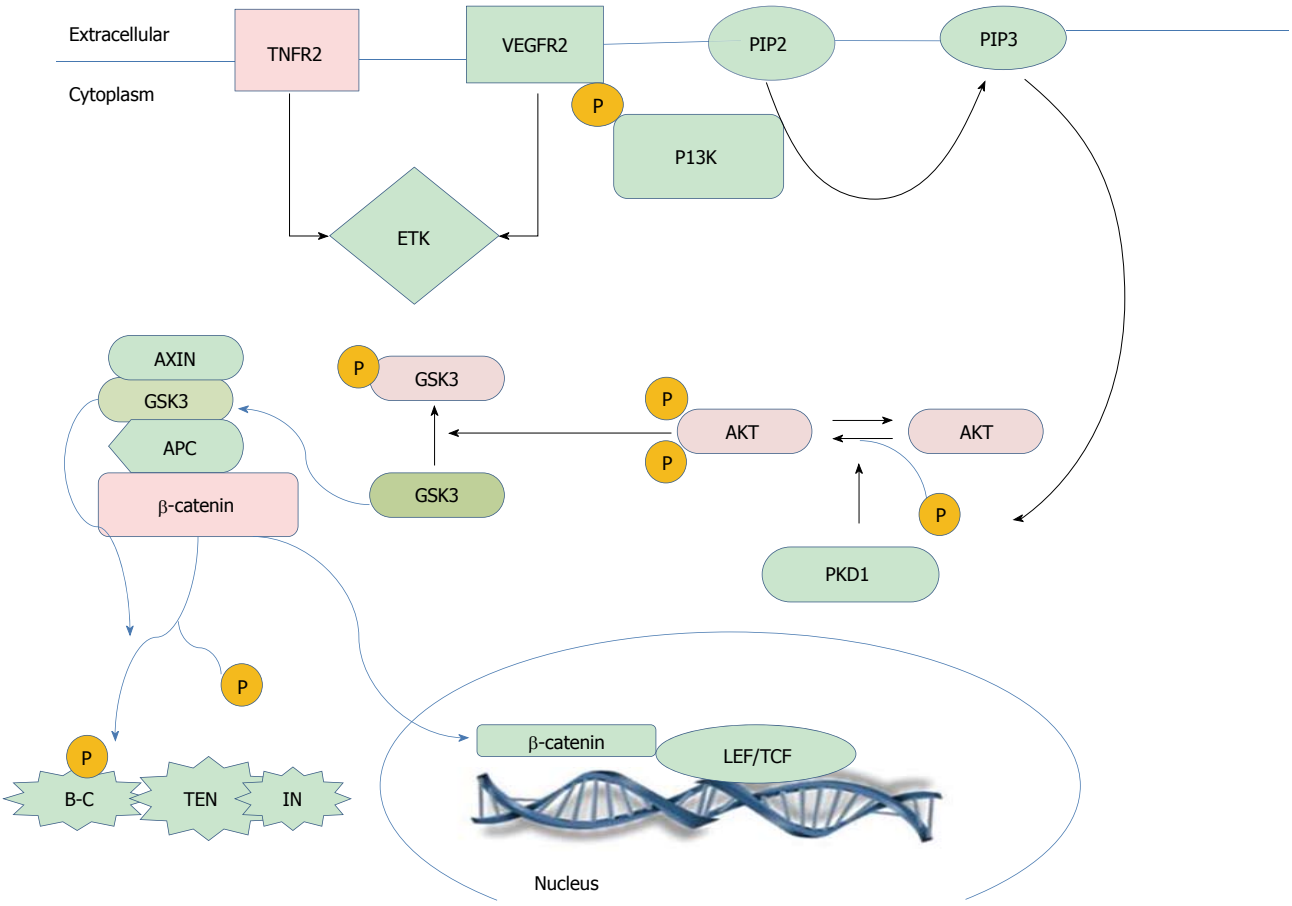

Figure 5 The hypothetical mechanism between tumor necrosis factor receptor Ⅱ and β-catenin. TNF-RⅡ: Tumor necrosis factor receptor Ⅱ.

× sICAM + 0.001858 × sTNF + (-0.2984) × β-catenin + 0.02169 × AFP] with a cutoff of 0.582.

In general, for the early detection of hepatocellular carcinoma in high risk patients; using the mathematical model based on the binary classifier (-11.33 + 7.38 × proteasome + 0.001081 × sICAM + 0.2574 × β-catenin + 0.01597 × AFP) with a cutoff of 0.655 improved the diagnostic accuracy of the discrimination of the HCC group from the LC group, with an AUC value of 0.961, 98.8% specificity, and 89.1% sensitivity. Additionally, using the mathematical model based on the binary classifier (-11.33 + 7.38 × Proteasome + 0.00108 × sICAM + 0.2574 × β-catenin + 0.01597 × AFP) with a cutoff of 0.655 improved the diagnostic performance in discriminating the HCC group from the CHC group, with an AUC value of 0.971, 96.8% specificity, and 89.7% sensitivity.

In conclusion, this disease predictor model may be a valuable tool for the early detection of the statuses of different liver diseases co-occurring HCV infection in an accurate, non-invasive, inexpensive, and rapid manner. Our recommendation is to perform further studies to evaluate the mathematical model on a larger scale (validation dataset) and to generalize the early detection of HCC for other etiologic agents rather than HCV.

ACKNOWLEDGMENTS

We acknowledge Mai Lotfy for helping format the manuscript and the virology and immunology staff members for their help in sample collection, as well as the NCI for financing the study.

COMMENTS

Background

Hepatocellular carcinoma (HCC) is considered to be a heterogeneous tumor due to the presence of inflammation and most probably cirrhosis, making the early detection of HCC as well as its treatment complicated. Early detection of HCC is usually associated with a proper clinical response; however, the existing markers differentiate only a very limited number of cases and lack sensitivity and specificity. Therefore, this study used a panel of serum proteins in association with AFP to build a mathematical model for the early detection of HCC and examined the cascade of complicated liver disease.

Research frontiers

This is the first time that a proper mathematical model has been developed from a serum protein panel for early disease detection of different states of liver disease co-occurring with hepatitis C virus (HCV) infection.

Innovations and breakthroughs

Although these studied markers have been previously addressed in relation to liver disease, a mathematical model had yet to be built from this panel in combination with standard α-fetoprotein (AFP) for the differentiation between

different states of liver disease co-occurring with HCV infection.

Applications

The proposed mathematical model using a panel of serum proteins in combination with AFP may be a useful method for the early detection of different liver disease states co-occurring with HCV infection.

Peer-review

This study was designed to explore a mathematical model for the early detection of hepatocellular carcinoma co-occurring with HCV infection, the authors provide a potential novel biomarker combination useful for the early diagnosis for patients with HCV. This is an interesting study.

REFERENCES

1 **Hiotis SP**, Rahbari NN, Villanueva GA, Klegar E, Luan W, Wang Q, Yee HT. Hepatitis B vs. hepatitis C infection on viral hepatitis-associated hepatocellular carcinoma. *BMC Gastroenterol* 2012; **12**: 64 [PMID: 22681852 DOI: 10.1186/1471-230X-12-64]

2 **Iakova P**, Timchenko L, Timchenko NA. Intracellular signaling and hepatocellular carcinoma. *Semin Cancer Biol* 2011; **21**: 28-34 [PMID: 20850540 DOI: 10.1016/j.semcancer.2010.09.001]

3 **Yamashita T**, Honda M, Kaneko S. Molecular mechanisms of hepatocarcinogenesis in chronic hepatitis C virus infection. *J Gastroenterol Hepatol* 2011; **26**: 960-964 [PMID: 21443660 DOI: 10.1111/j.1440-1746.2011.06723.x]

4 **El-Zanaty F**, Way AA. Knowledge and prevalence of hepatitis C. In: Egypt Demographic and Health Survey 2008. Egyptian Ministry of Health, El-Zanaty and Associates and Macro International, 2009 (accessed April 10, 2015). Available from: URL: http://www.dhsprogram.com/2008edhs/Knowledge and prevalence of hepatitis C

5 **Zhao YJ**, Ju Q, Li GC. Tumor markers for hepatocellular carcinoma. *Mol Clin Oncol* 2013; **1**: 593-598 [PMID: 24649215 DOI: 10.3892/mco.2013.119]

6 **Bruix J**, Llovet JM. Prognostic prediction and treatment strategy in hepatocellular carcinoma. *Hepatology* 2002; **35**: 519-524 [PMID: 11870363 DOI: 10.1053/jhep.2002.32089]

7 **Zhu K**, Dai Z, Zhou J. Biomarkers for hepatocellular carcinoma: progression in early diagnosis, prognosis, and personalized therapy. *Biomark Res* 2013; **1**: 10 [PMID: 24252133 DOI: 10.1186/2050-7771-1-10]

8 **Claudino WM**, Quattrone A, Biganzoli L, Pestrin M, Bertini I, Di Leo A. Metabolomics: available results, current research projects in breast cancer, and future applications. *J Clin Oncol* 2007; **25**: 2840-2846 [PMID: 17502626 DOI: 10.1200/JCO.2006.09.7550]

9 **McShane LM**, Altman DG, Sauerbrei W, Taube SE, Gion M, Clark GM. Reporting recommendations for tumor marker prognostic studies (REMARK). *J Natl Cancer Inst* 2005; **97**: 1180-1184 [PMID: 16106022 DOI: 10.1093/jnci/dji237]

10 **Ren Y**, Poon RT, Tsui HT, Chen WH, Li Z, Lau C, Yu WC, Fan ST. Interleukin-8 serum levels in patients with hepatocellular carcinoma: correlations with clinicopathological features and prognosis. *Clin Cancer Res* 2003; **9**: 5996-6001 [PMID: 14676125]

11 **Bradley JR**. TNF-mediated inflammatory disease. *J Pathol* 2008; **214**: 149-160 [PMID: 18161752 DOI: 10.1002/path.2287]

12 **McConnell BB**, Yang VW. The Role of Inflammation in the Pathogenesis of Colorectal Cancer. *Curr Colorectal Cancer Rep* 2009; **5**: 69-74 [PMID: 19756239]

13 **Henry L**, Lavabre-Bertrand T, Vercambre L, Ramos J, Carillo S, Guiraud I, Pouderoux P, Bismuth M, Valats JC, Demattei C, Duny Y, Chaze I, Funakoshi N, Bureau JP, Daurès JP, Blanc P. Plasma proteasome level is a reliable early marker of malignant transformation of liver cirrhosis. *Gut* 2009; **58**: 833-838 [PMID: 19201777 DOI: 10.1136/gut.2008.157016]

14 **Sorokin AV**, Kim ER, Ovchinnikov LP. Proteasome system of protein degradation and processing. *Biochemistry (Mosc)* 2009; **74**: 1411-1442 [PMID: 20210701 DOI: 10.1134/S000629790913001X]

15 **Lawson C**, Wolf S. ICAM-1 signaling in endothelial cells. *Pharmacol Rep* 2009; **61**: 22-32 [PMID: 19307690]

16 **Bernier AJ**, Zhang J, Lillehoj E, Shaw AR, Gunasekara N, Hugh JC. Non-cysteine linked MUC1 cytoplasmic dimers are required for Src recruitment and ICAM-1 binding induced cell invasion. *Mol Cancer* 2011; **10**: 93 [PMID: 21798038 DOI: 10.1186/1476-4598-10-93]

17 **Clevers H**. Wnt/beta-catenin signaling in development and disease. *Cell* 2006; **127**: 469-480 [PMID: 17081971 DOI: 10.1016/j.cell.2006.10.018]

18 **Laurent-Puig P**, Zucman-Rossi J. Genetics of hepatocellular tumors. *Oncogene* 2006; **25**: 3778-3786 [PMID: 16799619 DOI: 10.1038/sj.onc.1209547]

19 **Zekri AR**, Ashour MS, Hassan A, Alam El-Din HM, El-Shehaby AM, Abu-Shady MA. Cytokine profile in Egyptian hepatitis C virus genotype-4 in relation to liver disease progression. *World J Gastroenterol* 2005; **11**: 6624-6630 [PMID: 16425355 DOI: 10.3748/wjg.v11.i42.6624]

20 **Zekri AR**, Bahnassy AA, Abdel-Wahab SA, Khafagy MM, Loutfy SA, Radwan H, Shaarawy SM. Expression of pro- and anti-inflammatory cytokines in relation to apoptotic genes in Egyptian liver disease patients associated with HCV-genotype-4. *J Gastroenterol Hepatol* 2009; **24**: 416-428 [PMID: 19054267 DOI: 10.1111/j.1440-1746.2008.05699.x]

21 **Zekri AR**, Alam El-Din HM, Bahnassy AA, Zayed NA, Mohamed WS, El-Masry SH, Gouda SK, Esmat G. Serum levels of soluble Fas, soluble tumor necrosis factor-receptor II, interleukin-2 receptor and interleukin-8 as early predictors of hepatocellular carcinoma in Egyptian patients with hepatitis C virus genotype-4. *Comp Hepatol* 2010; **9**: 1 [PMID: 20051112 DOI: 10.1186/1476-5926-9-1]

22 **Zekri AR**, Bahnassy AA, Alam El-Din HM, Morsy HM, Shaarawy S, Moharram NZ, Daoud SS. Serum levels of β-catenin as a potential marker for genotype 4/hepatitis C-associated hepatocellular carcinoma. *Oncol Rep* 2011; **26**: 825-831 [PMID: 21701780 DOI: 10.3892/or.2011.1355]

23 **Zekri AR**, Youssef AS, Bakr YM, Gabr RM, El-Rouby MN, Hammad I, Ahmed EA, Marzouk HA, Nabil MM, Hamed HA, Aly YH, Zachariah KS, Esmat G. Serum biomarkers for early detection of hepatocellular carcinoma associated with HCV infection in egyptian patients. *Asian Pac J Cancer Prev* 2015; **16**: 1281-1287 [PMID: 25735368]

24 **GLOBOCAN database**. IARC, France. 2012 (accessed April 21, 2015). Available from: URL: http://globocan.iarc.fr

25 **Shaker MK**, Abdella HM, Khalifa MO, El Dorry AK. Epidemiological characteristics of hepatocellular carcinoma in Egypt: a retrospective analysis of 1313 cases. *Liver Int* 2013; **33**: 1601-1606 [PMID: 23714212 DOI: 10.1111/liv.12209]

26 **Mittal A**, Sathian B, Chandrashekharan N, Farooqui SM, Hussain A. Diagnostic significance of alpha fetoprotein in carcinomas of liver and biliary tract - a comparative study from the western region of Nepal. *Asian Pac J Cancer Prev* 2011; **12**: 3475-3478 [PMID: 22471500]

27 **Guan CN**, Chen XM, Lou HQ, Liao XH, Chen BY, Zhang PW. Clinical significance of axin and β-catenin protein expression in primary hepatocellular carcinomas. *Asian Pac J Cancer Prev* 2012; **13**: 677-681 [PMID: 22524844]

28 **Shimizu Y**, Minemura M, Tsukishiro T, Kashii Y, Miyamoto M, Nishimori H, Higuchi K, Watanabe A. Serum concentration of intercellular adhesion molecule-1 in patients with hepatocellular carcinoma is a marker of the disease progression and prognosis. *Hepatology* 1995; **22**: 525-531 [PMID: 7543436 DOI: 10.1002/hep.1840220223]

29 **Moriyama M**, Matsumura H, Shioda J, Aoki H, Nakamura H, Arakawa Y, Nirei K, Yamagami H, Kaneko M, Tanaka N, Arakawa Y. Measurement of human intercellular adhesion molecule 1 in the blood is useful for predicting the occurrence of hepatocellular carcinomas from chronic hepatitis C and liver cirrhosis. *Intervirology* 2006; **49**: 327-338 [PMID: 16926545 DOI: 10.1159/000095152]

30 **Li P**, Cao Y, Li Y, Zhou L, Liu X, Geng M. Expression of Wnt-5a

and β-catenin in primary hepatocellular carcinoma. *Int J Clin Exp Pathol* 2014; **7**: 3190-3195 [PMID: 25031739]
31 **Elewa H**, Abd-Elmeneem M, Hashem AM, Alshehaby A. Study of interleukin 8 (IL8) serum level in patients with chronic liver disease due to hepatitis C virus (HCV) with and without hepatocellular carcinoma (HCC). *Int J Hepatol* 2010; **1**: 9-17
32 **Zimmermann HW**, Seidler S, Gassler N, Nattermann J, Luedde T, Trautwein C, Tacke F. Interleukin-8 is activated in patients with chronic liver diseases and associated with hepatic macrophage accumulation in human liver fibrosis. *PLoS One* 2011; **6**: e21381 [PMID: 21731723 DOI: 10.1371/journal.pone.0021381]
33 **Roebuck KA**, Finnegan A. Regulation of intercellular adhesion molecule-1 (CD54) gene expression. *J Leukoc Biol* 1999; **66**: 876-888 [PMID: 10614768]
34 **Moelants EA**, Mortier A, Van Damme J, Proost P. Regulation of TNF-α with a focus on rheumatoid arthritis. *Immunol Cell Biol* 2013; **91**: 393-401 [PMID: 23628802 DOI: 10.1038/icb.2013.15]
35 **Clodfelder-Miller B**, De Sarno P, Zmijewska AA, Song L, Jope RS. Physiological and pathological changes in glucose regulate brain Akt and glycogen synthase kinase-3. *J Biol Chem* 2005; **280**: 39723-39731 [PMID: 16179343 DOI: 10.1074/jbc.M508824200]
36 **Jia J**, Zhang L, Zhang Q, Tong C, Wang B, Hou F, Amanai K, Jiang J. Phosphorylation by double-time/CKIepsilon and CKIalpha targets cubitus interruptus for Slimb/beta-TRCP-mediated proteolytic processing. *Dev Cell* 2005; **9**: 819-830 [PMID: 16326393 DOI: 10.1016/j.devcel.2005.10.006]

P- Reviewer: Gao C, Sunami Y **S- Editor**: Yu J **L- Editor**: A
E- Editor: Zhang DN

World Journal of Gastroenterology

Submit a Manuscript: http://www.wjgnet.com/esps/
Help Desk: http://www.wjgnet.com/esps/helpdesk.aspx
DOI: 10.3748/wjg.v22.i16.4183

World J Gastroenterol 2016 April 28; 22(16): 4183-4190
ISSN 1007-9327 (print) ISSN 2219-2840 (online)

ORIGINAL ARTICLE

Case Control Study

Effects of interactions between environmental factors and *KIF1B* genetic variants on the risk of hepatocellular carcinoma in a Chinese cohort

Jun-Hu Chen, Yan-Yan Wang, Wei-Biao Lv, Yu Gan, Wei Chang, Na-Na Tian, Xiao-Hui Huang, Li Liu, Xin-Fa Yu, Si-Dong Chen

Jun-Hu Chen, Wei Chang, Si-Dong Chen, Department of Epidemiology, School of Public Health and Tropical Medicine, Southern Medical University, Guangzhou 510515, Guangdong Province, China

Jun-Hu Chen, Li Liu, Yu Gan, Wei Chang, Na-Na Tian, Xiao-Hui Huang, Si-Dong Chen, Department of Epidemiology and Biostatistics, School of Public Health, Guangdong Pharmaceutical University, Guangzhou 510310, Guangdong Province, China

Yan-Yan Wang, Department of Obstetrics and Gynecology, Affiliated HouJie Hospital of Guangdong Medical College, Dongguan 523945, Guangdong Province, China

Wei-Biao Lv, Xin-Fa Yu, Department of Oncology, The First People's Hospital of Shunde, Foshan 528300, Guangdong Province, China

Author contributions: Chen JH and Liu L analyzed the data and wrote the manuscript; Chang W, Tian NN, and Lv WB collected materials and clinical data; Wang YY, Gan Y, and Huang XH performed the experiments; Yu XF and Chen SD conceived and designed the study.

Institutional review board statement: This study was reviewed and approved by the Ethics Committee of the First People's Hospital of Shunde, Foshan, China.

Informed consent statement: All study participants provided informed written consent prior to study enrollment.

Conflict-of-interest statement: The authors declare that they have no conflicts of interest related to this work.

Data sharing statement: Technical appendix, statistical code, and dataset are available from the corresponding author at chensidong1@126.com.

Correspondence to: Dr. Si-Dong Chen, Professor, Department of Epidemiology, School of Public Health and Tropical Medicine, Southern Medical University, No. 1838, North Guangzhou Avenue, Guangzhou 510515, Guangdong Province, China. chensidong1@126.com
Telephone: +86-20-34055180
Fax: +86-20-34055355

Received: December 25, 2015
Peer-review started: December 28, 2015
First decision: December 30, 2015
Revised: January 17, 2016
Accepted: February 20, 2016
Article in press: February 23, 2016
Published online: April 28, 2016

Abstract

AIM: To examine the effect of the potential interaction between *KIF1B* variants (rs17401966 and rs3748578) and environmental factors on the risk of hepatocellular carcinoma (HCC) in a high-risk region in China.

METHODS: Three hundred and six patients with HCC and 306 hospital-based control participants residing in the Shunde region of Guangdong Province, China were enrolled. Clinical characteristics were collected by reviewing the complete medical histories from the patient archives, and epidemiological data were collected using a questionnaire and clinical examination. Two single nucleotide polymorphisms (SNPs) of *KIF1B* (rs17401966 and rs3748578) were chosen for the current study. All subjects were genotyped

using a TaqMan real-time polymerase chain reaction. Multiplicative and additive logistic regression models were used to evaluate various gene-environment interactions.

RESULTS: Smoking, frequent consumption of raw freshwater fish, hepatitis B virus (HBV) infection, and a family history of HCC were important risk factors for HCC in this population. Chronic infection with HBV was the most important environmental risk factor for HCC [odds ratio (OR) = 12.02; 95% confidence interval (95%CI): 6.02-24.00]. No significant association was found between the *KIF1B* variants alone and the risk of HCC. Nevertheless, a significant additive effect modification was observed between rs17401966 and alcohol consumption (*P* for additive interaction = 0.0382). Compared with non-drinkers carrying either the AG or GG genotype of rs17401966, individuals classified as alcohol consumers with the AA genotype of rs17401966 had a significantly increased risk of HCC (OR = 2.36; 95%CI: 1.49-3.74).

CONCLUSION: The gene-environment interaction between the *KIF1B* rs17401966 variant and alcohol consumption may contribute to the development of HCC in Chinese individuals.

Key words: Hepatocellular carcinoma; Kinesin family member 1B; Environmental factors; Alcohol drinking; Gene-environment interaction

Core tip: *KIF1B* has been proposed as a promising susceptibility gene for hepatocellular carcinoma (HCC) by a recent genome-wide association study (GWAS) in Chinese populations. However, the most significant variant (rs17401966) in this GWAS yielded inconsistent results in subsequent replication studies. In this work, we evaluated the role of rs17401966 in genetic susceptibility to HCC and gene-environment interactions. Our study demonstrates that the gene-environment interaction between the *KIF1B* rs17401966 variant and drinking alcohol significantly contributed to the development of HCC in the Chinese population.

Chen JH, Wang YY, Lv WB, Gan Y, Chang W, Tian NN, Huang XH, Liu L, Yu XF, Chen SD. Effects of interactions between environmental factors and *KIF1B* genetic variants on the risk of hepatocellular carcinoma in a Chinese cohort. *World J Gastroenterol* 2016; 22(16): 4183-4190 Available from: URL: http://www.wjgnet.com/1007-9327/full/v22/i16/4183.htm DOI: http://dx.doi.org/10.3748/wjg.v22.i16.4183

INTRODUCTION

Hepatocellular carcinoma (HCC) is one of the most common malignancies worldwide. HCC ranks as the fifth most common cancer in men and seventh most common cancer in women[1]. Eastern Asia experiences a large burden of the geographical distribution of HCC; China alone accounts for approximately 55% of all HCC cases worldwide[2]. Prognosis of HCC patients is poor, with an average 3-year survival rate of 13%-21%[3,4]. Due to the high disease burden worldwide, it is important to identify individuals who are at a higher risk of HCC and to identify risk factors that may be modifiable. Several environmental factors that increase the risk of HCC have been found, including chronic infection with hepatitis B virus (HBV) or hepatitis C virus (HCV), exposure to aflatoxin, and consumption of alcohol[5-7].

However, only a small percentage of individuals who are exposed to these risk factors will eventually develop HCC, highlighting that genetic susceptibility is another factor for the development of HCC. HCC involves a complex interplay of multiple genetic and environmental factors[8]. However, underlying genetic mechanisms of hepatocellular carcinogenesis have not yet been fully elucidated.

Kinesin superfamily proteins (*KIFs*) make up a large gene family of microtubule motor proteins[9]. *KIF1B*, a member of the *KIF* family, maps to a gene locus at 1p36.22 and encodes two alternatively spliced isoforms, *KIF1B*α and *KIF1B*β; both isoforms form homodimers and transport mitochondria and synaptic vesicle precursors, respectively. It has been postulated that *KIF1B* acts as a tumor suppressor. Downregulation of *KIFs* has been shown to contribute to tumorigenesis of certain cancers, including brain, colon and breast cancers[10]. Recently, Zhang *et al*[11] performed a genome-wide association study (GWAS) and found that *KIF1B* is a promising susceptibility gene for HCC in five independent Chinese populations. In this GWAS, the most significant variant of *KIF1B* (rs17401966), located in the intron of the gene, was associated with a decreased risk of HCC [joint odds ratio (OR) = 0.61, $P = 1.7 \times 10^{-18}$]. However, more recent studies have not drawn the same conclusion. Al-Qahtani *et al*[12] reported no significant association between the rs17401966 variant of *KIF1B* and HBV-related HCC. Sawai *et al*[13] also showed no association between rs17401966 and HBV-related HCC in a Japanese cohort. These inconsistent results may partly be due to the distinct genetic architecture among the different study populations. Additionally, the significant findings obtained by Zhang *et al*[11] may have resulted from a phenomenon known as the "winner's curse," where the odds ratio of the candidate variant is overestimated in the population, leading to reporting a positive result[14]. Another reason for the discrepancy among studies could be the complex gene-environment interactions involved in the development of HCC that have been neglected. Hence, we conducted a case-control study with HCC patients and hospital-based controls to clarify the effect of rs17401966 in *KIF1B* on HCC. In addition, one single nucleotide polymorphism (SNP),

rs3748578, was in strong linkage disequilibrium (LD) with rs17401966[15], which was also associated with HBV-induced HCC. We also investigated the potential functional role of this variant rs3748578. We applied both additive and multiplicative models using a logistic regression analysis framework to assess the potential interactions between the variants and environmental factors in development of HCC in a Chinese cohort.

MATERIALS AND METHODS

Study population

Three hundred and six patients with HCC and 306 control patients were recruited from Shunde First People's Hospital (Foshan, China) from October 2010 to October 2012. A diagnosis of HCC was made through a combination of liver function tests, serum immunological markers, liver ultrasonography (US) or computed tomography (CT), and pathological confirmation. Patients were excluded if they were diagnosed with cancer other than HCC after the workup. Age and sex-matched control participants with no history of cancer were enrolled from the hospital at the same time as case enrollment. Clinical characteristics were collected by reviewing the complete medical histories from the patient archives, including age, gender, serum α-fetoprotein (AFP) levels, hepatitis B surface antigen (HBsAg) status, HBV-DNA titer, alanine aminotransferase (ALT) levels, aspartate aminotransferase (AST) levels, and total bilirubin levels. Chronic infection with hepatitis B virus (CHB) was diagnosed based on HBsAg seropositivity, positive serum HBV-DNA levels, and continuously elevated ALT over a period of 6 mo.

Epidemiological data were collected using a questionnaire and clinical examination. The main definitions of risk categories were as follows: (1) a cigarette smoker is a person who smokes one or more cigarettes per day for at least 6 mo; (2) an alcohol drinker is a person who consumes beer, wine, or hard liquor at least once weekly for at least 6 mo during their lifetime; and (3) a family history of cancer in the first degree relatives (parents, siblings, and children). Written informed consent was obtained from all subjects. The study was approved by the Ethics Committee of the First People's Hospital of Shunde.

Genetic variant genotyping

As previously described, rs1740966 variant was found to be the most significant HCC-associated variant with another candidate variant, rs3748578, in high-linkage to rs1740966. Zhang *et al*[15] predicted that both rs1740966 and rs3748578 may function in HCC tumor suppression. Therefore, we chose two SNPs (rs17401966 and rs3748578) of *KIF1B* for the current study.

DNA was extracted using the TIANamp Blood DNA Kit (Tiangen, Beijing, China) according to the manufacturer's protocol. Genomic DNA was extracted from peripheral whole blood. All subjects were genotyped using TaqMan real-time polymerase chain reaction (Applied Biosystems, Foster City, CA, United States) without knowledge of subjects' infection status. Samples were heated to 95 ℃ for 10 min followed by 45 cycles of 95 ℃ for 15 s and 60 ℃ for 1 min. The ABI Prism 7900HT Sequence Detection System (Applied Biosystems, Carlsbad, CA, United States) was used to analyze the endpoint fluorescence. To ensure the accuracy of genotyping, > 5% of the samples were randomly selected and repeated, yielding a 100% concordance.

Statistical analysis

Differences in the distribution of demographic characteristics, lifestyles, and HBV infection status between cases and controls were evaluated using χ^2 test and *t* test, where appropriate. Hardy-Weinberg equilibrium (HWE) was tested for the genetic variants in controls. Logistic regressions were used to estimate the associations of environmental factors with HCC and ORs and corresponding 95% confidence intervals (CIs) were calculated. Logistic regressions were also fit to explore associations of genetic variants and HCC, taking into account both dominant and recessive inheritance patterns. Potential gene-environment interactions were studied using a logistic regression framework that employed both multiplicative and additive interaction models with a bootstrapping procedure. All statistical analyses were conducted using Stata software, version 14.0 (College Station, TX, United States). All probability analyses were two-sided tests where a P value < 0.05 was considered statistically significant.

RESULTS

A total of 306 patients with HCC (264 males and 42 females) and 306 controls (264 males and 42 females) were enrolled in the study with a mean age (± standard deviation) of 55.84 (± 11.49) and 55.83 (± 11.67) years, respectively. The general characteristics of the subjects are presented in Table 1. No significant differences were found between healthy controls and patients with HCC with regard to age and gender (P = 0.992 and P = 0.998, respectively). Logistic regression analysis suggested that smoking, frequent consumption of raw freshwater fish, HBV infection, and family history of HCC were important risk factors for HCC in the Shunde region of China (Table 1).

The genotypic distributions of rs3748578 and rs17401966 did not differ significantly between the cases and controls (Table 2). Logistic regression analysis failed to show a significant association between HCC with either rs3748578 or rs17401966 for all genetic models (Table 3).

Tables 4 and 5 show the results of additive and multiplicative interaction analysis between the two

Table 1 Distribution of selected characteristics and environmental factors in hepatocellular carcinoma cases and controls *n* (%)

Variable	Case (*n* = 306)	Control (*n* = 306)	*P* value	OR[3]	95%CI
Age, yr (mean ± SD)	55.84 ± 11.49	55.83 ± 11.67	0.992[1]		
Sex					
Male	264 (86.27)	264 (86.27)			
Female	42 (13.73)	42 (13.73)	0.998[2]		
Tobacco smoking					
No	95 (31.05)	139 (45.42)			
Yes	211 (68.95)	167 (54.58)	< 0.014[2]		
Alcohol drinking					
No	133 (43.46)	188 (38.56)		1.00	-
Yes	173 (56.54)	118 (61.44)	0.012[2]	2.45	1.24-4.82
History of raw freshwater fish eating					
No	111 (36.27)	171 (55.88)		1.00	-
Yes	195 (63.73)	135 (44.12)	0.030[2]	1.99	1.06-3.75
Status of HBV infection					
No	77 (25.16)	252 (82.35)		1.00	-
Yes	229 (74.84)	54 (17.65)	< 0.013[2]	12.02	6.02-24.00
Family history of HCC					
No	256 (83.66)	294 (96.08)		1.00	-
Yes	50 (16.34)	12 (3.92)	< 0.011[2]	6.90	2.10-22.73

[1]*P* value was calculated by the *t* test; [2]*P* value was calculated by the χ^2 test; [3]ORs were adjusted for age. HBV: Hepatitis B virus; HCC: Hepatocellular carcinoma; OR: Odds ratio.

Table 2 Distribution of rs3748578 and rs17401966 in hepatocellular carcinoma cases and controls *n* (%)

Variants	Genotypes	Case (*n* = 306)	Control (*n* = 306)	χ^2	*P* value	HWE
rs3748578	GG	169 (55.22)	150 (49.02)			
	AG	122 (39.87)	138 (45.10)			
	AA	15 (4.91)	18 (5.88)	2.39	0.303	0.058
rs17401966	AA	159 (51.96)	150 (49.02)			
	AG	126 (41.18)	138 (45.10)			
	GG	21 (6.86)	18 (5.88)	1.04	0.595	0.058

HWE: Hardy-Weinberg equilibrium.

Table 3 Association analysis between *KIF1B* variants and risk of hepatocellular carcinoma development *n* (%)

Variants	Crude OR (95%CI)	*P* value	Adjusted OR[1] (95%CI)	*P* value[1]
rs3748578				
GG	1.00		1.00	
AG	0.74 (0.36-1.52)	0.411	0.71 (0.33-1.53)	0.380
AA	0.79 (0.57-1.09)	0.148	0.82 (0.58-1.62)	0.260
Dominant model	0.78 (0.57-1.07)	0.124	0.80 (0.57-1.13)	0.209
Recessive model	0.83 (0.41-1.67)	0.592	0.77 (0.36-1.65)	0.507
Additive model	0.82 (0.63-1.07)	0.137	0.83 (0.62-1.10)	0.193
rs17401966				
AA	1.00		1.00	
AG	0.86 (0.62-1.20)	0.374	0.86 (0.62-1.20)	0.379
GG	1.10 (0.56-2.15)	0.778	1.12 (0.57-2.21)	0.746
Dominant model	0.89 (0.65-1.22)	0.467	0.91 (0.64-1.27)	0.566
Recessive model	1.18 (0.62-2.26)	0.620	1.06 (0.52-2.15)	0.871
Additive model	0.95 (0.73-1.23)	0.692	0.94 (0.71-1.25)	0.685

[1]The adjusted ORs, 95% confidence intervals (CIs) and their corresponding *P* values were calculated in a logistic regression model by adjusting for age, alcohol drinking, history of raw freshwater fish eating, history of chronic hepatitis B virus infection, family history of HBV infection, and family history of hepatoma.

variants and the main environmental risk factors for HCC. A significant additive interaction was seen between rs17401966 and alcohol consumption (P = 0.0382). Compared with non-drinkers carrying the rs17401966 AG or GG genotype, individuals who consumed alcohol and carried the AA genotype had a significantly increased risk of HCC, with an adjusted OR of 2.36 (95%CI: 1.49-3.74, P = 0.0382). No

Table 4 Interaction analysis between rs3748578 and environmental factors in hepatocellular carcinoma development

Variant and environmental factors		Cases	Controls	OR	95%CI	*P* value[1]	P value[2]
rs3748578 and alcohol drinking						0.945	0.228
AG + AA	No	63	92	1.00			
GG	No	70	96	1.06	0.68-1.66		
AG + AA	Yes	74	64	1.69	1.06-2.68		
GG	Yes	99	54	2.68	1.69-4.25		
rs3748578 and history of raw freshwater fish eating						0.557	0.681
AG + AA	No	49	89	1.00			
GG	No	62	82	1.37	0.85-2.22		
AG + AA	Yes	88	67	2.39	1.49-3.82		
GG	Yes	107	68	2.86	1.80-4.54		
rs3748578 and history of chronic hepatitis B virus infection						0.850	0.815
AG + AA	No	30	126	1.00			
GG	No	47	126	1.57	0.93-2.64		
AG + AA	Yes	107	30	14.98	8.49-26.43		
GG	Yes	122	24	21.35	11.82-38.58		
rs3748578 and family history of HCC						0.372	0.555
AG + AA	No	117	152	1.00			
GG	No	136	142	1.24	0.89-1.74		
AG + AA	Yes	20	4	6.50	2.16-19.52		
GG	Yes	33	8	5.36	2.39-12.04		

[1]*P* values were calculated by the test for additive interaction; [2]*P* values were calculated by the test for multiplicative interaction.

Table 5 Interaction analysis between rs17401966 and major environmental factors in hepatocellular carcinoma development

Variant and environmental factors		Cases	Controls	OR	95%CI	*P* value[1]	*P* value[2]
rs17401966 and alcohol drinking						0.038	0.102
AG + GG	No	69	91	1.00			
AA	No	64	97	0.87	0.56-1.36		
AG + GG	Yes	78	65	1.58	1.00-2.49		
AA	Yes	95	53	2.36	1.49-3.74		
rs17401966 and history of raw freshwater fish eating						0.470	0.852
AG + GG	No	53	88	1.00			
AA	No	58	83	1.16	0.72-1.87		
AG + GG	Yes	94	68	2.30	1.45-3.64		
AA	Yes	101	67	2.50	1.58-3.96		
rs17401966 and history of chronic hepatitis B virus infection						0.269	0.753
AG + GG	No	32	126	1.00			
AA	No	45	126	1.41	0.84-2.36		
AG + GG	Yes	115	30	15.09	8.63-26.39		
AA	Yes	114	24	18.7	10.40-33.63		
rs17401966 and family history of hepatoma						0.697	0.524
AG + GG	No	125	152	1.00			
AA	No	128	142	1.10	0.78-1.53		
AG + GG	Yes	22	4	6.69	2.25-19.92		
AA	Yes	31	8	4.71	2.09-10.62		

[1]*P* values were calculated by test for additive interaction; [2]*P* values were calculated by test for multiplicative interaction.

significant interactions were observed between the rs3748578 variant and environmental factors.

DISCUSSION

The current study aimed to investigate whether two variants of *KIF1B* (rs17401966 and rs3748578) interacted with environmental risk factors of HCC to influence the risk of HCC. A significant additive interaction was observed between rs17401966 and alcohol consumption.

HCC is a complex disease associated with many risk factors and cofactors[16]. The major risk factor for HCC in China is clearly chronic HBV infection[17], with an 8%-20% prevalence of HBV[18] and approximately 93 million chronic HBV carriers[19]. The proportion of HBV-positive HCC has significantly increased, with 76% of HCC cases being HBV positive[20], which was consistent with 74.84% in our research. However, compared to China, the proportion of HCV-positive HCC was high in the United States, Italy, Japan, Brazil, Taiwan, Egypt, and other countries[20]. As we know, HCV prevalence

in China is low (< 1.5%)[21], which is transmitted primarily through intravenous drug use and invasive medical treatment, particularly hemodialysis[22]. The overall prevalence of anti-HCV antibody (anti-HCV) in Guangdong Province was about 0.50%[23-25], after the implementation of strict blood screening and other procedural measures, and we did not describe the relationship between HCV and HCC in the research.

In this study, we did not find a significant association between rs17401966 and HCC. This result is not consistent with the results reported in the GWAS study by Zhang *et al*[11]. One possible explanation for this discrepancy is the fact that the study samples were made up of individuals with different genetic architectures, who were from south China and Japan. Additionally, according to evolutionary theory, individual common variants often exert modest effects on common diseases[26]. In other words, sufficient statistical power to detect a disease with low penetrance due to a specific variant would require enrollment of thousands of subjects in the study. A recent meta-analysis of rs17401966 and HCC summarized data from 7596 HCC cases and 9614 controls; this meta-analysis supported Zhang *et al*'s[15] findings, indicating a significant association between rs17401966 and HCC. Nevertheless, according to the common disease-common variant (CDCV) hypothesis, cumulative effects of multiple common variants or their interactions with environment factors underlie common diseases. The finding in the present study on the interaction between rs17401966 and alcohol consumption fits the CDCV hypothesis. Zhang *et al*[11] suggested a significant association between rs17401966 genotypes and expression of *KIF1B* in liver tissues, with carriers of the G allele having a greater *KIF1B* level than individuals without G allele (AA carriers). However, several studies have found that the G allele of rs17401966 demonstrated a protective effect on the susceptibility to HCC[27-29]. This inconsistency might be attributed to the fact that there were heterogeneous population structures. It is necessary to investigate the exact effect of ethnicity on the association between *KIF1B* polymorphisms and HCC risk in future. It has been hypothesized that *KIF1B* can act as a tumor suppressor. The mechanism by which this occurs is still unclear, but *KIF1B* may induce apoptosis by acting downstream of *EglN3* prolyl hydroxylase[30], ultimately leading to inhibition of malignant transformation and progression.

Alcohol consumption is common in Guangdong Province, where the total drinking rate is 33.3%[31], with the region of Shunde having an even higher rate, especially in residents who habitually drink brewed Chinese rice wine[32]. Ethanol, the active compound in alcoholic beverages, is metabolized to acetaldehyde, which has been found to be mutagenic and carcinogenic[33,34], and other studies reported that alcohol was involved in hepatocarcinogenesis[35,36]. Therefore, a significant joint effect and interaction between rs17401966 and alcohol consumption was observed, suggesting that gene-environment interactions may provide further insights for comprehensive understanding of HCC in the Shunde area.

Our study is not without limitations. Hospital-based samples may lead to a selection bias of participants. Secondly, the sample size was limited and statistical power was insufficient for detection of a modest effect size of individual common variants. Thirdly, only two variants in the *KIF1B* gene were assessed in this study, which may fail to reflect the genetic mechanism of other *KIF1B* variants in the development of HCC.

In conclusion, we identified a statistically significant interaction between the rs17401966 variant of *KIF1B* and alcohol consumption that contributes to the development of HCC in the Shunde region of China. This study further supports the hypothesis that *KIF1B* is an important susceptibility gene for HCC in the Chinese population. Comprehensive studies with larger sample sizes and more diverse independent populations are warranted to better understand the underlying mechanisms of *KIF1B* genetic variants in the development of HCC.

COMMENTS

Background

Several environmental factors have been identified that increase the risk of hepatocellular carcinoma (HCC). However, only a small percentage of individuals who are exposed to these risk factors will eventually develop HCC, highlighting genetic susceptibility as another factor at play in the development of HCC. HCC involves a complex interplay of multiple genetic and environmental factors.

Research frontiers

According to a recent genome-wide association study, *KIF1B* has been identified as a promising susceptibility gene for HCC in Chinese adults. However, one of the significant variants (rs17401966) in this study yielded inconsistent results in the subsequent replication studies. Indeed, it is important to evaluate the role of rs17401966 in genetic susceptibility to HCC and gene-environment interactions.

Innovations and breakthroughs

The authors confirm the gene-environment interaction between the *KIF1B* rs17401966 variant and alcohol consumption in the development of HCC in Chinese individuals.

Applications

KIF1B SNPs and gene-environment interaction should be added as valuable knowledge in the field of hepatology.

Peer-review

The authors conducted a case-control study with HCC patients and hospital-based controls to clarify the effect of rs17401966 in *KIF1B* on HCC and further examined the potential interaction between variants in *KIF1B* and environmental factors on the risk of HCC in a high-risk region of China. They found a gene-environment interaction between the *KIF1B* rs17401966 variant and alcohol consumption influenced the development of HCC in Chinese individuals. Their findings add valuable knowledge in the field of hepatology.

REFERENCES

1 **El-Serag HB**. Epidemiology of viral hepatitis and hepatocellular carcinoma. *Gastroenterology* 2012; **142**: 1264-1273.e1 [PMID: 22537432 DOI: 10.1053/j.gastro.2011.12.061]

2 **Torre LA**, Bray F, Siegel RL, Ferlay J, Lortet-Tieulent J, Jemal A. Global cancer statistics, 2012. *CA Cancer J Clin* 2015; **65**: 87-108 [PMID: 25651787 DOI: 10.3322/caac.21262]

3 **Barbara L**, Benzi G, Gaiani S, Fusconi F, Zironi G, Siringo S, Rigamonti A, Barbara C, Grigioni W, Mazziotti A. Natural history of small untreated hepatocellular carcinoma in cirrhosis: a multivariate analysis of prognostic factors of tumor growth rate and patient survival. *Hepatology* 1992; **16**: 132-137 [PMID: 1352268 DOI: 10.1002/hep.1840160122]

4 **Ebara M**, Ohto M, Shinagawa T, Sugiura N, Kimura K, Matsutani S, Morita M, Saisho H, Tsuchiya Y, Okuda K. Natural history of minute hepatocellular carcinoma smaller than three centimeters complicating cirrhosis. A study in 22 patients. *Gastroenterology* 1986; **90**: 289-298 [PMID: 2416627]

5 **Lafaro KJ**, Demirjian AN, Pawlik TM. Epidemiology of hepatocellular carcinoma. *Surg Oncol Clin N Am* 2015; **24**: 1-17 [PMID: 25444466 DOI: 10.1016/j.soc.2014.09.001]

6 **Kim MN**, Han KH, Ahn SH. Prevention of hepatocellular carcinoma: beyond hepatitis B vaccination. *Semin Oncol* 2015; **42**: 316-328 [PMID: 25843736 DOI: 10.1053/j.seminoncol.2014.12.018]

7 **Goossens N**, Hoshida Y. Hepatitis C virus-induced hepatocellular carcinoma. *Clin Mol Hepatol* 2015; **21**: 105-114 [PMID: 26157746 DOI: 10.3350/cmh.2015.21.2.105]

8 **Nahon P**, Sutton A, Ziol M, Zucman-Rossi J, Trinchet J-C, Ganne-Carrié N. Genetic risk markers for hepatocellular carcinoma in patients with alcoholic liver disease. *Hepatic Oncol* 2015; **2**: 63-78 [DOI: 10.2217/hep.14.26]

9 **Nangaku M**, Sato-Yoshitake R, Okada Y, Noda Y, Takemura R, Yamazaki H, Hirokawa N. KIF1B, a novel microtubule plus end-directed monomeric motor protein for transport of mitochondria. *Cell* 1994; **79**: 1209-1220 [PMID: 7528108 DOI: 10.1016/0092-8674(94)90012-4]

10 **Munirajan AK**, Ando K, Mukai A, Takahashi M, Suenaga Y, Ohira M, Koda T, Hirota T, Ozaki T, Nakagawara A. KIF1Bbeta functions as a haploinsufficient tumor suppressor gene mapped to chromosome 1p36.2 by inducing apoptotic cell death. *J Biol Chem* 2008; **283**: 24426-24434 [PMID: 18614535 DOI: 10.1074/jbc.M802316200]

11 **Zhang H**, Zhai Y, Hu Z, Wu C, Qian J, Jia W, Ma F, Huang W, Yu L, Yue W, Wang Z, Li P, Zhang Y, Liang R, Wei Z, Cui Y, Xie W, Cai M, Yu X, Yuan Y, Xia X, Zhang X, Yang H, Qiu W, Yang J, Gong F, Chen M, Shen H, Lin D, Zeng YX, He F, Zhou G. Genome-wide association study identifies 1p36.22 as a new susceptibility locus for hepatocellular carcinoma in chronic hepatitis B virus carriers. *Nat Genet* 2010; **42**: 755-758 [PMID: 20676096 DOI: 10.1038/ng.638]

12 **Al-Qahtani A**, Al-Anazi M, Viswan NA, Khalaf N, Abdo AA, Sanai FM, Al-Ashgar H, Al-Ahdal M. Role of single nucleotide polymorphisms of KIF1B gene in HBV-associated viral hepatitis. *PLoS One* 2012; **7**: e45128 [PMID: 23028799 DOI: 10.1371/journal.pone.0045128]

13 **Sawai H**, Nishida N, Mbarek H, Matsuda K, Mawatari Y, Yamaoka M, Hige S, Kang JH, Abe K, Mochida S, Watanabe M, Kurosaki M, Asahina Y, Izumi N, Honda M, Kaneko S, Tanaka E, Matsuura K, Itoh Y, Mita E, Korenaga M, Hino K, Murawaki Y, Hiasa Y, Ide T, Ito K, Sugiyama M, Ahn SH, Han KH, Park JY, Yuen MF, Nakamura Y, Tanaka Y, Mizokami M, Tokunaga K. No association for Chinese HBV-related hepatocellular carcinoma susceptibility SNP in other East Asian populations. *BMC Med Genet* 2012; **13**: 47 [PMID: 22712471 DOI: 10.1186/1471-2350-13-47]

14 **Zheng X**, Wang L, Zhu Y, Guan Q, Li H, Xiong Z, Deng L, Lu J, Miao X, Cheng L. The SNP rs961253 in 20p12.3 is associated with colorectal cancer risk: a case-control study and a meta-analysis of the published literature. *PLoS One* 2012; **7**: e34625 [PMID: 22509336 DOI: 10.1371/journal.pone.0034625]

15 **Zhang Z**. Association between KIF1B rs17401966 polymorphism and hepatocellular carcinoma risk: a meta-analysis involving 17,210 subjects. *Tumour Biol* 2014; **35**: 9405-9410 [PMID: 24952890 DOI: 10.1007/s13277-014-2192-6]

16 **Venook AP**, Papandreou C, Furuse J, de Guevara LL. The incidence and epidemiology of hepatocellular carcinoma: a global and regional perspective. *Oncologist* 2010; **15** Suppl 4: 5-13 [PMID: 21115576 DOI: 10.1634/theoncologist.2010-S4-05]

17 **Yuen MF**, Hou JL, Chutaputti A. Hepatocellular carcinoma in the Asia pacific region. *J Gastroenterol Hepatol* 2009; **24**: 346-353 [PMID: 19220670 DOI: 10.1111/j.1440-1746.2009.05784.x]

18 **Zidan A**, Scheuerlein H, Schüle S, Settmacher U, Rauchfuss F. Epidemiological pattern of hepatitis B and hepatitis C as etiological agents for hepatocellular carcinoma in iran and worldwide. *Hepat Mon* 2012; **12**: e6894 [PMID: 23233864 DOI: 10.5812/hepatmon.6894]

19 **Liang X**, Bi S, Yang W, Wang L, Cui G, Cui F, Zhang Y, Liu J, Gong X, Chen Y, Wang F, Zheng H, Wang F, Guo J, Jia Z, Ma J, Wang H, Luo H, Li L, Jin S, Hadler SC, Wang Y. Evaluation of the impact of hepatitis B vaccination among children born during 1992-2005 in China. *J Infect Dis* 2009; **200**: 39-47 [PMID: 19469708 DOI: 10.1086/599332]

20 **de Martel C**, Maucort-Boulch D, Plummer M, Franceschi S. World-wide relative contribution of hepatitis B and C viruses in hepatocellular carcinoma. *Hepatology* 2015; **62**: 1190-1200 [PMID: 26146815 DOI: 10.1002/hep.27969]

21 **Mohd Hanafiah K**, Groeger J, Flaxman AD, Wiersma ST. Global epidemiology of hepatitis C virus infection: new estimates of age-specific antibody to HCV seroprevalence. *Hepatology* 2013; **57**: 1333-1342 [PMID: 23172780 DOI: 10.1002/hep.26141]

22 **Qin Q**, Smith MK, Wang L, Su Y, Wang L, Guo W, Wang L, Cui Y, Wang N. Hepatitis C virus infection in China: an emerging public health issue. *J Viral Hepat* 2015; **22**: 238-244 [PMID: 25131856 DOI: 10.1111/jvh.12295]

23 **Xie X**, Ma H, Lu Y, Fand Y, Ye X, Wu T, Dong S, Chen W, Cheng J. The seroepidemiological study on hepatitis C virus infection among general population in Shenzhen City (in Chinese). *Jibing Kongzhi Zazhi* 2012; **17**: 604-607

24 **Rong X**, Xia W, Wang M, Wang Y, Zheng Y, Ye X, Luo G, Wang C, Bei C, Fu Y. Seroepidemiological studies of HCV among first-time volunteer blood donors in Guangzhou,China (in Chinese). *Zhongguo Shuxue Zazhi* 2009; **22**: 883-885

25 **Lu J**, Zhou Y, Lin X, Jiang Y, Tian R, Zhang Y, Wu J, Zhang F, Zhang Y, Wang Y, Bi S. General epidemiological parameters of viral hepatitis A, B, C, and E in six regions of China: a cross-sectional study in 2007. *PLoS One* 2009; **4**: e8467 [PMID: 20041146 DOI: 10.1371/journal.pone.0008467]

26 **Sawcer S**, Hellenthal G, Pirinen M, Spencer CC, Patsopoulos NA, Moutsianas L, Dilthey A, Su Z, Freeman C, Hunt SE, Edkins S, Gray E, Booth DR, Potter SC, Goris A, Band G, Oturai AB, Strange A, Saarela J, Bellenguez C, Fontaine B, Gillman M, Hemmer B, Gwilliam R, Zipp F, Jayakumar A, Martin R, Leslie S, Hawkins S, Giannoulatou E, D'Alfonso S, Blackburn H, Martinelli Boneschi F, Liddle J, Harbo HF, Perez ML, Spurkland A, Waller MJ, Mycko MP, Ricketts M, Comabella M, Hammond N, Kockum I, McCann OT, Ban M, Whittaker P, Kemppinen A, Weston P, Hawkins C, Widaa S, Zajicek J, Dronov S, Robertson N, Bumpstead SJ, Barcellos LF, Ravindrarajah R, Abraham R, Alfredsson L, Ardlie K, Aubin C, Baker A, Baker K, Baranzini SE, Bergamaschi L, Bergamaschi R, Bernstein A, Berthele A, Boggild M, Bradfield JP, Brassat D, Broadley SA, Buck D, Butzkueven H, Capra R, Carroll WM, Cavalla P, Celius EG, Cepok S, Chiavacci R, Clerget-Darpoux F, Clysters K, Comi G, Cossburn M, Cournu-Rebeix I, Cox MB, Cozen W, Cree BA, Cross AH, Cusi D, Daly MJ, Davis E, de Bakker PI, Debouverie M, D'Hooghe M B, Dixon K, Dobosi R, Dubois B, Ellinghaus D, Elovaara I, Esposito F, Fontenille C, Foote S, Franke A, Galimberti D, Ghezzi A, Glessner J, Gomez R, Gout O, Graham C, Grant SF, Guerini FR, Hakonarson H, Hall P, Hamsten A, Hartung HP, Heard RN, Heath S, Hobart J, Hoshi M, Infante-Duarte C, Ingram G, Ingram W, Islam T, Jagodic M, Kabesch M, Kermode AG, Kilpatrick TJ, Kim C, Klopp N, Koivisto K, Larsson M, Lathrop M, Lechner-Scott JS, Leone MA, Leppa V, Liljedahl U, Bomfim IL, Lincoln RR, Link J, Liu J, Lorentzen AR, Lupoli S, Macciardi F, Mack T,

Marriott M, Martinelli V, Mason D, McCauley JL, Mentch F, Mero IL, Mihalova T, Montalban X, Mottershead J, Myhr KM, Naldi P, Ollier W, Page A, Palotie A, Pelletier J, Piccio L, Pickersgill T, Piehl F, Pobywajlo S, Quach HL, Ramsay PP, Reunanen M, Reynolds R, Rioux JD, Rodegher M, Roesner S, Rubio JP, Ruckert IM, Salvetti M, Salvi E, Santaniello A, Schaefer CA, Schreiber S, Schulze C, Scott RJ, Sellebjerg F, Selmaj KW, Sexton D, Shen L, Simms-Acuna B, Skidmore S, Sleiman PM, Smestad C, Sorensen PS, Sondergaard HB, Stankovich J, Strange RC, Sulonen AM, Sundqvist E, Syvanen AC, Taddeo F, Taylor B, Blackwell JM, Tienari P, Bramon E, Tourbah A, Brown MA, Tronczynska E, Casas JP, Tubridy N, Corvin A, Vickery J, Jankowski J, Villoslada P, Markus HS, Wang K, Mathew CG, Wason J, Palmer CN, Wichmann HE, Plomin R, Willoughby E, Rautanen A, Winkelmann J, Wittig M, Trembath RC, Yaouanq J, Viswanathan AC, Zhang H, Wood NW, Zuvich R, Deloukas P, Langford C, Duncanson A, Oksenberg JR, Pericak-Vance MA, Haines JL, Olsson T, Hillert J, Ivinson AJ, De Jager PL, Peltonen L, Stewart GJ, Hafler DA, Hauser SL, McVean G, Donnelly P, Compston A. Genetic risk and a primary role for cell-mediated immune mechanisms in multiple sclerosis. *Nature* 2011; **476**: 214-219 [PMID: 21833088 DOI: 10.1038/nature10251]

27 **Zhong R**, Tian Y, Liu L, Qiu Q, Wang Y, Rui R, Yang BF, Duan SY, Shi JX, Miao XP, Wang L, Li H. HBV-related hepatocellular carcinoma susceptibility gene KIF1B is not associated with development of chronic hepatitis B. *PLoS One* 2012; **7**: e28839 [PMID: 22363396 DOI: 10.1371/journal.pone.0028839]

28 **Sopipong W**, Tangkijvanich P, Payungporn S, Posuwan N, Poovorawan Y. The KIF1B (rs17401966) single nucleotide polymorphism is not associated with the development of HBV-related hepatocellular carcinoma in Thai patients. *Asian Pac J Cancer Prev* 2013; **14**: 2865-2869 [PMID: 23803045 DOI: 10.7314/APJCP.2013.14.5.2865]

29 **Huang M**, Pan Y, Liu J, Qi F, Wen J, Xie K, Ma H, Shen H, Liu Y, Dai J. A genetic variant at KIF1B predicts clinical outcome of HBV-related hepatocellular carcinoma in Chinese. *Cancer Epidemiol* 2014; **38**: 608-612 [PMID: 25153661 DOI: 10.1016/j.canep.2014.07.012]

30 **Schlisio S**, Kenchappa RS, Vredeveld LC, George RE, Stewart R, Greulich H, Shahriari K, Nguyen NV, Pigny P, Dahia PL, Pomeroy SL, Maris JM, Look AT, Meyerson M, Peeper DS, Carter BD, Kaelin WG. The kinesin KIF1Bbeta acts downstream from EglN3 to induce apoptosis and is a potential 1p36 tumor suppressor. *Genes Dev* 2008; **22**: 884-893 [PMID: 18334619 DOI: 10.1101/gad.1648608]

31 **Tan Y**, Jiang Q, Dun Z, Wang P, Chen Z, Ji G, Tan Y, Huang R, Xu Y, Xu X, Ma W, Zhang Y. Status and associated factors of alcohol consumption among residents aged 15 and above in Guang-dong Province (in Chinese). *Huanan Yufang Yixue* 2015; **31**: 213-217

32 **Hao W**, Su Z, Liu B, Zhang K, Yang H, Chen S, Biao M, Cui C. Drinking and drinking patterns and health status in the general population of five areas of China. *Alcohol Alcohol* 2003; **39**: 43-52 [PMID: 14691074 DOI: 10.1093/alcalc/agh018]

33 **Varela-Rey M**, Woodhoo A, Martinez-Chantar ML, Mato JM, Lu SC. Alcohol, DNA methylation, and cancer. *Alcohol Res* 2013; **35**: 25-35 [PMID: 24313162]

34 **Testino G**. The burden of cancer attributable to alcohol consumption. *Maedica (Buchar)* 2011; **6**: 313-320 [PMID: 22879847]

35 **Chiesa R**, Donato F, Tagger A, Favret M, Ribero ML, Nardi G, Gelatti U, Bucella E, Tomasi E, Portolani N, Bonetti M, Bettini L, Pelizzari G, Salmi A, Savio A, Garatti M, Callea F. Etiology of hepatocellular carcinoma in Italian patients with and without cirrhosis. *Cancer Epidemiol Biomarkers Prev* 2000; **9**: 213-216 [PMID: 10698484]

36 **Takeshita T**, Yang X, Inoue Y, Sato S, Morimoto K. Relationship between alcohol drinking, ADH2 and ALDH2 genotypes, and risk for hepatocellular carcinoma in Japanese. *Cancer Lett* 2000; **149**: 69-76 [PMID: 10737710 DOI: 10.1016/S0304-3835(99)00343-2]

P- Reviewer: Cerwenka HR, Iwasaki Y, Qadri I, Sergi C
S- Editor: Gong ZM **L- Editor**: Filipodia **E- Editor**: Zhang DN

World Journal of Gastroenterology

Submit a Manuscript: http://www.wjgnet.com/esps/
Help Desk: http://www.wjgnet.com/esps/helpdesk.aspx
DOI: 10.3748/wjg.v22.i16.4191

World J Gastroenterol 2016 April 28; 22(16): 4191-4200
ISSN 1007-9327 (print) ISSN 2219-2840 (online)

ORIGINAL ARTICLE

Retrospective Study

Urinary nuclear magnetic resonance spectroscopy of a Bangladeshi cohort with hepatitis-B hepatocellular carcinoma: A biomarker corroboration study

I Jane Cox, Abil E Aliev, Mary ME Crossey, Mahvish Dawood, Mamun Al-Mahtab, Sheikh M Akbar, Salimur Rahman, Antonio Riva, Roger Williams, Simon D Taylor-Robinson

I Jane Cox, Antonio Riva, Roger Williams, Institute of Hepatology, London, Foundation for Liver Research, London WC1E 6HX, United Kingdom

Abil E Aliev, Department of Chemistry, University College London, London WC1H 0AJ, United Kingdom

Mary ME Crossey, Mahvish Dawood, Simon D Taylor-Robinson, Division of Digestive Diseases, Department of Surgery and Cancer, Imperial College London, London W2 1NY, United Kingdom

Mamun Al-Mahtab, Salimur Rahman, Department of Hepatology, Bangabandhu Sheikh Mujib Medical University, Dhaka 1000, Bangladesh

Sheikh M Akbar, Department of Medical Sciences, Toshiba General Hospital, Tokyo 140-8522, Japan

Author contributions: Cox IJ, Williams R, Taylor-Robinson SD, Al-Mahtab M, Rahman S and Akbar SM designed the research; Cox IJ, Crossey MME, Dawood M and Aliev AE performed the research; Cox IJ, Aliev AE, Dawood M and Riva A analyzed the data; Riva A provided statistical advice; Cox IJ, Taylor-Robinson SD, Al-Mahtab M and Williams R wrote the paper.

Institutional review board statement: Ethical approval was granted by the research ethics committee at Bangabandhu Sheikh Mujib Medical University and Imperial College London (REC 09/H0712/82).

Informed consent statement: Informed consent was obtained from the study participants

Conflict-of-interest statement: To the best of our knowledge the authors declare no conflict of interest.

Correspondence to: I Jane Cox, PhD, Institute of Hepatology, London, Foundation for Liver Research, 69-75 Chenies Mews, London WC1E 6HX,
United Kingdom. j.cox@researchinliver.org.uk
Telephone: +44-207-2559830
Fax: +44-207-3800405

Received: December 1, 2015
Peer-review started: December 4, 2015
First decision: January 28, 2016
Revised: February 19, 2016
Accepted: March 1, 2016
Article in press: March 2, 2016
Published online: April 28, 2016

Abstract

AIM: To establish if a distinct urinary metabolic profile could be identified in Bangladeshi hepatitis-B hepatocellular carcinoma (HCC) patients compared to cirrhosis patients and controls.

METHODS: Urine samples from 42 Bangladeshi patients with HCC (39 patients with hepatitis-B HCC), 47 with cirrhosis on a background of hepatitis B, 46 with chronic hepatitis B, and seven ethnically-matched healthy controls were analyzed using nuclear magnetic resonance (NMR) spectroscopy. A full dietary and medication history was recorded for each subject. The urinary NMR data were analyzed using principal component analysis (PCA) and orthogonal partial least

squared discriminant analysis (OPLS-DA) techniques. Differences in relative signal levels of the most discriminatory metabolites identified by PCA and OPLS-DA were compared between subject groups using an independent samples Kruskal-Wallis one-way analysis of variance (ANOVA) test with all pairwise multiple comparisons. Within the patient subgroups, the Mann-Whitney U test was used to compare metabolite levels depending on hepatitis B e-antigen (HBeAg) status and treatment with anti-viral therapy. A Benjamini-Hochberg adjustment was applied to acquire the level of significance for multiple testing, with a declared level of statistical significance of $P < 0.05$.

RESULTS: There were significant differences in age ($P < 0.001$), weight ($P < 0.001$), and body mass index ($P < 0.001$) across the four clinical subgroups. Serum alanine aminotransferase (ALT) was significantly higher in the HCC group compared to controls ($P < 0.001$); serum α-fetoprotein was generally markedly elevated in HCC compared to controls; and serum creatinine levels were significantly reduced in the HCC group compared to the cirrhosis group ($P = 0.004$). A three-factor PCA scores plot showed clustering of the urinary NMR spectra from the four subgroups. Metabolites that contributed to the discrimination between the subgroups included acetate, creatine, creatinine, dimethyamine (DMA), formate, glycine, hippurate, and trimethylamine-*N*-oxide (TMAO). A comparison of relative metabolite levels confirmed that carnitine was significantly increased in HCC; and creatinine, hippurate, and TMAO were significantly reduced in HCC compared to the other subgroups. HBeAg negative patients showed a significant increase in creatinine ($P = 0.001$) compared to HBeAg positive patients in the chronic hepatitis B subgroup, whilst HBeAg negative patients showed a significant decrease in DMA ($P = 0.004$) in the cirrhosis subgroup compared to HBeAg positive patients. There were no differences in metabolite levels in HCC patients who did or did not receive antiviral treatment.

CONCLUSION: Urinary NMR changes in Bangladeshi HCC were identified, corroborating previous findings from Egypt and West Africa. These findings could form the basis for the development of a cost-effective HCC dipstick screening test.

Key words: Urinary metabolic profiling; Hepatocellular carcinoma; Nuclear magnetic resonance spectroscopy; Hepatitis B; Bangladesh

Core tip: Previous urinary metabolic profiling studies using nuclear magnetic resonance (NMR) spectroscopy of hepatocellular carcinoma (HCC) from Egypt and West Africa suggested the reproducibility of an identifying urinary metabolic profile in HCC. Here, a Bangladeshi HCC cohort was studied to identify similar changes. Urine samples from 142 subjects with hepatitis B HCC, cirrhosis, chronic hepatitis B, or no history of liver disease were analyzed using NMR. Urinary NMR from HCC differed across a range of metabolites, including reduced hippurate and creatinine and increased carnitine levels, consistent with the diverse effects of liver cancer on metabolic pathways and the interrelationship with the gut microbiome. Previous findings were corroborated, suggesting that a panel of metabolic markers could form the basis of a cost-effective HCC dipstick screening test.

Cox IJ, Aliev AE, Crossey MME, Dawood M, Al-Mahtab M, Akbar SM, Rahman S, Riva A, Williams R, Taylor-Robinson SD. Urinary nuclear magnetic resonance spectroscopy of a Bangladeshi cohort with hepatitis-B hepatocellular carcinoma: A biomarker corroboration study. *World J Gastroenterol* 2016; 22(16): 4191-4200 Available from: URL: http://www.wjgnet.com/1007-9327/full/v22/i16/4191.htm DOI: http://dx.doi.org/10.3748/wjg.v22.i16.4191

INTRODUCTION

The incidence of hepatocellular carcinoma (HCC) in Asia was estimated to be approximately 460000 in 2000, and since then, it has been increasing every year[1]. Studies have shown that hepatitis B virus (HBV) underlies 33% of the HCC cases in the People's Republic of Bangladesh, a small, but densely-populated country in the Indian sub-continent, bordering India and Myanmar[2]. Bangladesh is considered a region of intermediate prevalence for HBV infection, with the lifetime risk of HBV infection at 20%-60%[3]. While HBV infection is mainly transmitted during infancy and childhood in Bangladesh, all age groups are affected.

It is estimated that 2 billion people, one-third of the world-wide population, have been infected by HBV[4] and that approximately 400 million people are living with a chronic form of the disease[5]. Chronic HBV results in a wide range of liver diseases, spanning asymptomatic acute hepatitis to HCC. Recent studies have concluded that serum α-fetoprotein (AFP) lacks sufficient sensitivity to be widely used as a surveillance test for HCC[6]. Ultrasound-based surveillance is generally considered more sensitive than AFP, but the quality of the images can be both equipment- and user-dependent[6]. In addition, these procedures are generally unavailable in resource-constrained countries of Asia and Africa that harbor a majority population of HBV-related cirrhosis and HCC. A simple and versatile biomarker for the early stages of HCC, when treatment would still be effective, would, therefore, be of considerable value, both in resource-poor Bangladesh and in other parts of the world with a high HBV prevalence.

There has recently been considerable interest in analyzing the chemical composition of urine

to establish if one or more urinary biomarkers can be used to distinguish HCC from cirrhosis or uncomplicated chronic HBV infection. Urinary metabolic profiling using proton nuclear magnetic resonance (NMR) spectroscopy may provide objective diagnostic and prognostic assessment for a range of diseases[7]. It would be particularly valuable if subtle changes in the chemical composition of urine could be interpreted to improve early diagnosis of HCC. Diagnosis is currently often not made until such a late stage of disease that treatment measures are ineffective. Clinical cohorts from Egypt[8], Nigeria[9,10], and The Gambia[10] have been studied, and a consensus is emerging for a urinary fingerprint of HCC. The aim of this study was to establish if a similar urinary NMR fingerprint for HCC could be identified in a Bangladeshi cohort, since these patients have a different environmental and genetic background than the African populations.

MATERIALS AND METHODS

Study population

Urine samples were obtained with informed consent from patients attending the Department of Hepatology, Bangabandhu Sheikh Mujib Medical University, Dhaka, Bangladesh. Ethical approval was granted by the research ethics committee at Bangabandhu Sheikh Mujib Medical University and Imperial College London (REC 09/H0712/82), and the study conformed to the 1975 Declaration of Helsinki.

A total of 152 subjects, all of Indian ethnic origin, were recruited for the study between January 2013 and November 2014. The study cohort comprised 46 patients with HCC on a background of hepatitis B (43 patients) (HCC-HBV), hepatitis C (one patient), and cryptogenic (two patients); 50 patients with clinical or histologically confirmed hepatitis B related cirrhosis (CIR), 48 patients with non-cirrhotic chronic hepatitis B related liver disease (CHB), and eight healthy volunteers with no history of liver disease from the same Bangladeshi population (CTR). All patients with HBV-related HCC provided a 5-10 year history of their liver disease, and all were seropositive for hepatitis B surface antigen (HBsAg) and expressed antibodies to hepatitis B core antigen (anti-HBc) at the time of sampling. Forty two of these patients had hepatitis B e-antigen (HBeAg) status determined, and levels of HBV DNA were quantified in 35 subjects. The diagnosis of HCC was made from past history of HBV-related chronic liver disease, clinical presentation, ultrasound assessment of HCC nodules, and elevated AFP levels. The diagnosis was confirmed by fine needle aspiration cytology (FNAC).

Urine sample collection and preparation for NMR analysis

A full dietary and medication history was recorded for each subject. Mid-stream urine samples were collected in the morning into tubes and stored at -20 ℃, 2 to 4 h after collection, in Bangladesh until transport to the Institute of Hepatology, London, United Kingdom on dry ice and by air. Samples were prepared for NMR study according to previously published standard methodology[9]. Specifically, 400 μL of urine was added to 160 μL of phosphate buffer solution (0.2 mol/L Na_2HPO_4/0.2 mol/L NaH_2PO_4, pH 7.4) and 40 μL of 3-trimethylsilyl-(2,2,3,3-d_4)-1-propionate (TSP)/D_2O solution. After centrifuging, 550 μL of buffered urine was pipetted into an NMR tube of 5 mm diameter (Norell 502-7 from Glass Precision Engineering Ltd, Leighton Buzzard, United Kingdom) for proton NMR spectroscopy at the Department of Chemistry, University College London. Samples were placed in a sample queue at 21 ℃ on the auto sampler, and some samples may have remained in the queue for up to 6 h before NMR analysis.

Proton NMR spectral acquisition

The urine samples were prepared for proton NMR study and analyzed in a random order. NMR spectra were recorded on a Bruker Avance III 600 NMR spectrometer (Billerica, MA, United States) operating at proton NMR frequency of 600.13 MHz equipped with a 5 mm DCH cryoprobe and a 60-position sample changer BACS60. Data acquisition and processing were performed using standard TopSpin (version 3.2, Bruker) software. NMR spectra were recorded at 300 K. Temperature calibration was carried out using a sample of 99.8% deuterated methanol in a 5 mm NMR tube. A standard water suppression sample of 2 mmol/L sucrose in 90%H_2O + 10%D_2O with 4,4-dimethyl-4-silapentane-1-sulfonic acid (DSS) was used for manual iterative optimization of high-order shims (*z6* in particular) *via* inspection of the shape of the residual water signal after presaturation. Each sample was shimmed using a modified topshim routine, in which the *z* shim was incremented by +24 units at the final stage in order to achieve optimum resolution for organic species dissolved in water. The increment applied was determined using a sample of H_2O:CD_3CN (3:1) with a small amount of DSS added to it. This sample was shimmed using first deuterium of CD_3CN and then the protons of H_2O. The change of the *z* shim from the shimming using CD_3CN to that using H_2O was -24 units. The deuterium lock phase was autocorrected both before and after shimming. The presaturation frequency (o1, Hz) was determined using a single 360° pulse sequence followed by further manual iterations where the phase of the pre-saturated residual water signal was monitored and dispersive contributions were minimized. This was done for the first sample for each set of 20-25 samples, and the o1 value was then kept constant for the remaining samples. The variation in the o1 value for all samples was found to be within less than ± 0.5 Hz. Similarly, probe tuning and matching was carried out manually for the first sample

in each set of 20-25 samples and then kept unchanged for the remaining samples of the set. Proton NMR spectra with water presaturation during relaxation delay were acquired using a standard pulse sequence *noesygppr1d*, which suppressed effectively the probe background signal, giving a flat baseline. In addition, a digital filter (known as "BASEOPT" under TopSpin) with a pre-optimized correction for filter delay (1.0 μs in our case) was used to give spectra with a flat baseline, which required no first order phase correction. Prior to the start of data acquisition for each sample, the 90° pulse was determined (typically 14.0 μs) and the power level was adjusted for a 25 Hz-wide solvent presaturation automatically. Four dummy scans were used for equilibration followed by 64 scans collected into 144 K points with a total repetition time of 8.0 s at each scan (acquisition time = 4.0 s; relaxation delay = 4.0 s). NMR spectra were processed using the Bruker AMIX data processing package and the KnowItAll Informatics System v9.0 (Bio-Rad, Philadelphia, PA, United States). The Free Induction Decays were zero-filled, and an exponential 0.3 Hz line-broadening function was applied before Fourier transformation. All NMR spectra were automatically phased, and a baseline correction was applied. The TSP peak was assigned to be at δ 0.00 ppm for an internal chemical shift reference. NMR peaks in the range δ 0.50-9.50 ppm were analyzed, although the region δ 4.50-6.40 ppm was excluded to remove the residual water signal and the signal from urea. The urinary NMR peaks were assigned to metabolites on the basis of chemical shifts and coupling patterns and with reference to the published literature[8-13].

Statistical analysis

Demographic and blood biochemistry data between subject groups were compared using an independent sample Kruskal-Wallis one-way analysis of variance (ANOVA) test with pairwise multiple comparisons (IBM® SPSS® v21), and a *P* value of < 0.05 was considered significant.

The NMR data were analyzed using principal component analysis (PCA) (KnowItAll Informatics System v9.0) and orthogonal partial least squared discriminant analysis (OPLS-DA) techniques [SIMCA v14 (Umetrics AB, Umeå, Sweden)]. Using the intellibucketing option in KnowItAll v9.0, the NMR spectra were subdivided into smaller regions of about 0.02 ppm. Regions corresponding to particular metabolites were additionally selected, including those assigned to hippurate (7.82-7.85 ppm, 7.61-7.66 ppm, 7.52-7.58 ppm); creatinine (3.0425-3.0550 ppm, 4.04-4.07 ppm); creatine (3.035-3.0425 ppm); citrate (2.64-2.72 ppm, 2.52-2.58 ppm), and dimethylamine (2.72-2.74 ppm). All spectral regions were integrated, normalized to the sum of the total spectral integral, and mean-centred prior to multivariate analysis. PCA was performed to highlight outliers and clustering (KnowItAll v9.0). PCA was then repeated with all outliers excluded, and the metabolites contributing to the separation of groupings were identified from the loadings plot. This final data set was also analyzed by OPLS-DA using SIMCA v14. The discriminatory power of the model was validated using leave-one-out cross validation. An R^2 value was determined to give a measure of the goodness of fit by the model. A cross-validated Q^2 statistic (based on a 1:7 leave one out algorithm) was calculated as a quantitative measure of the predictability of the model for the Y variable, where a positive Q^2 indicated a good predictive.

The NMR spectral regions corresponding to the most important discriminatory metabolite peaks, as determined by the PCA and OPLS-DA loadings plots, were normalized to the sum of the total spectral integral, and differences in these relative metabolite signal levels were compared between the subject groups using an independent samples Kruskal-Wallis one-way ANOVA test with all pairwise multiple comparisons (IBM® SPSS® v21). Within the patient subgroups, the Mann-Whitney *U* test was used to compare relative metabolite levels depending on HBeAg status and treatment with anti-viral therapy. A Benjamini-Hochberg adjustment[14] was applied to the obtained *P* values to acquire the level of significance for multiple testing, with a declared level of statistical significance of $P < 0.05$.

RESULTS

Subject demographics

Nine samples from across the four cohorts were identified as outliers on subsequent NMR analysis (one CTR, two CHB, three CIR, and three HCC). In addition, one HCC subject was excluded for diagnostic uncertainty. The final study cohort, therefore, comprised 142 subjects (seven CTR, 46 CHB, 47 CIR, and 42 HCC). Subject demographics are summarized in Table 1, and the serum biochemistry results are shown in Table 2. All HCC patients had underlying cirrhosis, and the diagnosis of HCC was confirmed by FNAC in all cases. The levels of HBV DNA showed considerable variation. All HCC patients were considered to have advanced HCC, which is a typical finding in Bangladesh.

There were significant differences in age ($P < 0.001$), weight ($P < 0.001$), and body mass index (BMI) ($P < 0.001$) across the four subgroups. For example, the CHB cohort was significantly younger than both the CIR ($P = 0.000$) and HCC ($P < 0.001$) cohorts, and BMI was significantly lower in the HCC cohort compared to the CTR ($P = 0.001$) and CIR ($P < 0.001$) cohorts. While 83% of the CIR subgroup was male, the control group was entirely male, and so the urinary NMR data were analyzed both as a complete cohort and as a subset of males only.

The majority of subjects had eaten a similar diet of rice, dhal, water with vegetables, fish or chicken, in the

Table 1 Subject demographics of the Bangladeshi study cohort

Group	*n*	Age (yr), median (range)	M:F (%male)	Etiology, *n*	HBeAg positive	Height (cm), median (range)	Weight (kg), median (range)	BMI (kg/m^2), median (range)
CTR	7	37 (24-46)	7:0 (100%)	NA	NA	170 (152-173)	65 (54-85)	26.0 (18.7-29.4)
CHB	46	27 (15-45)	40:6 (87%)	HBV (100%)	27 (-59%)	166 (147- 180)	55 (35-79)	20.6 (13.9-26.6)
CIR	47	42 (15-67)	39:8 (83%)	HBV (98%) Cryptogenic HBV (2%)	21 (-45%)	165 (142–175)	58 (42-82)	21.9 (14.9-29.3)
HCC	42	48 (27-90)	38:3 (90%)	HBV (93%) HCV (2%) Cryptogenic (5%)	15 (-36%)	162 (145-180)	48 (38-75)	18.3 (12.3-25.2)

CTR: Healthy controls; CHB: Chronic hepatitis-B related liver disease; CIR: Cirrhosis; HCC: Hepatocellular carcinoma; NA: Unavailable; BMI: Body mass index.

Table 2 Serum biochemistry profiles

Group	ALT (U/L)	ALP (U/L)	Bil (mg/dL)	Alb (g/dL)	AFP (ng/mL)	Creatinine (mg/dL)
CTR	31 (18-42) [7/7]	NA	NA	NA	NA	NA
CHB	40 (22-232) [32/46]	96 (63-171) [14/46]	1.4 (0.4-2.2) [5/46]	3.4 (2.9-3.9) [2/46]	NA	1.4 (1.3-1.5) [2/46]
CIR	51 (10-243) [30/47]	286 (75-558) [5/47]	1.9 (0.3-22.4) [19/47]	2.7 (1.5-39.0) [20/47]	6 (2-12) [4/47]	1.4 (0.8-2.8) [17/47]
HCC	74 (28-332) [32/42]	259 (82-648) [25/42]	1.8 (0.3-21.5) [28/42]	3.1 (1.3-35.0) [26/42]	4900 (4-70000) [34/42]	0.9 (0.4-1.3) [23/42]

Data are represented as median (range) [number of subjects included/total number of subjects in subgroup]. CTR: Healthy controls; CHB: Chronic hepatitis-B related liver disease; CIR: Cirrhosis; HCC: Hepatocellular carcinoma; ALT: Alanine transaminase; ALP: Alkaline phosphatase; Bil: Bilirubin; Alb: Albumin; AFP: α-fetoprotein; NA: Unavailable.

6 h prior to collection of a urine sample. The patients reported a varied drug history: the majority of the CHB group were taking multivitamins, although some were also taking an oral antiviral drug (n = 10, entecavir or tenofovir) and/or an oral proton pump inhibitor (PPI) (omeprazole, pantoprazole); the CIR group reported a combination of non-absorbable sugars (lactulose), PPI (omeprazole, pantoprazole), oral antiviral (n = 7, entecavir, tenofovir or telbivudine), and/or multivitamins; and the HCC cohort reported a wider range of medication, including an oral antiviral (entecavir, tenofovir), hormonal therapy (tamoxifen), PPI (omeprazole, pantoprazole), beta blockers, non-absorbable sugars (lactulose), multivitamins, and pain killers (including tramadol).

Serum biochemical analysis

The median (range) values for the available serum alanine aminotransferase (ALT), alkaline phosphatase (ALP), bilirubin, albumin, AFP, and creatinine levels are summarized in Table 2. Serum ALT was significantly higher in the HCC group than controls (P < 0.001) and patients with CHB (P < 0.001) or CIR (P = 0.006); serum ALP was higher in the HCC group than the CHB group (P < 0.001). Serum AFP was generally markedly elevated in HCC, although two HCC patients showed AFP $\leqslant$ 20 ng/mL in the presence of large space occupying lesion(s) in the right lobe of the liver as observed on axial imaging. Serum creatinine levels were significantly lower in the HCC group than in the CIR group (P = 0.004).

Representative urinary NMR spectra

Illustrative urinary proton NMR spectra from each of the four subject groups are summarized in Figure 1. The spectral resolution was defined by a TSP linewidth of < 1 Hz in all NMR data sets. On visual inspection, a number of trends could be seen across the groups, including a reduction in hippurate and an increase in creatine, when comparing CTR, CHB, and CIR through to HCC (Figures 1A-D and 1A'-D', respectively).

Analyses of the urinary NMR spectra

Nine outliers were identified on five iterations of PCA: one CTR showing particularly high levels of hippurate; two CHB showing high levels of glucose and lactate and overlap of creatinine into the creatine peak; three CIR showing either high glucose, high glucose and lactate, or ethanol present; and three HCC showing either paracetamol resonances, absence of creatine and creatinine, or unassigned additional dominant peaks.

A three-factor PCA score plot of the final study cohort of 142 subjects is illustrated in Figure 2, showing clustering of each of the four subgroups. Metabolites that contributed to the discrimination between groups in the loadings plot included acetate, creatine, creatinine, dimethyamine (DMA), formate, glycine, hippurate, and trimethylamine-*N*-oxide (TMAO). An OPLS-DA plot is illustrated in Figure 3 and the $R^2(X)$, $R^2(Y)$ and Q^2 values were 0.468, 0.289, and 0.195, respectively.

Acetate, carnitine, citrate, creatine, creatinine,

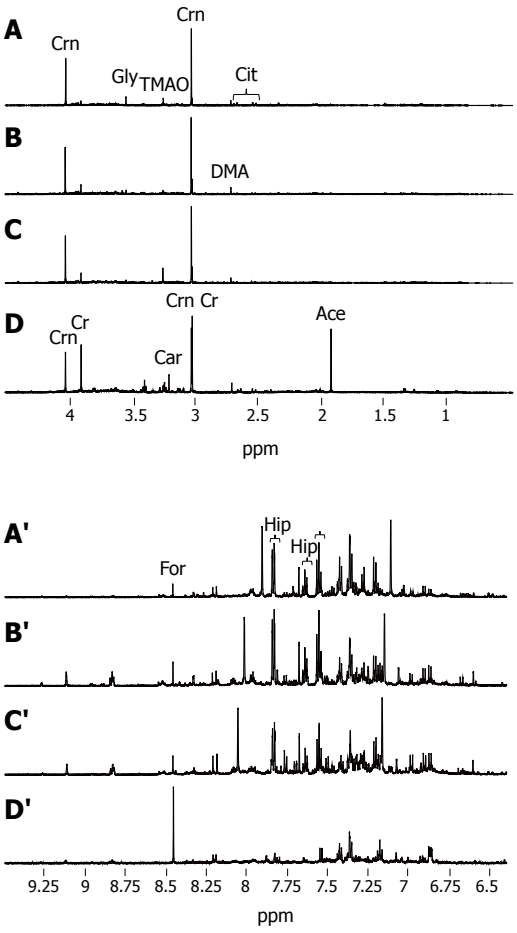

Figure 1 Illustrative urinary proton nuclear magnetic resonance spectra. From a 35 year old healthy control (CTR) (A, A'); a 22 year old male with chronic hepatitis-B related liver disease (CHB) (B, B'); a 36 year old male with hepatitis B virus (HBV)-cirrhosis (C, C'); and a 50 year old male with HBV-hepatocellular carcinoma (AFP > 30000 mg/dL) displaying (A-D) the aliphatic region 0.5-4.5 ppm and (A'-D') the aromatic region 6.4-9.5 ppm (D, D'). Each NMR spectrum is scaled independently. The more prominent peaks are assigned and include acetate (Ace), carnitine (Car), citrate (Cit), creatine (Cr), creatinine (Crn), dimethylamine (DMA), formate (For), glycine (Gly), hippurate (Hip), histidine (His), and trimethylamine-N-oxide (TMAO).

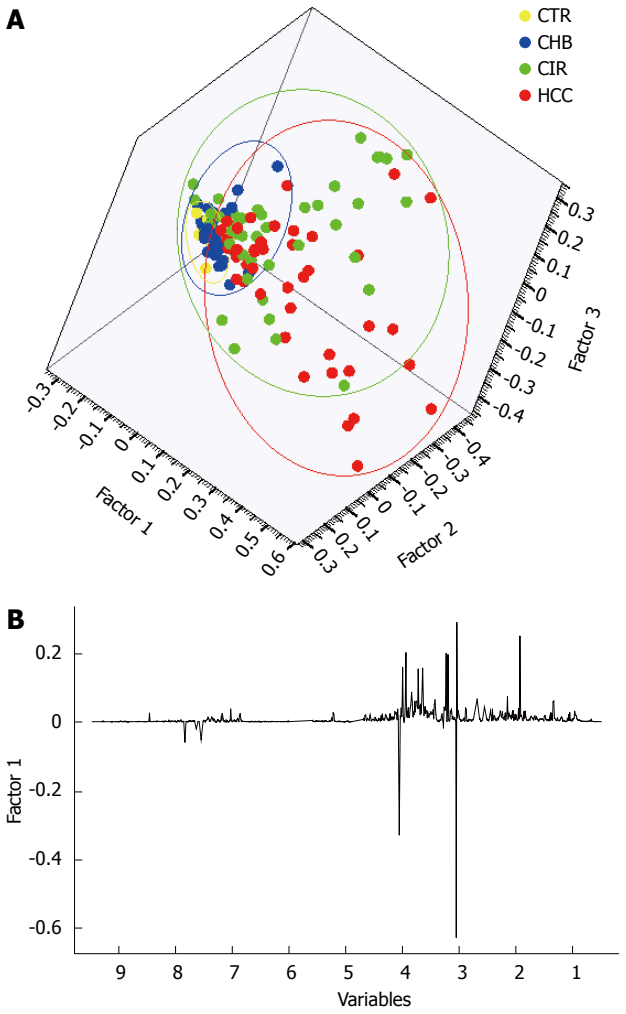

Figure 2 A three-factor principal components analysis scores plot of the cohort of 142 subjects and clustering of each of the four subgroups. A: Principal components analysis (PCA) scatter plot showing clustering and separation of healthy controls (CTR), chronic hepatitis-B related liver disease (CHB), cirrhosis (CIR), and hepatocellular carcinoma (HCC) subgroups; B: The associated loadings plot illustrating the metabolites contributing to the separation of the subgroups.

DMA, hippurate, and TMAO metabolite levels were significantly different across the four groups, when considering all subjects (Table 3) and only the males. A comparison of relative metabolite levels between HCC *vs* CTR and/or HCC *vs* CHB in all subjects confirmed that carnitine was significantly increased in HCC, and creatinine, hippurate, and TMAO were significantly reduced in HCC (Figure 4). A significant increase in carnitine and significant reductions in creatinine and hippurate were observed in the HCC group compared to the CIR group (Figure 4).

HBeAg negative patients showed a significant increase in creatinine (P = 0.001) compared to HBeAg positive patients in the CHB subgroup. In the CIR group, HBeAg negative patients showed a significant decrease in DMA (P = 0.004) compared to HBeAg positive patients; there were no significant differences in the HCC subgroup according to HBeAg status.

There were no differences in metabolite levels in the HCC or CHB groups when comparing subjects receiving antiviral treatment with those not. However, creatine levels were lower in subjects receiving antiviral therapy in the CIR group (n = 7) than those who were not (n = 40) (P = 0.002).

DISCUSSION

In this study of Bangladeshi subjects, all of Indian ethnic origin, the urinary NMR metabolic profile measured in patients with HCC was distinguishable from the urinary profile of patients with CIR and CHB and also healthy control subjects. The majority of the patients (131 patients) had a background of CHB, while one patient with cirrhosis and two patients with HCC were defined as cryptogenic and one HCC subject had a background of HCV. Metabolites that contributed to the differences in urinary NMR profiles of HCC, compared to CIR, CHB and/or CTR, included acetate,

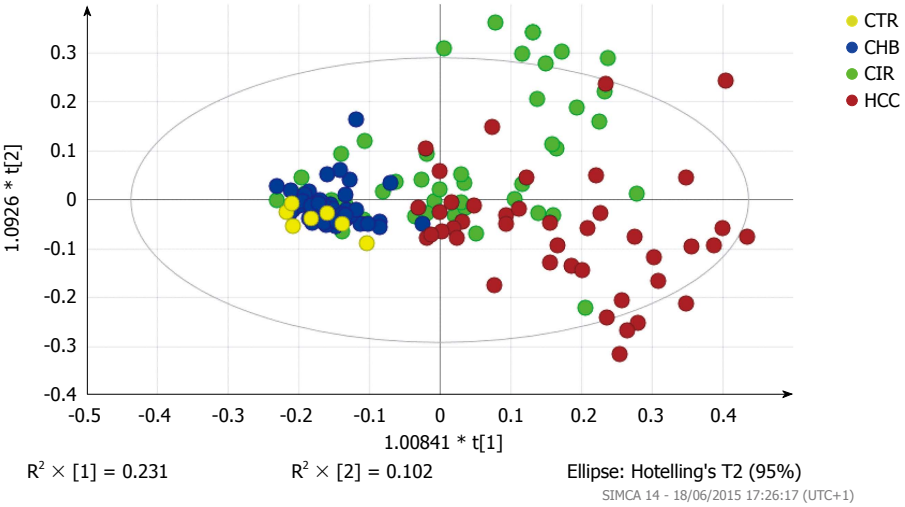

Figure 3 Scores plot of orthogonal partial least squares discriminant analysis (OPLS-DA) model of CTR, CHB, CIR, and HCC subgroups. $R^2(X)$, $R^2(Y)$ and Q^2 values were 0.468, 0.289, and 0.195, respectively.

Table 3 Comparison of relative signal levels (mean ± SD) of discriminatory metabolites between study cohorts[1]

Selected metabolites		Study cohort (number of subjects in group)				*P* value[2]
Metabolite	δ/ppm (multiplicity) of peak analysed	CTR (*n* = 7)	CHB (*n* = 46)	CIR (*n* = 47)	HCC (*n* = 42)	
Acetate	1.92 (s)	0.34 ± 0.03	0.57 ± 0.64	1.70 ± 2.14	1.24 ± 1.49	0.007
Carnitine	3.23 (s)	0.57 ± 0.41	0.42 ± 0.22	0.44 ± 0.53	1.19 ± 1.04	0.000
Citrate	2.52 (d)	1.49 ± 0.61	1.35 ± 0.61	1.19 ± 1.21	1.07 ± 0.46	0.005
Creatine	3.03 (s)	1.34 ± 0.35	1.24 ± 0.38	1.07 ± 0.95	1.54 ± 1.82	0.007
Creatinine	3.04 (s)	10.88 ± 1.30	10.06 ± 1.76	7.74 ± 3.00	5.85 ± 1.83	0.000
DMA	2.72 (s)	2.14 ± 0.57	2.11 ± 0.58	1.95 ± 1.21	1.91 ± 0.45	0.022
Formate	8.46 (s)	0.07 ± 0.03	0.07 ± 0.05	0.16 ± 0.16	0.16 ± 0.18	0.059
Glycine	3.56 (s)	1.04 ± 0.39	0.84 ± 0.42	0.74 ± 0.38	0.79 ± 0.63	0.129
Hippurate	7.85 (d)	0.99 ± 0.47	0.85 ± 0.47	0.44 ± 0.35	0.28 ± 0.30	0.000
TMAO	3.27 (s)	1.79 ± 0.44	1.95 ± 0.77	1.62 ± 1.04	1.32 ± 0.75	0.000

[1]Percentage normalised metabolite signal level relative to total NMR signal in the region 0.50-9.50 ppm (excluding 4.50-6.40 ppm); [2]Significance for independent samples Kruskal-Wallis one-way ANOVA test with pairwise multiple comparisons. CTR: Healthy controls; CHB: Chronic hepatitis-B related liver disease; CIR: Cirrhosis; HCC: Hepatocellular carcinoma.

carnitine, citrate, creatine, creatinine, DMA, hippurate, and TMAO. Within the CHB and CIR patient subgroups, metabolite differences were also observed according to HBeAg status and, only in CIR, to treatment with oral antiviral therapy.

Our findings extend previous studies using urinary NMR to identify metabolic changes in HCC. Previous studies showed that urinary NMR changes in HCC could be distinguished from CIR and CTR in patient cohorts from Egypt, Nigeria, and The Gambia, with HCC on a background of either chronic HCV[8,10] or chronic HBV[9,10]. An NMR pattern has emerged to separate HCC from CIR and CTR, which includes a reduction in hippurate, citrate, creatinine, and TMAO and an increase in acetate, carnitine, and creatine. In this population, neither glycine nor formate was significantly different in HCC between the other study cohorts, although both of these metabolites were identified as discriminators in the West African study. Overall, given that the urinary profile of HCC could be distinguished from CIR, CHB, and CTR, this study provides further support for the suggestion that a diagnostic marker may be feasible, as consistent urinary NMR changes are seen across differing ethnicities as well as varying disease etiologies.

The urinary metabolite changes observed in HCC subjects relate to alterations in both host and gut bacterial metabolism. For example, a reduced urinary concentration of citrate, which is a tricarboxylic acid intermediate, might be in agreement with Warburg's hypothesis of altered mitochondrial aerobic respiration and heightened physiological stress of cancer cells[8]. The alterations observed in carnitine are interesting, and its increase in HCC is consistent with the previous urinary NMR profiling studies in HCC[8-10]. Carnitine is required for energy metabolism, enabling fatty acids to enter the mitochondria for β-oxidation[15]. Carnitine can be absorbed from the diet or synthesised in the liver, testis, and kidney and reabsorbed *via* the renal system[8]. Increased urinary carnitine may, therefore,

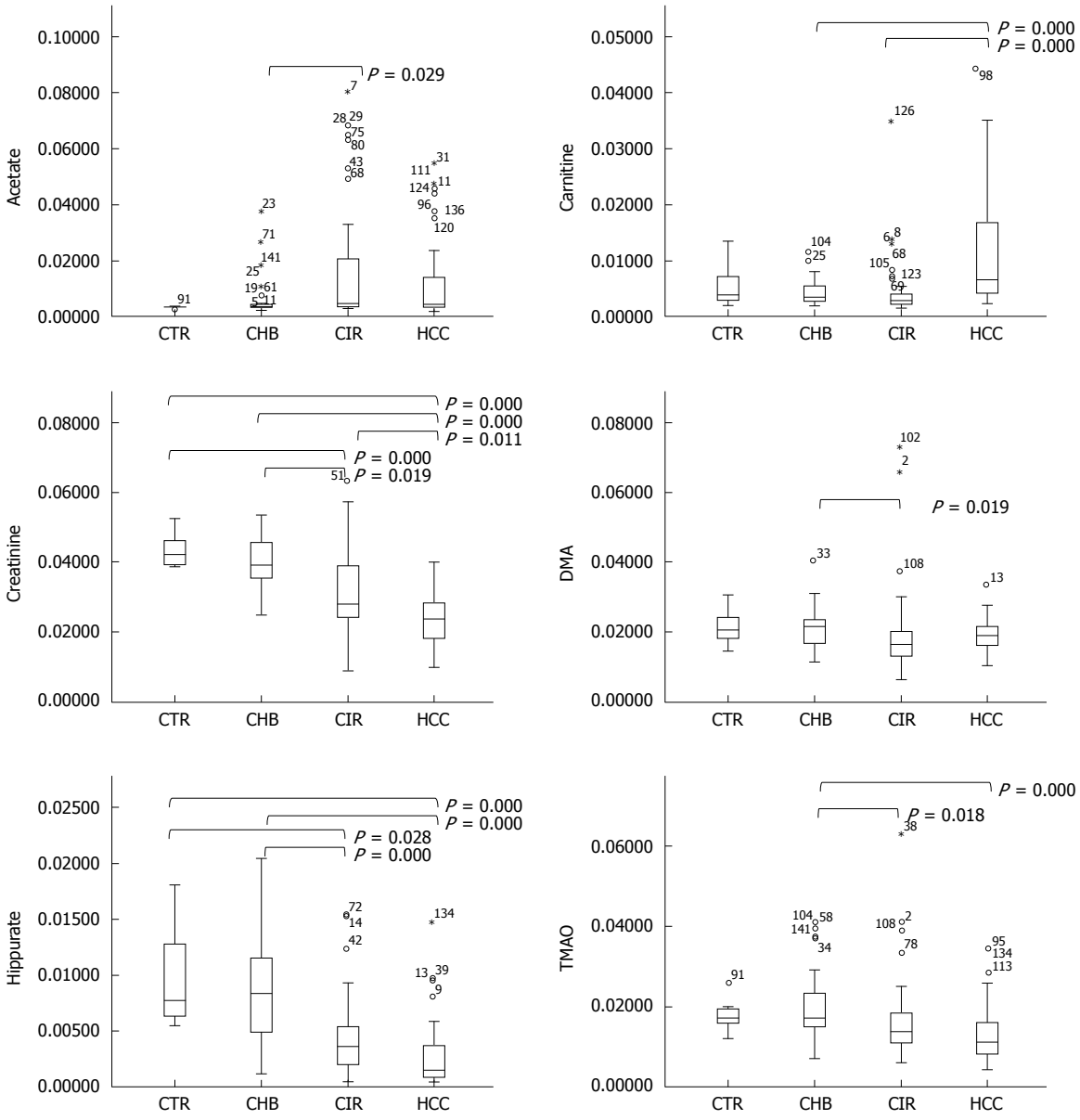

Figure 4 Boxplots of selected metabolites. Metabolites [acetate, carnitine, creatinine, dimethylamine (DMA), hippurate, and trimethylamine-*N*-oxide (TMAO)], showing the results of a comparison of signal levels (normalized to 1) using an independent-samples Kruskal-Wallis test.

correspond to excess carnitine ingestion, increased biosynthesis, or poor reabsorption and may reflect overproduction of tumor carnitine to maintain rapid growth and fuel mitochondrial activity[8]. Further evidence of heightened β-oxidation is shown by relatively higher acetate in the urine of HCC patients than in controls[10]. Advanced HCC can be complicated by cancer cachexia with associated sarcopenia, and urinary creatinine concentration has been suggested as a biomarker of sarcopenia[16]. In combination with other factors, however, urinary NMR creatinine concentration may contribute to a biomarker panel for HCC. Our findings on urinary creatine suggest that it is elevated in HCC in comparison to ethnically-matched healthy controls but is reduced in CIR patients in comparison to the same controls. Creatine has a direct function in cellular energy transport, and it may be that creatine is elevated in rapidly growing cells; and, indeed, urinary creatine levels may be increased 24 h after partial hepatectomy in rats[17].

The urinary changes in DMA, hippurate, and TMAO implicate alterations in the gut microbiome. TMAO is the oxidation product of trimethylamine (TMA), which can be produced by bacterial degradation of dietary phosphatidylcholine and choline. It is likely that a decrease in TMAO reflects dysregulation of the intestinal microbiota. DMA can also be a product of gut bacterial metabolism of dietary choline, although it can originate from the N-methylation of methylamines from the breakdown of creatine. While diet was not controlled for in the study, and such a proposition would be difficult to implement, the observation that HBeAg status has an influence on DMA levels does further suggest that gut bacterial metabolism

might have pathophysiological consequences in CHB and HCC. Hippurate is formed by the conjugation of benzoate with glycine in liver and kidney mitochondria. Benzoate is formed from dietary aromatic compounds *via* gut microbial metabolism. It has been suggested that less efficient benzoate conjugation and lower urinary hippurate excretion levels may result from reduced hepatic function in patients with HCC[8].

The differences observed in the urinary profiles according to HBeAg status within the CHB and CIR subgroups are worth exploring in more detail in future studies. In this cohort, differences were seen in DMA and creatinine levels between HBeAg positive and negative subjects in the CHB and CIR subgroups respectively. The rate of disease progression has been shown to be influenced by HBeAg status[18], and it would be particularly interesting if these urinary metabolic differences could be attributed to differences in cell turnover, for example.

An impact of antiviral treatment on relative urinary creatine levels was observed in patients with cirrhosis. While antiviral therapy may influence renal function[19], it is not clear why urinary creatine levels might be altered. Regardless, any influence of treatment effects do need to be considered when interpreting the urinary metabolite changes.

There are a number of limitations to this present study. There was a logistical delay between sample collection and sample analysis, as the Bangladeshi samples were archived, stored, and transported to London for NMR analysis, although this would not be expected to have had any impact on the urinary NMR profile. The NMR urinary profile from nine subjects were shown to be outliers using PCA, and confounding factors included high levels of glucose and overlapping peaks from unreported over-the-counter medication. These factors need to be considered for developing an NMR analysis protocol for inclusion of all NMR data sets, without obscuring overlapping peaks in the spectral regions with outlier resonances. There was gender imbalance between the subgroups, but analyzing males only as a separate cohort did not alter the urinary NMR differences seen across the patient groups. Increased study numbers would allow inclusion of training and validation data sets and also a more detailed comparison of NMR findings with currently available diagnostic serum and clinical biomarkers. Further prospective studies looking at the urinary NMR differences in patients with early HCC, for example stage 0 using the Barcelona Clinic Liver Cancer score[20] and also following treatment, would underline the potential of implementing a urinary screening test for HCC.

In conclusion, urinary NMR changes in HCC are consistent with the diverse effects of liver cancer on human physiology and gut bacterial action and may aid the development of a cost-effective HCC urinary dipstick screening test. Such a diagnostic urine test for HCC could be a paradigm shift in liver cancer screening. It could provide a practical and cost-effective test that is easy to use in primary care and particularly applicable to countries of Central and East Asia. Clinically and economically, such a simple approach could have a major impact, not only in the developed economies of Europe and North America, but also in severely resource limited settings, such as sub-Saharan Africa. Further validation work is required, but the pattern emerging from different studies around the world is promising.

ACKNOWLEDGMENTS

We thank colleagues at the Institute of Hepatology, London (Drs M Briones, S Chokshi, J Coombes, P Manka) and Imperial College London (Ms A Ledlie, Drs N Ladep, MJW McPhail, MIF Shariff, CA Wadsworth) for advice and helpful discussions. We thank Dr. Peter Gierth (Bruker, United Kingdom) for his help with the initial setup of NMR measurements at UCL Chemistry, including optimization of shimming routines. Crossey MME, Dawood M, and Taylor-Robinson SD are grateful to the United Kingdom NIHR Biomedical Facility at Imperial College London for infrastructure support.

COMMENTS

Background

Previous studies of hepatocellular carcinoma (HCC) from Egypt and West Africa suggest reproducibility of urinary metabolic profiling in HCC using nuclear magnetic resonance (NMR) spectroscopy techniques. This study aimed to establish if similar changes were found in a Bangladeshi HCC cohort.

Research frontiers

To explore the use of metabolic profiling of urine to provide markers of hepatocellular cancer, with the aim of developing a panel of metabolic markers to form the basis of a cost-effective dipstick test for hepatocellular cancer.

Innovations and breakthroughs

Urinary NMR from patients with HCC differed across a range of metabolites, including reduced hippurate and creatinine and increased carnitine levels, when compared to the urinary NMR profile of cirrhotics, chronic hepatitis B patients, and controls, consistent with the diverse effects of liver cancer on metabolic pathways and its interrelationship with the gut microbiome. These results corroborated previous urinary NMR findings from patients with HCC from Egypt and West Africa.

Applications

Urinary NMR changes in HCC are consistent with the diverse effects of liver cancer on human physiology and gut bacterial action and may aid in the development of a cost-effective HCC urinary dipstick screening test. Further validation work is required, but the pattern emerging from different studies around the world is promising.

Terminology

NMR spectroscopy describes a state-or-the-art analytical chemistry technique that enables a non-selective snap-shot assessment of sample composition.

Peer-review

The authors should ensure as much reliability as is possible to diagnose appropriately liver disease. The authors recommend subdividing the results from patients with HCC into early and advanced disease and comparing NMR findings to other biomarker results.

REFERENCES

1 **Al-Mahtab M**, Uddin H, Akbar SM. Epidemiology and Risk Factors of Hepatocellular Carcinoma in Asia. *Journal of Gastroenterology and Hepatology Research* 2014; **3**: 1019-1023 [DOI: 10.6051/j.issn.2224-3992.2014.03.306]

2 **Khan M**, Zaki KM, Ahmed KU, Ali SM, Islam N. Clinical profile: prognostic index in hepatocellular carcinoma. *Bangladesh Med Res Counc Bull* 1991; **17**: 49-62 [PMID: 1668711]

3 **Mahtab MA**, Rahman S, Karim MF, Khan M, Foster G, Solaiman S, Afroz S. Epidemiology of hepatitis B virus in Bangladeshi general population. *Hepatobiliary Pancreat Dis Int* 2008; **7**: 595-600 [PMID: 19073404]

4 **Franco E**, Bagnato B, Marino MG, Meleleo C, Serino L, Zaratti L. Hepatitis B: Epidemiology and prevention in developing countries. *World J Hepatol* 2012; **4**: 74-80 [PMID: 22489259 DOI: 10.4254/wjh.v4.i3.74]

5 **Thio CL**, Guo N, Xie C, Nelson KE, Ehrhardt S. Global elimination of mother-to-child transmission of hepatitis B: revisiting the current strategy. *Lancet Infect Dis* 2015; **15**: 981-985 [PMID: 26145195 DOI: 10.1016/S1473-3099(15)00158-9]

6 **Daniele B**, Bencivenga A, Megna AS, Tinessa V. Alpha-fetoprotein and ultrasonography screening for hepatocellular carcinoma. *Gastroenterology* 2004; **127**: S108-S112 [PMID: 15508073 DOI: 10.1053/j.gastro.2004.09.023]

7 **Dona AC**, Jiménez B, Schäfer H, Humpfer E, Spraul M, Lewis MR, Pearce JT, Holmes E, Lindon JC, Nicholson JK. Precision high-throughput proton NMR spectroscopy of human urine, serum, and plasma for large-scale metabolic phenotyping. *Anal Chem* 2014; **86**: 9887-9894 [PMID: 25180432 DOI: 10.1021/ac5025039]

8 **Shariff MI**, Gomaa AI, Cox IJ, Patel M, Williams HR, Crossey MM, Thillainayagam AV, Thomas HC, Waked I, Khan SA, Taylor-Robinson SD. Urinary metabolic biomarkers of hepatocellular carcinoma in an Egyptian population: a validation study. *J Proteome Res* 2011; **10**: 1828-1836 [PMID: 21275434 DOI: 10.1021/pr101096f]

9 **Shariff MI**, Ladep NG, Cox IJ, Williams HR, Okeke E, Malu A, Thillainayagam AV, Crossey MM, Khan SA, Thomas HC, Taylor-Robinson SD. Characterization of urinary biomarkers of hepatocellular carcinoma using magnetic resonance spectroscopy in a Nigerian population. *J Proteome Res* 2010; **9**: 1096-1103 [PMID: 19968328 DOI: 10.1021/pr901058t]

10 **Ladep NG**, Dona AC, Lewis MR, Crossey MM, Lemoine M, Okeke E, Shimakawa Y, Duguru M, Njai HF, Fye HK, Taal M, Chetwood J, Kasstan B, Khan SA, Garside DA, Wijeyesekera A, Thillainayagam AV, Banwat E, Thursz MR, Nicholson JK, Njie R, Holmes E, Taylor-Robinson SD. Discovery and validation of urinary metabotypes for the diagnosis of hepatocellular carcinoma in West Africans. *Hepatology* 2014; **60**: 1291-1301 [PMID: 24923488 DOI: 10.1002/hep.27264]

11 **Bouatra S**, Aziat F, Mandal R, Guo AC, Wilson MR, Knox C, Bjorndahl TC, Krishnamurthy R, Saleem F, Liu P, Dame ZT, Poelzer J, Huynh J, Yallou FS, Psychogios N, Dong E, Bogumil R, Roehring C, Wishart DS. The human urine metabolome. *PLoS One* 2013; **8**: e73076 [PMID: 24023812 DOI: 10.1371/journal.pone.0073076]

12 **Wishart DS**, Tzur D, Knox C, Eisner R, Guo AC, Young N, Cheng D, Jewell K, Arndt D, Sawhney S, Fung C, Nikolai L, Lewis M, Coutouly MA, Forsythe I, Tang P, Shrivastava S, Jeroncic K, Stothard P, Amegbey G, Block D, Hau DD, Wagner J, Miniaci J, Clements M, Gebremedhin M, Guo N, Zhang Y, Duggan GE, Macinnis GD, Weljie AM, Dowlatabadi R, Bamforth F, Clive D, Greiner R, Li L, Marrie T, Sykes BD, Vogel HJ, Querengesser L. HMDB: the Human Metabolome Database. *Nucleic Acids Res* 2007; **35**: D521-D526 [PMID: 17202168 DOI: 10.1093/nar/gks1065]

13 **Heinzmann SS**, Merrifield CA, Rezzi S, Kochhar S, Lindon JC, Holmes E, Nicholson JK. Stability and robustness of human metabolic phenotypes in response to sequential food challenges. *J Proteome Res* 2012; **11**: 643-655 [PMID: 21999107 DOI: 10.1021/pr2005764]

14 **Benjamini Y**, Hochberg Y. Controlling the False Discovery Rate: a practical and powerful approach to multiple testing. *J Royal Stat Soc Ser B* 1995; **57**: 289-300

15 **Vaz FM**, Wanders RJ. Carnitine biosynthesis in mammals. *Biochem J* 2002; **361**: 417-429 [PMID: 11802770 DOI: 10.1042/bj3610417]

16 **Pahor M**, Manini T, Cesari M. Sarcopenia: clinical evaluation, biological markers and other evaluation tools. *J Nutr Health Aging* 2009; **13**: 724-728 [PMID: 19657557 DOI: 10.1007/s12603-009-0204-9]

17 **Bollard ME**, Contel NR, Ebbels TM, Smith L, Beckonert O, Cantor GH, Lehman-McKeeman L, Holmes EC, Lindon JC, Nicholson JK, Keun HC. NMR-based metabolic profiling identifies biomarkers of liver regeneration following partial hepatectomy in the rat. *J Proteome Res* 2010; **9**: 59-69 [PMID: 19445528 DOI: 10.1021/pr900200v]

18 **Ribeiro RM**, Germanidis G, Powers KA, Pellegrin B, Nikolaidis P, Perelson AS, Pawlotsky JM. Hepatitis B virus kinetics under antiviral therapy sheds light on differences in hepatitis B e antigen positive and negative infections. *J Infect Dis* 2010; **202**: 1309-1318 [PMID: 20874517 DOI: 10.1086/656528]

19 **Gane EJ**, Deray G, Liaw YF, Lim SG, Lai CL, Rasenack J, Wang Y, Papatheodoridis G, Di Bisceglie A, Buti M, Samuel D, Uddin A, Bosset S, Trylesinski A. Telbivudine improves renal function in patients with chronic hepatitis B. *Gastroenterology* 2014; **146**: 138-146.e5 [PMID: 24067879 DOI: 10.1053/j.gastro.2013.09.031]

20 **Llovet JM**, Brú C, Bruix J. Prognosis of hepatocellular carcinoma: the BCLC staging classification. *Semin Liver Dis* 1999; **19**: 329-338 [PMID: 10518312 DOI: 10.1055/s-2007-1007122]

P- Reviewer: Guan YS **S- Editor**: Yu J **L- Editor**: Filipodia
E- Editor: Wang CH

World Journal of Gastroenterology

Submit a Manuscript: http://www.wjgnet.com/esps/
Help Desk: http://www.wjgnet.com/esps/helpdesk.aspx
DOI: 10.3748/wjg.v22.i16.4201

World J Gastroenterol 2016 April 28; 22(16): 4201-4210
ISSN 1007-9327 (print) ISSN 2219-2840 (online)

ORIGINAL ARTICLE

Retrospective Study

Influence of antibiotic-regimens on intensive-care unit-mortality and liver-cirrhosis as risk factor

Mireen Friedrich-Rust, Beate Wanger, Florian Heupel, Natalie Filmann, Reinhard Brodt, Volkhard AJ Kempf, Johanna Kessel, Thomas A Wichelhaus, Eva Herrmann, Stefan Zeuzem, Joerg Bojunga

Mireen Friedrich-Rust, Beate Wanger, Florian Heupel, Stefan Zeuzem, Joerg Bojunga, Department of Internal Medicine I (Gastroenterology, Pulmonology, Endocrinology), J.W. Goethe-University Hospital, 60590 Frankfurt, Germany

Natalie Filmann, Eva Herrmann, Institute of Biostatistics and Mathematical Modeling, Faculty of Medicine, J.W. Goethe-University, 60590 Frankfurt, Germany

Reinhard Brodt, Johanna Kessel, Department of Internal Medicine II (Infectious Disease, Oncology, Hematology), J.W. Goethe-University Hospital, 60590 Frankfurt, Germany

Volkhard AJ Kempf, Thomas A Wichelhaus, Institute of Medical Microbiology and Infection Control, J.W. Goethe-University Hospital, 60590 Frankfurt, Germany

Author contributions: Friedrich-Rust M, Herrmann E, Bojunga J participated in the design of the study; all authors participated in the clinical study, data acquisition and extraction; Friedrich-Rust M, Wanger B, Heupel F, Filmann N and Herrmann E performed the statistical analysis; Friedrich-Rust M, Wanger B, Heupel F, Filmann N, Bojunga J participated in the drafting of the manuscript; all authors read and approved the final manuscript.

Institutional review board statement: This study was reviewed and approved by the Ethics Committee of the University Clinic Frankfurt.

Informed consent statement: Patients were not required to give informed consent to the study because the analysis used anonymous clinical data that were obtained retrospectively.

Conflict-of-interest statement: We have no financial relationships to disclose.

Data sharing statement: No additional data are available.

Correspondence to: Dr. Mireen Friedrich-Rust, Professor, Department of Internal Medicine I (Gastroenterology, Pulmonology, Endocrinology), J.W. Goethe-University Hospital, Theodor-Stern-Kai 7, 60590 Frankfurt am Main, Germany. mireen.friedrich-rust@kgu.de
Telephone: +49-69-63015297
Fax: +49-69-63016247

Received: January 13, 2016
Peer-review started: January 16, 2016
First decision: January 28, 2016
Revised: February 9, 2016
Accepted: March 13, 2016
Article in press: March 14, 2016
Published online: April 28, 2016

Abstract

AIM: To assess the rate of infection, appropriateness of antimicrobial-therapy and mortality on intensive care unit (ICU). Special focus was drawn on patients with liver cirrhosis.

METHODS: The study was approved by the local ethical committee. All patients admitted to the Internal Medicine-ICU between April 1, 2007 and December 31, 2009 were included. Data were extracted retrospectively from all patients using patient charts and electronic documentations on infection, microbiological laboratory reports, diagnosis and therapy. Due to the large hepatology department and liver transplantation center, special interest was on the subgroup of patients with liver cirrhosis. The primary statistical-endpoint was the evaluation of the influence of appropriate versus

inappropriate antimicrobial-therapy on in-hospital-mortality.

RESULTS: Charts of 1979 patients were available. The overall infection-rate was 53%. Multiresistant-bacteria were present in 23% of patients with infection and were associated with increased mortality (P < 0.000001). Patients with infection had significantly increased in-hospital-mortality (34% *vs* 17%, P < 0.000001). Only 9% of patients with infection received inappropriate initial antimicrobial-therapy, no influence on mortality was observed. Independent risk-factors for in-hospital-mortality were the presence of septic-shock, prior chemotherapy for malignoma and infection with *Pseudomonas* spp. Infection and mortality-rate among 175 patients with liver-cirrhosis was significantly higher than in patients without liver-cirrhosis. Infection increased mortality 2.24-fold in patients with cirrhosis. Patients with liver cirrhosis were at an increased risk to receive inappropriate initial antimicrobial therapy.

CONCLUSION: The results of the present study report the successful implementation of early-goal-directed therapy. Liver cirrhosis patients are at increased risk of infection, mortality and to receive inappropriate therapy. Increasing burden are multiresistant-bacteria.

Key words: Intensive care unit; Sepsis-bundle; Early goal-directed therapy; Liver cirrhosis; Mortality

Core tip: This is a retrospective study evaluating the association of appropriate and inappropriate antimicrobial therapy on intensive care unit-mortality with special focus on patients with liver cirrhosis. Charts of 1979 patients were available for analysis. Patients with infection had significantly increased in-hospital mortality. Only 9% of patients with infection received inappropriate initial antimicrobial therapy. Multiresistant bacteria were detected in 23% of patients with infection and were associated with increased mortality. Infection increased mortality 2.24-fold in patients with cirrhosis. Patients with liver cirrhosis were at an increased risk to receive inappropriate initial antimicrobial therapy.

Friedrich-Rust M, Wanger B, Heupel F, Filmann N, Brodt R, Kempf VAJ, Kessel J, Wichelhaus TA, Herrmann E, Zeuzem S, Bojunga J. Influence of antibiotic-regimens on intensive-care unit-mortality and liver-cirrhosis as risk factor. *World J Gastroenterol* 2016; 22(16): 4201-4210 Available from: URL: http://www.wjgnet.com/1007-9327/full/v22/i16/4201.htm DOI: http://dx.doi.org/10.3748/wjg.v22.i16.4201

INTRODUCTION

Infections are a worldwide problem concerning patients admitted to intensive care units (ICU), since they are associated with an increased mortality, morbidity and financial burden[1-4]. A 51%-prevalence of infection has been reported for ICU-patients and previously 20% of patients admitted with septic-shock to an ICU received inappropriate antimicrobial-therapy[5]. This knowledge led to increased efforts to implement early-goal-directed therapy with timely initiation of appropriate antimicrobial-therapy in clinical practice[4].

The aim of the present study was to assess the rate of infection, as well as appropriate- and inappropriate antimicrobial-therapy after implementation of early-goal-directed therapy of infection and sepsis on an Internal-Medicine-ICU and to assess the association of appropriate-and inappropriate antimicrobial-therapy on mortality. In addition, special focus was drawn on the subgroup of patients with liver cirrhosis. This special interest was derived due to the hepatologic focus of our unit with a large hepatology outpatient and inn-patient clinic including transplantation unit. A previous meta-analysis reported a 4-fold increase in mortality in patients with liver-cirrhosis that acquire an infection[6].

MATERIALS AND METHODS

All patients admitted to the Internal-Medicine-ICU of the Goethe-University-Hospital-Frankfurt between April 1, 2007 and December 31, 2009 were included in the study. Data were extracted retrospectively from all patients using patient-charts and electronic-documentations on infection, microbial-isolates, diagnosis and therapy. The study was approved by the local ethical-committee. The study protocol included the special focus on liver cirrhosis patients and was approve prior to the study recruitment.

Demographic, physiological, antimicrobial and therapeutic-data were collected from all patients. Only the first seven days after ICU-admission were evaluated concerning microbial-isolates and antibiotic-regimen. Patient characteristics are shown in Tables 1 and 2.

Infection was defined according to the definitions of the International Sepsis-Forum[7] and adjudicated by the senior-physicians. Data concerning infection were extracted from the ICU-doctor´s final-report, from imaging (Computed-Tomogaphy, Magnetic-Resonance-Imaging, X-ray, ultrasound, endoscopy) and from the microbiological laboratory-reports.

Appropriate/inappropriate antimicrobial-therapy was determined for all patients with infection. Appropriate initial antimicrobial-therapy was defined as: (1) Initiation of appropriate empirical antimicrobial-therapy at symptom begin (recurrence or persistent hypotension) with *in vitro* activity appropriate to isolated pathogenic organisms according to the Sanford Guide on Antimicrobial Therapy 2010 (40th edition)[8] and the national guidelines 2010 of the Paul-Ehrlich-society for chemotherapy[9] or according to the antibiotic susceptibility-testing; and (2) Appropriate empiric therapy for culture negative infections accor-

Table 1 Characteristics of patients *n* (%)

Characteristic	All patients (*n* = 1979)	Patients without infection (*n* = 937)	Patients with infection (*n* = 1042)	OR (95%CI)	*P* value
Age (yr), mean ± SD (range)	61 ± 16 (16-96)	61 ± 16 (16-96)	61 ± 16 (16-95)	1.003 (0.997-1.008)	> 0.20
Male sex	1236 (62.5)	614 (65.5)	622 (60)	0.779 (0.649-0.935)	0.0074
Days on ICU, mean ± SD (range)	5.53 ± 9.88 (1-217)	2.89 ± 5.97 (1-76)	8.12 ± 12 (1-217)	0.877 (0.858-0.897)	< 0.000001
Hospital-mortality	489 (24.7)	140 (14.9)	349 (33.5)	2.883 (2.312-3.595)	< 0.000001
Severity score on admission day					
SAPS II, mean ± SD (range)	35 ± 16 (5-93)	30 ± 14 (5-80)	39 ± 16 (5-93)	0.958 (0.950-0.965)	< 0.000001
TISS, mean ± SD (range)	9.5 ± 8.8 (0-55)	6.3 ± 7.4 (0-35)	11.6 ± 9.1 (0-55)	0.925 (0.912-0.938)	< 0.000001
Highest severity score within 7 d after admission					
SAPS II, mean ± SD (range)	39 ± 17 (6-93)	32 ± 15 (6-91)	44 ± 17 (6-93)	0.954 (0.947-0.961)	< 0.000001
TISS, mean ± SD (range)	12.0 ± 9.4 (0-55)	7.5 ± 8.0 (0-35)	14.6 ± 9.1 (0-55)	0.909 (0.897-0.921)	< 0.000001
Type of admission					< 0.000001
Internal medicine ICU	825 (41.7)	275 (29.3)	550 (52.8)		
Cardiology ICU	1154 (58.3)	663 (70.8)	491 (47.1)		
Source of admission					< 0.000001
Emergency department	923 (46.6)	468 (49.9)	455 (43.7)	Reference	
Other hospital	274 (13.8)	87 (9.3)	187 (17.9)	2.211 (1.662-2.941)	< 0.000001
Hospital ward	613 (31.0)	276 (29.5)	337 (32.2)	1.256 (1.023-1.541)	0.029
Operating room	132 (67.0)	98 (10.5)	34 (3.3)	0.357 (0.237-0.538)	0.000001
Surgical IMC/ICU	38 (1.9)	9 (0.96)	29 (2.8)	3.314 (1.552-7.079)	0.0020
Comorbid conditions	1410 (71.2)	607 (64.8)	803 (77.1)	1.840 (1.511-2.241)	< 0.000001
COPD	233 (11.8)	84 (9.0)	149 (14.3)	1.696 (1.278-2.252)	0.00026
Heart failure (EF < 30%)	114 (5.8)	59 (6.3)	55 (5.3)	0.830 (0.569-1.212)	> 0.20
Coronary artery disease	455 (23.0)	244 (26.0)	211 (20.2)	0.722 (0.585-0.891)	0.0024
Chronic renal failure	342 (34.2)	140 (14.9)	202 (19.4)	1.371 (1.082-1.736)	0.0089
Diabetes mellitus	474 (24.0)	227 (24.2)	247 (23.7)	0.973 (0.791-1.197)	> 0.20
Liver-cirrhosis	175 (8.8)	57 (6.1)	118 (11.3)	1.974 (1.420-2.744)	0.000052
Cancer	229 (11.6)	89 (9.5)	140 (13.4)	1.481 (1.117-1.962)	0.0063
Hematologic neoplasia	111 (5.6)	39 (4.2)	72 (6.9)	1.711 (1.147-2.553)	0.0085
HIV	76 (3.8)	15 (1.6)	61 (5.9)	3.826 (2.160-6.779)	0.0000043
Immunosuppressive Tx	106 (5.4)	29 (3.1)	77 (7.4)	2.501 (1.616-3.870)	0.000039
Chemotherapy	108 (5.5)	32 (3.4)	76 (7.3)	2.230 (1.461-3.403)	0.00020
Number of cormobid conditions					0.000023
0	566 (28.6)	330 (35.2)	236 (22.6)		
1	593 (30.0)	257 (27.4)	336 (32.2)		
2	415 (21.0)	174 (18.6)	241 (23.1)		
3	260 (13.1)	109 (11.6)	151 (14.5)		
> 3	146 (7.4)	68 (7.3)	78 (7.5)		
Mechanical ventilation	942 (47.6)	265 (28.3)	677 (65.0)	4.710 (3.892-5.701)	<0.000001
Hemodialysis	274 (13.8)	61 (6.5)	213 (20.4)	3.694 (2.736-4.987)	<0.000001

SAPS II: Simplified Acute Physiology Score II; TISS: Therapeutic Intervention Scoring System; ICU: Intensive care unit; IMC: Intermediate care unit, Internal Medicine ICU includes patients from Gastroenterology, Hepatology, Pulmonology, Endocrinology, Oncology, Hematology, Infectiology, Rheumatology departments, while Cardiology-ICU include patients from Cardiology, Angiology, Nephrology department; EF: Ejection fraction.

ding to the underlying clinical syndrome, risk-factors (hospital-stay, previous antibiotics, immunosuppressive patient) in accordance to the Sanford Guide on Antimicrobial Therapy 2010 (40th edition)[8] and national guidelines 2010 of the Paul-Ehrlich-society for chemotherapy and the local hospital resistance-statistics[9] and initiation of appropriate antimicrobial-therapy at symptom begin.

In addition appropriate adjustment of antimicrobial-therapy within the first 7 d of ICU-stay was recorded.

Statistical analysis

The primary statistical-endpoint was the evaluation of the influence of appropriate versus inappropriate antimicrobial-therapy on in-hospital-mortality. Multivariate-logistic regression-analysis was performed. The statistical analysis was performed using SPSS-version-20 (SPSS-Inc, Chicago, IL, United States). Data were expressed as mean ± SD for normally distributed variables and median and range for others. All statistical tests were 2-sided and $P < 0.05$ was considered statistically significant. No correction for multiple-testing was done. Wilcoxon-Mann-Whitney-test was used to compare numeric variables between the main-groups of patients. Ordinal-variables were analyzed using Chi-square-test and *via* binary-logistic regression-analysis. A multivariate-logistic regression-analysis was performed by forward binary-logistic-regression including all relevant nominal-variables, in which the significant variables were selected.

RESULTS

Characteristics of infection

Between April 1, 2007 and December 31, 2009, 2148 patients were admitted to the Internal-Medicine-ICU

Table 2 Site of infection and types of microorganisms in culture-positive infected patients *n* (%)

	All patients with infection (*n* = 1042)	Appropriate therapy (*n* = 948)	Inappropriate therapy (*n* = 94)	*P* value
Site of primary infection				
Respiratory tract	716 (68.7)	658 (69.4)	58 (61.7)	0.12
Abdomen/GIT	49 (4.7)	46 (4.9)	3 (3.2)	> 0.20
Renal/urinary tract	33 (3.2)	32 (3.4)	1 (1.1)	> 0.20
Skin	13 (1.2)	13 (1.4)	0	> 0.20
CNS	12 (1.2)	10 (1.1)	2 (2.1)	> 0.20
Endocarditis	26 (2.5)	24 (2.5)	2 (2.3)	> 0.20
Bloodstream	5 (0.5)	5 (0.5)	0	> 0.20
Others	35 (3.4)	33 (3.5)	2 (2.1)	> 0.20
Sepsis	207 (19.8)	179 (18.9)	28 (29.8)	0.011
Sites with detection of microorganism				
Respiratory tract	400 (38.4)	345 (36.4)	55 (58.5)	0.000026
Gastrointestinal	215 (20.6)	184 (19.4)	31 (33.0)	0.0019
Bloodstream	156 (15.0)	130 (13.7)	26 (27.7)	0.00030
Renal/urinary tract	185 (17.8)	155 (16.4)	30 (31.9)	0.000165
Skin	174 (16.7)	145 (15.3)	29 (30.9)	0.00012
Catheter-related	51 (4.9)	39 (4.1)	12 (12.8)	0.00021
CNS	10 (1.0)	10 (1.1)	0	> 0.20
Others	87 (8.4)	70 (7.4)	17 (18.1)	0.00055
Culture-positive	697 (66.9)	606 (63.9)	91 (69.8)	< 0.000001
Gram-positive isolates	473 (45.4)	400 (42.2)	73 (77.7)	< 0.000001
S. aureus	187 (17.9)	171 (18.0)	16 (17.0)	> 0.20
MRSA	45 (4.3)	31 (3.3)	14 (14.9)	< 0.000001
S. epidermidis	17 (1.6)	15 (1.6)	2 (2.1)	> 0.20
S. pneumoniae	16 (1.5)	12 (1.3)	4 (4.3)	0.025
VSE	93 (8.9)	67 (7.1)	26 (27.7)	< 0.000001
VRE	91 (8.7)	68 (7.2)	23 (24.5)	< 0.000001
Others	172 (16.5)	138 (14.5)	34 (36.2)	< 0.000001
Gram-negative isolates	368 (35.3)	320 (33.8)	48 (51.1)	0.00081
E. coli	99 (9.5)	89 (9.4)	10 (10.6)	> 0.20
Enterobacter spp.	45 (4.3)	39 (4.1)	6 (6.4)	> 0.20
Klebsiella spp.	56 (5.4)	49 (5.2)	7 (7.4)	> 0.20
Pseudomonas spp.	93 (8.9)	79 (8.3)	14 (14.9)	0.033
Acinetobacter spp.	10 (1.0)	5 (0.5)	5 (5.3)	0.0000055
ESBL-producing Enterobacteriaceae	42 (4.0)	37 (3.9)	5 (5.3)	> 0.20
Others	148 (14.2)	122 (12.8)	26 (27.7)	0.00099
Other bacteria	17 (1.6)	11 (1.2)	6 (6.4)	0.00014
Fungi	484 (46,5)	421 (40,4)	63 (6,1)	0.00028
Candia albicans	406 (39.0)	359 (37.9)	47 (50)	0.021
Other *Candida* spp.	197 (18.9)	165 (17.4)	32 (3.4)	0.010
C. glabrata	128 (12.3)	108 (11.4)	20 (21.3)	
C. tropicalis	39 (3.7)	33 (3.5)	6 (6.4)	
C. krusei	17 (1.6)	13 (1.4)	4 (4.3)	
Others	13 (1.3)	11 (1.2)	2 (2.1)	
Aspergillus spp.	27 (2.6)	8 (0.8)	19 (20.2)	< 0.000001
Pneumocystis jiroveci	14 (1.3)	4 (0.4)	10 (10.6)	< 0.000001
Other fungi	10 (1.0)	10 (1.1)	0	> 0.20
Parasites	1 (0.1)	1 (0.1)	0	0.00072
Multiresistant-bacteria	235 (22.6)	180 (19.0)	55 (58.5)	< 0.000001
MRSA	45 (4.3)	31 (3.3)	14 (14.9)	
VRE	91 (8.7)	68 (7.2)	23 (24.5)	
ESBL-producing Enterobacteriaceae	42 (4.0)	37 (3.9)	5 (5.3)	
Pseudomonas spp.	16 (1.5)	14 (1.5)	2 (2.2)	
Stenotrophomonas spp.	19 (1.8)	12 (1.3)	7 (7.4)	
Acinetobacter spp.	3 (0.29)	1 (0.1)	2 (2.2)	
Others	21 (2.01)	19 (2.0)	2 (2.2)	

Appropriate therapy: Patients who received appropriate antimicrobial-therapy; Inappropriate therapy: Patients who received inappropriate antimicrobial-therapy; GIT: Gastrointestinal tract; CNS: Central nervous system; VSE: Vancomycin-sensitive *Enterococcus*; VRE: Vancomycin-resistant *Enterococcus*; ESBL: Extended-spectrum β-lactamase producing bacteria; MRSA: Methicilline-resistant *Staphylococcus aureus*.

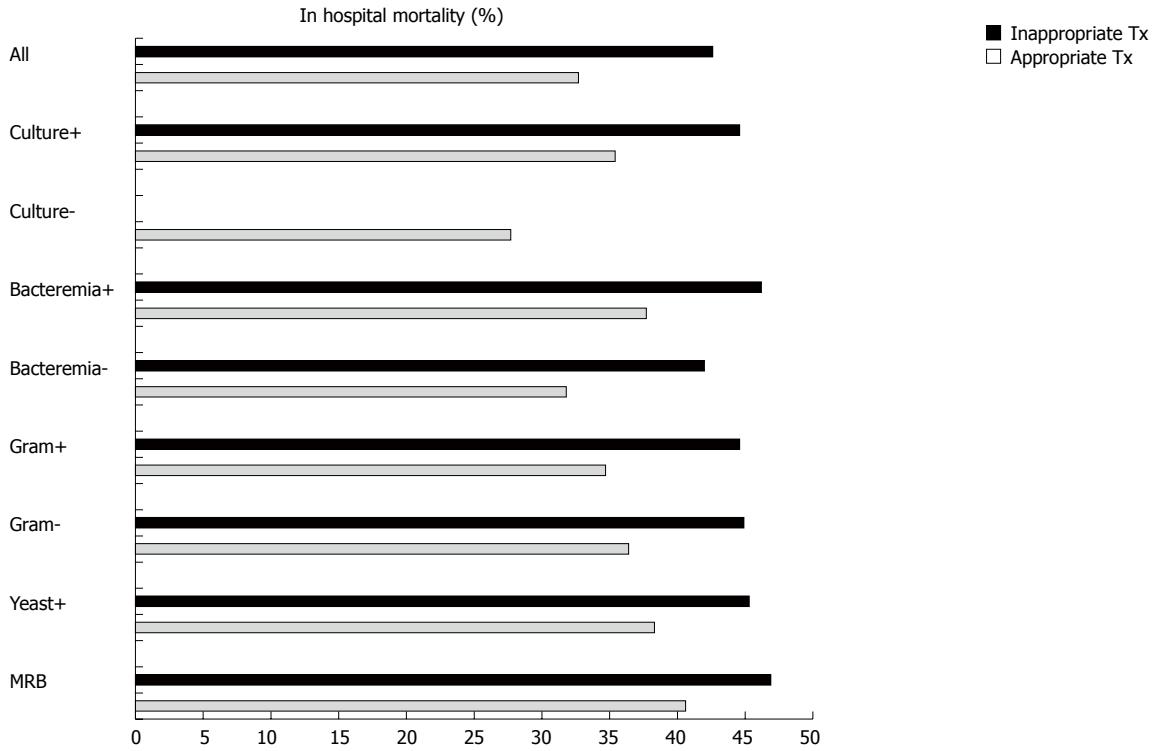

Figure 1 Impact of appropriate and inappropriate antimicrobial-therapy on in hospital-mortality. Culture+: Culture-positive infection; Culture-: Culture-negative infection; Bacteremia+: Patients with positive blood cultures; Bacteremia-: Patients with negative blood cultures; Gram+: Culture-positive for gram-positive bacteria; Gram-: Culture-positive for gram-negative bacteria; Yeast+: Culture-positive for yeast; MRB: Multiresistant-bacteria.

of the Goethe-University-Hospital-Frankfurt. From 1979 patients enough data were available to include them into the analysis. Of the 1979 patients, 1042 (53%) were classified as having an infection. Infected patients had more comorbid conditions, higher SAPS-II and TISS-scores, received more often mechanical-ventilation and hemodialysis, and had a higher in-hospital-mortality-rate than patients without infection. Details are shown in Table 1.

The most frequent site of infection was the respiratory-tract, followed by gastrointestinal-infections, genitourinary-infections, endocarditis and skin-infections (Table 2).

In 697 patients (67%) from overall 1042 patients with infection underlying microorganisms were identified. Gram-positive isolates (*S. aureos*, *S. epidermidis*, *S. pneumoniae*, VSE, VRE, and others) were found in 45% (473/1042) of patients with infections and gram-negative isolates (*E. coli*, *Enterobacter* spp., *Klebsiella* spp., Pseudomonas spp., Acinetobacter spp., ESBL-producing Enterobacteriaceae, and others) in 35% (368/1042). Details are shown in Table 2. Multiresistant-bacteria were present in 23% of patients with infection; these were most frequently vancomycin-resistant *Enterococcus faecium* (VRE) (8.7%), followed by methicilline-resistant *Staphylococcus aureus* (MRSA) (4.3%) and extended-spectrum-betalactamase (ESBL)-producing enterobacteriaceae (4.0%).

Overall, the rate of survival to hospital-discharge was 66% in patients with infection as compared to 83% of patients without infection ($P < 0.000001$).

Appropriateness of initial antimicrobial-therapy

From all patients with infection, 91% of patients received appropriate and 9% inappropriate initial antimicrobial-therapy. From the 697 patients with infection and positive blood-culture, 87% received appropriate initial antimicrobial-therapy. The survival-rate to hospital discharge was higher in the group of patients receiving appropriate antimicrobial-therapy (67% *vs* 57%). However, this difference was not statistically significant ($P = 0.054$). The rate of inappropriate antimicrobial-therapy in septic-shock was 13.5%. In the group of patients with septic-shock (20% of patients with infection) no significant difference in survival-rate to hospital discharge was found between patients receiving appropriate ($n = 179$) versus inappropriate ($n = 28$) initial antimicrobial-therapy (44% *vs* 36%, $P > 0.20$). Details are shown in Figure 1 and Table 3.

Patients who received inappropriate initial antimicrobial-therapy had a longer ICU stay and suffered from higher rates of liver-cirrhosis, HIV, and prior chemotherapy. In addition, patients with multiresistant-bacterial infection received significantly more often inappropriate initial antimicrobial-therapy as compared to patients with other bacterial-infection [58% *vs* 19%, $P < 0.000001$; OR = 6.25 (2.59-15.15), $P = 0.000046$]. Details are shown in Table 3.

Escalation of antimicrobial-therapy was documented

Table 3 Characteristics of patients with infection according to appropriate or inappropriate antimicrobial-therapy *n* (%)

Characteristic	All patients with infection (*n* = 1042)	Appropriate therapy (*n* = 948)	Inappropriate therapy (*n* = 94)	OR (95%CI)	*P* value
Age (yr), mean ± SD (range)	61 ± 16 (16-95)	61 ± 16 (16-95)	61 ± 14 (21-88)	1.003 (0.99-1.017)	> 0.20
Male sex	622 (60.0)	376 (39.7)		0.747 (0.488-1.143)	0.18
Days on ICU, mean ± SD (range)	8.12 ± 12 (1-217)	7.68 ± 11.958 (1-217)	10.02 ± 11.134 (1-59)	1.011 (0.998-0.024)	0.092
ICU-mortality	324 (31.3)	287 (30.3)	37 (39.4)	0.669 (0.432-1.035)	0.071
Hospital-mortality	350 (33.6)	310 (32.7)	40 (42.6)	0.656 (0.426-1.009)	0.055
Severity score on admission day					
SAPS II, mean ± SD (range)	38.67 ± 15.64 (5-93)	38.54 ± 15.82 (5-93)	39.95 ± 13.78 (8-68)	1.006 (0.992-1.020)	> 0.20
TISS, mean ± SD (range)	11.57 ± 9.11 (0-55)	11.74 ± 9.25 (0-55)	9.86 ± 7.42 (0-28)	0.976 (0.951-1.002)	0.071
Highest severity score within 7 d after admission					
SAPS II, mean ± SD (range)	43.88 ± 16.57 (6-93)	43.68 ± 16.71 (6-93)	45.87 ± 15.09 (8-81)	1.008 (0.994-1.022)	> 0.20
TISS. mean ± SD (range)	14.65 ± 9.14 (0-55)	14.68 ± 9.27 (0-55)	14.32 ± 7.73 (0-38)	0.996 (0.971-1.021)	> 0.20
Type of Admission					0.0022
Internal Medicine ICU	550 (52.8)	486 (51.3)	64 (68.1)		
Cardiology ICU	491 (47.1)	461 (48.7)	30 (31.9)		
Source of admission					> 0.20
Emergency department	455 (43.7)	418 (44.1)	37 (39.4)	Reference	
Other hospital	187 (17.9)	170 (17.9)	17 (18.1)	0.425 (0.153-1.179)	0.10
Hospital ward	337 (32.3)	305 (32.2)	32 (34.0)	0.48 (0.162-1.429)	0.19
Operating room	34 (3.3)	31 (3.3)	3 (3.2)	0.504 (0.18-1.411)	0.19
Surgical IMC/ICU	29 (2.7)	24 (2.6)	5 (5.3)	0.465 (0.101-2.14)	> 0.20
Comorbid conditions	806 (77.4)	729 (76.9)	77 (81.9)	0.842 (0.498-1.424)	> 0.20
COPD	149 (14.3)	137 (14.5)	12 (12.8)	1.154 (0.613-2.172)	> 0.20
Heart failure (EF < 30%)	55 (5.3)	50 (5.3)	5 (5.3)	0.991 (0.385-2.549)	> 0.20
Coronary artery disease	211 (20.2)	195 (20.6)	16 (17.0)	1.262 (0.721-2.211)	> 0.20
Chronic renal failure	202 (19.4)	182 (19.2)	20 (21.3)	0.879 (0.523-1.478)	> 0.20
Diabetes mellitus	247 (23.7)	220 (23.2)	27 (28.7)	0.750 (0.468-1.202)	> 0.20
Liver-cirrhosis	118 (11.3)	100 (10.5)	18 (19.1)	0.498 (0.286-0.866)	0.014
Cancer	140 (13.4)	122 (12.9)	18 (19.1)	0.624 (0.361-1.079)	0.091
Hematologic neoplasia	72 (6.9)	68 (7.2)	4 (4.3)	1.739 (0.620-4.877)	> 0.20
HIV	61 (5.9)	51 (5.4)	10 (10.6)	0.478 (0.234-0.975)	0.042
Immunosuppressive Tx.	77 (7.4)	69 (7.3)	8 (8.5)	0.844 (0.393-1.813)	> 0.20
Chemotherapy	53 (5.1)	47 (5.0)	6 (6.4)	2.634 (1.691-4.102)	0.000018
Number of cormobid conditions					> 0.20
0	236	219 (23.1)	17 (18.1)		
1	336	304 (32.1)	32 (34.0)		
2	241	219 (23.1)	22 (23.4)		
3	151	138 (14.6)	13 (13.8)		
> 3	78	68 (7.2)	10 (10.6)		
Mechanical ventilation	677 (65.0)	621 (65.5)	56 (59.6)	1.289 (0.836-1.987)	> 0.20
Hemodialysis	213 (20.4)	194 (20.5)	19 (20.2)	1.016 (0.599-1.721)	> 0.20

Appropriate therapy: Patients who received appropriate antimicrobial-therapy; Inappropriate therapy: Patients who received inappropriate antimicrobial-therapy; SAPS II: Simplified Acute Physiology Score II; TISS: Therapeutic Intervention Scoring System; ICU: Intensive care unit; IMC: Internal Medicine ICU includes patients from Gastroenterology, Hepatology, Pulmonology, Endocrinology, Oncology, Hematology, Infectiology, Rheumatology departments, while Cardiology-ICU include patients from Cardiology, Angiology, Nephrology department; EF: Ejection fraction.

within the first 7 d of ICU stay in 20% of patients with infection, and de-escalation in 31%, respectively. From the 94 patients with infection who received inappropriate initial antimicrobial-therapy, antimicrobial-therapy was adjusted appropriately within the first seven days in 38 (40%) of patients according to the AST.

Mortality

In hospital-mortality-rate was 25% in the overall ICU population and 34% in patients with infection. Details are shown in Table 4.

Multivariate-logistic regression-analysis including all significant variables revealed as independent risk-factors for in hospital-mortality the presence of septic-shock at admission [OR = 2.928 (1.246-6.787), *P* = 0.0057], chemotherapy for malignoma received within 3 mo prior to ICU admission [OR = 4.274 (1.37-13.33), *P* = 0.012] and infection with *Pseudomonas* spp.[OR = 4.187 (1.665-12.579), *P* = 0.0030].

Risk factors for in-hospital mortality in patients with infection are shown in Table 5.

Multivariate-logistic regression-analysis for patients with infection only revealed as independent risk-factors for in hospital-mortality the presence of septic-shock at admission [OR = 3.576 (2.347-5.448), *P* < 0.000001], SAPS-II-score at admission [OR = 1.014 (1.002-1.027), *P* = 0.017], presence of comorbid-disease [OR = 2.228 (1.443-3.627), *P* = 0.00043], mechanical-ventilation [OR = 1.712 (0.993-2.959), *P* = 0.034], pulmonary focus of infection [OR = 1.885 (1.200-2.963), *P* = 0.0061], liver-cirrhosis [OR =

Table 4 Risk factors for in hospital mortality *n* (%)

Characteristic	Patients who died in hospital	Patients surviving	Odds ratio	*P* value
Age (yr)	63	60		0.0011
SAPS II score (mean)	47	37		< 0.000001
TISS score (mean)	12.8	8.5		< 0.000001
Number of comorbid conditions			1.851 [1.446-2.369]	< 0.000001
Chemotherapy for malignoma within 3 mo prior to admission			2.385 [1.605-3.543]	0.000017
Clinical infection on admission			2.883 [2.312-3.595]	< 0.000001
Septic-shock on admission			4.993 [3.707-6.727]	< 0.000001
Bacteriemia			2.119 [1.515-2.962]	< 0.000001
Multiresistant-bacterial infections			2.189 [1.664-2.879]	< 0.000001
mechanical ventilation during ICU stay			5.018 [3.981-6.324]	< 0.000001
C-reactive-protein at admission (mg/dL)	8.76	6.23		< 0.000001
Creatinine-values at admission (mg/dL)	1.93	1.644		< 0.000001
Bilirubin-values at admission (mg/dL)	3.175	1.818		0.0014
INR	1.81	1.46		< 0.000001

SAPS II: Simplified Acute Physiology Score II; TISS: Therapeutic Intervention Scoring System; ICU: Intensive care unit.

Table 5 Risk factors for in hospital mortality of patients with infection

Characteristic	Patients who died in hospital	Patients surviving	Odds ratio	*P* value
SAPS II score (mean)	42	37		0.00021
TISS score (mean)	12.7	11.03		0.0084
Number of comorbid conditions			1.824 [1.311-2.539]	0.00036
mechanical ventilation during ICU stay			2.363 [1.765-3.164]	< 0.000001
pulmonary-infections			1.741 [1.301-2.33]	0.00020
catheter-related infection			2.578 [1.51-4.399]	0.00052
bilirubin-values at admission (mg/dL)	3.39	2.458		0.0300
INR	1.83	1.55		0.0000082

ICU: Intensive care unit.

1.816 (1.061-3.106), *P* = 0.029] and INR [OR = 1.248 (1.031-1.508), *P* = 0.022].

Liver disease

Chronic liver-disease was known in 272 patients (14%) with liver-cirrhosis present in 175 of these patients (64%). From these 272 patients with chronic liver disease, chronic viral hepatitis infection was present in 150 patients (55%), of whom 101 were infected with chronic hepatitis C and 49 with chronic hepatitis B. Only one patient had chronic alcoholic and one patient autoimmune liver disease. Patients with spontaneous bacterial infection as primary infection site were not included in the analysis.

Patients with chronic liver-disease had a higher infection-rate (69% *vs* 50%, *P* < 0.000001) and presented more often with septic-shock (15% *vs* 10%, *P* = 0.014) as compared to patients without chronic liver-disease. From all patients with chronic liver-disease, only patients infected with chronic hepatitis C had significantly higher risk of in hospital-mortality [OR = 1.660 (1.087-2.534), *P* = 0.019].

The presence of liver-cirrhosis significantly increased the risk of infection (OR = 1.974 (1.420-2.744), *P* = 0.000052], the risk of receiving inappropriate initial antimicrobial-therapy [OR = 2.008 (1.155-3.497), *P* = 0.014] and in hospital-mortality-rate [OR = 2.320 (1.684-3.195), *P* < 0.000001]. Infection-rate and sepsis-rate was significantly higher in patients with liver-cirrhosis as compared to patients without liver-cirrhosis (67% *vs* 51%, *P* = 0.000040 and 15% *vs* 10%, *P* = 0.046). In patients with liver-cirrhosis the presence of infection significantly increased in hospital-mortality (49% *vs* 25%, *P* = 0.0019). Liver-cirrhosis was an independent risk-factor for in hospital-mortality in patients with infection [OR = 1.816 (1.061-3.106), *P* = 0.029] (Figure 2).

MELD-score was significantly higher in patients with liver-cirrhosis who died in hospital as compared to survivors (MELD-score 28 *vs* 23, *P* = 0.012) and significantly more patients with liver-cirrhosis received hemodialysis (15% *vs* 8%, *P* = 0.043). In patients with liver-cirrhosis infections with multiresistant-bacteria were found in 32% (38/118) of patients. From these 38 patients, 18% were infected with ESBL-producing bacteria enterobacteriaceae, 18% with MRSA and 55% with VRE.

No significant difference was found for diagnostic-accuracy of MELD-score (AUROC 73%, 95%CI: 65%-82%) and SAPS-II-score (AUROC 72%, 95%CI: 63%-81%) at admission in identifying risk of in-hospital-mortality (*P* > 0.20).

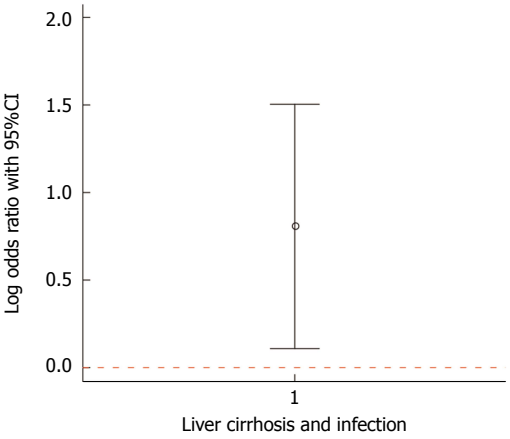

Figure 2 49% of patients with liver-cirrhosis and infection died in hospital, compared to 25% with liver-cirrhosis and without infection. The plot shows the log odds ratio (0.8063, marked by the dot) and its 95%CI [(0.1086-1.5039), marked by the whiskers], *i.e.* patients with liver-cirrhosis and infection had a 2.24 greater in-hospital-mortality than patients with liver-cirrhosis without infection.

DISCUSSION

In the present study the infection-rate of patients on the Internal Intensive Care Unit was 53%. Patients with infection had more often comorbid conditions and higher SAPS II scores on admission and during the first seven days of ICU treatment. The results of the present study are in accordance with a 1-d point international multicenter prevalence study by Vincent *et al*[5] reporting infections in 51% of ICU patients and similar associations. While the present study included Internal Medicine ICU only, the study by Vincent et al. included also surgery and trauma patients. The most common infection focus in the present study was the lung, followed by abdomen, and genitourinary tract infection. This again is in accordance with epidemiological studies concerning infections on ICU[10-12]. Positive microbiological cultures were obtained in 65% of infected patients with more gram-positive than gram-negative microorganisms. This is in accordance with previous studies that reported an increasing incidence of gram-positive microorganisms on ICUs[2]. In hospital-mortality was significantly higher in patients with infections and patients with sepsis as compared to patients without. This again supports results of previous studies[2,5].

Studies have reported higher hospital-mortality in patients with blood stream infections that receive inappropriate initial antimicrobial-therapy[13-15]. In 2006 Kumar *et al*[16] reported, that effective antimicrobial administration within the first hour of documented hypotension was associated with increased survival to hospital-discharge in patients with septic-shock. However, only 50% of septic-shock patients received effective antimicrobial-therapy within 6 h of documented hypotension[16]. In 2004, the Surviving-Sepsis-Campaign developed guidelines for the management of severe sepsis and septic-shock[17]. This included besides others, early cultures for microbial evaluation and "early-goal-directed therapy" with initiation of antimicrobial-therapy as soon as possible[17,18]. After implementation of the "sepsis-bundle" the Surviving-Sepsis-Campaign study group published a study performed at 165 sites with 15022 subjects and reported an increase in compliance with the sepsis bundle from 11 to 31% two years after implementation and a reduction in mortality[19]. Other studies have reported a similar association[20]. The present study also started after implementation of the sepsis-bundle with early-goal-directed antimicrobial-therapy with empiric calculated therapy on the ICU-ward. Only 9% of patients with infection and 13.5% of patients with septic-shock received inappropriate antimicrobial-therapy. This was lower than reported in a study of Kumar *et al*[16] published in 2009 including 5715 patients with septic-shock with 20% of inappropriate therapy of patients with septic-shock and significant reduction of survival in those receiving inappropriate therapy (10% *vs* 52%)[16]. Although these two studies cannot be directly compared, it shows a trend towards improvement of initial antimicrobial-therapy. While in the study of Kumar[16] a significant reduction of survival (42%) was found in patients receiving inappropriate antimicrobial-therapy as compared to patients receiving appropriate antimicrobial-therapy, no significant reduction was found in the present study (10%). Antimicrobial-therapy is only one aspect of the sepsis bundle, therefore other factors might have also played a role in the present study.

Multiresistant-microorganisms are an increasing burden on ICUs worldwide[21]. Also in the present study multiresistant-bacteria were detected in 23% of patients with infection. This is higher than the overall prevalence in German hospitals[22,23]. A reason might be the high proportion of patients colonized with such bacteria which arrive from countries with high prevalence of multiresistant-bacteria to be treated at Frankfurt-University-hospital due to its close location to Frankfurt international-airport. Therefore, successful infection control measurements are strictly implemented inhibiting transmission of such pathogens from patient to patient. In addition, Frankfurt-University-Hospital is a referral-hospital and therefore many severely ill patients, who received multiple antibiotic-regimens prior to referral, receive further treatment here.

Nevertheless, inappropriate therapy was significantly associated with the presence of multiresistant-bacteria in the present study, suggesting that empirical therapy has to cover multiresistant-bacteria more regularly. Studies have shown that inappropriate antimicrobial-therapy for gram negative ESBL producers was associated with significant increase in mortality (59.5% *vs* 18.5%, $P < 0.001$)[24]. Common risk factors for infection with multiresistant-bacteria are: residence in nursery home, recent hospital stay, mechanical ventilation, age, prior antibiotic therapy and foreign

citizenship[9,25]. Also in the present study prior anti-microbial-therapy was an independent risk-factor for infection.

Since the University-Hospital is a liver transplantation center, a high number of patients with liver-disease are treated here. Chronic liver-disease was present in 14% of patients admitted to the ICU with liver-cirrhosis in 64% of these patients. Patients with liver-cirrhosis had a significantly higher infection-rate than patients without liver-cirrhosis. This is in accordance with previous studies reporting infection-rates of 32%-34% in liver-cirrhosis as compared to 5%-7% in the general hospitalized population[26,27]. A meta-analysis reported a 4-fold increase in mortality in patients with liver-cirrhosis that acquire an infection[6]. In addition, patients with sepsis and liver-cirrhosis have a significant higher mortality-rate as compared to patients with sepsis in the general hospitalized population[27], this was supported by the results of the present study. The presence of liver-cirrhosis was an independent risk factor for in hospital-mortality in patients with infection. In addition, also in patients with liver-cirrhosis infection with multiresistant-bacteria is increasing. A recent study resported an incidence of 39% multiresistant-bacteria in patients with liver-cirrhosis and nosocomial infection[28]. In the present study an infection with multiresistant-bacteria could be found in 32% of patients with liver-cirrhosis. Inappropriate antimicrobial-therapy was significantly more often in patients with liver-cirrhosis. The high rate of multiresistant-bacteria could be an explanation herefore. A recent study revealed a significantly higher rate of septic-shock and in-hospital-mortality in patients with liver-cirrhosis infected with multiresistant-bacteria (26% *vs* 10% and 25% *vs* 12%)[29].

MELD-score and SAPS-II-score at admission performed equally good concerning the prediction of in-hospital-mortality with diagnostic accuracies of 73% and 72%. A previous systematic review including 21 studies reported diagnostic accuracies of 81% for MELD-score and 83% for SOFA (sequential-organ-failure-assessment)-score[29]. Therefore both studies report comparable results for general ICU prognostic-markers and liver-specific prognostic-markers for patients with liver-cirrhosis on ICU and therefore might supplement each other.

A limitation of the present study is its monocentric retrospective study-design. Nevertheless, the distribution of infections was comparable to previous multicenter-studies[5].

The inclusion of patients with culture-negative infection might be criticized and lead to bias. However, no difference in percentage of appropriate to inappropriate antimicrobial-therapy was found in a subanalysis of patients with culture-positive infections only.

In conclusion, the results of the present study report the successful implementation of early-goal-directed therapy. Increasing burden are multiresistant-bacteria, which are associated with increased mortality.

COMMENTS

Background

Infections are a worldwide problem concerning patients admitted to intensive care units, since they are associated with an increased mortality, morbidity and financial burden. A 51%-prevalence of infection has been reported for intensive care unit (ICU)-patients and previously 20% of patients admitted with septic-shock to an ICU received inappropriate antimicrobial-therapy.

Research frontiers

Infection rate and management on ICU with special focus on liver cirrhosis patients.

Innovations and breakthroughs

In the present study the infection-rate of patients on the Internal Intensive Care Unit was 53%. Infection increased mortality 2.24-fold in patients with cirrhosis.

Applications

Retrospective analysis reporting the high prevalence of infections and the importance of early goal-directed therapy.

Peer-review

The paper presents the influence of antibiotic-regimens on ICU-mortality. It underlines the successful implementation of early-goal-directed therapy in patients treated in ICU. The topic is interesting, especially considering the rate of mortality in these patients and financial burden.

REFERENCES

1 **Harrison DA**, Welch CA, Eddleston JM. The epidemiology of severe sepsis in England, Wales and Northern Ireland, 1996 to 2004: secondary analysis of a high quality clinical database, the ICNARC Case Mix Programme Database. *Crit Care* 2006; **10**: R42 [PMID: 16542492]

2 **Vincent JL**, Sakr Y, Sprung CL, Ranieri VM, Reinhart K, Gerlach H, Moreno R, Carlet J, Le Gall JR, Payen D. Sepsis in European intensive care units: results of the SOAP study. *Crit Care Med* 2006; **34**: 344-353 [PMID: 16424713 DOI: 10.1097/01.CCM.0000194725.48928.3A]

3 **Angus DC**, Linde-Zwirble WT, Lidicker J, Clermont G, Carcillo J, Pinsky MR. Epidemiology of severe sepsis in the United States: analysis of incidence, outcome, and associated costs of care. *Crit Care Med* 2001; **29**: 1303-1310 [PMID: 11445675 DOI: 10.1097/00003246-200107000-00002]

4 **Kumar A**, Ellis P, Arabi Y, Roberts D, Light B, Parrillo JE, Dodek P, Wood G, Kumar A, Simon D, Peters C, Ahsan M, Chateau D. Initiation of inappropriate antimicrobial therapy results in a fivefold reduction of survival in human septic shock. *Chest* 2009; **136**: 1237-1248 [PMID: 19696123 DOI: 10.1378/chest.09-0087]

5 **Vincent JL**, Rello J, Marshall J, Silva E, Anzueto A, Martin CD, Moreno R, Lipman J, Gomersall C, Sakr Y, Reinhart K. International study of the prevalence and outcomes of infection in intensive care units. *JAMA* 2009; **302**: 2323-2329 [PMID: 19952319 DOI: 10.1001/jama.2009.1754]

6 **Arvaniti V**, D'Amico G, Fede G, Manousou P, Tsochatzis E, Pleguezuelo M, Burroughs AK. Infections in patients with cirrhosis increase mortality four-fold and should be used in determining prognosis. *Gastroenterology* 2010; **139**: 1246-1256, 1256e1-e5 [PMID: 20558165 DOI: 10.1053/j.gastro.2010.06.019]

7 **Calandra T**, Cohen J. The international sepsis forum consensus conference on definitions of infection in the intensive care unit. *Crit Care Med* 2005; **33**: 1538-1548 [PMID: 16003060 DOI: 10.1097/01.CCM.0000168253.91200.83]

8 **Gilbert DN**, Moellering RC, Eliopoulos GM. Clinical approach to intitial choice of antimicrobial therapy. The Sanford Guide To Antimicrobial Therapy 2010, Antimicrobial Therapy Inc., 2010. Available from: URL: http://www.sanfordguide.com/

9 **Bodmann KF**, Grabein B, Expertenkommission der Paul-Ehrlich-Gesellschaft fur Chemotherapie e.V. [Empfehlungen zur

kalkulierten parenteralen Initialtherapie bakterieller Erkrankungen bei Erwachsenen-Update 2010. Available from: URL: http://www.p-e-g.org/aktuelles/435/

10 **Martin CM**, Priestap F, Fisher H, Fowler RA, Heyland DK, Keenan SP, Longo CJ, Morrison T, Bentley D, Antman N. A prospective, observational registry of patients with severe sepsis: the Canadian Sepsis Treatment and Response Registry. *Crit Care Med* 2009; **37**: 81-88 [PMID: 19050636 DOI: 10.1097/CCM.0b013e31819285f0]

11 **Brun-Buisson C**, Meshaka P, Pinton P, Vallet B. EPISEPSIS: a reappraisal of the epidemiology and outcome of severe sepsis in French intensive care units. *Intensive Care Med* 2004; **30**: 580-588 [PMID: 14997295 DOI: 10.1007/s00134-003-2121-4]

12 **Engel C**, Brunkhorst FM, Bone HG, Brunkhorst R, Gerlach H, Grond S, Gruendling M, Huhle G, Jaschinski U, John S, Mayer K, Oppert M, Olthoff D, Quintel M, Ragaller M, Rossaint R, Stuber F, Weiler N, Welte T, Bogatsch H, Hartog C, Loeffler M, Reinhart K. Epidemiology of sepsis in Germany: results from a national prospective multicenter study. *Intensive Care Med* 2007; **33**: 606-618 [PMID: 17323051 DOI: 10.1007/s00134-006-0517-7]

13 **Prowle JR**, Echeverri JE, Ligabo EV, Sherry N, Taori GC, Crozier TM, Hart GK, Korman TM, Mayall BC, Johnson PD, Bellomo R. Acquired bloodstream infection in the intensive care unit: incidence and attributable mortality. *Crit Care* 2011; **15**: R100 [PMID: 21418635 DOI: 10.1186/cc10114]

14 **Kollef MH**, Sherman G, Ward S, Fraser VJ. Inadequate antimicrobial treatment of infections: a risk factor for hospital mortality among critically ill patients. *Chest* 1999; **115**: 462-474 [PMID: 10027448 DOI: 10.1378/chest.115.2.462]

15 **Ibrahim EH**, Sherman G, Ward S, Fraser VJ, Kollef MH. The influence of inadequate antimicrobial treatment of bloodstream infections on patient outcomes in the ICU setting. *Chest* 2000; **118**: 146-155 [PMID: 10893372 DOI: 10.1378/chest.118.1.146]

16 **Kumar A**, Roberts D, Wood KE, Light B, Parrillo JE, Sharma S, Suppes R, Feinstein D, Zanotti S, Taiberg L, Gurka D, Kumar A, Cheang M. Duration of hypotension before initiation of effective antimicrobial therapy is the critical determinant of survival in human septic shock. *Crit Care Med* 2006; **34**: 1589-1596 [PMID: 16625125 DOI: 10.1097/01.CCM.0000217961.75225.E9]

17 **Dellinger RP**, Carlet JM, Masur H, Gerlach H, Calandra T, Cohen J, Gea-Banacloche J, Keh D, Marshall JC, Parker MM, Ramsay G, Zimmerman JL, Vincent JL, Levy MM. Surviving Sepsis Campaign guidelines for management of severe sepsis and septic shock. *Intensive Care Med* 2004; **30**: 536-555 [PMID: 14997291 DOI: 10.1007/s00134-004-2210-z]

18 **Rivers E**, Nguyen B, Havstad S, Ressler J, Muzzin A, Knoblich B, Peterson E, Tomlanovich M. Early goal-directed therapy in the treatment of severe sepsis and septic shock. *N Engl J Med* 2001; **345**: 1368-1377 [PMID: 11794169 DOI: 10.1056/NEJMoa010307]

19 **Levy MM**, Dellinger RP, Townsend SR, Linde-Zwirble WT, Marshall JC, Bion J, Schorr C, Artigas A, Ramsay G, Beale R, Parker MM, Gerlach H, Reinhart K, Silva E, Harvey M, Regan S, Angus DC. The Surviving Sepsis Campaign: results of an international guideline-based performance improvement program targeting severe sepsis. *Intensive Care Med* 2010; **36**: 222-231 [PMID: 20069275 DOI: 10.1007/s00134-009-1738-3]

20 **Shiramizo SC**, Marra AR, Durão MS, Paes ÂT, Edmond MB, Pavão dos Santos OF. Decreasing mortality in severe sepsis and septic shock patients by implementing a sepsis bundle in a hospital setting. *PLoS One* 2011; **6**: e26790 [PMID: 22073193 DOI: 10.1371/journal.pone.0026790]

21 **Burgmann H**, Hiesmayr JM, Savey A, Bauer P, Metnitz B, Metnitz PG. Impact of nosocomial infections on clinical outcome and resource consumption in critically ill patients. *Intensive Care Med* 2010; **36**: 1597-1601 [PMID: 20614212 DOI: 10.1007/s00134-010-1941-2]

22 **Kresken M**, Hafner D, Schmitz FJ, Wichelhaus TA. PEG-Resistenzstudie 2004. Paul-Ehrlich-Gesellschaft für Chemotherapie e.V. Available from: URL: http://www.p-e-g.org

23 **Geffers C**, Gastmeier P. Nosocomial infections and multidrug-resistant organisms in Germany: epidemiological data from KISS (the Hospital Infection Surveillance System). *Dtsch Arztebl Int* 2011; **108**: 87-93 [PMID: 21373275 DOI: 10.3238/arztebl.2011.0087]

24 **Tumbarello M**, Sanguinetti M, Montuori E, Trecarichi EM, Posteraro B, Fiori B, Citton R, D'Inzeo T, Fadda G, Cauda R, Spanu T. Predictors of mortality in patients with bloodstream infections caused by extended-spectrum-beta-lactamase-producing Enterobacteriaceae: importance of inadequate initial antimicrobial treatment. *Antimicrob Agents Chemother* 2007; **51**: 1987-1994 [PMID: 17387156 DOI: 10.1128/AAC.01509-06]

25 **Kaye KS**, Fraimow HS, Abrutyn E. Pathogens resistant to antimicrobial agents. Epidemiology, molecular mechanisms, and clinical management. *Infect Dis Clin North Am* 2000; **14**: 293-319 [PMID: 10829257 DOI: 10.1016/S0891-5520(05)70249-X]

26 **Gustot T**, Durand F, Lebrec D, Vincent JL, Moreau R. Severe sepsis in cirrhosis. *Hepatology* 2009; **50**: 2022-2033 [PMID: 19885876 DOI: 10.1002/hep.23264]

27 **Tandon P**, Garcia-Tsao G. Bacterial infections, sepsis, and multiorgan failure in cirrhosis. *Semin Liver Dis* 2008; **28**: 26-42 [PMID: 18293275 DOI: 10.1055/s-2008-1040319]

28 **Fernández J**, Acevedo J, Castro M, Garcia O, de Lope CR, Roca D, Pavesi M, Sola E, Moreira L, Silva A, Seva-Pereira T, Corradi F, Mensa J, Ginès P, Arroyo V. Prevalence and risk factors of infections by multiresistant bacteria in cirrhosis: a prospective study. *Hepatology* 2012; **55**: 1551-1561 [PMID: 22183941 DOI: 10.1002/hep.25532]

29 **Cholongitas E**, Senzolo M, Patch D, Kwong K, Nikolopoulou V, Leandro G, Shaw S, Burroughs AK. Risk factors, sequential organ failure assessment and model for end-stage liver disease scores for predicting short term mortality in cirrhotic patients admitted to intensive care unit. *Aliment Pharmacol Ther* 2006; **23**: 883-893 [PMID: 16573791 DOI: 10.1111/j.1365-2036.2006.02842.x]

P- Reviewer: Ampuero J, Cichoz-Lach H, He JY, Kayashima H
S- Editor: Gong ZM **L- Editor**: A **E- Editor**: Zhang DN

World Journal of Gastroenterology

Submit a Manuscript: http://www.wjgnet.com/esps/
Help Desk: http://www.wjgnet.com/esps/helpdesk.aspx
DOI: 10.3748/wjg.v22.i16.4211

World J Gastroenterol 2016 April 28; 22(16): 4211-4218
ISSN 1007-9327 (print) ISSN 2219-2840 (online)

ORIGINAL ARTICLE

Retrospective Study

Lymphocyte-to-monocyte ratio predicts survival after radiofrequency ablation for colorectal liver metastases

Antonio Facciorusso, Valentina Del Prete, Nicola Crucinio, Gaetano Serviddio, Gianluigi Vendemiale, Nicola Muscatiello

Antonio Facciorusso, Valentina Del Prete, Nicola Crucinio, Nicola Muscatiello, Gastroenterology Unit, Department of Medical Sciences, University of Foggia, 71100 Foggia, Italy

Gaetano Serviddio, Gianluigi Vendemiale, Internal Medicine Unit, University of Foggia, 71100 Foggia, Italy

Author contributions: Facciorusso A designed the study, performed the statistical analysis and wrote the paper; Crucinio N performed the treatment procedures; Del Prete V and Muscatiello N collected the data; Vendemiale G and Serviddio G revised the paper.

Institutional review board statement: This study was approved by the Institutional Review Board of the University of Foggia for retrospective evaluation of de-identified patients.

Informed consent statement: Patients were not required to give informed consent to the study because the analysis used anonymous clinical data that were obtained after each patient agreed to treatment by written consent.

Conflict-of-interest statement: None of the authors have received fees for serving as a speaker or are consultant/advisory board member for any organizations. None of the authors have received research funding from any organizations. None of the authors are employees of any organizations. None of the authors own stocks and/or share in any organizations. None of the authors own patents.

Data sharing statement: No additional data are available.

Correspondence to: Antonio Facciorusso, MD, Gastroenterology Unit, Department of Medical Sciences, University of Foggia, Viale L.Pinto, 1, 71100 Foggia, Italy. antonio.facciorusso@virgilio.it
Telephone: +39-881-732154
Fax: +39-881-732135

Received: December 12, 2015
Peer-review started: December 12, 2015
First decision: December 30, 2015
Revised: December 31, 2015
Accepted: January 30, 2016
Article in press: January 30, 2016
Published online: April 28, 2016

Abstract

AIM: To test the correlation between lymphocyte-to-monocyte ratio (LMR) and survival after radiofrequency ablation (RFA) for colorectal liver metastasis (CLMs).

METHODS: From July 2003 to Feb 2012, 127 consecutive patients with 193 histologically-proven unresectable CLMs were treated with percutaneous RFA at the University of Foggia. All patients had undergone primary colorectal tumor resection before RFA and received systemic chemotherapy. LMR was calculated by dividing lymphocyte count by monocyte count assessed at baseline. Treatment-related toxicity was defined as any adverse events occurred within 4 wk after the procedure. Overall survival (OS) and time to recurrence (TTR) were estimated from the date of RFA by Kaplan-Meier with plots and median (95%CI). The inferential analysis for time to event data was conducted using the Cox univariate and multivariate regression model to estimate hazard ratios (HR) and 95%CI. Statistically significant variables from the univariate Cox analysis were considered for the multivariate models.

RESULTS: Median age was 66 years (range 38-88) and patients were prevalently male (69.2%). Median LMR was 4.38% (0.79-88) whereas median number of nodules was 2 (1-3) with a median maximum diameter of 27 mm (10-45). Median OS was 38 mo (34-53) and survival rate (SR) was 89.4%, 40.4% and 33.3% at 1, 4 and 5 years respectively in the whole cohort. Running log-rank test analysis found 3.96% as the most significant prognostic cut-off point for LMR and stratifying the study population by this LMR value median OS resulted 55 mo (37-69) in patients with LMR > 3.96% and 34 (26-39) mo in patients with LMR $\leqslant$ 3.96% (HR = 0.53, 0.34-0.85, P = 0.007). Nodule size and LMR were the only significant predictors for OS in multivariate analysis. Median TTR was 29 mo (22-35) with a recurrence-free survival (RFS) rate of 72.6%, 32.1% and 21.8% at 1, 4 and 5 years, respectively in the whole study group. Nodule size and LMR were confirmed as significant prognostic factors for TTR in multivariate Cox regression. TTR, when stratified by LMR, was 35 mo (28-57) in the group > 3.96% and 25 mo (18-30) in the group $\leqslant$ 3.96% (P = 0.02).

CONCLUSION: Our study provides support for the use of LMR as a novel predictor of outcome for CLM patients.

Key words: Colorectal liver metastasis; Radiofrequency ablation; Survival; Prognosis; Regression

Core tip: This is a retrospective study to test the correlation between baseline lymphocyte-to-monocyte ratio (LMR) and survival outcomes in colorectal liver metastasis patients treated with radiofrequency ablation. Median overall survival (OS) was 55 mo in patients with LMR > 3.96% and 34 mo in patients with LMR $\leqslant$ 3.96% (P = 0.007). Time to recurrence (TTR) was 35 mo in the group > 3.96% and 25 mo in the group $\leqslant$ 3.96% (P = 0.02). Nodule size and LMR were the only significant predictors either for OS and for TTR in multivariate analysis. LMR was useful as clinical predictor of survival outcomes.

Facciorusso A, Del Prete V, Crucinio N, Serviddio G, Vendemiale G, Muscatiello N. Lymphocyte-to-monocyte ratio predicts survival after radiofrequency ablation for colorectal liver metastases. *World J Gastroenterol* 2016; 22(16): 4211-4218 Available from: URL: http://www.wjgnet.com/1007-9327/full/v22/i16/4211.htm DOI: http://dx.doi.org/10.3748/wjg.v22.i16.4211

INTRODUCTION

Colorectal cancer (CRC) is the second cause of cancer-related mortality in developed countries and the third most common malignancy worldwide[1]. Liver resection represents a valuable therapeutic option in patients who develop liver metastases, but unfortunately less than 20% of them is suitable for surgery mainly due to high tumor burden or extrahepatic tumoral disease which render systemic chemotherapy the more appropriate treatment in such cases[2,3]. When the surgical option is unfeasible due to patient comorbidities, unwillingness to undergo surgery or tumor location, local ablation may represent a valuable alternative.

Percutaneous radiofrequency ablation (RFA), an ablative technique which determines coagulation necrosis of the tumor by means of radiofrequency-induced heat, has proved effective in prolonging survival in a number of liver malignancies such as hepatocellular carcinoma (HCC)[4-6], liver metastases from CRC (CLMs)[7], breast[8] and ovarian cancer[9]. Cumulative evidence has demonstrated that inflammatory cells infiltrates in the tumor microenvironment have a large influence on the biological behavior of several malignancies, including HCC[10] and CRC[11]. In particular, macrophages constitute the most represented leukocyte lineage in such infiltrates and are well-known to promote tumor proliferation, neo-angiogenesis and metastasis occurrence[12-15]. As a consequence, immunohistochemical studies have validated the association between high monocyte/macrophage density in the tumoral stroma and unfavorable prognosis in a number of malignancies[10,16].

Several inflammatory bio-markers have been tested in CLMs, among them widely available and easy to use are those obtained from peripheral blood cell count such as neutrophil-to-lymphocyte ratio (NLR) and monocyte level (expressed as percentage) but none of them have been definitively and unequivocally validated[17,18]. Since the pre-operative lymphocyte-to-monocyte ratio (LMR) has been recently found to correlate accurately with clinical outcomes in CLM patients undergoing hepatic resection[19], we decided to test whether this marker exerts a prognostic role and therefore can be considered a predictor of overall survival (OS) and time to recurrence (TTR) in CRC patients with liver metastases treated with percutaneous RFA.

MATERIALS AND METHODS

Patients

From July 2003 to Feb 2012, 127 consecutive patients with 193 histologically-proven CLMs deemed unresectable by consensus of a multidisciplinary team or who refused surgery were treated with percutaneous RFA at the University of Foggia.

All patients had undergone primary colorectal tumor resection before RFA and tumor staging was assessed by multiphasic contrast-enhanced computed tomography (CT) or gadolinium-enhanced magnetic resonance imaging (MRI), according to current guidelines[3].

Inclusion criteria were: (1) confirmed proof of

malignancy of CLM; (2) patients not suitable to surgery (due to comorbidities, unfavorable tumor location or those requiring large/difficult surgery) or who refused liver resection; (3) nodule size < 5 cm; (4) no more than three lesions; (5) complete resection of primary neoplasm and no extrahepatic tumors; (6) platelet count > 40000/ mm^3 and prothrombin time ratio > 40%; and (7) no pre-treatment hematology disease, infection or hyperpyrexia.

All patients received systemic chemotherapy, mostly according to Douillard regimen (irinotecan, leucovorin, and 5-fluorouracil) for four to six cycles[20], as adjuvant treatment. In cases of tumor progression the FOLFOX (folinic acid, fluorouracil, oxaliplatin) regimen was adopted.

The absolute peripheral blood lymphocyte and monocyte counts were derived from the complete blood cell count before RFA, with LMR calculated by dividing lymphocyte count by monocyte count.

This study was approved by our Institutional Review Board for retrospective evaluation of de-identified patients.

Patients were followed up until July 2015 (median 63 mo, 95%CI: 54-71).

Treatment protocol

The technical details of the ablative procedures performed in our center have been described elsewhere[4-6]. Briefly, ultrasound-guided RFA was performed under conscious sedation with a 150W generator (Model 1500 L; RITA Medical System, Mountain View, California), connected to a 15-14-gauge probe with a 2.0-cm-long exposed tip able to deploy seven hooks. The needle was then inserted into the centre of the nodul maintaining the temperature of the tip at 80-110 ℃ for 10-12 min. At the end of the RFA cycle, track ablation was performed in order to prevent tumoral seeding or hemorrhage. In the case of multinodular disease, all nodules were treated in a single session. Aim of the procedure was to achieve complete nodule ablation with a 5 mm safety margin around the target area. All the cycles were performed with no pre-procedural antibiotic or anti-inflammatory drug administration.

Patient monitoring and response evaluation

Patients were followed-up by means of multiphasic CT scan imaging and adverse events were assessed according to Common Terminology Criteria for Adverse Events 4.0[4-6,21] at 1 mo after the procedure and, in the case of complete response, every 4 mo for the first 3 years and at 5-6 mo thereafter. Treatment-related toxicity was defined as any adverse events occurred within 4 wk after the procedure.

Response rate was defined according to commonly accepted criteria recently proposed by a group of experts and complete response was considered the absence of contrast enhancement in the target nodule[22].

When local tumor progression occurred, RFA was re-planned when technically feasible and on the basis of the likelihood of achieving complete response. For those who developed more extensive metastases or extrahepatic disease, systemic chemotherapy was given whenever possible.

Statistical analysis

Categorical variables were expressed as frequencies and percentages and continuous variables as medians and ranges.

OS and TTR were analyzed by Kaplan-Meier method and expressed in terms of median (95%CI).

Candidate predictors of survival outcomes were tested with Cox univariate and multivariate regression test and results were described as hazard ratios (HR) and 95%CI. Only those variables which resulted significant in univariate setting were inserted into multivariate model[23].

Running log-rank test was performed to identify a reliable LMR prognostic cut-off value[24]. With this method, all the observed LMR values were plotted against survival and log-rank test was performed for each value up to the level that covered 90% of the patients. The LMR value with the highest log-rank statistical value was finally chosen as the optimal cutoff point[24].

Furthermore, in order to assess the independence of LMR from other clinical and tumoral markers, linear and logistic regression models correlating this inflammatory index and the main laboratory and tumoral parameters at baseline were built.

The analysis was performed using R Statistical Software (Foundation for Statistical Computing, Vienna, Austria) and significance threshold was established at the 0.05 level (two-sided).

RESULTS

Clinical characteristics of patients

Clinical and demographic characteristics are summarized in Table 1. Median age was 66 years (range 38-88) and patients were prevalently male (69.2%). Median NLR was 1.74% (0.33-13.09) whereas LMR was 4.38% (0.79-88). Median carcinoembryonic antigen (CEA) level was 34.2 ng/mL (1.5-1198). Median number of nodules was 2 (1-3) with a median maximum diameter of 27 mm (10-45). Most metastatic lesions were synchronous (77.1%) and colon was the most common location of the primary tumor (74.8%).

Regression analysis found no significant correlation between LMR and the other clinical and tumoral markers at baseline. In fact, LMR did not correlate with age (rho = -0.21, P = 0.34), NLR (rho = 0.27, P = 0.10), gender (P = 0.49), CEA (rho = 0.19, P = 0.12), max nodule diameter (rho = 0.12, P = 0.31), timing of metastases occurrence (P = 0.24), and performance status (P = 0.62).

Table 1 Baseline characteristics of the study population

Variable	
Age (yr)	66 (38-88)
Gender (M/F)	88 (69.2%)/39 (30.8%)
Absolute lymphocyte count (10^3 cells/μL)	1.77 (0.45-5.98)
Absolute neutrophil count (10^3 cells/μL)	3.29 (0.98-12.17)
Absolute monocyte count (10^3 cells/μL)	0.35 (0.01-2.15)
NLR (%)	1.74 (0.33-13.09)
LMR (%)	4.38 (0.79-88)
CEA (ng/mL)	34.2 (1.5-1198)
Number of Nodules	2 (1-3)
Max diameter (mm)	27 (10-45)
Primary tumor (colon/rectum)	95 (74.8%)/32 (25.2%)
Timing of occurrence (synchronous/metachronous)	98 (77.1%)/29 (22.9%)
ECOG performance status (0/1)	112 (88.1%)/15 (11.9%)

Values are expressed as median (range) or absolute numbers (percentages) when appropriate. NLR: Neutrophil-to-lymphocyte ratio; LMR: Lymphocyte-to-monocyte ratio; CEA: Carcinoembryonic antigen; ECOG: Eastern Cooperative Oncology Group.

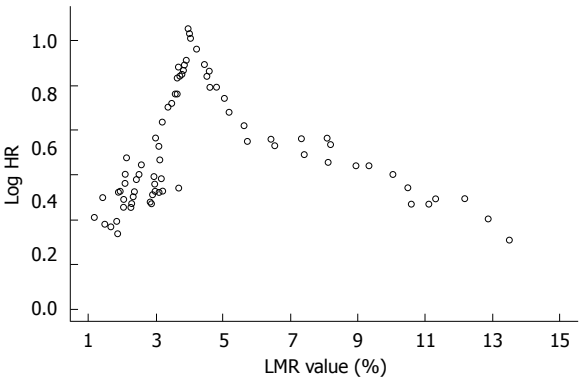

Figure 1 Scatter plot of log Hazard Ratios for overall survival plotted against Lymphocyte-to-neutrophil ratios. The most significant cut-off value LMR was 3.96%. HR: Hazard ratio; LMR: Lymphocyte-to-monocyte ratio.

Tumor response and safety data

Out of 127 treated patients, 115 reached the complete response (90.5%) after the first RFA and the remaining 12 patients needed a second procedure in order to achieve the complete tumor ablation.

Mean number of RFA sessions needed to achieve the complete ablation was 1.09 ± 0.23 with a median time to response of 3 mo (95%CI: 2-4).

No treatment-related deaths nor severe adverse events were observed.

Prognostic cut-off level of LMR

Running log-rank analysis was performed to find a reliable LMR cut-off value able to predict OS as described in Figure 1.

The most significant cut-off value was 3.96%. Stratifying the study population by this cut-off point, median OS resulted 55 mo (37-69) in patients with LMR > 3.96% and 34 (26-39) mo in patients with LMR ⩽ 3.96% (HR = 0.53, 0.34-0.85, P = 0.007) (Figure 2A).

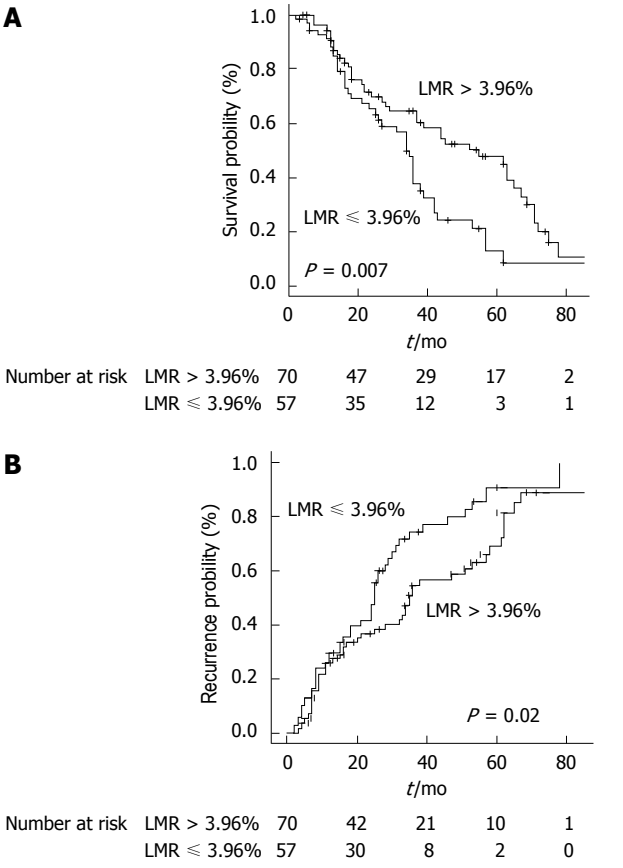

Figure 2 Kaplan-Meier curves. A: Overall survival. Median overall survival resulted 55 mo (37-69) in patients with LMR > 3.96% and 34 (26-39) mo in patients with LMR ⩽ 3.96% (P = 0.007). LMR: Lymphocyte-to-Monocyte Ratio. B: Time to recurrence. Median time to recurrence was 35 mo (28-57) in the group with LMR > 3.96% and 25 mo (18-30) in the group with LMR ⩽ 3.96% (P = 0.02). LMR: Lymphocyte-to monocyte ratio.

As for absolute monocyte count and NLR, the respective cut-off points used in uni/multivariate regression analysis were selected by means of receiver operating characteristic curve (data not shown).

Overall survival

During the study follow-up, 82 patients died.

Median OS was 38 mo (34-53) and survival rate (SR) was 89.4%, 40.4% and 33.3% at 1, 4 and 5 years respectively in the whole cohort.

NLR, LMR, CEA levels, number of nodules and nodule size were found to be predictors of OS in univariate analysis (Table 2). The multivariate Cox analysis restricted the significant predictors of OS to nodule size (P = 0.001) and LMR (P = 0.02) (Table 2).

Tumor recurrence

During the study follow-up, 90 patients experienced tumor recurrence, of which 26 (28.8%) were local recurrences (*i.e.,* in the same liver segment) and 64 (71.2%) new metastases. Median TTR was 29 mo (22-35) with a recurrence-free survival (RFS) rate of 72.6%, 32.1% and 21.8% at 1, 4 and 5 years, respectively.

Table 2 Cox univariate/multivariate regression for overall survival

Variables	Univariate analysis		Multivariate analysis	
	Hazard ratio (95%CI)	*P* value	Hazard ratio (95%CI)	*P* value
Age (reference ⩽ 65 yr)	1.16 (0.68-1.95)	0.39		
Gender (reference F)	1.41 (0.58-3.1)	0.14		
Monocyte ratio (reference ⩽ 5%)	1.38 (0.46-2.78)	0.16		
NLR (reference ⩽ 2.1)	1.62 (0.87-3.64)	0.03	1.48 (0.22- 2.79)	0.14
LMR (reference ⩽ 3.96)	0.53 (0.34-0.85)	0.007	0.49 (0.29-0.96)	0.02
CEA (reference ⩽ 34 ng/mL)	1.83 (1.24-4.07)	0.01	1.38 (1.03-2.54)	0.32
Number of nodules (reference 1)	1.69 (1.13-4.22)	0.02	1.27 (2.02-6.63)	0.48
Max diameter (reference ⩽ 30 mm)	2.1 (1.59-5.1)	0.002	2.49 (1.45-5.46)	0.001
Primary tumor (reference colon)	1.18 (0.46-1.43)	0.34		
Timing (reference synchronous)	1.29 (0.77-1.84)	0.21		
ECOG PS (reference 0)	1.54 (0.94-2.75)	0.09		

NLR: Neutrophil-to-lymphocyte ratio; LMR: Lymphocyte-to-monocyte ratio; CEA: Carcinoembryonic antigen; ECOG: Eastern Cooperative Oncology Group; PS: Performance status.

Table 3 Cox univariate/multivariate regression for time to recurrence

Variables	Univariate analysis		Multivariate analysis	
	HR (95%CI)	*P* value	HR (95%CI)	*P* value
Age (reference ⩽ 65 yr)	1.01 (0.57-1.59)	0.61		
Gender (reference F)	1.29 (0.63-1.91)	0.52		
Monocyte ratio (reference ⩽ 5%)	1.23 (0.47-2.11)	0.45		
NLR (reference ⩽ 2.1)	1.49 (0.88-2.89)	0.04	1.28 (0.21- 4.75)	0.26
LMR (reference ⩽ 3.96)	0.62 (0.40-0.95)	0.02	0.41 (0.25-0.89)	0.01
CEA (reference ⩽ 38 ng/mL)	1.69 (1.04-4.21)	0.02	1.38 (1.12-3.48)	0.22
Number of nodules (reference 1)	1.41 (1.11-3.64)	0.05	1.53 (1.23-3.49)	0.10
Max Diameter (reference ⩽ 30 mm)	2.29 (1.58-5.2)	< 0.001	3.59 (1.86-6.31)	0.003
Primary tumor (reference colon)	1.12 (0.52-1.64)	0.48		
Timing (reference synchronous)	1.21 (0.89-1.75)	0.41		
ECOG PS (reference 0)	1.01 (0.72-1.34)	0.87		

NLR: Neutrophil-to-lymphocyte ratio; LMR: Lymphocyte-to-monocyte ratio; CEA: Carcinoembryonic antigen; ECOG: Eastern Cooperative Oncology Group; PS: Performance status.

NLR, LMR, CEA levels, number of nodules and nodule size resulted predictors of TTR in univariate analysis, but only maximum diameter (P = 0.001) and LMR (P = 0.01) were confirmed in multivariate setting (Table 3).

TTR, when stratified by LMR, was 35 mo (28-57) in the group > 3.96% and 25 mo (18-30) in the group ⩽ 3.96% (P = 0.02) (Figure 2B).

DISCUSSION

RFA represents a valuable therapeutic option for primary and secondary hepatic malignancies in patients unsuitable to surgery or unwilling to undergo major liver resection[3,25].

Because of differences in inclusion criteria, local expertise and use of adjuvant chemotherapy, post-RFA outcomes vary widely between the different published series, with local recurrence rates ranging from 2% to 60%[26,27].

The significant difference in patient outcomes reported throughout the literature has raised an increasing interest on the research and characterization of the main prognostic factors able to influence post-treatment results. Among them, biomarkers of the infiltrating inflammatory microenvironment may represent an important determinant for the clinical outcome in several malignancies such as HCC and CLMs[10,17].

In fact, the immune system plays an important role in cancer as it can destroy cancer cells but also establish the tumor microenvironment that facilitates cancer cell proliferation and metastasis occurrence. Lymphocytes are key immune cells in both humoral and cellular antitumor immune responses while monocytes are recruited into tumors where they alter the tumor microenvironment to promote cancer progression through local immune suppression and angiogenesis[28]. As a consequence high monocyte counts have been reported to be a poor prognostic factor in patients with solid tumors[18,29] and a low LMR, defined as the absolute lymphocyte count divided by the absolute monocyte count, has been proposed as a more reliable predictor of poorer prognosis in a wide range of cancers[30]. Thus a low LMR, which reflects the imbalance in immune response in favor of monocytes/macrophages over lymphocytes, may be responsible of a week antitumor immunity and a favorable micro-

environment for tumor growth.

The interesting results of a recent study seem to support the use of pre-operative LMR as prognostic factor in CLMs patients after liver resection[19] but further studies are needed in order to confirm such findings; furthermore, whether this index may represent a reliable predictor of patients survival in other therapeutic fields such as loco-regional treatments is still unknown.

Therefore, aim of our study was to test the correlation between baseline LMR and survival outcomes in our series of CLM patients treated with RFA. To the best of our knowledge our study is the first report on the prognostic role of this novel inflammatory biomarker in metastatic CRC patients.

In order to exclude any theoretical influence of other tumoral and clinical parameters on LMR values, linear and logistic regression analyses were performed which confirmed the independence of lymphocyte-to-monocyte ratio from other baseline features. Afterwards, since LMR is a continuous variable, all values observed in our population were tested with log-rank analysis as predictors of survival in order to identify an accurate cut-off point aimed at stratifying the whole cohort in two different prognostic groups. The higher HR was obtained using as LMR cut-off level 3.96%.

Noteworthy, the cut-off point found in our analysis is consistent with other reports using LMR as predictor of patients survival in several cancers and this aspect further strengthens and puts our results in line with the current literature[19,30].

Patients presenting a higher pre-treatment LMR beyond the aforementioned cut-off showed significantly better survival outcomes with a median OS of 55 mo (*vs* 34 in patients with LMR $\leqslant$ 3.96%, $P = 0.007$) and median TTR of 35 mo (*vs* 25 in the group $\leqslant$ 3.96%, $P = 0.02$).

Cox multivariate analysis confirmed LMR, together with tumor size, as a significant predictor of either OS and TTR ($P = 0.02$ and 0.01; respectively).

Interestingly, LMR resulted superior to both NLR and absolute monocyte count in prognostic accuracy and this represents one of the most important findings in our study. If confirmed in larger prospective series our results could pave the way to the wide use of this useful and commonly available marker in the clinical field.

With regard to toxicity and tumor response, our results are in keeping with most of the published literature and confirm the effectiveness of RFA in CLM patients[3,26,27].

The main strength of the current study is the novelty of our findings that propose a novel, reliable and easily measurable prognostic factor for CLM patients. Second, our series constitutes one of the largest mono-institutional cohort of CLM patients treated with RFA and gives a further proof of the efficacy and safety of such an ablative technique in this oncological setting. Third, the very long recruitment period allowed us to report long-term data up to 10 years from the treatment. To the best of our knowledge only a minority of clinical papers[26,27] provided so complete and long-term data, which are indeed essential for the proper definition of patient prognosis in colorectal cancer.

On the other hand, our paper presents several limitations. First, the findings of the current study could be weakened by its retrospective design. However, completeness of the database and the long follow-up period allowed us to overcome this limitation. Furthermore, the single-center nature of our experience stands for an homogenous approach to CLM patients and exclude any difference in terms of operator expertise and follow-up accuracy. Second, the lack of an external validation cohort requires further studies in order to consider LMR as a reliable prognostic tool. Moreover, the relatively low number of patients with low LMR did not allow to observe a linear trend of log HR for survival. Therefore, LMR cut-off level we propose needs further confirmation in wider series with a larger range of baseline LMR values. Therefore, our study represents a pivotal report aimed at paving the way to well-designed prospective trials.

In conclusion, our study provides support for the use of a novel predictor of outcome for CLM patients. Hence, LMR should be tested in prospective trials in order to verify its accuracy and validate an unequivocal prognostic cut-off point.

COMMENTS

Background

Colorectal cancer (CRC) is the second cause of cancer-related mortality in developed countries and the third most common malignancy worldwide. Cumulative evidence has demonstrated that inflammatory cells infiltrates in the tumor microenvironment have a large influence on the biological behavior of several malignancies, including CRC. In particular, macrophages constitute the most represented leukocyte lineage in such infiltrates and are well-known to promote tumor proliferation, neo-angiogenesis and metastasis occurrence. As a consequence, immunohistochemical studies have validated the association between high monocyte/macrophage density in the tumoral stroma and unfavorable prognosis in a number of malignancies. Several inflammatory biomarkers have been tested in CRC liver metastases (CLMs), among them widely available and easy to use are those obtained from peripheral blood cell count such as neutrophil-to-lymphocyte ratio (NLR) and monocyte level (expressed as percentage) but none of them have been definitively and unequivocally validated. Since the pre-operative lymphocyte-to-monocyte ratio (LMR) has been recently found to correlate accurately with clinical outcomes in CLM patients undergoing hepatic resection, we decided to test whether this marker exerts a prognostic role in CRC patients with liver metastases treated with percutaneous RFA.

Research frontiers

This study provides support for the use of a novel predictor of outcome for CLM patients. Hence, LMR should be tested in prospective trials in order to verify its accuracy and validate an unequivocal prognostic cut-off point.

Innovations and breakthroughs

The cut-off point found in our analysis (3.96%) is consistent with other reports using LMR as predictor of patients survival in several cancers and this aspect further strengthens and puts the results in line with the current literature. Patients presenting a higher pre-treatment LMR beyond the aforementioned cut-off showed significantly better survival outcomes with a median OS of 55

mo (*vs* 34 in patients with LMR ≤ 3.96%) and median TTR of 35 mo (*vs* 25 in the group ≤ 3.96%). Interestingly, LMR resulted superior to both neutrophil-to-lymphocyte ratio and absolute monocyte count in prognostic accuracy and this represents one of the most important findings in our study. With regard to toxicity and tumor response, our results are in keeping with most of the published literature and confirm the effectiveness of RFA in CLM patients.

Applications

This study provides support for the use of LMR as a novel predictor of outcome for CLM patients treated with RFA. If a patient has a baseline LMR > 3.96%, it will show better survival outcomes after RFA.

Peer-review

Very good and interesting study focusing on use of biomarkers used to predict efficacy of locoregional treatment. Methodology appears to be correct, the rationale of the study is convincing, and results are useful in clinical practice.

REFERENCES

1 **Siegel RL**, Miller KD, Jemal A. Cancer statistics, 2015. *CA Cancer J Clin* 2015; **65**: 5-29 [PMID: 25559415 DOI: 10.3322/caac.21254]

2 **Kornprat P**, Jarnagin WR, Gonen M, DeMatteo RP, Fong Y, Blumgart LH, D'Angelica M. Outcome after hepatectomy for multiple (four or more) colorectal metastases in the era of effective chemotherapy. *Ann Surg Oncol* 2007; **14**: 1151-1160 [PMID: 17195913]

3 **Gillams A**, Goldberg N, Ahmed M, Bale R, Breen D, Callstrom M, Chen MH, Choi BI, de Baere T, Dupuy D, Gangi A, Gervais D, Helmberger T, Jung EM, Lee F, Lencioni R, Liang P, Livraghi T, Lu D, Meloni F, Pereira P, Piscaglia F, Rhim H, Salem R, Sofocleous C, Solomon SB, Soulen M, Tanaka M, Vogl T, Wood B, Solbiati L. Thermal ablation of colorectal liver metastases: a position paper by an international panel of ablation experts, The Interventional Oncology Sans Frontières meeting 2013. *Eur Radiol* 2015; **25**: 3438-3454 [PMID: 25994193 DOI: 10.1007/s00330-015-3779-z]

4 **Facciorusso A**, Del Prete V, Antonino M, Neve V, Amoruso A, Crucinio N, Di Leo A, Barone M. Conditional survival analysis of hepatocellular carcinoma patients treated with radiofrequency ablation. *Hepatol Res* 2015; **45**: E62-E72 [PMID: 25472869 DOI: 10.1111/hepr.12458]

5 **Facciorusso A**, Del Prete V, Antonino M, Crucinio N, Neve V, Di Leo A, Carr BI, Barone M. Post-recurrence survival in hepatocellular carcinoma after percutaneous radiofrequency ablation. *Dig Liver Dis* 2014; **46**: 1014-1019 [PMID: 25085684 DOI: 10.1016/j.dld.2014.07.012]

6 **Facciorusso A**, Del Prete V, Crucinio N, Muscatiello N, Carr BI, Di Leo A, Barone M. Angiotensin receptor blockers improve survival outcomes after radiofrequency ablation in hepatocarcinoma patients. *J Gastroenterol Hepatol* 2015; **30**: 1643-1650 [PMID: 25974743 DOI: 10.1111/jgh.12988]

7 **Wong SL**, Mangu PB, Choti MA, Crocenzi TS, Dodd GD, Dorfman GS, Eng C, Fong Y, Giusti AF, Lu D, Marsland TA, Michelson R, Poston GJ, Schrag D, Seidenfeld J, Benson AB. American Society of Clinical Oncology 2009 clinical evidence review on radiofrequency ablation of hepatic metastases from colorectal cancer. *J Clin Oncol* 2010; **28**: 493-508 [PMID: 19841322 DOI: 10.1200/JCO.2009.23.4450]

8 **Lee HY**, Ko HK, Kim SH, Lee KS, Ro J, Park IH. Percutaneous radiofrequency ablation for liver metastases in breast cancer patients. *Breast J* 2013; **19**: 563-565 [PMID: 24073730 DOI: 10.1111/tbj.12170]

9 **Gervais DA**, Arellano RS, Mueller PR. Percutaneous radiofrequency ablation of ovarian cancer metastasis to the liver: indications, outcomes, and role in patient management. *AJR Am J Roentgenol* 2006; **187**: 746-750 [PMID: 16928940]

10 **Lin ZX**, Ruan DY, Li Y, Wu DH, Ma XK, Chen J, Chen ZH, Li X, Wang TT, Lin Q, Wen JY, Wu XY. Lymphocyte-to-monocyte ratio predicts survival of patients with hepatocellular carcinoma after curative resection. *World J Gastroenterol* 2015; **21**: 10898-10906 [PMID: 26478681 DOI: 10.3748/wjg.v21.i38.10898]

11 **Song A**, Eo W, Lee S. Comparison of selected inflammation-based prognostic markers in relapsed or refractory metastatic colorectal cancer patients. *World J Gastroenterol* 2015; **21**: 12410-12420 [PMID: 26604648 DOI: 10.3748/wjg.v21.i43.12410]

12 **Allavena P**, Sica A, Solinas G, Porta C, Mantovani A. The inflammatory micro-environment in tumor progression: the role of tumor-associated macrophages. *Crit Rev Oncol Hematol* 2008; **66**: 1-9 [PMID: 17913510 DOI: 10.1016/j.critrevonc.2007.07.004]

13 **Facciorusso A**, Licinio R, Carr BI, Di Leo A, Barone M. MEK 1/2 inhibitors in the treatment of hepatocellular carcinoma. *Expert Rev Gastroenterol Hepatol* 2015; **9**: 993-1003 [PMID: 25915713 DOI: 10.1586/17474124.2015.1040763]

14 **Facciorusso A**, Antonino M, Del Prete V, Neve V, Scavo MP, Barone M. Are hematopoietic stem cells involved in hepatocarcinogenesis? *Hepatobiliary Surg Nutr* 2014; **3**: 199-206 [PMID: 25202697 DOI: 10.3978/j.issn.2304-3881.2014.06.02]

15 **Facciorusso A**. The influence of diabetes in the pathogenesis and the clinical course of hepatocellular carcinoma: recent findings and new perspectives. *Curr Diabetes Rev* 2013; **9**: 382-386 [PMID: 23845075]

16 **Liu T**, Fang XC, Ding Z, Sun ZG, Sun LM, Wang YL. Pre-operative lymphocyte-to-monocyte ratio as a predictor of overall survival in patients suffering from osteosarcoma. *FEBS Open Bio* 2015; **5**: 682-687 [PMID: 26380812 DOI: 10.1016/j.fob.2015.08.002]

17 **Chang Z**, Zheng J, Ma Y, Zhao J, Wang C, Liu Z. The neutrophil-to-lymphocyte ratio as a predictor for recurrence of colorectal liver metastases following radiofrequency ablation. *Med Oncol* 2014; **31**: 855 [PMID: 24477649 DOI: 10.1007/s12032-014-0855-1]

18 **Haruki K**, Shiba H, Fujiwara Y, Furukawa K, Wakiyama S, Ogawa M, Ishida Y, Misawa T, Yanaga K. Perioperative change in peripheral blood monocyte count may predict prognosis in patients with colorectal liver metastasis after hepatic resection. *J Surg Oncol* 2012; **106**: 31-35 [PMID: 22231029 DOI: 10.1002/jso.23033]

19 **Neofytou K**, Smyth EC, Giakoustidis A, Khan AZ, Williams R, Cunningham D, Mudan S. The Preoperative Lymphocyte-to-Monocyte Ratio is Prognostic of Clinical Outcomes for Patients with Liver-Only Colorectal Metastases in the Neoadjuvant Setting. *Ann Surg Oncol* 2015; **22**: 4353-4362 [PMID: 25773876 DOI: 10.1245/s10434-015-4481-8]

20 **Douillard JY**, Cunningham D, Roth AD, Navarro M, James RD, Karasek P, Jandik P, Iveson T, Carmichael J, Alakl M, Gruia G, Awad L, Rougier P. Irinotecan combined with fluorouracil compared with fluorouracil alone as first-line treatment for metastatic colorectal cancer: a multicentre randomised trial. *Lancet* 2000; **355**: 1041-1047 [PMID: 10744089]

21 **Facciorusso A**, Di Maso M, Antonino M, Del Prete V, Panella C, Barone M, Muscatiello N. Polidocanol injection decreases the bleeding rate after colon polypectomy: a propensity score analysis. *Gastrointest Endosc* 2015; **82**: 350-358.e2 [PMID: 25910664 DOI: 10.1016/j.gie.2015.01.003]

22 **Ahmed M**, Solbiati L, Brace CL, Breen DJ, Callstrom MR, Charboneau JW, Chen MH, Choi BI, de Baère T, Dodd GD, Dupuy DE, Gervais DA, Gianfelice D, Gillams AR, Lee FT, Leen E, Lencioni R, Littrup PJ, Livraghi T, Lu DS, McGahan JP, Meloni MF, Nikolic B, Pereira PL, Liang P, Rhim H, Rose SC, Salem R, Sofocleous CT, Solomon SB, Soulen MC, Tanaka M, Vogl TJ, Wood BJ, Goldberg SN. Image-guided tumor ablation: standardization of terminology and reporting criteria--a 10-year update. *J Vasc Interv Radiol* 2014; **25**: 1691-705.e4 [PMID: 25442132 DOI: 10.1016/j.jvir.2014.08.027]

23 **Facciorusso A**, Mariani L, Sposito C, Spreafico C, Bongini M, Morosi C, Cascella T, Marchianò A, Camerini T, Bhoori S, Brunero F, Barone M, Mazzaferro V. Drug-eluting beads versus conventional chemoembolization for the treatment of unresectable hepatocellular carcinoma. *J Gastroenterol Hepatol* 2016; **31**: 645-653 [PMID: 26331807 DOI: 10.1111/jgh.13147]

24 **Facciorusso A**, Del Prete V, Antonino M, Neve V, Crucinio N, Di Leo A, Carr BI, Barone M. Serum ferritin as a new prognostic factor in hepatocellular carcinoma patients treated with radiofrequency

ablation. *J Gastroenterol Hepatol* 2014; **29**: 1905-1910 [PMID: 24731153 DOI: 10.1111/jgh.12618]

25 **Facciorusso A**, Di Maso M, Muscatiello N. Microwave ablation versus radiofrequency ablation for the treatment of hepatocellular carcinoma: A systematic review and meta-analysis. *Int J Hyperthermia* 2016; 1-6 [PMID: 26794414]

26 **Solbiati L**, Ahmed M, Cova L, Ierace T, Brioschi M, Goldberg SN. Small liver colorectal metastases treated with percutaneous radiofrequency ablation: local response rate and long-term survival with up to 10-year follow-up. *Radiology* 2012; **265**: 958-968 [PMID: 23091175 DOI: 10.1148/radiol.12111851]

27 **Shady W**, Petre EN, Gonen M, Erinjeri JP, Brown KT, Covey AM, Alago W, Durack JC, Maybody M, Brody LA, Siegelbaum RH, D' Angelica MI, Jarnagin WR, Solomon SB, Kemeny NE, Sofocleous CT. Percutaneous Radiofrequency Ablation of Colorectal Cancer Liver Metastases: Factors Affecting Outcomes-A 10-year Experience at a Single Center. *Radiology* 2016; **278**: 601-611 [PMID: 26267832]

28 **Chanmee T**, Ontong P, Konno K, Itano N. Tumor-associated macrophages as major players in the tumor microenvironment. *Cancers* (Basel) 2014; **6**: 1670-1690 [PMID: 25125485 DOI: 10.3390/cancers6031670]

29 **Lee SD**, Kim SH, Kim YK, Lee SA, Park SJ. Prognostic significance of preoperative peripheral blood monocyte ratio in patients with hepatocellular carcinoma. *World J Surg* 2014; **38**: 2377-2385 [PMID: 24692003 DOI: 10.1007/s00268-014-2545-8]

30 **Nishijima TF**, Muss HB, Shachar SS, Tamura K, Takamatsu Y. Prognostic value of lymphocyte-to-monocyte ratio in patients with solid tumors: A systematic review and meta-analysis. *Cancer Treat Rev* 2015; **41**: 971-978 [PMID: 26481060 DOI: 10.1016/j.ctrv.2015.10.003]

P- Reviewer: Chen F, Lassandro F **S- Editor**: Qi Y
L- Editor: A **E- Editor**: Wang CH

World Journal of Gastroenterology

Submit a Manuscript: http://www.wjgnet.com/esps/
Help Desk: http://www.wjgnet.com/esps/helpdesk.aspx
DOI: 10.3748/wjg.v22.i16.4219

World J Gastroenterol 2016 April 28; 22(16): 4219-4225
ISSN 1007-9327 (print) ISSN 2219-2840 (online)

ORIGINAL ARTICLE

Retrospective Study

Predictors of poor outcome in gastrointestinal bleeding in emergency department

Ender Kaya, Mehmet Ali Karaca, Deniz Aldemir, M Mahir Ozmen

Ender Kaya, Dr. Nafiz Korez State Hospital, Sincan 06932, Ankara, Turkey

Mehmet Ali Karaca, Deniz Aldemir, Emergency Medicine Department, Faculty of Medicine, Hacettepe University, Sihhiye 06100, Ankara, Turkey

M Mahir Ozmen, General Surgery Department, Faculty of Medicine, Hacettepe University, Sihhiye 06100, Ankara, Turkey

Author contributions: Kaya E and Karaca MA contributed equally to planning the study, collecting and analyzing the data, and drafting the manuscript; Aldemir D contributed in collecting the data; Ozmen MM revised the manuscript for important intellectual content.

Conflict-of-interest statement: The authors have no commercial association or sources of support that might pose a conflict interest.

Correspondence to: Mehmet Ali Karaca, MD, Emergency Medicine Department, Faculty of Medicine, Hacettepe University, Sihhiye 06100, Ankara, Turkey. mehmetalikaraca@gmail.com
Telephone: +90-532-5918202
Fax: +90-312-3052512

Received: December 3, 2015
Peer-review started: December 4, 2015
First decision: January 28, 2016
Revised: February 10, 2016
Accepted: March 1, 2016
Article in press: March 2, 2016
Published online: April 28, 2016

Abstract

AIM: To determine the prognostic risk factors of gastrointestinal bleeding in emergency department cases.

METHODS: The trial was a retrospective single-center study involving 600 patients over 18-years-old and carried out with approval by the Institutional Ethics Committee. Patient data included demographic characteristics, symptoms at admission, past medical history, vital signs, laboratory results, endoscopy and colonoscopy results, length of hospital stay, need of intensive care unit (ICU) admission, and mortality. Mortality rate was the principal endpoint of the study, while duration of hospital stay, required interventional treatment, and admission to the ICU were secondary endpoints.

RESULTS: The mean age of patients was 61.92-years-old. Among the 600 total patients, 363 (60.5%) underwent upper gastrointestinal endoscopy and the most frequent diagnoses were duodenal ulcer (19.2%) and gastric ulcer (12.8%). One-hundred-and-fifteen (19.2%) patients required endoscopic treatment, 20 (3.3%) required surgical treatment, and 5 (0.8%) required angiographic embolization. The mean length of hospital stay was 5.21 ± 5.85 d. The mortality rate was 6.3%. The ICU admission rate was 5.3%. Patients with syncope, higher blood glucose levels, and coronary artery disease had significantly higher ICU admission rates (P = 0.029, P = 0.043, and P = 0.002, respectively). Patients with low thrombocyte levels, high creatinine, high international normalized ratio, and high serum transaminase levels had significantly longer hospital stay (P = 0.02, P = 0.001, P = 0.019, and P = 0.005, respectively). Patients who died had significantly higher serum blood urea nitrogen and creatinine levels (P = 0.016 and P = 0.038), and significantly lower mean blood pressure and oxygen saturation (P = 0.004 and P = 0.049). Malignancy and low Glasgow coma scale (GCS) were independent predictive factors of mortality.

CONCLUSION: Prognostic factors for gastrointestinal bleeding in emergency room cases are malignancy, hypotension on admission, low GCS, and impaired kidney function.

Key words: Gastrointestinal bleeding; Poor prognosis; Mortality; Emergency department; Kidney function; Malignancy

Core tip: Early diagnosis and identification of patients at high risk of poor prognosis with gastrointestinal bleeding may increase survival rates. Identification of factors associated with prognosis based upon findings at admission to the emergency department will help to improve management of patients with gastrointestinal bleeding.

Kaya E, Karaca MA, Aldemir D, Ozmen MM. Predictors of poor outcome in gastrointestinal bleeding in emergency department. *World J Gastroenterol* 2016; 22(16): 4219-4225 Available from: URL: http://www.wjgnet.com/1007-9327/full/v22/i16/4219.htm DOI: http://dx.doi.org/10.3748/wjg.v22.i16.4219

INTRODUCTION

Gastrointestinal (GI) bleeding is one of the clinical conditions that results in approximately 7000 admissions to emergency medicine departments (EDs) annually[1]. Acute GI bleeding can be life threatening in some patients, and the overall rate of mortality for patients admitted with acute GI bleeding has been reported at 7% to 8.2%[1]. Moreover, a large proportion of these patients (reported at 19% to 28%) are admitted and monitored in the intensive care unit (ICU)[2]. Determining the clinical variables that will facilitate identification of patients with GI bleeding, who are at high risk for poor prognosis, may aid in improving initial triage as well as the timing of primary endoscopic hemostasis and the management of therapy[2]. In addition, identifying those patients who are at low risk (*i.e.*, those with minor bleeding) will allow for their treatment as outpatients[3].

The aim of this study was to determine risk factors of patients with GI bleeding upon admission to the emergency department in order to improve triaging of the patients according to high risk for mortality and needs for ICU hospitalization, longer hospital stay, and surgical treatment.

MATERIALS AND METHODS

Data collection

This trial was carried out as a retrospective single-center study performed in the ED setting. All adult patients (18 years or older) who were admitted to the ED at Hacettepe University Faculty of Medicine (Ankara, Turkey) between January 1, 2001 and December 31, 2010 were identified from the hospital database using ICD-10 codes. Each patient's medical records were obtained with approval by the institutional ethics committee (IRB No. 410.01-907). Those patients who had been transferred from other centers with a diagnosis of GI bleeding, those whose GI bleeding started after admission, and those with inadequate data in their medical records were excluded from the study.

Patient data collected for analysis included demographic characteristics, health-related complaints, medical history, vital signs, laboratory values, endoscopy and colonoscopy results, duration of follow-up, and mortality. Mortality rate was the principal endpoint of the study. Duration of hospital stay, required interventional treatment, and admission to the ICU were secondary endpoints.

Statistical analysis

The SPSS, version 18.0, was used for data analysis. Inter-group (2 groups) comparison was carried out using the independent samples *t*-test, χ^2 test, and Fisher's χ^2 analysis. Multiple (> 2) group comparison was carried out using one-way analysis of variance (ANOVA) with averaged values. To determine which group was responsible for differences found in the ANOVA results, the Tukey's honest significant difference test was used. Relationship between categorical variables was assessed by χ^2 analysis, and relationship between quantitative measurements was assessed by Pearson's correlation analysis. A P value of < 0.05 was considered statistically significant.

RESULTS

A total of 721 patients with GI bleeding symptoms had been admitted to the ED between January 1, 2001 and December 31, 2010. Of those, 600 patients met the inclusion criteria and were included in the study. Of the 121 patients that were excluded, 38 had been transferred from another hospital, 42 had GI bleeding that occurred in-hospital, and 41 had incomplete data. The mean age of the included patients was 61.92 years (male: 60.83 ± 25.34, female: 63.66 ± 17.93). The demographic and clinical features of the study population are shown in Table 1.

Of the 600 total patients, 86.7% had at least one comorbid disease, with the most frequent being hypertension (28.3%), diabetes mellitus (15.5%), and coronary artery disease (15.2%).

Of the 600 total patients, 60.5% underwent upper gastrointestinal endoscopy, with the most frequent pathological diagnoses being duodenal ulcer (19.2%) and gastric ulcer (12.8%). Normal endoscopic results were reported in 10.2% of the patients. Esophageal

Table 1 Demographic and clinical characteristics of patients

Characteristic	*n*
Sex	
Male	369
Female	231
Admission symptoms	
Melena	423
Hematemesis	142
Hematochezia	76
Syncope	34
Systolic blood pressure (mmHg)	
< 90	26
90-139	546
⩾ 140	28
Diastolic blood pressure (mmHg)	
< 60	55
60-89	539
⩾ 90	6
Heart rate (bpm)	
< 60	2
60-100	448
> 100	150
Respiratory rate (rpm)	
12-20	545
> 20	55
Oxygen saturation (%)	
< 92	14
⩾ 92	586
Glasgow coma score	
< 15	21
15	579

Mean values: Blood pressure, 82.8 ± 13.1 mmHg; Systolic blood pressure, 110.2 ± 18.2 mmHg; Diastolic blood pressure, 69.2 ± 11.8 mmHg; Heart rate, 92.7 ± 18.37 bpm; Respiratory rate, 18.2 ± 2.6 rpm; SaO_2, 95.15% ± 1.66%; Glasgow coma score, 14.93 ± 0.45.

pathologies, such as esophageal varices (4.9%) and esophagitis (1.7%), were detected in 7.7% of the patients who underwent upper gastrointestinal endoscopy. Forrest classifications[4] of endoscopic findings are given in Table 2.

Of the 600 total patients, 7.5% underwent colonoscopy, with 44.4% of those having normal colonoscopic findings and anal pathologies being the most frequently detected diagnoses (20.0%). Furthermore, active bleeding was observed in 6.7% of the patients during colonoscopy (Table 3).

Of the 600 total patients, 76.7% received medical treatment, with 19.2% requiring endoscopy, 3.3% requiring surgery, and 0.8% requiring angiographic embolization. Endoscopic treatments included sclerotherapy, laser treatment, argon plasma coagulation, and mechanical interventions such as hemoclips.

For the 600 total patients, the most frequent admission symptoms were hematemesis (30.3%), melena (20.1%), hematochezia (15.8%), and syncope (29.4%). Rate of interventional treatment, including endoscopic, surgery and angiographic embolization, was significantly higher for the patients with hematemesis than for the patients with other admission symptoms (P = 0.002). In addition, patients with elevated levels of blood urea nitrogen (BUN; ⩾ 23 mg/dL) had a higher interventional treatment rate than the patients treated with medical therapy (23.9% *vs* 13.9%, P = 0.006). Statistical analyses of the patients that required interventional therapy showed non-significant differences regarding comorbidities; specifically, the interventional therapy rate was 22.9% for patients with chronic hepatic disease, 27.4% for patients with peptic ulcer, 21.1% for patients with malignancy, 14.3% for patients with bleeding diathesis, 17.6% for patients with hypertension, 21.5% for patients with diabetes mellitus, and 22.0% for patients with coronary artery disease (all P > 0.05).

Patients that required erythrocyte suspension replacement had higher surgery rates than patients that did not require erythrocyte replacement (4.8% *vs* 1.7%; P = 0.03), while surgery rates did not differ in patients between fresh frozen plasma replaced (FFP) and non-replaced groups (4.3% *vs* 3.1%, P = 0.561). The laboratory values of patients for whom surgery was required are given in Table 4. Comorbidities and admission symptoms were not significantly associated with the treatment modality.

Of the 600 patients, 5.3% were treated in the ICU, including 14.7% of the patients who presented with syncope (P = 0.029), 2.1% of those with hematemesis (P = 0.051), 5.7% of those with melena (P = 0.560), and 5.3% of those with hematochezia (P = 0.971). The ICU admission rate was significantly higher in patients with syncope (14.7%, P = 0.029). The ICU admission rate was higher in patients with diabetes mellitus than non diabetes mellitus (9.7% *vs* 4.5%, P = 0.043). Also the ICU admission rate for patients with coronary artery diseases was higher than for patients who did not have coronary artery diseases (12.1% *vs* 4.1%, P = 0.002).

The laboratory results and vital signs of patients who were treated in the general wards/ED as compared to those treated in the ICU are presented in Table 5. Patients who were treated in the general wards/ED or ICU showed no statistically significant differences in systolic blood pressure, diastolic blood pressure, heart rate, Glasgow coma scale (GCS), or oxygen saturation (SpO_2). However, serum glucose levels were higher in the ICU admission group than in the patients treated in general wards/ED (171.47 mg *vs* 144.53 mg, P = 0.05).

For the 600 study patients, the mean length of hospital stay was 5.21 ± 5.85 d. Patients with comorbid diseases had a longer length of hospital stay than patients without comorbidities (5.52 d *vs* 3.16 d, P < 0.001). There were no statistical differences between admission symptoms and length of hospital stay. Patients with low thrombocyte level (< 150000/L), high creatinine level (> 1.2 mg/dL), high international normalized ratio (INR) (> 1.5), and high serum transaminase levels (AST, ALT) had significantly longer hospital stay than the patients with normal thrombocyte, creatinine, INR and serum transaminase level (P = 0.02, P = 0.001, P = 0.019, P = 0.005,

Table 2 Upper endoscopy results, treatment modalities and mortality rates

Forrest classification[4]	*n* (%)	Medical treatment	Endoscopic treatment[1]	Surgery	Angiographic embolization	Exitus
Spurting hemorrhage (1a)	41 (12.2)	0	39	0	2	0
Oozing hemorrhage (1b)	41 (12.2)	0	39	2	0	2
Visible vessel (2a)	16 (4.8)	2	13	1	0	1
Adherent clot (2b)	16 (4.8)	5	9	2	0	1
Flat pigmented hematin on ulcer base (2c)	3 (0.9)	3	0	0	0	0
Lesions without signs of recent hemorrhage/ fibrin-covered clean ulcer base (3)	218 (65.1)	216	0	2[2]	0	2[3]
Total	335 (100)	226	100	7	2	6

[1]Sclerotherapy, laser, argon plasma coagulation, mechanical modalities; [2]Patients who underwent surgery due to gastric malignancy; [3]Causes of mortality include septic shock and pneumonia; Forrest classification is a classification that attempt to standardize the characterization of peptic ulcers.

Table 3 Colonoscopy findings, treatment modality, and mortality rates

Colonoscopic findings	*n* (%)	Active bleeding -	Active bleeding +	Medical treatment	Endoscopic treatment	Surgery	Angiographic embolization	Exitus
Normal findings	20 (44.4)	20	0	19	0	0	0	1[1]
Anal pathologies	9 (20.0)	9	0	7	0	2	0	0
Recto-sigmoid pathologies	7 (15.6)	5	2	5	0	1	1	0
Other colon pathologies	4 (8.9)	3	1	3	1	0	1	0
Other pathologies	5 (11.1)	5	0	4	1	0	0	0
Total	45 (100)	42	3	38	2	3	2	1

[1]Cause of mortality was septic shock.

Table 4 Laboratory results and treatment modalities

	Medical treatment	Endoscopic treatment	Angiographic embolization	Surgery	*P* value
Hb (g/dL)	9.92	9.74	8.32	8.85	0.283
Htc (g/dL)	29.12	28.61	24.82	25.85	0.273
Thrombocytes (10^3/L)	251.59	272.61	282.40	291.95	0.162
BUN (mg/dL)	38.57	37.73	33.60	35.06	0.177
Creatinine (mg/dL)	1.15	1.07	1.17	1.07	0.864
Glucose, (mg/dL)	144.25	148.50	173.40	164.05	0.539
AST (IU/L)	33.59	24.33	66.20	59.75	0.635
ALT (IU/L)	26.10	20.21	62.80	29.25	0.825
aPTT (s)	31.36	26.92	31.80	26.83	0.818
INR (s)	2.22	1.59	2.40	2.25	0.831
Mean blood pressure (mmHg)	83.74	81.47	75.33	72.83	0.001
Pulse (bpm)	91.81	95.04	108.00	98.05	0.043

Data represent mean values. Hb: Hemoglobin; Htc: Hematocrit; BUN: Blood urea nitrogen; AST: Aspartate aminotransferase; ALT: Alanine aminotransferase; aPTT: Active partial thromboplastin; INR: International normalization ratio.

respectively).

The overall mortality rate of the total 600 patients was 6.3%, with 20 patients dying in the ED, 7 in the general wards, and 11 in the ICU. Eight patients died within 48 hours of admission. The mean age of the patients that survived was 61.53 ± 23.16 years and of the patients who died was 67.74 ± 15.70 years (P = 0.027). Univariate analysis of the clinical risk factors for mortality showed no statistically significant differences in sex or admission symptoms. However, serum BUN and creatinine levels were significantly higher, and mean blood pressure and $Sp0_2$ were significantly lower for the patients who died compared to those who survived (respectively 46.39 mg/dL *vs* 36.24 mg/dL, P = 0.016; 1.65 mg/dL *vs* 1.10 mg/dL, P = 0.038; 76.92 mmHg *vs* 83.28 mmHg, P = 0.004; 94.63% *vs* 95.18%, P = 0.049). Malignancy was the independent predictive factor of mortality for the patients included in the study (P < 0.001). On the other hand, none of the patients with a previous history of peptic ulcer became exitus in this study group (P = 0.014). Lower GCS was independently correlated with increased mortality (P < 0.001). The analyses of surviving patients' data and mortality are shown in Tables 6 and 7.

For the exitus group, GI endoscopy was performed in 21.1% of the patients and upper endoscopy and colonoscopy was performed in only 2.6%. The

Table 5 Comparison of laboratory results according to departments of admission

	General wards/ED	ICU	*P* value
Hb (g/dL)	9.89	8.82	0.051
Htc (g/dL)	29.04	25.96	0.054
Thrombocytes (10^3/L)	254.87	298.88	0.086
BUN (mg/dL)	36.86	37.38	0.909
Creatinine (mg/dL)	1.13	1.18	0.787
Glucose (mg/dL)	144.53	171.47	0.050
AST (IU/L)	33.21	106.59	0.131
ALT (IU/L)	24.63	88.81	0.238
aPTT (s)	30.57	28.36	0.402
INR (s)	2.11	2.61	0.370
Mean blood pressure (mmHg)	83.09	79.11	0.097
Pulse (bpm)	92.73	93.56	0.803
SpO_2 (%)	95.16	94.96	0.467

Data represent mean values. Hb: Hemoglobin; Htc: Hematocrit; BUN: Blood urea nitrogen; AST: Aspartate aminotransferase; ALT: Alanine aminotransferase; aPTT: Active partial thromboplastin; INR: International normalization ratio; ICU: Intensive care unit; ED: Emergency medicine department.

Table 6 Comparison of laboratory results for surviving and exitus patients

	Surviving	Exitus	*P* value
Hb (g/dL)	9.85	9.63	0.072
Htc (g/dL)	28.90	28.54	0.085
Thrombocytes (10^3/L)	259.06	230.05	0.280
BUN (mg/dL)	36.24	46.39	0.016
Creatinine (mg/dL)	1.10	1.65	0.038
Glucose (mg/dL)	144.56	166.76	0.268
AST (IU/L)	33.06	97.29	0.150
ALT (IU/L)	26.53	50.58	0.061
aPTT (s)	30.45	30.43	0.991
INR (s)	2.18	1.99	0.072
Mean blood pressure (mmHg)	83.28	76.92	0.004
Pulse (bpm)	92.51	96.68	0.175
SpO_2 (%)	95.18	94.63	0.049

Data represent mean values. Hb: Hemoglobin; Htc: Hematocrit; BUN: Blood urea nitrogen; AST: Aspartate aminotransferase; ALT: Alanine aminotransferase; aPTT: Active partial thromboplastin; INR: International normalization ratio.

diagnoses made from upper GI endoscopy included esophageal varices (25.0%), gastritis (25.0%), gastric ulcer (12.5%), and duodenal ulcer (37.5%). Colonoscopy results were normal for all patients in the exitus group. Endoscopic procedures were not performed in 30 of the patients due to hemodynamic instability (60.0%), high INR (13.3%), and refusal to accept the endoscopic procedure (26.6%). Causes of mortality are listed in Table 8, and malignancy was the most noted concomitant cause of mortality.

DISCUSSION

Acute GI bleeding is a frequent cause of mortality and morbidity. Optimal management of patients and prognostic factors have been defined in guidelines

Table 7 Comparison of surviving and exitus patient history, need for transfusion, and mortality *n* (%)

	Surviving	Exitus	*P* value
Medical history	562 (93.7)	38 (6.3)	
Liver disease			
+	42 (87.5)	6 (12.5)	0.730
-	520 (94.2)	32 (5.8)	
Peptic ulcer			
+	62 (100)	0 (0.0)	0.014
-	500 (92.9)	38 (7.1)	
Malignancy			
+	64 (84.2)	12 (15.8)	0.001
-	498 (95.0)	26 (5.0)	
Bleeding diathesis			
+	7 (100)	0 (0.0)	0.631
-	555 (93.6)	38 (6.4)	
Anal disease			
+	9 (100)	0 (0.0)	0.553
-	553 (93.6)	38 (6.4)	
Hypertension			
+	164 (96.5)	6 (3.5)	0.051
-	398 (92.6)	32 (7.4)	
Diabetes mellitus			
+	86 (92.5)	7 (7.5)	0.373
-	476 (93.9)	31 (6.1)	
Coronary artery disease			
+	85 (93.4)	6 (6.6)	0.530
-	477 (93.7)	32 (6.3)	
Comorbid disease			
+	77 (96.3)	3 (3.8)	0.227
-	485 (93.3)	35 (6.7)	
ES replacement			
+	291 (93.3)	21 (6.7)	0.400
-	271 (94.1)	17 (5.9)	
FFP replacement			
+	106 (92.2)	456 (94)	0.290
-	9 (7.8)	29 (6.0)	
GCS			
15	549 (94.8)	30 (5.2)	0.000
< 15	13 (61.9)	8 (38.1)	

ES: Erythrocyte suspension; FFP: Fresh frozen plasma; GCS: Glasgow coma score.

and previous trials for both upper and lower GI bleeding. Nonetheless, no studies in the literature to date have adequately examined all the prognostic factors of GI bleeding. To the best of our knowledge, the study described herein is one of the largest studies to have analyzed the prognostic factors of all adult patients with GI bleeding presenting to an ED. The results indicate that having a concomitant malignancy, decreased GCS, decreased mean arterial blood pressure, increased serum creatinine level, or increased BUN level is associated with increased mortality rate.

More than half of patients with GI bleeding have a comorbid disease and according to the literature the most frequent of these diseases are hypertension, diabetes mellitus, coronary artery diseases, malignancies, and hepatic diseases[5-7]. Clinical guidelines published in 2008 in Scotland cited a mortality rate of 4% in GI bleeding patients without comorbidities, with the mortality rate increasing

Table 8 Causes of mortality

Causes of mortality	*n* (%)
Malignancy[1]	14 (36.8)
Esophageal varices bleeding	8 (21.1)
Sepsis/septic shock	6 (15.8)
Renal failure	4 (10.5)
Multi organ failure	3 (7.9)
Others[2]	3 (7.9)
Total	38 (100)

[1]Gastric cancer, esophageal adenocancer, hepatocellular carcinoma; [2]Anticoagulant therapy for venous thromboembolism, mesenteric ischemia.

1.8 times in cases with heart failure, 3.8 times in cases with malignancy, and 2.0 times in cases with liver disease[1]. According to the National Institute for Health and Clinical Excellence 2012 guidelines, patients with GI bleeding who also have chronic diseases are at a higher risk of death[8]; similarly, 86.7% of patients in our study had at least one comorbidity. Furthermore, in our study, the patients with malignancy had significantly higher mortality rate. Patients with diabetes mellitus and coronary artery diseases, however, had significantly higher rates of ICU admission. Acute bleeding causes hemodynamic instability, and this condition worsens in the condition of coronary artery disease, particularly in patients with heart failure. Another factor underlying the higher ICU admission rate of patients with coronary artery disease was anticoagulant, antithrombotic and antiplatelet therapy[9].

Previous studies have indicated prognostic factors for GI bleeding. The main factors of poor prognosis include hypotension, anemia, advanced age, changes in mental status, comorbid diseases, and coagulopathy[10-12]. Some of these risk factors were also identified in our study. Markers of hemodynamic instability, such as hypotension, oxygen desaturation and decreased GCS, may reflect blood loss and bleeding rate. In our study, the patients with syncope had a higher ICU admission rate. This is not surprising, however, as syncope is one of the consequences of hemodynamic instability.

In our study population, patients with increased BUN and serum creatinine levels also experienced higher mortality. Uremic bleeding is a well-recognized complication in patients with renal failure, and it affects platelet aggregation and/or the coagulation cascade[13]. In patients with chronic kidney disease, GI bleeding is also a common complication[14]. In addition, elevated BUN level in patients with GI bleeding can be due to ingested blood protein[15]. Therefore, bleeding and uremia affect the occurrence of one another. The Blatchford scale uses BUN as one of the variables to determine the prognostic outcome of patients with upper GI bleeding[16]. Anand *et al*[17] showed that elevated serum creatinine levels are associated with increased rates of mortality and re-bleeding. In addition, hypovolemia causes acute renal failure in patients with severe bleeding[18].

In our study, a large majority of the patients required medical treatment, with a very small proportion of those requiring surgery. The study by Bor *et al*[19] demonstrated that bleeding stopped in 66.9% of patients upon receipt of medical treatment, with only 3.7% of those patients undergoing surgery (proportions that were very similar to those in our study). In our study population, malignancy and severe bleeding with hemodynamic deterioration were the most common indications for surgical treatment. Severe bleeding, however, may cause a decrease in mean arterial blood pressure and, not surprisingly in our study, was associated with emergency surgery.

The study by Bor *et al*[19] also showed a mean length of hospital stay of 7 ± 5.7 d, and another study by Morales Uribe *et al*[7,19] showed a mean length of 7 d. The length of hospital stay for our study population was 5.21 d, similar to those previous studies.

In conclusion, our study revealed that the most important factors in determining morbidity and mortality of GI bleeding cases presenting to the ED were the presence of malignancy, hypotension on admission, low GCS, and impaired kidney function. These findings should prompt the identification of patients who present a poor prognosis and will contribute to improving the management of patients with GI bleeding in the ED setting.

COMMENTS

Background

Acute gastrointestinal (GI) bleeding can be life threatening in some patients; overall, the rate of mortality in patients admitted to the emergency department with acute GI bleeding is reported to be 7% to 8.2%. Determining clinical variables to identify patients with GI bleeding, who are at high risk for poor prognosis, may aid improvements in the initial triage, the timing of primary endoscopic hemostasis, and the management of therapy.

Research frontiers

Early identification of poor prognostic findings in GI bleeding can improve morbidity and mortality rates.

Related publications

Previous studies have indicated prognostic factors for GI bleeding. The main prognostic factors for poor outcome include hypotension, anemia, advanced age, changes in mental status, comorbid diseases, and coagulopathy.

Innovations and breakthroughs

Previous publications have reported that hypotension, anemia, and changes in mental status are related to poor prognosis for GI bleeding. These factors were confirmed in this study, and malignancy and impaired renal function were also found to be related to poor prognosis. In addition, the authors identified high blood glucose levels and heart failure as related to higher intensive care unit admission rate.

Applications

The study results suggest that hypotension, impaired renal function, and malignancy are related to higher mortality in patients presenting to the emergency department with GI bleeding.

Terminology

Gastrointestinal bleeding is bleeding in the gastrointestinal tract, at any point from the esophagus to the rectum.

Peer-review

This is a good descriptive study in which the authors analyzed the prognostic factors of GI bleeding on admission to the emergency department. The results are interesting and suggest that hypotension, impaired renal function and malignancy are related to poor prognosis in the study population. High blood glucose levels and heart failure were also found to be related to higher rate of admission to the intensive care unit.

REFERENCES

1 Management of acute upper and lower gastrointestinal bleeding A national clinical guideline. Scottish Intercollegiate Guidelines Network Elliott House. Edinburgh, September, 2008. (accessed October 1, 2015). Available from: URL: http://www.sign.ac.uk/pdf/sign105.pdf

2 **Das AM**, Sood N, Hodgin K, Chang L, Carson SS. Development of a triage protocol for patients presenting with gastrointestinal hemorrhage: a prospective cohort study. *Crit Care* 2008; **12**: R57 [PMID: 18430209 DOI: 10.1186/cc6878]

3 **Chiu PW**, Sung JJ. Acute nonvariceal upper gastrointestinal bleeding. *Curr Opin Gastroenterol* 2010; **26**: 425-428 [PMID: 20703110 DOI: 10.1097/MOG.0b013e32833d1746]

4 **Gralnek IM**, Dumonceau JM, Kuipers EJ, Lanas A, Sanders DS, Kurien M, Rotondano G, Hucl T, Dinis-Ribeiro M, Marmo R, Racz I, Arezzo A, Hoffmann RT, Lesur G, de Franchis R, Aabakken L, Veitch A, Radaelli F, Salgueiro P, Cardoso R, Maia L, Zullo A, Cipolletta L, Hassan C. Diagnosis and management of nonvariceal upper gastrointestinal hemorrhage: European Society of Gastrointestinal Endoscopy (ESGE) Guideline. *Endoscopy* 2015; **47**: a1-46 [PMID: 26417980 DOI: 10.1055/s-0034-1393172]

5 **Straube S**, Tramèr MR, Moore RA, Derry S, McQuay HJ. Mortality with upper gastrointestinal bleeding and perforation: effects of time and NSAID use. *BMC Gastroenterol* 2009; **9**: 41 [PMID: 19500343 DOI: 10.1186/1471-230X-9-41]

6 **Yavorski RT**, Wong RK, Maydonovitch C, Battin LS, Furnia A, Amundson DE. Analysis of 3,294 cases of upper gastrointestinal bleeding in military medical facilities. *Am J Gastroenterol* 1995; **90**: 568-573 [PMID: 7717312]

7 **Morales Uribe CH**, Sierra Sierra S, Hernández Hernández AM, Arango Durango AF, López GA. Upper gastrointestinal bleeding: risk factors for mortality in two urban centres in Latin America. *Rev Esp Enferm Dig* 2011; **103**: 20-24 [PMID: 21341933]

8 Acute upper gastrointestinal bleeding Management Clinical Guideline Methods, evidence and recommendations. National Clinical Guideline Centre. London, June 2012. (accessed October 3, 2015). Available from: URL: https://www.nice.org.uk/guidance/cg141

9 **Mega JL**, Simon T. Pharmacology of antithrombotic drugs: an assessment of oral antiplatelet and anticoagulant treatments. *Lancet* 2015; **386**: 281-291 [PMID: 25777662 DOI: 10.1016/S0140-6736(15)60243-4]

10 **Saltzman JR**, Tabak YP, Hyett BH, Sun X, Travis AC, Johannes RS. A simple risk score accurately predicts in-hospital mortality, length of stay, and cost in acute upper GI bleeding. *Gastrointest Endosc* 2011; **74**: 1215-1224 [PMID: 21907980 DOI: 10.1016/j.gie.2011.06.024]

11 **Inayet N**, Amoateng-Adjepong Y, Upadya A, Manthous CA. Risks for developing critical illness with GI hemorrhage. *Chest* 2000; **118**: 473-478 [PMID: 10936143 DOI: 10.1378/chest.118.2.473]

12 **Chiu PW**, Ng EK. Predicting poor outcome from acute upper gastrointestinal hemorrhage. *Gastroenterol Clin North Am* 2009; **38**: 215-230 [PMID: 19446255 DOI: 10.1016/j.gtc.2009.03.009]

13 **Hedges SJ**, Dehoney SB, Hooper JS, Amanzadeh J, Busti AJ. Evidence-based treatment recommendations for uremic bleeding. *Nat Clin Pract Nephrol* 2007; **3**: 138-153 [PMID: 17322926 DOI: 10.1038/ncpneph0421]

14 **Kalman RS**, Pedrosa MC. Evidence-based review of gastrointestinal bleeding in the chronic kidney disease patient. *Semin Dial* 2015; **28**: 68-74 [PMID: 25215610 DOI: 10.1111/sdi.12301]

15 **Bang CS**, Lee YS, Lee YH, Sung H, Park HJ, Kim HS, Kim JB, Baik GH, Kim YS, Yoon JH, Kim DJ, Suk KT. Characteristics of nonvariceal upper gastrointestinal hemorrhage in patients with chronic kidney disease. *World J Gastroenterol* 2013; **19**: 7719-7725 [PMID: 24282360 DOI: 10.3748/wjg.v19.i43.7719]

16 **Pang SH**, Ching JY, Lau JY, Sung JJ, Graham DY, Chan FK. Comparing the Blatchford and pre-endoscopic Rockall score in predicting the need for endoscopic therapy in patients with upper GI hemorrhage. *Gastrointest Endosc* 2010; **71**: 1134-1140 [PMID: 20598244 DOI: 10.1016/j.gie.2010.01.028]

17 **Anand D**, Gupta R, Dhar M, Ahuja V. Clinical and endoscopic profile of patients with upper gastrointestinal bleeding at tertiary care center of North India. *J Dig Endosc* 2014; **5**: 139-143 [DOI: 10.4103/0976-5042.150660]

18 **Lameire N**. The pathophysiology of acute renal failure. *Crit Care Clin* 2005; **21**: 197-210 [PMID: 15781157 DOI: 10.1016/j.ccc.2005.01.001]

19 **Bor S**, Dağli U, Sarer B, Gürel S, Tözün N, Sıvrı B, Akbaş T, Sahın B, Memık F, Batur Y. A retrospective study demonstrating properties of nonvariceal upper gastrointestinal bleeding in Turkey. *Turk J Gastroenterol* 2011; **22**: 249-254 [PMID: 21805414]

P- Reviewer: Sharma P, Shussman N, Souza JLS
S- Editor: Yu J **L- Editor**: A **E- Editor**: Liu XM

World Journal of Gastroenterology

Submit a Manuscript: http://www.wjgnet.com/esps/
Help Desk: http://www.wjgnet.com/esps/helpdesk.aspx
DOI: 10.3748/wjg.v22.i16.4226

World J Gastroenterol 2016 April 28; 22(16): 4226-4237
ISSN 1007-9327 (print) ISSN 2219-2840 (online)

ORIGINAL ARTICLE

Retrospective Study

Eukaryotic elongation factor-1α 2 knockdown inhibits hepatocarcinogenesis by suppressing PI3K/Akt/NF-κB signaling

Fu-Nan Qiu, Yi Huang, Dun-Yan Chen, Feng Li, Yan-An Wu, Wen-Bing Wu, Xiao-Li Huang

Fu-Nan Qiu, Yi Huang, Dun-Yan Chen, Feng Li, Yan-An Wu, Wen-Bing Wu, Xiao-Li Huang, Provincial Clinical College, Fujian Medical University, Fuzhou 350001, Fujian Province, China

Fu-Nan Qiu, Department of Hepatobiliary Surgery, Fujian Provincial Hospital, Fuzhou 350001, Fujian Province, China

Yi Huang, Dun-Yan Chen, Yan-An Wu, Wen-Bing Wu, Xiao-Li Huang, Department of Clinical Laboratory, Fujian Provincial Hospital, Fuzhou 350001, Fujian Province, China

Feng Li, Department of Pathology, Fujian Provincial Hospital, Fuzhou 350001, Fujian Province, China

Author contributions: Qiu FN and Huang Y contributed equally to this study; Qiu FN and Huang Y were the guarantors of integrity of the entire study, study concepts, study design, definition of intellectual content, literature research, experimental studies, data acquisition, data analysis, and statistical analysis; Chen DY, Li F and Wu WB participated in experimental studies and data acquisition; Chen DY, Wu YA and Huang XL participated in data analysis and statistical analysis; Huang Y and Wu YA prepared the manuscript; Huang Y edited and reviewed the manuscript; all authors read and approved the final manuscript.

Supported by the Middle-Young Age Backbone Talent Cultivation Program of Fujian Health System, No. 2013-ZQN-JC-2; and Key Projects of Science and Technology Plan of Fujian Province, No. 2014Y0009.

Institutional review board statement: This study was approved by the Ethics Committee of Fujian Provincial Hospital and conducted in accordance with the Declaration of Helsinki and international guidelines.

Informed consent statement: All patients provided signed informed consent.

Conflict-of-interest statement: All the authors declare that they have no conflict of interest.

Data sharing statement: No additional data available.

Correspondence to: Yi Huang, PhD, Provincial Clinical College, Fujian Medical University, No. 134 Dong Street, Fuzhou 350001, Fujian Province, China. yihuang8070@sina.com
Telephone: +86-591-88216378
Fax: +86-591-87532356

Received: November 10, 2015
Peer-review started: November 10, 2015
First decision: December 21, 2015
Revised: January 13, 2016
Accepted: January 30, 2016
Article in press: January 30, 2016
Published online: April 28, 2016

Abstract

AIM: To assess the impact of eukaryotic elongation factor 1 alpha 2 (eEF1A2) on hepatocellular carcinoma (HCC) cell proliferation, apoptosis, migration and invasion, and determine the underlying mechanisms.

METHODS: eEF1A2 levels were detected in 62 HCC tissue samples and paired pericarcinomatous specimens, and the human HCC cell lines SK-

HEP-1, HepG2 and BEF-7402, by real-time PCR and immunohistochemistry. Experimental groups included eEF1A2 silencing in BEL-7402 cells with lentivirus eEF1A2-shRNA (KD group) and eEF1A2 overexpression in SK-HEP-1 cells with eEF1A2 plasmid (OE group). Non-transfected cells (control group) and lentivirus-based empty vector transfected cells (NC group) were considered control groups. Cell proliferation (MTT and colony formation assays), apoptosis (Annexin V-APC assay), cell cycle (DNA ploidy assay), and migration and invasion (Transwell assays) were assessed. Protein levels of PI3K/Akt/NF-κB signaling effectors were evaluated by Western blot.

RESULTS: eEF1A2 mRNA and protein levels were significantly higher in HCC cancer tissue samples than in paired pericarcinomatous and normal specimens. SK-HEP-1 cells showed lower eEF1A2 mRNA levels; HepG2 and BEL-7402 cells showed higher eEF1A2 mRNA levels, with BEL-7402 cells displaying the highest amount. Efficient eEF1A2 silencing resulted in reduced cell proliferation, migration and invasion, increased apoptosis, and induced cell cycle arrest. The PI3K/Akt/NF-κB signaling pathway was notably inhibited. Inversely, eEF1A2 overexpression resulted in promoted cell proliferation, migration and invasion.

CONCLUSION: eEF1A2, highly expressed in HCC, is a potential oncogene. Its silencing significantly decreases HCC tumorigenesis, likely by inhibiting PI3K/Akt/NF-κB signaling.

Key words: Hepatocellular carcinoma; Carcinogenesis; Eukaryotic elongation factor 1 alpha 2; Proliferation; PI3K/Akt/NF-κB signaling pathway

Core tip: Whether eukaryotic elongation factor 1 alpha 2 (eEF1A2) affects hepatocellular carcinoma (HCC) biology is largely unknown. In this study, eEF1A2 mRNA and protein levels were significantly higher in HCC cancer tissue samples than in paired control specimens. Efficient eEF1A2 silencing resulted in reduced cell proliferation, migration and invasion, increased apoptosis, and induced cell cycle arrest; the PI3K/Akt/NF-κB signaling pathway was notably inhibited. Inversely, eEF1A2 overexpression resulted in promoted cell proliferation, migration and invasion. Our findings indicate that eEF1A2 is a potential oncogene, whose silencing significantly decreases HCC tumorigenesis, likely by inhibiting PI3K/Akt/NF-κB signaling.

Qiu FN, Huang Y, Chen DY, Li F, Wu YA, Wu WB, Huang XL. Eukaryotic elongation factor-1α 2 knockdown inhibits hepatocarcinogenesis by suppressing PI3K/Akt/NF-κB signaling. *World J Gastroenterol* 2016; 22(16): 4226-4237 Available from: URL: http://www.wjgnet.com/1007-9327/full/v22/i16/4226.htm DOI: http://dx.doi.org/10.3748/wjg.v22.i16.4226

INTRODUCTION

Human eukaryotic elongation factor 1 alpha 2 (eEF1A2) gene is located on chromosome 20q13.3 and participates in peptide chain elongation during protein translation, therefore playing a critical role in protein synthesis[1]. Traditionally, eEF1A2 was considered a housekeeping protein, with expression limited to the heart, brain and skeletal muscle[1,2]. However, recent studies have attributed more biological functions to eEF1A2 besides its role as an elongation factor. eEF1A2 has carcinogenic potential due to these diverse functions. Recent studies have demonstrated that eEF1A2 is highly expressed in tumors from multiple tissues, indicating a tight relation between eEF1A2 and tumor genesis, development and biological behaviors[3-7]. eEF1A2 is known to transmit signals from the cytoplasm to the nucleus through interaction with zinc finger protein 1 and subsequent interactions with a set of receptors with tyrosine kinase ability, thus promoting efficient cell proliferation[8]. Besides, eEF1A2 can also regulate cell apoptosis; high levels of rat eEF1A2 protect muscle cells from caspase-3-mediated apoptosis[9]. In addition, the interaction between eEF1A2 and peroxidase Ⅰ protects cells from oxidative stress-induced apoptosis, involving the suppression of caspase-3 and caspase-8 pyrolysis[10]. Taken together, these findings indicate that eEF1A2 regulation of tumorigenesis may be associated with its apoptosis inhibitory ability[11]. In addition to cell proliferation and apoptosis regulation, eEF1A2 is also involved in cytoskeleton rearrangement, interacting with F-actin and shortening microtubules, thus playing an important role in tumor invasion and migration[11,12]. High eEF1A2 levels were reported to induce filopodia generation in breast cancer cells, enhancing their migration and invasion abilities[11]. Conversely, targeted silencing of eEF1A2 reduces the migration and invasion abilities of some tumor cells. Highly expressed in human breast cancer BT-549 cells and mouse plasmacytoma ABPC4 cells, eEF1A2 efficiently binds Akt and induces its phosphorylation, promoting tumor cell invasion and migration, and thereby increasing malignancy[13].

Primary hepatocellular carcinoma (HCC) is a common malignancy in China, whose annual cases exceed 50% of the global incidence[14]. The mechanism and potential therapeutic targets of HCC are hotspots in global liver cancer research. Recently, the microarray-discrepant genome hybridization technology was applied to analyze gene expression profiles and functions of candidate genes in HCC cancer tissues and cell lines. The results revealed exceptionally high expression of eEF1A2 in HCC, which is quite intriguing[15-17]. Akt is a major regulator in the PI3K/Akt/NF-κB signaling pathway, and can be activated upon phosphorylation to subsequently phosphorylate a series of downstream targets[18]. As an important target downstream of Akt, NF-κB participates in multiple biological processes such as cell proliferation,

apoptosis, invasion and migration, by regulating the transcription of various genes[19]. EEF1A2 was identified as an upstream inducer of PI3K[17], which promotes cell migration, invasion and metastasis in pancreatic cancer[12]. However, there is no report about the effects of eEF1A2 silencing on HCC progression, and the mechanism underlying eEF1A2 involved in HCC is largely unknown.

This study aimed to assess the effect of eEF1A2 on HCC cell proliferation, apoptosis, invasion, and migration, and determine its effect on PI3K/Akt/NF-κB signaling in HCC. We found that eEF1A2 promotes HCC tumorigenicity, likely by regulating the PI3K/Akt/NF-κB signaling pathway. These findings indicate that eEF1A2 is a potential novel therapeutic target for HCC.

MATERIALS AND METHODS

Patients

A total of 62 HCC patients were enrolled, who had surgical excision and pathology confirmation from October 2012 to December 2013 in Fujian Provincial Hospital. They included 52 males and 10 females of 54.3 ± 12.2 (18.0-73.0) years old. None of them had radiotherapy or chemotherapy before surgery. Liver cancer and paired pericarcinomatous tissue specimens in each patient were excised. A part of each tissue sample was fixed in 10% neutral buffered formalin for immunohistochemistry, while the remaining portion was kept in RNA preserving fluid (Beijing ComWin Biotech Co., Ltd.) overnight, before storage at -80 ℃ for real-time polymerase chain reaction (PCR).

Normal liver tissue specimens were obtained from 20 patients with liver hemangioma who had surgical excision from October 2012 to December 2013 in Fujian Provincial Hospital. They included 12 men and 8 women of 40.8 ± 10.4 (25.0-66.0) years old. These control patients were hepatitis and liver cirrhosis free. The excised peripheral liver hemangioma tissue specimens were treated as described above for liver cancer and paired pericarcinomatous tissue samples.

This study was approved by the Ethics Committee of Fujian Provincial Hospital; all patients provided signed informed consent.

Cell culture

The human HCC cell lines SK-HEP-1, HepG2 and BEL-7402 were purchased from Institute of Biochemistry and Cell Biology, Shanghai Institutes for Biological Sciences, Chinese Academy of Sciences (China). Cells were cultured in DMEM (Gibco, United States) supplemented with 10% fetal bovine serum (FBS, Gibco) and incubated at 37 ℃ in a humid environment containing 5% CO_2.

Lentivirus-based short hairpin RNA silencing in BEL-7402 cells and experimental grouping

According to eEF1A2 sequence in GenBank database (NM_001958), an interfering shRNA sequence targeting site 418 was designed as ACTACATCACCATCATCGA, with the control scrambled siRNA sequence TTCTCCGAACGTGTCACGT. Both shRNA fragments were cloned into the GV115 vector (Shanghai Genechem Biotech Co, Ltd, China) with *Age* Ⅰ/*EcoR* Ⅰ double restriction enzyme digestion sites. Reconstructed lentivirus vectors expressing GV115-eEF1A2-shRNA and the negative control were transformed into competent *E. coli* DH5α, and positive colonies were selected for PCR and sequencing. Reconstructed lentivirus expressing vectors, packing plasmids pHelper 1.0 and pHelper 2.0 were co-transfected into 293T cells with Lipofectamine 2000 (Invitrogen). Forty-eight hours after transfection, the lentivirus containing culture medium was collected and concentrated. After titration, lentiviruses were stored at -80 ℃.

To assess the role of eEF1A2 in tumor cell proliferation, apoptosis and migration, a lentivirus expressing eEF1A2-shRNA was used to infect log-phase BEL-7402 cells. The virus containing culture medium was replaced with fresh DMEM supplemented with 10% FBS at 12 h after infection. Five days post lentivirus infection, three BEL-7402 cell groups were set up: KD (knockdown, cells infected with eEF1A2-shRNA lentivirus), NC (negative control, cells infected with negative control-shRNA lentivirus) and CON (cells without lentivirus infection). Cells were used for subsequent experiments, when lentiviral transfection efficiency was above 80%.

Lentivirus-based eEF1A2 overexpression in SK-HEP-1 cells and experimental grouping

According to eEF1A2 sequence in GenBank database (NM_001958), the following primers were designed: forward 5'-GAGGATCCCCGGGTACCGGTCGCCACCATGGGCAAGGAGAAGACCCAC-3, and reverse 5'-TCCTTGTAGTCCATACCCTTGCCCGCCTTCTGCGCCTTCTGCGCCGACTTG-3' for eEF1A2 cloning. Exogenous eEF1A2 was expressed in SK-HEP-1 cells *via* transduction of the lentivirus plasmid pGLV5-eEF1A2 (pGLV5 was from GenePharma Co, Ltd, China), to assess the role of eEF1A2 in tumor cell proliferation, apoptosis and migration. Three groups of cells were set up: OE (overexpression, cells infected with eEF1A2 lentivirus), NC (negative control, cells infected with negative control lentivirus) and CON (cells without lentivirus infection). The SK-HEP-1 cells were collected 5 d after infection, and used for RT-PCR or Western blot.

RT-PCR

Total RNA was extracted from homogenized samples using TRIzol Reagent (Invitrogen, United States) and treated with DNase. A total of 62 HCC liver cancer and paired pericarcinomatous tissue specimens, 20 normal liver tissue samples, and log-phase HCC SK-HEP-1 and HepG2 cells were assessed. In addition, the three BEL-7402 cell groups (KD, NC, and CON) were analyzed after 5 d of culture post-lentiviral infection, as described above. For each sample, 2 μg of RNA were

Table 1 Primers used in this study

Gene	Primers (5′-3′)	Length (bp)
eEF1A2	GTCAAGGAAGTCAGCGCCTAC TGAACCACGGCATGTTGGG	124
GAPDH	TGACTTCAACAGCGACACCCA CACCCTGTTGCTGTAGCCAAA	121

used for cDNA synthesis with a specific kit (Promega, United States). Real-time PCR was performed with SYBR Green Ⅰ (Applied Biosystems, United States) on ABI 7300 (Applied Biosystems). The primers used are described in Table 1.

Immunohistochemistry

Liver tissues were fixed in 10% neutral formalin, and paraffin embedded. After sectioning, an SP immunohistochemistry kit (Fuzhou Maixin Biotech Co., Ltd, China) was used for staining. Rabbit anti-human eEF1A2 polyclonal antibody (1:50, Novus Biologicals, United States) was used for eEF1A2 detection according to the manufacturer's instructions. Positive cells were identified by claybank particles in the cytoplasm. Five hundred cells were counted under a high power lens, and positive and negative staining considered with ≥ 10% and < 10% dyed cells, respectively.

Western blot

BEL-7402 cells were cultured for 5 d post lentivirus infection, and lysed with cell lysis buffer (Hyclone-Pierce, United States) for total protein extraction. After quantification, 50 μg protein were separated by SDS-PAGE and electro-transferred onto PVDF membranes. After blocking, the membranes were incubated with primary antibodies, including rabbit anti-GAPDH, Akt, p-Akt, IκB, p-IκB (Ser32), p-NF-κB p65 (ser468), Bcl-2, MMP-9 and MMP-2 (Cell Signaling Technology, United States), rabbit anti-eEF1A2 (Novus Biologicals), rabbit anti-c-Myc (Santa Cruz, United States), and rabbit anti- NF-κB p65 (eBioscience, United States). Horseradish peroxidase (HRP)-conjugated goat-anti-rabbit IgG (KPL, United States) was used as a secondary antibody. After exposure and film development, protein bands were scanned with a Gel Doc gel image analyzer (Bio-Rad, United States). Relative protein levels were determined with GAPDH as a reference.

MTT assay and cell proliferation curve

HCC cells infected with lentivirus for 3 d were seeded in 96-well plates at a density of 2 × 10^3 cells/well in 100 μL culture medium. Three replicates were set up for each group. After lentiviral infection of BEL-7402 cells followed by 1-5 d of culture, 10 μL of 5 mg/mL MTT (Sigma) were added into wells, and further incubated for 4 h at 37 ℃. Then, culture medium was carefully removed followed by addition of 100 μL DMSO to dissolve the purple crystals. Finally, absorbance was read at 490 nm on an American stat Fax-2100microplate reader (Awareness Technology, United States). Cell proliferation curve was obtained with absorbance values and time on the vertical and horizontal axes, respectively.

Colony formation assay

HCC cells infected with lentivirus for 3 d were seeded in 6-well plates at a density of 4 × 10^2 cells /well. Three replicate wells were set up for each group, and cultured continuously for 14 d. Then, cells were washed twice with PBS, fixed with paraformaldehyde for 30 min, and submitted to Giemsa staining for 20 min. Cell colonies were counted under a microscope. Colony formation rate was derived as (colony numbers/inoculated cell numbers) × 100%.

Cell cycle analysis

Five days after lentivirus infection, cells were washed with PBS, and fixed with 70% ethanol (pre-cooled at 4 ℃) for 1 h. After ethanol removal, cells were loaded with propidium iodide (PI) for 15 min in the dark, according to the DNA ploidy detection kit (Sigma, United States). Cell cycle distribution was analyzed by flow cytometry on FACS Calibur (BD Biosciences, United States) with > 10000 cells assessed for each sample.

Evaluation of cell apoptosis

After 5 d of lentivirus infection, HCC cells were washed with PBS, and assessed for apoptosis using the Annexin V-APC apoptosis detection kit (eBioscience) according to the manufacturer's instructions. Flow cytometry was carried out on FACS Calibur (BD Biosciences).

Cell migration and invasion assays

Transwell chambers for cell migration assessment were purchased from Corning (United States). Those used for cell invasion assays were from BD Biosciences, with Matrigel on the filter membrane. The chambers were placed in 24-well plates, and 1 × 10^6 cells added to the upper chambers in 200 μL of serum free DMEM; meanwhile, 500 μL of complete medium were added to the bottom chambers. Incubation was carried out for 24 h at 37 ℃ with 5% CO_2. Then, the culture medium in the upper chamber as well as cells on the filter membrane (invasion assay) were removed. The cells that had passed through the filter membrane were submitted to Giemsa staining for 30 min and dissolved in 180 μL of 10% acetic acid. 100 μL of the resulting solution were used for absorbance measurements at 570 nm on an American stat Fax-2100 microplate reader. Finally, cell migration and invasion rates were calculated, respectively.

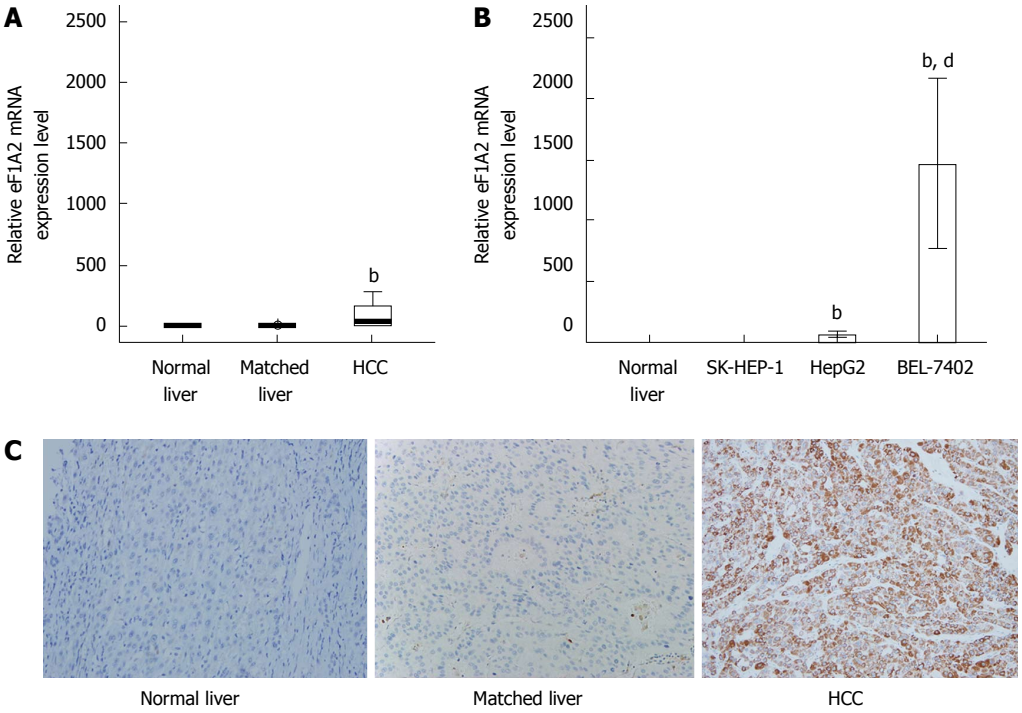

Figure 1 Relative eEF1A2 mRNA expression levels in hepatocellular carcinoma tissue samples and cells. GAPDH was used as an internal control. Expression data were obtained as $2^{-\Delta\Delta CT}$ or -ΔΔCT relative to normal liver tissue values. A: Relative eEF1A2 mRNA expression levels in HCC tissue samples analyzed by the -ΔΔCT method. Normal liver tissue specimens (n = 20); matched liver tissue samples (n = 62); HCC tissue specimens (n = 62); B: Relative eEF1A2 mRNA expression levels in SK-HEP-1, HepG2 and BEL-7402 cells analyzed by $2^{-\Delta\Delta CT}$ method (n = 3); C: eEF1A2 protein levels in matched liver tissue and HCC tissue specimens from a HCC patient, and normal liver tissue samples were analyzed by immunohistochemistry (SP × 200). Data are mean ± SD. $^{b}P < 0.01$ *vs* Normal liver tissue and Matched liver tissue samples. $^{d}P < 0.01$ *vs* SK-HEP-1 and HepG2.

Table 2 eEF1A2 expression in hepatocellular carcinoma, paired pericarcinomatous and normal liver tissue samples

	eEF1A2 positive tissue/total tissue	Positive rate
HCC	47/62	75.8%
Paired pericarcinomatous	5/62	8.1%
Normal liver	0/20	0%

eEF1A2: Eukaryotic elongation factor 1 alpha 2; HCC: Hepatocellular carcinoma.

Statistical analysis

Data are mean ± SD of at least three replicates. Student's *t*-test was used to compare continuous measurement data with a normal distribution between two groups. One way analysis of variance (ANOVA) was employed while comparing three groups. Mann-Whitney *U* test was used to evaluate continuous data with a non-normal distribution; χ^2 test was used to compare positive rates. Statistical analyses were performed with the SPSS13.0 software (SPSS, United States). $P < 0.05$ was considered statistically significant.

RESULTS

eEF1A2 is highly expressed in HCC liver cancer tissues and HCC cell lines

To determine the relationship between eEF1A2 and HCC, we assessed eEF1A2 expression levels in 62 HCC and paired pericarcinomatous tissue samples, 20 normal liver tissue specimens, and HCC cell lines. We found that median eEF1A2 mRNA levels in HCC tissue samples [35.27 (2.45-166.15)] were significantly higher compared with paired pericarcinomatous specimens [1.34 (0.78-1.68)] and normal liver tissue samples [1.22 (0.72-1.63)] ($P < 0.01$; Figure 1A). Besides, the HCC cell lines HepG2 and BEL-7402, but not SK-HEP-1, showed higher eEF1A2 mRNA levels compared with normal liver tissues (Figure 1B). Furthermore, immunohistochemistry data revealed that eEF1A2 was mainly expressed in the cytoplasm. Importantly, 47 HCC tissues showed positive eEF1A2 expression (a positive rate of 75.8%), while only 8.1% of paired pericarcinomatous tissue samples stained for eEF1A2 (47/62) (Table 2). No eEF1A2 positive sample was found in normal liver tissues (Table 2). Accordingly, eEF1A2 protein levels in HCC were significantly higher than values obtained for paired pericarcinomatous and normal liver tissues ($P < 0.01$) (Figure 1C).

Lentiviral silencing of eEF1A2 expression in BEL-7402 cells

BEL-7402 cells were selected for subsequent studies for its higher eEF1A2 expression compared with the other cell lines (Figure 1B). BEL-7402 cells were infected with lentivirus expressing eEF1A2-shRNA for 5 d. Then, eEF1A2 mRNA levels were decreased

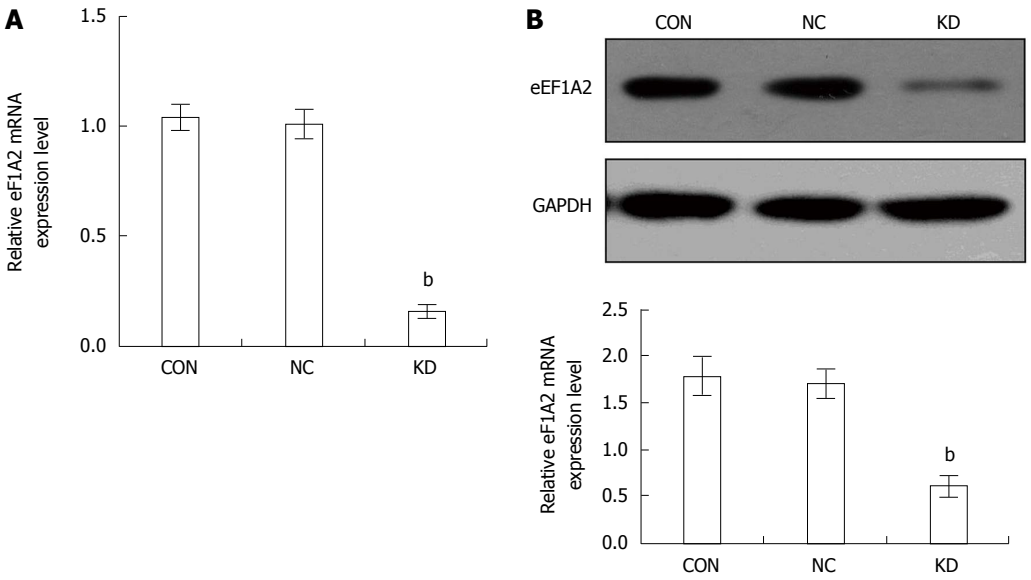

Figure 2 Effect of eEF1A2-shRNA on eEF1A2 expression in BEL-7402 cells (*n* = 3). GAPDH was used as an internal control. A: Relative expression of eEF1A2 mRNA; B: eEF1A2 protein levels as detected by the Western blot method (upper, Western blot; lower, quantification of Western blot normalized by GADPH). Data are mean ± SD (*n* = 3). $^{b}P < 0.01$ *vs* NC and CON. CON: Blank control group not infected; NC: Negative control group infected with GV115-LV; KD: eEF1A2 RNAi group infected with GV115-eEF1A2-shRNA-LV.

by 84.10 ± 3.32% in the KD group compared with the NC group ($P < 0.01$) as shown in Figure 2A. In agreement, eEF1A2 protein amounts in the KD group were reduced by 64.47% ± 7.07% compared with the values obtained for the NC group ($P < 0.01$) (Figure 2B). There were no differences between the NC and CON groups in eEF1A2 mRNA or protein levels (Figure 2A and B).

eEF1A2 knockdown significantly reduces BEL-7402 cell proliferation

The accelerated proliferation of tumor cells is a crucial mechanism in tumor deterioration. MTT results showed that BEL-7402 cells of the NC and CON groups began to proliferate at 2 d of culture, entering into log-phase at 3 d, with a normal growth curve. In contrast, cell proliferation in the KD group was remarkably suppressed, with significantly lower proliferation obtained at 4 and 5 d compared with the NC group ($P < 0.01$): inhibition rates of 34.36% ± 4.65% and 39.44% ± 3.94% were obtained, respectively (Figure 3A). These results were further confirmed by the colony formation assay; compared with the NC group, the KD group showed an overtly declined colony formation rate of 6.70% ± 6.08% ($P < 0.01$) (Figure 3B and C).

eEF1A2 knockdown blocks cell cycle progression in BEL-7402 cells

To determine the cause of decreased cell proliferation in eEF1A2 deprived BEL-7402 cells, the effect of eEF1A2 knockdown on cell cycle progression was analyzed by flow cytometry. DNA ploidy detection indicated that after lentivirus infection, BEL-7402 cells showed 60.13% ± 2.16% of G0/G1 cells, a much higher rate than that of the NC group (49.28% ± 1.29%, $P < 0.05$); consequently, S phase rates were significantly decreased in the KD group compared with the NC group ($P < 0.01$) (Figure 4A and B).

eEF1A2 knockdown enhances BEL-7402 cell apoptosis

Another effective way to inhibit tumor progression is to promote apoptosis. In an Annexin V-APC assay, we showed that after lentivirus infection, BEL-7402 cells in the KD group showed a high apoptosis rate (6.09% ± 0.40%), significantly increased compared with those of the NC (3.24% ± 0.39%) and CON (3.12% ± 0.25%) groups ($P < 0.01$) as shown in Figure 5.

eEF1A2 silencing decreases migration and invasion abilities in BEL-7402 cells

Migration and invasion are important strategies in tumor worsening, and their inhibition effectively prevents tumor progression. Transwell assays demonstrated that the migration rate of BEL-7402 cells in the KD group (1.76 ± 0.22) was much lower compared with the NC group (5.62 ± 0.31) (Figure 6A and B). Similarly, BEL-7402 cells in the KD group showed a significantly decreased invasion rate (2.26 ± 0.27) compared with the NC group (7.06 ± 0.50, $P < 0.01$) (Figure 6C and D).

eEF1A2 knockdown inhibits PI3K/Akt/NF-κB signaling

To further explore the molecular mechanism underlying the eEF1A2 effect in BEL-7402 cells, activation of the PI3K/AKT/NF-κB signaling pathway was assessed. As shown in Figure 7A and B, eEF1A2 knockdown significantly suppressed p-Akt, p-IκB (Ser32), p-NF-κB ($P < 0.01$) and NF-κB ($P < 0.05$) protein levels in BEL-7402 cells. In addition, c-Myc, MMP-2 ($P < 0.01$),

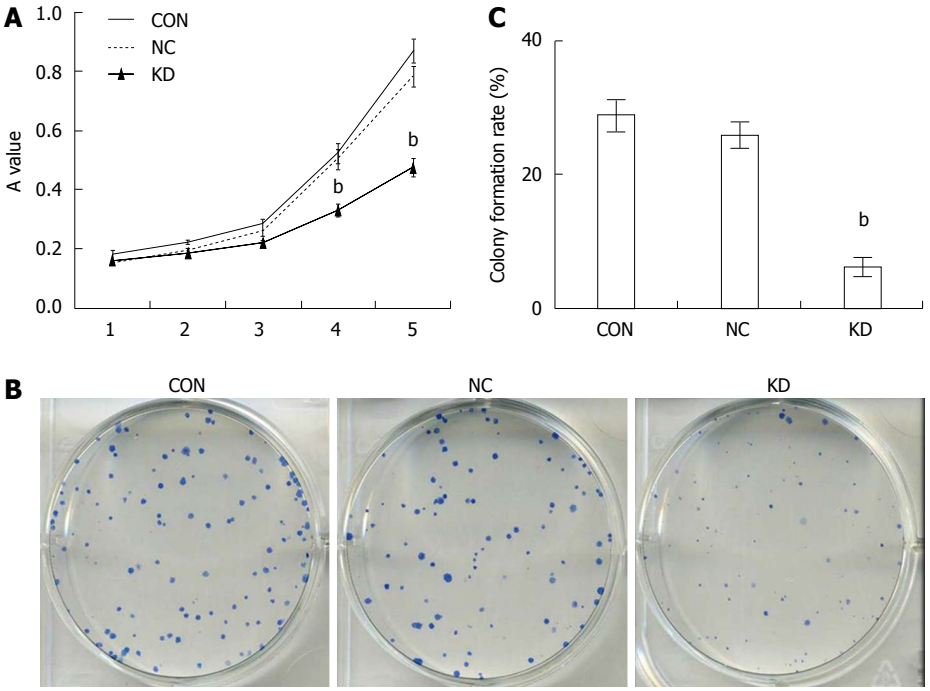

Figure 3 Effect of eEF1A2-shRNA on BEL-7402 cell proliferation. A: Effect of eEF1A2-shRNA on BEL-7402 cell colony formation; B: Colony formation as detected by the Giemsa staining method (× 100); C: Colony formation rates of Bel-7402 cells. Data are mean ± SD (n = 3). $^{b}P < 0.01$ *vs* NC and CON.

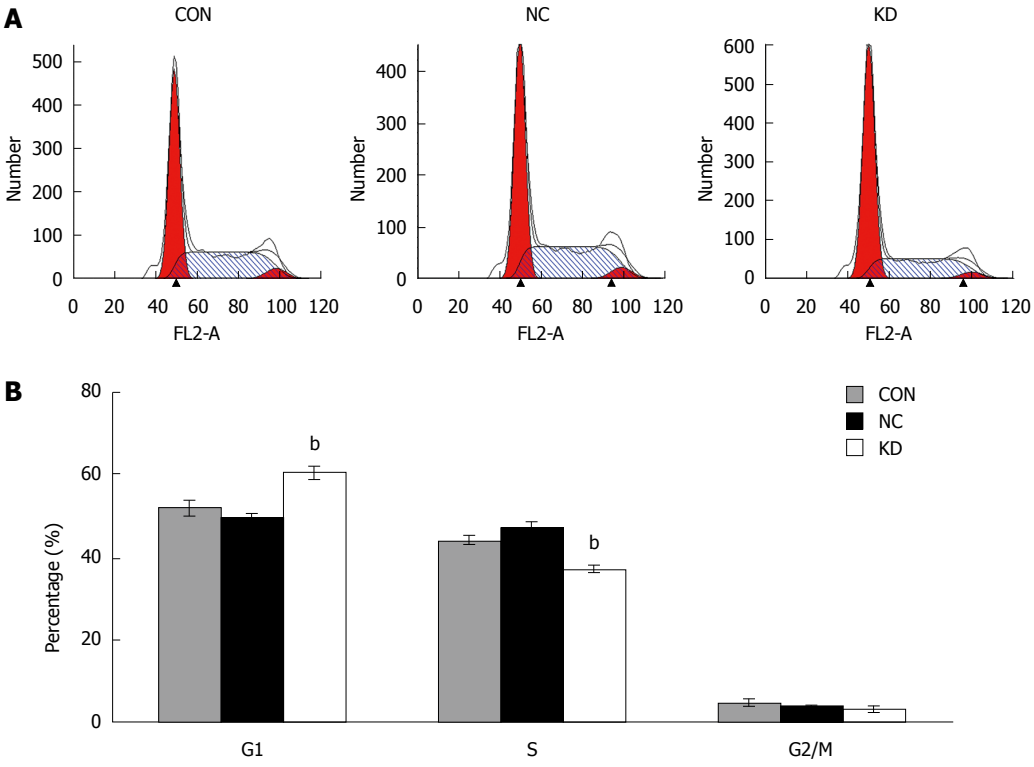

Figure 4 Effect of eEF1A2-shRNA on BEL-7402 cell cycle. A: Cell cycle distribution detected by DNA ploidy analysis; B: Percentages of Bel-7402 cells in the G0/G1, S and G2/M phases, respectively. Data are mean ± SD (n = 3). $^{b}P < 0.01$ *vs* NC and CON.

Bcl-2 and MMP-9 ($P < 0.05$) as downstream target genes regulated by NF-κB, were downregulated in the KD group compared with the NC group (Figure 7C and D).

Overexpression of eEF1A2 promotes cell proliferation, cell cycle, migration and invasion in SK-HEP-1 cells

To evaluate how eEF1A2 affects the proliferation and

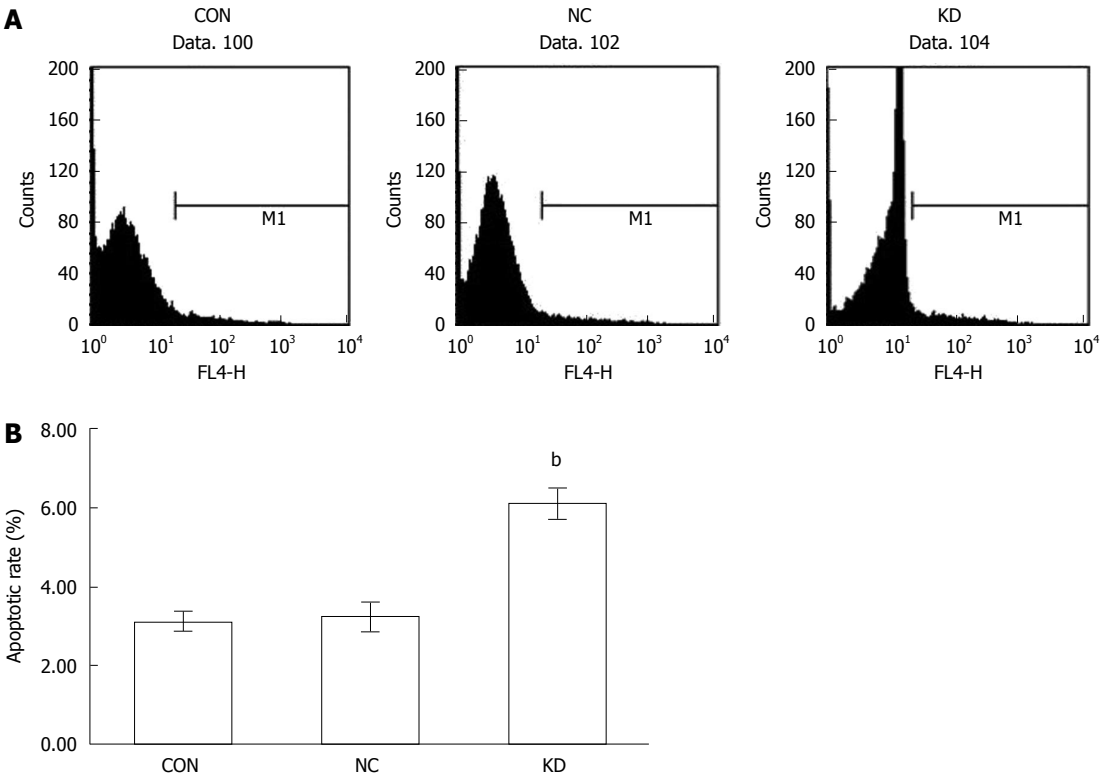

Figure 5 Effect of eEF1A2-shRNA on BEL-7402 apoptosis. A: Flow-cytograms after Annexin V-APC staining; B: Apoptotic rates of Bel-7402 cells. Data are mean ± SD (n = 3). $^{b}P < 0.01$ *vs* NC and CON.

invasion of HCC cells, we established SK-HEP-1 cell lines that overexpressed eEF1A2 using lentivirus-based overexpression eEF1A2 system. The levels of ectopic eEF1A2 mRNA and protein expression were considerably higher than those of endogenous eEF1A2 in the negative lentiviurs control (NC) and blank control cells (CON) as determined by qRT–PCR and Western blot (Figure 8A and B). Increased proliferation properties of the eEF1A2-expressing cells were observed by MTT assay (Figure 8C). Cell cycle progression was analyzed by flow cytometry. DNA ploidy detection indicated that overexpression of eEF1A2 induced lower G0/G1 and higher S and G2/M rates (Figure 8D and E). Transwell assays demonstrated that overexpression of eEF1A2 significantly increased the migration and invasion rates of SK-HEP cells (Figure 8F and G).

DISCUSSION

eEF1A2 has an important role in carcinogenesis and tumour metastasis; however, the mechanism underlying its activity remains unclear. In the present work, we indicated that eEF1A2, highly expressed in HCC, is a potential oncogene. Its silencing significantly suppresses cell proliferation, promotes apoptosis, and decreases migration and invasion rates in HCC cells, likely by inhibiting the PI3K/Akt/NF-κB signaling pathway. These findings indicate that eEF1A2 is a potential novel therapeutic target for HCC.

eEF1A2 is a multifunctional protein and potential oncogene. Anand *et al*[3] first proposed a possible role for eEF1A2 in the development of ovarian cancer. Besides ovarian cancer, the abnormally high expression of eEF1A2 has been described in breast, prostate, lung and gastrointestinal cancers[4-7]. The high eEF1A2 expression in malignant liver tumors has aroused increasing attention recently[15-17]. In the present work, we also found exceptionally high eEF1A2 expression in HCC cancer, which showed a positive rate of 75.8% as determined by immunohistochemistry. Taken together, these findings indicate a relationship between high eEF1A2 expression and HCC occurrence.

Due to the high eEF1A2 levels in the BEL-7402 cell line, the latter was selected for lentivirus-mediated knockdown of eEF1A2. As shown above, eEF1A2 silencing in BEL-7402 cells significantly inhibited cell proliferation, induced apoptosis, and caused cell cycle arrest in the G0/G1 phase. In addition, eEF1A2 suppression efficiently inhibited BEL-7402 migration and invasion. Inversely, overexpression of eEF1A2 in SK-HEP-1 cells increased cell proliferation, and promoted migration and invasion. These results was consistent with the role of eEF1A2 in pancreatic cancer, which indicated that overexpression of eEF1A2 promoted cell growth, survival, and invasion in pancreatic cancer[20]. These findings indicate a carcinogenic role for eEF1A2 in HCC, and its abnormally high expression is tightly related to proliferation, apoptosis, invasion and migration in HCC cells.

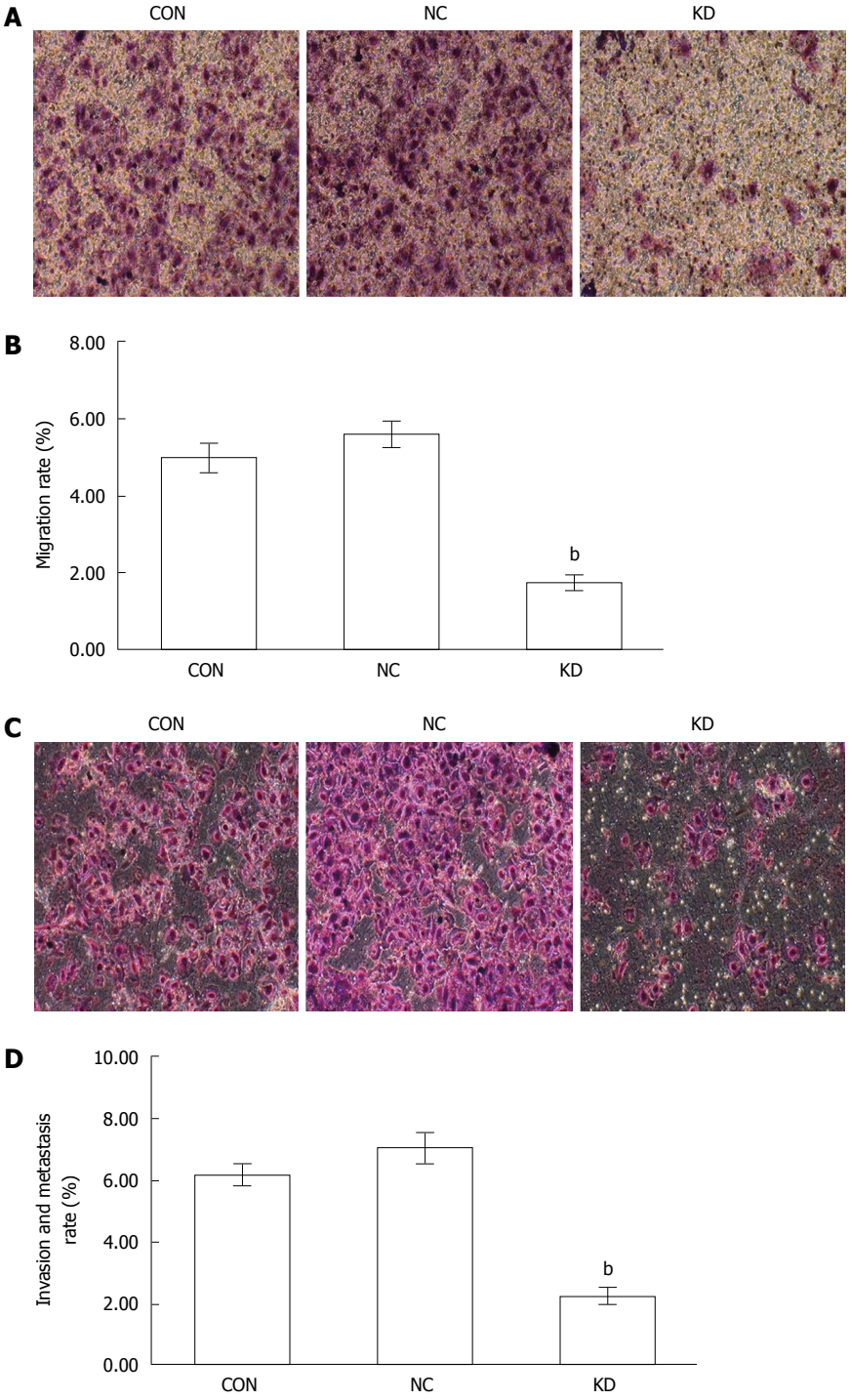

Figure 6 Effect of eEF1A2-shRNA on BEL-7402 cell migration and metastasis. A: Cell migration as detected by the Giemsa staining method; B: Quantitation of A. Data are mean ± SD (n = 3). $^{b}P < 0.01$ *vs* NC and CON; C: Cell invasion and metastasis as assessed by the Giemsa staining method; D: Quantitation of C. Data are mean ± SD (n = 3). $^{b}P < 0.01$ *vs* NC and CON.

eEF1A2 promotes phosphorylation of tyrosine residues[8], and PI3K/Akt is an important pathway activated downstream of tyrosine phosphorylation. Constitutive activation of PI3K/Akt leads to decreased apoptosis and/or accelerated cell cycle, which result in cell malignancy[21]. Indeed, genesis and development of multiple malignant tumors are closely related to abnormal activation of the PI3K/Akt signaling pathway. Akt, a major regulator of PI3K/Akt signaling, is activated upon phosphorylation. Recent findings have revealed an Akt-specific binding site in eEF1A2[22], which is involved in the regulation of Akt phosphorylation and activity[11,13]. As shown above, eEF1A2 knockdown significantly inhibited Akt activity, indicating the ability of eEF1A2 to efficiently regulate Akt phosphorylation in HCC cells. As an important downstream target of Akt, NF-κB exerts its role by transmitting and amplifying Akt signal, which makes the PI3K/Akt/NF-κB signaling

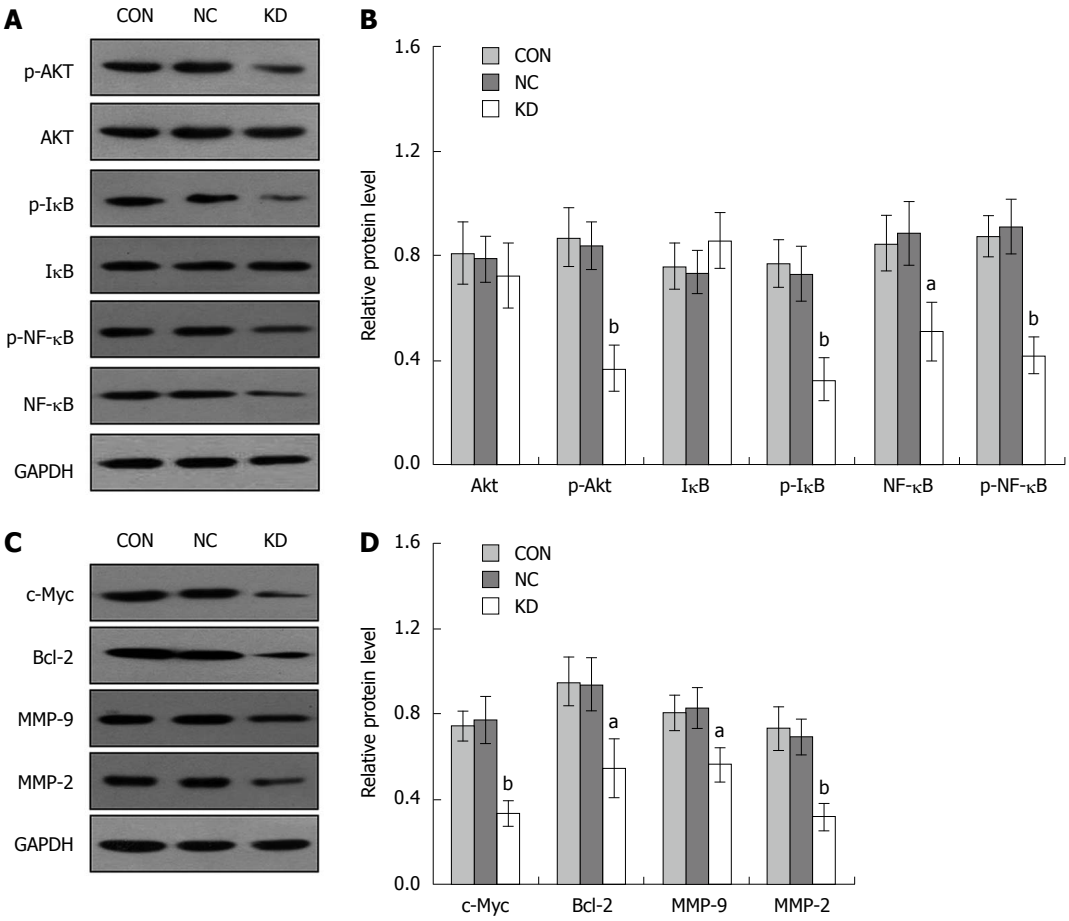

Figure 7 Effect of eEF1A2-shRNA on Akt, p-Akt, IκB, p-IκB, NF-κB, p-NF-κB, c-Myc, Bcl-2, MMP-9 and MMP-2 protein expression in BEL-7402 cells. GAPDH was used as an internal control. A: Western blots showing Akt, p-Akt, IκB, p-IκB, NF-κB, p-NF-κB and GAPDH protein bands; B: Relative expression of Akt, p-Akt, IκB, p-IκB, NF-κB and p-NF-κB; C: Western blots showing expression of c-Myc, Bcl-2, MMP-9, MMP-2 and GAPDH protein bands; D: Relative expression of c-Myc, Bcl-2, MMP-9 and MMP-2. Data are mean ± SD (n = 3). $^{a}P < 0.05$ *vs* NC and CON; $^{b}P < 0.01$ *vs* NC and CON.

pathway a critical target for anti-malignant tumor treatment[19]. As a transcription factor, NF-κB usually forms the IκB/NF-κB complex under normal conditions, where its transcriptional activity is suppressed. Activated Akt separates and activates NF-κB from the IκB/NF-κB complex by phosphorylating IκB. On the other hand, by directly phosphorylating Ser529 and Ser536 sites on NF-κB already interacting with the related binding sites, Akt promotes its transcriptional activity. Upon activation, NF-κB regulates the expression of multiple genes involved in cell proliferation, apoptosis, invasion and migration, thus augmenting cell malignancy[19]. We demonstrated that eEF1A2 silencing inhibits IκB and NF-κB phosphorylation. These findings indicate the inhibitory impact of eEF1A2 knockdown on NF-κB transcriptional activity, which likely translates into altered NF-κB-mediated effects on proliferation, apoptosis, invasion and migration in tumor cells. Moreover, with NF-κB-binding sites in their gene sequences, the oncoprotein c-Myc[23], the anti-apoptosis factor Bcl-2[24], MMP-9[25] and MMP-2[26] are considered important targets downstream of NF-κB. As shown above, c-Myc, Bcl-2, MMP-9 and MMP-2 expression levels were significantly reduced in eEF1A2-deficient cells. These findings indicate that eEF1A2 affects HCC proliferation, migration, invasion and apoptosis likely by regulating the PI3K/Akt/NF-κB signaling pathway. Further studies are needed to unveil the mechanisms underlying the regulatory activity of eEF1A2 on PI3K/Akt/NF-κB signaling.

In conclusion, we propose a potential carcinogenic role of eEF1A2 in HCC cells. Indeed, eEF1A2 is involved in cell proliferation, apoptosis, migration and invasion during HCC carcinogenesis and development *via* regulation of PI3K/Akt/NF-κB signaling. Further studies are warranted to determine whether other signaling pathways play a role in eEF1A2-mediated carcinogenesis. Overall, our findings indicate eEF1A2 as a novel diagnostic marker and therapeutic target in HCC.

COMMENTS

Background

Human eukaryotic elongation factor 1 alpha 2 (eEF1A2) participates in peptide chain elongation during protein translation, therefore playing a critical role in protein synthesis and other biological pathways. Consequently, eEF1A2 has

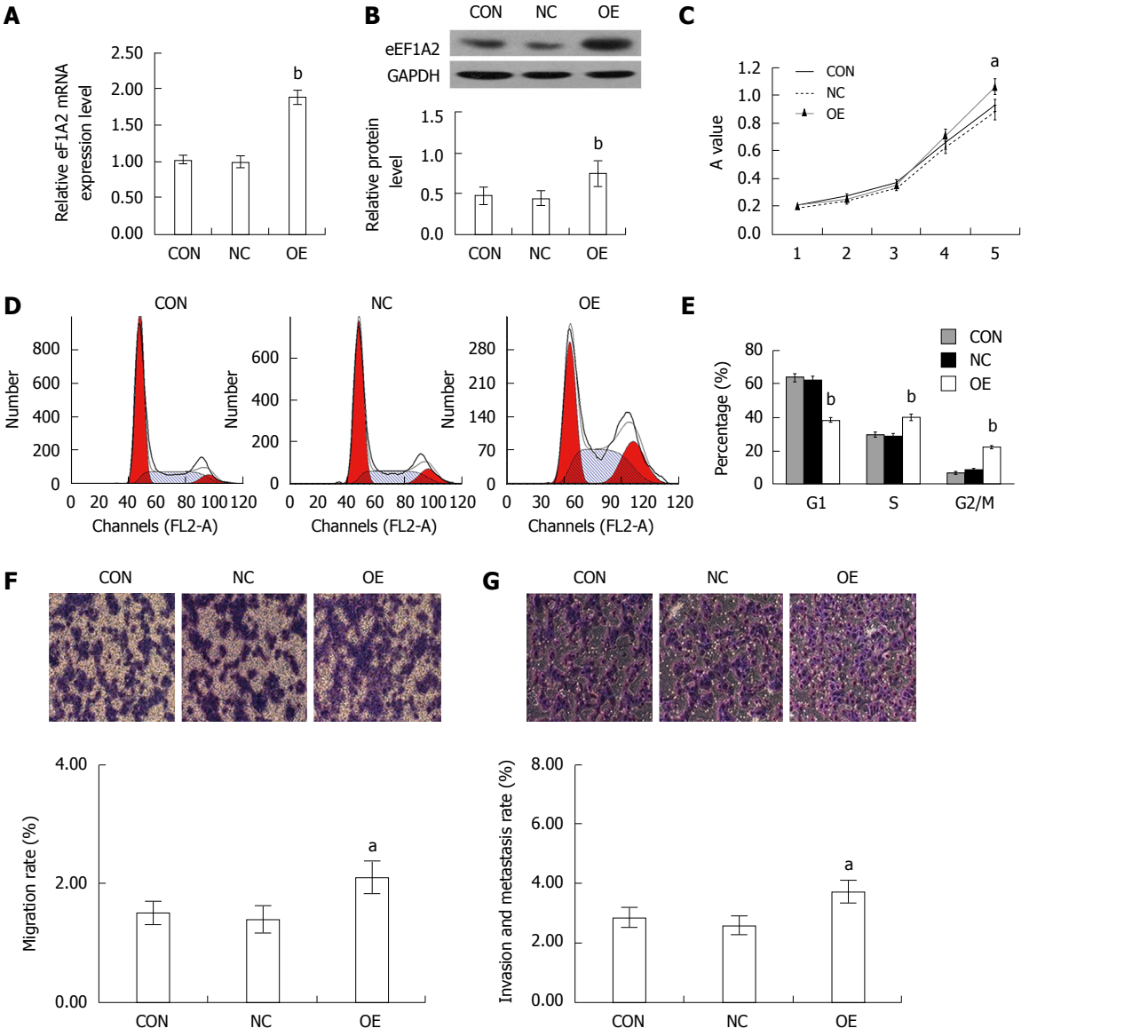

Figure 8 Overexpression of eEF1A2 promotes the proliferation, migration and invasion of SK-HEP-1 cells. SK-HEP-1 cells were infected with the negative lentivirus (NC), without lentivirus transfection (CON), or lentivirus-based eEF1A2 overexpression (OE). A: qRT–PCR; B: Western blot analysis confirmed the expression of eEF1A2 in the SK-HEP-1 cells; C: eEF1A2 promoted the proliferation of SK-HEP-1 cells in MTT assay; D: Cell cycle distribution detected by DNA ploidy analysis; E): Percentages of SK-HEP-1 cells in the G0/G1, S and G2/M phases; F: Migration; G: Metastasis in a Transwell chamber invasion assay. Data are mean ± SD (n = 3). $^{a}P < 0.05$, $^{b}P < 0.01$ *vs* NC and CON.

carcinogenic potential due to its diverse functions. However, the role of eEF1A2 in hepatocellular carcinoma (HCC) remains largely unknown.

Research frontiers

High eEF1A2 levels induce filopodia generation in breast cancer cells, enhancing their malignancy, at least in part by modulating the Akt signaling pathway.

Innovations and breakthroughs

eEF1A2 overexpression resulted in promoted hepatocellular carcinoma cell proliferation, migration and invasion. Conversely, its silencing resulted in opposite effects, with decreased activity of the PI3K/Akt/NF-κB signaling pathway.

Applications

These findings suggest a potential carcinogenic role for eEF1A2 in HCC cells. Therefore, eEF1A2 should be considered a novel diagnostic marker and therapeutic target in HCC.

Terminology

The human eukaryotic elongation factor 1 alpha 2 (*eEF1A2*) gene is located on chromosome 20q13.3.

Peer-review

In this study, the authors found significantly higher eEF1A2 mRNA and protein levels in HCC cancer tissue samples compared with paired control specimens. In accordance, they demonstrated that eEF1A2 knockdown resulted in decreased HCC malignancy, with PI3K/Akt/NF-κB signaling markedly repressed. Meanwhile, eEF1A2 overexpression resulted in increased malignancy potential of HCC cells. These data reveal eEF1A2 as a potential oncogene, which likely acts through PI3K/Akt/NF-κB signaling.

REFERENCES

1 **Knudsen SM**, Frydenberg J, Clark BF, Leffers H. Tissue-dependent variation in the expression of elongation factor-1 alpha isoforms:

isolation and characterisation of a cDNA encoding a novel variant of human elongation-factor 1 alpha. *Eur J Biochem* 1993; **215**: 549-554 [PMID: 8354261]

2 **Kahns S**, Lund A, Kristensen P, Knudsen CR, Clark BF, Cavallius J, Merrick WC. The elongation factor 1 A-2 isoform from rabbit: cloning of the cDNA and characterization of the protein. *Nucleic Acids Res* 1998; **26**: 1884-1890 [PMID: 9518480]

3 **Anand N**, Murthy S, Amann G, Wernick M, Porter LA, Cukier IH, Collins C, Gray JW, Diebold J, Demetrick DJ, Lee JM. Protein elongation factor EEF1A2 is a putative oncogene in ovarian cancer. *Nat Genet* 2002; **31**: 301-305 [PMID: 12053177 DOI: 10.1038/ng904]

4 **Kulkarni G**, Turbin DA, Amiri A, Jeganathan S, Andrade-Navarro MA, Wu TD, Huntsman DG, Lee JM. Expression of protein elongation factor eEF1A2 predicts favorable outcome in breast cancer. *Breast Cancer Res Treat* 2007; **102**: 31-41 [PMID: 16897428 DOI: 10.1007/s10549-006-9315-8]

5 **Zhu H**, Lam DC, Han KC, Tin VP, Suen WS, Wang E, Lam WK, Cai WW, Chung LP, Wong MP. High resolution analysis of genomic aberrations by metaphase and array comparative genomic hybridization identifies candidate tumour genes in lung cancer cell lines. *Cancer Lett* 2007; **245**: 303-314 [PMID: 16517066 DOI: 10.1016/j.canlet.2006.01.020]

6 **Scaggiante B**, Dapas B, Bonin S, Grassi M, Zennaro C, Farra R, Cristiano L, Siracusano S, Zanconati F, Giansante C, Grassi G. Dissecting the expression of EEF1A1/2 genes in human prostate cancer cells: the potential of EEF1A2 as a hallmark for prostate transformation and progression. *Br J Cancer* 2012; **106**: 166-173 [PMID: 22095224 DOI: 10.1038/bjc.2011.500]

7 **Duanmin H**, Chao X, Qi Z. eEF1A2 protein expression correlates with lymph node metastasis and decreased survival in pancreatic ductal adenocarcinoma. *Hepatogastroenterology* 2013; **60**: 870-875 [PMID: 23165190 DOI: 10.5754/hge12869]

8 **Panasyuk G**, Nemazanyy I, Filonenko V, Negrutskii B, El'skaya AV. A2 isoform of mammalian translation factor eEF1A displays increased tyrosine phosphorylation and ability to interact with different signalling molecules. *Int J Biochem Cell Biol* 2008; **40**: 63-71 [PMID: 17936057 DOI: 10.1016/j.biocel.2007.08.014]

9 **Ruest LB**, Marcotte R, Wang E. Peptide elongation factor eEF1A-2/S1 expression in cultured differentiated myotubes and its protective effect against caspase-3-mediated apoptosis. *J Biol Chem* 2002; **277**: 5418-5425 [PMID: 11724805 DOI: 10.1074/jbc.M110685200]

10 **Chang R**, Wang E. Mouse translation elongation factor eEF1A-2 interacts with Prdx-I to protect cells against apoptotic death induced by oxidative stress. *J Cell Biochem* 2007; **100**: 267-278 [PMID: 16888816 DOI: 10.1002/jcb.20969]

11 **Amiri A**, Noei F, Jeganathan S, Kulkarni G, Pinke DE, Lee JM. eEF1A2 activates Akt and stimulates Akt-dependent actin remodeling, invasion and migration. *Oncogene* 2007; **26**: 3027-3040 [PMID: 17130842 DOI: 10.1038/sj.onc.1210101]

12 **Xu C**, Hu DM, Zhu Q. eEF1A2 promotes cell migration, invasion and metastasis in pancreatic cancer by upregulating MMP-9 expression through Akt activation. *Clin Exp Metastasis* 2013; **30**: 933-944 [PMID: 23739844 DOI: 10.1007/s10585-013-9593-6]

13 **Li Z**, Qi CF, Shin DM, Zingone A, Newbery HJ, Kovalchuk AL, Abbott CM, Morse HC. Eef1a2 promotes cell growth, inhibits apoptosis and activates JAK/STAT and AKT signaling in mouse plasmacytomas. *PLoS One* 2010; **5**: e10755 [PMID: 20505761 DOI: 10.1371/journal.pone.0010755]

14 **Parkin DM**, Bray F, Ferlay J, Pisani P. Global cancer statistics, 2002. *CA Cancer J Clin* 2005; **55**: 74-108 [PMID: 15761078]

15 **Grassi G**, Scaggiante B, Farra R, Dapas B, Agostini F, Baiz D, Rosso N, Tiribelli C. The expression levels of the translational factors eEF1A 1/2 correlate with cell growth but not apoptosis in hepatocellular carcinoma cell lines with different differentiation grade. *Biochimie* 2007; **89**: 1544-1552 [PMID: 17825975 DOI: 10.1016/j.biochi.2007.07.007]

16 **Schlaeger C**, Longerich T, Schiller C, Bewerunge P, Mehrabi A, Toedt G, Kleeff J, Ehemann V, Eils R, Lichter P, Schirmacher P, Radlwimmer B. Etiology-dependent molecular mechanisms in human hepatocarcinogenesis. *Hepatology* 2008; **47**: 511-520 [PMID: 18161050 DOI: 10.1002/hep.22033]

17 **Pellegrino R**, Calvisi DF, Neumann O, Kolluru V, Wesely J, Chen X, Wang C, Wuestefeld T, Ladu S, Elgohary N, Bermejo JL, Radlwimmer B, Zörnig M, Zender L, Dombrowski F, Evert M, Schirmacher P, Longerich T. EEF1A2 inactivates p53 by way of PI3K/AKT/mTOR-dependent stabilization of MDM4 in hepatocellular carcinoma. *Hepatology* 2014; **59**: 1886-1899 [PMID: 24285179 DOI: 10.1002/hep.26954]

18 **Hanada M**, Feng J, Hemmings BA. Structure, regulation and function of PKB/AKT--a major therapeutic target. *Biochim Biophys Acta* 2004; **1697**: 3-16 [PMID: 15023346 DOI: 10.1016/j.bbapap.2003.11.009]

19 **Ma Y**, Wang J, Liu L, Zhu H, Chen X, Pan S, Sun X, Jiang H. Genistein potentiates the effect of arsenic trioxide against human hepatocellular carcinoma: role of Akt and nuclear factor-κB. *Cancer Lett* 2011; **301**: 75-84 [PMID: 21078540 DOI: 10.1016/j.canlet.2010.10.022]

20 **Cao H**, Zhu Q, Huang J, Li B, Zhang S, Yao W, Zhang Y. Regulation and functional role of eEF1A2 in pancreatic carcinoma. *Biochem Biophys Res Commun* 2009; **380**: 11-16 [PMID: 19138673 DOI: 10.1016/j.bbrc.2008.12.171]

21 **Martini M**, De Santis MC, Braccini L, Gulluni F, Hirsch E. PI3K/AKT signaling pathway and cancer: an updated review. *Ann Med* 2014; **46**: 372-383 [PMID: 24897931 DOI: 10.3109/07853890.2014.912836]

22 **Lau J**, Castelli LA, Lin EC, Macaulay SL. Identification of elongation factor 1alpha as a potential associated binding partner for Akt2. *Mol Cell Biochem* 2006; **286**: 17-22 [PMID: 16652225 DOI: 10.1007/s11010-005-9006-5]

23 **La Rosa FA**, Pierce JW, Sonenshein GE. Differential regulation of the c-myc oncogene promoter by the NF-kappa B rel family of transcription factors. *Mol Cell Biol* 1994; **14**: 1039-1044 [PMID: 8289784]

24 **Viatour P**, Bentires-Alj M, Chariot A, Deregowski V, de Leval L, Merville MP, Bours V. NF- kappa B2/p100 induces Bcl-2 expression. *Leukemia* 2003; **17**: 1349-1356 [PMID: 12835724 DOI: 10.1038/sj.leu.2402982]

25 **Andela VB**, Gordon AH, Zotalis G, Rosier RN, Goater JJ, Lewis GD, Schwarz EM, Puzas JE, O'Keefe RJ. NFkappaB: a pivotal transcription factor in prostate cancer metastasis to bone. *Clin Orthop Relat Res* 2003; (415 Suppl): S75-S85 [PMID: 14600595 DOI: 10.1097/01.blo.0000093048.96273.aa]

26 **Felx M**, Guyot MC, Isler M, Turcotte RE, Doyon J, Khatib AM, Leclerc S, Moreau A, Moldovan F. Endothelin-1 (ET-1) promotes MMP-2 and MMP-9 induction involving the transcription factor NF-kappaB in human osteosarcoma. *Clin Sci* (Lond) 2006; **110**: 645-654 [PMID: 16417466 DOI: 10.1042/CS20050286]

P- Reviewer: Iqbal M **S- Editor**: Qi Y **L- Editor**: Wang TQ
E- Editor: Wang CH

World Journal of Gastroenterology

Submit a Manuscript: http://www.wjgnet.com/esps/
Help Desk: http://www.wjgnet.com/esps/helpdesk.aspx
DOI: 10.3748/wjg.v22.i16.4238

World J Gastroenterol 2016 April 28; 22(16): 4238-4249
ISSN 1007-9327 (print) ISSN 2219-2840 (online)

ORIGINAL ARTICLE

Observational Study

Transient elastography compared to liver biopsy and morphometry for predicting fibrosis in pediatric chronic liver disease: Does etiology matter?

Behairy El-Sayed Behairy, Mostafa Mohamed Sira, Khaled Refat Zalata, El-Sayed Ebrahem Salama, Mohamed Ahmed Abd-Allah

Behairy El-Sayed Behairy, Mostafa Mohamed Sira, El-Sayed Ebrahem Salama, Mohamed Ahmed Abd-Allah, Department of Pediatric Hepatology, National Liver Institute, Menofiya University, Shebin El-koom 32511, Menofiya, Egypt

Khaled Refat Zalata, Department of Pathology, Faculty of Medicine, Mansura University, Dakahliya Governorate 35516, Egypt

Author contributions: Behairy BE, Sira MM, Zalata KR, Salama EE and Abd-Allah MA were involved in the study concept and design; Behairy BE, Sira MM and Abd-Allah MA were involved in recruitment of patients, clinical management, follow up and contributed to data acquisition; Sira MM performed the statistical analysis and designed the figures; Behairy BE, Sira MM, Zalata KR, Salama EE and Abd-Allah MA performed the data interpretation; Behairy BE, Sira MM, Abd-Allah MA wrote the manuscript; Zalata KR performed histopathological assessment; all the authors reviewed and agreed the final manuscript.

Supported by the National Liver Institute, Menofiya University, Egypt, No. 2011.MDT013.

Institutional review board statement: The study was reviewed and approved by the Institutional Review Board of National Liver Institute, Menofiya University (Egypt).

Informed consent statement: All the legal guardians of the study participants provided informed written consent prior to study enrollment.

Conflict-of-interest statement: There are no conflicts of interest to report.

Data sharing statement: No additional data are available.

Correspondence to: Mostafa Mohamed Sira, MD, Department of Pediatric Hepatology, National Liver Institute, Menofiya University, Gamal Abd El-Nasir, Shebin El-koom 32511, Menofiya, Egypt. msira@liver-eg.org
Telephone: +20-48-2222740
Fax: +20-48-2234586

Received: January 7, 2016
Peer-review started: January 8, 2016
First decision: February 18, 2016
Revised: March 4, 2016
Accepted: March 18, 2016
Article in press: March 18, 2016
Published online: April 28, 2016

Abstract

AIM: To evaluate transient elastography (TE) as a noninvasive tool in staging liver fibrosis compared with liver biopsy and morphometry in children with different chronic liver diseases.

METHODS: A total of 90 children [50 with chronic hepatitis C virus (HCV), 20 with autoimmune hepatitis (AIH) and 20 with Wilson disease] were included in the study and underwent liver stiffness measurement (LSM) using TE. Liver biopsies were evaluated for fibrosis, qualitatively, by Ishak score and quantitatively by fibrosis area fraction (FAF) using digital image analysis (morphometry). LSM was correlated with fibrosis and other studied variables using spearman correlation. A stepwise multiple regression analysis was also

performed to examine independent factors associated with LSM. Different cut-off values of LSM were calculated for predicting individual fibrosis stages using receiver-operating characteristic curve. Cut-off values with optimal clinical performance (optimal sensitivity and specificity simultaneously) were selected.

RESULTS: The majority of HCV group had minimal activity (80%) and no/mild fibrosis (72%). On the other hand, the majority of AIH group had mild to moderate activity (70%) and moderate to severe fibrosis (95%) and all Wilson disease group had mild to moderate activity (100%) and moderate to severe fibrosis (100%). LSM correlated significantly with both FAF and Ishak scores and the correlation appeared better with the latter (r = 0.839 *vs* 0.879, P < 0.0001 for both). LSM discriminated individual stages of fibrosis with high performance. Sensitivity ranged from 81.4% to 100% and specificity ranged from 75.0% to 97.2%. When we compared LSM values for the same stage of fibrosis, they varied according to the different etiologies. Higher values were in AIH (16.15 ± 7.23 kPa) compared to Wilson disease (8.30 ± 0.84 kPa) and HCV groups (7.43 ± 1.73 kPa). Multiple regression analysis revealed that Ishak fibrosis stage was the only independent variable associated with higher LSM (P < 0.0001).

CONCLUSION: TE appears reliable in distinguishing different stages of liver fibrosis in children. However, its values vary according to the disease type. For that, a disease-specific estimation of cut-off values for fibrosis staging is worthy.

Key words: Autoimmune hepatitis; Chronic hepatitis C; Liver fibrosis; Liver stiffness; Morphometry; Pediatrics; Transient elastography; Wilson disease

Core tip: Noninvasive prediction of liver fibrosis is a challenging issue especially in pediatric population. Liver stiffness, as assessed by transient elastography, was reported to be associated with liver fibrosis and therefore proposed as a candidate for fibrosis prediction. The accuracy of transient elastography has been shown to be excellent in a large number of adult studies, most of which are concerned with viral hepatitis. A few studies have also been performed in children. In addition to viral etiology, the current study is concerned with noninvasive assessment of fibrosis in other etiologies of pediatric chronic liver diseases. We compared the liver stiffness measurements with both the Ishak fibrosis score and the quantitative assessment of fibrosis using morphometry.

Behairy BE, Sira MM, Zalata KR, Salama EE, Abd-Allah MA. Transient elastography compared to liver biopsy and morphometry for predicting fibrosis in pediatric chronic liver disease: Does etiology matter? *World J Gastroenterol* 2016; 22(16): 4238-4249 Available from: URL: http://www.wjgnet.com/1007-9327/full/v22/i16/4238.htm DOI: http://dx.doi.org/10.3748/wjg.v22.i16.4238

INTRODUCTION

Severity of liver fibrosis and its progression are the most important factors for the treatment policy and its outcome in children with chronic liver disease. Those with more advanced stages of fibrosis are more likely to develop cirrhosis[1]. Evidence of significant fibrosis is an indication to commence treatment in certain conditions, such as chronic hepatitis C[2]. Evaluation of treatment efficacy and fibrosis regression in autoimmune hepatitis (AIH)[3] and Wilson disease[4] is also important. In those with cirrhosis, surveillance for gastroesophageal varices is of utmost importance[5].

Liver biopsy has been considered the gold standard for evaluating fibrosis. However, it is limited by the need for hospital admission and sedation in children. The accuracy of liver histology assessment has been challenged because of sampling error (1/50000 of the liver is sampled with needle biopsy) and up to 30% of cirrhotic cases might be missed, especially when the liver specimens are small or fragmented[6], in addition to serious risks including bleeding[7,8].

Development of reliable and accurate noninvasive methods for determining fibrosis stage is important across all chronic liver diseases of childhood. Several noninvasive methods have achieved acceptance in adults during the past decade. Biochemical, hematological and serological markers were derived, including the aspartate transaminase-to-platelet ratio index (APRI)[9], the Forns index[10], the fibrotest[11], the hepascore[12], and the Egy-Score[13]. However, most of these fibrosis markers have been evaluated only in chronic hepatitis C virus (HCV) infected patients.

Serum markers often discriminate higher stages of fibrosis, but do not discriminate adequately between earlier stages of fibrosis[14-16]. Identifying early stages of liver fibrosis is essential to initiate therapy and to prevent disease progression. An efficient tool allowing the detection of a slight variation in liver fibrosis would be essential for antifibrotic trials[17].

During the past few years, liver stiffness measurement (LSM) by the use of transient elastography (TE) has become increasingly accepted as a non-invasive marker of liver disease[18]. The accuracy of TE has been shown to be excellent in a large number of adult studies[18-21]. A few studies have also been performed in children[22-26].

The narrow step changes between categorical Ishak or Metavir fibrosis stages are defined by qualitative criteria, which may not closely reflect quantitative fibrosis changes. Digital image analysis (morphometry) allows quantitative assessment of fibrosis area fraction (FAF) on picrosirius red stained liver tissue sections.

It provides more objective data and detecting smaller changes between biopsies particularly in patients with early stages of fibrosis[27-29].

We aimed to study the value of transient elastography as a noninvasive tool in staging liver fibrosis compared with liver biopsy and morphometry in children with different chronic liver diseases.

MATERIALS AND METHODS

Study population

This prospective cross-sectional study included a total of 90 children with three different etiologies of chronic liver disease (50 with chronic HCV infection, 20 with AIH, and 20 with Wilson disease). Patients were recruited consecutively from the Pediatric Hepatology department, National Liver Institute, Menofiya University and Pediatric Hepatology and Gastroenterology Unit, Mansoura University Children Hospital, Egypt in the period between 2012 and 2014. Those with systemic diseases such as cardiac, pulmonary or renal diseases were excluded from the study. Patients with ascites or decompensated liver disease or those with body mass index more than 28 were also excluded. A signed informed consent was obtained from the parents of the patients before enrollment in the study. The study was approved by the Research Ethics Committee of National Liver Institute, Menofiya University, Egypt.

Etiological diagnosis and group allocation

After complete history taking, thorough clinical examination and routine investigations, diagnosis of chronic hepatitis C was based on the presence of serum anti-HCV antibody (Ab) and persistently positive HCV-RNA for six months or more[30,31], negative hepatitis B viral markers and absence of any associated liver disease; supported by the histopathological feature of HCV infection in liver biopsy. AIH was defined according to the simplified AIH score[32]. Wilson disease was diagnosed by clinical and laboratory evidence of chronic hepatitis, the presence of low plasma ceruloplasmin level in some patients, significant urinary copper excretion with penicillamine challenge test, positive Kayser-Flischer ring by slit lamp examination, positive staining for copper in liver biopsy with absent evidence for any other associated liver disease. Severity of liver disease was assessed by the pediatric end-stage liver disease (PELD) score or the model for end-stage liver disease (MELD) score according to the age of the patient[33].

Serum autoantibodies, protein electrophoresis and urinary copper excretion

All patients were tested for serum autoantibodies and gammaglobulins at presentation. Antinuclear antibody (ANA), anti-smooth muscle antibody (ASMA), liver kidney microsomal antibody- 1 (LKM1), and anti-mitochondrial antibody (AMA) were tested by indirect immunofluorescence technique using a Fluoro-Kit™ Combo Pak (All from DiaSorin, Stillwater, Minnesota, United States). Protein electrophoresis was performed using Titan III Cellulose Acetate Plate and scanned using Helena QuickScan 2000 (both from Helena laboratories, Beaumont, Texas, United States). Twenty-four hours urinary copper was determined by spectrophotometry (Biosystems, BTS-310)[4].

Serum viral markers and ultrasonography

Hepatitis B surface antigen (HBsAg), anti-hepatitis B core immunoglobulin (Ig)M and IgG types were tested by enzyme linked immunosorbent assay (ELISA) kit (All from Sorin Biomedica Co, Spain). Anti-HCV Ab was tested by 4th generation ELISA (Innogenetics, Ghent-Belgium). Real-time polymerase chain reaction for HCV-RNA was performed using COBAS® Ampliprep/ COBAS® TaqMan®, Roche Molecular Systems, Inc., Branchburg, NJ, 08876 United States. Ultrasonography was performed by using 2-5-MHz curved linear and 4-8-MHz linear transducers (Xario XG; Toshiba, Tokyo, Japan).

Transient elastography

TE was performed by a single operator who was unaware of the fibrosis stage or blood biomarkers results. TE was performed using the standard M probe using the right lobe of the liver through the intercostal space. Liver stiffness was measured through a device called FibroScan which is composed of an ultrasound transducer probe mounted on the axis of a vibrator. Vibrations of mild amplitude and low frequency are transmitted by the transducer, inducing an elastic shear wave that propagates through the underlying tissues. Pulse echo ultrasound acquisition is used to follow the propagation of the shear wave and to measure its velocity in kilopascals (kPa), which is directly related to tissue stiffness: the stiffer the tissue, the faster the shear wave propagates[34]. Ten successful acquisitions were performed on each patient. The success rate was calculated as the ratio of the number of successful acquisitions over the total number of acquisitions. The median value was kept as representative of the liver elastic modulus. The LSM was considered reliable only if 10 successful acquisitions were obtained, with interquartile range $\leqslant$ 30% of liver stiffness and success rate > 60%. A 10-mm diameter core of tissue was measured in depth between 25 mm and 65 mm. The liver stiffness was expressed in kPa. A higher kPa reflects a stiffer liver and more severe liver fibrosis.

Liver biopsy and histopathological evaluation

Liver biopsy was performed by percutaneous ultrasonography-guided Tru-Cut needle 14 G using local anesthesia and sedation. A core of at least 1.5

cm length or encompassing five portal areas was considered suitable for interpretation. Specimens were fixed in formalin, embedded in paraffin and stained with hematoxylin and eosin, Masson's trichrome, reticulin, Perl's stains, Prussian blue and picrosirius red (for collagen). Hepatic necroinflammatory activity and liver fibrosis were evaluated according to Ishak score. Necroinflammatory activity was classified into minimal (score A1-A3), mild (score A4-A8), moderate (score A9-A12), and severe (score A13-A18)[35]. Fibrosis was classified into mild (F1), moderate (F2-F3), and severe fibrosis or cirrhosis (F4-F6)[36].

FAF by morphometery

The morphometric assessment of liver fibrosis was performed as previously described[3] using the fully automated X-Y motorized stage Leica microscope (Leica, Cambridge, England) and Leica image processor with Leica Qwin software 2004. Liver biopsy assessment by Ishak score and morphometry was performed by a highly experienced hepatopathologist (KRZ) who was unaware of the clinical data or the final diagnosis of the patients. Assessment of liver fibrosis was performed within a week from serological tests.

Statistical analysis

Values were expressed as mean ± SD or number (percentage) of individuals with a condition. For quantitative data, statistical significance was tested by either independent samples *t*-test or by the non-parametric Mann-Whitney *U* test according to the nature of the data. For qualitative data, significance was tested by χ^2 test or Fisher's exact test. Correlation was tested by Spearman test. A stepwise multiple regression analysis was also performed to examine independent factors associated with LSM. The final model was determined using $P_{in} < 0.05$ and $P_{out} < 0.10$. Standardized coefficient (β), R squared (R^2) and *P* values of the independent variables are presented. The diagnostic value of liver stiffness was assessed by calculating the area under the receiver-operating characteristic (AUROC) curves. The diagnostic performance was measured as sensitivity, specificity, positive predictive value and negative predictive value. The cut-off values for optimal clinical performance (optimal sensitivity and specificity simultaneously) were determined from the ROC curves (The upper most left point). Results were considered significant if *P*-value was < 0.05. Statistical analysis was performed using SPSS, version 13 (SPSS Inc, Chicago, IL, United States).

RESULTS

Study population characteristics

A total of 90 children were recruited to the study between 2012 and 2014; 50 children with chronic HCV, 20 children with AIH (18 patients were type-1 AIH and 2 patients were seronegative AIH), and 20 children with Wilson disease. None of the HCV group had jaundice, hepatomegaly or splenomegaly and their liver enzymes were significantly lower compared to the other studied groups ($P < 0.0001$ for all) (Table 1). The majority of HCV group had minimal activity (80%) and no/mild fibrosis (72%). On the other hand, the majority of AIH group had mild to moderate activity (70%) and moderate to severe fibrosis (95%) and all Wilson disease group had mild to moderate activity (100%) and moderate to severe fibrosis (100%) (Table 1).

Correlation of LSM with liver fibrosis in liver biopsy

LSM correlated significantly with both FAF and Ishak fibrosis scores and the correlation appeared better with the latter (Figure 1). The mean value of LSM increases successively with higher stages of fibrosis. Comparing the individual fibrosis stages in all the patients, a significant increase in LSM was found except between F0 and F1 and between F5 and F6 (Figure 2A). Comparing LSM of each fibrosis stage within different etiological groups revealed higher LSM with higher fibrosis stages (Figure 2B-D). Comparing FAF in different Ishak fibrosis stages revealed a significant difference between individual stages except between F4 and F5 ($P = 0.376$) (Figure 3).

Performance of transient elastography in predicting individual fibrosis stages

LSM was a good discriminator of any fibrosis ($\geq$ F1) from absent fibrosis (F0) ($P = 0.039$); of fibrosis $\geq$ F2 from < F2 ($P < 0.0001$); of fibrosis $\geq$ F3 from < F3 ($P < 0.0001$); of fibrosis $\geq$ F4 from < F4 ($P < 0.0001$), of fibrosis $\geq$ F5 from < F5 ($P < 0.0001$) and cirrhosis (F6) from < F6 ($P < 0.0001$) (Table 2). The performance of LSM in the etiological subgroups was calculated as the AUROC and its *P*-value, but the number of patients in each fibrosis category was too small to calculate sensitivity and specificity (Table 3). When we compared LSM values for the same stage of fibrosis, they varied according to the different etiologies with higher values in AIH (16.15 ± 7.23 kPa) compared to Wilson disease (8.30 ± 0.84 kPa) and HCV groups (7.43 ± 1.73 kPa) (Table 4).

Correlation of LSM with the studied variables

LSM correlated significantly with age, serum bilirubin, hepatocellular enzymes, prothrombin time, activity grade and fibrosis stage in liver biopsy; $P = 0.011$ for age, $P = 0.013$ for alkaline phosphatase, $P = 0.002$ for prothrombin time and $P < 0.0001$ for the remaining studied parameters (Table 5). Subsequently, stepwise multiple regression analysis was performed. As a result, Ishak fibrosis stage was the only independent variable associated with higher LSM ($\beta = 0.855$; $R^2 = 0.731$). Other variables were excluded from the model.

Table 1 Basic clinical characteristics of the studied groups

Parameter	HCV (n = 50)	AIH (n = 20)	Wilson disease (n = 20)	P value
Age (yr)	8.50 ± 3.51	8.98 ± 2.98	12.05 ± 4.25	0.003
Sex [male, n (%)]	39 (78)	7 (35)	13 (65)	0.003
Jaundice, n (%)	0 (0)	18 (90)	5 (25)	< 0.0001
Abdominal enlargement, n (%)	0 (0)	5 (25)	15 (75)	< 0.0001
Liver US, n (%)				< 0.0001
Normal	50 (100)	0 (0)	1 (5)	
Enlarged	0 (0)	20 (100)	13 (65)	
Shrunken	0 (0)	0 (0)	6 (30)	
Splenomegaly US, n (%)	0 (0)	16 (80)	20 (100)	< 0.0001
Total bilirubin (mg/dL)	0.97 ± 0.24	7.70 ± 3.72	3.37 ± 2.85	< 0.0001
Direct bilirubin (mg/dL)	0.24 ± 0.17	5.58 ± 3.24	1.8 ± 1.30	< 0.0001
Albumin (g/dL)	4.40 ± 0.61	3.71 ± 1.71	3.55 ± 0.71	< 0.0001
Aspartate transaminase (U/L)	27.21 ± 14.75	225.10 ± 21.7	76.59 ± 68.43	< 0.0001
Alanine transaminase (U/L)	29.52 ± 14.93	218.65 ± 14.2	87.05 ± 56.26	< 0.0001
Gamma-glutamyl transpeptidase (U/L)	28.66 ± 13.80	52.50 ± 19.22	51.25 ± 37.89	< 0.0001
Alkaline phosphatase (U/L)	127.82 ± 74.13	122.25 ± 45.03	222.30 ± 134.23	< 0.0001
Prothrombin time (s)	13.2 ± 1.1	14.87 ± 3.13	16.18 ± 5.31	0.003
Activity grade, n (%)				< 0.0001
Minimal (A1-A3)	40 (80)	6 (30)	0 (0)	
Mild (A4-A8)	8 (16)	8 (40)	18 (90)	
Moderate (A9-A12)	2 (4)	6 (30)	2 (10)	
Fibrosis category, n (%)				< 0.0001
Absent (F0)	4 (8)	0 (0)	0 (0)	
Mild (F1)	32 (64)	1 (5)	0 (0)	
Moderate (F2-F3)	14 (28)	7 (35)	6 (30)	
Severe (F4-F6)	0 (0)	12 (60)	14 (70)	
Fibrosis area fraction (%)	2.72 ± 1.66	17.41 ± 9.24	12.68 ± 4.59	< 0.0001
Liver stiffness (kPa)	5.75 ±1.81	22.13 ± 14.23	20.05 ± 10.57	< 0.0001

AIH: Autoimmune hepatitis; HCV: Hepatitis C virus; US: Ultrasonography.

FAF according to Ishak scores and correlation of both with disease severity

FAF varied significantly with increasing stage of Ishak score. There was overlap in the values of FAF in F5 and F6 with no significant statistical difference (P = 0.376) (Figure 3). PELD/MELD scores correlated significantly with both FAF and Ishak score, nonetheless, the correlation with Ishak score appeared better than with FAF (P = 0.001 and 0.022 respectively) (Figure 4).

DISCUSSION

The current study showed a significant correlation between LSM and both the Ishak fibrosis stage and FAF with better correlation with Ishak fibrosis stage. The close correlation of TE readings with the extent of fibrosis suggests that TE is an ideal tool to follow liver fibrosis over years. In previous studies, among patients with viral hepatitis, the diagnostic performance of LSM was best for histologic cirrhosis and was less satisfactory for earlier stages of liver fibrosis[19,37-40].

Our results demonstrated that LSM could significantly discriminate individual stages of fibrosis even the earlier stages (≥ F1) from absent fibrosis (F0). Different LSM cut-off values have been proposed by different investigators for various stages of liver fibrosis. The optimal LSM cut-off for cohorts with predominantly chronic hepatitis C patients was between 10.4 and 17.6 kPa, and the AUROC for liver cirrhosis was 0.93-0.96[19,37-39].

de Lédinghen *et al*[22] reported a significant correlation of LSM with Metavir score in children with chronic liver disease but the performance was studied only for discriminating cirrhosis bacause F2 and F3 values were comparable. The better results in our study may be due to the wider range of Ishak score (7 stages) compared to Metavir score (5 stages).

The performance of LSM in discriminating individual stages of fibrosis was highly significant (P < 0.0001) for stages ≥ F2 with AUROC more than 0.94, and for ≥ F1 (*i.e.*, discriminating F0) the AUROC was 0.807 and P = 0.039. The significance for discriminating F0 was abolished when comparing LSM according to the etiology (P = 0.192). F0 was found only in patients with chronic HCV in our study, but in none of the other studied groups. This may be due to the milder course of the HCV disease which induces mild changes in the liver with a low level of fibrosis and a low rate of progression[41].

The higher LSM values for different Ishak stages in AIH patients compared to the other studied groups in our study was in agreement with that of Fitzpatrick *et al*[26] and others[42]. In our study, AIH patients had higher stages of fibrosis and higher grades of inflammatory activity. Increased histologic necroinflammation, which is a logical cause of

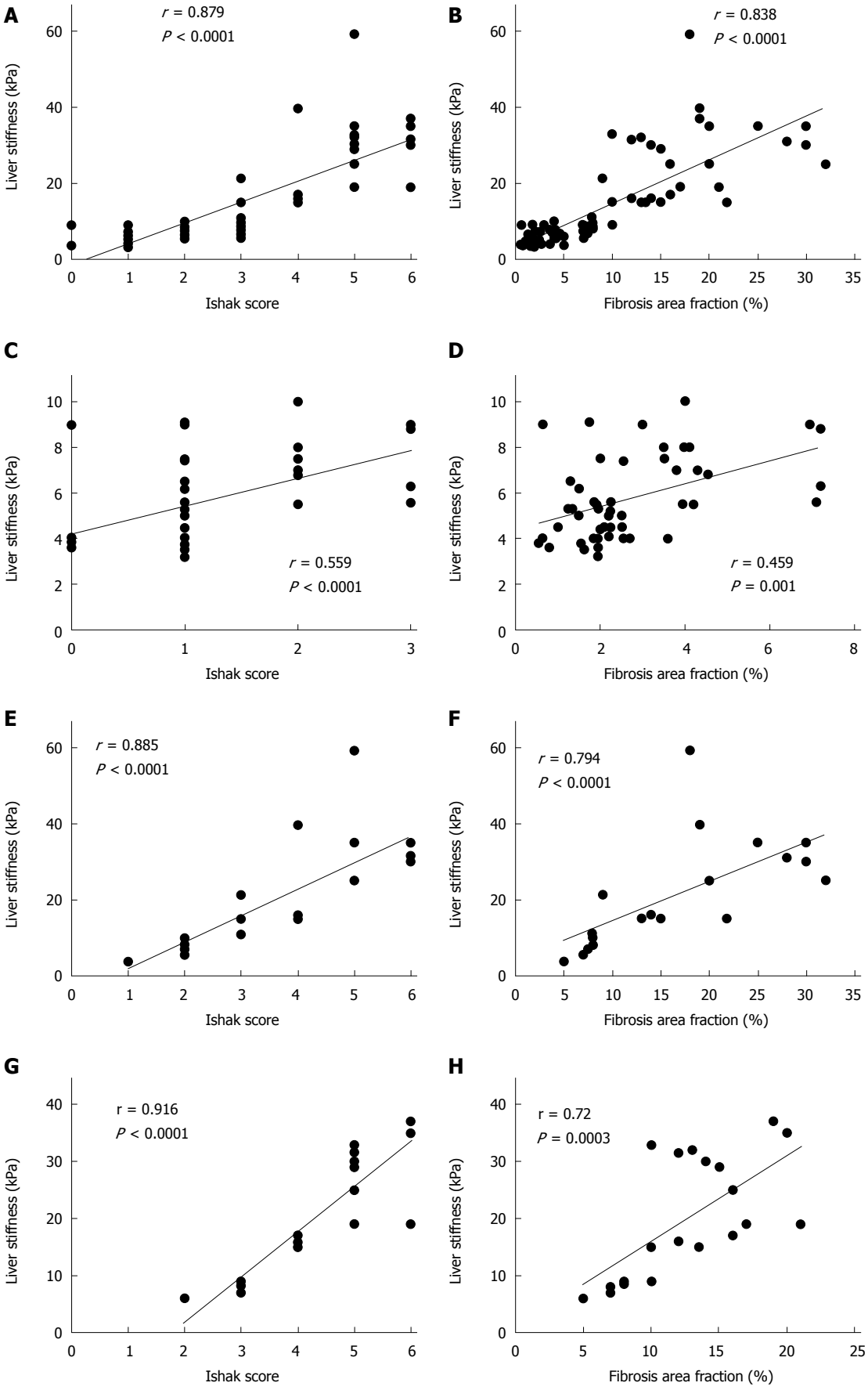

Figure 1 Correlation of LSM with fibrosis category by Ishak scores (left panel) and fibrosis area fraction (right panel). A and B: All patients; C and D: HCV patients; E and F: AIH patients; G and H: Wilson disease patients.

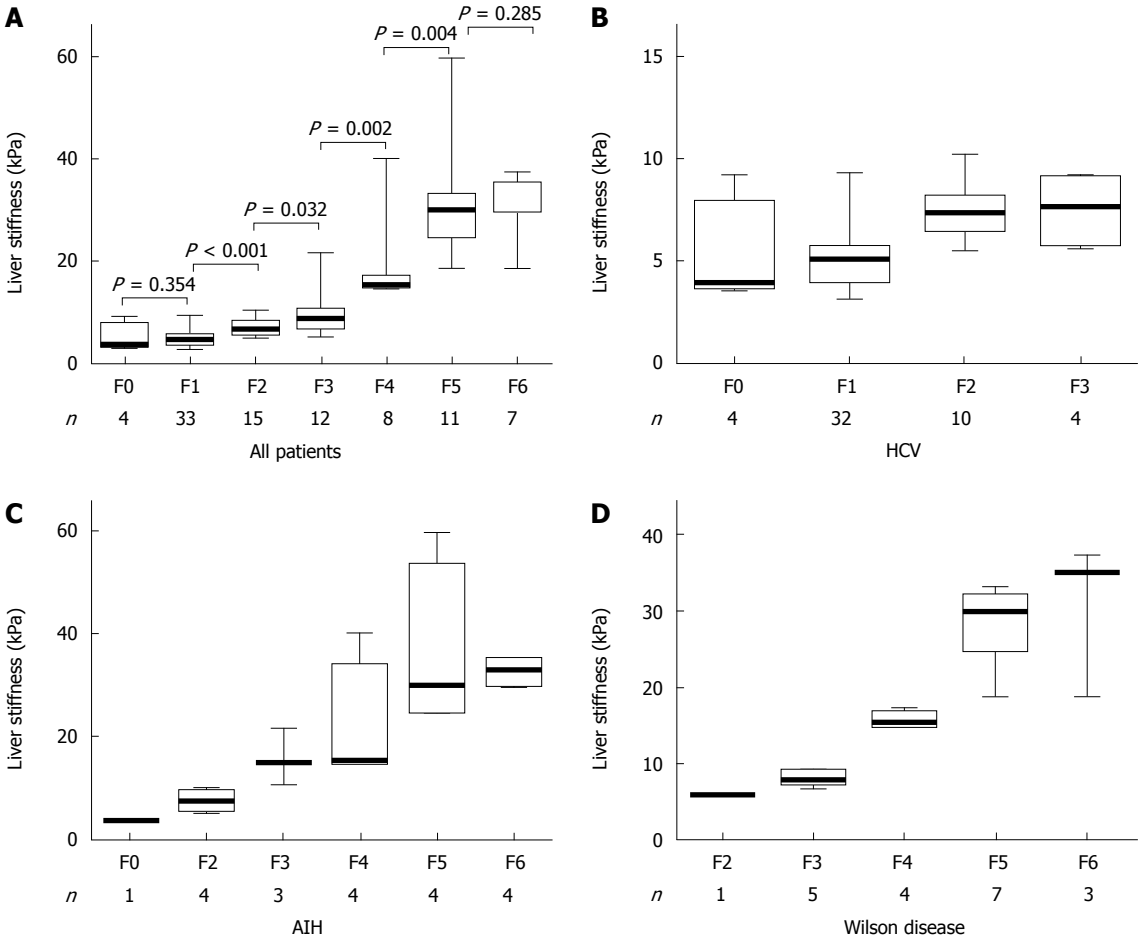

Figure 2 Distribution of liver stiffness measurement according to categorical fibrosis scores. A: All patients; B: HCV group; C: AIH group; D: Wilson disease group. Box-and-whiskers plot for liver stiffness measurement. The top and bottom of each box are the 75th and 25th percentiles. The line through the box is the median and the error bars are the maximum and minimum. The horizontal bar represents the significance between the designated groups.

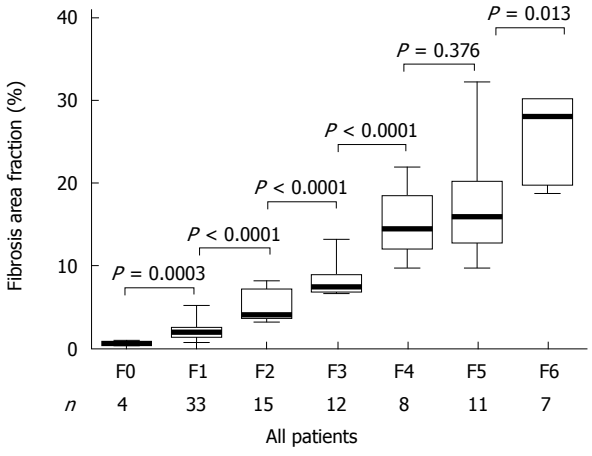

Figure 3 Distribution of fibrosis area fraction according to the categorical fibrosis scores. Box-and-whiskers plot for liver stiffness measurement. The top and bottom of each box are the 75th and 25th percentiles. The line through the box is the median and the error bars are the maximum and minimum. The horizontal bar represents the significance between the designated groups.

increased hepatic fibrosis, may explain the higher results of LSM in AIH patients compared with HCV and Wilson disease groups. One possible explanation for the higher LSM was a stiffer liver during active inflammation[1].

When we compared LSM for the same stage of fibrosis, it varied according to the etiology. This carries the possibility that, patients only having mild fibrosis would be misdiagnosed as moderate to severe fibrosis and even cirrhosis if they had increase histological activity. That is why it is better to estimate disease-specific cut-off values for predicting different stages of fibrosis due to the variable nature of liver diseases. For that, we checked the performance of LSM in the etiological subgroups which showed wide variability among the calculated AUROC and their *P*-values, but the number of patients in each fibrosis category was too small to calculate sensitivity and specificity. Similar to our results, other reports found that LSM was associated with the Ishak score in AIH[3,43], in HCV[44,45] and in Wilson disease patients[46].

The better correlation of the LSM in our study with Ishak scores compared to FAF suggests that LSM reflect the pattern (or quality) of fibrosis better than the quantity of hepatic collagen deposition. Liver diseases involve several types of cell injury, each of which leads to wound healing by fibrosis of distinct

Table 2 Clinical performance of liver stiffness in predicting individual Ishak fibrosis stages in all the patients

Ishak fibrosis stage	Cut-off (kPa)	AUROC	*P* value	Sensitivity	Specificity	PPV	NPV
≥ F1	4.75	0.807	0.039	81.4	75.0	98.6	15.7
≥ F2	6.65	0.947	< 0.0001	88.7	86.5	90.4	84.2
≥ F3	8.25	0.960	< 0.0001	89.5	90.4	87.2	92.2
≥ F4	13.0	0.993	< 0.0001	100	96.9	92.9	100
≥ F5	18.0	0.985	< 0.0001	100	97.2	90.0	100
F6	29.5	0.941	< 0.0001	85.7	91.6	46.2	98.7

AUROC: Area under receiver operating characteristic curve; PPV: Positive predictive value; NPV: Negative predictive value.

Table 3 Area under receiver operating characteristic curve for liver stiffness in predicting individual Ishak fibrosis stages in the different etiological groups

Ishak fibrosis stage	HCV		AIH		Wilson disease	
	AUROC	*P* value	AUROC	*P* value	AUROC	*P* value
≥ F1	0.698	0.192	NA	--	NA	--
≥ F2	0.870	< 0.0001	1.000	< 0.0001	NA	--
≥ F3	0.799	0.049	1.000	< 0.0001	1.000	< 0.0001
≥ F4	NA	--	0.958	0.001	1.000	< 0.0001
≥ F5	NA	--	0.927	0.002	1.000	< 0.0001
F6	NA	--	0.828	0.047	0.837	0.044

AIH: Autoimmune hepatitis; AUROC: Area under receiver operating characteristic; HCV: Hepatitis C virus.

Table 4 Liver stiffness measurement in every fibrosis stage by the disease group

Ishak fibrosis stage	All patients (*n* = 90) kPa	HCV (*n* = 50) kPa	AIH (*n* = 20) kPa	Wilson disease (*n* = 20) kPa
F0	5.10 ± 2.61	5.10 ± 2.61	--	--
F1	5.10 ± 1.45	5.13 ± 1.45	3.70	--
F2	7.32 ± 1.4	7.33 ± 1.32	7.50 ± 0.71	6.00
F3	9.88 ± 4.33	7.43 ± 1.73	16.15 ± 7.23	8.30 ± 0.84
F4	18.58 ± 8.57	--	21.43 ± 12.19	15.75 ± 0.96
F5	31.25 ± 10.38	--	36.08 ± 16.19	28.49 ± 4.93
F6	31.71 ± 6.13	--	32.75 ± 3.63	30.33 ± 9.87

AIH: Autoimmune hepatitis; HCV: Hepatitis C virus.

Table 5 Correlation of liver stiffness with age, laboratory, and histopathological parameters of the studied patients

Parameter	Correlation	
	r	*P* value
Age (yr)	0.267	0.011
Total bilirubin (mg/dL)	0.433	< 0.0001
Direct bilirubin (mg/dL)	0.506	< 0.0001
Albumin (g/dL)	-0.419	< 0.0001
Alanine transaminase (U/L)	0.622	< 0.0001
Aspartate transaminase (U/L)	0.559	< 0.0001
Alkaline phosphatase (U/L)	0.261	0.013
gamma-glutamyl transpeptidase (U/L)	0.559	< 0.0001
Prothrombin time (s)	0.322	0.002
Ishak activity grade	0.760	< 0.0001
Ishak fibrosis stage	0.879	< 0.0001

types and location. In chronic hepatitis (seen most often in chronic viral hepatitis, as well as in AIH, drug reactions, and some metabolic disorders as Wilson disease), fibrosis mainly develop from portal myofibroblasts and give rise to a dense, stellate, and regularly-distributed portal and periportal fibrosis that may form septa. On the other hand, fibrosis is mainly located in the perisinusoidal space of the centrilobular area, and in the wall of the centrilobular vein in alcoholic and nonalcoholic steatohepatitis[17,47,48].

Sandrini *et al*[49] investigated what type of fibrosis influences LSM. They found that the area of portal-bridging fibrosis better correlated with the liver stiffness than did the area of whole fibrosis or the area of perisinusoidal fibrosis. In the early fibrosis stages, there was a significant increase of perisinusoidal fibrosis from F0 to F2 Metavir, more than that of portal-bridging fibrosis. In subsequent stages F3 and F4, the area of perisinusoidal fibrosis stabilized[49]. Ishak scoring system is based on the pattern and extension of portal fibrosis, while FAF evaluates the whole amount of collagen whether portal or perisinusoidal.

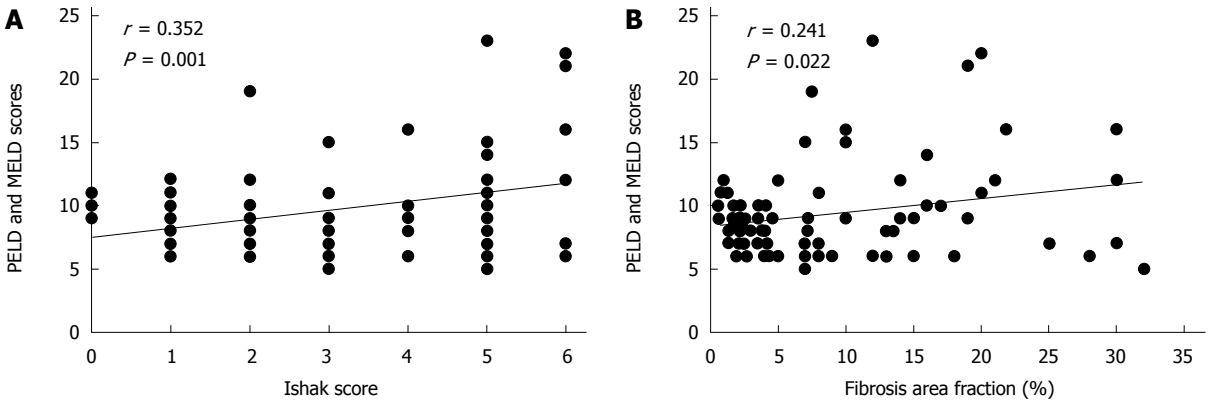

Figure 4 Correlation of PELD/MELD scores of all studied patients with categorical Ishak fibrosis scores (A) and fibrosis area fraction (B). PELD: Pediatric end-stage liver disease; MELD: Model for end-stage liver disease.

Taken together, this may explain the better correlation of LSM with Ishak scores in our study.

In contrast to semiquantitative fibrosis scores that rely on the pattern of architectural distortion caused by fibrosis, morphometry determines the proportion of collagenous tissue in a specimen, regardless of the pattern, and provides precise measurements on a continuous scale. Within any given semiquantitative stage, a wide range of collagen may be present, and considerable overlap exists within Metavir and Ishak stages[45]. In our study, FAF was largely overlapping between F4 and F5 with no significant difference (P = 0.376).

Biopsy sampling error will always be present to some extent, so it must be emphasized that morphometry is not appropriate for evaluation of changes in individual patients but should be reserved for statistical analysis and comparison of changes in large cohorts[45].

The question whether the severity and deterioration of liver disease is related to the pattern (quality) or to the quantity of fibrosis remains to be answered. The PELD/MELD scores were developed to create an integrated system of deceased donor liver allocation based on the severity of the chronic liver disease[50]. In our study, PELD/MELD scores were significantly correlated with both Ishak score and FAF but the correlation appeared better with Ishak scores (P = 0.001 *vs* 0.022). This may suggest that the information about the pattern (or quality) of fibrosis by semiquantitative Ishak score is more important than the overall amount of fibrosis by FAF in predicting the outcome of liver disease.

In the current study, LSM at cut-off values of 4.75, 6.65, 8.25, 13.0, 18.0, and 29.5 kPa was able to discriminate ≥ F1, ≥ F2, ≥ F3, ≥ F4, ≥ F5, and F6 respectively. Fitzpatrick *et al*[26] using Metavir score in pediatric patients with chronic liver diseases reported an LSM cut-off values of 6.1, 6.9, 7.5 and 14.1 kPa in discriminating ≥ F1, ≥ F2, ≥ F3, and F4. Other studies reported only the discrimination of cirrhosis. de Lédinghen *et al*[22] studied LSM performance in children with chronic liver disease. Using Metavir score, they reported that LSM was able to discriminate cirrhosis with AUROC of 0.88.

Wong *et al*[1] reported that a cut-off value of 8.4 kPa was associated with cirrhosis in adults with chronic liver disease at a very high sensitivity (93%) and a specificity of 79%. On the other hand, a cut-off value of 13.4 kPa was associated with high specificity (95%) but with low sensitivity (41%). In addition, Wang *et al*[51] reported that values below 6 kPa are considered as normal and exclude ongoing liver disease, while cut-off values of 8 and 12.5 kPa represent generally accepted values for discriminating F3 and F4 fibrosis in adults with chronic liver disease.

Staging of fibrosis with biopsy will always carry a risk, albeit low, of misclassification thus making the term "best" standard more appropriate than "gold" standard for liver biopsy[52]. As liver biopsy with its limitations[53] is used as a reference, a perfect surrogate will never reach maximal value[52].

Because LSM represents a volume of liver tissue at least 100 times bigger than a biopsy sample, a possibility that the performance of LSM has been underestimated can not be excluded. Yet it represents an efficient, noninvasive rapid painless and reproducible tool for fibrosis evaluation[54].

The limitation of the present study was the relatively small numbers in each of the etiological groups. In addition, the paucity of children with no fibrosis (F0) made it difficult to differentiate between no and minimal fibrosis. Future studies on larger population number are advisable.

In conclusion, TE appears reliable in distinguishing different stages of liver fibrosis in children with different chronic liver diseases. Routine use of this technique may significantly decrease the number of biopsies performed and provide a reliable method of noninvasive monitoring of liver disease progression or regression in children. Patients with increased necroinflammatory activity tend to have higher LSM values. For that, a disease-specific estimation of cut-

off values for fibrosis staging is worthy.

ACKNOWLEDGMENTS

The authors would like to thank the doctors and nursing staff of Pediatric Hepatology and Gastroenterology Unit, Mansoura University Children Hospital, for their help and contribution.

COMMENTS

Background

The need for repetition of liver biopsy in patients with chronic liver disease, especially in assessing the degree of fibrosis and follow-up of treatment protocols, justifies an intensive search for non-invasive alternatives. Of these alternatives, liver stiffness measurement, as assessed by transient elastography, has been proposed. The accuracy of transient elastography has been shown to be excellent in a large number of adult studies. A few studies have also been performed in children.

Research frontiers

The natural course of hepatitis C viral infection in children differs from that in adults since the infection is relatively benign and induces mild changes in the liver with a low level of fibrosis. Progression of liver fibrosis in other liver diseases such as autoimmune hepatitis and Wilson disease is somehow faster. In patients with no or minimal fibrosis at presentation, treatment could possibly be delayed or withheld. On the other hand, patients with significant fibrosis progress almost invariably to cirrhosis more rapidly and treatment should be strongly considered. The decision to stop treatment in some cases, such as autoimmune hepatitis, may necessitate a second liver biopsy.

Innovations and breakthroughs

Most of liver stiffness studies have been conducted only in chronic hepatitis C virus infected patients. The current study includes different etiologies of pediatric chronic liver diseases. When the authors compared liver stiffness values for the same stage of fibrosis, they varied according to the different etiologies. Patients with increased necroinflammatory activity tend to have higher liver stiffness values. For that, a disease-specific estimation of cut-off values is worthy.

Terminology

Hepatic fibrosis is the final common path of liver injury in most chronic liver diseases and can lead to cirrhosis, which is responsible for the majority of clinical complications. Fibrosis is characterized by excess deposition of extracellular matrix components including different collagens and non-collagenous proteins. The more deposition of extracellular matrix in the liver the stiffer it gets. Liver stiffness is directly correlated with the amount of liver fibrosis. Digital image analysis (morphometry) allows quantitative assessment of fibrosis area fraction in liver tissue sections regardless of the pattern (or quality) of fibrosis. It detects smaller changes between biopsies particularly in patients with early stage fibrosis.

Peer-review

The authors demonstrated that Ishak fibrosis stage was the only independent variable associated with liver stiffness measurement assessed by TE. They concluded that TE may be useful for distinguishing different stages of liver fibrosis in pediatric patients with chronic liver diseases. Overall impression: The authors well demonstrated usefulness of TE for assessing liver fibrosis in pediatric patients with different chronic liver diseases.

REFERENCES

1 **Wong GL**, Wong VW, Choi PC, Chan AW, Chum RH, Chan HK, Lau KK, Chim AM, Yiu KK, Chan FK, Sung JJ, Chan HL. Assessment of fibrosis by transient elastography compared with liver biopsy and morphometry in chronic liver diseases. *Clin Gastroenterol Hepatol* 2008; **6**: 1027-1035 [PMID: 18456573 DOI: 10.1016/j.cgh.2008.02.038]

2 **Strader DB**, Wright T, Thomas DL, Seeff LB. Diagnosis, management, and treatment of hepatitis C. *Hepatology* 2004; **39**: 1147-1171 [PMID: 15057920 DOI: 10.1002/hep.20119]

3 **Abdalla AF**, Zalata KR, Ismail AF, Shiha G, Attiya M, Abo-Alyazeed A. Regression of fibrosis in paediatric autoimmune hepatitis: morphometric assessment of fibrosis versus semiquantiatative methods. *Fibrogenesis Tissue Repair* 2009; **2**: 2 [PMID: 19341455 DOI: 10.1186/1755-1536-2-2]

4 **Roberts EA**, Schilsky ML. Diagnosis and treatment of Wilson disease: an update. *Hepatology* 2008; **47**: 2089-2111 [PMID: 18506894 DOI: 10.1002/hep.22261]

5 **Garcia-Tsao G**, Sanyal AJ, Grace ND, Carey W. Prevention and management of gastroesophageal varices and variceal hemorrhage in cirrhosis. *Hepatology* 2007; **46**: 922-938 [PMID: 17879356 DOI: 10.1002/hep.21907]

6 **Bedossa P**, Dargère D, Paradis V. Sampling variability of liver fibrosis in chronic hepatitis C. *Hepatology* 2003; **38**: 1449-1457 [PMID: 14647056 DOI: 10.1016/j.hep.2003.09.022]

7 **Cadranel JF**, Rufat P, Degos F. Practices of liver biopsy in France: results of a prospective nationwide survey. For the Group of Epidemiology of the French Association for the Study of the Liver (AFEF). *Hepatology* 2000; **32**: 477-481 [PMID: 10960438 DOI: 10.1053/jhep.2000.16602]

8 **Terjung B**, Lemnitzer I, Dumoulin FL, Effenberger W, Brackmann HH, Sauerbruch T, Spengler U. Bleeding complications after percutaneous liver biopsy. An analysis of risk factors. *Digestion* 2003; **67**: 138-145 [PMID: 12853725 DOI: 10.1159/000071293]

9 **Wai CT**, Greenson JK, Fontana RJ, Kalbfleisch JD, Marrero JA, Conjeevaram HS, Lok AS. A simple noninvasive index can predict both significant fibrosis and cirrhosis in patients with chronic hepatitis C. *Hepatology* 2003; **38**: 518-526 [PMID: 12883497 DOI: 10.1053/jhep.2003.50346]

10 **Forns X**, Ampurdanès S, Llovet JM, Aponte J, Quintó L, Martínez-Bauer E, Bruguera M, Sánchez-Tapias JM, Rodés J. Identification of chronic hepatitis C patients without hepatic fibrosis by a simple predictive model. *Hepatology* 2002; **36**: 986-992 [PMID: 12297848 DOI: 10.1053/jhep.2002.36128]

11 **Imbert-Bismut F**, Ratziu V, Pieroni L, Charlotte F, Benhamou Y, Poynard T. Biochemical markers of liver fibrosis in patients with hepatitis C virus infection: a prospective study. *Lancet* 2001; **357**: 1069-1075 [PMID: 11297957 DOI: 10.1016/S0140-6736(00)04258-6]

12 **Adams LA**, Bulsara M, Rossi E, DeBoer B, Speers D, George J, Kench J, Farrell G, McCaughan GW, Jeffrey GP. Hepascore: an accurate validated predictor of liver fibrosis in chronic hepatitis C infection. *Clin Chem* 2005; **51**: 1867-1873 [PMID: 16055434 DOI: 10.1373/clinchem.2005.048389]

13 **Alboraie M**, Khairy M, Elsharkawy A, Elsharkawy M, Asem N, Abo El-Seoud AR, Elghamry FG, Esmat G. Egy-score as a noninvasive score for the assessment of hepatic fibrosis in chronic hepatitis C: a preliminary approach. *Saudi J Gastroenterol* 2014; **20**: 170-174 [PMID: 24976280 DOI: 10.4103/1319-3767.133003]

14 **Abdel-Ghaffar TY**, Behairy EB, Abd El-Shaheed A, Mahdy K, El-Batanony M, Hussein MH, Sira MM. Clinical Benefits of Biochemical Markers of Fibrosis in Egyptian Children With Chronic Liver Diseases. *Gastroenterol Res* 2010; **3**: 262-271 [DOI: 10.4021/gr246w]

15 **Sira MM**, Behairy BE, Abd-Elaziz AM, Abd Elnaby SA, Eltahan EE. Serum Inter-Alpha-Trypsin Inhibitor Heavy Chain 4 (ITIH4) in Children with Chronic Hepatitis C: Relation to Liver Fibrosis and Viremia. *Hepat Res Treat* 2014; **2014**: 307942 [PMID: 25295185 DOI: 10.1155/2014/307942]

16 **Behairy BE**, El-Mashad GM, Abd-Elghany RS, Ghoneim EM, Sira MM. Serum complement C4a and its relation to liver fibrosis in children with chronic hepatitis C. *World J Hepatol* 2013; **5**: 445-451 [PMID: 24023984 DOI: 10.4254/wjh.v5.i8.445]

17 **Ziol M**, Kettaneh A, Ganne-Carrié N, Barget N, Tengher-

Barna I, Beaugrand M. Relationships between fibrosis amounts assessed by morphometry and liver stiffness measurements in chronic hepatitis or steatohepatitis. *Eur J Gastroenterol Hepatol* 2009; **21**: 1261-1268 [PMID: 19478678 DOI: 10.1097/MEG.0b013e32832a20f5]

18 **Friedrich-Rust M**, Ong MF, Martens S, Sarrazin C, Bojunga J, Zeuzem S, Herrmann E. Performance of transient elastography for the staging of liver fibrosis: a meta-analysis. *Gastroenterology* 2008; **134**: 960-974 [PMID: 18395077 DOI: 10.1053/j.gastro.2008.01.034]

19 **Fraquelli M**, Rigamonti C, Casazza G, Conte D, Donato MF, Ronchi G, Colombo M. Reproducibility of transient elastography in the evaluation of liver fibrosis in patients with chronic liver disease. *Gut* 2007; **56**: 968-973 [PMID: 17255218 DOI: 10.1136/gut.2006.111302]

20 **Arena U**, Vizzutti F, Abraldes JG, Corti G, Stasi C, Moscarella S, Milani S, Lorefice E, Petrarca A, Romanelli RG, Laffi G, Bosch J, Marra F, Pinzani M. Reliability of transient elastography for the diagnosis of advanced fibrosis in chronic hepatitis C. *Gut* 2008; **57**: 1288-1293 [PMID: 18448567 DOI: 10.1136/gut.2008.149708]

21 **Chon YE**, Choi EH, Song KJ, Park JY, Kim do Y, Han KH, Chon CY, Ahn SH, Kim SU. Performance of transient elastography for the staging of liver fibrosis in patients with chronic hepatitis B: a meta-analysis. *PLoS One* 2012; **7**: e44930 [PMID: 23049764 DOI: 10.1371/journal.pone.0044930]

22 **de Lédinghen V**, Le Bail B, Rebouissoux L, Fournier C, Foucher J, Miette V, Castéra L, Sandrin L, Merrouche W, Lavrand F, Lamireau T. Liver stiffness measurement in children using FibroScan: feasibility study and comparison with Fibrotest, aspartate transaminase to platelets ratio index, and liver biopsy. *J Pediatr Gastroenterol Nutr* 2007; **45**: 443-450 [PMID: 18030211 DOI: 10.1097/MPG.0b013e31812e56ff]

23 **Nobili V**, Vizzutti F, Arena U, Abraldes JG, Marra F, Pietrobattista A, Fruhwirth R, Marcellini M, Pinzani M. Accuracy and reproducibility of transient elastography for the diagnosis of fibrosis in pediatric nonalcoholic steatohepatitis. *Hepatology* 2008; **48**: 442-448 [PMID: 18563842 DOI: 10.1002/hep.22376]

24 **Alkhouri N**, Sedki E, Alisi A, Lopez R, Pinzani M, Feldstein AE, Nobili V. Combined paediatric NAFLD fibrosis index and transient elastography to predict clinically significant fibrosis in children with fatty liver disease. *Liver Int* 2013; **33**: 79-85 [PMID: 23146095 DOI: 10.1111/liv.12024]

25 **Breton E**, Bridoux-Henno L, Guyader D, Daniélou H, Jouan H, Beuchée A, Nousbaum JB, Dabadie A. [Value of transient elastography in noninvasive assessment in children's hepatic fibrosis]. *Arch Pediatr* 2009; **16**: 1005-1010 [PMID: 19446446 DOI: 10.1016/j.arcped.2009.03.021]

26 **Fitzpatrick E**, Quaglia A, Vimalesvaran S, Basso MS, Dhawan A. Transient elastography is a useful noninvasive tool for the evaluation of fibrosis in paediatric chronic liver disease. *J Pediatr Gastroenterol Nutr* 2013; **56**: 72-76 [PMID: 22922372 DOI: 10.1097/MPG.0b013e31826f2760]

27 **Caballero T**, Pérez-Milena A, Masseroli M, O'Valle F, Salmerón FJ, Del Moral RM, Sánchez-Salgado G. Liver fibrosis assessment with semiquantitative indexes and image analysis quantification in sustained-responder and non-responder interferon-treated patients with chronic hepatitis C. *J Hepatol* 2001; **34**: 740-747 [PMID: 11434621 DOI: 10.1016/S0168-8278(01)00006-X]

28 **Lazzarini AL**, Levine RA, Ploutz-Snyder RJ, Sanderson SO. Advances in digital quantification technique enhance discrimination between mild and advanced liver fibrosis in chronic hepatitis C. *Liver Int* 2005; **25**: 1142-1149 [PMID: 16343064 DOI: 10.1111/j.1478-3231.2005.01155.x]

29 **O'Brien MJ**, Keating NM, Elderiny S, Cerda S, Keaveny AP, Afdhal NH, Nunes DP. An assessment of digital image analysis to measure fibrosis in liver biopsy specimens of patients with chronic hepatitis C. *Am J Clin Pathol* 2000; **114**: 712-718 [PMID: 11068544 DOI: 10.1309/D7AU-EYW7-4B6C-K08Y]

30 **Alisi A**, Comparcola D, Nobili V. Treatment of chronic hepatitis C in children: is it necessary and, if so, in whom? *J Hepatol* 2010; **52**: 472-474 [PMID: 20185196 DOI: 10.1016/j.jhep.2009.12.018]

31 **Chen SL**, Morgan TR. The natural history of hepatitis C virus (HCV) infection. *Int J Med Sci* 2006; **3**: 47-52 [PMID: 16614742 DOI: 10.7150/ijms.3.47]

32 **Hennes EM**, Zeniya M, Czaja AJ, Parés A, Dalekos GN, Krawitt EL, Bittencourt PL, Porta G, Boberg KM, Hofer H, Bianchi FB, Shibata M, Schramm C, Eisenmann de Torres B, Galle PR, McFarlane I, Dienes HP, Lohse AW. Simplified criteria for the diagnosis of autoimmune hepatitis. *Hepatology* 2008; **48**: 169-176 [PMID: 18537184 DOI: 10.1002/hep.22322]

33 **Freeman RB**, Wiesner RH, Harper A, McDiarmid SV, Lake J, Edwards E, Merion R, Wolfe R, Turcotte J, Teperman L. The new liver allocation system: moving toward evidence-based transplantation policy. *Liver Transpl* 2002; **8**: 851-858 [PMID: 12200791 DOI: 10.1053/jlts.2002.35927]

34 **Ji D**, Shao Q, Han P, Li F, Li B, Zang H, Niu X, Li Z, Xin S, Chen G. The frequency and determinants of liver stiffness measurement failure: a retrospective study of "real-life" 38,464 examinations. *PLoS One* 2014; **9**: e105183 [PMID: 25122123 DOI: 10.1371/journal.pone.0105183]

35 **Ishak K**, Baptista A, Bianchi L, Callea F, De Groote J, Gudat F, Denk H, Desmet V, Korb G, MacSween RN. Histological grading and staging of chronic hepatitis. *J Hepatol* 1995; **22**: 696-699 [PMID: 7560864 DOI: 10.1016/0168-8278(95)80226-6]

36 **Esmat G**, Metwally M, Zalata KR, Gadalla S, Abdel-Hamid M, Abouzied A, Shaheen AA, El-Raziky M, Khatab H, El-Kafrawy S, Mikhail N, Magder LS, Afdhal NH, Strickland GT. Evaluation of serum biomarkers of fibrosis and injury in Egyptian patients with chronic hepatitis C. *J Hepatol* 2007; **46**: 620-627 [PMID: 17316875 DOI: 10.1016/j.jhep.2006.12.010]

37 **Castéra L**, Vergniol J, Foucher J, Le Bail B, Chanteloup E, Haaser M, Darriet M, Couzigou P, De Lédinghen V. Prospective comparison of transient elastography, Fibrotest, APRI, and liver biopsy for the assessment of fibrosis in chronic hepatitis C. *Gastroenterology* 2005; **128**: 343-350 [PMID: 15685546 DOI: 10.1053/j.gastro.2004.11.018]

38 **Foucher J**, Chanteloup E, Vergniol J, Castéra L, Le Bail B, Adhoute X, Bertet J, Couzigou P, de Lédinghen V. Diagnosis of cirrhosis by transient elastography (FibroScan): a prospective study. *Gut* 2006; **55**: 403-408 [PMID: 16020491 DOI: 10.1136/gut.2005.069153]

39 **Ganne-Carrié N**, Ziol M, de Ledinghen V, Douvin C, Marcellin P, Castera L, Dhumeaux D, Trinchet JC, Beaugrand M. Accuracy of liver stiffness measurement for the diagnosis of cirrhosis in patients with chronic liver diseases. *Hepatology* 2006; **44**: 1511-1517 [PMID: 17133503 DOI: 10.1002/hep.21420]

40 **Ziol M**, Handra-Luca A, Kettaneh A, Christidis C, Mal F, Kazemi F, de Lédinghen V, Marcellin P, Dhumeaux D, Trinchet JC, Beaugrand M. Noninvasive assessment of liver fibrosis by measurement of stiffness in patients with chronic hepatitis C. *Hepatology* 2005; **41**: 48-54 [PMID: 15690481 DOI: 10.1002/hep.20506]

41 **Camarero C**, Ramos N, Moreno A, Asensio A, Mateos ML, Roldan B. Hepatitis C virus infection acquired in childhood. *Eur J Pediatr* 2008; **167**: 219-224 [PMID: 17464514 DOI: 10.1007/s00431-007-0472-5]

42 **Wilder J**, Patel K. The clinical utility of FibroScan(®) as a noninvasive diagnostic test for liver disease. *Med Devices* (Auckl) 2014; **7**: 107-114 [PMID: 24833926 DOI: 10.2147/mder.s46943]

43 **Wang QX**, Shen L, Qiu DK, Bao H, Chen XY, Zeng MD, Mao YM, Ma X. [Validation of transient elastography (Fibroscan) in assessment of hepatic fibrosis in autoimmune hepatitis]. *Zhonghua Ganzangbing Zazhi* 2011; **19**: 782-784 [PMID: 22409854 DOI: 10.3760/cma.j.issn.1007-3418.2011.10.015]

44 **Muñoz R**, Ramírez E, Fernandez I, Martin A, Romero M, Romero E, Dominguez-Gil B, Hernandez A, Morales E, Andres A, Castellano G, Morales JM. Correlation between fibroscan, liver biopsy, and clinical liver function in patients with hepatitis C virus infection after renal transplantation. *Transplant Proc* 2009; **41**: 2425-2426 [PMID: 19715940 DOI: 10.1016/j.transproceed.2009.06.103]

45 **Goodman ZD**, Stoddard AM, Bonkovsky HL, Fontana RJ, Ghany

MG, Morgan TR, Wright EC, Brunt EM, Kleiner DE, Shiffman ML, Everson GT, Lindsay KL, Dienstag JL, Morishima C. Fibrosis progression in chronic hepatitis C: morphometric image analysis in the HALT-C trial. *Hepatology* 2009; **50**: 1738-1749 [PMID: 19824074 DOI: 10.1002/hep.23211]

46 **Karlas T**, Hempel M, Tröltzsch M, Huster D, Günther P, Tenckhoff H, Mössner J, Berg T, Keim V, Wiegand J. Non-invasive evaluation of hepatic manifestation in Wilson disease with transient elastography, ARFI, and different fibrosis scores. *Scand J Gastroenterol* 2012; **47**: 1353-1361 [PMID: 22943453 DOI: 10.3109/00365521.2012.719924]

47 **Sokol RJ**. Copper metabolism and copper storage disorders. In: Suchy FJ, Sokol RJ, Balistreri WF, editors. Liver Disease in Children. 4th ed. New York: Cambridge University Press, 2014: 465-492

48 **Goodman ZD**, Becker RL, Pockros PJ, Afdhal NH. Progression of fibrosis in advanced chronic hepatitis C: evaluation by morphometric image analysis. *Hepatology* 2007; **45**: 886-894 [PMID: 17393526 DOI: 10.1002/hep.21595]

49 **Sandrini J**, Boursier J, Chaigneau J, Sturm N, Zarski JP, Le Bail B, de Ledinghen V, Calès P, Rousselet MC. Quantification of portal-bridging fibrosis area more accurately reflects fibrosis stage and liver stiffness than whole fibrosis or perisinusoidal fibrosis areas in chronic hepatitis C. *Mod Pathol* 2014; **27**: 1035-1045 [PMID: 24390214 DOI: 10.1038/modpathol.2013.225]

50 **McDiarmid SV**, Merion RM, Dykstra DM, Harper AM. Selection of pediatric candidates under the PELD system. *Liver Transpl* 2004; **10**: S23-S30 [PMID: 15384170 DOI: 10.1002/lt.20272]

51 **Wang JH**, Changchien CS, Hung CH, Eng HL, Tung WC, Kee KM, Chen CH, Hu TH, Lee CM, Lu SN. FibroScan and ultrasonography in the prediction of hepatic fibrosis in patients with chronic viral hepatitis. *J Gastroenterol* 2009; **44**: 439-446 [PMID: 19308312 DOI: 10.1007/s00535-009-0017-y]

52 **Bedossa P**, Carrat F. Liver biopsy: the best, not the gold standard. *J Hepatol* 2009; **50**: 1-3 [PMID: 19017551 DOI: 10.1016/j.jhep.2008.10.014]

53 **Regev A**, Berho M, Jeffers LJ, Milikowski C, Molina EG, Pyrsopoulos NT, Feng ZZ, Reddy KR, Schiff ER. Sampling error and intraobserver variation in liver biopsy in patients with chronic HCV infection. *Am J Gastroenterol* 2002; **97**: 2614-2618 [PMID: 12385448]

54 **Mendoza J**, Trapero-Marugán M, González-Moreno L, Jones EA, Gómez-Domínguez E, Moreno-Otero R. Hepatic fibrosis in patients with chronic hepatitis C assessed by transient elastography: implications for determining the efficacy of antiviral therapy. *Rev Esp Enferm Dig* 2010; **102**: 426-434 [PMID: 20617863 DOI: 10.4321/S1130-01082010000700005]

P- Reviewer: Konno T, Wang R **S- Editor**: Qi Y
L- Editor: A **E- Editor**: Liu XM

World Journal of Gastroenterology

Submit a Manuscript: http://www.wjgnet.com/esps/
Help Desk: http://www.wjgnet.com/esps/helpdesk.aspx
DOI: 10.3748/wjg.v22.i16.4250

World J Gastroenterol 2016 April 28; 22(16): 4250-4258
ISSN 1007-9327 (print) ISSN 2219-2840 (online)

ORIGINAL ARTICLE

Prospective Study

Predictive effects of bilirubin on response of colorectal cancer to irinotecan-based chemotherapy

Qian-Qian Yu, Hong Qiu, Ming-Sheng Zhang, Guang-Yuan Hu, Bo Liu, Liu Huang, Xin Liao, Qian-Xia Li, Zhi-Huan Li, Xiang-Lin Yuan

Qian-Qian Yu, Hong Qiu, Ming-Sheng Zhang, Guang-Yuan Hu, Bo Liu, Liu Huang, Qian-Xia Li, Xiang-Lin Yuan, Department of Oncology, Tongji Hospital, Tongji Medical College, Huazhong University of Science and Technology, Wuhan 430030, Hubei Province, China

Xin Liao, Department of Geriatrics, Tongji Hospital, Tongji Medical College, Huazhong University of Science and Technology, Wuhan 430030, Hubei Province, China

Zhi-Huan Li, Department of Genetics and Complex Diseases, Harvard T.H. Chan School of Public Health, Boston, MA 02115, United States

Author contributions: Yuan XL designed the study; Yu QQ, Qiu H, Zhang MS and Hu GY performed the research; Yu QQ, Liu B, Huang L, Liao X and Li QX analyzed the data; Yu QQ and Li ZH wrote the paper; and Yuan XL revised the manuscript for final submission.

Supported by the National Natural Science Foundation of China, No. 81372664.

Institutional review board statement: The study was reviewed and approved by the Ethical Committee of Huazhong University of Science and Technology Institutional Review Board.

Clinical trial registration statement: This study is registered at http://www.clinicaltrials.gov. The registration identification number is NCT01282658.

Informed consent statement: All study participants, or their legal guardian, provided informed written consent prior to study enrollment.

Conflict-of-interest statement: The authors have no conflict of interest related to the manuscript.

Data sharing statement: Technical appendix, statistical code, and dataset available from the corresponding author at yxl@medmail.com.cn. Participants gave informed consent for data sharing. No additional data are available.

Correspondence to: Xiang-Lin Yuan, PhD, MD, Professor of Medicine, Department of Oncology, Tongji Hospital, Tongji Medical College, Huazhong University of Science and Technology, 1095 Jiefang Avenue, Wuhan 430030, Hubei Province, China. yxl@medmail.com.cn
Telephone: +86-27-83663342
Fax: +86-27-83663342

Received: January 20, 2016
Peer-review started: January 21, 2016
First decision: February 18, 2016
Revised: March 1, 2016
Accepted: March 14, 2016
Article in press: March 14, 2016
Published online: April 28, 2016

Abstract

AIM: To examine the predictive effects of baseline serum bilirubin levels and UDP-glucuronosyltransferase (UGT) 1A1*28 polymorphism on response of colorectal cancer to irinotecan-based chemotherapy.

METHODS: The present study was based on a prospective multicenter longitudinal trial of Chinese metastatic colorectal cancer (mCRC) patients treated with irinotecan-based chemotherapy (NCT01282658). Baseline serum bilirubin levels, including total bilirubin (TBil) and unconjugated bilirubin (UBil), were measured,

and genotyping of *UGT1A1*28* polymorphism was performed. Receiver operating characteristic curve (ROC) analysis was used to determine cutoff values of TBil and UBil. The TBil values were categorized into > 13.0 or ⩽ 13.0 groups; the UBil values were categorized into > 4.1 or ⩽ 4.1 groups. Combining the cutoff values of TBil and UBil, which was recorded as CoBil, patients were classified into three groups. The classifier's performance of *UGT1A1*28* and CoBil for predicting treatment response was evaluated by ROC analysis. Associations between response and CoBil or *UGT1A1*28* polymorphism were estimated using simple and multiple logistic regression models.

RESULTS: Among the 120 mCRC patients, the serum bilirubin level was significantly different between the *UGT1A1*28* wild-type and mutant genotypes. Patients with the mutant genotype had an increased likelihood of a higher TBil (P = 0.018) and a higher UBil (P = 0.014) level compared with the wild-type genotype. Patients were stratified into three groups based on CoBil. Group 1 was patients with TBil > 13.0 and UBil > 4.1; Group 2 was patients with TBil ⩽ 13.0 and UBil > 4.1; and Group 3 was patients with TBil ⩽ 13.0 and UBil ⩽ 4.1. Patients in Group 3 had more than a 10-fold higher likelihood of having a response in the simple (OR = 11.250; 95%CI: 2.286-55.367; P = 0.003) and multiple (OR = 16.001; 95%CI: 2.802-91.371; P = 0.002) analyses compared with the Group 1 individuals. Patients carrying the *UGT1A1*28* (TA)7 allele were 4-fold less likely to present with a response compared with the individuals harboring a homozygous (TA)6 genotype in the simple (OR = 0.267; 95%CI: 0.100-0.709; P = 0.008) and multiple (OR = 0.244; 95%CI: 0.088-0.678; P = 0.007) analyses. Classifier's performance of CoBil and *UGT1A1*28* were comparable.

CONCLUSION: CoBil and *UGT1A1*28* are both independent biomarkers for predicting the treatment response of mCRC patients to irinotecan-based chemotherapy. After validation, CoBil, an easily determinable index in the clinic, might be helpful in facilitating stratification of mCRC patients for individualized treatment options.

Key words: Bilirubin; Irinotecan; Metastatic colorectal cancer; Response; *UGT1A1*28*

Core tip: Serum bilirubin was reported to be associated with irinotecan-induced toxicity. The current study evaluated whether baseline bilirubin levels could predict treatment response of metastatic colorectal cancer patients given irinotecan-based chemotherapy in a Chinese population and found that a lower bilirubin level was an independent predictor of irinotecan treatment response.

Yu QQ, Qiu H, Zhang MS, Hu GY, Liu B, Huang L, Liao X, Li QX, Li ZH, Yuan XL. Predictive effects of bilirubin on response of colorectal cancer to irinotecan-based chemotherapy. *World J Gastroenterol* 2016; 22(16): 4250-4258 Available from: URL: http://www.wjgnet.com/1007-9327/full/v22/i16/4250.htm DOI: http://dx.doi.org/10.3748/wjg.v22.i16.4250

INTRODUCTION

Colorectal cancer (CRC) is the third most common cancer and a major cause of cancer related death worldwide[1]. More than 40% of CRC patients will eventually develop metastases and require palliative chemotherapy[2,3]. Irinotecan-based therapy is one of the most important fundamental chemotherapy regimens for metastatic CRC (mCRC)[4,5]. As a first-line treatment, the response rate to irinotecan-based therapy is approximately 35%-55%[6,7]. Patients who do not benefit from first-line therapy will miss the best opportunity for disease palliation or control. To date, no prospective tool has been validated for selecting the best therapy for an individual patient. Biomarkers with predictive effects on therapeutic efficacy warrant further investigations[8].

Circulating levels of 7-ethyl-10-hydroxycamptothecin (SN-38), the active metabolite of irinotecan, is associated with irinotecan-treatment efficacy[9]. Through the glucuronidation pathway, SN-38 is converted to an inactive form and eliminated in the bile[10]. UGT1A1 is the most important enzyme that metabolizes SN-38, and it is the only physiological enzyme that converts bilirubin to water-soluble glucuronides[11]. Pharmacological studies demonstrate that glucuronidation rates of both SN-38 and bilirubin are decreased when the TATAA box of the gene contains an extra TA insertion (*UGT1A1*28*)[12]. Additionally, *UGT1A1*28* is involved in the pathogenesis of Gilbert syndrome (GS), which is an inherited disorder of hepatic bilirubin metabolism characterized by unconjugated hyperbilirubinemia[13]. Even in populations without GS, *UGT1A1*28* has a strong impact on serum bilirubin levels[14]. Although it is reported that *UGT1A1*28* is linked to SN-38 glucuronidation and irinotecan-related toxicity, the predictive role of the *UGT1A1*28* polymorphism regarding treatment outcome of irinotecan-based therapy has been conflicting[15-18].

In the current study, we investigated the association between serum bilirubin levels, *UGT1A1*28* polymorphism and the therapeutic response in a prospective series of patients with mCRC undergoing irinotecan-based first-line chemotherapy to determine whether serum bilirubin levels and *UGT1A1*28* polymorphism could be predictors of therapeutic response.

MATERIALS AND METHODS

Methods

Study design and patients: The study was based on a prospective longitudinal Chinese clinical trial sponsored by Huazhong University of Science and Technology. Patients treated with irinotecan-based therapy were consecutively recruited between November 2010 and December 2014 from the Tongji Hospital, Tongji Medical College, Huazhong University of Science and Technology and 5 other cancer centers in south-central China.

Eligibility criteria were as follows: histologically confirmed adenocarcinoma of the colon or rectum; unresectable metastases; age from 18 to 75 years; measurable disease defined according to the Response Evaluation Criteria In Solid Tumors version 1.1 (RECIST1.1)[19]; no prior chemotherapy for metastatic disease (adjuvant chemotherapy except for irinotecan was allowed); Eastern Cooperative Oncology Group Performance Status Scale (PS) ≤ 2 or Karnofsky index of performance status (KPS) > 60%; total bilirubin ≤ 1.5 times the upper limit of normal (ULN); aspartate aminotransferase (AST) and alanine aminotransferase (ALT) ≤ 2.5 times ULN (≤ 5 times ULN if liver metastases present); creatinine clearance > 50 mL/min or serum creatinine ≤ 1.5 times ULN; and no history of Gilbert's syndrome.

This study was approved by the Ethical Committee of Huazhong University of Science and Technology under reference number NCT01282658 (registered at http://www.clinicaltrials.gov). Written informed consent was required, and blood samples were obtained.

In the current study, only participants recruited from Tongji Hospital or Tongji Medical College were included because they were provided with recorded numerical values of baseline serum bilirubin.

Clinical data collection

Baseline clinical information, including demographics, KPS, tumor-related details and medical history, was collected prior to the commencement of chemotherapy. Total bilirubin (TBil) and conjugated bilirubin levels were measured in the participants recruited from Tongji Hospital. The unconjugated bilirubin (UBil) level was calculated by subtracting the conjugated bilirubin level from the TBil level. Reference value ranges were 3.4-20.5 μmol/L and 0.00-6.84 μmol/L for TBil and conjugated bilirubin, respectively.

Objective tumor response was categorized using computed tomography or magnetic resonance imaging every 6-8 weeks according to RECIST1.1. The disease was considered to be stable only if the duration of stabilization was at least 2 mo. Patients who received fewer than 3 cycles of chemotherapy were not evaluated for tumor response, except for those with rapid progression. Evaluations were performed blindly with respect to biochemical markers.

Genotyping of UGT1A1*28 polymorphism

Genomic DNA was extracted from peripheral blood samples using the QIAGEN DNA Blood Mini Kit (Qiagen, Valencia, CA). TA repeats in the *UGT1A1* promoter (*UGT1A1*28*) was genotyped by fragment sizing. Polymerase chain reaction (PCR) was performed in a total volume of 20 μL containing template DNA (80 ng/μL) according to the manufacturer's instructions (2 × Taq PCR MasterMix; Tiangen Biotech, Beijing, China). A forward primer that was modified by adding a 5′ fluorescent label FAM (FAM_F: 5′-GAACTCCCT-GCTACCTTT-3′) and an unlabeled reverse primer (R: 5′-GAACTCCCTGCTACCTTT-3′) were used. The amplification was performed with a GeneAmp PCR system 9700 (Applied Biosystems, Foster City, CA, United States), started with initial denaturation at 95 ℃ for 3 min, followed by 30 cycles of denaturation at 95 ℃ for 30 s, annealing at 58 ℃ for 30 s, and extension at 72 ℃ for 30 s. Then, the mixtures of the PCR product (TA6, 242 bp; TA7, 244 bp) and Hi-Di formamide (containing the internal size standard Genescan 500 [Applied Biosystems]) were run in the ABI 3730 Genetic Analyzer (Applied Biosystems). Fragment sizes were determined by comparison with Genescan 500 using the local Southern algorithm and analyzed by GeneMapper 3.2 (Applied Biosystems). For quality control purposes, heterozygous and homozygous sequenced samples were included in each run. Genotypes were determined based on the number of TA repeats in each allele (*i.e.*, [TA]6/6, [TA]6/7 and [TA]7/7). Repeat genotyping of 25% of the samples was 100% concordant with original results.

Statistical analysis

Statistical analyses were performed using SPSS 16.0 statistical software (SPSS Inc., Chicago, IL, United States). Continuous variables are presented as the mean with SD and range and compared using two-sided *t*-tests or Wilcoxon tests, when appropriate. Categorical variables are expressed as the frequencies and percentages and compared using Pearson's χ^2 test. The cutoff values for TBil and UBil were determined using receiver operating curve (ROC) analysis based on optimal Youden Index. The TBil values were categorized into two groups: > 13.0 or ≤ 13.0; and the UBil values were categorized into two groups: > 4.1 or ≤ 4.1. The parameter combining the TBil and UBil cutoff values (CoBil) was used to further stratify patients. Associations between the objective tumor response and bilirubin indicators or *UGT1A1*28* polymorphism were estimated using simple and multiple logistic regression models. Multiple logistic regression analyses were adjusted for age, sex, KPS (≥ 80% or < 80%), histology (glandular or others), primary tumor site (left- or right-side) and treatment regimens. The classifier's performance of CoBil and *UGT1A1*28* was evaluated using a ROC analysis. All tests were two-sided, and $P \leq 0.05$ indicated statistical significance. The statistical

Table 1 Demographic and clinical characteristics of the patients *n* (%)

Characteristics	Value
Total	120 (100)
Age, yr	
mean ± SD	49.6 ± 10.5
Median (range)	18-72
Gender	
Male	71 (59.2)
Female	49 (40.8)
KPS	
⩾ 80%	96 (80.0)
70%	20 (16.7)
60%	4 (3.3)
Primary tumor	
Right-sided	33 (27.5)
Left-sided	87 (72.5)
Histology	
Glandular	89 (74.2)
Mucinous	13 (10.8)
Signet-ring cell	3 (2.5)
Mixed	10 (8.3)
Unfixed	5 (4.2)
First-line chemotherapy	
FOLFIRI	109 (90.8)
mXELIRI	7 (5.8)
Irinotecan	4 (3.3)
Serum total bilirubin, μmol/L	
mean ± SD	10.2 ± 4.3
Range	3.1-26.9
Serum unconjugated bilirubin, μmol/L	
mean ± SD	7.2 ± 3.1
Range	2.5-19.2
UGT1A1*28 genotype[1]	
(TA)6/6	84 (70.0)
(TA)6/7	34 (28.3)
(TA)7/7	2 (1.7)

[1]Variants were in Hardy-Weinberg equilibrium ($P > 0.05$). KPS: Karnofsky performance status.

review of the study was performed by a biomedical statistician.

RESULTS

Demographic and clinical characteristics of patients

A total of 120 Han Chinese patients with recorded serum bilirubin data and who were available for response assessment were enrolled. Follow-up information was updated in April 2015 when 58% of the patients were deceased. The mean duration of follow-up is 26 mo (range 5-55 mo).

The baseline patient characteristics and tumor biological factors are shown in Table 1. The median age by the time of diagnosis was 50 years (range 18-72 years); 59.2% were males; 20.0% of patients had a KPS less than 80%; and 74.2% of patients were characterized as having a glandular histology. The primary tumors that were proximal or distal to the splenic flexure were categorized as right-sided (n = 33) or left-sided (n = 87), respectively, as described by Loupakis *et al*[20]. One hundred and nine (90.8%) patients received the FOLFIRI regimen[21], 7 (5.8%) patients received the mXILIRI regimen[21], and the rest (3.3%), who could not bear combined chemotherapy, were treated with irinotecan alone[22].

Table 2 Demographic and clinical characteristics between patients with objective response and patients without objective response *n* (%)

Characteristics	Objective response		*P* value	*P* value[1]
	No	Yes		
Age, yr (mean ± SD)	48.2 ± 10.9	52.1 ± 9.0	0.047[2]	0.066
Gender				
Male	44 (62.0)	27 (38.0)	0.402[3]	0.492
Female	34 (69.4)	15 (30.6)		
KPS				
⩾ 80%	64 (66.7)	32 (33.3)	0.444[3]	0.42
< 80%	14 (58.3)	10 (41.7)		
Primary tumor				
Right-sided	22 (66.7)	11 (33.3)	0.814[3]	0.885
Left-sided	56 (64.4)	31 (35.6)		
Histology				
Glandular	55 (61.8)	34 (38.2)	0.213[3]	0.407
Other	23 (74.2)	8 (25.8)		
First-line chemotherapy				
FOLFIRI	71 (65.1)	38 (34.9)	0.882[4]	0.832
mXELIRI	4 (57.1)	3 (42.9)		
Irinotecan	3 (75.0)	1 (25.0)		

[1]*P*-values were adjusted for age, sex, KPS, primary tumor site, histology and treatment regimen in logistic regression models; [2]*P*-value was calculated using two-sided *t* tests; [3]*P*-values were calculated using two-sided χ^2 tests; [4]*P*-value was calculated using Fisher' exact tests. KPS: Karnofsky performance status.

The mean ± SD of TBil was 10.2 ± 4.3 (range 3.1-26.9), and the mean ± SD of UBil was 7.2 ± 3.1 (range 2.5-19.2). Eighty-four (70%) patients harbored the *UGT1A1*28* (TA)6/6 genotype, and 36 (30%) patients harbored variant genotypes, including 34 (28.3%) (TA)6/7 and 2 (1.7%) (TA)7/7 genotypes.

As shown in Table 2, there were no significant differences between patients who had an objective tumor response [complete response (CR) + partial response (PR)] and those who had stable disease or progressive disease (PD) with respect to sex, KPS, primary tumor site, histology and treatment regimen. The mean age was slightly different between the two groups classified by objective response (P = 0.047). Patients with older age tended to have an increased likelihood of objective response (P = 0.066).

Serum bilirubin levels and UGT1A1*28 genotypes

As shown in Figure 1, patients with *UGT1A1*28* (TA)6/7 or (TA)7/7 genotype had an increased likelihood of having a higher TBil (P = 0.018, t tests) and a higher UBil (P = 0.014, t tests) level compared with the (TA)6/6 genotype. The mean and SD of TBil was 11.9 ± 5.5 for (TA)6/7 or (TA)7/7 patients, and 9.5 ± 3.4 for (TA)6/6 patients. The mean and SD of UBil was 8.5 ± 3.9 for (TA)6/7 or (TA)7/7 patients, and 6.7 ± 2.5 for (TA)6/6 patients.

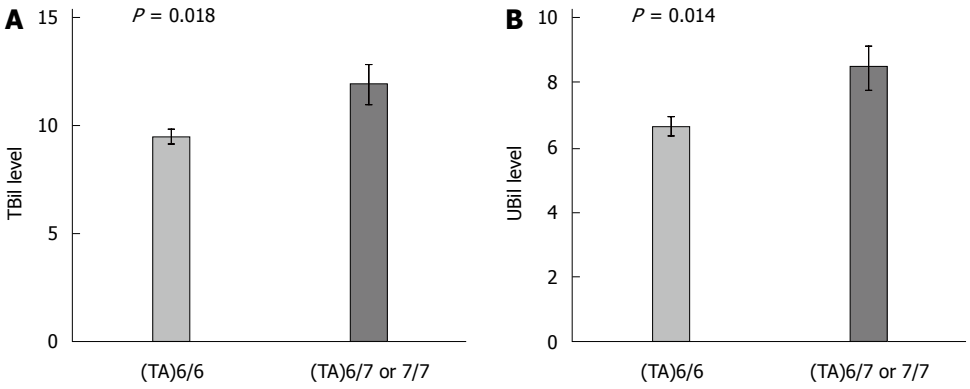

Figure 1 Serum total bilirubin and unconjugated bilirubin levels between *UGT1A1*28* (TA)6/6 and (TA)6/7 or (TA)7/7 genotype. Patients with *UGT1A1*28* (TA)6/7 or (TA)7/7 genotype had an increased likelihood of (A) higher TBil (P = 0.018) and (B) higher UBil (P = 0.014) levels compared with (TA)6/6 genotype. TBil: Total bilirubin; UBil: Unconjugated bilirubin.

Table 3 Association between *UGT1A1*28* genotypes and response to treatment *n* (%)

*UGT1A1*28* genotype	Complete response	Partial response	Stable disease	Progressive disease	Objective response[2]		Simple analysis			Multiple analysis[3]		
					n	Yes	OR	95%CI	*P* value	OR	95%CI	*P* value
(TA)6/6	3 (3.6)	33 (39.3)	34 (40.5)	14 (16.7)	84	36 (42.9)	1.000 (ref.)			1.000 (ref.)		
(TA)6/7 or (TA)7/7[1]	1 (2.8)	5 (13.9)	18 (50.0)	12 (33.3)	36	6 (16.7)	0.267	0.100-0.709	0.008	0.244	0.088-0.678	0.007

[1]In the dominant model; [2]Yes, partial and complete response; [3]Multiple analyses were adjusted for age, sex, KPS, histology, primary tumor site and treatment regimen. KPS: Karnofsky performance status.

Table 4 Association between serum total/unconjugated bilirubin levels and response to treatment

	Objective response[1]		Simple analysis		Multiple analysis[2]	
	n	Yes (%)	OR (95%CI)	*P* value	OR (95%CI)	*P* value
Serum total bilirubin						
> 13.0	24	4 (16.7)	1.000 (ref.)		1.000 (ref.)	
≤ 13.0	96	38 (39.6)	3.276 (1.038-10.333)	0.043	3.874 (1.127-13.319)	0.032
Serum unconjugated bilirubin						
> 4.1	107	33 (30.8)	1.000 (ref.)		1.000 (ref.)	
≤ 4.1	13	9 (69.2)	5.045 (1.450-17.561)	0.011	5.923 (1.561-22.479)	0.009

[1]Yes, partial and complete response; [2]Multiple analyses were adjusted for age, sex, KPS, histology, primary tumor site and treatment regimen. KPS: Karnofsky performance status.

*UGT1A1*28 polymorphism and objective response*

As shown in Table 3, the objective response was observed in 42 (35.0%) of 120 patients, including 4 CRs (3.3%) and 38 PRs (31.7%). Stable disease was observed in 52 (43.3%) patients, and PD was observed in 26 (21.7%) patients.

Patients harboring the minor allele of *UGT1A1**28 (TA)6>(TA)7 had a reduced likelihood of objective response compared with the wild-type genotype (OR = 0.267; 95%CI: 0.100-0.709; P = 0.008). In the multiple logistic regression model, the (TA)6/7 or (TA)7/7 genotype remained significantly associated with a decreased objective response rate (OR = 0.244; 95%CI: 0.088-0.678; P = 0.007) compared with the (TA)6/6 genotype.

TBil and UBil values and objective response

The optimal Youden Index-based cut-off points were 13.0 μmol/L and 4.1 μmol/L for TBil and UBil, respectively. As shown in Table 4, in the simple analysis, patients with TBil ≤ 13.0 had an increased likelihood of an objective response to treatment compared with the TBil > 13.0 individuals (OR = 3.276; 95%CI: 1.038-10.333; P = 0.043). The association remained significant in multiple analyses adjusted for age, sex, KPS, histology, primary tumor site and treatment regimen (OR = 3.874; 95%CI: 1.127-13.319; P = 0.032). Patients with UBil ≤ 4.1 had approximately a 5-fold higher likelihood of having an objective response compared with the UBil > 4.1 individuals (OR = 5.045; 95%CI: 1.450-17.561; P =

Table 5 Association between combined bilirubin levels and response to treatment

Combined bilirubin levels[1]	Objective response[2]		Simple analysis		Multiple analysis[3]	
	n	Yes (%)	OR (95%CI)	*P* value	OR (95%CI)	*P* value
Group 1	24	4 (16.7)	1.000 (ref.)		1.000 (ref.)	
Group 2	83	29 (34.9)	2.685 (0.838-8.604)	0.096	3.215 (0.918-11.255)	0.068
Group 3	13	9 (69.2)	11.250 (2.286-55.367)	0.003	16.001 (2.802-91.371)	0.002

[1]Group 1: individuals with total bilirubin > 13.0 and unconjugated bilirubin > 4.1; Group 2: individuals with total bilirubin ⩽ 13.0 and unconjugated bilirubin > 4.1; Group 3: individuals with total bilirubin ⩽ 13.0 and unconjugated bilirubin ⩽ 4.1; [2]Yes, partial and complete response; [3]Multiple analyses were adjusted for age, sex, KPS, histology, primary tumor site and treatment regimen; KPS: Karnofsky performance status.

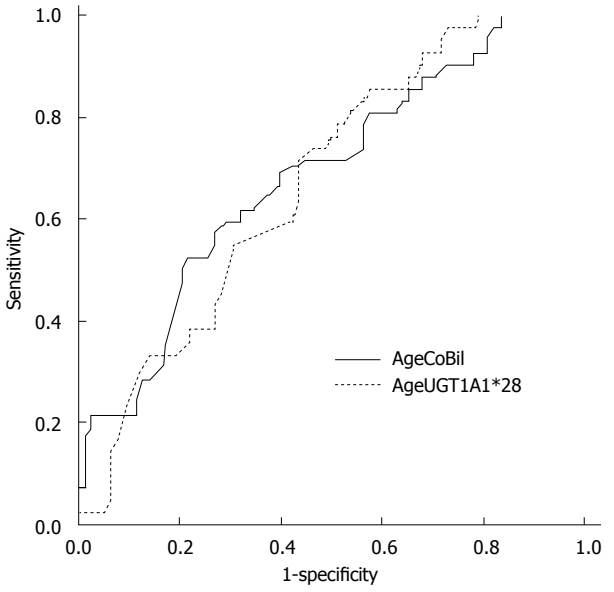

Variables	AUC	SE	*P* value	95%CI
AgeCoBil	0.686	0.050	0.001	0.576-0.785
AgeUGT1A1*28	0.672	0.049	0.002	0.576-0.768

Figure 2 Receiver operating characteristic analysis of AgeCoBil and AgeUGT1A1*28 in predicting objective response. AgeCoBil included age (as a continuous variable) and CoBil (as a trichotomous variable). AgeUGT1A1*28 included age and *UGT1A1*28* genotypes (as a dichotomous variable). Classifier's performance of CoBil and *UGT1A1*28* was comparable. AUC: Area under the curve; TBil: Total bilirubin; UBil: Unconjugated bilirubin; CoBil: Combined TBil and UBil.

0.011) in the simple analyses. The multiple analysis also showed a significantly increased likelihood of an objective response in patients with UBil ⩽ 4.1 compared with the UBil > 4.1 individuals (OR = 5.923; 95%CI: 1.561-22.479; *P* = 0.011).

Combined TBil and UBil and objective response

Based on the combined TBil and UBil values (CoBil), patients were classified into three groups: Group 1 patients harbored TBil > 13.0 and UBil > 4.1; Group 2 patients harbored TBil ⩽ 13.0 and UBil > 4.1; and Group 3 patients harbored TBil ⩽ 13.0 and UBil ⩽ 4.1. Compared with Group 1, Group 2 had a trend towards an increased likelihood of an objective response in the simple (OR = 2.685; 95%CI: 0.838-8.604; *P* = 0.096) and multiple (OR = 3.215; 95%CI: 0.918-11.255; *P* = 0.068) analyses, and Group 3 had more than a 10-fold increase in the likelihood of an objective response in the simple (OR = 11.250; 95%CI: 2.286-55.367; *P* = 0.003) and multiple (OR = 16.001; 95%CI: 2.802-91.371; *P* = 0.002) analyses (Table 5).

To compare the classifier's performance of CoBil and *UGT1A1*28*, an ROC analysis was used. Considering that age may be a potential predictor of objective response, we drew ROC curves of age + CoBil (AgeCoBil) and age + *UGT1A1*28* (AgeUGT1A1*28), as shown in Figure 2. The areas under the curves (AUCs) were 0.686 (95%CI: 0.587-0.785) and 0.672 (95%CI: 0.576-0.768) for AgeCoBil and Age*UGT1A1*28*, respectively. Therefore, CoBil had a comparable performance for predicting objective response to *UGT1A1*28*.

DISCUSSION

This study evaluated whether serum bilirubin levels and *UGT1A1*28* polymorphism could predict treatment response of mCRC patients treated with irinotecan-based chemotherapy in a Chinese population. We found that patients with TBil ⩽ 13.0 and UBil ⩽ 4.1 had a 16-fold higher likelihood of objective response compared with the TBil > 13.0 and UBil > 4.1 individuals; patients carrying the *UGT1A1*28* (TA)7 allele were 4-fold less likely to present with an objective response compared with the individuals harboring the homozygous (TA)6 genotype.

Consistent with previous observations, we also found that the *UGT1A1*28* variant genotypes were correlated with higher serum TBil and UBil levels[13,14,21,23]. Patients harboring the *UGT1A1*28* variant genotypes have a decreased ability to glucuronidate bilirubin, resulting in relatively elevated levels of unconjugated bilirubin as well as total bilirubin[24,25]. At the same time, the metabolism of SN-38 is reduced, leading to higher SN-38 exposures in those patients[26,27].

However, either in patients with the higher bilirubin levels or in patients harboring the *UGT1A1*28* variant genotypes, the response rate to irinotecan-based therapy was lower than in the others. The reduced response rate is not due to the toxicity-related dose-reduction because no significant difference in terms of dose-reduction and chemotherapy cycles was observed between the groups classified by the *UGT1A1*28* genotypes or CoBil (data shown in the Supplementary Material).

It is pharmacologically plausible that the *UGT1A1*28* genotype is associated with irinotecan treatment efficacy. However, published data from different clinical studies are inconsistent[16,28]. Our result was in agreement with the observations by McLeod *et al*[29] that the homozygous *UGT1A1*28* patients showed a trend toward a decreased response rate, but our result was opposite to the findings by Toffoli *et al*[30] that the homozygous *UGT1A1*28* patients had a higher response rate than the wild genotype patients. These inconsistencies may be due to different study populations, distinct study designs and diverse schedules of irinotecan treatment used.

Data with respect to bilirubin and irinotecan-based therapy were limited. Two articles based on previous clinical trials suggested that baseline bilirubin was predictive of grade 3 to 4 neutropenia but not severe diarrhea or therapeutic efficacy[31,32]. These trials were conducted in mCRC patients administered with single-agent irinotecan as second-line chemotherapy, and the analyses were performed retrospectively. In contrast, the current study was conducted prospectively in a Chinese patient population treated with irinotecan-based first-line chemotherapy. The treatment response in first-line therapy is less likely to be confounded by other regimens than that in second-line therapy, and prospective data has a higher level of evidence than retrospective data.

It is proverbial that initial treatment provides the best opportunity for disease palliation or control. The response rate could be reduced from 56% in first-line chemotherapy to 4% in second-line chemotherapy[7]. Hence, biomarkers that could improve therapeutic efficacy by stratifying patients using their predictive effects are of great importance to practitioners and patients alike[33]. For the inconsistency of *UGT1A1*28* as a predictor for therapeutic efficacy, *UGT1A1*28* genotyping has not been used as a routine test in clinic. However, serum bilirubin level is detected prior to the commencement of each cycle of chemotherapy. The predictive value of baseline bilirubin in tumor response to irinotecan-based therapy is a novel finding in Chinese mCRC patients. As predictors of irinotecan-treatment response, CoBil has a comparable classifier's performance to *UGT1A1*28*, and the predictive power is more significant. With validation, CoBil could facilitate stratification of patients for optimal first-line therapy options without extra examinations.

There are some limitations in the current study. First, the study is limited by the restricted number of samples, and requires confirmation in independent external patient cohorts. Second, the result is derived from a unicentral population. Although the research is based on a multicenter clinical trial, only participants at Tongji Hospital are equipped with complete records of baseline bilirubin. Finally, for the longitudinal design, not all patients received standardized treatment schedules as strict as those described in international clinical trials. However, from another perspective, the longitudinal study may represent the treatment experience of patients in a more literal way.

In conclusion, CoBil, as a parameter combining TBil and UBil values, might be clinically useful for predicting treatment response in mCRC patients treated with irinotecan and may help clinicians make informed decisions about first-line treatment selection without extra examinations. We also found that *UGT1A1*28* polymorphism is a predictor of treatment response. However, the results need to be validated in other independent prospective studies, and the classifiers for bilirubin warrant verification in cohorts with sufficient power to detect their predictive accuracy.

ACKNOWLEDGMENTS

We thank Guohui Pan from NYU Langone Medical Center for biostatistics assistance and statistical review.

COMMENTS

Background

Irinotecan-based therapy is one of the most important fundamental chemotherapy regimens for metastatic colorectal cancer (mCRC). More than 40% of CRC patients will eventually develop metastases and possibly receive irinotecan treatment during the course of the disease. As a first-line treatment, the response rate to irinotecan-based therapy is approximately 35%-55%. No biomarker has been validated for predicting the individual likelihood of response to irinotecan treatment in mCRC patients. The current study was designed to evaluate the predictive effects of baseline serum bilirubin levels and UDP-glucuronosyltransferase (UGT)1A1*28 polymorphism on treatment response of mCRC to irinotecan-based chemotherapy.

Research frontiers

Baseline bilirubin has been reported to be associated with irinotecan-induced toxicity. Pharmacological studies demonstrate that SN-38 (the active metabolite of irinotecan) and bilirubin are glucuronidated in the same pathway, and the activity of glucuronidation is influenced by *UGT1A1*28* polymorphism.

Innovations and breakthroughs

Literature suggested a connection between circulating bilirubin, *UGT1A1*28* polymorphism and irinotecan-induced toxicity. However, the predictive role of bilirubin and *UGT1A1*28* regarding treatment outcome of irinotecan-based therapy has been conflicting. For the first time, the authors found that CoBil (an indicator combining the cutoff values of total bilirubin and unconjugated bilirubin) and *UGT1A1*28* were both independent biomarkers for predicting the treatment response of mCRC to irinotecan-based chemotherapy in a Chinese population.

Applications

After validation, CoBil, an easily determinable index in the clinic, might be helpful in facilitating stratification of mCRC patients for individualized treatment options.

Terminology

TBil and UBil are total bilirubin and unconjugated bilirubin for short, respectively. CoBil is an indicator combining the cutoff values of TBil and UBil. SN-38 is 7-ethyl-10- hydroxycamptothecin for short. SN-38 is the active metabolite of irinotecan and associated with irinotecan-treatment efficacy.

Peer-review

The authors have performed a good study, and the manuscript is interesting and has clinical relevance.

REFERENCES

1 **Torre LA**, Bray F, Siegel RL, Ferlay J, Lortet-Tieulent J, Jemal A. Global cancer statistics, 2012. *CA Cancer J Clin* 2015; **65**: 87-108 [PMID: 25651787 DOI: 10.3322/caac.21262]

2 **McPhail S**, Johnson S, Greenberg D, Peake M, Rous B. Stage at diagnosis and early mortality from cancer in England. *Br J Cancer* 2015; **112** Suppl 1: S108-S115 [PMID: 25734389 DOI: 10.1038/bjc.2015.49]

3 **Yoo PS**, Lopez-Soler RI, Longo WE, Cha CH. Liver resection for metastatic colorectal cancer in the age of neoadjuvant chemotherapy and bevacizumab. *Clin Colorectal Cancer* 2006; **6**: 202-207 [PMID: 17026789 DOI: 10.3816/CCC.2006.n.036]

4 **André T**, Louvet C, Maindrault-Goebel F, Couteau C, Mabro M, Lotz JP, Gilles-Amar V, Krulik M, Carola E, Izrael V, de Gramont A. CPT-11 (irinotecan) addition to bimonthly, high-dose leucovorin and bolus and continuous-infusion 5-fluorouracil (FOLFIRI) for pretreated metastatic colorectal cancer. GERCOR. *Eur J Cancer* 1999; **35**: 1343-1347 [PMID: 10658525]

5 **Fuchs CS**, Marshall J, Mitchell E, Wierzbicki R, Ganju V, Jeffery M, Schulz J, Richards D, Soufi-Mahjoubi R, Wang B, Barrueco J. Randomized, controlled trial of irinotecan plus infusional, bolus, or oral fluoropyrimidines in first-line treatment of metastatic colorectal cancer: results from the BICC-C Study. *J Clin Oncol* 2007; **25**: 4779-4786 [PMID: 17947725 DOI: 10.1200/JCO.2007.11.3357]

6 **Saltz LB**, Cox JV, Blanke C, Rosen LS, Fehrenbacher L, Moore MJ, Maroun JA, Ackland SP, Locker PK, Pirotta N, Elfring GL, Miller LL. Irinotecan plus fluorouracil and leucovorin for metastatic colorectal cancer. Irinotecan Study Group. *N Engl J Med* 2000; **343**: 905-914 [PMID: 11006366 DOI: 10.1056/NEJM200009283431302]

7 **Tournigand C**, André T, Achille E, Lledo G, Flesh M, Mery-Mignard D, Quinaux E, Couteau C, Buyse M, Ganem G, Landi B, Colin P, Louvet C, de Gramont A. FOLFIRI followed by FOLFOX6 or the reverse sequence in advanced colorectal cancer: a randomized GERCOR study. *J Clin Oncol* 2004; **22**: 229-237 [PMID: 14657227 DOI: 10.1200/JCO.2004.05.113]

8 **De Divitiis C**, Nasti G, Montano M, Fisichella R, Iaffaioli RV, Berretta M. Prognostic and predictive response factors in colorectal cancer patients: between hope and reality. *World J Gastroenterol* 2014; **20**: 15049-15059 [PMID: 25386053 DOI: 10.3748/wjg.v20.i41.15049]

9 **Cai X**, Cao W, Ding H, Liu T, Zhou X, Wang M, Zhong M, Zhao Z, Xu Q, Wang L. Analysis of UGT1A1*28 genotype and SN-38 pharmacokinetics for irinotecan-based chemotherapy in patients with advanced colorectal cancer: results from a multicenter, retrospective study in Shanghai. *J Cancer Res Clin Oncol* 2013; **139**: 1579-1589 [PMID: 23892411 DOI: 10.1007/s00432-013-1480-7]

10 **Iyer L**, King CD, Whitington PF, Green MD, Roy SK, Tephly TR, Coffman BL, Ratain MJ. Genetic predisposition to the metabolism of irinotecan (CPT-11). Role of uridine diphosphate glucuronosyltransferase isoform 1A1 in the glucuronidation of its active metabolite (SN-38) in human liver microsomes. *J Clin Invest* 1998; **101**: 847-854 [PMID: 9466980 DOI: 10.1172/Jci915]

11 **Bosma PJ**, Seppen J, Goldhoorn B, Bakker C, Oude Elferink RP, Chowdhury JR, Chowdhury NR, Jansen PL. Bilirubin UDP-glucuronosyltransferase 1 is the only relevant bilirubin glucuronidating isoform in man. *J Biol Chem* 1994; **269**: 17960-17964 [PMID: 8027054]

12 **Iyer L**, Hall D, Das S, Mortell MA, Ramírez J, Kim S, Di Rienzo A, Ratain MJ. Phenotype-genotype correlation of in vitro SN-38 (active metabolite of irinotecan) and bilirubin glucuronidation in human liver tissue with UGT1A1 promoter polymorphism. *Clin Pharmacol Ther* 1999; **65**: 576-582 [PMID: 10340924 DOI: 10.1016/S0009-9236(99)70078-0]

13 **Monaghan G**, Ryan M, Seddon R, Hume R, Burchell B. Genetic variation in bilirubin UPD-glucuronosyltransferase gene promoter and Gilbert's syndrome. *Lancet* 1996; **347**: 578-581 [PMID: 8596320]

14 **Chen YH**, Hung SC, Tarng DC. Serum bilirubin links UGT1A1*28 polymorphism and predicts long-term cardiovascular events and mortality in chronic hemodialysis patients. *Clin J Am Soc Nephrol* 2011; **6**: 567-574 [PMID: 21411679 DOI: 10.2215/CJN.06130710]

15 **Cecchin E**, Innocenti F, D'Andrea M, Corona G, De Mattia E, Biason P, Buonadonna A, Toffoli G. Predictive role of the UGT1A1, UGT1A7, and UGT1A9 genetic variants and their haplotypes on the outcome of metastatic colorectal cancer patients treated with fluorouracil, leucovorin, and irinotecan. *J Clin Oncol* 2009; **27**: 2457-2465 [PMID: 19364970 DOI: 10.1200/JCO.2008.19.0314]

16 **Liu X**, Cheng D, Kuang Q, Liu G, Xu W. Association between UGT1A1*28 polymorphisms and clinical outcomes of irinotecan-based chemotherapies in colorectal cancer: a meta-analysis in Caucasians. *PLoS One* 2013; **8**: e58489 [PMID: 23516488 DOI: 10.1371/journal.pone.0058489]

17 **Xu JM**, Wang Y, Ge FJ, Lin L, Liu ZY, Sharma MR. Severe irinotecan-induced toxicity in a patient with UGT1A1 28 and UGT1A1 6 polymorphisms. *World J Gastroenterol* 2013; **19**: 3899-3903 [PMID: 23840132 DOI: 10.3748/wjg.v19.i24.3899]

18 **Wang Y**, Shen L, Xu N, Wang JW, Jiao SC, Liu ZY, Xu JM. UGT1A1 predicts outcome in colorectal cancer treated with irinotecan and fluorouracil. *World J Gastroenterol* 2012; **18**: 6635-6644 [PMID: 23236239 DOI: 10.3748/wjg.v18.i45.6635]

19 **Eisenhauer EA**, Therasse P, Bogaerts J, Schwartz LH, Sargent D, Ford R, Dancey J, Arbuck S, Gwyther S, Mooney M, Rubinstein L, Shankar L, Dodd L, Kaplan R, Lacombe D, Verweij J. New response evaluation criteria in solid tumours: revised RECIST guideline (version 1.1). *Eur J Cancer* 2009; **45**: 228-247 [PMID: 19097774 DOI: 10.1016/j.ejca.2008.10.026]

20 **Loupakis F**, Yang D, Yau L, Feng S, Cremolini C, Zhang W, Maus MK, Antoniotti C, Langer C, Scherer SJ, Müller T, Hurwitz HI, Saltz L, Falcone A, Lenz HJ. Primary tumor location as a prognostic factor in metastatic colorectal cancer. *J Natl Cancer Inst* 2015; **107**: pii dju427 [PMID: 25713148 DOI: 10.1093/jnci/dju427]

21 **Liu CY**, Chen PM, Chiou TJ, Liu JH, Lin JK, Lin TC, Chen WS, Jiang JK, Wang HS, Wang WS. UGT1A1*28 polymorphism predicts irinotecan-induced severe toxicities without affecting treatment outcome and survival in patients with metastatic colorectal carcinoma. *Cancer* 2008; **112**: 1932-1940 [PMID: 18300238 DOI: 10.1002/cncr.23370]

22 **Fuchs CS**, Moore MR, Harker G, Villa L, Rinaldi D, Hecht JR. Phase III comparison of two irinotecan dosing regimens in second-line therapy of metastatic colorectal cancer. *J Clin Oncol* 2003; **21**: 807-814 [PMID: 12610178]

23 **Sugatani J**, Yamakawa K, Yoshinari K, Machida T, Takagi H, Mori M, Kakizaki S, Sueyoshi T, Negishi M, Miwa M. Identification of a defect in the UGT1A1 gene promoter and its association with hyperbilirubinemia. *Biochem Biophys Res Commun* 2002; **292**: 492-497 [PMID: 11906189 DOI: 10.1006/bbrc.2002.6683]

24 **Bosma PJ**, Chowdhury JR, Bakker C, Gantla S, de Boer A, Oostra BA, Lindhout D, Tytgat GN, Jansen PL, Oude Elferink RP. The genetic basis of the reduced expression of bilirubin UDP-glucuronosyltransferase 1 in Gilbert's syndrome. *N Engl J Med* 1995; **333**: 1171-1175 [PMID: 7565971 DOI: 10.1056/NEJM199511023331802]

25 **Beutler E**, Gelbart T, Demina A. Racial variability in the UDP-glucuronosyltransferase 1 (UGT1A1) promoter: a balanced polymorphism for regulation of bilirubin metabolism? *Proc Natl Acad Sci USA* 1998; **95**: 8170-8174 [PMID: 9653159]

26 **Iyer L**, Das S, Janisch L, Wen M, Ramírez J, Karrison T, Fleming GF, Vokes EE, Schilsky RL, Ratain MJ. UGT1A1*28 polymorphism as a determinant of irinotecan disposition and toxicity. *Pharmacogenomics J* 2002; **2**: 43-47 [PMID: 11990381]

27 **Stewart CF**, Panetta JC, O'Shaughnessy MA, Throm SL, Fraga CH, Owens T, Liu T, Billups C, Rodriguez-Galindo C, Gajjar A, Furman WL, McGregor LM. UGT1A1 promoter genotype correlates with SN-38 pharmacokinetics, but not severe toxicity

in patients receiving low-dose irinotecan. *J Clin Oncol* 2007; **25**: 2594-2600 [PMID: 17577039 DOI: 10.1200/JCO.2006.10.2301]

28 **Dias MM**, Pignon JP, Karapetis CS, Boige V, Glimelius B, Kweekel DM, Lara PN, Laurent-Puig P, Martinez-Balibrea E, Páez D, Punt CJ, Redman MW, Toffoli G, Wadelius M, McKinnon RA, Sorich MJ. The effect of the UGT1A1*28 allele on survival after irinotecan-based chemotherapy: a collaborative meta-analysis. *Pharmacogenomics J* 2014; **14**: 424-431 [PMID: 24709690 DOI: 10.1038/tpj.2014.16]

29 **McLeod HL**, Sargent DJ, Marsh S, Green EM, King CR, Fuchs CS, Ramanathan RK, Williamson SK, Findlay BP, Thibodeau SN, Grothey A, Morton RF, Goldberg RM. Pharmacogenetic predictors of adverse events and response to chemotherapy in metastatic colorectal cancer: results from North American Gastrointestinal Intergroup Trial N9741. *J Clin Oncol* 2010; **28**: 3227-3233 [PMID: 20530282 DOI: 10.1200/JCO.2009.21.7943]

30 **Toffoli G**, Cecchin E, Corona G, Russo A, Buonadonna A, D' Andrea M, Pasetto LM, Pessa S, Errante D, De Pangher V, Giusto M, Medici M, Gaion F, Sandri P, Galligioni E, Bonura S, Boccalon M, Biason P, Frustaci S. The role of UGT1A1*28 polymorphism in the pharmacodynamics and pharmacokinetics of irinotecan in patients with metastatic colorectal cancer. *J Clin Oncol* 2006; **24**: 3061-3068 [PMID: 16809730 DOI: 10.1200/JCO.2005.05.5400]

31 **Freyer G**, Rougier P, Bugat R, Droz JP, Marty M, Bleiberg H, Mignard D, Awad L, Herait P, Culine S, Trillet-Lenoir V. Prognostic factors for tumour response, progression-free survival and toxicity in metastatic colorectal cancer patients given irinotecan (CPT-11) as second-line chemotherapy after 5FU failure. CPT-11 F205, F220, F221 and V222 study groups. *Br J Cancer* 2000; **83**: 431-437 [PMID: 10945486 DOI: 10.1054/bjoc.2000.1303]

32 **Meyerhardt JA**, Kwok A, Ratain MJ, McGovren JP, Fuchs CS. Relationship of baseline serum bilirubin to efficacy and toxicity of single-agent irinotecan in patients with metastatic colorectal cancer. *J Clin Oncol* 2004; **22**: 1439-1446 [PMID: 15084617 DOI: 10.1200/JCO.2004.10.043]

33 **Dréanic J**, Maillet M, Dhooge M, Mir O, Brezault C, Goldwasser F, Chaussade S, Coriat R. Prognostic value of the Glasgow Prognostic Score in metastatic colorectal cancer in the era of anti-EGFR therapies. *Med Oncol* 2013; **30**: 656 [PMID: 23839775 DOI: 10.1007/s12032-013-0656-y]

P- Reviewer: Demir Y **S- Editor**: Ma YJ **L- Editor**: Wang TQ
E- Editor: Ma S

World Journal of Gastroenterology

Submit a Manuscript: http://www.wjgnet.com/esps/
Help Desk: http://www.wjgnet.com/esps/helpdesk.aspx
DOI: 10.3748/wjg.v22.i16.4259

World J Gastroenterol 2016 April 28; 22(16): 4259-4263
ISSN 1007-9327 (print) ISSN 2219-2840 (online)

CASE REPORT

Pancreaticoduodenal artery aneurysm associated with coeliac artery occlusion from an aortic intramural hematoma

Akihiko Sakatani, Yoshinori Doi, Toshiaki Kitayama, Takaaki Matsuda, Yasutaka Sasai, Naohiro Nishida, Megumi Sakamoto, Naoto Uenoyama, Kazuo Kinoshita

Akihiko Sakatani, Department of Gastroenterology and Hepatology, Osaka University Graduate School of Medicine, Suita 565-0871, Japan

Akihiko Sakatani, Yoshinori Doi, Takaaki Matsuda, Yasutaka Sasai, Naohiro Nishida, Megumi Sakamoto, Naoto Uenoyama, Kazuo Kinoshita, Department of Gastroenterology, Otemae Hospital, Osaka 540-0008, Japan

Toshiaki Kitayama, Department of Radiology, Otemae Hospital, Osaka 540-0008, Japan

Author contributions: Sakatani A wrote the manuscript; Doi Y, Kitayama T, Matsuda T, Sasai Y, Nishida N, Sakamoto M, Uenoyama N and Kinoshita K proofread and revised the manuscript.

Institutional review board statement: Otemae Hospital Clinical Ethics Review Board does not require approval for case reports.

Informed consent statement: The patient involved in this case report authorized the disclosure of his protected health information for academic purposes.

Correspondence to: Akihiko Sakatani, MD, Department of Gastroenterology and Hepatology, Osaka University Graduate School of Medicine, 2-2 Yamadaoka, Suita 565-0871, Osaka, Japan. akihiko-sakatani@umin.net
Telephone: +81-6-68793621
Fax: +81-6-68793629

Received: December 2, 2015
Peer-review started: December 4, 2015
First decision: December 31, 2015
Revised: January 27, 2016
Accepted: February 20, 2016
Article in press: February 22, 2016
Published online: April 28, 2016

Abstract

Pancreaticoduodenal artery aneurysms are a rare type of visceral artery aneurysm, whose rupture is associated with high mortality. These aneurysms are of particular interest because local haemodynamic change caused by coeliac artery obstruction plays an important role in their development. However, the pathophysiological mechanism of coeliac artery obstruction is not completely understood. Pressure from the median arcuate ligament is most frequently reported cause. Although it is well-known that stenosis or occlusion of the visceral vessels may be caused by aortic syndrome, reports of pancreaticoduodenal artery aneurysm associated with coeliac artery occlusion due to aortic syndrome are extremely rare. Our case indicates a new aetiology for a pancreaticoduodenal artery aneurysm and demonstrates the rapid deterioration of the patient affected.

Key words: Pancreaticoduodenal artery; Coeliac artery; Visceral artery aneurysm; Aortic dissection

Core tip: Approximately 60% of patients with pancreaticoduodenal artery aneurysms presented with rupture have an attending mortality rate of 50%. With the development of the device and techniques,

transcatheter arterial embolotherapy has decreased the mortality to as low as 0%. Therefore, early detection and treatment is necessary to improve prognosis of the case.

Sakatani A, Doi Y, Kitayama T, Matsuda T, Sasai Y, Nishida N, Sakamoto M, Uenoyama N, Kinoshita K. Pancreaticoduodenal artery aneurysm associated with coeliac artery occlusion from an aortic intramural hematoma. *World J Gastroenterol* 2016; 22(16): 4259-4263 Available from: URL: http://www.wjgnet.com/1007-9327/full/v22/i16/4259.htm DOI: http://dx.doi.org/10.3748/wjg.v22.i16.4259

INTRODUCTION

Sutton and Lawton first reported a pancreaticoduodenal artery (PDA) aneurysm associated with coeliac axis occlusion in 1973 and since then 93 such cases have been reported[1]. Obstruction of the coeliac artery leads to collateralization of the hepatic and splenic arteries through the superior mesenteric artery (SMA). Increased blood flow in the small and fragile pancreaticoduodenal arcade vessels may contribute to aneurysm development[1,2]. Here we report what is, to the best of our knowledge, the second case in the English-language literature of a PDA aneurysm associated with occlusion of the coeliac artery due to aortic syndrome.

CASE REPORT

An apparently healthy 60-year-old man developed sudden and severe upper abdominal pain and was admitted to a local hospital. He did not feel nausea or other symptoms of visceral ischemia. There was no history of any cardiovascular disorder, connective tissue disorders, chest injury, and familial history of aortic syndrome. The aortic dissections detection risk score was 1. Initial plain computed tomography (CT) performed 5 h after onset of symptoms showed a dilated descending aorta and hyperattenuated collection located eccentrically within the aortic wall (Figure 1A). However, the attending physician could not recognize it and the cause of abdominal pain remained unclear. Therefore, contrast-enhanced CT had to be performed 6 h after the onset of symptoms, which revealed crescentic and asymmetric wall thickening of the descending aorta: Contrast is not visualized within the aortic media. Intimal flap was not detected. A diagnosis of aortic intramural hematoma (IMH) extending from the distal aortic arch to the level of the coeliac artery was made (Figure 1B-D). The root of the coeliac artery was compressed by IMH (Figures 1D and 2A). The patient was transferred to our hospital 8 h after symptom onset. This patient was not administered any drug which would affect the coagulation during the period of pre-hospital to hospital care.

On arrival, his vital signs were normal and initial laboratory data were: white blood cell count 20190/mm^3, D-dimer 85.9 μg/mL, and C-reactive protein 3.0 mg/dL, with other parameters, including haemoglobin, prothrombin time, activated partial thromboplastin time, and serum amylase levels within normal limits. However, the patient lost consciousness and became hypotensive (74/40 mmHg) during transfer to the CT room 10 min after arrival in the emergency room. Contrast-enhanced CT revealed an aortic IMH and a large retroperitoneal haematoma involving the head of the pancreas and duodenum (Figure 2A and B).

The patient underwent visceral angiography for localization of the site of injury and to control bleeding. The arteriogram showed complete occlusion at the root of the coeliac artery, collateralization from SMA through the pancreaticoduodenal arcade and a saccular aneurysm of the inferior PDA (Figure 2C). The patient was, therefore, diagnosed with retroperitoneal bleeding caused by a ruptured PDA aneurysm. Selective microcoil embolization proximal and distal to the aneurysm was successfully performed. A clear CT performed at our hospital revealed anterior branch aneurism of inferior PDA (Figure 2B). The patient recovered completely and has been doing well for 5 mo.

DISCUSSION

PDA aneurysms are rare and account for 2% of all the splanchnic artery aneurysms[3]. PDA aneurysms may either be true aneurysms, resulting from a primary abnormality of the vessel wall, or false aneurysms, resulting from injury and erosion of the vessel wall, most commonly after trauma or inflammation (*e.g.*, pancreatitis). Most cases of true PDA aneurysm are reported in patients in their 50s[1,2], suggesting a different aetiology from that of atherosclerotic aneurysms reported in the elderly. In fact, coeliac axis stenosis has been identified in 60%-75% of patients diagnosed with true PDA aneurysm[4]. In contrast, the reported incidence of coeliac axis stenosis ranges from 12.5% to 24% in the general population[2].

Obstruction of the coeliac artery leads to collateralization of the hepatic and splenic arteries through the SMA. Increased blood flow in the small and fragile pancreaticoduodenal arcade vessels is likely to contribute to aneurysm development[1]. However, the pathophysiological mechanism of coeliac artery obstruction remains to be elucidated. Pressure from the median arcuate ligament (MAL) is the most frequently reported cause[1]. Although it is well known that spontaneous aortic syndrome may cause occlusion of the aortic side branch, to the best of our knowledge, only one Japanese patient with ruptured PDA aneurysm associated with acute aortic syndrome involving the coeliac axis has been reported[5]. In that report, CT at symptom onset confirmed the presence of MAL

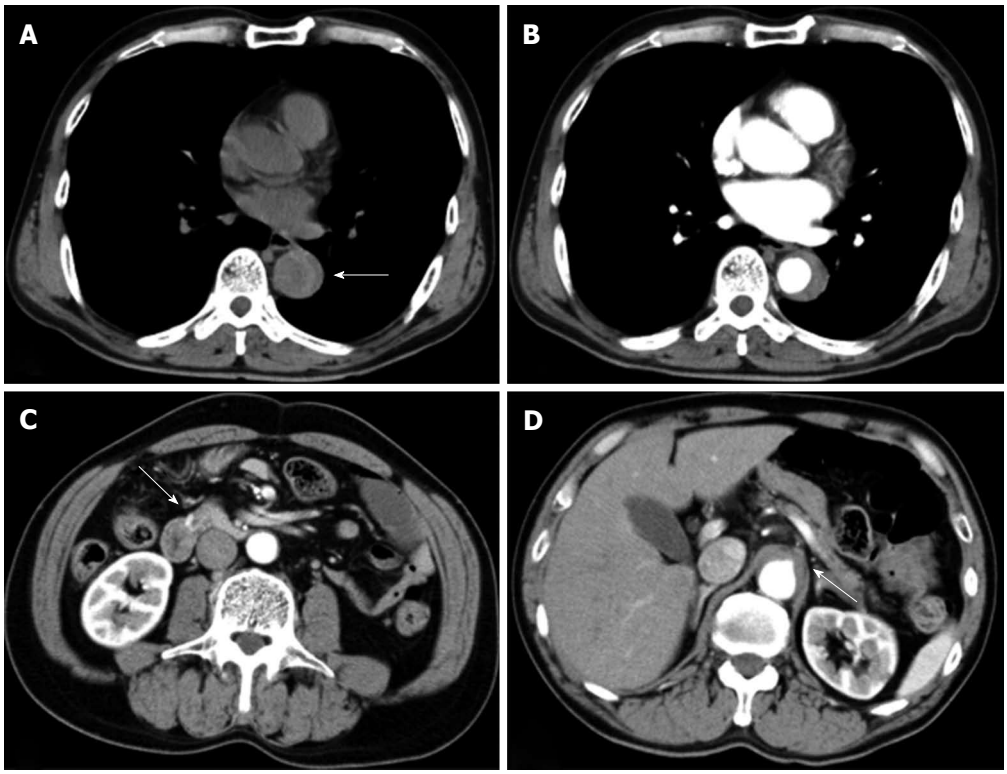

Figure 1 Initial computed tomography performed at local hospital before the onset of hypotension. A: Plain computed tomography (CT) demonstrating dilated descending aorta and hyperattenuated collection located eccentrically within the aortic wall (arrow); B: Contrast-enhanced CT revealed crescentic and asymmetric wall thickening of the descending aorta: Contrast is not visualized within the aortic media. Intimal flap was not detected; C: An aneurysm at the anteroinferior pancreaticoduodenal artery (arrow); D: The occluded root of the coeliac artery (arrow).

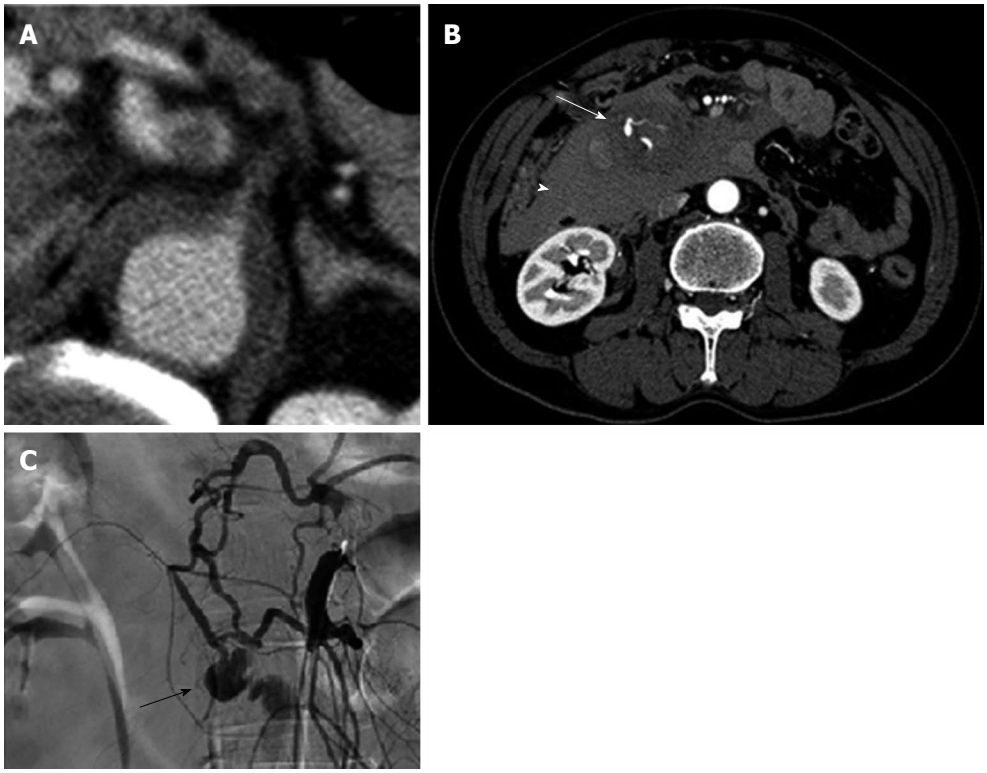

Figure 2 Subsequent contrast-enhanced computed tomography and arteriography performed at our hospital, after the onset of hypotension. A: Multidetector computed tomography (CT) performed at our hospital showing the root of the coeliac artery compressed and occluded by the false lumen more clearly than that performed at a local hospital; B: CT scan showing a large haematoma in the right prerenal space (arrow head) and the aneurysm of anteroinferior pancreaticoduodenal artery (arrow); C: Arteriogram of the superior mesenteric artery (SMA) showing blood flow reversal from the SMA to the hepatic artery through the pancreaticoduodenal arcade, due to coeliac trunk occlusion and a saccular aneurysm of the inferior pancreaticoduodenal artery (PDA) (arrow).

with acute aortic dissection. Therefore, the authors speculated that both MAL and aortic dissection played a role of causative factor to develop the aneurysm. However, our patient showed no other factor causing coeliac artery occlusion without aortic IMH. Aortic IMH are considered as a variant of aortic dissection, accounting for 10%-30% of all acute aortic syndromes. Despite the difference in the pathophysiology, the prognosis for thoracic aortic dissections and IMH is similar. Although IMH is less likely to be associated with the branch artery occlusion compared with the typical aortic dissection, there have been some reports on ischemia due to IMH[6-8].

Although the duration of the coeliac artery occlusion from aortic IMH was limited in our case, we speculate that this is a causative factor contributing to PDA aneurysm development and rupture because of an interesting characteristic of PDA aneurysms. Although most visceral artery aneurysms show a correlation between the size and the frequency of rupture, this does not apply to PDA aneurysms[1,9,10]. Because true aneurysms of the splenic and hepatic artery, accounting for 70% of all visceral artery, rarely rupture when they are < 2 cm[11,12], it is generally believed that visceral aneurysm require a lot of time to develop and rupture. However, PDA aneurysms have not shown a clear correlation between size and propensity to rupture[1,9,10]. Brocker *et al*[1] reported a size variance from 3 to 40 mm (mean 15.2 mm) for ruptured PDA aneurysm. In his report, at least 24 patients bled from aneurysm < 2 cm and 14 patients bled from aneurysm < 1 cm. This suggests PDA aneurysms may rupture within short time after development. Therefore, we conclude that the celiac artery obstruction due to aortic IMH played an important role in the development and rupture of PDA aneurysm in this case, even in a limited duration of time.

It is difficult to make diagnosis of PDA aneurysms before the occurrence of rupture because of the low prevalence and nonspecific symptoms. Approximately 60% of patients with PDA aneurysms presented with rupture have an attending mortality rate of 50%[2]. With the development of the device and techniques, transcatheter arterial embolotherapy has decreased the mortality to as low as 0%[2]. Therefore, early detection and treatment is necessary to improve prognosis of the case.

COMMENTS

Case characteristics

An apparently healthy 60-year-old man diagnosed aortic intramural hematoma at local hospital lost consciousness and became hypotensive after transfering to Otemae Hospital.

Clinical diagnosis

Type B aortic intramural hematoma complicated retroperitoneal bleeding of a ruptured pancreaticoduodenal artery (PDA) aneurysm.

Differential diagnosis

Acute aortic ruputure, cardiac tamponade.

Laboratory diagnosis

Initial laboratory data showed elevation only of white blood cell count, D-dimer and C-reactive protein.

Imaging diagnosis

Contrast-enhanced computed tomography showed retroperitoneal hematoma and pancreaticoduodenal artery aneurysm associated with occlusion of the coeliac artery due to aortic intramural hematoma.

Treatment

Transcatheter arterial embolization.

Related reports

Only one Japanese patient with ruptured PDA aneurysm associated with acute aortic syndrome involving the coeliac axis has been reported.

Term explanation

Aortic intramural hematoma is a life-threatening aortic disease included within acute aortic syndrome, together with aortic dissection and penetrating aortic ulcer.

Experiences and lessons

PDA aneurysms, which is uncommon but life-threatening complications may occur in patients with aortic syndrome involving the visceral arteries.

Peer-review

This case report describes the case of a 60-year old man affected by type B aortic intramural hematoma, complicated by retroperitoneal bleeding of a ruptured PDA aneurysm.

REFERENCES

1 **Brocker JA**, Maher JL, Smith RW. True pancreaticoduodenal aneurysms with celiac stenosis or occlusion. *Am J Surg* 2012; **204**: 762-768 [PMID: 22578409 DOI: 10.1016/j.amjsurg.2012.03.001]

2 **Dave B**, Sharma A, Kwolek C, Demoya M, Wicky S, Kalva S. Percutaneous transcatheter arterial embolization of inferior pancreatico-duodenal artery aneurysms associated with celiac artery stenosis or occlusion. *Catheter Cardiovasc Interv* 2010; **75**: 663-672 [PMID: 20155804 DOI: 10.1002/ccd.22395]

3 **Lakin RO**, Kashyap VS. Splanchnic Artery Aneurysms. In: Cronenwett JL, Johnston KW, editor. Rutherford's Vascular Surgery. 8th ed. Philadelphia: W.B.Saunders, 2014: 2220-2235

4 **Roger DB**. Personal space, body image and leadership: an exploratory study. *Percept Mot Skills* 1976; **43**: 25-26 [PMID: 958818 DOI: 10.1007/s100169900155]

5 **Miyayama S**, Terada T, Tamaki M. Ruptured pancreaticoduodenal artery aneurysm associated with median arcuate ligament compression and aortic dissection successfully treated with embolotherapy. *Ann Vasc Dis* 2015; **8**: 40-42 [PMID: 25848431 DOI: 10.3400/avd.cr.14-00117]

6 **Sawhney NS**, DeMaria AN, Blanchard DG. Aortic intramural hematoma: an increasingly recognized and potentially fatal entity. *Chest* 2001; **120**: 1340-1346 [PMID: 11591580 DOI: 10.1378/chest.120.4.1340]

7 **Evangelista A**, Mukherjee D, Mehta RH, O'Gara PT, Fattori R, Cooper JV, Smith DE, Oh JK, Hutchison S, Sechtem U, Isselbacher EM, Nienaber CA, Pape LA, Eagle KA. Acute intramural hematoma of the aorta: a mystery in evolution. *Circulation* 2005; **111**: 1063-1070 [PMID: 15710757 DOI: 10.1161/01.CIR.0000081776.49923.5A]

8 **von Kodolitsch Y**, Csösz SK, Koschyk DH, Schalwat I, Loose R, Karck M, Dieckmann C, Fattori R, Haverich A, Berger J,

Meinertz T, Nienaber CA. Intramural hematoma of the aorta: predictors of progression to dissection and rupture. *Circulation* 2003; **107**: 1158-1163 [PMID: 12615795 DOI: 10.1161/01.CIR.0000052628.77047.EA]

9 **Ducasse E**, Roy F, Chevalier J, Massouille D, Smith M, Speziale F, Fiorani P, Puppinck P. Aneurysm of the pancreaticoduodenal arteries with a celiac trunk lesion: current management. *J Vasc Surg* 2004; **39**: 906-911 [PMID: 15071464 DOI: 10.1016/j.jvs.2003.09.049]

10 **Suzuki K**, Kashimura H, Sato M, Hassan M, Yokota H, Nakahara A, Muto H, Yuzawa K, Fukao K, Tanaka N. Pancreaticoduodenal artery aneurysms associated with celiac axis stenosis due to compression by median arcuate ligament and celiac plexus. *J Gastroenterol* 1998; **33**: 434-438 [PMID: 9658327 DOI: 10.1007/s005350050109]

11 **Lakin RO**, Bena JF, Sarac TP, Shah S, Krajewski LP, Srivastava SD, Clair DG, Kashyap VS. The contemporary management of splenic artery aneurysms. *J Vasc Surg* 2011; **53**: 958-64; discussion 965 [PMID: 21215563 DOI: 10.1016/j.jvs.2010.10.055]

12 **Abbas MA**, Stone WM, Fowl RJ, Gloviczki P, Oldenburg WA, Pairolero PC, Hallett JW, Bower TC, Panneton JM, Cherry KJ. Splenic artery aneurysms: two decades experience at Mayo clinic. *Ann Vasc Surg* 2002; **16**: 442-449 [PMID: 12089631 DOI: 10.1007/s10016-001-0207-4]

P- Reviewer: Gao BL, Morello F **S- Editor**: Yu J **L- Editor**: A
E- Editor: Zhang DN

World Journal of Gastroenterology

Submit a Manuscript: http://www.wjgnet.com/esps/
Help Desk: http://www.wjgnet.com/esps/helpdesk.aspx
DOI: 10.3748/wjg.v22.i16.4264

World J Gastroenterol 2016 April 28; 22(16): 4264-4269
ISSN 1007-9327 (print) ISSN 2219-2840 (online)

CASE REPORT

Urgent endoscopic ultrasound-guided choledochoduodenostomy for acute obstructive suppurative cholangitis-induced sepsis

Kosuke Minaga, Masayuki Kitano, Hajime Imai, Kentaro Yamao, Ken Kamata, Takeshi Miyata, Shunsuke Omoto, Kumpei Kadosaka, Tomoe Yoshikawa, Masatoshi Kudo

Kosuke Minaga, Masayuki Kitano, Hajime Imai, Kentaro Yamao, Ken Kamata, Takeshi Miyata, Shunsuke Omoto, Kumpei Kadosaka, Tomoe Yoshikawa, Masatoshi Kudo, Department of Gastroenterology and Hepatology, Kinki University Faculty of Medicine, Osaka-Sayama 589-8511, Japan

Author contributions: All authors helped to perform the research; Minaga K wrote the manuscript; Kitano M and Kudo M drafted the conception and design; Kitano M performed endoscopic interventions; Imai H, Yamao K, Kamata K, Miyata T, Omoto S, Kadosaka K and Yoshikawa T contributed to writing the manuscript.

Supported by The Japan Society for the Promotion of Science and the Japanese Foundation for the Research and Promotion of Endoscopy, No. 22590764 and 25461035.

Institutional review board statement: This study was approved by the Institutional Review Board of Kinki University Faculty of Medicine.

Informed consent statement: All study participants, or their legal guardian, provided informed written consent prior to study enrollment.

Conflict-of-interest statement: All authors declare no conflicts-of-interest related to this article.

Correspondence to: Masayuki Kitano, MD, PhD, Department of Gastroenterology and Hepatology, Kinki University Faculty of Medicine, 377-2 Ohno-Higashi, Osaka-Sayama 589-8511, Japan. m-kitano@med.kindai.ac.jp

Telephone: +81-72-3660221
Fax: +81-72-3672880

Received: December 10, 2015
Peer-review started: December 12, 2015
First decision: December 30, 2015
Revised: January 7, 2016
Accepted: January 30, 2016
Article in press: January 30, 2016
Published online: April 28, 2016

Abstract

Acute obstructive suppurative cholangitis (AOSC) due to biliary lithiasis is a life-threatening condition that requires urgent biliary decompression. Although endoscopic retrograde cholangiopancreatography (ERCP) with stent placement is the current gold standard for biliary decompression, it can sometimes be difficult because of failed biliary cannulation. In this retrospective case series, we describe three cases of successful biliary drainage with recovery from septic shock after urgent endoscopic ultrasound-guided choledochoduodenostomy (EUS-CDS) was performed for AOSC due to biliary lithiasis. In all three cases, technical success in inserting the stents was achieved and the patients completely recovered from AOSC with sepsis in a few days after EUS-CDS. There were no procedure-related complications. When initial ERCP fails, EUS-CDS can be an effective life-saving endoscopic biliary decompression procedure that shortens the procedure time and prevents post-ERCP pancreatitis, particularly in patients with AOSC-induced sepsis.

Key words: Endoscopic ultrasound-guided biliary drainage; Choledochoduodenostomy; Acute obstructive

suppurative cholangitis; Sepsis; Life-saving endoscopy

Core tip: We present 3 cases of urgent endoscopic ultrasound-guided choledochoduodenostomy (EUS-CDS) performed for acute obstructive suppurative cholangitis (AOSC)-induced sepsis due to benign lesions. In all three cases, technical success in inserting the stents was achieved and the patients completely recovered from AOSC with sepsis in a few days after EUS-CDS. Although endoscopic retrograde cholangiopancreatography (ERCP) with transpapillary stent placement is the current gold standard for biliary decompression, this technique is not always successful. In this situation, EUS-CDS can be an effective life-saving biliary decompression procedure that can shorten the procedure time and prevent post-ERCP pancreatitis, particularly in patients with AOSC-induced sepsis.

Minaga K, Kitano M, Imai H, Yamao K, Kamata K, Miyata T, Omoto S, Kadosaka K, Yoshikawa T, Kudo M. Urgent endoscopic ultrasound-guided choledochoduodenostomy for acute obstructive suppurative cholangitis-induced sepsis. *World J Gastroenterol* 2016; 22(16): 4264-4269 Available from: URL: http://www.wjgnet.com/1007-9327/full/v22/i16/4264.htm DOI: http://dx.doi.org/10.3748/wjg.v22.i16.4264

INTRODUCTION

Acute obstructive suppurative cholangitis (AOSC) due to biliary lithiasis is a life-threatening condition that requires urgent biliary decompression. Endoscopic retrograde cholangiopancreatography (ERCP) with transpapillary stent placement is the current gold standard for biliary decompression. Endoscopic transpapillary stent placement can sometimes be difficult because of failed biliary cannulation. Recently, endoscopic ultrasound (EUS) guided biliary drainage (EUS-BD) has been increasingly used as an alternative in patients with malignant biliary obstruction after failed initial ERCP[1-4]. However, this technique is not usually indicated for benign biliary lesions. Here we describe three cases of successful biliary drainage with full recovery from septic shock after urgent EUS-guided choledochoduodenostomy (EUS-CDS) was performed for AOSC-induced sepsis. All procedures were carried out by a single experienced endoscopist (M.K.) at a tertiary-care referral center. All EUS procedures were performed using a therapeutic linear echoendoscope (GF-UCT260; Olympus Medical Systems, Tokyo, Japan) with carbon dioxide insufflation. The collection of clinical data for this study was approved by the Institutional Review Board of Kinki University Faculty of Medicine and all study participants, or their legal guardian, provided informed written consent prior to study enrollment.

CASE REPORT

Patient 1

An 83-year-old woman with septic shock due to common bile duct (CBD) stones was referred to our hospital. Urgent ERCP had been performed at a neighboring general hospital; however, biliary cannulation was unsuccessful even with needle-knife precut papillotomy. Intravenous norepinephrine had been administered to maintain systolic blood pressure. Her vital signs were as follows: Glasgow coma scale (GCS) conscious level of E3V4M3, blood pressure of 75/55 mmHg, heart rate of 108 beats/min, and body temperature of 39.2 ℃. Laboratory tests showed an elevated inflammatory reaction [white blood cell count (WBC), 38300/μL; serum C-reactive protein (CRP) level, 17.7 mg/dL; and serum procalcitonin (PCT), 64.3 ng/mL]. Elevated levels of serum liver function parameters and bilirubin were also noted [aspartate aminotransferase (AST), 123 IU/L; alanine aminotransferase (ALT), 169 IU/L; alkaline phosphatase (ALP), 220 IU/L; and total bilirubin, 5.2 mg/dL]. Computed tomography (CT) revealed large piled-up CBD stones and dilatation of CBD. Because the intrahepatic bile ducts were not dilated, percutaneous transhepatic biliary drainage (PTBD) seemed to be difficult. Thus, we decided to perform EUS-CDS. The procedure was performed without intubation after administration of a small amount of intravenous midazolam. The depth of the patient's sedation was titrated by continuous monitoring with a bispectral index monitor and a pulse oximetry. On EUS, the dilated CBD was accessed from the duodenum bulb. First, the CBD was punctured using a 19-gauge needle (Sono Tip Pro Control; Medi-Globe, Rosenheim, Germany) under echoendoscopic guidance (Figure 1A). Bile was aspirated, and then contrast medium was injected. A 0.025-inch guidewire (VisiGlide 2; Olympus Medical Systems) was placed into the CBD. The fistula was dilated using a 4-mm balloon catheter (ZARA; Century Medical, Tokyo, Japan) (Figure 1B), and a covered metallic stent (8-mm wide, 80-mm long; WallFlex partially covered stent; Boston Scientific, Natick, MA, United States) and a 6-Fr endoscopic nasobiliary drainage catheter were inserted (Figure 1C). The duration for the procedure was 21 min. The patient completely recovered in a few days and was discharged 14 d after admission. One month later, we removed the metallic stents and inserted two 7-Fr plastic stents *via* the EUS-CDS fistula to keep it patent (Figure 2). When we suggested options for performing rendezvous technique *via* the CDS fistula or surgery to extract the CBD stones, the patient and her family did not choose to undergo these procedures because she did not have any new symptoms. Therefore, we decided to exchange stents semiannually. During 8 mo

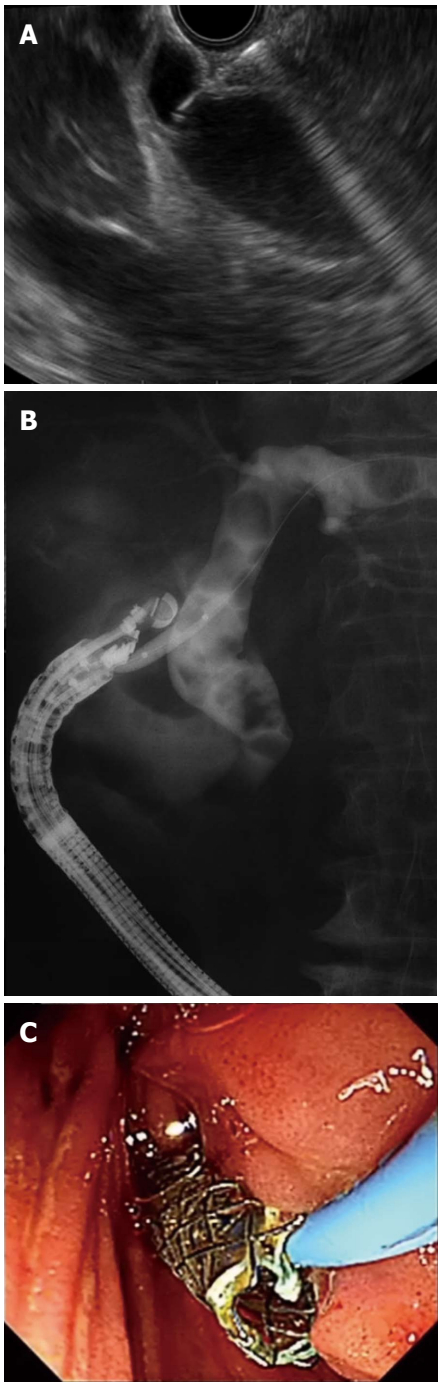

Figure 1 Images of patient 1 who underwent urgent endoscopic ultrasound-guided choledochoduodenostomy. A: EUS-guided common bile duct (CBD) puncture; B: EUS-guided cholangiography showed large piled-up CBD stones. Fistula track was dilated using a 4-mm balloon catheter; C: A covered metallic stent and an endoscopic nasobiliary drainage catheter were successfully placed *via* the duodenum bulb. EUS: Endoscopic ultrasound.

of follow-up, the patient was free of any symptoms and we exchanged the stents endoscopically 6 mo after the initial procedure.

Patient 2

An 85-year-old woman with septic shock due to CBD stones was referred to our hospital. Urgent

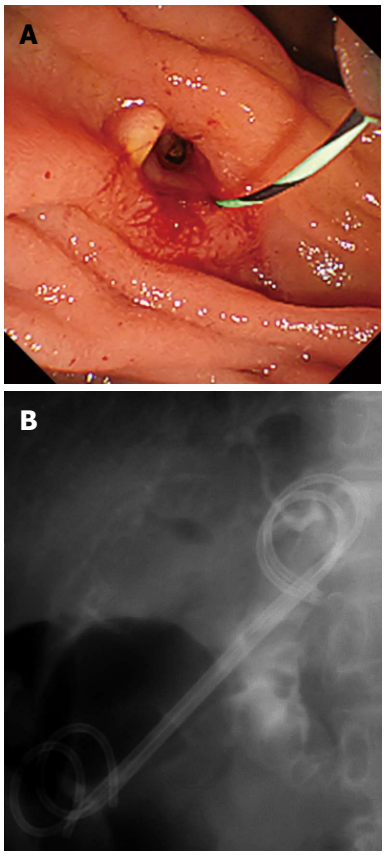

Figure 2 Images of biliary cannulation and plastic stent placement *via* an endoscopic ultrasound-guided choledochoduodenostomy fistula. A: A matured fistula was created where the removed metallic stent was placed. The common bile duct (CBD) was cannulated *via* the EUS-CDS fistula using an ERCP catheter and a guidewire was inserted; B: Two 7-Fr double pigtail plastic stents were placed into the CBD *via* the EUS-CDS fistula. EUS-CDS: Endoscopic ultrasound-guided choledochoduodenostomy; ERCP: Endoscopic retrograde cholangiopancreatography.

ERCP had been attempted at a neighboring general hospital. Biliary cannulation had failed because of the presence of juxtapapillary diverticulum. The patient's vital signs were as follows: GCS conscious level of E2V2M3, blood pressure of 193/92 mmHg, heart rate of 120 beats/min, and body temperature of 39.8 ℃. Laboratory tests showed an elevated inflammatory reaction (WBC, 93600/μL; serum CRP, 11.6 mg/dL; and serum PCT, 30.1 ng/mL). Elevated levels of serum liver function parameters and bilirubin were also remarkable (AST, 567 IU/L; ALT, 372 IU/L; ALP, 1312 IU/L; and total bilirubin, 5.0 mg/dL). CT revealed large multiple CBD stones, and the CBD was dilated approximately 18 mm. Because urgent biliary drainage was required to treat septic shock, we performed EUS-CDS. The intrahepatic bile ducts were slightly dilated on EUS; therefore, the dilated CBD was punctured from the duodenum bulb using a 19-gauge needle. A 0.025-inch guidewire was placed into the CBD. Then, the fistula was dilated using a 7-Fr dilation catheter, and a covered metallic stent (8-mm-wide and 60-mm-long; WallFlex) was placed. The duration

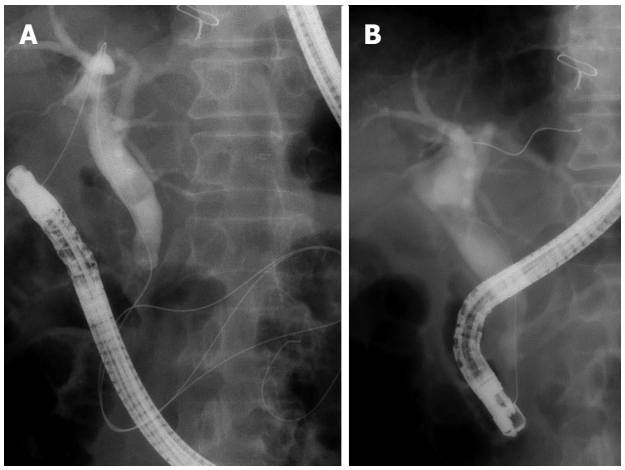

Figure 3 Images of a rendezvous technique *via* the endoscopic ultrasound-guided choledochoduodenostomy fistula. A: The common bile duct was cannulated *via* the EUS-CDS fistula and a guidewire was advanced into the duodenum through the papilla; B: The guidewire was caught in the duodenum and transpapillary biliary cannulation was succeeded.

for the procedure was 18 min. The patient recovered completely in a few days and was discharged 12 d after admission. One month later, we removed the metallic stents and inserted two 7-Fr plastic stents *via* the EUS-CDS fistula. We suggested options for performing rendezvous technique or surgery in the same manner as described in case 1, she did not wish for these invasive procedures. Therefore, we decided to exchange stents semiannually. During 4 mo of follow-up, the patient was free of any symptoms.

Patient 3

An 80-year-old man with severe cholangitis due to CBD stones was referred to our hospital. His vital signs were as follows: GCS conscious level of E3V4M5, blood pressure of 170/77 mmHg, heart rate of 102 beats/min, and body temperature of 38.6 ℃. Laboratory tests showed an elevated inflammatory reaction (WBC, 13200/μL and serum CRP, 6.7 mg/dL). Elevated liver function parameters and bilirubin level were also noted (AST, 306 IU/L; ALT, 324 IU/L; ALP, 1510 IU/L; and total bilirubin, 1.8 mg/dL). His platelet count decreased to 96000/μL. He also had disseminated intravascular coagulation (DIC) (defined as an acute DIC score ⩾ 4) complicated by acute cholangitis induced-sepsis. CT revealed two CBD stones with a diameter of 12 mm. Recombinant human soluble thrombomodulin was administered to treat DIC. Then, urgent ERCP was attempted. Deep biliary cannulation failed even after using a double-guidewire technique. To treat the sepsis, we performed EUS-CDS in the same session. The dilated CBD was punctured from the duodenum bulb using a 19-gauge needle. A 0.025-inch guide wire was placed into the CBD. Then, the fistula was dilated using a 7-Fr dilation catheter, and a 7-Fr straight plastic stent (70-mm-long; Flexima, Boston Scientific) was placed. The duration for ERCP and EUS-CDS procedures was 43 min and 18 min, respectively. The patient recovered fully in a few days. One month later, we removed the plastic stent, and because the guidewire was successfully advanced through the papilla, we performed a rendezvous technique *via* the EUS-CDS fistula (Figure 3). After achieving transpapillary biliary cannulation, endoscopic sphincterotomy was performed, and two stones were removed using a retrieval balloon. Follow-up MRCP obtained 6 mo later showed no recurrence of bile duct stones.

DISCUSSION

Acute cholangitis is a systemic infectious disease characterized by acute inflammation and biliary tract infection. AOSC is a severe form of cholangitis in which pus collects in the biliary tract. According to the newly published Updated Tokyo Guidelines for management of acute cholangitis and cholecystitis (TG13), biliary tract drainage should be performed as soon as possible in patients with AOSC[5]; otherwise, translocation of bacteria into the bloodstream causes sepsis, which is a fatal complication of acute cholangitis that induces severe organ damage and high mortality. Endoscopic retrograde biliary stenting is the current gold standard treatment for acute cholangitis due to biliary lithiasis; however, it may be impossible in patients with selective cannulation failure of the major papilla. In this situation, PTBD is an alternative method, but is sometimes difficult when the intrahepatic bile ducts are not dilated.

Since being first reported in 2001 by Giovannini *et al*[1] EUS-BD has been increasingly performed as an alternative in patients with malignant biliary obstruction for failed ERCP[1-4]. Various techniques of EUS-BD have been described, including EUS-CDS, EUS-guided rendezvous (EUS-RV), and EUS-guided antegrade stent placement. Among these, because EUS-RV preserves the anatomical integrity of the biliary tree and avoids permanent fistula creation, it can be a first-line EUS-BD technique in patients with an endoscopically accessible papilla[6]. There still remain technically challenging aspects, including difficulty in negotiating the guidewire across the obstruction and papilla[6]. Furthermore, EUS-RV needs scope exchange and may require a long procedure time[7]. Püspök *et al*[8] indicated that, compared with EUS-RV, EUS-CDS has several advantages. One is that the fistulous tract created by a puncture of the bile duct is immediately sealed within the same session, which minimizes the risk of significant bile leakage. However, the main indication for EUS-CDS was malignant distal biliary obstruction due to pancreato-biliary malignancies. A recent review, which included 36 studies of EUS-CDS, found that EUS-CDS for benign biliary stricture was performed in only two cases[9]. For acute cholangitis due to choledocholithiasis, EUS-CDS was performed

in only one case[10]. Therefore, the indication for benign biliary disease has not been established. In our series, we experienced three cases of successful urgent EUS-CDS for AOSC due to choledocholithiasis, and there were no procedure-related complications in any of the cases. We suggest that patients with AOSC due to biliary lithiasis after failed ERCP could be preferred candidates for EUS-CDS because endoscopic procedure of long duration may lead to causing increase in morbidity and mortality especially in elderly patients with AOSC-induced sepsis.

The drainage of the CBD can be achieved by two different types of stents, metal and plastic. In cases 1 and 2, covered metallic stents were deployed and in case 3, plastic stent was deployed. According to a recent systematic analysis, the post-procedure adverse events were lower in the metallic stents although there were no differences in technical and functional success rates between metallic and plastic stents[11]. In case 3, the patient had increased risk of bleeding due to DIC. Concerning this risk, we avoided to insert a metallic stent for it needs fistula dilation using a balloon catheter. We placed a nasobiliary tube through the metallic stent in case 1 because the previous report recommended the use of a nasobiliary drain for 48 h to decrease the pressure in the punctured bile duct[12]. In case 2, we attempted to place the nasobiliary tube but the guidewire slipped and failed to place it.

In one case, we extracted CBD stones using a RV technique, and in the other two cases, the patients and their families didn't wish for RV technique or surgery due to advanced age, we routinely exchanged the plastic stents to keep the fistula patent. Endoscopic transpapillary biliary stenting remains an effective alternative for patients with stones difficult to manage by conventional endoscopic methods and those who are unfit for surgery or have high surgical risks[13,14]. There is no standardized time period for routine stent replacement of endoscopic transpapillary biliary stenting. Stent patency rates declined rapidly from 94% at 6 mo to 79% at 12 mo and 58% at 24 mo[15]. Therefore we decided to exchange stents semiannually in case 1 and 2.

Recent large studies have identified repeated cannulation attempts with standard approach as a risk factor for post-ERCP pancreatitis (PEP)[16]. It is important to change the procedure early to achieve safe and effective bile cannulation with a shorter procedure time. For prevention of PEP, EUS-CDS is a more advantageous procedure because the pancreas is untouched.

Although endoscopic retrograde biliary stenting has been well-established technique for providing biliary decompression in patients with bile duct obstruction, we believe that EUS-CDS will be a suited salvage to patients whom ERCP cannot be performed. There are still some problems to be solved. One is that bile leak is a concern during EUS-guided biliary interventions and previous studies have demonstrated that biliary leakage into the peritoneal space is the most common complications of EUS-BD[3,4,17]. Therefore, the development of new comfortable stenting device that facilitates simultaneous puncture/dilation is needed. If it becomes available, EUD-CDS will become easier and safer in the future.

The limitations of this study were the small number of patients, lack of a control group, and the inclusion of only a single operator at a single tertiary-care referral center.

In conclusion, with regards to a failed standard ERCP, EUS-CDS can be an effective life-saving biliary decompression procedure that can shorten the procedure time and prevent PEP, particularly in patients with AOSC-induced sepsis. Further long-term studies with a larger cohort are needed to prove the efficacy and safety of this technique.

COMMENTS

Case characteristics

Three elderly patients (1 male, 2 female) presented with sepsis from acute cholangitis.

Clinical diagnosis

Acute obstructive suppurative cholangitis (AOSC) with sepsis due to biliary lithiasis.

Differential diagnosis

Tumors (pancreatic cancer, cholangiocarcinoma, ampullary cancer or metastasis) or benign bile duct stricture/stenosis.

Laboratory diagnosis

The laboratory findings showed an elevated inflammatory reaction and elevated levels of serum liver function parameters and bilirubin.

Imaging diagnosis

Computed tomography revealed common bile duct (CBD) stones and dilatation of CBD.

Pathological diagnosis

Pathological examination was not performed in any of the patients.

Treatment

Urgent endoscopic ultrasound-guided choledochoduodenostomy (EUS-CDS) *via* the duodenum bulb.

Related reports

EUS-CDS is commonly performed in patients with malignant distal biliary obstruction due to pancreato-biliary malignancies. In contrast, there are few reports performing this technique for benign biliary lesions.

Term explanation

EUS-CDS is a novel alternative technique for biliary drainage in patients for whom endoscopic retrograde cholangiopancreatography (ERCP) has failed and who prefer internal rather than percutaneous biliary drainage or surgical bypass procedures.

Experiences and lessons

Urgent EUS-CDS for AOSC-induced sepsis due to biliary lithiasis can be an effective life-saving endoscopic biliary decompression procedure that can

shorten the procedure time and prevent post-ERCP pancreatitis.

Peer-review

This case report is well written and the topic is interesting. This report describes the successful use of EUS-CDS in three patients with AOSC-induced sepsis due to biliary lithiasis.

REFERENCES

1 **Giovannini M**, Moutardier V, Pesenti C, Bories E, Lelong B, Delpero JR. Endoscopic ultrasound-guided bilioduodenal anastomosis: a new technique for biliary drainage. *Endoscopy* 2001; **33**: 898-900 [PMID: 11571690 DOI: 10.1055/s-2001-17324]

2 **Artifon EL**, Aparicio D, Paione JB, Lo SK, Bordini A, Rabello C, Otoch JP, Gupta K. Biliary drainage in patients with unresectable, malignant obstruction where ERCP fails: endoscopic ultrasonography-guided choledochoduodenostomy versus percutaneous drainage. *J Clin Gastroenterol* 2012; **46**: 768-774 [PMID: 22810111 DOI: 10.1097/MCG.0b013e31825f264c]

3 **Kahaleh M**, Hernandez AJ, Tokar J, Adams RB, Shami VM, Yeaton P. Interventional EUS-guided cholangiography: evaluation of a technique in evolution. *Gastrointest Endosc* 2006; **64**: 52-59 [PMID: 16813803]

4 **Park do H**, Jang JW, Lee SS, Seo DW, Lee SK, Kim MH. EUS-guided biliary drainage with transluminal stenting after failed ERCP: predictors of adverse events and long-term results. *Gastrointest Endosc* 2011; **74**: 1276-1284 [PMID: 21963067 DOI: 10.1016/j.gie.2011.07.054]

5 **Miura F**, Takada T, Strasberg SM, Solomkin JS, Pitt HA, Gouma DJ, Garden OJ, Büchler MW, Yoshida M, Mayumi T, Okamoto K, Gomi H, Kusachi S, Kiriyama S, Yokoe M, Kimura Y, Higuchi R, Yamashita Y, Windsor JA, Tsuyuguchi T, Gabata T, Itoi T, Hata J, Liau KH. TG13 flowchart for the management of acute cholangitis and cholecystitis. *J Hepatobiliary Pancreat Sci* 2013; **20**: 47-54 [PMID: 23307003 DOI: 10.1007/s00534-012-0563-1]

6 **Iwashita T**, Yasuda I, Mukai T, Iwata K, Ando N, Doi S, Nakashima M, Uemura S, Mabuchi M, Shimizu M. EUS-guided rendezvous for difficult biliary cannulation using a standardized algorithm: a multicenter prospective pilot study (with videos). *Gastrointest Endosc* 2016; **83**: 394-400 [PMID: 26089103 DOI: 10.1016/j.gie.2015.04.043]

7 **Kim YS**, Gupta K, Mallery S, Li R, Kinney T, Freeman ML. Endoscopic ultrasound rendezvous for bile duct access using a transduodenal approach: cumulative experience at a single center. A case series. *Endoscopy* 2010; **42**: 496-502 [PMID: 20419625 DOI: 10.1055/s-0029-1244082]

8 **Püspök A**, Lomoschitz F, Dejaco C, Hejna M, Sautner T, Gangl A. Endoscopic ultrasound guided therapy of benign and malignant biliary obstruction: a case series. *Am J Gastroenterol* 2005; **100**: 1743-1747 [PMID: 16086710]

9 **Ogura T**, Higuchi K. Technical tips of endoscopic ultrasound-guided choledochoduodenostomy. *World J Gastroenterol* 2015; **21**: 820-828 [PMID: 25624715 DOI: 10.3748/wjg.v21.i3.820]

10 **Horaguchi J**, Fujita N, Noda Y, Kobayashi G, Ito K, Obana T, Takasawa O, Koshita S, Kanno Y. Endosonography-guided biliary drainage in cases with difficult transpapillary endoscopic biliary drainage. *Dig Endosc* 2009; **21**: 239-244 [PMID: 19961522 DOI: 10.1111/j.1443-1661.2009.00899.x]

11 **Wang K**, Zhu J, Xing L, Wang Y, Jin Z, Li Z. Assessment of efficacy and safety of EUS-guided biliary drainage: a systematic review. *Gastrointest Endosc* 2015; Epub ahead of print [PMID: 26542374 DOI: 10.1016/j.gie.2015.10.033]

12 **Giovannini M**, Pesenti Ch, Bories E, Caillol F. Interventional EUS: difficult pancreaticobiliary access. *Endoscopy* 2006; **38** Suppl 1: S93-S95 [PMID: 16802236]

13 **Jain SK**, Stein R, Bhuva M, Goldberg MJ. Pigtail stents: an alternative in the treatment of difficult bile duct stones. *Gastrointest Endosc* 2000; **52**: 490-493 [PMID: 11023565]

14 **Yang J**, Peng JY, Chen W. Endoscopic biliary stenting for irretrievable common bile duct stones: Indications, advantages, disadvantages, and follow-up results. *Surgeon* 2012; **10**: 211-217 [PMID: 22647840 DOI: 10.1016/j.surge.2012.04.003]

15 **Li KW**, Zhang XW, Ding J, Chen T, Wang J, Shi WJ. A prospective study of the efficacy of endoscopic biliary stenting on common bile duct stones. *J Dig Dis* 2009; **10**: 328-331 [PMID: 19906114 DOI: 10.1111/j.1751-2980.2009.00404.x]

16 **Cheng CL**, Sherman S, Watkins JL, Barnett J, Freeman M, Geenen J, Ryan M, Parker H, Frakes JT, Fogel EL, Silverman WB, Dua KS, Aliperti G, Yakshe P, Uzer M, Jones W, Goff J, Lazzell-Pannell L, Rashdan A, Temkit M, Lehman GA. Risk factors for post-ERCP pancreatitis: a prospective multicenter study. *Am J Gastroenterol* 2006; **101**: 139-147 [PMID: 16405547]

17 **Poincloux L**, Rouquette O, Buc E, Privat J, Pezet D, Dapoigny M, Bommelaer G, Abergel A. Endoscopic ultrasound-guided biliary drainage after failed ERCP: cumulative experience of 101 procedures at a single center. *Endoscopy* 2015; **47**: 794-801 [PMID: 25961443 DOI: 10.1055/s-0034-1391988]

P- Reviewer: Amornyotin S, Giannopoulos GA, Kayaalp C, Muguruma N, Skok P, Yan SL **S- Editor**: Qi Y **L- Editor**: A **E- Editor**: Ma S

World Journal of Gastroenterology

Submit a Manuscript: http://www.wjgnet.com/esps/
Help Desk: http://www.wjgnet.com/esps/helpdesk.aspx
DOI: 10.3748/wjg.v22.i16.4270

World J Gastroenterol 2016 April 28; 22(16): 4270-4274
ISSN 1007-9327 (print) ISSN 2219-2840 (online)

CASE REPORT

Occult gastric cancer with distant metastasis proven by random gastric biopsy

Sang Hyuk Lee, Kyu-Hyoung Lim, Seo-Young Song, Hui-Young Lee, Sung Chul Park, Chang Don Kang, Sung Joon Lee, Dong Wook Choi, Sung Bae Park, Young-Joon Ryu

Sang Hyuk Lee, Kyu-Hyoung Lim, Seo-Young Song, Hui-Young Lee, Sung Chul Park, Chang Don Kang, Sung Joon Lee, Dong Wook Choi, Department of Internal Medicine, Kangwon National University School of Medicine, Chuncheon 24341, South Korea

Sung Bae Park, Department of General Surgery, Kangwon National University School of Medicine, Chuncheon 24341, South Korea

Young-Joon Ryu, Department of Pathology, Kangwon National University School of Medicine, Chuncheon 24341, South Korea

Author contributions: Lee SH and Lim KH designed the case report, analyzed the data and wrote the paper; Song SY, Lee HY, Park SC, Kang CD, Lee SJ and Park SB collected the patient's clinical data; Ryu YJ performed the pathologic review.

Supported by 2013 Research Grant from Kangwon National University, No. C1010351-01-01.

Institutional review board statement: This case report was exempt from the Institutional Review Board standards of Kangwon National University Hospital (Approval No. 2015-11-015).

Informed consent statement: Because the patient involved in this study passed away, we were allowed an exemption of informed consent from the Institutional Review Board standards of Kangwon National University Hospital (Approval No. 2015-11-015).

Conflict-of-interest statement: All the authors declare they have no conflicts of interests related to the publication of this case report.

Correspondence to: Kyu-Hyoung Lim, MD, Assistant Professor, Division of Hemato-Oncology, Department of Internal Medicine, Kangwon National University School of Medicine, 156 Baengnyeong-ro, Chuncheon-Si, Gangwon-Do 24341, South Korea. kyuhyoung.lim@gmail.com
Telephone: +82-33-2589173
Fax: +82-33-2582404

Received: October 25, 2015
Peer-review started: October 26, 2015
First decision: November 13, 2015
Revised: December 10, 2015
Accepted: January 17, 2016
Article in press: January 18, 2016
Published online: April 28, 2016

Abstract

Krukenberg tumor, a rare metastatic ovarian tumor arising from gastrointestinal adenocarcinoma mainly, tends to occur in premenopausal females. Finding the origin of a Krukenberg tumor is crucial for determining prognosis. In Eastern countries, the most common origin of Krukenberg tumor is stomach cancer, which is generally diagnosed *via* endoscopic biopsy to investigate an abnormal mucosal lesion. Here, we describe a case of huge adnexal mass in a 33-year-old woman who presented with abdominal distension. Two independent endoscopic examinations performed by experts in two tertiary university hospitals revealed no abnormal mucosal lesion. The patient was diagnosed with a Krukenberg tumor according to findings from random endoscopic biopsies taken from normal-looking gastric mucosa in our hospital. It is very rare to be diagnosed *via* a random biopsy in cases where three well-trained endoscopists had not found any mucosal lesion previously. Thus, in this case, random biopsy was helpful in finding the origin of a Krukenberg tumor.

Key words: Gastric cancer; Krukenberg tumor; Biopsy; Endoscopy; Diagnosis

Core tip: We describe a 33-year-old woman who was diagnosed with Krukenberg tumor of gastric origin after random biopsy taken during endoscopy for normal-looking mucosa. Although three well-trained endoscopists confirmed that there was no mucosal lesion in the stomach, the random biopsy from the corpus showed signet ring cell carcinoma. Clinical significance of this case is that clinicians should consider gastric malignancy for patients who have Krukenberg tumor of which the origin has not been found, even when the gastric mucosa appears to be intact. For these patients, random gastric biopsy may help to reveal the primary cancer.

Lee SH, Lim KH, Song SY, Lee HY, Park SC, Kang CD, Lee SJ, Choi DW, Park SB, Ryu YJ. Occult gastric cancer with distant metastasis proven by random gastric biopsy. *World J Gastroenterol* 2016; 22(16): 4270-4274 Available from: URL: http://www.wjgnet.com/1007-9327/full/v22/i16/4270.htm DOI: http://dx.doi.org/10.3748/wjg.v22.i16.4270

INTRODUCTION

Stomach cancer is the fourth most frequent malignancy and the second leading cause of cancer death worldwide[1]. In South Korea, it is the second most common type of cancer and the third leading cause of cancer deaths[2]. A Krukenberg tumor is an ovarian metastatic carcinoma from a primary site, such as the gastrointestinal tract. Patients with this tumor type are generally between the ages of 40-years-old and 46-years-old, and present with variable symptoms. Because Krukenberg tumors are initially diagnosed at the highly advanced state, they have a poor prognosis; the median overall survival period has been reported as 7-14 mo[3]. In Asian countries, stomach cancer primary origin accounts for approximately 70% of the Krukenberg tumor cases[4-6], with this origin generally diagnosed *via* an endoscopic biopsy of an abnormal mucosal lesion. Although there has been a similar case report from Japan with identification during autopsy[7], the case we are reporting here is the first of Krukenberg tumor for which the primary origin was confirmed *via* random endoscopic biopsy. Herein, we report a case of Krukenberg tumor of gastric origin diagnosed *via* random endoscopic biopsy of apparently normal-looking gastric mucosa.

CASE REPORT

A 33-year-old woman with complaints of nausea and abdominal distension for 3 mo was admitted to a university hospital near her home. Examination by abdomino-pelvic computed tomography (CT) (Figure 1A) and positron emission tomography (PET)-CT (Figure 1B) revealed a left, huge ovarian mass and peritoneal metastatic lesions. To identify primary origins, gastroscopy and colonoscopy were performed, but showed no abnormal lesions (Figure 2A). Thereafter, she visited another tertiary university hospital for a second opinion; the diagnostic tests included repeat gastroscopy, which showed grossly normal mucosa similar to the previous findings (Figure 2B). A fine-needle biopsy was then conducted at the left supraclavicular lymph node (SCN), which yielded positive findings for signet ring cell carcinoma in the chest CT and the PET-CT (Figure 3A).

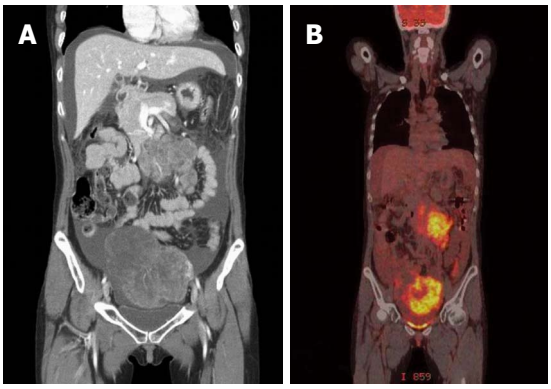

Figure 1 A huge heterogeneous enhancing ovarian mass and peritoneal metastatic lesions were observed. A: Computed tomography (CT) scan; B: Positron emission tomography-CT scan.

The patient was clinically diagnosed with Krukenberg tumor of an unknown primary origin. She was transferred to our hospital for supportive care, as she complained of severe pain and had poor oral intake. Upon physical examination, her abdomen was soft and distended, with a huge palpable mass in the lower abdomen. Anemia, leukocytosis, electrolyte imbalance, and high carbohydrate antigen (CA)125 level were found. Tests for carcinoembryonic antigen (CEA) and CA19-9 markers were within normal ranges. Based on the clinical aspects and outside medical records that included radiologic imaging and histological findings for the left SCN, we considered the primary origin likely to be the upper digestive tract; thus, we decided to conduct random endoscopic gastric biopsy. It is important to note that the patient's performance status contraindicated an invasive procedure, and consequently we did not perform any surgical procedures, such as staging laparoscopy. The endoscopic examination showed no abnormal mucosal lesion in the region from the cardia to the antrum, similar to the two previous endoscopic findings (Figure 2C). Random biopsies were taken from antrum (2 biopsies on the lesser curvature and 2 on the greater curvature) and body (1 biopsy on

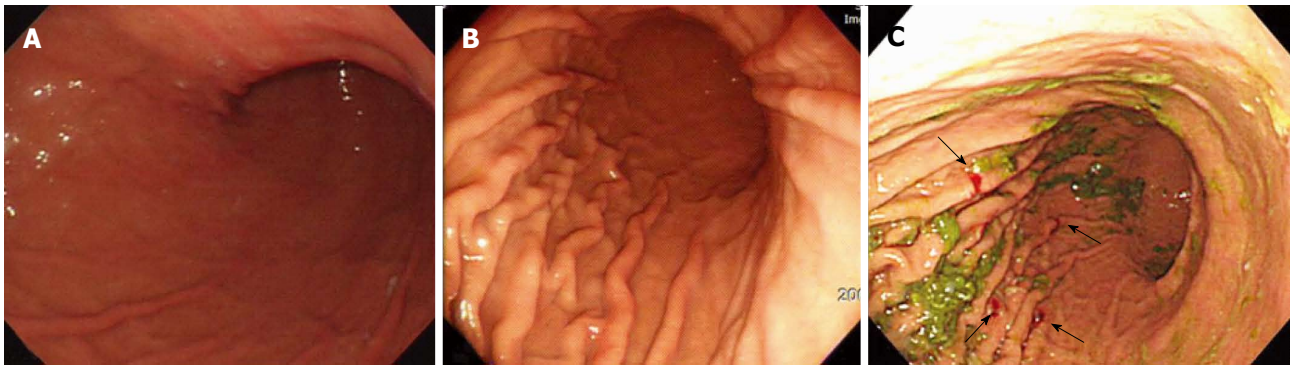

Figure 2 No grossly abnormal lesion was observed in gastroscopy. A: Examination at first visit to the first hospital; B: At repeat visit to the second hospital; C: At the last visit to our hospital. The black arrows indicate the random biopsy sites. Green matter is remnant gastric content.

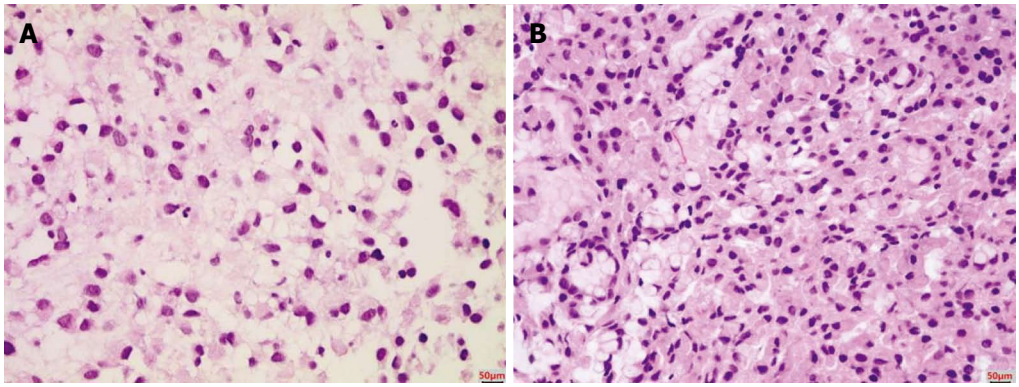

Figure 3 Histopathologic findings. A: Lymph node needle biopsy; B: Gastric random biopsy; A and B: Hematoxylin-eosin staining and magnification × 400.

the lesser curvature and 4 on the greater curvature). The morphological finding of carcinoma was signet ring cell type adenocarcinoma, which was the same as that of the left SCN (Figure 3B). Immunohistochemical staining showed strong positivity for C-erbB2 (score of 3) and negativity for cytokeratin 7 and cytokeratin 20. Therefore, the final diagnosis was Krukenberg tumor of gastric origin.

On the day 9 after the patient's hospital admission, she underwent combination chemotherapy (trastuzumab, 5-FU, and cisplatin). However, the tumor had an aggressive course and the patient died of systemic fungal infection 2 mo later.

DISCUSSION

A Krukenberg tumor is considered a metastatic cancer of the ovary, usually from the gastrointestinal tract[8]. There are some differences between Asian and Western countries in the prevalence and primary origin of metastatic cancer of the ovary. In Europe, Krukenberg tumors reportedly account for 15% of all ovarian malignancies, with the primary sites of such cancers being gastrointestinal tract (39%), breast (28%), and endometrium (20%)[9]. On the other hand, Krukenberg tumor has been reported in 29% of cases of metastatic ovarian cancer in Japan, with the most common primary lesion being gastric cancer, with an incidence range of 69.6%-72.0%[5,6]. Similar prevalence of metastatic ovarian cancers has been reported for Korea; however, the most common primary origin is the stomach (66.7%), followed by the colon (17.6%) and the breast (5.6%)[4]. Al-Agha and Nicastri[10] reported that the prognosis of Krukenberg tumor was worse for cases in which the primary tumor was unidentified.

Krukenberg tumor often develops in premenopausal females[3,5,8]. Yang *et al*[11] reported that more than 80% of signet ring cell carcinomas are the absorptive and mucus-producing functional differentiation type (AMPFDT). Since AMPFDT expresses estrogen receptors, the proliferation and infiltration of signet ring cell carcinoma are affected by the estrogen level. Therefore, gastric signet ring cell carcinoma commonly metastasizes to the ovary or the uterine cervix, where the estrogen level is high[11]. Other possible pathways of metastasis of gastric cancer to the ovary are the lymphatic routes. Krukenberg tumor is an example of the selective spread of cancers, as is very common in the stomach-ovarian axis. Retrograde lymphatic spread is the most powerful candidate for the metastatic route for several reasons[10]. First, microscopic lymphatic permeation at the hilum and cortex has been observed in many cases. Second, there have been several reported cases of Krukenberg tumor with early gastric cancer that was limited to the

mucosa and the submucosa, where a rich lymphatic plexus exists[12]. Lymphatic invasion can account for the spread of early gastric cancer. Third, some studies have demonstrated that greater number of metastatic lymph nodes is associated with higher risk of ovarian metastasis in gastric cancer[13].

Optimal treatment strategies for Krukenberg tumors have not been established yet. The role of surgical cytoreduction remains controversial; although, cytoreductive surgery combined with chemotherapy has been evidenced as an effective treatment of primary ovarian cancer[14]. A few studies have demonstrated surgery as capable of improving overall survival of patients with Krukenberg tumor of primary colorectal or breast cancer; on the contrary, patients with Krukenberg tumor from primary gastric cancer did not appear to benefit from cytoreductive surgery[14,15]. Therefore, treatment plans need to be individualized according to the type of primary cancer. The treatment for our patient, described herein, followed the standard guidelines for metastatic gastric cancer.

Prognosis of Krukenberg tumors is poorer than that of primary ovarian cancer. In addition, the overall survival of patients with Krukenberg tumor depends on the primary origin. Jiang *et al*[15] reported that the overall survival period of patients with Krukenberg tumor of gastric origin was about 12 mo, similar to that of patients with metastatic gastric cancer, whereas the overall survival periods of patients with Krukenberg tumor of the colon and other origins were 29.6 and 48.2 mo, respectively. Another study reported that the presence of peritoneal seeding was the only significant prognostic factor for Krukenberg tumor from gastric primary cancer[16].

At times, gastric cancers can be overlooked, even by expert gastroscopists. According to a Korean study, Bormann type 3 advanced gastric cancer (AGC) in the cardia of the stomach and Bormann type 4 AGC at the greater curvature were the most commonly overlooked types of gastric cancer[17]. Overlooking the lesions in the cardia was conjectured to be related to the technical difficulty of the endoscopic approach. In general, it is also considered difficult to find lesions in the side of the body with greater curvature, because they can be hidden by the gastric folds. In our case, there was little possibility of a lesion being overlooked, because three other endoscopists, who were sufficiently trained in a university hospital, had performed examination for abnormal mucosal lesions specifically; no area was found to be covered with the gastric folds during the endoscopy and the gastric contents were completely emptied in the two previous procedures. Besides, the patient did not show any gastric fold thickening with poor expansibility, which is one of the characteristic features of submucosal spreading AGC.

In conclusion, it is very important to know the origin of a Krukenberg tumor in order to plan the treatment strategy and determine prognosis. Unfortunately, about 10% of patients with Krukenberg tumor continue to have an unknown primary origin despite various efforts at identification. In such cases, multiple random gastric biopsies to further examine endoscopically normal-looking mucosa can be helpful, especially for Asian patients.

COMMENTS

Case characteristics

A 33-year-old woman with no significant medical history complained of a 3-mo history of nausea and abdominal distension.

Clinical diagnosis

The patient's abdomen was soft and distended, with a huge palpable mass in the lower abdomen.

Differential diagnosis

Primary ovarian cancer with metastasis, peritoneal carcinomatosis with ovary involvement.

Laboratory diagnosis

Anemia, leukocytosis, electrolyte imbalance, and high carbohydrate antigen (CA) 125 level were shown.

Imaging diagnosis

Computed tomography showed a 13.2 cm × 9.1 cm heterogeneous enhancing mass in the left ovary and peritoneal infiltration, thickening, and ascites suggesting peritoneal seeding.

Pathological diagnosis

Signet ring cell type adenocarcinoma.

Treatment

Combination chemotherapy (trastuzumab, 5-FU, and cisplatin).

Related reports

Krukenberg tumor is considered a metastatic cancer. However, for some cases, primary cancer of the tumor may not be revealed. Outcomes can be different according to knowledge of the origin.

Term explanation

Recently, a new cell-functional classification of gastric carcinomas was proposed, and includes the absorptive and mucus-producing functional differentiation type (AMPFDT). Most of the signet ring cell type adenocarcinomas found in this case were AMPFDT.

Experiences and lessons

In selected cases, multiple random gastric biopsies obtained from endoscopically normal-looking mucosa can aid in identifying the primary cancer of Krukenberg tumor.

Peer-review

It's an interesting report regarding the application of random biopsy in detecting the primary origin site of the patient with a Krukenberg tumor.

REFERENCES

1 **Parkin DM**, Bray F, Ferlay J, Pisani P. Global cancer statistics, 2002. *CA Cancer J Clin* 2005; **55**: 74-108 [PMID: 15761078 DOI: 10.3322/canjclin.55.2.74]

2 **Jung KW**, Won YJ, Kong HJ, Oh CM, Lee DH, Lee JS. Cancer statistics in Korea: incidence, mortality, survival, and prevalence in 2011. *Cancer Res Treat* 2014; **46**: 109-123 [PMID: 24851102 DOI:

10.4143/crt.2014.46.2.109]
3 **McGill FM**, Ritter DB, Rickard CS, Kaleya RN, Wadler S, Greston WM, O'Hanlan KA. Krukenberg tumors: can management be improved? *Gynecol Obstet Invest* 1999; **48**: 61-65 [PMID: 10394095 DOI: 10.1159/000010136]
4 **Kim YW**, Lee HW, Kang JS. Clinical Analysis of Krukenberg Tumor -A Review of 18 Cases-. *Obstet Gynecol Sci* 1991; **34**: 1451-1456
5 **Yakushiji M**, Tazaki T, Nishimura H, Kato T. Krukenberg tumors of the ovary: a clinicopathologic analysis of 112 cases. *Nihon Sanka Fujinka Gakkai Zasshi* 1987; **39**: 479-485 [PMID: 3031182]
6 **Yada-Hashimoto N**, Yamamoto T, Kamiura S, Seino H, Ohira H, Sawai K, Kimura T, Saji F. Metastatic ovarian tumors: a review of 64 cases. *Gynecol Oncol* 2003; **89**: 314-317 [PMID: 12713997 DOI: 10.1016/S0090-8258(03)00075-1]
7 **Nakamura Y**, Hiramatsu A, Koyama T, Oyama Y, Tanaka A, Honma K. A Krukenberg Tumor from an Occult Intramucosal Gastric Carcinoma Identified during an Autopsy. *Case Rep Oncol Med* 2014; **2014**: 797429 [PMID: 25386374 DOI: 10.1155/2014/797429]
8 **Hale RW**. Krukenberg tumor of the ovaries. A review of 81 records. *Obstet Gynecol* 1968; **32**: 221-225 [PMID: 4316071]
9 **de Waal YR**, Thomas CM, Oei AL, Sweep FC, Massuger LF. Secondary ovarian malignancies: frequency, origin, and characteristics. *Int J Gynecol Cancer* 2009; **19**: 1160-1165 [PMID: 19823050 DOI: 10.1111/IGC.0b013e3181b33cce]
10 **Al-Agha OM**, Nicastri AD. An in-depth look at Krukenberg tumor: an overview. *Arch Pathol Lab Med* 2006; **130**: 1725-1730 [PMID: 17076540]
11 **Yang XF**, Yang L, Mao XY, Wu DY, Zhang SM, Xin Y. Pathobiological behavior and molecular mechanism of signet ring cell carcinoma and mucinous adenocarcinoma of the stomach: a comparative study. *World J Gastroenterol* 2004; **10**: 750-754 [PMID: 14991954 DOI: 10.3748/wjg.v10.i5.750]
12 **Kakushima N**, Kamoshida T, Hirai S, Hotta S, Hirayama T, Yamada J, Ueda K, Sato M, Okumura M, Shimokama T, Oka Y. Early gastric cancer with Krukenberg tumor and review of cases of intramucosal gastric cancers with Krukenberg tumor. *J Gastroenterol* 2003; **38**: 1176-1180 [PMID: 14714257 DOI: 10.1007/s00535-003-1227-3]
13 **Kim NK**, Kim HK, Park BJ, Kim MS, Kim YI, Heo DS, Bang YJ. Risk factors for ovarian metastasis following curative resection of gastric adenocarcinoma. *Cancer* 1999; **85**: 1490-1499 [PMID: 10193938]
14 **Kim WY**, Kim TJ, Kim SE, Lee JW, Lee JH, Kim BG, Bae DS. The role of cytoreductive surgery for non-genital tract metastatic tumors to the ovaries. *Eur J Obstet Gynecol Reprod Biol* 2010; **149**: 97-101 [PMID: 20018420 DOI: 10.1016/j.ejogrb.2009.11.011]
15 **Jiang R**, Tang J, Cheng X, Zang RY. Surgical treatment for patients with different origins of Krukenberg tumors: outcomes and prognostic factors. *Eur J Surg Oncol* 2009; **35**: 92-97 [PMID: 18632244 DOI: 10.1016/j.ejso.2008.05.006]
16 **Yook JH**, Oh ST, Kim BS. Clinical prognostic factors for ovarian metastasis in women with gastric cancer. *Hepatogastroenterology* 2007; **54**: 955-959 [PMID: 17591102]
17 **Sung IK**, Kim YC, Yun JW, Seo HI, Park DI, Cho YK, Kim HJ, Park JH, Sohn CI, Jeon WK, Kim BI, Oh SJ, Son BH, Yoo CH, Sohn JH, Lee HY, Won KH. Characteristics of advanced gastric cancer undetected on gastroscopy. *Korean J Gastroenterol* 2011; **57**: 288-293 [PMID: 21623137 DOI: 10.4166/kjg.2011.57.5.288]

P- Reviewer: Arigami T, Wang YH
S- Editor: Gong ZM **L- Editor**: A **E- Editor**: Liu XM

Published by **Baishideng Publishing Group Inc**
8226 Regency Drive, Pleasanton, CA 94588, USA
Telephone: +1-925-223-8242
Fax: +1-925-223-8243
E-mail: bpgoffice@wjgnet.com
Help Desk: http://www.wjgnet.com/esps/helpdesk.aspx
http://www.wjgnet.com

ISSN 1007-9327
16>